frontiers | Research Topics

Current advances in Fusarium wilt

Edited by
Mahyar Mirmajlessi, Inmaculada Larena, María Del Mar Guerrero and María Del Carmen Rodríguez-Molina

Published in
Frontiers in Plant Science
Frontiers in Microbiology

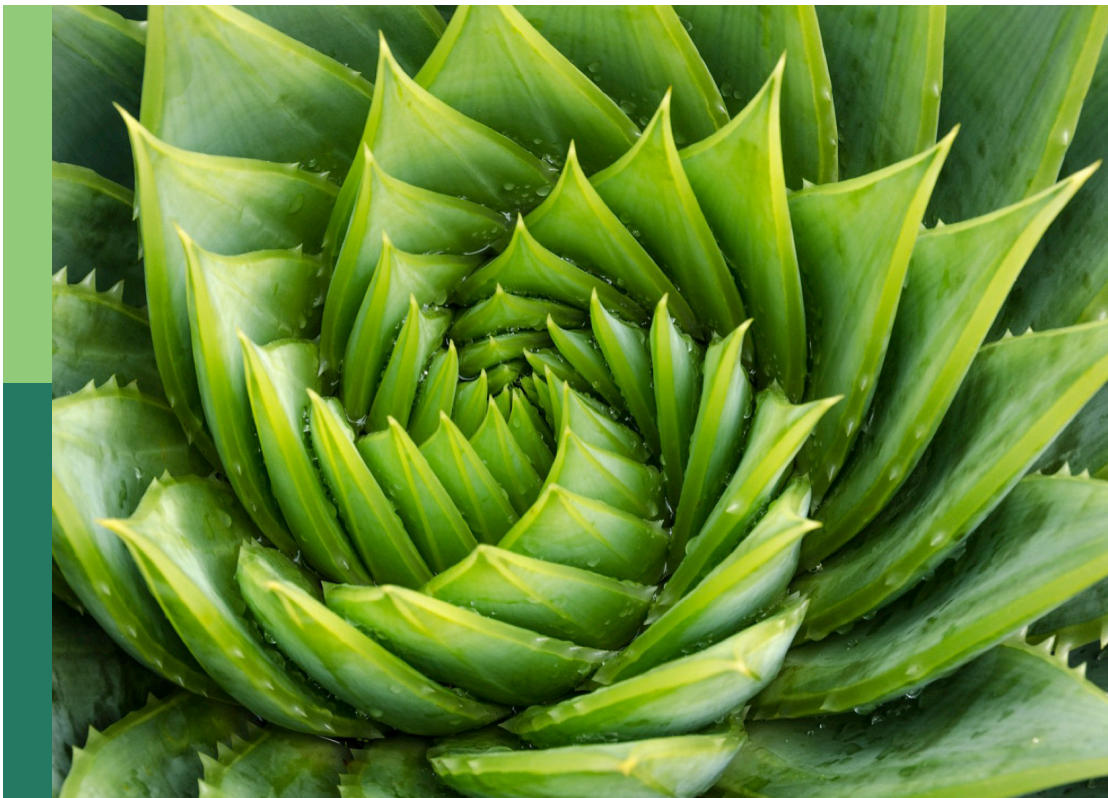

ISSN 1664-8714
ISBN 978-2-8325-6958-0
DOI 10.3389/978-2-8325-6958-0

Generative AI statement
Any alternative text (Alt text) provided alongside figures in the articles in this ebook has been generated by Frontiers with the support of artificial intelligence and reasonable efforts have been made to ensure accuracy, including review by the authors wherever possible. If you identify any issues, please contact us.

About Frontiers

Frontiers is more than just an open access publisher of scholarly articles: it is a pioneering approach to the world of academia, radically improving the way scholarly research is managed. The grand vision of Frontiers is a world where all people have an equal opportunity to seek, share and generate knowledge. Frontiers provides immediate and permanent online open access to all its publications, but this alone is not enough to realize our grand goals.

Frontiers journal series

The Frontiers journal series is a multi-tier and interdisciplinary set of open-access, online journals, promising a paradigm shift from the current review, selection and dissemination processes in academic publishing. All Frontiers journals are driven by researchers for researchers; therefore, they constitute a service to the scholarly community. At the same time, the *Frontiers journal series* operates on a revolutionary invention, the tiered publishing system, initially addressing specific communities of scholars, and gradually climbing up to broader public understanding, thus serving the interests of the lay society, too.

Dedication to quality

Each Frontiers article is a landmark of the highest quality, thanks to genuinely collaborative interactions between authors and review editors, who include some of the world's best academicians. Research must be certified by peers before entering a stream of knowledge that may eventually reach the public - and shape society; therefore, Frontiers only applies the most rigorous and unbiased reviews. Frontiers revolutionizes research publishing by freely delivering the most outstanding research, evaluated with no bias from both the academic and social point of view. By applying the most advanced information technologies, Frontiers is catapulting scholarly publishing into a new generation.

What are Frontiers Research Topics?

Frontiers Research Topics are very popular trademarks of the *Frontiers journals series*: they are collections of at least ten articles, all centered on a particular subject. With their unique mix of varied contributions from Original Research to Review Articles, Frontiers Research Topics unify the most influential researchers, the latest key findings and historical advances in a hot research area.

Find out more on how to host your own Frontiers Research Topic or contribute to one as an author by contacting the Frontiers editorial office: frontiersin.org/about/contact

Current advances in Fusarium wilt

Topic editors

Mahyar Mirmajlessi — Ghent University, Belgium

Inmaculada Larena — Instituto Nacional de Investigación y Tecnología Agraria y Alimentaria (INIA-CSIC), Spain

María Del Mar Guerrero — Instituto Murciano de Investigación y Desarrollo Agrario y Alimentario (IMIDA), Spain

María Del Carmen Rodríguez-Molina — Center for Scientific and Technological Research of Extremadura (CICYTEX), Spain

Citation

Mirmajlessi, M., Larena, I., Guerrero, M. D. M., Del Carmen Rodríguez-Molina, M., eds. (2025). *Current advances in Fusarium wilt*. Lausanne: Frontiers Media SA. doi: 10.3389/978-2-8325-6958-0

Table of contents

frontiers | Frontiers in Plant Science

TYPE Editorial
PUBLISHED 23 September 2025
DOI 10.3389/fpls.2025.1683977

OPEN ACCESS

EDITED AND REVIEWED BY
Brigitte Mauch-Mani,
Retired, Fribourg, Switzerland

*CORRESPONDENCE
Seyed Mahyar Mirmajlessi
mahyar.mirmajlessi@ugent.be

RECEIVED 11 August 2025
ACCEPTED 09 September 2025
PUBLISHED 23 September 2025

CITATION
Mirmajlessi M, Larena I, Guerrero MDM and del Carmen Rodríguez-Molina M (2025) Editorial: Current advances in Fusarium wilt. *Front. Plant Sci.* 16:1683977. doi: 10.3389/fpls.2025.1683977

Editorial: Current advances in Fusarium wilt

Mahyar Mirmajlessi[1]*, Inmaculada Larena[2], María Del Mar Guerrero[3] and María del Carmen Rodríguez-Molina[4]

[1]Department of Plants and Crops, Faculty of Bioscience Engineering, Ghent University, Ghent, Belgium, [2]Department of Plant Protection, Instituto de Investigación y Tecnología Agraria y Alimentaria-CSIC, Madrid, Spain, [3]Instituto Murciano de Investigacion y Desarrollo Agrario y Medioambiental, Mayor La Alberca Murcia, Spain, [4]Centro de Agricultura Ecologica y de Montana (CAEM), Centro de Investigaciones Cientificas y Tecnologicas de Extremadura (CICYTEX), Plasencia, Spain

KEYWORDS

***Fusarium* wilt, harnessing antagonistic fungi and soil amendments, bioactive plant compounds, microbial interactions and community dynamics, integrating host resistance and genomic approaches**

Editorial on the Research Topic
Current advances in Fusarium wilt

Fusarium wilt, caused by a diverse group of *Fusarium* spp., remains one of the most formidable soilborne threats to agricultural productivity worldwide. The persistence of its propagules in soil, its broad host range, and its capacity to compromise both yield and quality make it a particularly intractable challenge across cropping systems. With chemical control options constrained by environmental and regulatory concerns, and host resistance often incomplete or unstable, sustainable and integrated disease management solutions have gained renewed urgency. This Research Topic brings together innovative studies aimed at improving the understanding of and control of *Fusarium* wilt through biological, ecological, molecular, and formulation-based approaches.

Harnessing antagonistic fungi and soil amendments

A recurrent theme across multiple contributions is the potential of antagonistic fungi, particularly *Trichoderma* spp., to serve as biocontrol agents against *Fusarium* wilt. Pradhan et al. conducted a performance evaluation of novel tablet and powder formulations based on *T. viride* ITCC 7764 in chickpeas. These formulations demonstrated both superior biocontrol efficacy and agronomic benefits under field conditions compared to synthetic fungicides and talc-based formulations. These formulations were characterized by desirable physical properties and were enriched with volatile organic compounds including octan-3-one and 1-octen-3-ol, which are known for their antifungal activity. In addition, Long et al. isolated a promising *T. parareesei* strain (N4-3) from banana rhizospheres exhibiting potent antifungal activity against *F. oxysporum* f. sp. *cubense* TR4. This strain exhibited hyperparasitic behavior by deploying a range of cell wall-degrading enzymes, including 21 chitinases and 26 β-1,3-glucanases, resulting in severe structural disruption of the pathogen. Its application in pot trials significantly reduced the pathogen load and disease

index while improving plant growth, highlighting its potential as an eco-friendly solution for controlling banana Fusarium wilt. Chen et al. identified two efficient biocontrol fungi *T. harzianum* and *Pestalotiopsis* sp. that can be used for *F. oxysporum* control in *Morinda officinalis*. To explore the control mechanisms of these biocontrol fungi, the authors used transcriptome sequencing analyses. They showed that expression levels in *M. officinalis* roots varied significantly following treatment with different biocontrol fungi, regulating signal transduction pathways and phytohormones related to pathogen resistance, such as the MAPK signaling pathway and the ethylene signaling pathway. This could improve the disease resistance and growth of *M. officinalis*. The biocontrol effects of some biological strains in field experiments are not ideal. Therefore, more efficient and locally adapted antagonistic strains still need to be selected. Zhou et al. identified the strain YNF2217 as the native endophytic fungus *Pochonia chlamydosporia*. This strain was selected from the root nodules of *Dolichos lablab* in the mulch of banana fields. This fungus demonstrated great potential for the management of *F. oxysporum* f.sp *cubense* race TR4 in banana.

Bioactive plant compounds and formulation innovations

The use of plant-derived compounds as green fungicides received significant attention. Saghrouchni et al. evaluated carvacrol, a phenolic monoterpenoid, for its dual function as a plant growth promoter and bio-fungicide in perennial ryegrass. In both *in vitro* and greenhouse experiments, carvacrol significantly suppressed disease symptoms caused by *F. oxysporum*, *F. solani*, and *F. nivale*, while simultaneously enhancing seedling vigor and root development. The compound's preventive role and biostimulatory effects make it a promising tool for sustainable disease management. Mirmajlessi et al. proposed an implementation framework for evaluating the biocidal potential of essential oils against *F. oxysporum* in spinach. Moving from *in vitro* assays to *in planta* trials, the authors assessed key disease and growth parameters, providing strong evidence for essential oils as viable components in integrated pest management strategies. Together, these studies reflect a shift toward natural, multifunctional compounds capable of addressing plant health and productivity holistically.

Exploring microbial interactions and community dynamics

Beyond direct biocontrol, insights into microbial ecology are vital for the sustainable management of *Fusarium* diseases. The work of Todorovic et al. examined the microbial consortia in suppressive soils using high-throughput sequencing and co-occurrence network analysis to identify dominant taxa associated with disease suppression in watermelon. Notably, *Trichoderma*, *Bacillus*, and *Pseudomonas* spp. emerged as key microbial players, suggesting that understanding soil microbial assembly and community structure can inform more targeted biocontrol interventions. In a parallel study, Choi et al. investigated *Fusarium graminearum* and *F. asiaticum* using community ecology frameworks. These frameworks revealed how stress tolerance and infectivity traits influence fungal community assembly. Phenotypic clustering, as evidenced by the Net Relatedness Index and the Nearest Taxon Index, was observed under stress and competition, indicating that local environmental pressures drive convergence among pathogenic strains. These findings underscore the importance of ecological filtering and resource competition in shaping pathogen populations, a critical consideration when designing long-term, evolutionarily robust control measures.

Integrating host resistance and genomic approaches

While biocontrol is a key pillar of sustainable disease management, its success is often enhanced by host genetic resistance. In a genome-wide association study (GWAS) of 249 Canadian spring wheat lines, Semagn et al. identified multiple quantitative trait loci (QTLs) linked to Fusarium head blight resistance. Several of these QTLs overlapped with traits related to plant height and flowering time, reflecting the complexity and pleiotropy inherent in disease resistance breeding. Four QTLs were found to be consistently associated with disease incidence, severity, and visual rating index across environments, accounting for up to 33.2% of phenotypic variance. Conversely, Xu et al. were the first to create a high-density map of QTLs for yield-related traits, seed color and sesame Fusarium wilt disease using an F2 population. This study provides a solid basis for further genetic analyses of Fusarium wilt disease-related traits in sesame, including map-based gene cloning and marker-assisted selection breeding.

Host-induced gene silencing (HIGS) is a relatively new approach to managing plant diseases. Based on the pharmacological inhibition of calcineurin in *F. fujikuroi*, Hou et al. discovered that the calcineurin inhibitors FK506 and cyclosporin A can prevent the growth of *F. fujikuroi*. They then used an HIGS strategy to silence the calcineurin genes of *F. fujikuroi* in rice, finding that the transgenic rice seedlings exhibited enhanced resistance to infection by *F. fujikuroi*, which suggests that calcineurin is essential for F. fujikuroi to infect rice plants. Furthermore, these results provide valuable insights into the HIGS mechanism in plants and offer a promising approach to enhancing resistance against rice bakanae disease.

Comparative genomic and transcriptomic analyses of the different *F. oxysporum* races would reveal the most significant genetic differences between them, providing a better understanding of the pathogen's evolution and potentially enabling more lasting resistance in crops. For this reason, Bates et al. presented the first full genome and transcriptome data of *F. oxysporum* f.sp. *lactucae* (Fola). This has enabled the identification of key differences in the effector repertoire and its expression in the globally significant Fola1 and Fola4 races in lettuce. Mestdagh et al. employed molecular detection methods (such as race-specific real-time PCR

assays) to detect *F.* Fola races 1 and 4 in plant tissue and optimized sample preparation. These methods can now be used to study the pathogen's spread and evaluate the impact of control measures, including various soil disinfestation methods, new resistant varieties, and alternative crops. This study provides the first quantitative data on the presence of Fola in greenhouse soil. Bhutia et al. employed an RNA sequencing-based approach to analyze the shoot transcriptome in order to understand the molecular mechanisms conferring resistance to *Fusarium* wilt infection in chickpeas. The authors concluded that efficient energy metabolism, activation of environmental adaptation mechanisms, and DNA stability were key to resistance against *Fusarium* wilt infection in chickpea genotypes.

On the other hand, charting the *F. oxysporum* f.sp. *pangenome* (the characterization of the complete set of genes of a species or an infra-species taxa) blueprint and studying its diversity is an essential and imperative initial step toward uncovering the mechanisms that underlie plant-fungal interactions, and devising new disease control strategies. Logachev et al. conducted an analysis of the pangenome of 13 *F. oxysporum* f.sp. *lini* isolates that belong to 4 clonal lineages with varying virulence, shedding new light on its genomic diversity. Moreover, these studies strongly support the hypothesis that *Fusarium oxysporum* isolates utilize different virulence factors during the infection of crops, enabling them to evade plant defense mechanisms. All these studies enrich the -omics tools available to crop breeders and support the integration of molecular and agronomic strategies for combating Fusarium diseases.

Closing remarks

The studies presented in this Research Topic reflect the richness and diversity of approaches currently being pursued to manage *Fusarium* wilt diseases in different crops and agroecosystems. From novel *Trichoderma* strains and essential oil formulations to genomic mapping and microbial ecology, the Research Topic exemplifies the convergence of traditional plant pathology with modern tools in genomics, formulation science, and ecological modeling tools. Importantly, several contributions moved beyond proof-of-concept, offering scalable solutions with practical relevance under field conditions. The integration of biocontrol agents with plant-based compounds and host resistance strategies appears especially promising, pointing toward multi-layered approaches capable of withstanding pathogen evolution and environmental variability. Future research should emphasize long-term field validation, compatibility with agricultural inputs, and farmer-centered implementation strategies. As we continue to navigate the global challenge of sustainable food production, these interdisciplinary efforts will be indispensable.

Author contributions

SM: Methodology, Supervision, Writing – original draft, Visualization, Validation, Writing – review & editing, Conceptualization, Investigation. IL: Writing – review & editing. MG: Writing – review & editing. MC: Writing – review & editing.

Conflict of interest

The authors declare that the research was conducted in the absence of any commercial or financial relationships that could be construed as a potential conflict of interest.

Generative AI statement

The author(s) declare that no Generative AI was used in the creation of this manuscript.

Any alternative text (alt text) provided alongside figures in this article has been generated by Frontiers with the support of artificial intelligence and reasonable efforts have been made to ensure accuracy, including review by the authors wherever possible. If you identify any issues, please contact us.

Publisher's note

frontiers | Frontiers in Plant Science

TYPE Original Research
PUBLISHED 07 October 2022
DOI 10.3389/fpls.2022.990392

OPEN ACCESS

EDITED BY
Prem Lal Kashyap,
Indian Institute of Wheat and Barley Research (ICAR), India

REVIEWED BY
Elsherbiny A. Elsherbiny,
Mansoura University, Egypt
Manoj Kumar Solanki,
University of Silesia in Katowice, Poland

*CORRESPONDENCE
Anupama Singh
anupamanil2000@gmail.com

SPECIALTY SECTION
This article was submitted to Plant Pathogen Interactions, a section of the journal Frontiers in Plant Science

RECEIVED 09 July 2022
ACCEPTED 05 September 2022
PUBLISHED 07 October 2022

CITATION
Pradhan PC, Mukhopadhyay A, Kumar R, Kundu A, Patanjali N, Dutta A, Kamil D, Bag TK, Aggarwal R, Bharadwaj C, Singh PK and Singh A (2022) Performance appraisal of *Trichoderma viride* based novel tablet and powder formulations for management of *Fusarium* wilt disease in chickpea.
Front. Plant Sci. 13:990392.
doi: 10.3389/fpls.2022.990392

Performance appraisal of *Trichoderma viride* based novel tablet and powder formulations for management of *Fusarium* wilt disease in chickpea

Prakash Chandra Pradhan[1], Arkadeb Mukhopadhyay[1], Randeep Kumar[1], Aditi Kundu[1], Neeraj Patanjali[1], Anirban Dutta[1], Deeba Kamil[2], Tusar Kanti Bag[2], Rashmi Aggarwal[2], Chellapilla Bharadwaj[3], P. K. Singh[1] and Anupama Singh[1]*

[1]Division of Agricultural Chemicals, Indian Council of Agricultural Research (ICAR)-Indian Agricultural Research Institute, New Delhi, India, [2]Division of Plant Pathology, Indian Council of Agricultural Research (ICAR)-Indian Agricultural Research Institute, New Delhi, India, [3]Division of Genetics, (ICAR)-Indian Agricultural Research Institute, New Delhi, India

In developing a *Trichoderma viride*-based biocontrol program for *Fusarium* wilt disease in chickpea, the choice of the quality formulation is imperative. In the present study, two types of formulations *i.e.* powder for seed treatment (TvP) and tablet for direct application (TvT), employing *T. viride* as the biocontrol agent, were evaluated for their ability to control chickpea wilt under field conditions at three dosages *i.e.* recommended (RD), double of recommended (DD) and half of recommended (1/2 RD). A screening study for the antagonistic fungi strains based on volatile and non-volatile bioassays revealed that *T. viride* ITCC 7764 has the most potential among the five strains tested (ITCC 6889, ITCC 7204, ITCC 7764, ITCC 7847, ITCC 8276), which was then used to develop the TvP and TvT formulations. Gas Chromatography-Mass Spectrometry (GC-MS) analysis of volatile organic compounds (VOCs) of *T. viride* strain confirmed the highest abundance of compositions comprising octan-3-one (13.92%), 3-octanol (10.57%), and 1-octen-3-ol (9.40%) in the most potential *T. viride* 7764. Further Physico-chemical characterization by standard Collaborative International Pesticides Analytical Council (CIPAC) methods revealed the optimized TvP formulation to be free flowing at pH 6.50, with a density of 0.732 g cm^{-3}. The TvT formulation showed a pH value of 7.16 and density of 0.0017 g cm^{-3} for a complete disintegration time of 22.5 min. The biocontrol potential of TvP formulation was found to be superior to that of TvT formulation in terms of both seed germination and wilt incidence in chickpea under field conditions. However, both the developed formulations (TvP and TvT) expressed greater bioefficacy compared to the synthetic fungicide (Carbendazim 50% WP) and the conventional talc-based formulation. Further research should be carried out on the compatibility of

the developed products with other agrochemicals of synthetic or natural origin to develop an integrated disease management (IDM) schedule in chickpea.

KEYWORDS

Trichoderma viride, VOCs, tablet, seed treatment, *Fusarium* wilt, chickpea, IDM

Introduction

Chickpea (*Cicer arietinum* L.) is one of the most important legume crops (Sunkad et al., 2019) grown in the Mediterranean basin and worldwide. It is the third pulse crop in the world after dry bean (*Phaseolous vulgans* L.) and dry pea (*Pisum sativum* L.). In India, chickpea production occupies an area of 112 lakh hectares, resulting in approximately 116.20 lakh tonnes, with 1036 kg ha^{-1} in 2020-21. It covers approximately 38% of the area under pulse and contributes to around 50% of the total pulse production in India. Chickpea is an important source of protein for millions of people in developing countries. In addition to having high protein content (20-22%), chickpea is also rich in fiber, minerals (phosphorus, calcium, magnesium, iron, and zinc), and β-carotene (Yegrem, 2021).

Chickpea is exposed to several biotic and abiotic stresses among which pathogenic diseases are a major challenge. Chickpea is prone to attack by numerous pathogens, of which the most destructive is *Fusarium oxysporum* f. sp. *ciceris* causing wilt disease in chickpea crops (Golakiya et al., 2018). Wilt disease in chickpea caused by *F. oxysporum* f. sp. *ciceris* is one of the major causes of biotic stress to the crop. An average annual yield loss of 10-15% is reported due to this disease and under severe conditions, the damage may reach up to 100% (Navas-Cortes et al., 2000). Soil moisture stress and high-temperature conditions are conducive to soil-borne disease (Chand and Khirbat., 2009; Zaim et al., 2016; Alloosh et al., 2019). Carbendazim is the most widely used and recommended fungicide for the management of wilt disease in legumes (Srivastava et al., 2011). However, sole reliance on synthetic pesticides, due to injudicious and misuse is being discouraged globally, particularly in India, with more focus being given to greener options such as integrated disease management, and use of biopesticides, etc.

Biocontrol agent based products hold a major share of the biopesticides sector in agriculture. Biocontrol agents not only provide effective disease control but present safe and environmentally friendly options. The concept of biocontrol embodies the introduction of antagonists into cropping systems. A living multiplying biocontrol agent potentially provides continuous, non-chemical control of the pathogen. Moreover, chemical measures may establish an imbalance in the microbiological community *i.e.*, an unfavorable situation for the activity of beneficial organisms (Anusha et al., 2019). Therefore, direct application of antagonist would be a safer method for introducing microorganisms into the soil for biological control of soil-borne plant pathogens. It has been known for many years that biocontrol agents produce a wide range of antibiotic substances and that they parasitize other pathogenic fungi (Kumar et al., 2021). Among biocontrol agents, *T. viride* has been extensively reported as being effective at combating soil-borne diseases in field crops, including Fusarium wilt (Mei et al., 2019). A constraint in the large-scale adoption of bioagents despite their potential, is the lack of quality formulations with adequate cfu counts and viability. The most commonly reported and marketed products in this context are wettable powder formulations that employ talc as a carrier (Ramanujam et al., 2010). In India, wettable powder of *T. viride* (1% WP) is recommended for the management of chickpea wilt (CIBRC, 2022). Poor load of cfu in stored WP formulations coupled with the poor coating efficacy of dry powders and dust hazards necessitate precision formulation approaches for biocontrol products. Furthermore, WP or dust powder for seed treatments employs a carrier only. Since the performance of *Trichoderma* is positively related to moisture availability in the zone of its application, the addition of adjuvants like carbon sources and moisture enriching polymers can provide additional benefits for biocontrol (John et al., 2011). As per the Central Insecticides Board and Registration Committee (CIBRC, India), an authentic biocontrol formulation of *Trichoderma* spp. should have 2×10^6 cfu g^{-1} of formulation at the time of its application in the field (CIBRC, 2011).

The present work reports on the development, characterization, and performance assessment of two innovative formulations of *T. viride*, namely, tablets (TvT) and dustable powder for seed coating (TvP), employing biopolymer, clay, neem leaf powder as an environmentally benign alternative to conventionally used synthetic fungicides to manage *Fusarium* wilt in chickpea. Excipients have previously been used to provide a moist environment in the formulation's application zone. With this in mind, the objectives of the present study were (1) to develop and characterize a novel tablet formulation of *T. viride*; (2) to evaluate the potential of the developed tablets against

chickpea wilt under *in vivo* conditions; and (3) to ascertain the dose-response and relative performance of the optimized tablet formulation with a powder formulation under field conditions to provide an alternative to the conventional talc-based WP formulation and synthetic fungicide, Carbendazim 50% WP.

Materials and methods

Culture medium and reagents

Dehydrated potato dextrose agar medium (PDA) and potato dextrose broth (PDB) were procured from HiMedia® laboratories (Mumbai, India) and used as culture media for the pathogen, *F. oxysporum* f. sp. *ciceris* and the biocontrol agent *T. viride*, obtained from Indian Type Culture Collection (ITCC), ICAR-Indian Agricultural Research Institute, New Delhi, India. Neem leaves were collected from trees on the institute premises, dried, and powdered to around 100 -240 mesh size (62.5 -150µ) before use. Biopolymer (pH 6.0-6.5; water absorption capacity 80 g g^{-1} was purchased from the local market and used. Aluminosilicate clay mineral (80-90% silica, 2-3% alumina) was obtained from Casa De Amor, Madhya Pradesh, India. Bentonite clay (Al_2O_3. 4 SiO_2. H_2O; pH of 2% suspension in water: 9.00-10.50) was obtained from Hi-Media Laboratories Pvt. Limited, Mumbai, India. The xerogel used was sugarcane bagasse-based biopolymeric grafted and crosslinked polyacrylate hydrogel composite prepared in our laboratory (Particle size: 120 -200 mesh size (75 -125µ), WAC 600 g g^{-1}). Carboxymethyl cellulose sodium salt (CMC) (LR grade; viscosity: 1100-1900 cps as per label claim) was purchased from Merck® Life Science Pvt. Ltd., Mumbai, India.

Pathogen and antagonistic fungi

Pure culture of *F. oxysporum* f. sp. *ciceris* in slants was obtained from the Indian Type Culture Collection (ITCC), Division of Plant Pathology, ICAR-Indian Agricultural Research Institute, New Delhi, India. Pure cultures of five *T. viride* strains (ITCC 6889, ITCC 7204, ITCC 7764, ITCC 7847, ITCC 8276) were also obtained from ITCC. The pathogenic and biocontrol fungi were sub-cultured for one week and four days in Petri plates using potato dextrose agar (PDA) and mass produced on sterilized sorghum (*Sorghum bicolor*) grains (Khan et al., 2001).

For mass culturing, sorghum grains were soaked in distilled water for 12h, strained, and filled into various conical flasks (500 mL). The flasks containing sorghum grains were autoclaved for two subsequent days at 1.1 kg cm^{-2} for 30 min and inoculated with a 7-day-old culture of *T. viride* ITCC 7764. The flasks were incubated at 25 ± 1 °C for 15 days. Well-colonized sorghum grains were then taken out from the flask, dried at room temperature, and finally made into a fine powder.

In vitro evaluation of *T. viride* strains against *F. oxysporum*

T. viride strains (ITCC 6889, ITCC 7204, ITCC 7764, ITCC 7847, and ITCC 8276) were tested *in vitro* for antagonistic activity against *F. oxysporum*. To select the most potential biocontrol *T. viride* strain, two-way assays namely, volatile and non-volatile *in-vitro* antifungal methods were performed.

Effect of volatiles of *T. viride* on growth of *F. oxysporum*

The test was carried out using the inverted plate technique as described by Sheoran et al. (2015). Briefly, the upper lid of the PDA plate was inoculated with the pathogen and the lower lid with a strain of *T. viride* separately under aseptic conditions. The two lids were taped together to facilitate the exposure of the pathogen to volatile organic compounds released by the biocontrol fungi, then incubated at 27 ± 1°C for seven days. The experiment was conducted in triplicate and negative control was maintained with *F. oxysporum*. Relative radial growth and inhibition (%) were computed with reference to control, according to the equation suggested by Tapwal et al. (2011):

$$N = ((A\text{-}B)/A)*100$$

where N is growth inhibition percentage, A is the average diameter of the control colony and B is the average diameter of the treatment colony

Effect of non-volatile components of *T. viride* on growth of *F. oxysporum*

The test was carried out using the method reported by Choi and Ahsan (2022). Briefly, the *T. viride* cultures were inoculated in conical flasks (250 mL) containing sterile potato dextrose broth (PDB) and incubated at 27 ± 1°C for two weeks. The culture was filtered through a micropore filter (0.22 µ) and filtrates were collected in a sterile flask. The culture filtrate was added to the molten PDA medium to obtain a final concentration of 10% (v v^{-1}). Upon its solidification, a 5 mm disc of the pathogen was inoculated. Negative control plates were also maintained. The radial growth (mm) of colonies was recorded and inhibition (%) was calculated relative to control.

GC-MS analysis of volatile organic components

GC-MS analysis was carried out to characterize VOCs from potential *T. viride* strains using a 5590C Gas Chromatograph, equipped with a Mass Spectrometer (Agilent Technologies®, USA). Volatiles were separated through an HP-5MS capillary column (30 m × 0.25 µm; 0.25 µm). The VOCs were allowed to adsorb on Tenax TA polymer (80-100 mesh) for 8h and then extracted in GC-MS grade hexane (Kumar et al., 2021). Samples were injected (1µL, each) through an autoinjector following the split mode, 1:10. Helium (>99.9% purity) was used as carrier gas with a flow rate of 0.75 mL min^{-1} and pressure of 15 psi. Oven temperature ramping started at 40°C and raised at the rate of 3°C min^{-1} to reach 130°C and held for 2 min. Again, the temperature was raised at the rate of 5°C min^{-1} to reach 200°C and held for 2 min. Finally, the oven temperature was increased at the rate of 10°C min^{-1} to reach 300°C. The total run time was 58 min. Besides, other mass acquisition parameters were tuned before analysis and fixed with the ion source temperature of 200°C, transfer line temperature of 200°C, solvent delay of 3 min, and E.M voltage 1420 V. The scanning rate per second was fixed with the mass range m/z 50-550 amu. Identification of volatile compounds was carried out based on their retention indices (RI) and calculated using the homologous series of *n*-alkanes (C_9-C_{24}) before being matched with the library database of the NIST (National Institute of Standards and Technology) Version 3.02 (Keerthiraj et al., 2021).

Compatibility evaluation of neem leaf powder with *T. viride* and *F. oxysporum*

The random choice of formulation adjuvants may result in poor efficacy. For the selection of the neem leaf powder as filler material for the development of the tablet and powder formulations of *T.viride*, it is imperative to generate information on its compatibility with the biocontrol agent as neem leaf powder is known to be rich in various secondary metabolites having pesticidal properties (Patil et al., 2018). Therefore, *in vitro* studies were performed to assess the compatibility of neem leaf powder with the biocontrol agent and the biocontrol potential singly and in combination with the biocontrol agent. The PDA culture media was prepared as described by Bunbury-Blanchette and Walker (2019).

Test concentrations of neem leaf powder

The compatibility of *T. viride* was tested with neem leaf powder under laboratory conditions at test concentrations of 800µg/mL, 400 µg/mL, and 200 µg/mL. Test concentrations were prepared using acetone as solvent. At these concentrations of neem leaf powder, TvT or TvP formulations at double the recommended dose, the recommended dose, and half of the recommended dose were applied for *in vivo* experiments.

Compatibility evaluation of neem leaf powder with *T. viride* and *F. oxysporum*

A definite volume of neem leaf powder in acetone was thoroughly dispersed into a sterilized PDA medium to furnish different test concentrations of 800 -200 µg/mL. Acetone (1 mL) solution was taken as control. Media containing neem leaf powder (20 mL) was poured into each Petri dish. The culture (5 mm diameter disc) of both the fungi was placed separately in the center of each dish. Three replicates were maintained for each treatment along with the negative control and the experiment was repeated twice. Petri dishes were incubated in a BOD incubator at 28 ± 1°C. Data were recorded after 3 days and 7 days in the case of *T. viride* and *F. oxysporum*, respectively.

Preparation of biocontrol formulations

The best performing *T. viride* strain (Tv, ITCC 7764) was used as an active ingredient (*a.i.* Biomass) to develop two novel biocontrol formulations, the tablet for direct application (TvT) and powder for seed treatment (TvP). To optimize the composition for TvT, a standardization study was conducted at different concentrations of ingredients. The tablet formulation for direct application (TvT) was developed by using *T. viride* spores as a biocontrol agent, carboxy methyl cellulose (CMC), neem leaf powder as fillers, xerogel, and bentonite as carriers. The tablets were prepared by hand operated tablet making machine at room temperature (26-28 °C). The present study used an optimized composition of powder formulation named TvP2, which was previously developed for seed treatment by our laboratory for the comparative evaluation of the bioefficacy of the tablet (TvT) formulation in managing chickpea wilt disease under field conditions. The excipients used for the development of the TvP formulation included a pre-standardized ratio of biopolymer, neem leaf powder, xerogel, and a porous clay mineral carrier other than talc. The general procedure involved a pre-standardized sequence of mixing the fungal biomass with the carrier and the excipients under ambient conditions. The developed compositions were stored in air-tight glass bottles at 25°C. The composition variations of the prepared formulations are depicted in Table 1. The optimized TvP formulation has shown potential bioefficacy against *F. oxysporum* f. sp. *ciceris* under *in vivo* conditions, as reported elsewhere. Briefly, the application of TvP formulation at recommended doses resulted in 3.33% wilting in chickpea under *in vivo* conditions. However, the bioefficacy of the TvP formulation under field conditions has yet not been evaluated.

TABLE 1 Compositions of developed TvT and TvP formulations.

Code	Bentonite (% w w^{-1})	CMC (% w w^{-1})	Neem leaf powder (% w w^{-1})	Optimized xerogel (% w w^{-1})
TvT1	80.94-81.99	2.5-3.5	9.8-10.3	4.7-5.5
TvT2	83.98-84.99	2.5-3.5	9.8-10.3	2.0-2.4
TvT3	78.99-79.99	2.5-3.5	9.8-10.3	6.9-7.3
TvT4	86.50-86.99	2.5-3.5	4.8-5.2	4.8-5.2
TvT5	75.99-76.99	2.5-3.5	14.5-15.2	4.8-5.2
TvT6	83.00-83.49	1.3-1.7	9.8-10.3	4.7-5.5
TvT7	80.50-80.99	1.8-2.1	9.8-10.3	4.7-5.5
TvT8	71.50-71.99	12.5-13.5	9.8-10.3	4.7-5.5
TvT9	86.70-86.99	0.90-1.20	7.0-7.3	4.8-5.2
	Neem leaf powder (% w w^{-1})	**Biopolymer (% w w^{-1})**	**Porous clay mineral (% w w^{-1})**	**Optimized xerogel (% w w^{-1})**
TvP2	28.38-29.03	20.97-21.62	20.97-21.62	28.38-29.03

Following on from this previous research, the present study undertook a comparative evaluation of the TvT and TvP formulations (previously developed in our laboratory) under field conditions.

Physico-chemical characterization of optimized TvP and TvT formulations

The pH, flowability, density and sieve analysis of the optimized TvP formulation (TvP2) were carried out by following MT 75, MT 44, MT 3.2.1, and MT 59.1 of the standard CIPAC guidelines. We undertook a standardization study of TvT composition at different levels of ingredients as a function of physicochemical characteristics, the procedure for which is described below.

pH

For TvT, the pH of each composition was measured by using the CIPAC method MT 75. Briefly, around 1 g of sample tablet was put into a 250 mL glass beaker and completely dissolved in 100 mL of water. After the complete disintegration of the tablets, the beaker was stirred for 1 min and the pH of the supernatant was recorded.

Visible extraneous matter

The tablets were immediately weighed and then kept undisturbed for 1h on Petri plates. After one hour, the tablets were whisked thoroughly and then the extraneous formulation residue left on the plate was weighed and recorded as grams per tablet.

Moisture content

The moisture content of the developed tablets was measured gravimetrically (Sun et al., 2020). The pre-weighed (W1) tablets were placed in an oven at 60 °C and weighed periodically until they attained a constant weight (W2). The percent moisture content of the TvT compositions was calculated using the following formula:

$$\%\text{Moisture}\quad\text{content} = (W1 - W2/W1)*100$$

Disintegration time

The time for complete disintegration of the tablets was determined by the CIPAC method MT 197. Briefly, one tablet was added to standard hard water D (1800 mL) and gently stirred until it completely disintegrated. The suspension was passed through a 2000 μ sieve. The time taken for complete disintegration using standard procedure was recorded.

Tablet integrity

Tablet integrity was determined visually by observing whether any tablet of the table pack prepared in each batch was broken or not.

Density

First, the volume of the tablet was determined using the vernier caliper scale, followed by density calculation as per the standard formula, d=m/v (Eiliazadeh et al., 2003).

In-vivo assessment of optimized TvT formulation against wilt disease in chickpea

A pot experiment was conducted in the net house of the Division of Plant Pathology, ICAR-IARI, New Delhi, India. The soil of the sick plot (*Fusarium oxysporum* f. sp. *ciceris* infested) of the institute farm was used (pH-7.8, EC- 5.6 dS m^{-1}, organic matter 0.4%) to fill the pot (18 cm×15 cm) dimension. In total, 2kg of soil was used to fill each pot. The treatment details for the pot experiment are depicted in Table 2. Briefly, six treatments with three replications per treatment were employed for the experiment. A total of 10 seeds per pot (for each replication) were sown to record different observations. The parameters recorded to assess the performance of formulation were the wilting incidence and seed germination. The percentage of germination of seeds without infection was 94% as received as the foundation seeds from the Division of Genetics, ICAR-IARI, New Delhi, India. In pot experiments, the seed emergence was recorded 21 days after sowing (DAS). Observations on the number of plants wilted in each pot were recorded at 30, 45, and 60 DAS. The plants that showed dropping petioles, rachis, and leaflets without any external rotting in the roots, but dark brown discoloration of the internal xylem were considered wilted (Nene et al., 2012).

The causal agent of wilt incidence was confirmed after re-isolation of the pathogen from the infected root and stems of chickpea plants. The wilt incidence (%) was calculated based on the initial plant count and the total number of wilted plants in each pot. The disease was monitored for 6-8 weeks and assayed as the total percentage of plants showing any wilt symptoms due to the pathogen (yellowing and dropping of leaves, vascular discoloration, and wilting). The stem sections of wilted plants were surface disinfested in 0.5% sodium hypochlorite and plated on a Pentachloronitrobenzene (PCNB) medium to confirm the presence of the wilt pathogen. The stem sections of asymptomatic plants were also plated at the conclusion of the experiment to evaluate potential pathogen infection.

Comparative bio-efficacy assessment of TvT and TvP against wilt disease under field condition

The two bioformulations (TvT and TvP) were assessed for their performance in affecting wilting incidence, inhibition of seed germination, and mortality of chickpea seedlings caused by the pathogen under *Fusarium* wilt sick field conditions. The field experiment was conducted at the institute farm of ICAR-IARI, New Delhi, India, during the rabi season (2021-2022). The natural abundance of Fusarium in the sick field was 2× 10^7 cfu g^{-1} of soil at the time of sowing. A randomized block design with nine treatments along with three replications per treatment was applied. Moderately susceptible chickpea variety, Pusa-372 was taken for the experiment. The treatment details for the field experiment were used to check the comparative bio-efficacy of the developed TvT and TvP formulations against *Fusarium* wilt in chickpea have been depicted in Table 2. The crop was sown with 30×10 cm spacing having a gross plot size of 9.0×9.0 m and a net plot size of 2.0×0.6 m. The seed rate used was 60 kg ha^{-1}. Seeds were sown in microplots in rows (20 seeds per row, 2 rows per microplot), *i.e.* a total of forty seeds were sown in each microplot of each treatment. The pathogen population in the sick field was determined at the pre-sowing stage. Seed germination (%) was recorded two weeks after sowing and computed based on the number of germinated seeds (emerged seedlings) out of the total number of seeds sown in a microplot (40 seeds).

The seed emergence was recorded 21 days after sowing (DAS). Observations on the number of plants that wilted in each microplot were recorded at 30, 45, and 60 DAS. The wilting incidence (%) was calculated based on the initial plant count and

TABLE 2 Treatment details from bio-efficacy studies of developed formulations under pot and field experiments.

S. No.	Treatments*	Treatment details
1	T1	Absolute control
2	T2	Carbendazim 50% WP
3	T3	Talc formulation
4	T4	Test formulation (TvT) at RD
5	T5	Test formulation (TvT) at DD
6	T6	Test formulation (TvT) at HD
7	T7	Test formulation (TvP) at RD
8	T8	Test formulation (TvP) at DD
9	T9	Test formulation (TvP) at HD

*[Treatments for pot experiment: T1-T6; Treatments for field experiment: T1-T9].
(RD, Recommended dose; DD, Double dose; HD, Half dose; TvT, Tablet for direct application; TvP, Powder for seed treatment).

the total number of wilted plants in each microplot. At maturity, seed weight and grain yield were recorded for each treatment.

Statistical analysis

The *in vitro* bioefficacy of the selected *T. viride* strains using volatile and non-volatile methods along with the efficacy of the neem leaf powder singly and in combination with the antagonistic fungi at three different concentrations against *F. oxysporum* were analyzed by comparing mean differences using a completely randomized design by Duncan Multiple Range test at $p< 0.05$. Different test parameters such as germination (%), relative disease incidence (%), and yield parameters such as percent yield, shoot length, root length, and shoot dry matter in test treatments were analyzed by randomized complete block design using a one-way analysis of variance (ANOVA) and grouped by Duncan Multiple Range test at $p< 0.05$ using PROC GLM procedure of SAS 9.3 (SAS Institute, Cary, North Carolina, USA).

Results

In-vitro evaluation of *Trichoderma viride* strains against *Fusarium* wilt pathogen

Based on the *in-vitro* bio-efficacy assessment of five strains of *T. viride* strains against *F. oxysporum* f. sp. *ciceris* suggested the suitability of *Trichoderma* (ITCC 7764) as a potential biocontrol agent to manage wilting in chickpea (Figures 1, S1, and S2). In the volatile assay, the volatile components produced by all the strains significantly inhibited the pathogen but did so relatively less than the non-volatile method. Pathogen growth inhibition ranged between 21.15-26.45% with the volatiles, out of which TV-3 (26.45%) recorded the maximum inhibition followed by TV-1 (23.15%), TV-5 (22.58%), TV-2 (22.56%) and TV-4 (21.15%). Furthermore, all the strains of *Trichoderma* were assessed to inhibit the radial growth of the *F. oxysporum*, attributed to the effect of non-volatile organic compounds. Strains TV-3 (74.45%) and TV-2 (71.2%) recorded maximum inhibition of mycelial growth, significant potential over the other strains. Strains TV-1 (69.5%), TV-4 (67.58%), and TV-5 (59.54%) performed moderately to control the growth of the pathogen.

Characterization of VOCs

Volatile metabolites of the potential *T. viride* strains were characterized using GC-MS, which displayed identification of a total of twenty-seven VOCs, listed as per their elution from the HP-5MS column (Table 3). Total Ion Chromatogram (TIC) of *T. viride* 7764 showed the maximum number of peaks corresponding to nineteen components. Among the identified VOCs of *T. viride* 7764, octan-3-one (13.92%), 3-octanol (10.57%) and 1-octen-3-ol (9.40%) were most abundant. Other major components were 6-methyl-bicyclo-octan-7-ol (5.34%), 9-octadecenoic acid-methyl ester (4.98%), hexadecanoic acid-methyl ester (4.17%), methyl-6-arachidonate (3.46%), 2-Mthyl-butanol (1.79%), 2-ethyl-hexanal (1.72%), and heptadecanoic acid-methyl ester (1.40%). Besides, 2-pentyl-furan (0.91%), 2-nonanone (0.83%), phenylethyl alcohol (0.72%), 3-methyl-butanal (0.64%), 2,4-Decadienal (0.58%), 2-undecanone (0.39%), 3-hexene-1-ol (0.33%), 2-heptyl-furan (0.26%), and octacosanol (0.18%) were identified as minor components of *T. viride* 7764.

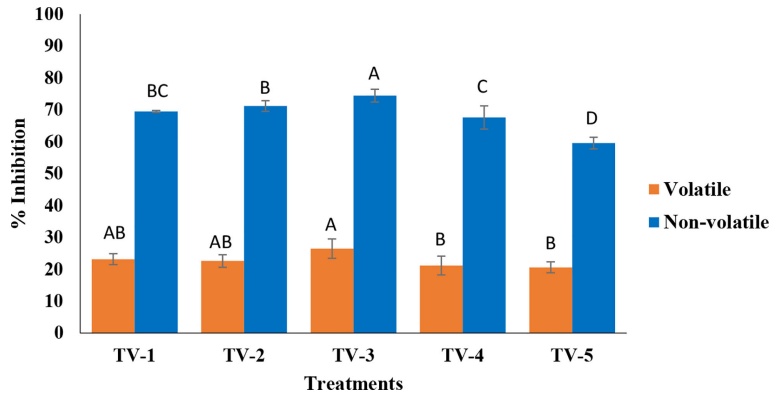

FIGURE 1
Assessment of secondary metabolites of *T. viride* against pathogenic wilt causing fungus, *F. oxysporum* f. sp. *ciceris* by volatile and nonvolatile methods. (Tv1- ITCC 6889, Tv2- ITCC 7204, Tv3- ITCC 7764, Tv4- ITCC 7847, Tv5- ITCC 8276, Control-without *Trichoderma* strain). (For each method, treatment bars having at least one letter common are not statistically significant using Duncan's Multiple Range Test at $p<0.05$, n=3, error bars represent standard deviations).

TABLE 3 Chemical composition of the volatile organic compounds of potential *trichoderma viride* strains as analysed in gc-ms.

S No.	[a]Compound	[b]RI[exp]	[c]Area %					[d]Detection
			T. viride 6889	*T. viride* 7204	*T. viride* 7764	*T. viride* 7847	*T. viride* 8276	
1	2-Methylpropanal	554	0.37 ± 0.12	0.19 ± 0.00	–	0.24 ± 0.10	–	NIST, RI
2	3-Methyl-butanal	648	1.09 ± 0.39	–	0.64 ± 0.15	–	–	NIST, RI
3	2-Pentanone	682	–	–	–	0.73 ± 0.12	0.14 ± 0.00	NIST, RI
4	2-Mthyl-butanol	737	1.60 ± 0.21	0.36 ± 0.12	1.79 ± 0.28	–	–	NIST, RI
5	3-Hexene-1-ol	855	tr	1.02 ± 0.00	0.33 ± 0.05	2.25 ± 0.31	7.29 ± 1.14	NIST, RI
6	2-Heptanone	891	–	0.46 ± 0.09	tr	1.78 ± 0.42	–	NIST, RI
7	2-Ethyl-hexanal	953	2.06 ± 0.53	1.11 ± 0.20	1.72 ± 0.37	2.29 ± 0.36	6.64 ± 0.88	NIST, RI
8	1-Octen-3-ol	984	3.35 ± 0.19	7.42 ± 1.41	9.40 ± 1.71	–	0.98 ± 0.10	NIST, RI
9	Octan-3-one	986	5.27 ± 0.67	6.79 ± 0.78	13.92 ± 2.65	tr	tr	NIST, RI
10	2-Pentyl-furan	990	–	tr	0.91 ± 0.12	–	–	NIST, RI
11	3-Octanol	997	0.74 ± 0.12	11.06 ± 2.26	10.57 ± 1.33	0.63 ± 0.12	0.15 ± 0.00	NIST, RI
12	2-Nonanone	1094	–	–	0.83 ± 0.15	–	–	NIST, RI
13	Phenylethyl alcohol	1120	–	0.23 ± 0.00	0.72 ± 0.00	1.54 ± 0.29	0.27 ± 0.12	NIST, RI
14	2-Methyl-1-undecene	1182	1.02 ± 0.16	tr	–	–	tr	NIST, RI
15	2-Heptyl-furan	1202	0.12 ± 0.00	–	0.26 ± 0.10	–	–	NIST, RI
16	2-Undecanone	1289	–	3.47 ± 0.98	0.39 ± 0.00	0.63 ± 0.12	–	NIST, RI
17	2,4-Decadienal	1318	tr	0.60 ± 0.12	0.58 ± 0.17	2.92 ± 0.11	4.82 ± 0.55	NIST, RI
18	Dodecane	1461	5.32 ± 0.92	–	–	9.38 ± 2.17	17.44 ± 3.48	NIST, RI
19	2,4-Dodecadienal	1515	–	0.41 ± 0.12	tr	1.18 ± 0.21	0.54 ± 0.19	NIST, RI
20	1-Hexadecene	1598	–	0.38 ± 0.00	tr	–	0.12 ± 0.00	NIST, RI
21	6-Methyl-bicyclo-octan-7-ol	1720	tr	1.27 ± 0.34	5.34 ± 0.96	–	–	NIST, RI
22	Hexadecane		–	–	tr	3.22 ± 0.15	1.46 ± 0.58	NIST, RI
23	Hexadecanoic acid-methyl ester	1925	1.18 ± 0.00	3.92 ± 0.96	4.17 ± 0.82	–	0.93 ± 0.25	NIST, RI
24	Heptadecanoic acid-methyl ester	2030	0.24 ± .12	2.58 ± 0.14	1.40 ± 0.23	1.51 ± 0.12	1.24 ± 0.69	NIST, RI
25	9-Octadecenoic acid-methyl ester	2105	–	1.34 ± 0.13	4.98 ± 0.17	–	–	NIST, RI
26	Methyl-6- arachidonate	2208	–	1.00 ± 0.19	3.46 ± 0.45	–	–	NIST, RI
27	Octacosanol	3110	0.67 ± 0.00	–	0.18 ± 0.00	tr	0.35 ± 0.00	NIST, RI

[a]Compounds are listed in order of their elution from an HP-5MS column.
[b]Retention index (RI^{exp}) on HP-5MS column, experimentally determined using homologous series of C_8-C_{30} alkanes.
[c]Relative area % values are expressed as means ± SD.
[d]Detection: RI, NIST (matching with the mass library), and mass fragments.
* tr-trace<0.1%.

T. viride 7204 produces a high amount of 3-octanol (11.06%), 1-Octen-3-ol (7.42%), and octan-3-one (6.79%). Other prominent components were identified as hexadecanoic acid-methyl ester (3.92%), 2-undecanone (3.47%), heptadecanoic acid-methyl ester (2.58%), 9-octadecenoic acid-methyl ester (1.34%), 6-methyl-bicyclo-octan-7-ol (1.27%), 2-ethyl-hexanal (1.11%), 3-hexene-1-ol (1.02%), and methyl-6-arachidonate (1.00%). Similarly, the GC-MS chromatogram of volatiles of *T. viride* 6889 exhibited a relatively smaller number of components than the previous two strains. Structural long chain hydrocarbon dodecane (5.32%) was the major compound followed by octan-3-one (5. 27%). A similar observation of the high content of dodecane was estimated in *T. viride* 7847 (9.38%) and *T. viride* 8276 (17.44%). Except dodecane, other major volatile components of *T. viride* 7847 were hexadecane (3.22%), 2,4-decadienal (2.92%), 2-ethyl-hexanal (2.29%), 3-hexene-1-ol (2.25%). Likewise, 3-hexene-1-ol (7.29%), 2-ethyl-hexanal (6.64%), 2,4-decadienal (4.82%), hexadecane (1.46%), and heptadecanoic acid-methyl ester (1.24%) were identified in *T. viride* 8276.

Compatibility evaluation of neem leaf powder against *T. viride*

The *in-vitro* efficacy of neem leaf powder was assessed against *T. viride* using the poisoned food technique. The result suggested that there was no inhibition of the biocontrol agent upon the addition of neem leaf powder in the formulation at all three test dosage levels. This result confirmed that neem leaf powder could be used as an adjuvant to *T. viride*- based formulation.

Compatibility evaluation of neem leaf powder against *F. oxysporum*

The neem leaf powder was further assessed to diagnose the effect on the target pathogen and revealed significant inhibition of the test fungus, *F. oxysporum i.e.* 18.6%, 12.8%, and 5.8% at double, recommended, and half doses, respectively. The result signifies that the neem leaf powder can be utilized in the formulation to enhance the synergistic effect against the target pathogen (Table 4).

Effect of *T. viride* and neem leaf powder on *F. oxysporum*

To assess the synergistic effect of neem leaf powder and *T. viride*, both the components were assessed in dual culture technique against the target pathogen. The result suggested that there was direct synergism in the combined application of neem leaf powder and *T. viride*. Upon application of respective concentrations at three test dosage levels (double, recommended, and half dose), 50.6%, 34.9%, and 16.5% inhibition of the test fungus were observed, respectively (Table 4).

Physico-chemical properties of optimized TvP and developed TvT formulations

The preparation of optimized TvP and developed TvT formulations are outlined in Table 1. The different physicochemical properties of the developed optimized TvP formulation (TvP2) and developed TvT formulations used in this study are presented in Table 5. Briefly, the optimized TvP2 formulation was found to be free flowing, with a pH of 6.50 and a density of 0.732 g cm^{-3}.

The physicochemical characteristics of the prepared TvT formulations for optimization of the most suitable composition revealed variations depending on the formulation compositions. The pH is considered one of the most important parameters of any bioformulation. The recorded pH of the prepared tablets was found to be slightly alkaline having a nominal value from 7.16 to 7.48. The positive effect of the amount of bentonite clay on pH increment was recorded. The composition TvT9 with the maximum amount of bentonite clay (86.70-86.99%, w w^{-1}) revealed the highest pH value of 7.48. The amount of visible extraneous materials in the prepared tablets was in the range of 0.0043-0.0083 g per tablet. The percent moisture content of the developed tablets was found to be in the range of 7.55% (TvT1) to 10.07% (TvT2). No specific pattern was observed in the changing of the moisture content of the prepared tablets due to variation in compositions. The complete disintegration time is an important factor for the efficacy of the tablets intended for direct application. The longer time of disintegration may affect the desired bio-efficacy of the developed product. In our case, the prepared tablets showed 22.5 min to 26.5 min time for complete degradation of a single tablet. The lowest disintegration time (22.5 min) was recorded in the TvT1 formulation. All the prepared tablets irrespective of their composition were found to be non-breakable. The density of the tablets varied from 0.0015 g cm^{-3} (TvT8) to 0.0018 g cm^{-3} (TvT9). There was not much variation in the density of the developed tablets. The variations in xerogel, neem leaf powder, and CMC content in the composition did not show any kind of correlation with the density recorded. However, the reason for the highest density, which was recorded in TvT9, might be due to the presence of it having the highest amount of bentonite clay (86.70-86.99%) in the formulation composition.

The biocontrol agent, *T. viride*, prefers to grow and function best at slightly acidic pH (Belal, 2008). Therefore, because the TvT1 composition has the lowest pH value of 7.16, it might be the best choice. This composition also exerted the lowest percentage of moisture content (7.55%, w w^{-1}) and disintegration time (22.50 min). The composition of TvT1 was therefore selected for further experiments.

TABLE 4 Effect of Neem Leaf powder and *Trichoderma viride* + Neem Leaf Powder on *Fusarium oxysporum* f. sp. *ciceris* (*in vitro*).

Dose	% Inhibition*	
	Neem leaf powder	*Trichoderma viride* + neem leaf powder
Double dose (800 ppm)	18.6 ± 2.9^{A}	50.6 ± 3.4 ^{A}
Recommended dose (400 ppm)	12.8 ± 1.2 ^{B}	34.9 ± 4.5 ^{B}
Half dose (200 ppm)	5.8 ± 1.3 ^{C}	16.5 ± 1.1 ^{C}
CV (%)	13.97	2.94

*Means with at least one letter common are not statistically significant using DUNCAN's Multiple Range Test at $p<0.05$, n=3.

10.3389/fpls.2022.990392

TABLE 5 Effect of formulation compositions on the physico-chemical characteristics of developed TvT and TvP formulations.

TvT formulations	Parameters					
	pH	Visible extraneous matter(g tablet^{-1})	Moisture content(%)	Disintegration time (min)	Tablet integrity	Density (g cm^{-3})
TvT1	7.16	0.0046	7.55	22.50	No broken tablets	0.0017
TvT2	7.33	0.0044	10.07	24.00	No broken tablets	0.0016
TvT3	7.24	0.0082	9.77	26.50	No broken tablets	0.0017
TvT4	7.34	0.0056	9.97	23.50	No broken tablets	0.0017
TvT5	7.45	0.0062	9.31	25.00	No broken tablets	0.0016
TvT6	7.32	0.0083	9.84	26.50	No broken tablets	0.0017
TvT7	7.41	0.0055	9.76	23.50	No broken tablets	0.0016
TvT8	7.21	0.0043	9.48	26.00	No broken tablets	0.0015
TvT9	7.48	0.0070	9.88	24.50	No broken tablets	0.0018

TvP formulation	Parameters									
	pH	Flowability	Density (g cm^{-3})	% Retention of powder (mesh size wise)						
				BSS 5	BSS16	BSS 30	BSS60	BSS 100	BSS 120	BSS 240	BSS 325
TvP2	6.50	Free-flowing	0.732	0	1.1	4.4	14.6	1.9	3.6	41.9	0.2

Effect of tablet formulation (TvT) of *T. viride* against *F. oxysporum* on chickpea germination and wilting in pot experiment

Treatments were found to be significant ($p<0.05$) at all the replications under pot experiments for the germination percentage and wilting percentage at each time point (30, 45, and 60 DAS) (Table S1). As far as germination is concerned, a wide range of germination percentages were observed, ranging from 66.67-90.00%. The highest germination was recorded in T_4 (TvT formulation at recommended dose level) while the lowest was in T_1 (Absolute control). The TvT formulation at the three dose levels also performed significantly better than the commercial fungicide formulation treatment (T_2) (Figures 2, 3).

Wilting incidence was to be recorded lowest in the TvT formulation at the recommended dose level (T_4), while it was at

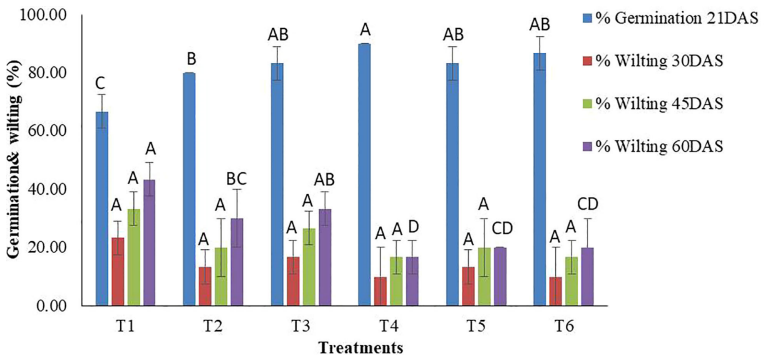

FIGURE 2
In-vivo assessment of percent seed germination and wilting of chickpea by TvT formulation of *T. viride* against pathogenic funus, *F. oxysporum* f. sp. *Ciceris*. (T1- Absolute control; T2- Carbendazim 50% WP; T3- Talc formulation; T4- TvT formulation at recommended dose; T5- TvT formulation at double dose; T6- TvT formulation at ½ of recommended dose). (For each parameter, treatment bars having at least one letter common are not statistically significant using Duncan's Multiple Range Test at $p<0.05$, n=3, error bars represent standard deviations).

FIGURE 3
In-vivo assessment of wilt incidence in chickpea caused by wilt causing fungi, *F. oxysporum* f. sp. *ciceris* post application of TvT formulation of *T. viride*. (**A**- Absolute control; **B**- Carbendazim 50% WP; **C**- Talc formulation; **D**- TvT formulation at recommended dose; **E**- TvT formulation at double dose; **F**- TvT formulation at ½ of recommended dose).

its highest in the absolute control (T_1) for the three-time intervals (30, 45, 60 DAS). At 30 DAS, the highest wilting recorded was 23.33% (T_1), while, 10.00% (T_4 and T_6) was the lowest. All the treatments were found to inhibit disease incidence more than that the commercial pesticide formulation (13.33%) as well as the talc-based formulation (16.67%) (Figures 2, 3). At 45 DAS, the highest wilting recorded was 33.33% (T_1) while 16.67% (T_4) was the lowest. All the treatments were found to inhibit the disease incidence more than the commercial pesticide formulation (20.00%) as well as the talc formulation (26.67%). At 60 DAS, the highest wilting recorded was 43.33% (T_1), while 16.67% (T_4) was the lowest. All the treatments were found to inhibit the disease incidence higher than that of the commercial pesticide formulation (30.00%) as well as the talc-based formulation (33.33%).

Bio-efficacy evaluation of TvP and TvT formulations on chickpea germination and wilting under field condition

Treatments were found to be significant ($p<0.05$) under field conditions concerning the germination percentage and wilting percentage at the three-time intervals *i.e.* 30, 45, and 60 DAS (Table S2). As far as germination is concerned, a wide range of germination percentages were observed *i.e.* ranging from 80.83-94.17%. The highest germination was recorded in T_7 (TvP formulation at the recommended dose level) while the lowest was in T_1 (Absolute control). (Figures 4, 5).

Wilting incidence was recorded as being lowest in powder formulation (TvP) at the recommended dose level (T_7) while it was

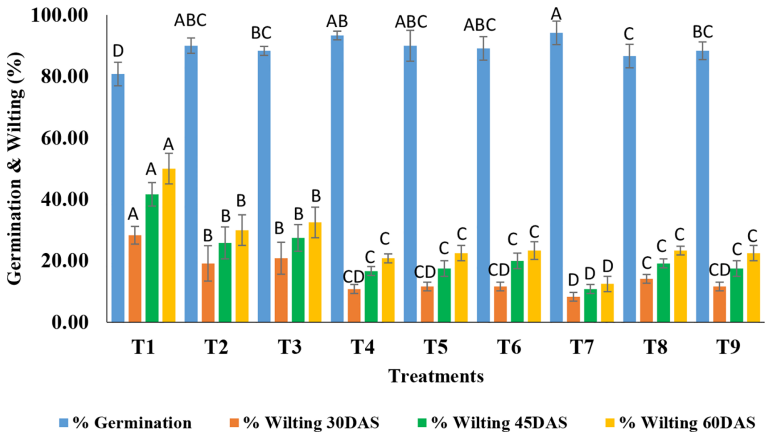

FIGURE 4
Effect of application of optimized TvT and TvP formulations against *F. oxysporum* f. sp. *ciceris* on percent seed germination and wilting of chickpea under field condition. (T1- Absolute control; T2- Carbendazim 50% WP; T3- Talc formulation; T4- TvT formulation at recommended dose; T5- TvT formulation at double dose; T6- TvT formulation at ½ of recommended dose; T7- TvP formulation at recommended dose; T8- TvP formulation at double dose; T9- TvP formulation at ½ of recommended dose.

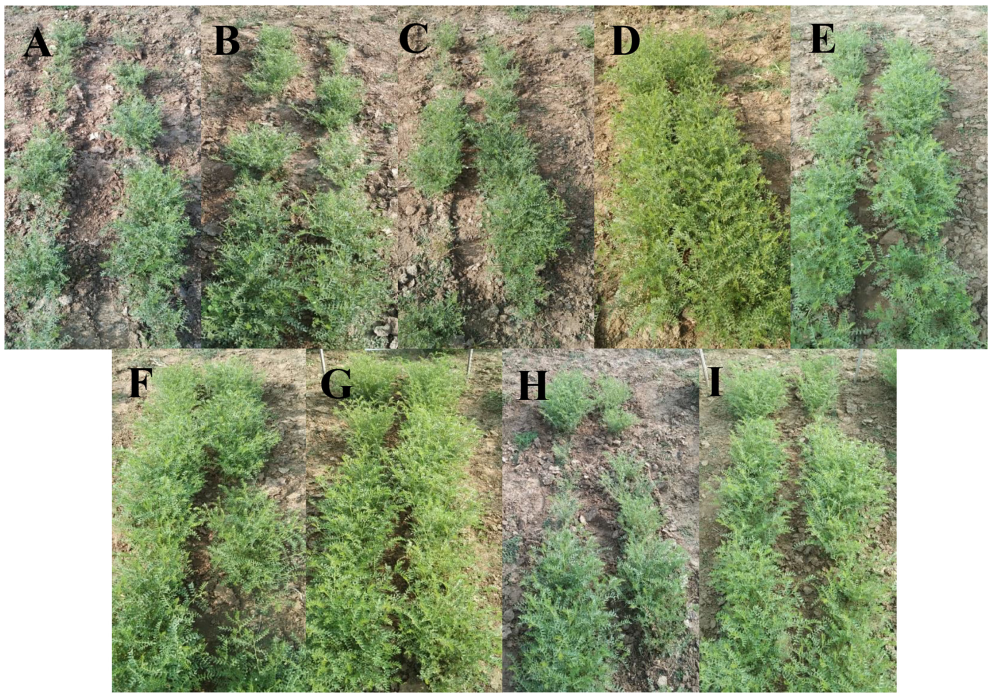

FIGURE 5
Field assessment of wilt incidence in chickpea caused by *F. oxysporum* f. sp. *ciceris* post application of TvT and TvP formulations of *T. viride*. (**A**- Absolute control; **B**- Carbendazim 50% WP; **C**- Talc formulation; **D**- TvT formulation at recommended dose; **E**- TvT formulation at double dose; **F**- TvT formulation at ½ of recommended dose; **G**- TvP formulation at recommended dose; **H**- TvP formulation at double dose; **I**- TvP formulation at ½ of recommended dose).

highest in the absolute control (T_1) at the three time points time intervals (30, 45, 60 DAS). At 30 DAS, the highest wilting recorded was 28.33% (T_1) while 8.33% (T_7) was the lowest. All the treatments were found to inhibit the disease incidence significantly higher than that of the commercial pesticide formulation (19.17%) as well as the talc formulation (20.83%) (Figure 4). At 45 DAS, the highest wilting recorded was 41.67% (T_1) while 10.83% (T_7) was the lowest. All the treatments were found to inhibit the disease incidence significantly higher than the commercial fungicide, Carbendazim 50% WP formulation (25.83%) as well as the talc formulation (27.50%). At 60 DAS, the highest wilting recorded was 50.00% (T_1) while 12.50% (T_7) was the lowest. All the treatments were found to inhibit the disease incidence significantly more than Carbendazim (30.00%) as well as the talc formulation (32.50%).

Effect of TvP and TvT formulations on chickpea yield parameters under field condition

Treatments were found to be significant ($p<0.05$) at all three replications under field conditions concerning the yield attributes *i.e.* root length, shoot length, shoot dry weight, and yield analysis. As shown in Table 6, the yield attributes follow the same trend as the germination and wilting studies. A wide range of differences in root length between the treatments were observed to be highest in T_7 (24.9 cm) while the lowest was in T_1 (10.03 cm). The biocontrol formulation-based treatment was the most effective compared to the commercial fungicide formulation (13.67 cm) and the talc-based formulation (16.00 cm). Similarly, shoot length ranged from T_1 (32.43 cm) to T_7 (44.40 cm) while no such effective difference was observed in the commercial pesticide formulation (38.53 cm) and the talc-based formulation (37.7 cm). Shoot dry weight was recorded in T_7 (16.40 g) as being highest while T_1 (8.23 g) was the lowest, meaning that all the treatments were superior over the talc-based formulation (11.37 g) and commercial pesticide formulation (11.73 g). Like other plant growth parameters, yield also followed the same trend, keeping the highest yield in T_7 (21.29 q ha^{-1}), whereas the lowest yield was obtained in T_1 (15.16 q ha^{-1}). The formulations developed in terms of yield were much more effective than the talc-based formulation (18.16 q ha^{-1}) and commercial pesticide formulation (19.83 q ha^{-1}).

Discussion

F. oxysporum f. sp. *ciceris* is one the most potent yield-limiting factors of chickpea (*Cicer arietinum* L.) worldwide. It

TABLE 6 Effect of application of *T. viride*-based tablet (TvT) and powder (TvP) formulations against *F. oxysporum* f. sp. *ciceris* on plant growth and yield of chickpea in field conditions.

Treatment	Root length (cm)	Shoot length (cm)	Shoot dry weight (g)	Yield (q ha^{-1})
T1	10.03 ± 2.35^{D}	32.43 ± 1.16^{E}	8.23 ± 1.59^{E}	15.16 ± 1.53^{D}
T2	13.67 ± 2.22^{C}	38.53 ± 2.00^{D}	11.73 ± 1.37^{CD}	19.83 ± 3.61^{AB}
T3	16.00 ± 1.30^{C}	37.70 ± 2.46^{D}	11.37 ± 2.42^{D}	18.16 ± 1.53^{C}
T4	22.50 ± 0.65^{B}	44.07 ± 0.25^{AB}	15.30 ± 3.27^{A}	20.46 ± 3.51^{AB}
T5	21.57 ± 1.52^{B}	42.47 ± 0.35^{BC}	12.67 ± 2.58^{BCD}	19.57 ± 2.00^{BC}
T6	21.63 ± 1.16^{B}	41.40 ± 0.36^{C}	13.93 ± 2.60^{ABC}	19.76 ± 2.08^{AB}
T7	24.90 ± 0.80^{A}	44.40 ± 0.46^{A}	16.40 ± 1.42^{A}	21.29 ± 2.52^{A}
T8	21.50 ± 0.92^{B}	42.80 ± 0.35^{ABC}	14.30 ± 3.10^{AB}	19.68 ± 3.06^{BC}
T9	21.63 ± 0.21^{B}	41.70 ± 0.53^{C}	14.33 ± 2.95^{AB}	19.93 ± 2.08^{AB}
CV(%)	7.02	2.65	11.26	4.62

Means with at least one letter common are not statistically significant using DUNCAN's Multiple Range Test at $p<0.05$, n=3.
(T1- Absolute control; T2- Carbendazim 50% WP; T3- Talc formulation; T4- TvT formulation at recommended dose; T5- TvT formulation at double dose; T6- TvT formulation at ½ of recommended dose; T7- TvP formulation at recommended dose; T8- TvP formulation at double dose; T9- TvP formulation at ½ of recommended dose).

enters through the roots and the germ tube enters plant epidermal cells. Eventually, the hyphae expand to the root cortical region and invade the xylem vessels, preventing water and other critical solutes from being transported upward and causing wilt. Additionally, the saprophytic fungus can live in soil or debris for up to 6 years and cause a reduction in yield (Caballo et al., 2019). Therefore, extensive research has been undertaken with an economical and feasible approach to manage the disease and a biological control-based approach has been found suitable (Dubey et al., 2007). Several efforts toward the management of soil or seed-borne diseases support the *Trichoderma* spp. as the best antagonist of pathogens (Dubey, 2002; Poddar et al., 2004). The antagonism caused by *Trichoderma* against *Fusarium* spp. is due to the coiling of antagonistic fungal hyphae, thereby causing lysis (Kumar and Dubey, 2001; Naglot et al., 2015; El-Debaiky, 2017; Chen et al., 2021). In the present work, the selection study of the best performing strain of *T. viride* revealed the efficacy of the strain ITCC 7764 as the most efficient. GC-MS analysis of the VOCs released by the fungal strain showed the highest content of octan-3-one (13.92%), 3-octanol (10.57%), and 1-octen-3-ol (9.40%). These compounds did not appear in the less potential strains, *T. viride* 8276 and *T. viride* 7847, where long-chain hydrocarbon contributed maximum in their respective composition. According to some of the studies, several species of *Trichoderma* have been found to generate different chemicals that prevent the growth and development of pathogenic fungi and also mycoparasitize them in crops, such as *T. harzianum* on *R. solani* (Poveda, 2021). In another investigation by Kumar et al. (2019), *T. viride* and *T. harzianum* exhibited inhibition zones of 70.10% and 76.90% against the FOC strain of *F. oxysporum*, respectively.

Based on the screening study, the strain ITCC 7764 was selected as the bioagent to develop *T. viride*-based biocontrol formulations. Two types of biocontrol formulations of *T. viride* strain ITCC 7764, TvP for seed treatment and TvT for direct application, have been developed in the present study with different compositions of biopolymer, optimized xerogel, neem leaf powder, and clay. The present study undertook the selection of formulation auxiliaries critically to prepare the powder and tablet matrix suitable for bioagent survival and bioefficacy. Clay is generally used in formulations as a filler material (Le Bras and Bourbigot, 1996). Biopolymer has been extensively used in the development of biocontrol formulations due to their nontoxicity, wider availability, and cost-effectiveness (Mukhopadhyay et al., 2019; Meena et al., 2020; Oszust et al., 2021). The presence of xerogel in the formulation matrix may provide a sustained moisture-enriched environment during storage (Mukhopadhyay et al., 2020) and supply moisture to the crop after getting released to the field through formulation application (Akhter et al., 2004; Prakash et al., 2021). Moreover, the neem leaf powder, which was taken as an excipient of the prepared formulations expressed, no negative impact on test antagonistic fungi, *T. viride*, expressing its compatibility and suitability as an adjuvant of the formulations. The neem leaf powder expressed 12.80% and 34.90% inhibition of *F. oxysporum* f. sp. *ciceris* singly and in combination with *T. viride* at the concentration present in the recommended dose of the formulation. A similar finding was observed by Patil et al. (2018), where the application of neem leaves at the rate of 30 g per pot revealed a lower percentage of damping-off caused by *F. oxysporum* f. sp. *cucumerinum* as compared to bavistin and untreated inoculated check of the fungus alone in cucumber at 30 DAS. The azadirachtin content has been reported to be 0.0244 percent (w w^{-1}) in neem leaves (Radhakrishnan et al., 2010). In another study by Prashanth and Krishnaiah (2014), the alkaloids, reducing sugars, saponins, and other phytochemicals were detected in the ethanolic and aqueous extracts of neem leaves. Numerous other substances, including acetyloxy acetic acid, germanicol, 1,3-diphenyl-2-azafluorene, phytol, and hydroxy pivalic acid, were also detected in the ethanolic

extract of the neem leaves by GC-MS. Singh et al. (2010) prepared a controlled release fungicidal formulation of thiram by employing alginate beads and neem leaf powder.

The various physicochemical parameters of the developed formulations were also analyzed using standard CIPAC guidelines. For the selection of the optimized formulations, the pH of the formulations was selected as the most important criterion. The biocontrol agent, *T. viride*, has been previously reported to grow best and function at pH 6.50 (Belal, 2008). Therefore, the formulations TvP2 (pH: 6.50) and TvT1 (pH 7.16) were selected for further experimentation. Immobilizing wet or dry biomass inside cross-linked polymers like alginate and carrageenan is one of the most current techniques for generating biocontrol formulations (Saberi-Riseh et al., 2021). Bejarano and Puopolo (2020) reported the formulation of pellets by dry and wet immobilization of the biocontrol agents. For the entrapment of bio-agent conidia, sodium alginate, aluminum silicate, and sabudana powder were utilized by Dubey et al. (2009) to develop *Trichoderma*-based formulations for soil application. Furthermore, granular and liquid formulations of *Trichoderma* have been developed for the control of *R. solani* (Herrera et al., 2020).

The wilt disease caused by *F. oxysporum* is one the most prominent yield-limiting diseases affecting chickpea worldwide. Yield losses have been recorded from 10 to 100%, varying with the differences in the prevailing climatic conditions (Jiménez-Díaz et al., 2015; Sharma et al., 2019). Fungal soil-borne diseases have been hard to manage, especially when the pathogen adopts some resistant means of survival such as chlamydospores or sclerotia, enabling the pathogen to infect the crop and soil for up to several years (Maitlo et al., 2019). Being soil-borne, chemical control measures are applied several times for controlling the wilt in chickpea crops. However, the biological control based approach is more suitable compared to chemical methods (Dubey et al., 2007). In the present findings, the observed wilting percentage was only 16.67% after 60 DAS at the recommended dose of the formulation TvT1 under *in vivo* conditions. Moreover, the bioefficacy of the TvT1 formulation was significantly higher as compared to the carbendazim and *Trichoderma* talc-based formulation.

Several efforts toward the management of soil or seed-borne diseases support the *T. viride* and *T. harzianum* to be the best antagonists of pathogens (Dubey, 2002; Poddar et al., 2004). The same biocontrol agent has been assessed against *Fusarium* species, resulting in the production of various volatiles and non-volatiles having antagonistic potential towards the pathogen and resulting in its suppression (Kumar and Dubey, 2001; Bubici et al., 2019). A bioefficacy study under field conditions expressed the superior performance of TvP formulation as compared to the Carbendazim and talc-based biocontrol formulation. Moreover, at 60 DAS, the highest wilting recorded was 50.00% in the negative control while 12.50% was the lowest in the TvP formulation at the recommended dose. In another *in vitro* study, the biopolymeric hydrogel-based formulation composition containing *Trichoderma* sp. spores and/or mycelia was found to be more effective at combating *R. solani* compared to *Trichoderma* sp. alone (Mondal et al., 2020). A similar observation was also reported by Animisha et al. (2012), suggesting only 19% occurrence of wilt disease after application of *T. viride* compared to the 21% incidence observed on treatment with Carbendazim.

Different herbicide tablets have already been developed for sustained release applications (Shahena et al., 2020). However, the preparation of antagonistic fungi-loaded tablet formulations for direct applications to the field employed in this study is novel. The performance of a tablet formulation depends on several factors such as dissolution, tablet breaking force, disintegration, the homogeneity of composition, etc. (Akseli et al., 2017) Similarly, the effect of *Trichoderma* based formulation depends on different factors namely p^H, moisture content, inoculum concentration, storage temperature, inoculum age, and the incubation period (Mulatu et al., 2021). Therefore, integrating knowledge of material science and fungal physiological behavior is paramount for the development of antagonistic fungi-based tablet bioformulations. In the present investigation, the TvT formulation showed improved bioefficacy compared to the positive controls (Carbendazim 50% WP and talc formulation), but it expressed inferior performance compared to TvP under field conditions. This might be due to the presence of alkaline formulation components resulting in the p^H of the matrix being higher than 6.50, which was not conducive to the growth and functioning of the biocontrol agent. The high disintegration time (22.5 min) might also be responsible for the slower release and buildup of antagonistic fungal growth in the soil. Moreover, the proximity to the seeds being further away in the case of the TvT formulation might account for its worse performance in terms of wilting incidence compared to the TvP formulation.

Conclusion

In total, five different strains of *T. viride* (ITCC 6889, ITCC 7204, ITCC 7764, ITCC 7847, and ITCC 8276) were screened against *F. oxysporum* f. sp. *ciceris*, causing devastating wilt disease in chickpea. The selection of the most effective *Trichoderma* strain for the development of biocontrol formulations was based on *in-vitro* inhibition tests using volatile and non-volatile assays. The best strain ITCC-7764 recorded an inhibition of 26.45% and 74.45%, respectively. Furthermore, strain TV-3 (ITCC 7764) was used to formulate powder for seed treatment (TvP) and tablet (TvT) formulations applied at the three dose levels (recommended dose, double of the recommended dose, and half of the recommended dose), the effectivity of which were assessed in terms of germination and wilting percentage for Carbendazim as commercial formulation

and talc-based formulations under field conditions. Under field conditions, the powder formulation TvP for seed treatment at the recommended dose was recorded to be more effective against the pathogen than a tablet (TvT) applied treatment, though both recorded superior performance to Carbendazim 50% WP and talc based formulation. Overall, the research undertaken reports two different types of bio-control formulations (TvP and TvT) of *T. viride* as effective environmentally sustainable options for managing wilting disease in chickpeas. These findings on the novel powder and tablet formulations of *T. viride* will be taken forward to validate their product performance under shelf-life assessment and integrated disease management programs.

Supplementary information

Xerogel preparation method

An *in-situ* solution polymerization was used to synthesize the biopolymeric agri-waste reinforced superabsorbent composites taking various ratios of backbone, agriwaste, monomer, cross-linker and initiator in a definite volume of water at a particular temperature. The alkali was used after gel formation. Gel was suitably treated to attain pH of 7.0 and dried to get xerogel.

Data availability statement

The original contributions presented in the study are included in the article/Supplementary Material. Further inquiries can be directed to the corresponding author.

Author contributions

PP, AM, RK, AK and PS conducted the investigation. NP, AD and DK validated the study. AS and RA provided resources. AS conceptualized the study. PP, AM, RK and AK prepared the original draft. AS, CB and TB supervised the experiment. All authors contributed to the article and approved the submitted version.

Acknowledgments

The authors thank the Director of the Indian Council of Agricultural Research-Indian Agricultural Research Institute (ICAR-IARI), New Delhi, India.

Conflict of interest

The authors declare that the research was conducted in the absence of any commercial or financial relationships that could be construed as a potential conflict of interest.

Publisher's note

All claims expressed in this article are solely those of the authors and do not necessarily represent those of their affiliated organizations, or those of the publisher, the editors and the reviewers. Any product that may be evaluated in this article, or claim that may be made by its manufacturer, is not guaranteed or endorsed by the publisher.

Supplementary material

The Supplementary Material for this article can be found online at: https://www.frontiersin.org/articles/10.3389/fpls.2022.990392/full#supplementary-material

SUPPLEMENTARY FIGURE 1
Bioefficacy assessment of different strains of *T. viride* against *F. oxysporum* f. sp. *ciceris* using volatile method

SUPPLEMENTARY FIGURE 2
Bioefficacy assessment of different strains of *T. viride* against *F. oxysporum* f. sp. *ciceris* using non-volatile method

SUPPLEMENTARY TABLE 1
Effect of Application of *T. viride*-based Tablet (TvT) Formulation against *F. oxysporum* f. sp. *ciceris* on Seed Germination and Wilting Incidence on Chickpea *in-vivo*

SUPPLEMENTARY TABLE 2
Effect of Application of *T. viride*-based tablet (TvT) and Powder (TvP) Formulations against *F. oxysporum* f. sp. *ciceris* on Seed Germination and Wilting Incidence on Chickpea in Field Conditions

References

Akhter, J., Mahmood, K., Malik, K. A., Mardan, A., Ahmad, M., and Iqbal, M. M. (2004). Effects of hydrogel amendment on water storage of sandy loam and loam soils and seedling growth of barley, wheat and chickpea. *Plant Soil Environ.* 50, 463–469. doi: 10.17221/4059-pse

Akseli, I., Xie, J., Schultz, L., Ladyzhynsky, N., Bramante, T., He, X., et al. (2017). A practical framework toward prediction of breaking force and disintegration of tablet formulations using machine learning tools. *J. Pharm. Sci.* 106, 234–247. doi: 10.1016/j.xphs.2016.08.026

Alloosh, M., Hamwieh, A., Ahmed, S., and Alkai, B. (2019). Genetic diversity of fusarium oxysporum f. sp. ciceris isolates affecting chickpea in Syria. *Crop Prot.* 124, 104863. doi: 10.1016/j.cropro.2019.104863

Animisha,, Zacharia, S., Jaiswal, K. K., and Pandey, P. (2012). Integrated management of chickpea wilt incited by *Fusarium oxysporum f.* sp. *ciceris*. *Int. J. Agric. Res.* 7, 284–290. doi: 10.3923/ijar.2012.284.290

Anusha, B. G., Gopalakrishnan, S., Naik, M. K., and Sharma, M. (2019). Evaluation of streptomyces spp. and bacillus spp. for biocontrol of fusarium wilt in chickpea (Cicer arietinum l.). *Arch. Phytopathol. Plant Prot.* 52 (5-6), 417–442. doi: 10.1080/03235408.2019.1635302

Bejarano, A., and Puopolo, G. (2020). "Bioformulation of microbial biocontrol agents for a sustainable agriculture," in *Progress in biological control* (Cham: Springer), 275–293. doi: 10.1007/978-3-030-53238-3_16

Belal, E. B. (2008). Biodegradation of wastepaper by trichoderma viride and using bioprocessed materials in biocontrol of damping-off of pea caused by. *Pythium debaryanum J. Agric. Res. Kafrelsheikh Univ.* 34, 567–587.

Bubici, G., Kaushal, M., Prigigallo, M. I., Cabanás, C. G. L., and Mercado-Blanco, J. (2019). Biological control agents against fusarium wilt of banana. *Front. Microbiol.* 10. doi: 10.3389/fmicb.2019.00616

Bunbury-Blanchette, A. L., and Walker, A. K (2019). Trichoderma species show biocontrol potential in dual culture and greenhouse bioassays against Fusarium basal rot of onion. *Biological Control* 130, 127–135.

Caballo, C., Castro, P., Gil, J., Millan, T., Rubio, J., and Die, J. V. (2019). Candidate genes expression profiling during wilting in chickpea caused by fusarium oxysporum f. sp. ciceris race 5. *PloS One* 14, e0224212. doi: 10.1371/journal.pone.0224212

Chand, H., and Khirbat, S. K. (2009). Chickpea wilt and its management - a review. *Agric. Rev.* 30, 1–12.

Chen, J., Zhou, L., Din, I. U., Arafat, Y., Li, Q., Wang, J., et al. (2021). Antagonistic activity of trichoderma spp. against fusarium oxysporum in rhizosphere of radix pseudostellariae triggers the expression of host defense genes and improves its growth under long-term monoculture system. *Front. Microbiol.* 12. doi: 10.3389/fmicb.2021.579920

Choi, H. W., and Ahsan, S. M. (2022). Biocontrol activity of aspergillus terreus ANU-301 against two distinct plant diseases, tomato fusarium wilt and potato soft rot. *Plant Pathol. J.* 38 (1), 33. doi: 10.5423/PPJ.OA.12.2021.0187

CIBRC (2011). Guidelines/data requirements for registration of antagonistic fungi under section 9(3b) and 9(3) of the insecticide act 1–8.

CIBRC *Microsoft word—major uses of pesticides (biopesticides)* (2022).docx (ppqs.gov.in). Accessed on 01–06–2022.

Dubey, S. C. (2002). Bio-agent based integrated management of collar rot of French bean. *Indian Phytopathol.* 55, 230–231.

Dubey, S. C., Bhavani, R., and Singh, B. (2009). Development of pusa 5SD for seed dressing and pusa biopellet 10G for soil application formulations of trichoderma harzianum and their evaluation for integrated management of dry root rot of mungbean (Vigna radiata). *Biol. Control* 50, 231–242. doi: 10.1016/j.biocontrol.2009.04.008

Dubey, S. C., Suresh, M., and Singh, B. (2007). Evaluation of trichoderma species against fusarium oxysporum f. sp. ciceris for integrated management of chickpea wilt. *Biol. Control* 40, 118–127. doi: 10.1016/J.BIOCONTROL.2006.06.006

Eiliazadeh, B., Briscoe, B. J., Sheng, Y., and Pitt, K. (2003). Investigating density distributions for tablets of different geometry during the compaction of pharmaceuticals. *Part. Sci. Technol.* 21 (4), 303–316. doi: 10.1080/716100572

El-Debaiky, S. A. (2017). Antagonistic studies and hyphal interactions of the new antagonist *Aspergillus piperis* against some phytopathogenic fungi in vitro in comparison with trichoderma harzianum. *Microb. Pathog.* 113, 135–143. doi: 10.1016/j.micpath.2017.10.041

Golakiya, B. B., Bhimani, M. D., and Akbari, L. F. (2018). Efficacy of different fungicides for the management of chickpea wilt (Fusarium oxysporum f. sp. ciceri). *Int. J. Chem. Stud.* 6 (2), 199–205.

Herrera, W., Valbuena, O., and Pavone-Maniscalco, D. (2020). Formulation of trichoderma asperellum TV190 for biological control of rhizoctonia solani on corn seedlings. *Egypt J. Biol. Pest Control* 30, 1–8. doi: 10.1186/s41938-020-00246-9

Jiménez-Díaz, R. M., Castillo, P., Jiménez-Gasco, M., del, M., Landa, B. B., and Navas-Cortés, J. A. (2015). Fusarium wilt of chickpeas: Biology, ecology and management. *Crop Prot.* 73, 16–27. doi: 10.1016/j.cropro.2015.02.023

John, R. P., Tyagi, R. D., Brar, S. K., Surampalli, R. Y., and Prévost, D. (2011). Bio-encapsulation of microbial cells for targeted agricultural delivery. *Critic. Rev. Biotechnol.* 31 (3), 211–226. doi: 10.3109/07388551.2010.513327

Keerthiraj, M., Mandal, A., Dutta, T. K., Saha, S., Dutta, A., Singh, A., et al. (2021). Nematicidal and molecular docking investigation of essential oils from pogostemon cablin ecotypes against meloidogyne incognita. *Chem. Biodiv.* 18 (9), e2100320.

Khan, M. R., Khan, N., and Khan, S. M.. (2001). Evaluation of agricultural materials as substrate for mass culture of fungal biocontrol agents of fusarial wilt and root-knot nematode diseases. *Tests Agrochem. Cultivars* (22), 50–51.

Kumar, D., and Dubey, S. C. (2001). Management of collar rot of pea by the integration of biological and chemical methods. *Indian Phytopathol.* 57, 62–66.

Kumar, R., Kundu, A., Dutta, A., Saha, S., Das, A., and Bhowmik, A. (2021). Chemo-profiling of bioactive metabolites from chaetomium globosum for biocontrol of sclerotinia rot and plant growth promotion. *Fungal Biol.* 125 (3), 167–176. doi: 10.1016/j.funbio.2020.07.009

Kumar, M., Vipul, K., Meenakshi, R., and Seweta, S. (2019). Effect of volatile and non volatile compounds of trichoderma spp. against fusarium isolates causing chickpea wilt in punjab. *Plant Archiv.* 19, 159–162.

Le Bras, M., and Bourbigot, S. (1996). Mineral fillers in intumescent fire retardant formulations–criteria for the choice of a natural clay filler for the ammonium polyphosphate/pentaerythritol/polypropylene system. *Fire Mater.* 20, 39–49. doi: 10.1002/(SICI)1099-1018(199601)20:1<39::AID-FAM556>3.0.CO;2-Z

Maitlo, S. A., Rajput, N. A., Syed, R. N., Khanzada, M. A., Rajput, A. O., and Lodhi, A. M. (2019). Microbial control of fusarium wilt of chickpea caused by fusarium oxysporum f. sp. ciceris. *Pakistan J. Bot.* 51, 2261–2268. doi: 10.30848/PJB2019-6(23)

Mei, L. I., Hua, L. I. A. N., Su, X. L., Ying, T. I. A. N., Huang, W. K., Jie, M. E. I., et al. (2019). The effects of trichoderma on preventing cucumber fusarium wilt and regulating cucumber physiology. *J. Integr. Agric.* 18 (3), 607–617. doi: 1016/S2095-3119(18)62057-X

Meena, B. R., Chittora, D., Mittholiya, S., and Sharma, K.. (2020). Herbal Bio-Formulation: An Effective Mean To Control Alterneria Solani. *Plant Archive* 20 (1), 3243–3247.

Mondal, P., Singh, A., Dhruba, J. S., Dubey, S. C., and Kumar, A.. (2020). Trichoderma harzianum Formulations based on a Biopolymeric Hydrogel, ZnSO4 and their Combination. *Pesticide Res. J.* 32 (1), 107–116.

Mukhopadhyay, A., Singh, A., Somvanshi, V. S., Manna, S., Rudra, S. G., Kundu, A., et al. (2019). Effect of pH and viscosity of gel carrier and lipid metabolism arresting adjuvants on shelf life of entomopathogenic nematodes. *Pestic. Res. J.* 31, 160–171. doi: 10.5958/2249-524X.2019.00030.X

Mukhopadhyay, A., Singh, A., Somvanshi, V., and Patanjali, N. (2020). Novel bioinsecticidal gel formulation with improved shelf life and infectivity. *Allelopathy J.* 49, 257–269. doi: 10.26651/allelo.j/2020-49-2-1269

Mulatu, A., Alemu, T., Megersa, N., and Vetukuri, R. R. (2021). Optimization of culture conditions and production of bio-fungicides from trichoderma species under solid-state fermentation using mathematical modeling. *Microorganisms* 9, 1675. doi: 10.3390/microorganisms9081675

Naglot, A., Goswami, S., Rahman, I., Shrimali, D. D., Yadav, K. K., Gupta, V. K., et al. (2015). Antagonistic potential of native trichoderma viride strain against potent tea fungal pathogens in north east India. *Plant Pathol. J.* 31, 278–289. doi: 10.5423/PPJ.OA.01.2015.0004

Navas-Cortes, J. A., Hau, B., and Jimenez-Diaz, R. M. (2000). Yield loss in chickpeas in relation to development of fusarium wilt epidemics. *Phytopathol.* 90, 1269–1278. doi: 10.1094/PHYTO.2000.90.11.1269

Nene, Y. L., Reddy, M. V., Haware, M. P., Ghanekar, A. M., and Amin, K. S. (2012). *Field diagnosis of chickpea diseases and their control science with a human face. f. diagnosis chickpea dis. their control. inf. bull. no. 28* (Patancheru, India: Int. Crop. Res. Inst. Semi-Arid Trop).

Oszust, K., Pylak, M. , and Frąc, M. (2021). Trichoderma-based biopreparation with prebiotics supplementation for the naturalization of raspberry plant rhizosphere. *Int. J. Mol. Sci.* 22, 6356. doi: 10.3390/ijms22126356

Patil, J., Kumar, A., Yadav, S., Goel, S. R., and Bhatia, A. K. (2018). Bio-efficacy of phytotherapeutic substances against meloidogyne incognita and fusarium oxysporum f. sp. cucumerinum affecting cucumberin polyhouse under protected cultivation. *Indian J. Nematol.* 48, 190–197.

Poddar, R. K., Singh, D. V., and Dubey, S. C. (2004). Lntegrated application of chickpea, trichoderma harzianum mutants and carbendazim to manage wilt (Fusarium oxysporum ciceri). *Indian J. Agric. Sci.* 74, 346–348.

Poveda, J. (2021). Biological control of fusarium oxysporum f. sp. ciceri and ascochyta rabiei infecting protected geographical indication fuentesaúco-chickpea by trichoderma species. *Eur. J. Plant Pathol.* 160, 825–840. doi: 10.1007/s10658-021-02286-9

Prakash, V., Kavitha, J. R., and Maheshwari, P. (2021). Moisture conservation practice by using hydrogel in agriculture: A review. *Plant Archiv.* 21, 526–528. doi: 10.51470/PLANTARCHIVES.2021.v21

Prashanth, G. K., and Krishnaiah, G. M. (2014). Chemical composition of the leaves of azadirachta indica Linn (Neem). *Int. J. Eng. Technol. Manage. Appl. Sci.* 1, 21–31.

Radhakrishnan, L., Gomathinayagam, S., and Balakrishnan, V. (2010). Evaluation of anthelmintic effect of neem (Azadirachta indica) leaves on haemonchus contortus in goats. *J. Parasitol.* 5, 292–297. doi: 10.17311/jp.2007.57.62

Ramanujam, B., Prasad, R. D., Sriram, S., and Rangeswaran, R. (2010). Mass production, formulation, quality control and delivery of trichoderma for plant disease management. *J. Plant Prote. Sci.* 2 (2), 1–8.

Saberi-Riseh, R., Moradi-Pour, M., Mohammadinejad, R., and Thakur, V. K. (2021). Biopolymers for biological control of plant pathogens: advances in microencapsulation of beneficial microorganisms. *Polymers (Basel)* 13, 1938. doi: 10.3390/polym13121938

Shahena, S., Rajan, M., Chandran, V., and Mathew, L. (2020). "Controlled release herbicides and allelopathy as sustainable alternatives in crop production," in *Controlled release of pesticides for sustainable agriculture* (Cham: Springer), 237–252.

Sharma, M., Ghosh, R., Tarafdar, A., Rathore, A., Chobe, D. R., Kumar, A. V., et al. (2019). Exploring the genetic cipher of chickpea (Cicer arietinum l.) through identification and multi-environment validation of resistant sources against fusarium wilt (Fusarium oxysporum f. sp. ciceris). *Front. Sustain. Food Syst.* 3. doi: 10.3389/fsufs.2019.00078

Sheoran, N., Nadakkakath, A. V., Munjal, V., Kundu, A., Subaharan, K., Venugopal, V., et al. (2015). Genetic analysis of plant endophytic pseudomonas putida BP25 and chemo-profiling of its antimicrobial volatile organic compounds. *Microbiol. Res.* 173, 66–78. doi: 10.1016/j.micres.2015.02.001

Singh, B., Sharma, D. K., Kumar, R., and Gupta, A. (2010). Development of a new controlled pesticide delivery system based on neem leaf powder. *J. Hazard Mater.* 177, 290–299. doi: 10.1016/j.jhazmat.2009.12.031

Srivastava, S., Singh, V. P., Kumar, R., Srivastava, M., Sinha, A., and Simon, S. (2011). In vitro evaluation of carbendazim 50% WP, antagonists and botanicals against fusarium oxysporum f. sp. psidii associated with rhizosphere soil of guava. *Asian J. Plant Pathol.* 5, 46–53. doi: 10.3923/ajppaj.2011.46.53

Sunkad, G., Deepa, H., Shruthi, T. H., and Singh, D. (2019). Chickpea wilt: status, diagnostics and management. *Indian Phytopathol.* 72 (4), 619–627. doi: 10.1007/s42360-019-00154-5

Sun, H., Wang, X., Wang, J., Shi, G., and Chen, L. (2020). Influence of the formula on the properties of a fast dispersible fruit tablet made from mango, chlorella, and cactus powder. *Food Sci. Nutr.* 8 (1), 479–488. doi: 10.1002/fsn3.1330

Tapwal, A., Singh, U., Singh, G., Garg, S., and Kumar, R. (2011). In vitro antagonism of trichoderma viride against five phytopathogens. *Pest Technol.* 5, 59–62.

Yegrem, L. (2021). Nutritional composition, antinutritional factors, and utilization trends of Ethiopian chickpea (Cicer arietinum l.). *Int. J. Food Sci*, 1–10. doi: 10.1155/2021/5570753

Zaim, S., Belabid, L., Bayaa, B., and Bekkar, A. A. (2016). "Biological control of chickpea fusarium wilts using rhizobacteria 'pgpr," in *Microbial-mediated induced systemic resistance in plants* (Singapore: Springer Singapore), 147–162. doi: 10.1007/978-981-10-0388-2_10

frontiers | Frontiers in Plant Science

TYPE Original Research
PUBLISHED 10 February 2023
DOI 10.3389/fpls.2023.973207

OPEN ACCESS

EDITED BY
Rachid Lahlali,
Ecole Nationale d'Agriculture de Meknès, Morocco

REVIEWED BY
Göksel Özer,
Abant Izzet Baysal University, Türkiye
Said Ibrahim Behiry,
Alexandria University, Egypt

*CORRESPONDENCE
Hamza Saghrouchni
hsaghrouchni@student.cu.edu.tr
Mohammed Bourhia
bouriamohammed@gmail.com

SPECIALTY SECTION
This article was submitted to Plant Pathogen Interactions, a section of the journal Frontiers in Plant Science

RECEIVED 21 June 2022
ACCEPTED 12 January 2023
PUBLISHED 10 February 2023

CITATION
Saghrouchni H, Barnossi AE, Mssillou I, Lavkor I, Ay T, Kara M, Alarfaj AA, Hirad AH, Nafidi H-A, Bourhia M and Var I (2023) Potential of carvacrol as plant growth-promotor and green fungicide against fusarium wilt disease of perennial ryegrass.
Front. Plant Sci. 14:973207.
doi: 10.3389/fpls.2023.973207

Potential of carvacrol as plant growth-promotor and green fungicide against fusarium wilt disease of perennial ryegrass

Hamza Saghrouchni[1]*, Azeddin El Barnossi[2], Ibrahim Mssillou[3], Isilay Lavkor[4], Tahsin Ay[4], Mohammed Kara[5], Abdullah A. Alarfaj[6], Abdurahman Hajinur Hirad[6], Hiba-Allah Nafidi[7], Mohammed Bourhia[8]* and Isil Var[9]

[1]Department of Biotechnology, Institute of Natural and Applied Sciences, Çukurova University, Adana, Türkiye, [2]Laboratory of Biotechnology, Environment, Agri-Food and Health, Faculty of Sciences Dhar El Mehraz, Sidi Mohammed Ben Abdellah University, Fez, Morocco, [3]Laboratory of Natural Substances, Pharmacology, Environment, Modeling, Health & Quality of Life, Faculty of Sciences Dhar El Mehraz, Sidi Mohamed Ben Abdallah University, Fez, Morocco, [4]Mycology unit Biological Control Research Institute, Adana, Türkiye, [5]Laboratory of Biotechnology, Conservation and Valorisation of Natural Resources, Faculty of Sciences Dhar El Mehraz, Sidi Mohamed Ben Abdallah University, Fez, Morocco, [6]Department of Botany and Microbiology College of Science, King Saud University, Riyadh, Saudi Arabia, [7]Department of Food Science, Faculty of Agricultural and Food Sciences, Laval University, Quebec City, QC, Canada, [8]Laboratory of Chemisty and Biochemistry, Faculty of Medicine and Pharmacy, Ibn Zohr University, Laayoune, Morocco, [9]Department of Food Engineering, Faculty of Agriculture, Çukurova University, Adana, Türkiye

Perennial ryegrass (*Lolium perenne* L.) is a valuable forage and soil stabilisation crop. Perennial crops have long been associated with good environmental performance and ecosystem stability. Vascular wilt diseases caused by *Fusarium* species are the most damaging plant diseases affecting both woody perennials and annual crops. Therefore, the aim of the present study was the assessment of the preventive and growth-promoting effects of carvacrol against *Fusarium oxysporum*, *F. solani*, and *F. nivale* (phylogenetically analyzed on the basis of internal transcribed spacer (ITS) regions) causing vascular wilt of ryegrass *in vitro* and under greenhouse conditions. To accomplish this aim, various parameters were monitored including coleoptile development, rhizogenesis, the incidence of coleoptile lesions, disease index, the visual appearance of ryegrass health, ryegrass organic matter and soil fungal load. The results obtained showed that *F. nivale* was highly harmful to ryegrass seedlings compared to other *Fusarium* species. Furthermore, carvacrol with 0.1 and 0.2 mg/mL protected significantly the seedlings against Fusarium wilt diseases both *in vitro* and in the greenhouse. Simultaneously, carvacrol also functioned as a seedling growth promoter, as is reflected in all monitored parameters, such as the recovery of seedling height and root length, and the development of new leaf buds and secondary roots. Carvacrol proved to be effective plant growth promoter and a bio-fungicide against Fusarium vascular diseases.

KEYWORDS

***Lolium perenne*, perennial ryegrass, fusarium wilt, carvacrol, bio-fungicide, plant growth promotor**

Introduction

Perennial ryegrass (*Lolium perenne* L.) is a cool-season grass grown throughout temperate regions of the world (Wilkins & Humphreys, 2003; Wiering et al., 2021). Perennial plants have long been associated with good environmental performance and improved ecosystem health, perennials protect and stabilizer the soil against wind and water erosion, while increasing soil quality and organic matter thanks to biomass accumulation (Blanco-canqui, 2010). An increased proportion of perennials increase biodiversity by providing habitat for animals and insects. Additionally, perennial crops can increase the quantity and diversity of mineral nutrients available in the rhizosphere by establishing complex and often long-term relationships with the microbiome (Davis et al., 2010; Nehls et al., 2010). Perennial grasses with their large and active root system, play a crucial role in scavenging available nutrients and preventing them from leaching away where they may become pollutants (Heaton et al., 2010). Further, though a popular species in the turf industry, perennial ryegrass has desirable grazing characteristics and high nutritive value (Sampoux et al., 2011). Therefore, the main role of this species is to provide forage for ruminant animals. Consequently, perennial ryegrass forage breeders have focused on improving biomass, nutritive value, persistence, disease resistance, and winter-hardiness (Sampoux et al., 2011).

Vascular wilt diseases caused by fungal pathogens are the most damaging plant diseases that affect both woody perennials and annual crops (Boutaj et al., 2022). The *Fusarium* genus is one of the utmost complex and adaptive genus in the Eumycota (Gordon, 2017). Fusarium species which cause destructive vascular wilts, rots, and damping-off diseases, are ubiquitous soil-borne pathogens of a wide range of horticultural and food crops (Bodah, 2017; Saghrouchni et al., 2021). In addition to the damages caused in the pre-harvest period, many *Fusarium* species are capable of producing mycotoxins in agricultural and food commodities, as well as in perennial forage (Juraschek et al., 2022). These phytopathogens attack the vascular system made up of xylem arteries, tracheary elements that transport water and minerals from the roots to the photosynthetic organs, and phloem elements, which transport organic photosynthesis products (Agrios, 2005). High number of harmful mycotoxins produced by Fusarium can be commonly detected in ruminant diets, such as deoxynivalenol and fumonisins, which can interfere with ruminant animals and human health (Escrivá et al., 2015; Gallo et al., 2021).

Fusarium spp., *Microdochium* spp., and *Neocosmospora* spp. can cause destructive vascular wilt disease. *Fusarium nivale* (Fr.) Samuels and I.C. Hallet, *Fusarium oxysporum* described by Schltdl., and *Fusarium solani* (Mart.) L. Lombard and Crous, three species owning to the "Fusarium complex" have devastating effects on species belonging to wild gramineae, *Lolium perenne* L. (ryegrass) (Saghrouchni et al., 2021). These species usually limit the production of economically important crops since these strains attack several types of plants especially gramineae family including rice, maize, wheat, barley, oats, and rye, and therefore induce significant losses especially when the environmental conditions are favourable (Servin et al., 2015).

To control Fusarium wilt, several strategies were used such as soil solarisation and fumigation with various pesticides. However, the presence of chemical residues is harmful to the public health and can affect the quality of soil and groundwater (Boutaj et al., 2022). These products can be used before planting to treat soil and/or during cultivation, e.g., chloropicrin and benomyl (Dorugade et al., 2021; Karki et al., 2022). Due to excessive use, some fungicides can no longer be effective towards resistant strains among fungal species (Chaves et al., 2022). Therefore, it is necessary to identify alternative weapons to control Fusarium wilt disease.

Pathogen control and disease management can only be achieved through an integrative approach in which biological control can play a major role. Nowadays, biological agents including botanical agents (Plant extracts, essential oils and their major compounds) are used as alternative solutions (Lecomte et al., 2016; Agour et al., 2020; Jawhari et al., 2021; Amrati et al., 2021). Carvacrol is a natural low-molecular weight product, this secondary metabolite derived from plants (*Thymus vulgaris* and *Origanum vulgare* described by Linnaeus). Carvacrol has been the subject of many investigations that place a higher priority on natural products with biological activities to control such diseases. This monoterpene has been shown to possess a wide range of biological effects, such as antibacterial, antifungal, insecticidal, antioxidant, antimutagenic, antigenotoxic, and antitumor (Aprotosoaie et al., 2019). Previous investigations demonstrated that carvacrol is one of the potent monoterpenes that can be used to control fungal species (Saghrouchni et al., 2021; Gonçalves et al., 2021).

Based on the previously discussed reasons, the main aim of the current paper was to evaluate the preventive and stimulatory effects of carvacrol on Fusarium wilt disease of ryegrass *in vitro* and under greenhouse conditions. For this purpose, an infestation of three fungal strains was carried out on ryegrass pre-treated with carvacrol, and several parameters were monitored including coleoptile development and rhizogenesis, incidence of lesions on coleoptiles, disease index, visual aspect of the health status, the weight of organic matter and the Fusarium load of the soil.

Material and methods

Chemicals

The agar medium used in this study was 3% malt extract agar (MEA) amended with 0.5% mycological peptone, and potato dextrose agar (PDA) (Biokar, France). The monoterpene carvacrol (99%) used in this study was obtained from Flagresso, Austria.

Fungal strains

Fusarium oxysporum, *F. solani*, and *F. nivale* strains used in the present study were isolated from diseased leaves, stems, and roots of ryegrass and from soil samples before being identified. For morphological characterisation, macroscopic traits such as the colony appearance, colour, pigmentation and growth rate were observed on potato dextrose agar (PDA) according to Leslie & Summerell (2006). Morphological identification was also performed based on the morphological characteristics observed at optical microscope as described by Booth (1971) and Leslie & Summerell (2006).

Fungal DNA extraction

The morphological identification was further confirmed by DNA sequencing. Single hyphal tip isolates were grown on cellophane overlain on PDA for 10 days. The mycelium was lyophilized and 10 mg of lyophilized mycelium, grinded with 5 mm iron beads. Then, fungal DNA was extracted using a DNeasy Plant Mini Kit (Qiagen, Hilden, Germany) according to the manufacturer's protocol (Fallahi et al., 2019). The quality and quantity of the DNA obtained were evaluated by measuring the concentration (ng/µL) in a NanoDrop ND-1000 spectrophotometer (Thermo Fisher Scientific). The quality of the DNA yielded by each method was determined by gel electrophoresis in a 1% agarose gel at 90 V for 15-20 min, stained with Ethidium bromide

Molecular identification

To confirm the identity of the fungus, ITS-5 (5`-GGAAGTAAAAGTCGTAACAAGG-3`-) and ITS-4 (5`-CCTCCGCTTATTGATATGC-3') were used to amplify complete internal transcribed spacer (ITS) as described by White et al. (1990). The ITS region was amplified in a 25 µL reaction using 25 ng DNA, 1 x Dream Taq buffer (1.5 mM $MgCl_2$), 0.3 µM pimer, 200 µM dNTP, 0.2 U Taq DNA Polymerase. The PCR conditions were as follows: 95°C for 1 min, 35 cycles of 95°C for 15 s, 55°C for 30 s, and 72°C for 90 s, and a final cycle at 72°C for 5 min. PCR products were electrophoresed on a 1% (w/v) agarose gel in 1x THE (20 mM Tris-HEPES, pH 8.06) at 90 V for 1 hour. The product was purified and then sequenced. The nitrogen base sequence was analyzed using an automated DNA sequencer. Sequencing data were trimmed and assembled using ChromasPro program version 1.5. The program Molecular Evolutionary Genetic Analysis software, ver. 5.0 (MEGA4.0; http://www.megasoftware.net) was performed in order to edit and align the sequence files, which were manually adjusted. In order to assess the relationships between the major taxa, ambiguous parts of the ITS regions were removed from further analysis and more conserved and alignable parts of the region and all genes were used to generate phylogenetic trees containing representative taxa from major groups. The assembled data were BLASTED with genomic data that has been registered in NCBI/National Center for Biotechnology Information (http://www.ncbi.nlm.nih.gov/BLAST/). The aligned sequences were BLAST in GenBank database, to identify all the strains. In this study, phylogenetic tree was generated using maximum parsimony (MP) in MEGA5.0 (Tamura et al., 2011). Bootstrap values for the maximum parsimony tree (MPT) were calculated for 1,000 replicates (Felsenstein, 1985). The edited ITS sequences were compared with other available Fusarium species sequences in the GenBank. Furthermore, the sequences of some known species were downloaded from GenBank and used to reconstruct a combined ITS region and phylogenetic trees.

Preparation of fungal inoculants

Sporulation was obtained by culturing the fungal strains in a MEA medium after 7 days of incubation at 28°C (Pujol et al., 1997). Afterwards, the spores were collected by flooding the plate with 1 mL water, including 0.05% Tween 20, using a sterile spread rod. Then, the number of spores was counted manually with a haemocytometer (Merck, Germany) with light microscopy (Optika, Italy) before being diluted to an inoculum of about 10^6 spores/mL (Noman et al., 2016).

Plant material

Ryegrass seeds of the English Ryegrass variety were kindly offered by the technical service of the Golf Royal Dar Es-salaam, Rabat, Morocco.

Culturing substrate

The substrate used for the cultivation of the ryegrass consists of 100% vegetable soil. Topsoil sieved through a 2-mm sieve was autoclaved twice at 121°C/0.1MPa for 30 minutes.

Evaluation *in vitro* of the growth-promoting and preventive effects of carvacrol on ryegrass

Thirty seeds were disinfected with 0.5% sodium hypochlorite solution for 20 min and then rinsed twice with sterile distilled water for 10 min and dried before being transferred to Petri plates containing sterile layers of filter paper (Kordali et al., 2007; Kordali et al., 2008). Afterward, each group received 1 mL of sterile water daily. After seeds germination, 1 mL of 99% carvacrol diluted in agar 0.2% (1:10) was dispensed into the plates. Afterwards, the infestation of the groups was carried out by adding 1 mL of spores' suspension (10^6 spores/mL) of the *F. oxysporum*, *F. solani*, and *F. nivale* and with a consortium (1:1:1) of all the spores' strains. The experiment was carried out for 4 weeks under ambient temperature (28 ± 2°C). The experimental protocol has been presented in the Table 1. Plant height (PH), root length (RL), percentage of second leaf appearance (SL) and percentage of second root appearance (SR) were measured weekly. Moreover, the lesions developed on the coleoptile were also noted and the incidence of the disease (I) was estimated by the following equation (Mironenko, 1960):

$$I(\%) = (n1 - n2)/n1 \quad x \quad 100$$

TABLE 1 Experimental protocol for the carvacrol treatment *in vitro*.

Groups distribution	
Negative control	30 uninfested and untreated seeds
Positive control	30 infested and untreated seeds
Group I	30 infested seeds + 1 mL of 0.05 mg/mL carvacrol
Group II	30 infested seeds + 1 mL of 0.10 mg/mL carvacrol
Group III	30 infested seeds + 1 mL of 0.20 mg/mL carvacrol

Where n1 and n2, respectively, represent the total number of seeds per Petri plate and the number of seeds with unaltered coleoptile of seedlings.

Evaluation of the preventive effect of carvacrol on ryegrass grown in soil under greenhouse conditions

One gram of ryegrass' seeds (approximately 200 seeds) was seeded into pots containing 150 g of topsoil. Each group received a constant volume of 15 mL (in order to wet the soil completely) of carvacrol (diluted in agar 0.2% (1:10)) twice a week. After that, infection was carried out with 15 mL of the spores' suspension (10^6 spores/mL) of *F. oxysporum*, *F. solani*, and *F. nivale* and with a mixture of all strain's spores. The experimental protocol has been presented in the Table 2. The evolution of the fungal charge of Fusarium was followed once a week using the serial dilution technique. One gram from each sample was transferred to test tube containing 9 mL of 0.9% NaCl. From this solution, a series of dilutions (10^{-2} to 10^{-6}) were made (El Barnossi et al., 2019). From each dilution 0.1 mL was spread on Petri plates containing MEA medium. The plates were incubated at 27°C for 4 days. Colonies of Fusarium species were then counted by the enumeration technique. Consequently, plates containing 15 to 150 colonies were selected for counting and the result was expressed in log (CFU/g) of three replicates (Ribeiro et al., 2020). As regards the virulence of each fungal strain, it was estimated after 7 weeks based on the disease index (DI) technique using the 0-4 scale established by Hernandez et al. (1998) which was based on visible symptoms on each seedling, where code 4: dead turf, code 3: 67 to 99% affected plant, code 2: 34 to 66% affected plant, code 1: 1 to 33% affected plant and code 0: no visible symptoms. The experiment was carried out under greenhouse conditions using both normal topsoil and disinfected topsoil.

Measurements of fresh and dry weights

To determine the fresh shoots and roots weight, the shoots and roots were carefully washed under running tap water. Prior to weight determination, excess moisture was blotted using paper towels, and the weight was determined. While for the dry weight determination, the samples were dried in an oven at 70°C for 72 h till constant weight was reached after the dry weight was determined (Huang et al., 2017).

TABLE 2 Distribution groups for the carvacrol treatment under greenhouse.

Distribution groups	
Negative control	200 uninfested and untreated seeds
Positive control	200 infested and untreated seeds
Group I	200 infested seeds + 15 mL of 0.05 mg/mL carvacrol
Group II	200 infested seeds + 15 mL of 0.10 mg/mL carvacrol
Group III	200 infested seeds + 15 mL of 0.20 mg/mL carvacrol

Statistical analysis

Quantitative results were expressed as means, of triplicate experiments ± SD (standard deviation). To determine statistical significance, Two way-ANOVA and Tukey's multiple range tests at $p< 0.05$ were performed using GraphPad Prism 8.0.1 (Graph Pad Software Inc., San Diego, USA).

Results

Molecular identification

Molecular identification was confirmed by sequencing the ITS. BLAST analysis using ITS sequences revealed a threshold of 100% similarity between the sequences from the isolates in this study and sequences from strains which were previously deposited in Genbank. The ITS sequences were deposited in GenBank as: *F. solani* (accession no. OP810954), *F. oxysporum* (accession no. OP824842), and *F. nivale* (accession no. OP810953).

All strains isolated from soils and ryegrass represented two different lineages (Figure 1). The isolates of *F. solani* and *F. oxysporum* were divided into subgroups. *F. nivale* was included in other branches. Phylogenetic tree demonstrated that all strains are closely related with a strong bootstrap support (100%). All isolates described as *F. solani, F. oxysporum* and *F. nivale*, based on morphological characteristics, were identified as *F. solani, F. oxysporum* and *F. nivale* through molecular analyses.

Evaluation *in vitro* of the growth-promoting and preventive effects of carvacrol on ryegrass

Table 3 shows the results of the effect of carvacrol treatment on the coleoptile growth and on rhizogenesis of ryegrass *in-vitro*. After infestation of the seedlings with fungal spores, Fusarium significantly reduced plant height and root length for all tested strains compared to the negative control, especially *F. nivale* which was the most virulent on ryegrass seedlings. In contrast, after treatment, plant height and root length recovered well with all tested concentration of carvacrol. As a consequence, the measurement values of the treated plants were almost equal to those of the negative control and sometimes better.

On the other hand, Table 3 shows also the results of the carvacrol effect on plant development. According to the result portrayed by the table plants in both the positive and negative control did not develop a second leaf. However, in the treated groups between 10 and 23.33% of the plants have developed a second leaf during the experiment time. In addition, as regards the carvacrol effect on the appearance of the second root, 10% of the plants in the negative control developed the second root. After infestation with *F. nivale*, the fungus inhibited the development of the second root, and consequently the percentage was decreased to 1.37%. Treatment with 0.05, 0.1, and 0.2 mg/mL carvacrol significantly allowed the emergence of the second root in all plants with a percentage reaching 20.33, 26.67 and 34% respectively.

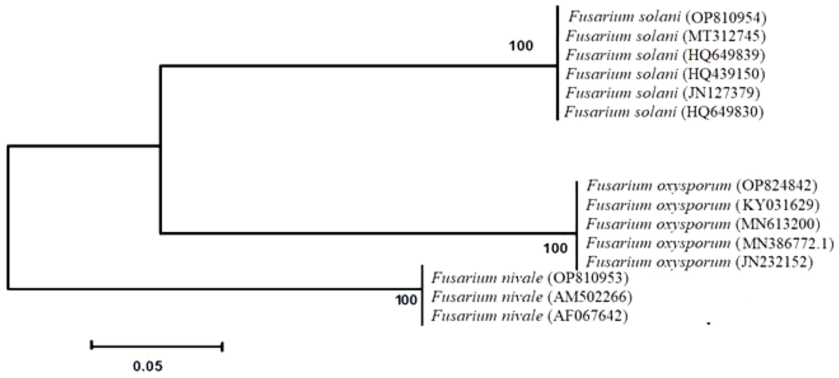

FIGURE 1
Phylogenetic analysis obtained by sequence analysis of *Fusarium* isolates 18S rDNA-ITS-region. Bootstrap tests were performed with 1,000 replications.

TABLE 3 The effect of carvacrol treatment on the coleoptile growth and on rhizogenesis of the ryegrass *in vitro*.

F. nivale	PH (cm)	RL (cm)	SL (%)	SR (%)
Negative control	7.77 ± 0.25^{a}	2.10 ± 0.10^{b}	0.00^{d}	10.00 ± 1.00^{b}
Positive control	1.70 ± 0.20^{a}	0.47 ± 0.05^{a}	1.70 ± 0.20^{a}	1.37 ± 0.47^{a}
0.05 mg/mL	5.70 ± 0.10^{b}	2.27 ± 0.15^{b}	3.33 ± 0.58^{b}	13.00 ± 10.00^{c}
0.1 mg/mL	6.33 ± 80.00^{b}	2.23 ± 0.15^{b}	16.67 ± 0.58^{c}	13.33 ± 0.58^{c}
0.2 mg/mL	5.33 ± 0.05^{b}	2.23 ± 0.05^{b}	3.30 ± 0.58^{b}	10.33 ± 0.58^{b}
F. oxysporum				
Negative control	7.77 ± 0.25^{c}	2.10 ± 0.10^{b}	0.00^{d}	10.00 ± 1.00^{b}
Positive control	2.60 ± 0.10^{a}	1.07 ± 0.05^{a}	2.90 ± 0.10^{a}	2.93 ± 0.11^{a}
0.05 mg/mL	6.60 ± 0.10^{b}	2.07 ± 0.05^{a}	10.33 ± 0.58^{c}	20.33 ± 0.58^{d}
0.1 mg/mL	8.13 ± 0.05^{c}	1.93 ± 0.05^{a}	10 ± 10.00^{c}	26.67 ± 0.58^{c}
0.2 mg/mL	6.60 ± 0.10^{b}	2.03 ± 0.05^{a}	23.33 ± 0.58^{b}	34.00 ± 10.00^{e}
F. solani				
Negative control	7.77 ± 0.25^{c}	2.10 ± 0.10^{b}	0.00^{a}	10.00 ± 1.00^{b}
Positive control	2.10 ± 0.10^{a}	0.50 ± 0.10^{a}	0.00^{a}	6.67 ± 0.58^{a}
0.05 mg/mL	7 ± 0.00^{c}	2.77 ± 0.05^{b}	17.33 ± 1.15^{d}	17.00 ± 1.00^{d}
0.1 mg/mL	7.67 ± 0.58^{c}	2.87 ± 0.05^{b}	21.00 ± 1.00^{c}	27.00 ± 1.00^{c}
0.2 mg/mL	5.07 ± 0.11^{b}	1.67 ± 0.58^{ab}	10.33 ± 0.58^{b}	23.67 ± 0.58^{e}
Spores' mixture				
Negative control	7.77 ± 0.25^{c}	2.10 ± 0.10^{b}	0.00^{d}	10.00 ± 1.00^{a}
Positive control	2.30 ± 0.10^{a}	1.03 ± 0.05^{a}	1.00 ± 0.00^{a}	11.00 ± 1.00^{a}
0.05 mg/mL	7.70 ± 0.27^{b}	2.13 ± 0.05^{a}	10.33 ± 0.58^{b}	10.00 ± 1.00^{a}
0.1 mg/mL	6.10 ± 3.47^{b}	2.13 ± 0.05^{a}	16.33 ± 3.78^{c}	14.67 ± 0.58^{b}
0.2 mg/mL	6.50 ± 0.50^{b}	1.43 ± 0.05^{a}	12.67 ± 0.58^{b}	14.67 ± 0.58^{b}

PH, plant height; RL, root length; SL, second leaf and SR, second root. Mean values (± SD, n = 3) followed by different letters in same row are significantly different (Tow-way ANOVA; Tukey's test, $p \leq 0.05$). Two results read from the same column and marked with the same letter do not differ significantly at a threshold $\alpha = 5\%$.

10.3389/fpls.2023.973207

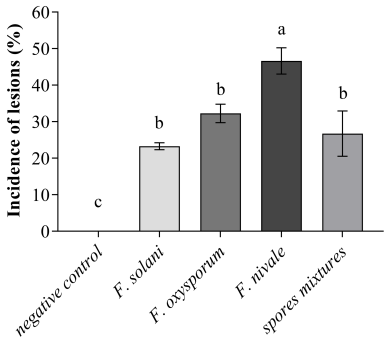

FIGURE 2
Incidence of lesions on coleoptiles of ryegrass seedlings. Means (± SD, n = 3) denoted by the same letter indicate no significant difference according to Tukey's multiple range tests at p< 0.05.

Regarding the incidence of lesions on coleoptiles of ryegrass seedlings, the Figure 2 shows that the incidence was high with *F. nivale* with a percentage of 50%. *Fusarium solani*, *F. oxysporum* and the spores mixtures did not induce severe lesions on coleoptiles, where the incidence percentage ranged between 23 an 33%.

According to the results, carvacrol showed protective effect on ryegrass against Fusarium wilt disease. Furthermore, carvacrol showed growth-promoting effect on both the leaves and the rhizogenesis.

Evaluation of the preventive effect of carvacrol on ryegrass grown in soil under greenhouse conditions

To evaluate the preventive effect of carvacrol and the virulence of the Fusarium species, the disease index (DI) was used. This index is an

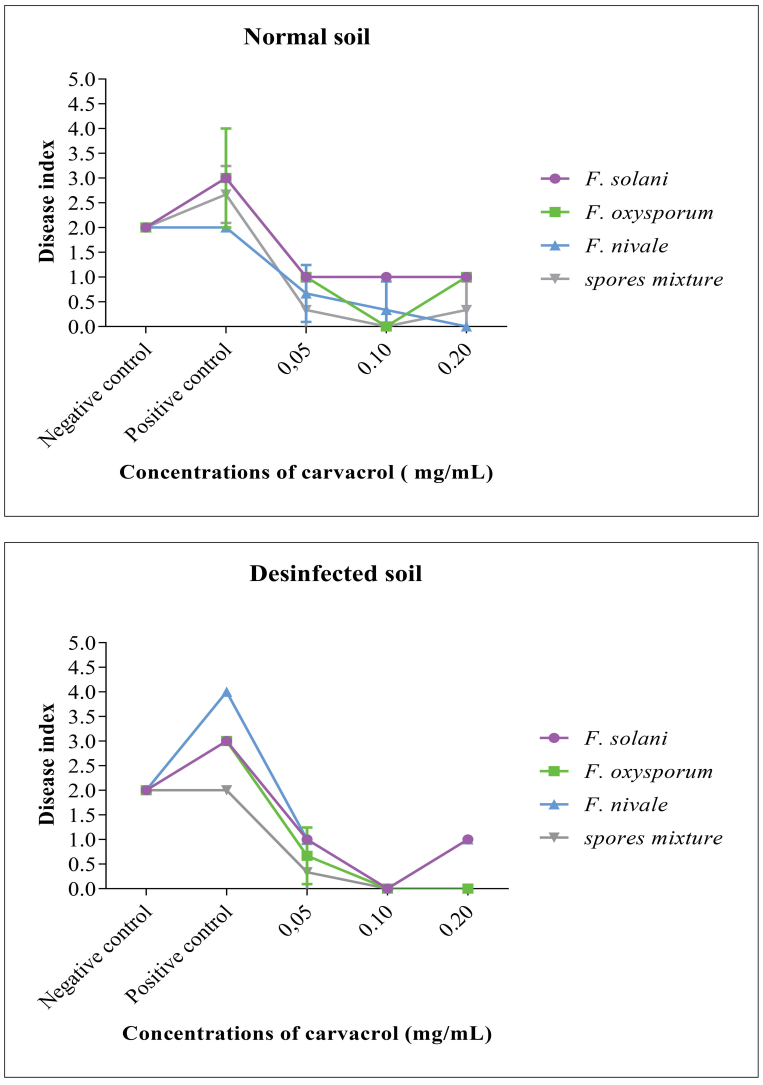

FIGURE 3
The disease index and the evolution of the average symptom severity on infested ryegrass after 7 weeks of preventive treatment with carvacrol. The results differ significantly at a threshold α = 5% (Two-way ANOVA, Turkey test). Error bars show standard deviations.

indication of the health status of the plant, the more it tends towards 4 the more affected the plant is. The results presented in Figure 3 demonstrate that before infestation, the DI was equal to 2, whereas, after the infestation the DI was increased to 3 and 4. In contrast, after the treatment with carvacrol, the DI decreased to 1 and 0. In the disinfected soil, *F. nivale* - with a DI tending towards 4 - was found to be the most virulent, however in the normal soil this virulence was reduced which was reflected by the elevation of DI to 2 as the negative control. The aggresivity of *F. nivale* is manifested by the total death of almost all plants of the infested and untreated lot in the disinfected soil (Figure 4). Regarding the most effective concentrations of carvacrol, 0.1 and 0.2 mg/mL were shown to have a better protective effect with a DI ranging between 1 and 0 against all tested strains and in both normal and disinfected soil.

Figures 5, 6 show the appearance of the health status of all pots in the greenhouse in disinfected and normal soil. The pictures show that the plants in the infested and treated lots with carvacrol were healthier than those in the infested and untreated lots.

The fungal load of Fusarium was measured during the whole period of ryegrass cultivation. Figures 7, 8 show the results of the follow-up of this load in both disinfected and normal soil. According to the figures, after the infestation, the Fusarium load was much higher in the disinfected soil than in the normal soil compared with negative control. In the normal soil, after treatment, the load of *F. solani* became null from the third week of treatment with 0.2 mg/mL and at the end of the fourth week the load was nulled with 0.1 mg/mL of carvacrol. In the disinfected soil, *F. solani* was eliminated with 0.2 mg/mL of carvacrol from the second week. Furthermore, with this concentration, the fungal load of all the spores' mixture was well eliminated after three weeks in both soil types. We noticed also that the disinfected soil remained without any apparition of fungal charge until the last week, we found a little of Fusarium charge (Figure 8).

FIGURE 4
Visual appearance of the health status of ryegrass in disinfected soil. **(A)**: dead plants due to fusarium wilt disease induced by **(*F*)** *nivale* and **(B)**: negative control.

Measurements of fresh and dry weights

Figures 9, 10 show the results of the quantitative evaluation of the vegetative growth variables such as fresh and dry weight of ryegrass shoots and roots after 4 weeks of treatment with carvacrol in normal and disinfected soil under greenhouse. In Figure 9, where we used normal soil, after infestation with Fusarium spores, the amount of organic matter has reduced significantly for all the groups and also for all growth parameters. After treatment, the amount of organic matter recovered and sometimes even increased especially with 0.1 and 0.2 mg/mL of carvacrol, compared to the negative control. On the other hand, in disinfected soil (Figure 10), *F. nivale* showed more damage on ryegrass. As a result, the amount of organic matter decreased from 7.4 to 4.9 g, from 2.17 to 0.26 g and from 1.87 to 0.17 g for the fresh shoots weight, dry shoots weight and dry root weight respectively.

Discussion

From the results obtained, we found that all three strains tested negatively influenced the development and growth of coleoptiles and seedling roots. Furthermore, the incidence of lesions on coleoptiles was very high for *F. nivale*. After *in vitro* treatment with carvacrol, the height of the seedlings was restored and also the length of the roots. During the treatment we noticed that the carvacrol treated seedlings fared better than the negative control plants due to the effect of carvacrol on the development of new leaf buds and also on the emergence of secondary roots.

The results obtained were in agreement with what Boudoudou et al. (2009) reported, infestation with *F. graminearum*, *F. nivale, F. solani* and *F. semitectum* influenced coleoptile and root development of seedlings of five rice varieties. The length of coleoptiles decreased from 4.0-6.1 to 2.6-5.3 cm. The number of roots decreases from 6.0-8.4 to 4.0-7.5 and the length of roots decreases from 5.5-7.0 to 3.2-6.9 cm. This decrease was high with *F. graminearum* and *F. nivale* in contrast to *F. solani*. In the same study, the researchers evaluated the lesion incidence on coleoptiles, therefore *F. solani* did not induce lesions on coleoptiles as opposed to the other three species. The incidence was high with *F. semitectum* for two rice varieties (28.5 and 25.1%) and with *F. nivale* for one variety (29.9%). All varieties were affected by *F. graminearum* (6.5 to 21.46%). The fact that Fusarium penetrates through the roots of the plant and damages the whole plant through the vessels of the plant, is why it is called vascular disease (Shaban et al., 2018). Therefore, we thought to apply a systematic (in soil) preventive treatment in order to avoid the penetration of Fusarium into the roots and thus the establishment of the disease.

The results obtained on the disease index showed that infected plants treated with 0.1 and 0.2 mg/mL carvacrol were well protected. It should also be noted that the isolates expressed more virulence in the disinfected soil than in the normal soil. This would be in favour of a competition between the *Fusarium* and the soil flora which would exert an inhibition on Fusarium. And this was reflected by the visual appearance of the ryegrass seedlings.

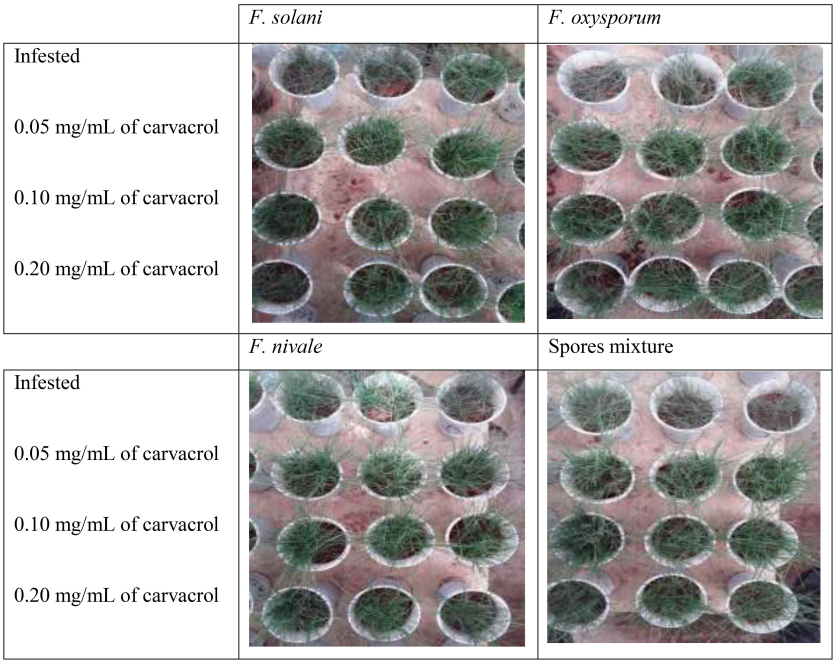

FIGURE 5
The visual appearance of the health status of ryegrass in normal soil after 4 weeks of preventive treatment with carvacrol under greenhouse conditions.

The improvement of the disease index following the carvacrol treatment can be explained by the results obtained on the *Fusarium* load of the soil. Indeed, the fungal load of the soil was decreased in the function of the dose and time. These results are in accordance with other study findings, the treatment of disinfected soil with carvacrol resulted in a reduction in dose-dependence of *F. oxysporum* load. 0.8 mg/mL of carvacrol was capable of reducing the load to 0 after 3 weeks. In normal soil, the total disinfection has taken 4 weeks of treatment with the same concentration (Saghrouchni et al., 2020). In another study undertaken on soil disinfection using thymol, another major compound of *T. vulgaris* and *O. vulgare*. the treated lot with 0.5 mg/mL of thymol has shown a decrease after 21 days from 5.26 Log10 to 3.56 Log10. For the treated lot with 2 mg/mL of thymol, a total disappearance of *F. oxysporum* occurred after 14 days (Oukhouia et al., 2017).

After providing an idea of the visual and qualitative aspects of ryegrass, we assessed vegetative growth variables such as fresh and dry

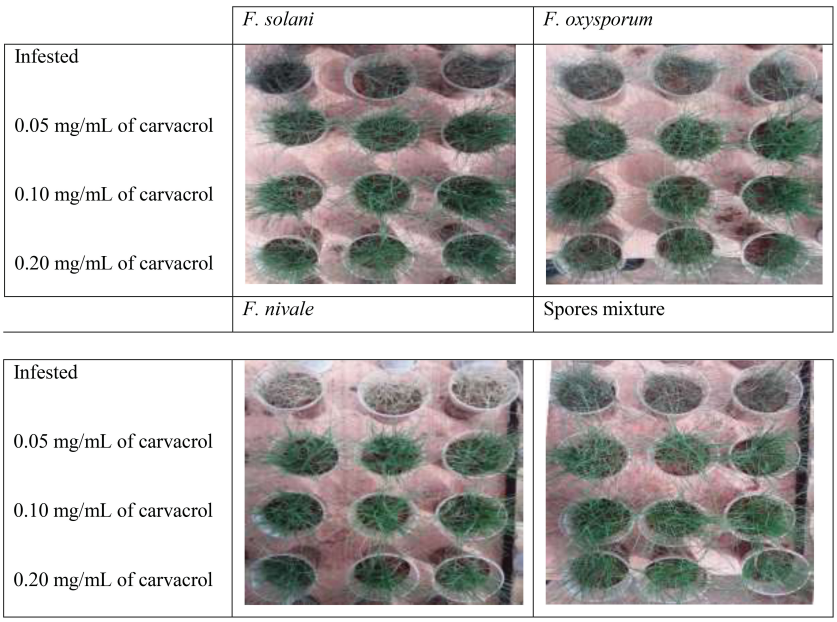

FIGURE 6
The visual appearance of the health status of ryegrass in disinfected soil after 4 weeks of preventive treatment with carvacrol under greenhouse conditions.

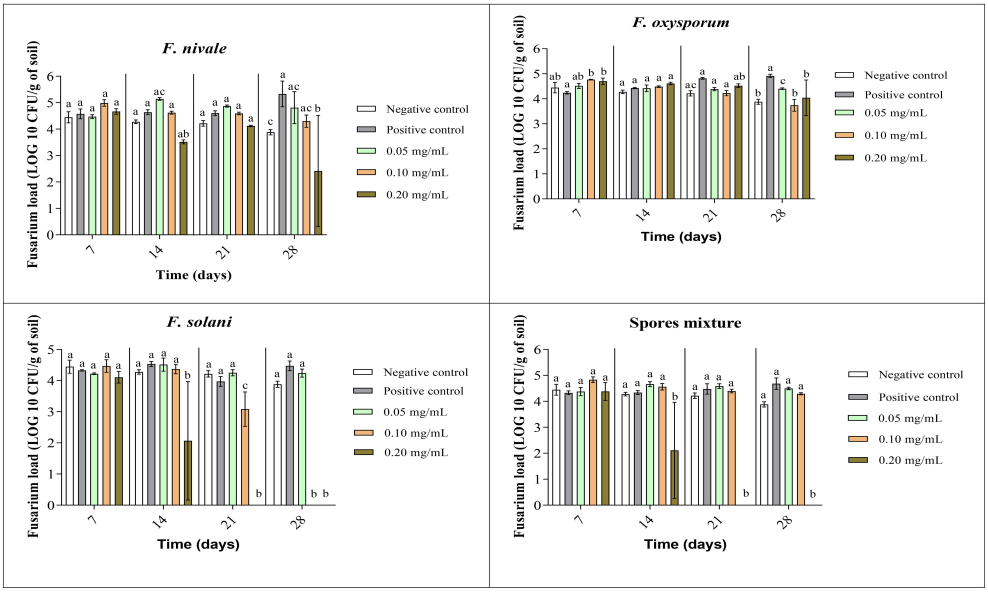

FIGURE 7
Fusarium load during treatment of ryegrass pots with carvacrol for four weeks in normal soil under greenhouse. Means (± SD, n = 3) denoted by the same letter indicate no significant difference according to Tukey's multiple range tests at p< 0.05.

shoots and root weights of the ryegrass. The results of the quantitative evaluation of the vegetative growth variables showed that the amount of organic matter was recovered after being decreased after infestation and sometimes even increased compared to negative control especially with 0.1 and 0.2 mg/mL of carvacrol. These findings evidently showed that carvacrol is an effective plant growth promoter. Therefore, this monoterpene can be used as biostimulator for plant development. Nowadays, there is increasing interest in the use of naturally occurring 'biostimulators' for enhancing the growth of agricultural and horticultural crops (Kurepin et al., 2014). The activity of biostimulators to promote plant growth is often attributed to their ability to directly or indirectly provide mineral nutrients (mostly N, but also P, S and other macro- and micro-nutrients) to plants. Although optimal growth of plants depends on the availability of adequate mineral nutrients, that growth (and also development, including reproduction) is also regulated by plant hormones (phytohormones), including gibberellins, auxins, cytokinins, abscisic acid, ethylene and other phytohormones (Bassanezi et al., 2021; Wu et al., 2021; Liu et al., 2022). For example, auxin is involved in the stimulation of cell elongation in

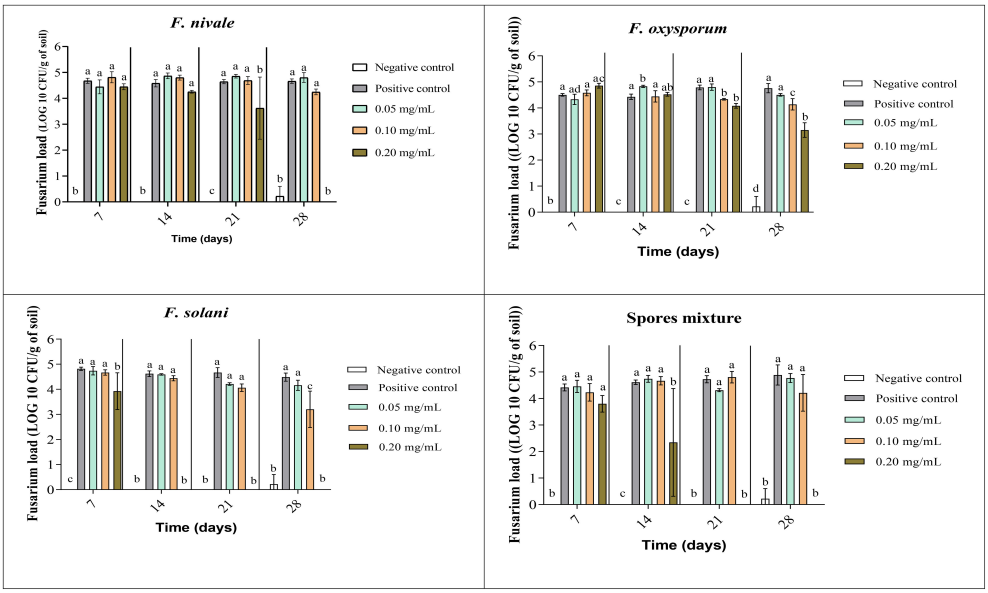

FIGURE 8
Fusarium load during treatment of ryegrass pots with carvacrol for four weeks in disinfested soil under greenhouse. Means (± SD, n = 3) denoted by the same letter indicate no significant difference according to Tukey's multiple range tests at p< 0.05.

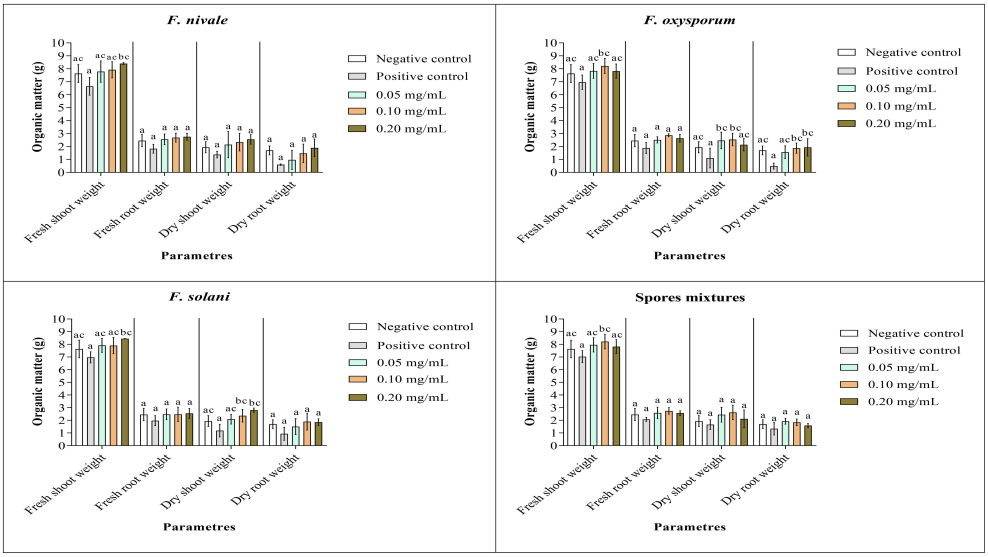

FIGURE 9
Organic matter of ryegrass after four weeks of treatment with carvacrol in normal soil under greenhouse. Means (± SD, n = 3) denoted by the same letter indicate no significant difference according to Tukey's multiple range tests at $p < 0.05$.

shoots and root initiation. Gibberellins, can also increase stem elongation. Cytokinins, which are usually found in high concentrations in meristematic regions and other areas of active growth, such as actively expanding portions of roots and stem, young leaves, developing fruits and seeds, are involved in the stimulation of cell division, shoot growth, root development, leaf expansion and the inhibition or slowing of leaf or organ senescence.

Carvacrol and other plant products can be useful in crop production due to their antimicrobial and growth-promoting potential. On the other hand, in livestock production, the use of medicinal plants is gaining more recognition as a result of numerous efforts (Oluwafemi et al., 2020). The worldwide interest on botanical products has grown significantly as described by (Oluwafemi et al., 2020), cattle, goat, sheep, horses and pigs represents about 70% of the animals treated with herbal remedies followed by poultry (9.1%), dogs (5.3%) and rabbits (4.3%). Medicinal plants are mostly used especially by rural and small-scale farmers because they are inexpensive, readily available and effective. Recently, researchers have suggested the use plant extracts and essential oils as alternative growth promoters in poultry feed because they have antimicrobial, anti-parasitic, antioxidant and anti-helminthic properties due to the presence of phytochemical or bioactive chemicals in plants (Oluwafemi et al., 2020).

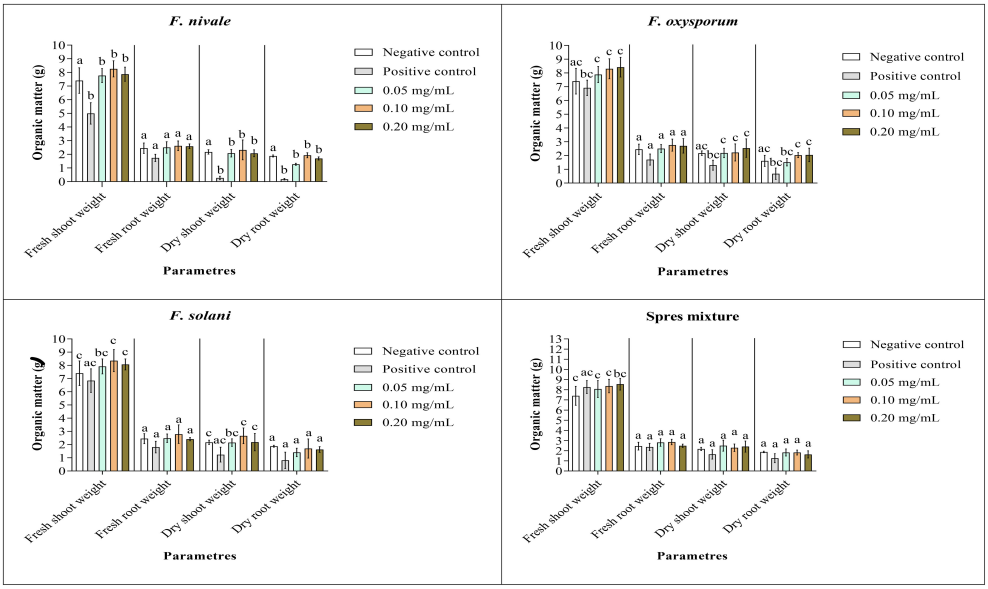

FIGURE 10
Organic matter of ryegrass after four weeks of treatment with carvacrol in disinfected soil under greenhouse. Means (± SD, n = 3) denoted by the same letter indicate no significant difference according to Tukey's multiple range tests at $p < 0.05$.

Fusarium appears to be phytopathogenic, It alters the early stages of development of the ryegrass seedlings tested (Saghrouchni et al., 2021). This genus is capable of invading other host plants with intense virulence, including other grasses and cereals. Treating seedlings with carvacrol has effectively protected them against Fusarium wilt disease. In addition to the anti-Fusarium action, carvacrol is thought to exert a growth-promoting effect on the seedlings. When left untreated, the fungus contained in the seeds becomes fully established. Thus, damaged seeds may harbour masses of conidia, when the seeds were able to germinate, diseased seedlings emerge (Saghrouchni et al., 2021). To control Fusarium, seeds treatment has been recommended (Mironenko, 1960). The alterations observed in seedlings from inoculated seeds show that these species can be troublesome in the early stages of seedling development. Therefore, it is important to monitor their development especially when using susceptible varieties.

Conclusion

Carvacrol and other plant products may be utilized in controlling diseases like Fusarium wilt, as well as improving plant yield. Further, to understand how carvacrol act as a growth-promotor and biostimulator for enhancing coleoptile growth and rhizogenesis, future studies are recommended. Carvacrol may interact with phytohormones such as auxins, cytokinins, gibberellins, etc. It remains a molecule of plant origin!

Data availability statement

The raw data supporting the conclusions of this article will be made available by the authors, without undue reservation.

Author contributions

HS, Writing—original draft preparation; HS, IL, and TA, formal analysis; HS, MB, AB, IM, AA, AH, IV, and HN, writing—review and editing. All authors contributed to the article and approved the submitted version.

Acknowledgments

The authors extend their appreciation to the Researchers supporting Project number (RSP-2023/98) King Saud University, Riyadh, Saudi Arabia for financial support. The authors also gratefully thank Biological Control Research Institute Adana, Turkey for their kind collaboration during the conduction of the study.

Conflict of interest

The authors declare that the research was conducted in the absence of any commercial or financial relationships that could be construed as a potential conflict of interest.

Publisher's note

References

Agour, A., Mssillou, I., Saghrouchni, H., Bari, A., Lyoussi, B., and Derwich, E. (2020). Chemical composition, antioxidant potential and antimicrobial properties of the essential oils of haplophyllum tuberculatum (Forsskal) a. juss from Morocco. *Trop. J. Natural Product Res. Available* 4 (12), 1108–1115. doi: 10.26538/tjnpr/v4i12.13

Agrios, N. G. (2005). *Plant pathology (5th ed.)* (Academic Press, Elsevier: USA).

Amrati, F. E.-Z., Bourhia, M., Saghrouchni, H., Slighoua, M., Grafov, A., Ullah, R., et al. (2021). *Caralluma europaea* (Guss.) N.E.Br.: Anti Inflammatory, Antifungal, and Antibacterial Activities against Nosocomial Antibiotic-Resistant Microbes of Chemically Characterized Fractions. *Molecules* (26), 636. doi: 10.3390/molecules26030636

Aprotosoaie, A. C., Vlad, S., Adriana, T., and Anca, M. (2019). "Antigenotoxic potential of some dietary non-phenolic phytochemicals," in *Studies in natural products chemistry* (Elsevier: USA), 223–297.

Bassanezi, R. B., Primiano, I. V., and Vescove, H. V. (2021). Effect of enhanced nutritional programs and exogenous auxin spraying on huanglongbing severity , fruit drop , yield and economic profitability of orange orchards. *Crop Prot.* 145, 105609. doi: 10.1016/j.cropro.2021.105609

Blanco-canqui, H. (2010). Energy crops and their implications on soil and environment. *Agron. J.* 102 (2), 403–419. doi: 10.2134/agronj2009.0333

Bodah, T. E. (2017). Root rot diseases in plants: A review of common causal agents and management strategies. *Agric. Res. Technol.* 5 (3), 1–9. doi: 10.19080/artoaj.2017.05.555661

Booth, C. (1971). *The genus fusarium* (Kew, Surray: Commonwealth Mycological Institute).

Boudoudou, H., Hassikou, R., Ouazzani Touhami, A., Badoc, A., and Douira, A. (2009). First demonstrations of fusariose on rice germination and plantlets. *Bull. Soc Pharm. Bordeaux* 148, 45–54.

Boutaj, H., Meddich, A., Roche, J., Mouzeyar, S., and El, C. (2022). The effects of *mycorrhizal fungi* on vascular wilt diseases. *Crop Prot.* 155, 105938. doi: 10.1016/j.cropro.2022.105938

Chaves, M. A., Reginatto, P., Souza, B., and Itiki, R. (2022). Fungicide resistance in *fusarium graminearum* species complex. *Curr. Microbiol.* 79 (2), 1–9. doi: 10.1007/s00284-021-02759-4

Davis, S. C., Parton, W. J., Dohleman, F. G., Candice, M., Grosso, S., Del, Kent, A. D., et al. (2010). Comparative biogeochemical cycles of bioenergy crops reveal nitrogen-fixation and low greenhouse gas emissions in a miscanthus 3 giganteus. *Ecosystems* 13, 144–156. doi: 10.1007/s10021-009-9306-9

Dorugade, S., Sardesai, V., and Kamble, S. (2021). Survival ability of benoyl resistant isolate of fusarium solani causing dry rot of elephant foot yam. *Bioinfolet* 18, 197–198.

El Barnossi, A., Saghrouchni, H., Moussaid, F., Chahmi, N., and Housseini, A. I. (2019). Microbiological study of effects of solid organic waste (chicken droppings and sheep manure) decomposed in the soil used for pisum sativum cultivation. *Int. J. Environ. Stud.* 77 (5), 830–842. doi: 10.1080/00207233.2019.1704116

Escrivá, L., Font, G., and Manyes, L. (2015). *In vivo* toxicity studies of fusarium mycotoxins in the last decade : A review. *Food Chem. Toxicol.* 78, 185–206. doi: 10.1016/j.fct.2015.02.005

Fallahi, M., Saremi, H., Javan-Nikkhah, M., Somma, S., Haidukowski, M., Logrieco, A. F., et al. (2019). Isolation, molecular identification and mycotoxin profile of fusarium species isolated from maize kernels in Iran. *Toxins* 11 (5), 297. doi: 10.3390/toxins11050297

Felsenstein, J. (1985). Confidence limits on phylogenies: an approach using the bootstrap. *Evolution* 39, 783–791.

Gallo, A., Ghilardelli, F., Doupovec, B., Faas, J., Schatzmayr, D., and Masoero, F. (2021). Kinetics of gas production in the presence of *fusarium mycotoxins* in rumen fluid of lactating dairy cows kinetics of gas production in the presence of fusarium mycotoxins in rumen fluid of lactating dairy cows. *JDS Commun.* 2, 243–247. doi: 10.3168/jdsc.2021-0100

Gonçalves, D. C., Tebaldi de Queiroz, V., Costa, A. V., Lima, W. P., Belan, L. L., Moraes, W. B., et al. (2021). Reduction of fusarium wilt symptoms in tomato seedlings following seed treatment with origanum vulgare l. essential oil and carvacrol. *Crop Prot.* 141 (3), 105487. doi: 10.1016/j.cropro.2020.105487

Gordon, T. R. (2017). *Fusarium oxysporum* and the fusarium wilt syndrome. *Annu. Rev. Phytopathol.* 55, 23–39. doi: 10.1146/annurev-phyto-080615-095919

Heaton, E. A., Dohleman, F. G., Miguez, A. F., Juvik, J. A., Lozovaya, V., Widholm, J., et al. (2010). "Miscanthus : A promising biomass crop," in *A role for biomass crops*, vol. Vol. 56. , 76–136). Advances in Botanical Research. St. Louis, MO, USA. doi: 10.1016/B978-0-12-381518-7.00003-0

Hernandez, M. E. S., D´avila, A. R., Algaba, A. P., de L´opez, M. A. B., and Casas, A. T. (1998). Occurrence and etiology of death of young olive trees in southern Spain. *Eur. J. Plant Pathol.* 104, 347–357.

Huang, P., de-Bashan, L., Crocker, T., Kloepper, J. W., and Bashan, Y. (2017). Evidence that fresh weight measurement is imprecise for reporting the effect of plant growth-promoting (rhizo)bacteria on growth promotion of crop plants. *Biol. Fertility Soils* 53 (2), 199–208. doi: 10.1007/s00374-016-1160-2

Jawhari, F. Z., Moussaoui, A. E. L., Bourhia, M., Imtara, H., Saghrouchni, H., Ammor, K., et al. (2021). *Anacyclus pyrethrum var. pyrethrum* (l.) and *anacyclus pyrethrum var. depressus* (ball) maire: Correlation between total phenolic and flavonoid contents with antioxidant and antimicrobial activities of chemically characterized extracts. *Plants* 10 (149). doi: 10.3390/plants10010149

Juraschek, L. M., Kappenberg, A., and Amelung, W. (2022). Mycotoxins in soil and environment. *Sci. Total Environ.* 814, 152425. doi: 10.1016/j.scitotenv.2021.152425

Karki, K., Grant, J., Luiz, A., Ribeiro, B., Petkar, A., Hajihassani, A., et al. (2022). Evaluation of pic-clor 60 [choloropicrin pre-mixed with 1 , 3 dicholoropropene] and soil-applied fungicides for the fusarium wilt management in watermelon. *Crop Prot.* 154, 105894. doi: 10.1016/j.cropro.2021.105894

Kordali, S., Cakir, A., Ozer, H., Cakmakci, R., Kesdek, M., and Mete, E. (2008). Antifungal, phytotoxic and insecticidal properties of essential oil isolated from Turkish origanum acutidens and its three components, carvacrol, thymol and p-cymene. *Bioresource Technol.* 99 (18), 8788–8795. doi: 10.1016/j.biortech.2008.04.048

Kordali, S., Cakir, A., and Sutay, S. (2007). Inhibitory effects of monoterpenes on seed germination and seedling growth. *Z. Fur Naturforschung - Section C J. Biosci.* 62 (3–4), 207–214. doi: 10.1515/znc-2007-3-409

Kurepin, L. V., Zaman, O., and Pharis, R. P. (2014). Phytohormonal basis for the plant growth promoting action of naturally occurring biostimulators. *Soc. Chem. Industry* 94, 1715–1722. doi: 10.1002/jsfa.6545

Lecomte, C., Alabouvette, C., Edel-hermann, V., Robert, F., and Steinberg, C. (2016). Biological control of ornamental plant diseases caused by fusarium oxysporum : A review. *Biol. Control* 101, 17–30. doi: 10.1016/j.biocontrol.2016.06.004

Leslie, J., and Summerell, B. (2006). *The fusarium laboratory manual* (Oxford: Wiley-Blackwell).

Liu, S., Adibi, M., Huijser, P., Smith, R. S., Tsiantis, M., Adibi, M., et al. (2022). Cytokinin promotes growth cessation in the arabidopsis root. *Curr. Biol.* 32, 1–12. doi: 10.1016/j.cub.2022.03.019

Mironenko, P. V. (1960). Fusarium wilt of rice in the caspian area. *Trud. Vses. Inst. Zashch. Rast.* 14, 123–128.

Nehls, U., Gohringer, F., Wittulsky, S., and Dietz, S. (2010). Fungal carbohydrate support in the ectomycorrhizal symbiosis : a review. *Plant Biol.* 12, 292–301. doi: 10.1111/j.1438-8677.2009.00312.x

Noman, E. A., Rahman, N. N. N. A., Shahadat, M., Nagao, H., Al-Karkhi, A. F. M., Al-Gheethi, A., et al. (2016). Supercritical fluid CO2 technique for destruction of pathogenic fungal spores in solid clinical wastes. *Clean - Soil Air Water* 44 (12), 1700–1708. doi: 10.1002/clen.201500538

Oluwafemi, R. A., Olawale, A. I., and Alagbe, J. O. (2020). Recent trends in the utilization of medicinal plants as growth promoters in poultry nutrition – a review. *J. Anim. Physiol. Anim. Nutr.* 104 (1), 5–11.

Oukhouia, M., Hamdani, H., Remmal, A., Sennouni, C., and Jabeur, I. (2017). In-vitro study of anti-fusarium effect of thymol, carvacrol, eugenol and menthol. *J. Plant Pathol. Microbiol.* 8 (423), 1–7. doi: 10.4172/2157-7471.1000423

Pujol, I., Guarro, J., Sala, J., and Riba, M. D. (1997). Effects of incubation temperature, inoculum size, and time of reading on broth microdilution susceptibility test results for amphotericin b against fusarium. *Antimicrobial Agents Chemotherapy* 41 (4), 808–811. doi: 10.1128/aac.41.4.808

Ribeiro, M. S. S., Freitas-Silva, O., Castro, I. M., Teixeira, A., Marques-da-Silva, S. H., Sales-Moraes, A. C. S., et al. (2020). Efficacy of sodium hypochlorite and peracetic acid against aspergillus nomius in Brazil nuts. *Food Microbiol.* 90, 103449. doi: 10.1016/j.fm.2020.103449

Saghrouchni, H., El Barnossi, A., Chefchaou, H., Mzabi, A., Tanghort, M., Remmal, A., et al. (2020). Study the effect of carvacrol, eugenol and thymol on fusariums sp responsible for lolium perenne fusariosis. *EM Int.* 26 (3), 2020–1059.

Saghrouchni, H., El Barnossi, A., Salamatullah, A. M., Bourhia, M., Alzahrani, A., Alkaltham, M. S., et al. (2021). Carvacrol : A promising environmentally friendly agent to fight seeds damping-off diseases induced by fungal species. *Agronomy* 11, 985. doi: 10.3390/agronomy11050985

Sampoux, J. P., Baudouin, P., Bayle, B., Béguier, V., Bourdon, P., Chosson, J. F., et al. (2011). Breeding perennial grasses for forage usage: An experimental assessment of trait changes in diploid perennial ryegrass (*Lolium perenne* l.) cultivars released in the last four decades. *Field Crops Res.* 123, 117–129. doi: 10.1016/j.fcr.2011.05.007

Servin, A., Elmer, W., Mukherjee, A., de la Torre-Roche, R., Hamdi, H., White, J. C., et al. (2015). A review of the use of engineered nanomaterials to suppress plant disease and enhance crop yield. *J. Nanoparticle Res.* 17, 1–21. doi: 10.1007/s11051-015-2907-7

Shaban, M., Miao, Y., Ullah, A., Khan, A. Q., Menghwar, H., Khan, A. H., et al. (2018). Physiological and molecular mechanism of defense in cotton against verticillium dahliae. *Plant Physiol. Biochem.* 125, 193–204. doi: 10.1016/j.plaphy.2018.02.011

Tamura, K., Peterson, D., Peterson, N., Stecher, G., Nei, M., and Kumar, S. (2011). MEGA5: Molecular evolutionary genetics analysis using maximum likelihood, evolutionary distance, and maximum parsimony methods. *Mol. Biol. Evol.* 28 (10), 2731–2739. doi: 10.1093/molbev/msr121

White, T. J., Bruns, T., Lee, S., and Taylor, J. W. (1990). "Amplification and direct sequencing of fungal ribosomal RNA genes for phylogenetics," in *PCR proto- cols: A guide to methods and applications*, vol. 64 . Eds. M. Innis, D. Gelfand, J. Sninsky and T. White (New York: Academic Press, Inc.), 315–322.

Wiering, N. P., Sheaffer, C. C., Ehlke, N. J., Catalano, D., and Martinson, K. (2021). Forage potential of winter-hardy perennial ryegrass populations in monoculture and binary alfalfa mixture. *Agron. J.* 113, 5183–5195. doi: 10.1002/agj2.20837

Wilkins, P. W., and Humphreys, M. O. (2003). Progress in breeding perennial forage grasses for temperate agriculture. *J. Agric. Sci.* 140, 129–150. doi: 10.1017/S0021859603003058

Wu, K., Xu, H., Gao, X., and Fu, X. (2021). New insights into gibberellin signaling in regulating plant growth – metabolic coordination. *Curr. Opin. Plant Biol.* 63, 102074. doi: 10.1016/j.pbi.2021.102074

frontiers | Frontiers in Plant Science

TYPE Original Research
PUBLISHED 23 August 2023
DOI 10.3389/fpls.2023.1190358

OPEN ACCESS

EDITED BY
Francis Chuks Ogbonnaya,
Grains Research and Development Corporation, Australia

REVIEWED BY
Bhoja Raj Basnet,
International Maize and Wheat Improvement Center, Mexico
Francesca Desiderio,
Council for Agricultural and Economics Research, Italy

*CORRESPONDENCE
Kassa Semagn
fentaye@ualberta.ca
Dean Spaner
dean.spaner@ualberta.ca

†Deceased

RECEIVED 20 March 2023
ACCEPTED 18 July 2023
PUBLISHED 23 August 2023

CITATION
Semagn K, Henriquez MA, Iqbal M, Brûlé-Babel AL, Strenzke K, Ciechanowska I, Navabi A, N'Diaye A, Pozniak C and Spaner D (2023) Identification of Fusarium head blight sources of resistance and associated QTLs in historical and modern Canadian spring wheat. *Front. Plant Sci.* 14:1190358. doi: 10.3389/fpls.2023.1190358

Identification of Fusarium head blight sources of resistance and associated QTLs in historical and modern Canadian spring wheat

Kassa Semagn[1*], Maria Antonia Henriquez[2], Muhammad Iqbal[1], Anita L. Brûlé-Babel[3], Klaus Strenzke[1], Izabela Ciechanowska[1], Alireza Navabi[4†], Amidou N'Diaye[5], Curtis Pozniak[5] and Dean Spaner[1*]

[1]Department of Agricultural, Food, and Nutritional Science, 4-10 Agriculture-Forestry Centre, University of Alberta, Edmonton, AB, Canada, [2]Morden Research and Development Centre, Agriculture and Agri-Food Canada, Morden, MB, Canada, [3]Department of Plant Science, University of Manitoba, Winnipeg, MB, Canada, [4]Department of Plant Agriculture, Crop Science Building, University of Guelph, Guelph, ON, Canada, [5]Crop Development Centre and Department of Plant Sciences, University of Saskatchewan, Saskatoon, SK, Canada

Fusarium head blight (FHB) is one the most globally destructive fungal diseases in wheat and other small grains, causing a reduction in grain yield by 10–70%. The present study was conducted in a panel of historical and modern Canadian spring wheat (*Triticum aestivum* L.) varieties and lines to identify new sources of FHB resistance and map associated quantitative trait loci (QTLs). We evaluated 249 varieties and lines for reaction to disease incidence, severity, and visual rating index (VRI) in seven environments by artificially spraying a mixture of four *Fusarium graminearum* isolates. A subset of 198 them were genotyped with the Wheat 90K iSelect single nucleotide polymorphisms (SNPs) array. Genome-wide association mapping performed on the overall best linear unbiased estimators (BLUE) computed from all seven environments and the International Wheat Genome Sequencing Consortium (IWGSC) RefSeq v2.0 physical map of 26,449 polymorphic SNPs out of the 90K identified sixteen FHB resistance QTLs that individually accounted for 5.7–10.2% of the phenotypic variance. The positions of two of the FHB resistance QTLs overlapped with plant height and flowering time QTLs. Four of the QTLs (*QFhb.dms-3B.1*, *QFhb.dms-5A.5*, *QFhb.dms-5A.7*, and *QFhb.dms-6A.4*) were simultaneously associated with disease incidence, severity, and VRI, which accounted for 27.0–33.2% of the total phenotypic variance in the combined environments. Three of the QTLs (*QFhb.dms-2A.2*, *QFhb.dms-2D.2*, and *QFhb.dms-5B.8*) were associated with both incidence and VRI and accounted for 20.5–22.1% of the total phenotypic variance. In comparison with the VRI of the checks, we identified four highly resistant and thirty-three moderately resistant lines and varieties. The new FHB sources of resistance and the physical map of the associated QTLs would provide wheat breeders valuable information towards their efforts in developing improved varieties in western Canada.

KEYWORDS

association mapping, diversity panel, *Fusarium graminearum*, international wheat genome sequencing consortium, physical map, Western Canada

Introduction

Fusarium head blight (FHB) is one the most globally destructive fungal diseases in wheat and other small grains. It is characterized by premature blighting of the spikes (plant death) and a reduction in grain yield by 10–70% due to shriveled kernels (Shah et al., 2018; Yi et al., 2018). FHB-infected grains are of unacceptable quality for marketing due to contamination with mycotoxins, which makes them not suitable for feed and food (Del Ponte et al., 2007). FHB is caused by several *Fusarium* species that may be present simultaneously in the same field. The prevalence of FHB species varies depending on geographical regions (temperate, sub-tropical, and tropical), weather conditions, the genetics of the varieties, and cultural practices (Waalwijk et al., 2003; Xu et al., 2005; Xu et al., 2008; Xue et al., 2019). Researchers from the Canadian Grain Commission identified a total of 13 *Fusarium* species in 454 durum (*Triticum turgidum subsp. durum (Desf.) Husn.*) and bread wheat (*Triticum aestivum* L.) samples collected in 1986-1987 of which six of the species accounted for 95% of the pathogen's populations. *Fusarium avenaceum*, *F. acuminatum*, and *F. sporotrichioides* were the most prevalent species in both Manitoba and Saskatchewan, while *F. graminearum* was most prevalent in eastern Canada and southern Manitoba but was rarely observed in both Saskatchewan and Alberta (Clear and Patrick, 1990). A follow-up study confirmed the high prevalence of *F. graminearum* in eastern Canada, accounting for ~90% of nine fungal species identified in 492 spring wheat sampled between 2001 and 2017 in Ontario (Xue et al., 2019). In recent years, however, *F. graminearum* has become the predominant causal agent of FHB not only in eastern Canada but also in the three major wheat-producing Prairie provinces of Manitoba, Saskatchewan, and Alberta (Valverde-Bogantes et al., 2020; Bamforth et al., 2022). For example, Bamforth et al. (2022) studied a total of 7,783 durum and bread wheat samples originated from several farms between 2014 and 2020 in eastern and western Canada. Although their results showed a fluctuation in species abundance over the years, *F. graminearum* was the most abundant species in both eastern and western Canada and accounted for 75–95% of the total pathogen populations, followed by *F. avenaceum* (10%), and *F. acuminatum* (5%).

The most common strategies used to reduce the introduction, spread, and severity of FHB include varietal selection, planting clean seeds, seed treatment, increasing seeding rate, staggered planting dates among fields to avoid all fields from flowering at the same time, limiting irrigation before and during the flowering period, crop rotation, fungicide application, and use of biological controls (Bai and Shaner, 2004; Bergstrom et al., 2011). The development and planting of varieties with stable and durable resistance to FHB and mycotoxin accumulation have been frequently cited as the most economical and environmentally friendly approach for long-term control. However, the development of FHB-resistant varieties is more complicated for multiple reasons, including the presence of different mechanisms of resistance, the difficulty in identifying reliable sources of resistance germplasm with combinations of different mechanisms, the polygenic nature of FHB resistance (Buerstmayr et al., 2020), and the negative correlations between FHB resistance traits with plant height and flowering time (Miedaner and Voss, 2008; Skinnes et al., 2010; Lu et al., 2011; Lu et al., 2013; Buerstmayr and Buerstmayr, 2016; He et al., 2016; Ruan et al., 2020). Of the five types of FHB resistance mechanisms described in the literature (Schroeder and Christensen, 1963; Mesterházy, 1995), Type I (resistance to initial infection) and Type II (resistance to the spread of infection in the spike) are the two most widely studied forms of resistance (Hales et al., 2020). For that reason, the major focuses in the global FHB research involve the identification of new sources of Type I and Type II resistance, mapping of quantitative trait loci (QTLs), and developing FHB resistance germplasm by pyramiding multiple resistance alleles using conventional and/or modern breeding methods (Steiner et al., 2017; Buerstmayr et al., 2020; Mesterhazy, 2020; Zhang et al., 2021).

Most sources of FHB resistance are controlled by numerous QTLs with minor effects and a few QTLs with major effects (Venske et al., 2019; Singh et al., 2021). Two recent synthesis studies compiled a list of 556 QTLs (Venske et al., 2019) and 883 QTLs (Singh et al., 2021) associated with FHB resistance in several populations. Those QTLs were distributed in all 21 wheat chromosomes with each chromosome consisting of a cluster of numerous resistance QTLs. A meta-analysis conducted on 323 FHB resistance QTLs identified 56 meta-QTLs (Venske et al., 2019), which is a six-fold reduction in the initial number of QTLs. Such results suggest the possibility of reporting a cluster of the same QTLs as potentially novel. Although consensus genetic maps have been used to compare QTLs identified in different populations and independent studies, they are prone to substantial errors for multiple reasons, including a smaller number of common markers among populations for consensus map constructions, lack of physical positions for most types of markers, and genotyping errors (Zhang et al., 2020a). Most meta-QTLs were physically located within a short interval, which requires further refinement using the International Wheat Genome Sequencing Consortium (IWGSC) RefSeq (Zhu et al., 2021a) physical map. In previous studies, we have used the IWGSC physical positions of the Wheat 90K iSelect array (Wang et al., 2014) to characterize QTLs associated with agronomic traits and grain characteristics (Semagn et al., 2022b) and reaction to leaf rust, stripe rust, common bunt,

and leaf spot (Iqbal et al., 2023) in a historical and modern Canadian spring wheat association mapping panel.

In western Canada, wheat diseases are divided into three priority groups with at least intermediate levels of resistance to priority-one diseases, which include FHB, stripe rust, leaf rust, stem rust, and common bunt (Brar et al., 2019b). FHB resistance QTLs were reported in biparental wheat populations derived from AAC Innova/AAC Tenacious (Dhariwal et al., 2020), FL62R1/Stettler and FL62R1/Muchmore (Zhang et al., 2018; Zhang et al., 2020b), DH181/AC Foremost (Yang et al., 2005), Vienna/25R47 (Tamburic-Ilincic and Barcellos Rosa, 2017), and Maxine/FTHP Redeemer (Tamburic-Ilincic and Rosa, 2019). Some of the issues of QTLs discovered in biparental populations include (i) poor resolution due to a limited number of recombination events, (ii) only alleles originating from two parents used in developing a given population are captured, and (iii) high multicollinearity among pairs of polymorphic markers in each population, which results to the exclusion of markers that differ by< 1 cM in the final data analyses (Semagn et al., 2006; Wang et al., 2006). Genome-wide association study surveys historical recombination frequencies in diverse genetic backgrounds and unrelated pedigrees developed for a wide range of purposes. It tend to be superior to linkage-based QTL mapping in biparental populations by testing genetic variants across the whole genome and finding genotypes statistically associated with phenotypes in unrelated individuals (Uffelmann et al., 2021). This methodology was used to map QTLs associated with FHB resistance in a Canadian durum wheat association mapping panel (Ruan et al., 2020) and durum wheat breeding lines assembled from 72 diverse crosses (Sari et al., 2020). We are not aware of previous GWAS to map QTLs associated with FHB resistance in historical and modern Canadian spring wheat varieties. The objectives of this study were, therefore, to (i) map QTLs associated with FHB incidence, severity, and visual rating index using genome-wide association analysis and the IWGSC RefSeq v2.0 physical map of the Wheat 90K iSelect array, (ii) understand if the positions of FHB resistance QTLs overlaps with QTLs for flowering time and plant height, and (iii) identify new sources of FHB resistance in historical and modern Canadian spring wheat varieties and lines.

Materials and methods

We used a total of 249 spring wheat varieties and lines adapted to the western Canada growing conditions (Supplementary Table S1), which included 200 historical and modern varieties registered for commercialization in Canada from 1905 to 2022, 47 unregistered lines developed by Canadian breeders, and 2 exotic lines (Sumai 3 and Saar). Sumai 3 (Yong-Fang et al., 1997) is one of the most widely studied Chinese cultivars, while Saar is a line developed by the International Maize and Wheat Improvement Center (Lillemo et al., 2008) and characterized by a moderate level of resistance to FHB (Wiśniewska et al., 2016). AC Vista and CDC Teal were used as FHB susceptible checks, both AC Cora and AC Barrie as intermediately resistant checks, 5602HR as a moderately resistant check, and both Sumai 3 and FHB37 as highly resistant checks. FHB37 is an experimental line developed from the cross HY611/Ning8331 and has the same *Qfhb-5AS* allele as Ning 8331 derived from Sumai 3 (Pandurangan et al., 2020).

Reactions to *F. graminearum* were evaluated at seven environments in eastern and western Canada, which included the Elora Research Station, Pilkington, Ontario in 2017 (Elora-2017), the Ian N. Morrison Research Farm, Carman, Manitoba in 2020 (Carm-2020), and the Morden Research and Development Center, Morden, Manitoba from 2017-2019 and 2021-2022 (Mord-2017, Mord-2018, Mord-2019, Mord-2021, and Mord-2022). To minimize the confounding effects of other wheat diseases, reactions to FHB were evaluated within 13 acres of land dedicated to *F. graminearum* screening. In addition, we also planted two meters wide border rows around the FHB nurseries to minimize infection by stray pathogens with tools, vehicles, and field equipment exclusively assigned to the FHB nursery. The detailed FHB evaluation method has been described in a previous study (Semagn et al., 2022a). Briefly, a suspension of four *F. graminearum* isolates at a concentration of 50,000 macroconidia mL^{-1} was prepared by mixing an equal amount of two 3-ADON (HSW-15-39 and HSW-15-87) and two 15-ADON (HSW-15-27 and HSW-15-57) chemotypes with sterile water and Tween 20 (Dhariwal et al., 2020). Wheat spikes were sprayed using a backpack sprayer when about 50% of the plants within a plot reached flowering. Inoculation was repeated 2-3 days later to infect tillers with delayed flowering time. Inoculated plants were irrigated three times weekly using an overhead mist irrigation system or Cadman Irrigations travelers with Briggs booms.

Disease incidence (the proportion of diseased plants) and severity (the area of plant tissue that was visibly diseased) were recorded on a scale of 0 (highly resistant) to 10 (highly susceptible) in three environments (Mord-2017, Mord-2018, and Mord-2019) and from 0 to 100% at the remaining four environments (Elora-2017, Carm-2020, Mord-2021, and Mord-2022) after 18-21 days from the first inoculation. To get the same disease rating in all environments, however, we converted the percent scores into a 0 to 10 scale. Visual rating index (VRI) was calculated by multiplying disease incidence and severity recorded into a 0 to 10 scale as described in a previous study (Gilbert and Morgan, 2000). Flowering time was recorded as the number of days from planting to the emergence of a few anthers in the middle of spikes at three environments (Mord-2017, Mord-2018, and Mord-2019). Plant height was measured from the base of the stem to the tip of the terminal spikelet excluding the awns at five environments (Mord-2017, Mord-2018, Mord-2019, Mord-2021, and Mord-2022).

The 249 lines and varieties evaluated for reaction to FHB were genotyped with Wheat 90K iSelect in two sets. The first set of 203 lines and varieties was genotyped at the University of Saskatchewan, Saskatoon, Canada in 2018. The remaining 46 lines and varieties were genotyped along with other samples at the Agriculture and Agri-Food Canada (AAFC) lab in Morden. All samples were also genotyped with 14 Kompetitive Allele-Specific PCR (KASP) markers associated with *Fhb1* (wMAS000008, wMAS000009, BS00003814, BS00009393, BS00009992, and BS00012531), *Rht-B1* (wMAS000001), *Rht-D1* (wMAS000002), *Glu-A1* (wMAS000012

and wMAS000013), *Glu-D1* (wMAS000014), *Lr34* (wMAS000003 and wMAS000004), and *Sr2* (wMAS000005). KASP genotyping was done using the Biosearch Technologies (https://www.biosearchtech.com/; accessed on 15 Feb 2023) service lab, Beverly, MA, USA. However, merging of the 90K SNPs genotype datasets generated by the University of Saskatchewan and AAFC labs was problematic due to inconsistencies in allele calls of the positive controls (Carberry, Glenn, and Park), and differences in the total number of SNPs successfully called by in both datasets (24,926 of the 90K SNPs by AAFC vs. 55,404 SNPs by the University of Saskatchewan). Challenges in merging SNP data generated by different labs and groups are a common constraint for different reasons, including strand orientation (Zuvich et al., 2011; Verma et al., 2014). Therefore, we only used the genotype data of 198 of the 203 lines and varieties after excluding five samples that had high missing genotype data and/or residual heterozygosity.

Of the 90K SNP array and KASP markers used to genotype the 198 lines and varieties, we used 26,449 polymorphic SNPs (Supplementary Table S2) for statistical analysis after removing markers with a minor allele frequency of<5%, heterozygosity of >20%, missing data of >30%, and those with unknown chromosomes based on the IWGSC RefSeq v2.0 (Zhu et al., 2021a). Sequences of the polymorphic SNPs were retrieved from the GrainGenes database (https://wheat.pw.usda.gov/GG3/) and blasted against the IWGSC RefSeq v2.0 in the Wheat@URGI portal (http://wheat-urgi.versailles.inra.fr/Seq-Repository/BLAST). The default blast parameters were used, followed by filtering based on the best scores (Okada et al., 2019). The final genotype data was imputed using LinkImpute implemented in TASSEL v5.2.86 (Bradbury et al., 2007).

Multi Environment Trial Analysis with R (META-R) v.6.04 (Alvarado et al., 2020) was used to compute the best linear unbiased predictors (BLUP), best linear unbiased estimators (BLUE), genetic and phenotypic correlation coefficients, and variance component analyses. Broad-sense heritability (H^2) in the combined environments and repeatability between replications within each environment (H) were computed from the variance components as follows:

$$H^2 = \frac{\sigma^2_g}{\sigma^2_g + \frac{\sigma^2_{ge}}{nEnv} + \frac{\sigma^2_\varepsilon}{nEnv \times nRep}} \text{ and } H = \frac{\sigma^2_g}{\sigma^2_g + \frac{\sigma^2_\varepsilon}{nRep}}$$

where σ^2_g, σ^2_{ge}, σ^2_ε, nEnv, and nRep refer to genotypic variance, G×E interaction variance, residual error variance, number of environments, and number of replications, respectively (Alemu et al., 2021). We used JMP v16 statistical software (Jones and Sall, 2011) for coefficients of determination (R^2) analysis and to generate different types of graphs from the phenotype data. Using the Prairie Recommending Committee for wheat, rye, and triticale operating protocol (PRCWRT, 2020), we assigned lines and varieties into five groups by comparing their overall VRI computed from all seven environments with checks as follows: highly resistant (VRI< 7.0), moderately resistant (7–20.0), intermediate (20.1–30.0), moderately susceptible (30.1-40.0), and highly susceptible (VRI > 40.0). These ranges were modified from previous threshold values described in Chinese wheat germplasm: highly resistant (VRI< 10%), moderately resistant (10–25%), moderately susceptible (25–45%), and highly susceptible (VRI > 45%) (Yan et al., 2020; Yan et al., 2022).

Identity by state (IBS)-based genetic distance matrices and principal component analysis (PCA) were computed using TASSEL v5.2.86 (Bradbury et al., 2007). Phylogenetic trees were constructed from the IBS-based distance matrices using the neighbor-joining method implemented in Molecular Evolutionary Genetics Analysis (MEGA) v11 (Tamura et al., 2021). Scatter plots were generated as an indicator of the population structure in the germplasm by plotting the first three principal components from PCA in CurlyWhirly v1.21.08.16 (The James Hutton Institute, Information & Computational Sciences). Marker trait associations (MTA) were identified using the weighted mixed linear model method implemented in TASSEL. The input data consisted of the imputed SNP genotype data, a kinship matrix to account for relatedness, PC1 to PC3 from a principal component analysis to account for population structure and BLUEs of each trait computed within each environment and combined across all environments. The number of polymorphic SNPs used in the final analysis varied from 307 on chromosome 4D to 2,276 on 2B (Supplementary Table S2) with an overall average of 1,259 SNPs per chromosome. The BLUEs used for marker-trait association analyses included disease incidence, severity, and VRI as the primary traits. Flowering time and plant height were used to explore if any of the SNPs significantly associated with disease incidence, severity, and VRI were also simultaneously associated with these two agronomic traits. Markers were declared as significant at a false discovery rate of $p< 3.1 \times 10^{-4}$ or $-\log_{10}$ (p) value of ≥ 3.5. Genome-wide Manhattan plots were obtained using SNPevg (Wang et al., 2012), while quantile-quantile (QQ) plots were generated in TASSEL. Two or more adjacent SNPs significantly associated with the same trait that differs by less than 15 Mb were assigned to the same QTL designation using a trait acronym (Fhb, Flt, or Pht), lab designation (dms = Dean Michael Spaner), and chromosome number. The positions of QTLs that consisted of a cluster of two or more SNPs significantly associated with each trait were given as an interval using the minimum and maximum positions. QTLs associated with two or more traits but differ by<15 Mb were considered coincident. QTL map of each chromosome was constructed using MapChart v2.32 (Voorrips, 2002).

Results

Phenotypic variation

The coefficients of determination (R^2) between BLUPs and BLUEs computed for each trait within each environment and combined environments were very high for disease incidence, severity, and VRI, which varied from 0.96 to 1.00 (Supplementary Figure S1). As a result, all the subsequent results are based on the BLUEs. The overall mean BLUE values of disease incidence, severity, VRI, flowering time, and plant height computed in each environment varied from 0.5 to 10, 0.5 to 9.9, 0.5 to 89.9%, 47 to 69 days, and from 54 to 120 cm, respectively. Disease incidence,

10.3389/fpls.2023.1190358

severity, and VRI of the 249 varieties and lines recorded in individual and combined environments showed continuous distribution in each environment but tend to be less severe at Morden both in 2018 and 2021 than in all other environments (Figure 1; Supplementary Table S1). The Shapiro-Wilk tests for normality performed on individual environments showed significantly skewed ($p< 0.05$) distributions for most trait-environments combinations, except the VRI both at Carm-2020 and Elora-2017, plant height at Mord-2018, Mord-2019, and Mord-2021. However, the distributions of mean BLUEs computed from all combined environments were normal or nearly so for all five traits. In the combined analyses of all environments, mean disease incidence, severity, VRI, flowering time and plant height ranged from 1.8 to 8.8, 1.9 to 8.2, 1.6 to 69.1%, 54 to 62 days and 67 to 104 cm, respectively (Supplementary Table S1).

Analysis of variance performed across all environments revealed highly significant ($p< 0.01$) differences among lines/varieties, environments, and G×E interaction (Table 1). However, differences among environments accounted for 39.3–81.4%, which is up to 12-fold greater than the genotypic variance. G×E interactions and residual error variances accounted for 1.7–10.0% and 7.6–29.7% of the total variances, respectively (Figure 2). Broad-sense heritability computed from all environments varied from 0.79 for disease incidence to 0.90 for plant height (Table 1). Repeatability computed between replications within each environment varied from 0.42 to 0.76 for disease incidence, 0.44 to 0.86 for disease severity, 0.50 to 0.89 for VRI, 0.41 to 0.90 for plant height, and 0.69 to 0.98 for flowering time (Supplementary Table S3). For each trait, we observed highly variable genetic correlation coefficients between pairs of environments, which ranged from 0.35 to 0.97 for the three

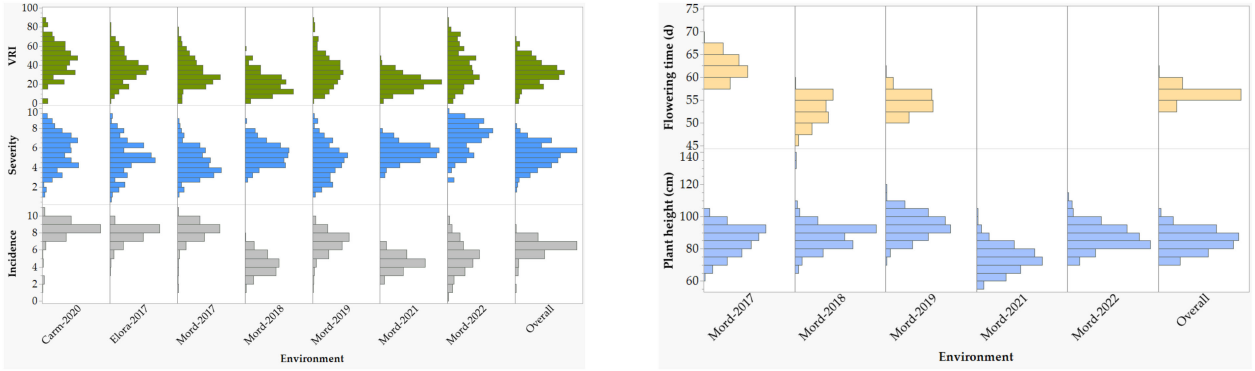

FIGURE 1
Frequency distributions of reactions to Fusarium head blight (FHB) incidence, severity, and visual rating index of 249 spring wheat varieties and lines evaluated at seven environments: the Ian N. Morrison Research Farm in Carman (Carm-2020), the Elora Research Station (Elora-2017), and the Morden Research and Development Center (Mord-2017, Mord-2018, Mord-2019, Mord-2021, and Mord-2022). Plant height and flowering time were evaluated at five and three environments, respectively. For each trait, the overall refers to the means of all combined environments.

TABLE 1 Variance components of Fusarium head blight incidence, severity, visual rating index, plant height, and flowering time recorded at 3–7 environments.

Statistics	Disease incidence	Disease severity	Visual rating index	Flowering time	Plant height
Genotype variance (σ^2g)	0.54	0.93	82.40	3.08	38.21
Environment variance (σ^2e)	6.61	3.36	274.66	26.86	53.47
Genotype × environment interaction (σ^2ge)	0.38	0.30	53.24	0.55	3.91
Residual error variance ($\sigma^2\varepsilon$)	1.43	1.66	121.37	2.49	40.42
Grand mean	5.72	4.25	27.77	58.30	85.04
Least significance difference (LSD)	1.03	1.12	11.08	2.34	6.26
Coefficient of variation (CV)	20.94	30.32	39.68	2.71	7.48
Mean number of replicates	2.29	2.29	2.29	2.50	2.40
No. of environments	7	7	7	3	5
P value for genotypes	< 0.01	< 0.01	< 0.01	< 0.01	< 0.01
P value for environments	< 0.01	< 0.01	< 0.01	< 0.01	< 0.01
P value for G×E interaction	< 0.01	< 0.01	< 0.01	< 0.01	< 0.01
Broad-sense heritability	0.79	0.86	0.84	0.80	0.90

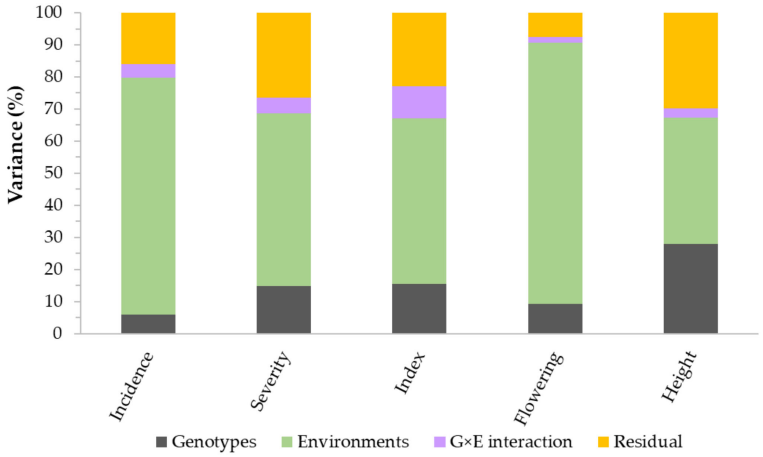

FIGURE 2
Partitioning of the total variance of genotypes (G), environments (E), G×E interaction, and residual error variances. The plot is based on 249 spring wheat varieties and lines evaluated for Fusarium head blight (FHB) incidence, severity, and visual rating index at seven environments, plant height at five environments, and flowering time at three environments.

FHB resistance traits, 0.24 to 0.84 for flowering time, and 0.77 to 0.98 for plant height. Phenotypic correlation coefficients between pairs of environments varied from 0.16 to 0.69 for the three FHB resistance traits, 0.48 to 0.77 for plant height, and 0.22 to 0.65 for flowering time (Supplementary Table S3). The coefficients of determination between pairs of traits within each environment varied from 0.05 to 0.48 between disease incidence and severity, 0.19 to 0.83 between incidence and VRI, and 0.52 to 0.93 between severity and VRI (Supplementary Figure S2). In the combined data of all seven environments, the overall correlations were 0.48 between disease incidence and severity, 0.68 between incidence and VRI, and 0.91 between severity and VRI. Both flowering time and plant height showed very small R^2 with disease incidence, severity, and VRI ($0.01< R^2< 0.11$).

FHB resistance QTLs

The first three principal components (PCs) from a principal component analysis accounted for 24.0% of the total variation. A plot of the PC1 (11.7%), PC2 (7.5%), and PC3 (4.8%) revealed two major groups based primarily on kernel hardness/texture, gluten strength, and/or grain protein content (Supplementary Figure S3 and Supplementary Table S1). Varieties and lines with medium to hard kennels and high grain protein content (> 11% measured as N x 5.7 on a 13.5% moisture basis) formed the first group, which included CWRS, CNHR, and CWHWS classes. Lines and varieties with soft and medium hard kernels (CPSR, CPSW, CWSP, and CWSWS) plus hard kennels with extra strong gluten strength (CWES) formed the second group. Details on the extent of molecular diversity, relatedness, linkage disequilibrium, and population structure of the diversity panel have been described in a previous study (Semagn et al., 2021). Genome-wide association analyses performed on the BLUEs computed within each environment and overall means of all combined environments identified a total of 559 significant marker-trait associations (MTAs). Of these 559 SNPs, 394 SNPs were associated with FHB resistance, six SNPs with FHB and plant height, one SNP with FHB and flowering time, 67 SNPs with flowering time, and 91 SNPs with plant height. One of the 559 SNPs located at 760.0 Mb on chromosome 2A (wsnp_Ex_c2137_4014383) was associated with both FHB severity and flowering time. Six SNPs located at 575.2 Mb on 2D (BobWhite_c17572_339), 379.7 Mb on 3A (wsnp_Ex_c22766_31972812), 597.6 Mb on 6A (both BobWhite_c14882_143 and Excalibur_c18632_1700), and 14.9 on 7B (BobWhite_c4253_568 and Excalibur_c34807_206) were associated with disease incidence and plant height.

The 559 SNPs were clustered into 185 QTLs and were associated with plant height (37 QTLs), flowering time (36), disease incidence (38), severity (12), VRI (12), incidence and severity (1), incidence and VRI (7), severity and VRI (14), and disease incidence, severity and VRI (28). The 185 QTLs were distributed in all 21 wheat chromosomes, each consisting of 1a cluster of up to 27 significant SNPs, and individually accounted for 6.1–15.9% of either the individual or combined environments (Supplementary Table S4). However, only 75 out of the 559 SNPs (Figure 3) and twenty-eight out of the 185 QTLs (Table 2; Figure 4 ; Supplementary Figure S4) were identified using BLUEs computed from all combined environments, which included sixteen FHB resistance, four plant height, and eight flowering time QTLs. Below, we provided detailed results of only the 28 QTLs identified in the overall phenotype data of all environments and their expression in individual environments.

Four out of the sixteen FHB resistance QTLs (*QFhb.dms-3B.1*, *QFhb.dms-5A.5*, *QFhb.dms-5A.7*, and *QFhb.dms-6A.4*) were associated with all three resistance traits (disease incidence, severity, and VRI) in the combined environments and accounted for 5.7–10.2% individually and 27.1-35.6% of the total (cumulative) phenotypic variance (Table 2). *QFhb.dms-3B.1* consisted of a cluster of sixteen SNPs, including wMAS000009 (one of the *Fhb1* linked KASP markers widely used for marker-assisted selection), and was mapped at 10.2–23.5 Mb.

10.3389/fpls.2023.1190358

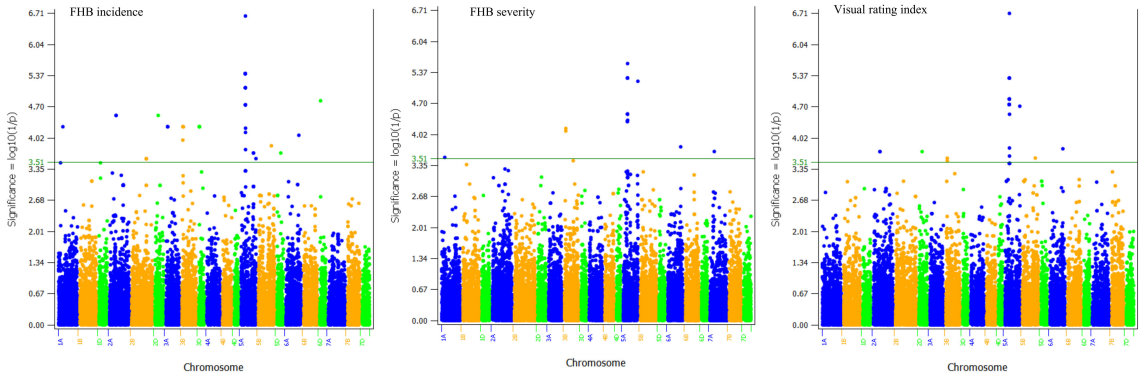

FIGURE 3
Genome-wide p values of 26,449 polymorphic SNPs based on a weighted mixed linear model and the best linear unbiased estimators (BLUEs) of Fusarium head blight (FHB) incidence, severity, and visual rating index computed from all seven environments. The horizontal line shows the threshold p-value of 3.1×10^{-4} or Log10 (1/p) value of 3.51. The A, B, and D genomes are in blue, orange, and green colors, respectively. Chromosomes and physical positions are shown on the x-axis.

TABLE 2 Summary of QTLs associated with Fusarium head blight incidence (Inc), severity (Sev), visual rating index (VRI), plant height (Pht), and flowering time (Flt) associated with individual and combined environments.

QTL	No. of SNPs	Chr	Position (Mb)	P-value	PVE (%) in overall environments*					PVE (%) in individual and combined environments				
					Inc	Sev	VRI	Pht	Flt	Inc	Sev	VRI	Pht	Flt
QFhb.dms-1A.1	4	1A	12.4-48.8	1.8×10^{-4}		6.5				7.6	6.5	6.9		
QFhb.dms-1A.2	1	1A	123.9	4.8×10^{-5}	7.1					7.6		7.7		
QFhb.dms-2A.2	2	2A	170.8	8.0×10^{-5}	7.6		6.9			8.0		7.0		
QFhb.dms-2B.8	4	2B	691.1-700.1	2.1×10^{-4}	6.7					6.0				
QFhb.dms-2D.2	1	2D	159.1	8.0×10^{-5}	7.6		6.9			8.0		7.0		
QFhb.dms-3A.1	9	3A	10.5-26.0	1.1×10^{-4}	7.1					7.0	8.0	7.9		
QFhb.dms-3B.1	16	3B	10.2-23.5	9.9×10^{-5}	7.0	7.7	6.5			7.0	10.2	7.9		
QFhb.dms-3D.1	9	3D	3.1-11.7	6.9×10^{-5}	7.1					7.5	7.8	7.6		
QFhb.dms-5A.5	33	5A	414.2-522.7	6.9×10^{-5}	7.7	8.7	9.2			7.5	8.4	9.1		
QFhb.dms-5A.6	11	5A	596.2-617.1	8.5×10^{-5}	5.9					7.8	7.8	9.5		
QFhb.dms-5A.7	5	5A	683.3-710.1	1.1×10^{-4}	5.7	9.8	8.9			6.6	8.6	9.2		
QFhb.dms-5B.8	1	5B	640.0	2.1×10^{-4}	6.2		6.6			6.2	6.8	6.6		
QFhb.dms-5D.3	1	5D	477.8	1.3×10^{-4}	5.9					6.5				
QFhb.dms-6A.4	5	6A	597.6-609.4	9.2×10^{-5}	6.7	6.9	7.0			7.5	8.4	7.0		
QFhb.dms-6D.1	2	6D	3.5-12	7.6×10^{-5}	7.2					8.2				
QFhb.dms-7A.1	5	7A	43.0-89.2	1.6×10^{-4}		6.7				6.9	7.3	6.6		
QPht.dms-2A.3	11	2A	679.8-680.0	1.1×10^{-4}				7.2					7.4	
QPht.dms-2A.5	3	2A	748.8-762.1	1.3×10^{-4}				7.0					7.5	
QPht.dms-6A.2	14	6A	565.7-615.3	1.4×10^{-4}				7.1					7.5	
QPht.dms-7B	2	7B	14.9	2.3×10^{-4}				6.7					6.7	
QFlt.dms-1A.4	1	1A	579.0	4.3×10^{-5}					8.3					8.0
QFlt.dms-1B.2	1	1B	675.7	9.2×10^{-5}					7.6					7.3

(Continued)

TABLE 2 Continued

QTL	No. of SNPs	Chr	Position (Mb)	P-value	PVE (%) in overall environments*					PVE (%) in individual and combined environments				
					Inc	Sev	VRI	Pht	Flt	Inc	Sev	VRI	Pht	Flt
QFlt.dms-2A.1	1	2A	511.5	1.3×10^{-4}					6.9					6.9
QFlt.dms-2A.2	2	2A	760.1-776.7	2.9×10^{-4}					6.1					6.1
QFlt.dms-2B.3	2	2B	800.7-803.2	8.0×10^{-5}					8.2					7.9
QFlt.dms-2D	1	2D	382.6	7.4×10^{-5}					7.4					7.4
QFlt.dms-7A.1	1	7A	65.8	2.4×10^{-4}					6.4					6.4
QFlt.dms-7B	1	7B	578.2	2.2×10^{-4}					6.5					6.5

Chromosome and physical positions are based on the International Wheat Genome Sequencing Consortium (IWGSC) RefSeq 2.0. See Figure 5 and Supplementary Table S4 for details. PVE refers to the mean phenotypic variance explained by each QTL either in the combined environments or each environment. *The proportion of phenotypic variance explained (PVE) by the QTL based on all combined environments.

QFhb.dms-3B.1 was detected using the overall mean disease incidence, severity, and VRI plus up to three of the seven tested environments (incidence: Carm-2020, Mord-2017, and Mord-2022; severity: Mord-2019; VRI: Carm-2020 and Mord-2019) and accounted for 6.5–10.2% of the phenotypic variances (Table 2, Supplementary Table S4). Lines and varieties that were homozygous for the resistance alleles at each of the significant SNPs had on average 11.2–30.5% (mean 20.5%), 21.9–33.5% (mean 25.6%), and 33.4–62.9% (mean 41.9%) less disease incidence, severity, and VRI, respectively, than those with the alternative alleles.

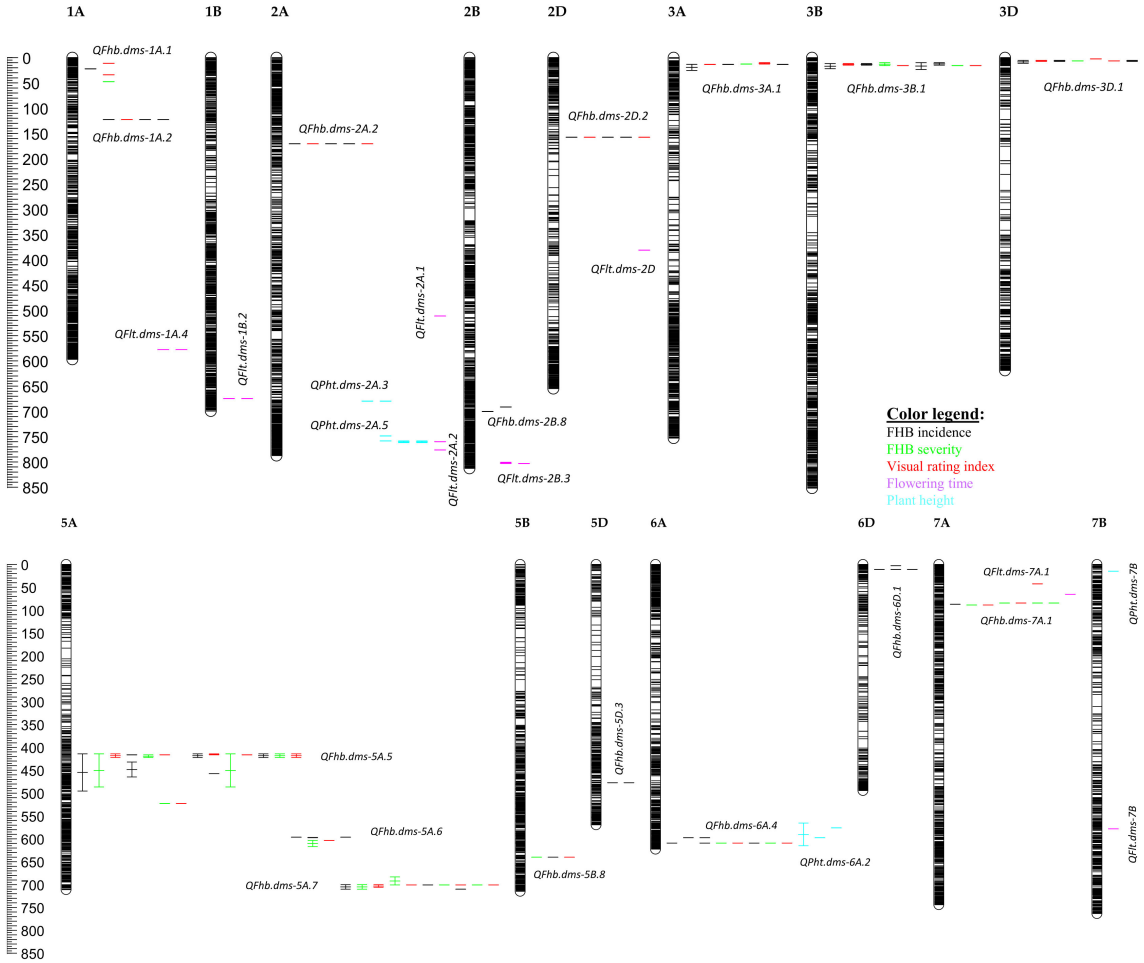

FIGURE 4
Visual rating index of seven checks, four highly resistant, and thirty-three moderately resistant varieties and lines based on overall mean best linear unbiased estimators (BLUE) computed from all seven environments. See Supplementary Table S1 for details.

QFhb.dms-5A.5 was the second QTL associated with disease incidence, severity, and VRI in the combined environments. It consisted of a cluster of 33 SNPs located at 414.2–522.7 Mb and accounted for 7.5–9.2% of the phenotypic variances of disease incidence, severity, and VRI in the individual and combined environments. *QFhb.dms-5A*.5 was a very stable QTL as it was identified not only in the overall means but also up to five out of the seven tested environments for each resistance trait (incidence: Carm-2020, Elora-2017, Mord-2017, Mord-2019, and Mord-2021; severity: Carm-2020, Mord-2017, Mord-2018, and Mord-2022; VRI: Carm-2020, Mord-2017, Mord-2018, Mord-2019, and Mord-2022) (Supplementary Table S4). Lines and varieties that were homozygous for the resistance alleles at each of the SNPs for *QFhb.dms-5A*.5 displayed 12.8–18.8% (mean 15.6%), 19.6–32.1% (mean 24.8%), and 27.5–54.5% (mean 38.8%) less disease incidence, severity, and VRI, respectively, than those with the alternative alleles. *QFhb.dms-5A*.7 was the third FHB resistance QTL associated with disease incidence, severity, and VRI in the combined environments plus up to three of the seven tested environments (incidence: Carm-2020 and Mord-2022; severity and VRI: Carm-2020, Elora-2017, and Mord-2022). This QTL was mapped at 683.3–710.1 Mb, consisted of a cluster of 5 SNPs, and accounted for 5.7-9.8% of the phenotypic variances of each trait in the combined and individual environments. Lines and varieties that were homozygous for the resistance alleles at each of the SNPs for *QFhb.dms-5A*.7 showed an average of 7.0%, 10.2%, and 12.6% less disease incidence, severity, and VRI, respectively, than those with the alternative alleles. *QFhb.dms-6A.4* was the fourth resistance QTL associated with disease incidence, severity, and VRI in the combined environments plus up to four of the seven tested environments (incidence: Carm-2020, Mord-2017, Mord-2021, and Mord-2022 plus both severity and VRI recorded in Mord-2022). It consisted of a cluster of 5 SNPs that mapped at 597.6-609.4 Mb and explained 6.7–8.4% of the phenotypic variances of each FHB resistance trait in the individual and combined environments. Lines and varieties that were homozygous for the FHB resistance alleles at each of the significant SNPs for *QFhb.dms-6A.4* showed an average of 25.3%, 35.6%, and 51.6% less disease incidence, severity, and VRI, respectively, than those with the alternative alleles.

QFhb.dms-2A.2, *QFhb.dms-2D*.2, and *QFhb.dms-5B.8* were the other FHB resistance QTLs located at 170.8 Mb, 159.1 Mb, and at 640.0 Mb, respectively, which were associated with both disease incidence and VRI recorded in all combined environments. These three QTLs accounted for 6.2-8.0% individually and 20.4–22.2% of the total disease incidence and VRI (Table 2). Lines and varieties harboring the FHB resistance alleles showed 7.4–12.2%, 5.1–7.8%, and 1.6–12.9% less disease incidence, severity, and VRI, respectively, than those with the alternative alleles. In the analysis performed on individual environments, however, these three QTLs were less stable because *QFhb.dms-2A*.2 and *QFhb.dms-2D.2* were associated with both disease incidence and VRI recorded in Carm-2020, and incidence in Mord-2017, whereas *QFhb.dms-5B.8* was associated with only disease severity recorded in Mord-2017 (Supplementary Table S4).

Seven of the sixteen FHB resistance QTLs identified using the overall means of all combined environments (Table 2) were associated with only disease incidence and accounted for 5.9–9.5% individually. These seven QTLs included *QFhb.dms-1A.2* that mapped at 123.9 Mb, *QFhb.dms-2B*.8 (691.1–700.1 Mb), *QFhb.dms-3A*.1 (10.5–26.0 Mb), *QFhb.dms-3D*.1 (3.1–11.7 Mb), *QFhb.dms-5A*.6 (596.2–617.1 Mb), *QFhb.dms-5D*.3 (477.8 Mb), and *QFhb.dms-6D*.1 (3.5–12.0 Mb). Each of these QTLs consisted

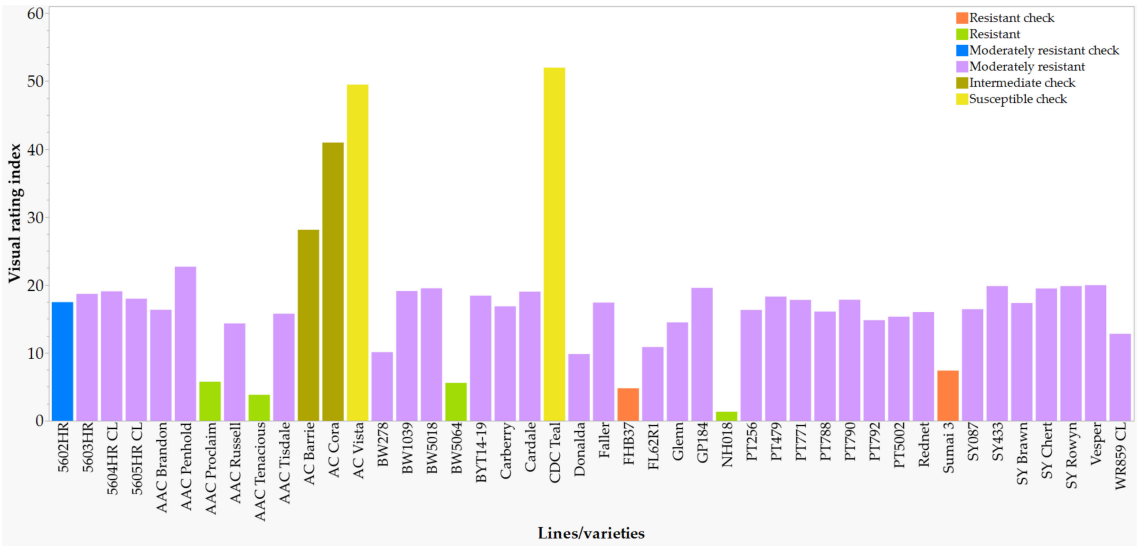

FIGURE 5
Physical positions of the 28 quantitative trait loci (QTLs) associated with Fusarium head blight (FHB) incidence (black), severity (green), visual rating index (red), flowering time (lavender), and plant height (Skye blue) based on individual environments and all combined environments. The IWGSC RefSeq v2.0 physical map position (Mb) is shown on the left side of the chromosomes, with each horizontal line representing each SNP. QTLs are shown on the right side of each chromosome. See Supplementary Table S4 for details of SNPs significantly associated with each trait and Supplementary Figure S4 for details of each QTL. Note the two coincident genomic regions associated with FHB resistance and flowering time on 6A and FHB resistance and flowering time on 7A.

of a cluster of up to eleven SNPs significantly associated with disease incidence. Lines and varieties that were homozygous for the resistance allele(s) at each QTL showed an average of 23.4–30.5% less disease incidence than those with the alternative alleles. In the GWAS analyses performed on individual environments, *QFhb.dms-2B.8* and *QFhb.dms-5D.3* were associated only with disease incidence recorded at one environment, *QFhb.dms-6D.1* with only disease incidence at three environments, and the remaining four QTLs (*QFhb.dms-1A.2*, *QFhb.dms-3A.1*, *QFhb.dms-3D.1*, and *QFhb.dms-5A.6*) were associated with disease incidence at two environments, disease severity at one environment, and VRI up to three environments (Supplementary Table S4).

QFhb.dms-1A.1 and *QFhb.dms-7A*.1 were mapped at 12.4–48.4 Mb and 43.0–89.2 Mb, respectively, each consisting of a cluster of 4–5 SNPs, and individually accounted for 6.5– 6.7% of disease severity in the combined environments (Table 2). Lines and varieties that harbored *QFhb.dms-1A.1* and *QFhb.dms-7A.1* resistance alleles showed an average of 16.9% and 2.8% less disease severity, respectively, than those with the alternative alleles. In the analyses performed on individual environments, *QFhb.dms-1A*.1 was associated with both disease incidence recorded at Mord-2017 and VRI recorded both at Mord-2018 and Mord-2021, but not disease severity recorded at any of the individual environments. *QFhb.dms-7A.1* was associated with disease incidence recorded at Carm-2020, disease severity recorded at three environments (Elora-2017, Mord-2017, and Mord-2022), and VRI recorded at three environments (Elora-2017, Mord-2017, and Mord-2018) (Supplementary Table S4).

QPht.dms-2A.3, *QPht.dms-2A*.5, *QPht.dms-6A.2*, and *QPht.dms-7B* were the four QTLs associated with the overall mean plant height recorded in all five combined environments, which were mapped at 679.8–680.0 Mb, 748.8–762.1 Mb, 565.7–615.3 Mb, and 14.9 Mb, respectively. These four QTLs accounted for 6.7–7.5% individually and 28.0% of the total phenotypic variance of plant height recorded in the combined environments (Table 2). In contrast to *QPht.dms-7B* which was detected only in the combined environments, the other three plant height QTLs were detected in the over means plus up to three of the five individual environments: *QPht.dms-2A.3* in Mord-2019, *QPht.dms-6A.2* in Mord-2019 and Mord-2022, and *QPht.dms-2A.5* in Mord-2018, Mord-2021, and Mord-2022. The eight flowering time QTLs identified in the combined environments were *QFlt.dms-1A*.4 that was mapped at 579.0 Mb, *QFlt.dms-1B*.2 (675.7 Mb), *QFlt.dms-2A*.1 (511.5 Mb), *QFlt.dms-2A*.2 (760.1–776.7 Mb), *QFlt.dms-2B*.3 (800.7-803.2 Mb), *QFlt.dms-2D* (382.6 Mb), *QFlt.dms-7A*.1 (65.8 Mb), and *QFlt.dms-7B* (578.2 Mb). These QTLs accounted for 6.1–8.3% individually and 57.4% of the total phenotypic variance in the combined environments. In the GWAS analysis performed using BLUEs from individual environments, four out of the eight flowering time QTLs (*QFlt.dms-2A.1*, *QFlt.dms-2D*, *QFlt.dms-7A.1*, and *QFlt.dms-7B*) were not identified in any of the individual environments and the remaining four QTLs (*QFlt.dms-1A.4*, *QFlt.dms-1B.2*, *QFlt.dms-2A.2*, and *QFlt.dms-2B.3*) were detected at one of the three tested environments (Supplementary Table S4).

FHB resistant sources

In comparison with the VRI of the checks computed from all seven combined environments (Supplementary Table S1), four of the 249 lines and varieties (AAC Proclaim, AAC Tenacious, NH018, and BW5064) were found to be highly resistant (R), 33 moderately resistant (MR), 60 intermediate (I), 83 moderately susceptible (MS), and 62 susceptible (S). Of the thirty-seven lines and varieties that displayed R and MR (Figure 5), twenty-seven belong to the Canada Western Red Spring market class (5603HR, 5604HR CL, 5605HR CL, AAC Brandon, AAC Russell, AAC Tisdale, BW1039, BW278, BW5018, BW5064, BYT14-19, Carberry, Cardale, Donalda, Glenn, PT256, PT479, PT5002, PT771, PT788, PT790, PT792, Rednet, SY433, SY Brawn, SY Chert, and WR859 CL). The remaining ten R and MR lines and varieties were from the Canada Northern Hard Red (Faller, NH018, and Vesper), the Canada Prairie Spring Red (AAC Penhold, AAC Tenacious, and SY Rowyn), and the Canada Western Special Purpose (AAC Proclaim, GP184, and SY087), and an Eastern Canadian spring wheat line (FL62R1). We observed clear differences among the overall visual rating index of the R, MR, I, MS, and S lines and varieties in all sixteen FHB resistant QTLs regardless of the specific linked SNPs (Figure 6). Similar trends were observed when the comparisons were made on each SNP linked with the FHB resistant QTLs, which is demonstrated in Figure 7 using a subset of seven of the sixteen SNPs for *QFhb.dms-3B*.1.

A detailed diversity assessment and relationship of the germplasm used in this study has been published in a previous study (Semagn et al., 2021). To get insight into the genetic relationship of the panel with emphasis on FHB reactions, we computed genetic distance matrices between pairs of varieties/lines from all 26,449 polymorphic SNPs (matrix-1) and 401 SNPs significantly associated with FHB incidence, severity, and VRI in the individual and combined environments (matrix-2). The pairwise distance varied from 0.012 to 0.484 for matrix-1 and 0 to 0.771 for matrix-2 (data not shown), suggesting biased estimates with a decrease in the number of markers. The phylogenetic trees constructed from the distance matrix computed from the 401 SNPs significantly associated with FHB resistance tend to cluster the R and MR lines/varieties better than all SNPs in matrix-1 (Supplementary Figure S5). One of the clusters constructed from the 401 SNPs consisted of eleven R and MR cultivars: AAC Penhold, WR859 CL, BW278, Glenn, SY087, Faller, AAC Brandon, AAC Tenacious, AAC Proclaim, FL62R1, and Sumai 3.

Discussion

FHB resistance QTLs

The historical and modern Canadian spring wheat varieties and lines used in the present study have been previously used for GWAS to map QTLs associated with agronomic traits and grain characteristics (Semagn et al., 2022b) and resistance to stripe rust, leaf rust, leaf spot, and common bunt (Iqbal et al., 2022). Using the IWGSC RefSeq v2.0 physical information and the overall mean

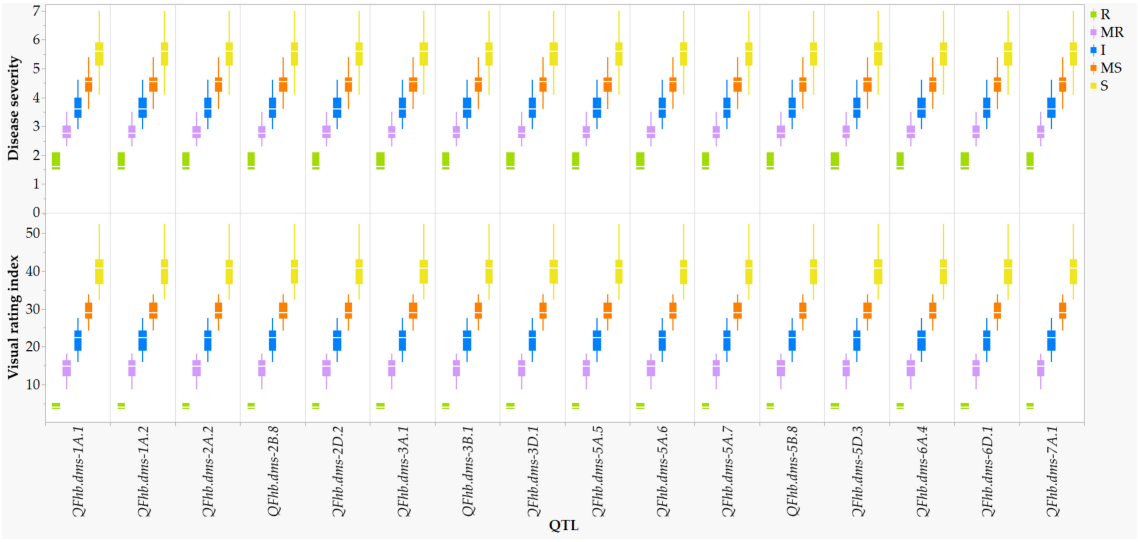

FIGURE 6
Comparison of the overall Fusarium head blight visual rating index of 198 varieties and lines at each of the 16 disease resistant QTLs: highly resistant (R), moderately resistant (MR), intermediate (I), moderately susceptible (MS), and susceptible (S).

phenotype data of four conventionally and three organically managed environments, we uncovered a total of 108 QTLs associated with days to heading (9), days to maturity (12), plant height (15), lodging tolerance (12), thousand kernel weight (13), test weight (13), grain yield (16), and grain protein content (18). These QTLs accounted for 4.4–11.5% individually and 13.8–73.4% of the total phenotypic variance of each agronomic trait and grain characteristic (Semagn et al., 2022b). For resistance to diseases, we uncovered a total of 37 QTLs associated with the overall means of common bunt (12), leaf rust (13), stripe rust (5), and leaf spot (7), which accounted for 6.6–16.9% individually and 39.4–97.9% of the total phenotypic variance of each disease combined across all environments (Iqbal et al., 2022). The physical positions of *QFhb.dms-1A.1* associated with the combined and individual environments in the present study was mapped 1 Mb away from a QTL previously reported for common bunt resistance (*QCbt.dms-1A.2*) in the same germplasm. *QFhb.dms-4B.3* was about 5.1 Mb away from the stripe rust resistance QTL (*QYr.dms-4B*). The number of lines and varieties used in two previous studies and the current study varied from 192–198, which agrees with the 150–

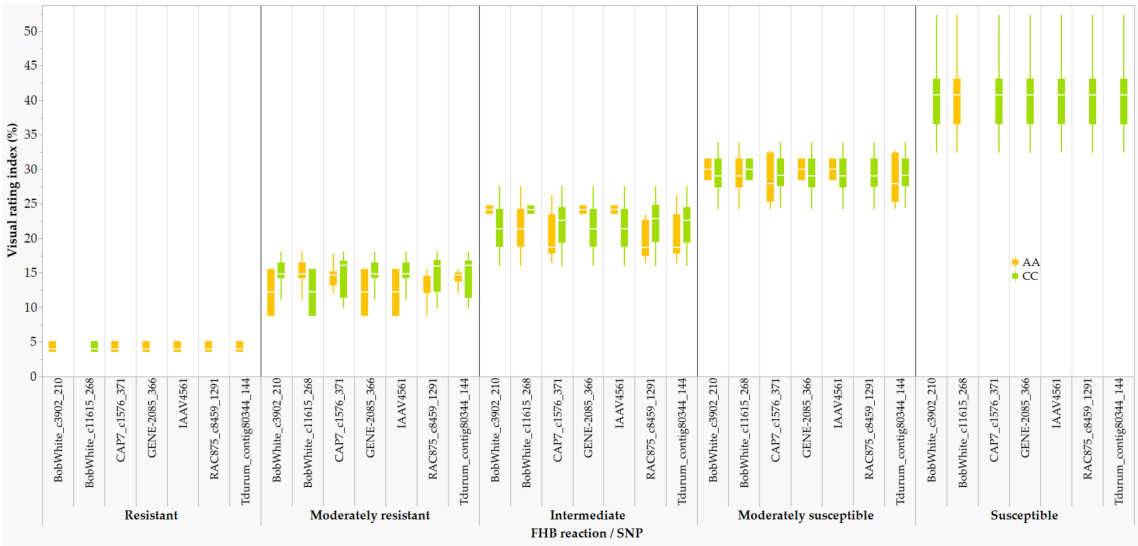

FIGURE 7
Comparison of the overall Fusarium head blight visual rating index of 198 varieties and lines that were homozygous for AA or CC at the seven SNPs associated with the *QFhb.dms-3B.1*: highly resistant (R), moderately resistant (MR), intermediate (I), moderately susceptible (MS), and susceptible (S).

200 population size widely used in QTL discovery studies (Wang et al., 2022). A few examples include 186 durum wheat association mapping panel (Ruan et al., 2020), an association panel of 171 common wheat cultivars (Hu et al., 2020), 187 spring wheat recombinant inbred lines (Poudel et al., 2022), and 171 bread wheat doubled haploid lines (Zhu et al., 2021b).

Flowering time in wheat is controlled primarily by the photoperiod response genes (*Ppd*), vernalization genes (*Vrn*), and "earliness per se". *Ppd* genes are located on chromosomes 2A (*Ppd-A1*), 2B (*Ppd-B1*), and 2D (*PPd-D1*), while *Vrn* genes are located on 5A (*Vrn-A1*), 5B (*Vrn-B1*), and 5D (*Vrn-D1*) (Laurie, 1997; Worland et al., 1998; Wilhelm et al., 2009; Chen et al., 2013). The physical position of *QFlt.dms-5A.3* (576.3 Mb) associated with flowering time recorded in Mord-2017 was ~11 Mb away from the *Vrn-A1* (*TraesCS5A02G391700*) gene located at 587.4–590.4 Mb depending on the version of the IWGSC RefSeq. Of the five SNPs associated with *QFlt.dms-5B* (553.0–574.4 Mb) in the Mord-2017, the physical positions of both Tdurum_contig32812_325 and BS00022000_51 were 0.6 Mb away from *Vrn-B1* (*TraesCS5B02G396600*) that is located at 573.8–577.1 Mb. Similarly, the position of *QFlt.dms-5D.3* (467.0 Mb) associated with Mord-2017 was 0.1 Mb away from the *Vrn-D1* (*TraesCS5D02G401500*) that is located at 467.1–470.0 Mb. However, the positions of none of the flowering time QTLs discovered in the present study were near the *Ppd-A1*, *Ppd-B1*, and *Ppd-D1* genes.

Flowering time, plant height, and/or anther extrusion/retention have often shown a significant negative correlation with FHB resistance (Miedaner and Voss, 2008; Skinnes et al., 2010; Lu et al., 2011; Lu et al., 2013; Buerstmayr and Buerstmayr, 2016; He et al., 2016; Ruan et al., 2020). For those reasons, the positions of several QTLs associated with FHB resistance overlapped with plant height and/or flowering time QTLs in multiple wheat populations (McCartney et al., 2016; Prat et al., 2017; Ruan et al., 2020; Zhang et al., 2020b). In the combined analysis of all environments, the physical position of FHB resistance QTL on chromosome 7A (*QFhb.dms-7A.1*) overlapped with the flowering time QTL (*QFlt.dms-7A.1*) and another FHB resistance QTL on 6A (*QFhb.dms-6A.4*) overlapped with a plant height QTL (*QPht.dms-6A.2*) (Table 2; Figure 4; Supplementary Figure S3). Liu and colleagues identified eight QTLs associated with five different FHB traits in a biparental population derived from the cross VA00W-38 × Pioneer brand 26R46 of which four coincided with flowering time QTLs (Liu et al., 2012). Colocalization of FHB resistance and plant height QTLs have also been reported on 14 wheat chromosomes (Buerstmayr et al., 2020), which could be due to the pleiotropic effect or tight linkage (Tuberosa et al., 2002; Martinez et al., 2021). The physical positions of the remaining fourteen FHB resistance QTLs identified in the combined environments were different from those QTLs associated with plant height and flowering time.

QFhb.dms-3B.1 was one of the QTLs that accounted for 6.5–10.2% of disease incidence, severity, and VRI (Table 2). *QFhb.dms-3B.*1 is likely the same as the *Fhb1* (syn. *Qfhs.ndsu-3BS*) gene that originated from Sumai 3 (Anderson et al., 2001; Liu and Anderson, 2003) for two reasons. First, the physical positions of *Fhb1* reported in the literature varied from 8 Mb to 21 Mb (Brar et al., 2019a), which overlapped with the 10.2–23.5 Mb interval for *QFhb.dms-3B.*1 (Table 2). Second, one of a cluster of SNPs significantly associated with *QFhb.dms-3B.1* in the present study was wMAS000009, which is a KASP marker developed from UMN10_SNP to introgress the *Fhb1* resistance allele through marker-assisted selection (Liu et al., 2008). Lines and varieties that were homozygous for GG at wMAS000009 had on average 18.4%, 34.8%, and 14.3% less disease incidence, severity, and VRI, respectively, than those that were homozygous for AA. Further study in biparental populations is needed to narrow the physical position of *QFhb.dms-3B.1* and determine specific allele(s) present in the Canadian sping wheat panel. Although *Fhb1* is the most consistent and the best source of resistance to a broad spectrum of *Fusarium* species (Anderson et al., 2001; Liu and Anderson, 2003), the phenotypic variance explained by this gene is highly erratic (3–60%) depending on the genetic background (Anderson et al., 2001; Buerstmayr et al., 2002; Bernardo et al., 2012; Wu et al., 2019; Zhang et al., 2020b).

Both *Qfhs.ifa-5A* (Buerstmayr et al., 2003) and *Qfhi.nau-5A* (Lin et al., 2006; Xue et al., 2011) have been reported as major FHB resistance QTLs on chromosome 5A and have been given *Fhb5* gene designation. The position of *Fhb5* ranged from 46 Mb to 111 Mb depending on the flanking markers (Brar et al., 2019a). For example, BS00045284_51 located at 110.8 Mb on 5A was one of the SNPs significantly associated with both VRI and disease incidence in two backcross populations derived from CDC Go*4/04GC0139 and CDC Alsask*4/04GC0139. We uncovered two QTLs associated with disease incidence, severity, and VRI (*QFhb.dms-5A.5* and *QFhb.dms-5A.7*) plus a third QTL (*QFhb.dms-5A.6*) located at 414.2–522.7 Mb, 683.3–710.1 Mb, and 596.2–617.2 Mb, respectively (Table 2). However, the positions of these three QTLs are far from the *Fhb5* gene. Several other FHB resistance QTLs have also been reported on chromosome 5A, including interspecific populations (Ollier et al., 2020), a durum wheat population derived from Joppa/10Ae564(Zhao et al., 2018a), a RIL population derived from Ningmai 9/Yangmai 158 (Jiang et al., 2020) between IAAV5294 and BS00060445_51 SNP markers. The IWGSC RefSeq v2.0 positions of both IAAV5294 and BS00060445_51 is 503.7 Mb, which overlaps with *QFhb.dms-5A.5* identified in the present study. In a Canadian DH spring wheat population derived from FL62R1/Stettler, a QTL that accounted for 6.3% of FHB resistance has been reported between BS00036839_51 and BobWhite_c2236_111 on 5A (Zhang et al., 2018) located at 397.6–445.4 Mb, which again overlaps with the *QFhb.dms-5A.5*.

Brar et al. (2019a) reported a QTL associated with disease incidence, severity, VRI, and deoxynivalenol (DON) accumulation (*Qfhb.ndwp-6A*) at 602.5–611.8 Mb on chromosome 6A, which accounted for 3.3–9.4% of the phenotypic variance in CDC Alsask/CDC Go near-isogenic lines. The position of *Qfhb.ndwp-6A* overlapped with another QTL reported in a RIL population derived from the cross of ND2603/Grandin population (Zhao et al., 2018b). In the present study, *QFhb.dms-6A.4* was located at 597.6–609.4 Mb (Table 2), which overlaps with that of *Qfhb.ndwp-6A* reported in the CDC Alsask/CDC Go and ND2603/Grandin populations. Other studies conducted in wheat have also reported QTLs on chromosome 6A that were associated with disease

incidence, severity, and DON accumulation in a winter wheat population derived from NC-Neuse/AGS 2000 (Petersen et al., 2016), disease severity in a winter wheat population derived from Dream/Lynx (Schmolke et al., 2005), and a spring wheat population derived from Surpresa/Wheaton (Poudel et al., 2022).

QFhb.dms-2A.2 was mapped at 170.8 Mb and was associated with disease incidence and VRI in the combined environments (Table 2). Several previous studies reported FHB resistance QTLs on chromosome 2A (Semagn et al., 2007; Zhang et al., 2014; Giancaspro et al., 2016; Sari et al., 2018; Zhang et al., 2018; Gadaleta et al., 2019; Tamburic-Ilincic and Rosa, 2019; Zhang et al., 2020b), including *QFhb.mgb-2A* between IWB43373 (syn. Kukri_c27040_309) and IWB63138 (syn. RAC875_rep_c78744_228) (Giancaspro et al., 2016; Gadaleta et al., 2019). Kukri_c27040_309 and RAC875_rep_c78744_228 are located at 35.0 and 36.5 Mb, respectively (Supplementary Table S2), which is more than 134 Mb away from *QFhb.dms-2A.2*. In Canada, FHB resistance QTL on 2A has also been reported at 37–55 Mb in two DH spring wheat populations derived from the cross of FL62R1/Stettler and FL62R1/Muchmore (Zhang et al., 2018; Zhang et al., 2020b), which is also very far from the position of *QFhb.dms-2A.2* (Table 2). *QFhb.dms-2D.2* was mapped at 159.1 Mb on chromosome 2D and accounted for 6.9-8.6% of disease incidence and VRI in the combined environments (Table 2). FHB resistance QTLs have been reported on chromosome 2D in a winter wheat DH population derived from the cross of Maxine/FTHP Redeemer (Tamburic-Ilincic and Rosa, 2019), in a winter wheat population derived from the cross of Vienna/25R47 (Tamburic-Ilincic and Barcellos Rosa, 2017), and a DH spring wheat population derived from the cross of DH181/AC Foremost (Yang et al., 2005). *QFhb.dms-5B.8* was located at 640.0 Mb and accounted for 6.6–7.2% of the disease incidence and VRI in all combined environments (Table 2). FHB resistance QTLs on chromosome 5B have been reported at 448–583 Mb in the FL62R1/Stettler populations (Zhang et al., 2018; Zhang et al., 2020b) and *Qfhs.ndsu-5BL* in durum wheat (Ghavami et al., 2011). *QFhb.dms-5B.8* identified in the present study was, therefore, different from the two FHB resistance QTLs reported on 5B in previous studies.

FHB resistance sources

Canadian breeders have been able to develop several varieties with moderate-to-intermediate levels of FHB resistance through stepwise accumulations of resistant alleles originated primarily from the Brazilian cv. Frontana and the Chinese cv. Sumai 3 (Gilbert and Tekauz, 2000; Zhu et al., 2019). Frontana has been used as the primary source of resistance in the early stage of Canadian spring wheat breeding, which may have contributed to intermediate level of resistance in Katepwa, AC Barrie, AC Cora, CDC Bounty, Kane, and 5602HR (Gilbert and Tekauz, 2000; McCartney et al., 2016). Sumai 3 has contributed to the release of more than 20 modern varieties, including Cardale, Glenn, Faller, Prosper, AAC Brandon, AAC Elie, Cardale, Carberry, and CDC VR Morris (Zhu et al., 2019). Most varieties with Sumai 3 in their pedigrees displayed moderate-to-intermediate levels of FHB resistance as compared to the intermediate-to-moderate susceptibility of varieties derived from Frontana. Linkage drag is one of the major weakness of heavy dependence on a few exotic FHB resistance sources from Asia and South America, which introduced undesirable genes and QTLs that negatively affect agronomic traits, grain yield, end use quality traits, and susceptibility to other diseases (Brar et al., 2019a).

In the present study, we confirmed and/or identified new FHB resistance sources among the locally adapted spring wheat varieties/lines by evaluating them using the same method and at the same environments. Of the 249 lines/varieties evaluated for FHB reactions, only 2.4% of them displayed a high level of resistance and 13.6% a moderate level of resistance as compared with 60% of them that showed moderate to high levels of FHB susceptibility (Supplementary Table S1). We used the VRI of the check varieties/lines with modified threshold values described in previous studies (Yan et al., 2020; Yan et al., 2022) to assign each tested variety/line to the different resistance categories. In contrast to Yan et al. (2020, 2022) who classified entries with a VRI of< 10% into highly resistant and 10-25% as moderately resistant, we considered lines and varieties with a VRI of <7% as highly resistant and those with 10-20% as moderately resistant. The proportion of lines and varieties that were considered highly and moderately resistant agree with a previous study that reported 2.3%, 15.5%, 41.1%, and 41.1% of the wheat samples that expressed high resistance, moderate resistance, moderate susceptibility, and high susceptibility, respectively (Yan et al., 2020). Of a total of 302 Chinese wheat cultivars released from 2005 to 2016, about 96% of them were either moderately susceptible or highly susceptible to FHB and only 4% were moderately resistant to the disease (Ma et al., 2019).

AAC Proclaim (CWSP), AAC Tenacious (CPSR), BW5064 (CWRS), and NH018 (CNHR) were the only varieties that displayed a good level of FHB resistance with an overall VRI of <7%. AAC Proclaim and AAC Tenacious were developed from the cross FHB37/AC Reed (Randhawa et al., 2015) and HY665/BW346 (Brown et al., 2015), respectively, and are characterized by resistance to FHB. Using a DH population derived from the cross AAC Innova/AAC Tenacious, Dhariwal et al. (2020) reported five FHB resistance QTLs that originated from AAC Tenacious at 253.4 Mb on chromosome 2B (*QFhi.lrdc-2B*), at 36.2 Mb (*QFhs.lrdc-2D.1*) and 555.1 Mb (*QFhs.lrdc-2D.2*) on 2D, 279.5 Mb on 5D (*QFhi.lrdc-5D*), and 673.7 Mb on 7A (*QFhi.lrdc-7A*). Comparative histological and transcriptomic analyses performed in AAC Tenacious and a susceptible control (Roblin) following inoculation with *F. graminearum* revealed a restricted infection at the point of inoculation (POI) as compared with a severe infection observed in Robin florets, which was due to a significant cell wall thickening within the rachis node below the POI, and activation of genes putatively involved in cell wall modification and defense response (Nilsen et al., 2021).

Thirty-three varieties and lines expressed a moderate level of VRI based on all seven combined environments (Supplementary Table S1) of which twelve (BW278, BW5018, PT256, PT479, PT788, FL62R1, BW1039, BYT14-19, GP184, PT5002, PT790, PT792) were unregistered lines and twenty-one (5603HR, 5604HR CL, 5605HR CL, AAC Brandon, AAC Penhold, AAC Russell, AAC Tisdale, Carberry, Cardale, Donalda, Faller, Glenn, PT771, Rednet, SY433, SY Brawn, SY Chert, SY Rowyn,

SY087, Vesper, and WR859 CL) were registered varieties. In previous studies, sixteen of the 25 lines and varieties expressed different levels of resistance to FHB, although they were not simultaneously evaluated for their reaction using the same inoculation method in the same environments. Three of the varieties (5603HR, 5604HR CL, and 5605HR CL) were developed by Syngenta Canada Inc. from a cross of McKenzie//FHB5227/Lars, AC Barrie//Butte86*4/FS4/3/CDC Teal/4/McKenzie/5/(BW288) AC Domain*2/AC Cora, and 99S2232-10 and 99S3228-4, respectively (https://inspection.canada.ca/; accessed 3 May 2023). AAC Brandon was developed from a cross of Superb/CDC Osler//ND744 and expressed moderate resistance to FHB (Cuthbert et al., 2016). AAC Tisdale (PT250) was derived from a cross of Somerset/BW865//Waskada and expressed a moderate level of FHB resistance and low DON accumulation (https://ensqualityseed.com/wp-content/uploads/2021/01/AAC-Tisdale-CWRS.pdf, accessed 23 Feb2023). Carberry was developed from the cross Alsen/Superb and expressed a moderate resistance to FHB (DePauw et al., 2011). Cardale was derived from the cross McKenzie/Alsen and expressed moderate level of resistance to FHB (Fox et al., 2013) originated from Alsen that has Sumai 3 in its pedigree (Zhu et al., 2019). Donalda was developed by the University of Alberta from a cross of Peace/Carberry and displayed an intermediate to moderate levels of FHB resistance (Spaner et al., 2022). Glenn originated from the cross ND 2831/Steele-ND and expressed moderate resistance to FHB (http://ndsuresearchfoundation.org/files/pdf/Ag%20Brochures/Glenn_brochure.pdf; accessed 23 Feb 2023). SY433 (BW433) originated from a cross BW275W/N99-2587 and expressed moderate resistance to FHB (https://inspection.canada.ca/english/plaveg/pbrpov/cropreport/whe/app00008453e.shtml; accessed 23 Feb 2023). WR859 CL was developed from a cross of BW267/3/(97S2199-105-1) AC Barrie//Butte 86*4/FS4 and expressed moderate resistance to FHB (https://inspection.canada.ca/english/plaveg/pbrpov/cropreport/whe/app00007331e.shtml; accessed 23Feb2023). PT771 was developed from the cross of Lovitt//Ning 8331/BiggarBSR/3/BW297 and expressed resistance to FHB originating from Ning 8331 (Spaner et al., 2014). Variety 5604HR CL was developed from the cross AC Barrie//Butte86*4/FS4/3/CDC Teal/4/McKenzie/5/(BW288) AC Domain*2/AC Cora, and has shown moderate susceptibility to FHB (https://inspection.canada.ca/english/plaveg/pbrpov/cropreport/whe/app00007753e.shtml; accessed 23 Feb 2023).

Faller was developed from the cross ND2710/ND688/3/Kitt/Amidon//Grandin/Stoa Sib and expressed intermediate resistance to FHB (https://www.fosterag.ca/seed-products/cereals/31-faller; accessed 23 Feb 2023). Vesper was derived from a cross between female F_1s (Augusta/Hard White Alpha//3*AC Barrie) and male F_1s (BW150*2//Tp/Tm/3/2*Superb/4/94B35-R5C/5/Superb), and expressed moderate resistance to FHB (Thomas et al., 2013). AAC Penhold was developed from the cross 5700PR/HY644-BE//HY469 and expressed moderate resistance to FHB (Cuthbert et al., 2017). SY Rowyn was developed from the cross 00S0323-7/N92-0098/99S0051-3-1 and expressed moderately resistant to moderately susceptible to FHB (https://inspection.canada.ca/english/plaveg/pbrpov/cropreport/whe/app00010368e.shtml; accessed 23 Feb 2023). SY087 was developed from the cross between BW361/Alsen and expressed moderate resistance to FHB (https://www.topcropmanager.com/new-cereal-varieties-update-19624/, accessed 23 Feb 2023). FL62R1 is an Eastern Canada hard red spring wheat line derived from a four-way cross involving QG22.24/Alsen//SS Blomidon/Alsen (Comeau et al., 2008; Zhang et al., 2020b). FL62R1 carry both *Fhb1* and *FHb5* genes (Zhang et al., 2018) but expressed different levels of FHB resistance across different studies, including moderate resistance in the present study (Figure 5), moderate susceptibility (Zhang et al., 2020b), and high resistance nearly comparable with Sumai 3 (Comeau et al., 2008).

The phylogenetic tree constructed from the 401 SNPs that were associated with FHB resistance in individual and combined environments showed a cluster that consisted of AAC Penhold, WR859 CL, BW278, Glenn, SY087, Faller, AAC Brandon, AAC Tenacious, AAC Proclaim, FL62R1, and Sumai 3 (Supplementary Figure S5). AAC Proclaim is related to Sumai 3 in its pedigree because it was derived using FHB37 (HY611/Ning 8331) as one of the parents with Ning 8331 being a Sumai 3 derivative. AAC Tenacious likely carry FHB resistance from one of its moderately resistant progenitor (grandparent) cv. Neepawa (through the male parent BW346) and its FHB-resistant female parent HY665 (Brown et al., 2015). Glenn, Faller, and AAC Brandon inherited FHB resistance from Sumai 3 (Zhu et al., 2019).

All selected varieties and lines are well adapted to western Canada growing conditions and would be valuable resources to further improve the level of FHB resistance through stepwise accumulations of resistant alleles from multiple sources. The University of Alberta breeding program has developed multiple populations using the newly identified resistant sources for selection against *F. graminearum*. Examples include FL62R1/Cardale//5603HR, FL62R1/Cardale//Waskada, PT771/Cardale//Waskada, AAC Tenacious//PT771/Cardale, AAC Tenacious/Cardale, FL62R1/Cardale//Carberry, PT771/Cardale//FL62R1/Cardale, PT771/Cardale//PT588, PT771/Cardale//PT584, PT771/Cardale//Carberry, PT771/Cardale//Cardale, and Cardale//FL62R1/PT584.

Conclusion

The present study contributed to the identification of new sources of FHB resistance and the associated QTLs in historical and modern Canadian spring wheat varieties and lines. The four varieties and lines that expressed a high level of VRI and the thirty-three varieties and lines that expressed a moderate level of resistance, and the sixteen FHB resistant QTLs provide additional information and data to wheat breeders to develop modern varieties with an enhanced level of FHB resistance in western Canada. Seven of the sixteen FHB resistance QTLs (*QFhb.dms-3B.1*, *QFhb.dms-5A.5*, *QFhb.dms-5A.7*, *QFhb.dms-6A.4*, *QFhb.dms-2A.2*, *QFhb.dms-2D.2*, and *QFhb.dms-5B.8*) are of particular importance as they were associated with disease incidence, visual rating index, and/or disease severity in the overall combined environments and up to five out of the seven tested environments. Two of the sixteen FHB resistance QTLs coincided with flowering time or plant height and the remaining fourteen were physically far from QTLs associated with both agronomic traits.

Data availability statement

The original contributions presented in the study are included in the article/Supplementary Material. Further inquiries can be directed to the corresponding authors.

Author contributions

KSe, MI, MH, and DS designed the study. KSe analyzed the data and drafted the paper. AB-B and DS acquired funding. MH, KSt, IC, AB-B, and AN evaluated the germplasm. AN'D and CP genotyped the germplasm with the Wheat 90K iSelect array. All authors contributed to the article and approved the submitted version.

Funding

This study was supported by grants to the University of Alberta wheat breeding program from the Alberta Crop Industry Development Fund (ACIDF), Canadian Wheat Research Coalition (Alberta Wheat Commission, Saskatchewan Wheat Development Commission, and Manitoba Crop Alliance), Natural Sciences and Engineering Research Council of Canada (NSERC) Discovery and Collaborative Grant, Agriculture and Agri-Food Canada (AAFC), Western Grains Research Foundation Endowment Fund (WGRF), Results Driven Agriculture Research (RDAR), and Core Program Check-off funds to DS. The FHB evaluation at the University of Manitoba was financed by the Western Grains Research Foundation Endowment check-off fund to AB-B.

Acknowledgments

The authors would like to express appreciation for the field staff at the Morden Research and Development Centre, the University of Guelph (Elora Research Station), and Roger Larios at the University of Manitoba for phenotype data collection.

Conflict of interest

The authors declare that the research was conducted in the absence of any commercial or financial relationships that could be construed as a potential conflict of interest.

Publisher's note

Supplementary material

The Supplementary Material for this article can be found online at: https://www.frontiersin.org/articles/10.3389/fpls.2023.1190358/full#supplementary-material

References

Alemu, A., Brazauskas, G., Gaikpa, D. S., Henriksson, T., Islamov, B., Jørgensen, L. N., et al. (2021). Genome-wide association analysis and genomic prediction for adult-plant resistance to Septoria tritici blotch and powdery mildew in winter wheat. *Front. Genet.* 12, 661742. doi: 10.3389/fgene.2021.661742

Alvarado, G., Rodríguez, F. M., Pacheco, A., Burgueño, J., Crossa, J., Vargas, M., et al. (2020). META-R: A software to analyze data from multi-environment plant breeding trials. *Crop J.* 8, 745–756. doi: 10.1016/j.cj.2020.03.010

Anderson, J. A., Stack, R. W., Liu, S., Waldron, B. L., Fjeld, A. D., Coyne, C., et al. (2001). DNA markers for Fusarium head blight resistance QTLs in two wheat populations. *Theor. Appl. Genet.* 102, 1164–1168. doi: 10.1007/s001220000509

Bai, G., and Shaner, G. (2004). Management and resistance in wheat and barley to Fusarium head blight. *Annu. Rev. Phytopathol.* 42, 135–161. doi: 10.1146/annurev.phyto.42.040803.140340

Bamforth, J., Chin, T., Ashfaq, T., Gamage, N. W., Pleskach, K., Tittlemier, S. A., et al. (2022). A survey of Fusarium species and ADON genotype on Canadian wheat grain. *Front. Fungal Biol.* 3, 1062444. doi: 10.3389/ffunb.2022.1062444

Bergstrom, G. C., Waxman, K. D., Bradley, C. A., Hazelrig, A. L., Hershman, D. E., Nagelkirk, M., et al. (2011). "Effects of local corn debris management on FHB and DON levels in seven U.S. wheat environments in 2011," in *National Fusarium Head Blight Forum*. Eds. S. Canty, A. Clark, S. A. Anderson and D. Van Sanford (Lansing, MI, USA: U.S. Wheat & Barley Scab Initiative and ASAP Printing, Inc), 119–121.

Bernardo, A. N., Ma, H. X., Zhang, D. D., and Bai, G. H. (2012). Single nucleotide polymorphism in wheat chromosome region harboring Fhb1 for Fusarium head blight resistance. *Mol. Breed.* 29, 477–488. doi: 10.1007/s11032-011-9565-y

Bradbury, P. J., Zhang, Z., Kroon, D. E., Casstevens, T. M., Ramdoss, Y., and Buckler, E. S. (2007). TASSEL: software for association mapping of complex traits in diverse samples. *Bioinformatics* 23, 2633–2635. doi: 10.1093/bioinformatics/btm308

Brar, G. S., Brûlé-Babel, A. L., Ruan, Y., Henriquez, M. A., Pozniak, C. J., Kutcher, H. R., et al. (2019a). Genetic factors affecting Fusarium head blight resistance improvement from introgression of exotic Sumai 3 alleles (including Fhb1, Fhb2, and Fhb5) in hard red spring wheat. *BMC Plant Biol.* 19, 179. doi: 10.1186/s12870-019-1782-2

Brar, G. S., Fetch, T., McCallum, B. D., Hucl, P. J., and Kutcher, H. R. (2019b). Virulence dynamics and breeding for resistance to stripe, stem, and leaf rust in Canada since 2000. *Plant Dis.* 103, 2981–2995. doi: 10.1094/PDIS-04-19-0866-FE

Brown, P. D., Randhawa, H. S., Fetch, J. M., Meiklejohn, M., Fox, S. L., Humphreys, D. G., et al. (2015). AAC Tenacious red spring wheat. *Can. J. Plant Sci.* 95, 805–810. doi: 10.4141/cjps-2015-011

Buerstmayr, M., and Buerstmayr, H. (2016). The semidwarfing alleles Rht-D1b and Rht-B1b show marked differences in their associations with anther-retention in wheat heads and with fusarium head blight susceptibility. *Phytopathology* 106, 1544–1552. doi: 10.1094/PHYTO-05-16-0200-R

Buerstmayr, H., Lemmens, M., Hartl, L., Doldi, L., Steiner, B., Stierschneider, M., et al. (2002). Molecular mapping of QTLs for Fusarium head blight resistance in spring wheat. I. Resistance to fungal spread (type II resistance). *Theor. Appl. Genet.* 104, 84–91. doi: 10.1007/s001220200009

Buerstmayr, M., Steiner, B., and Buerstmayr, H. (2020). Breeding for Fusarium head blight resistance in wheat—Progress and challenges. *Plant Breed.* 139, 429–454. doi: 10.1111/pbr.12797

Buerstmayr, H., Steiner, B., Hartl, L., Griesser, M., Angerer, N., Lengauer, D., et al. (2003). Molecular mapping of QTLs for Fusarium head blight resistance in spring wheat. II. Resistance to fungal penetration and spread. *Theor. Appl. Genet.* 107, 503–508. doi: 10.1007/s00122-003-1272-6

Chen, F., Gao, M., Zhang, J., Zuo, A., Shang, X., and Cui, D. (2013). Molecular characterization of vernalization and response genes in bread wheat from the Yellow and Huai Valley of China. *BMC Plant Biol.* 13, 199. doi: 10.1186/1471-2229-13-199

Clear, R. M., and Patrick, S. K. (1990). Fusarium species isolated from wheat samples containing tombstone (scab) kernels from Ontario, Manitoba, and Saskatchewan. *Can. J. Plant Sci.* 70, 1057–1069. doi: 10.4141/cjps90-128

Comeau, A., Langevin, F., Caetano, V. R., Haber, S., Savard, M. E., Voldeng, H., et al. (2008). A systemic approach for the development of fhb resistant germplasm accelerates genetic progress. *Cereal Res. Commun.* 36, 5–9. doi: 10.1556/CRC.36.2008.Suppl.B.2

Cuthbert, R. D., DePauw, R. M., Knox, R. E., Singh, A. K., McCaig, T. N., McCallum, B., et al. (2016). AAC Brandon hard red spring wheat. *Can. J. Plant Sci.* 97, 393–401. doi: 10.1139/CJPS-2016-0150

Cuthbert, R. D., DePauw, R. M., Knox, R. E., Singh, A. K., McCaig, T. N., McCallum, B., et al. (2017). AAC penhold Canada prairie spring red wheat. *Can. J. Plant Sci.* 98, 207–214. doi: 10.1139/CJPS-2017-0186

Del Ponte, EM, Fernandes, JMC, and Bergstrom, GC (2007). Influence of growth stage on Fusarium Head Blight and deoxynivalenol production in wheat. *J Phytopathology* 155:577–581. doi: 10.1111/j.1439-0434.2007.01281.x

DePauw, R. M., Knox, R. E., McCaig, T. N., Clarke, F. R., and Clarke, J. M. (2011). Carberry hard red spring wheat. *Can. J. Plant Sci.* 91, 529–534. doi: 10.4141/cjps10187

Dhariwal, R., Henriquez, M. A., Hiebert, C., McCartney, C. A., and Randhawa, H. S. (2020). Mapping of major Fusarium head blight resistance from Canadian wheat cv. AAC Tenacious. *Int. J. Mol. Sci.* 21, 4497. doi: 10.3390/ijms21124497

Fox, S. L., Humphreys, D. G., Brown, P. D., McCallum, B. D., Fetch, T. G., Menzies, J. G., et al. (2013). Cardale hard red spring wheat. *Can. J. Plant Sci.* 93, 307–313. doi: 10.4141/cjps2012-236

Gadaleta, A., Colasuonno, P., Giove, S. L., Blanco, A., and Giancaspro, A. (2019). Map-based cloning of QFhb.mgb-2A identifies a WAK2 gene responsible for Fusarium Head Blight resistance in wheat. *Sci. Rep.* 9, 6929. doi: 10.1038/s41598-019-43334-z

Ghavami, F., Elias, E. M., Mamidi, S., Ansari, O., Sargolzaei, M., Adhikari, T., et al. (2011). Mixed model association mapping for fusarium head blight resistance in Tunisian-derived durum wheat populations. *G3 (Bethesda)* 1, 209–218. doi: 10.1534/g3.111.000489

Giancaspro, A., Giove, S. L., Zito, D., Blanco, A., and Gadaleta, A. (2016). Mapping QTLs for Fusarium head blight resistance in an interspecific wheat population. *Front. Plant Sci.* 7, 1381. doi: 10.3389/fpls.2016.01381

Gilbert, J., and Morgan, K. (2000). "Field-based rating of spring wheat infected with Fusarium graminearum, cause of Fusarium head blight," in *The 6th European Seminar on Fusarium—Mycotoxins, Taxonomy and Pathogenicity. MITTEILUNGEN-BIOLOGISCHEN BUNDESANSTALT FUR LAND UND FORSTWIRTSCHAFT*, Berlin, Germany, 11–16 September 2000. 73.

Gilbert, J., and Tekauz, A. (2000). Review: Recent developments in research on fusarium head blight of wheat in Canada. *Can. J. Plant Pathol.* 22, 1–8. doi: 10.1080/07060660009501155

Hales, B., Steed, A., Giovannelli, V., Burt, C., Lemmens, M., Molnár-Láng, M., et al. (2020). Type II Fusarium head blight susceptibility conferred by a region on wheat chromosome 4D. *J. Exp. Bot.* 71, 4703–4714. doi: 10.1093/jxb/eraa226

He, X., Singh, P. K., Dreisigacker, S., Singh, S., Lillemo, M., and Duveiller, E. (2016). Dwarfing genes Rht-B1b and Rht-D1b are associated with both type I FHB susceptibility and low anther extrusion in two bread wheat populations. *PloS One* 11, e0162499. doi: 10.1371/journal.pone.0162499

Hu, W., Gao, D., Wu, H., Liu, J., Zhang, C., Wang, J., et al. (2020). Genome-wide association mapping revealed syntenic loci QFhb-4AL and QFhb-5DL for Fusarium head blight resistance in common wheat (Triticum aestivum L.). *BMC Plant Biol.* 20, 29. doi: 10.1186/s12870-019-2177-0

Iqbal, M., Semagn, K., Jarquin, D., Randhawa, H., McCallum, B. D., Howard, R., et al. (2022). Identification of disease resistance parents and genome-wide association mapping of resistance in spring wheat. *Plants* 11, 2905. doi: 10.3390/plants11212905

Iqbal, M., Semagn, K., Randhawa, H., Aboukhaddour, R., Ciechanowska, I., Strenzke, K., et al. (2023). Identification and characterization of stripe rust, leaf rust, leaf spot, and common bunt resistance in spring wheat. *Crop Sci* 63:2310–2328. doi: 10.1002/csc2.20953

Jiang, P., Zhang, X., Wu, L., He, Y., Zhuang, W., Cheng, X., et al. (2020). A novel QTL on chromosome 5AL of Yangmai 158 increases resistance to Fusarium head blight in wheat. *Plant Pathol.* 69, 249–258. doi: 10.1111/ppa.13130

Jones, B., and Sall, J. (2011). JMP statistical discovery software. *Wiley Interdiscip Rev. Comput. Stat.* 3, 188–194. doi: 10.1002/wics.162

Laurie, D. A. (1997). Comparative genetics of flowering time. *Plant Mol. Biol.* 35, 167–177. doi: 10.1023/A:1005726329248

Lillemo, M., Asalf, B., Singh, R. P., Huerta-Espino, J., Chen, X. M., He, Z. H., et al. (2008). The adult plant rust resistance loci Lr34/Yr18 and Lr46/Yr29 are important determinants of partial resistance to powdery mildew in bread wheat line Saar. *Theor. Appl. Genet.* 116, 1155–1166. doi: 10.1007/s00122-008-0743-1

Lin, F., Xue, S. L., Zhang, Z. Z., Zhang, C. Q., Kong, Z. X., Yao, G. Q., et al. (2006). Mapping QTL associated with resistance to Fusarium head blight in the Nanda2419 x Wangshuibai population. II: Type I resistance. *Theor. Appl. Genet.* 112, 528–535. doi: 10.1007/s00122-005-0156-3

Liu, S., and Anderson, J. A. (2003). Marker assisted evaluation of fusarium head blight resistant wheat germplasm. *Crop Sci.* 43, 760–766. doi: 10.2135/cropsci2003.7600

Liu, S., Christopher, M. D., Griffey, C. A., Hall, M. D., Gundrum, P. G., and Brooks, W. S. (2012). Molecular characterization of resistance to Fusarium head blight in U.S. soft red winter wheat breeding line VA00W-38. *Crop Sci.* 52, 2283–2292. doi: 10.2135/cropsci2012.03.0144

Liu, S., Pumphrey, M. O., Gill, B. S., Trick, H. N., Zhang, J. X., Dolezel, J., et al. (2008). Toward positional cloning of Fhb1, a major QTL for Fusarium head blight resistance in wheat. *Cereal Res. Commun.* 36, 195–201. doi: 10.1556/CRC.36.2008.Suppl.B.15

Lu, Q., Lillemo, M., Skinnes, H., He, X., Shi, J., Ji, F., et al. (2013). Anther extrusion and plant height are associated with Type I resistance to Fusarium head blight in bread wheat line 'Shanghai-3/Catbird'. *Theor. Appl. Genet.* 126, 317–334. doi: 10.1007/s00122-012-1981-9

Lu, Q., Szabo-Hever, A., Bjørnstad, Å, Lillemo, M., Semagn, K., Mesterhazy, A., et al. (2011). Two major resistance quantitative trait loci are required to counteract the increased susceptibility to Fusarium head blight of the Rht-D1b dwarfing gene in wheat. *Crop Sci.* 51, 2430–2438. doi: 10.2135/cropsci2010.12.0671

Ma, H., Zhang, X., Yao, J., and Cheng, S. (2019). Breeding for the resistance to Fusarium head blight of wheat in China. *Front. Agric. Sci. Eng.* 6, 251–264. doi: 10.15302/J-FASE-2019262

Martinez, A. F., Lister, C., Freeman, S., Ma, J., Berry, S., Wingen, L., et al. (2021). Resolving a QTL complex for height, heading, and grain yield on chromosome 3A in bread wheat. *J. Exp. Bot.* 72, 2965–2978. doi: 10.1093/jxb/erab058

McCartney, C. A., Brûlé-Babel, A. L., Fedak, G., Martin, R. A., McCallum, B. D., Gilbert, J., et al. (2016). Fusarium head blight resistance QTL in the spring wheat cross Kenyon/86ISMN 2137. *Front. Microbiol.* 7, 1542. doi: 10.3389/fmicb.2016.01542

Mesterházy, A. (1995). Types and components of resistance to Fusarium head blight of wheat. *Plant Breed.* 114, 377–386. doi: 10.1111/j.1439-0523.1995.tb00816.x

Mesterhazy, A. (2020). Updating the breeding philosophy of wheat to fusarium head blight (Fhb): Resistance components, qtl identification, and phenotyping—a review. *Plants* 9, 1–33. doi: 10.3390/plants9121702

Miedaner, T., and Voss, H. H. (2008). Effect of dwarfing Rht genes on Fusarium head blight resistance in two sets of near-isogenic lines of wheat and check cultivars. *Crop Sci.* 48, 2115–2122. doi: 10.2135/cropsci2008.02.0107

Nilsen, K. T., Walkowiak, S., Kumar, S., Molina, O. I., Randhawa, H. S., Dhariwal, R., et al. (2021). Histology and RNA sequencing provide insights into Fusarium head blight resistance in AAC Tenacious. *Front. Plant Sci.* 11, 570418. doi: 10.3389/fpls.2020.570418

Okada, T., Jayasinghe, JEARM, Eckermann, P., Watson-Haigh, N. S., Warner, P., Hendrikse, Y., et al. (2019). Effects of Rht-B1 and Ppd-D1 loci on pollinator traits in wheat. *Theor. Appl. Genet.* 132, 1965–1979. doi: 10.1007/s00122-019-03329-w

Ollier, M., Talle, V., Brisset, A. L., Le Bihan, Z., Duerr, S., Lemmens, M., et al. (2020). QTL mapping and successful introgression of the spring wheat-derived QTL Fhb1 for Fusarium head blight resistance in three European triticale populations. *Theor. Appl. Genet.* 133, 457–477. doi: 10.1007/s00122-019-03476-0

Pandurangan, S., Nilsen, K. T., and Kumar, S. (2020). Validation of a SNP-KASP marker for the Fusarium head blight resistance quantitative trait loci on chromosome 5AS. *Can. J. Plant Sci.* 101, 135–139. doi: 10.1139/cjps-2020-0099

Petersen, S., Lyerly, J. H., Maloney, P. V., Brown-Guedira, G., Cowger, C., Costa, J. M., et al. (2016). Mapping of Fusarium head blight resistance quantitative trait loci in winter wheat cultivar NC-Neuse. *Crop Sci.* 56, 1473–1483. doi: 10.2135/cropsci2015.05.0312

Poudel, B., Mullins, J., Puri, K. D., Leng, Y., Karmacharya, A., Liu, Y., et al. (2022). Molecular mapping of quantitative trait loci for fusarium head blight resistance in the Brazilian spring wheat cultivar "Surpresa". *Front. Plant Sci.* 12, 778472. doi: 10.3389/fpls.2021.778472

Prat, N., Guilbert, C., Prah, U., Wachter, E., Steiner, B., Langin, T., et al. (2017). QTL mapping of Fusarium head blight resistance in three related durum wheat populations. *Theor. Appl. Genet.* 130, 13–27. doi: 10.1007/s00122-016-2785-0

PRCWRT (2020). The Prairie recommending committee for wheat, rye and triticale (PRCWRT) operating procedures. *Can. Food Inspection Agency (CFIA)*, 1–62.

Randhawa, H. S., Graf, R. J., Fox, S. L., and Sadasivaiah, R. S. (2015). AAC proclaim general purpose spring wheat. *Can. J. Plant Sci.* 95, 1265–1269. doi: 10.4141/cjps-2015-006

Ruan, Y., Zhang, W., Knox, R. E., Berraies, S., Campbell, H. L., Ragupathy, R., et al. (2020). Characterization of the genetic architecture for Fusarium head blight resistance in durum wheat: the complex association of resistance, flowering time, and height genes. *Front. Plant Sci.* 11, 592064. doi: 10.3389/fpls.2020.592064

Sari, E., Berraies, S., Knox, R. E., Singh, A. K., Ruan, Y., Cuthbert, R. D., et al. (2018). High density genetic mapping of Fusarium head blight resistance QTL in tetraploid wheat. *PloS One* 13, e0204362. doi: 10.1371/journal.pone.0204362

Sari, E., Knox, R. E., Ruan, Y., Henriquez, M. A., Kumar, S., Burt, A. J., et al. (2020). Historic recombination in a durum wheat breeding panel enables high-resolution mapping of Fusarium head blight resistance quantitative trait loci. *Sci. Rep.* 10, 7567. doi: 10.1038/s41598-020-64399-1

Schmolke, M., Zimmermann, G., Buerstmayr, H., Schweizer, G., Miedaner, T., Korzun, V., et al. (2005). Molecular mapping of Fusarium head blight resistance in the winter wheat population Dream/Lynx. *Theor. Appl. Genet.* 111, 747–756. doi: 10.1007/s00122-005-2060-2

Schroeder, H. W., and Christensen, J. J. (1963). Factors affecting resistance of wheat to scab caused by Gibberella zeae. *Phytopathology* 53, 831–838.

Semagn, K., Bjornstad, A., Skinnes, H., Maroy, A. G., Tarkegne, Y., and William, M. (2006). Distribution of DArT, AFLP, and SSR markers in a genetic linkage map of a doubled-haploid hexaploid wheat population. *Genome* 49, 545–555. doi: 10.1139/g06-002

Semagn, K., Iqbal, M., Alachiotis, N., N'Diaye, A., Pozniak, C., and Spaner, D. (2021). Genetic diversity and selective sweeps in historical and modern Canadian

spring wheat cultivars using the 90K SNP array. *Sci. Rep.* 11, 23773. doi: 10.1038/s41598-021-02666-5

Semagn, K., Iqbal, M., Jarquin, D., Crossa, J., Howard, R., Ciechanowska, I., et al. (2022a). Genomic predictions for common bunt, FHB, stripe rust, leaf rust, and leaf spotting resistance in spring wheat. *Genes* 13, 565. doi: 10.3390/genes13040565

Semagn, K., Iqbal, M., N'Diaye, A., Pozniak, C., Ciechanowska, I., Barbu, S.-P., et al. (2022b). Genome-wide association mapping of agronomic traits and grain characteristics in spring wheat under conventional and organic management systems. *Crop Sci.* 62, 1069–1087. doi: 10.1002/csc2.20739

Semagn, K., Skinnes, H., Bjornstad, A., Mary, A. G., and Tarkegne, Y. (2007). Quantitative trait loci controlling Fusarium head blight resistance and low deoxynivalenol content in hexaploid wheat population from 'Arina' and NK93604. *Crop Sci.* 47, 294–303. doi: 10.2135/cropsci2006.02.0095

Shah, L., Ali, A., Yahya, M., Zhu, Y., Wang, S., Si, H., et al. (2018). Integrated control of Fusarium head blight and deoxynivalenol mycotoxin in wheat. *Plant Pathol.* 67, 532–548. doi: 10.1111/ppa.12785

Singh, K., Batra, R., Sharma, S., Saripalli, G., Gautam, T., Singh, R., et al. (2021). WheatQTLdb: a QTL database for wheat. *Mol. Genet. Genomics* 296, 1051–1056. doi: 10.1007/s00438-021-01796-9

Skinnes, H., Semagn, K., Tarkegne, Y., Maroy, A. G., and Bjornstad, A. (2010). The inheritance of anther extrusion in hexaploid wheat and its relationship to Fusarium head blight resistance and deoxynivalenol content. *Plant Breed.* 129, 149–155. doi: 10.1111/j.1439-0523.2009.01731.x

Spaner, D., Iqbal, M., Strenzke, K., Ciechanowska, I., and Beres, B. (2022). Donalda hard red spring wheat. *Can. J. Plant Sci.* 102, 1067–1072. doi: 10.1139/cjps-2022-0094

Spaner, D., Navabi, A., Strenzke, K., Asif, M., and Brule-Babel, A. (2014). Registration of hard red spring wheat germplasm PT771. *J. Plant Regist.* 8, 221–225. doi: 10.3198/jpr2013.05.0023crg

Steiner, B., Buerstmayr, M., Michel, S., Schweiger, W., Lemmens, M., and Buerstmayr, H. (2017). Breeding strategies and advances in line selection for Fusarium head blight resistance in wheat. *Trop. Plant Pathol.* 42, 165–174. doi: 10.1007/s40858-017-0127-7

Tamburic-Ilincic, L., and Barcellos Rosa, S. (2017). Alleles on the two dwarfing loci on 4B and 4D are main drivers of FHB-related traits in the Canadian winter wheat population "Vienna" × "25R47". *Plant Breed.* 136, 799–808. doi: 10.1111/pbr.12527

Tamburic-Ilincic, L., and Rosa, S. B. (2019). QTL mapping of Fusarium head blight and Septoria tritici blotch in an elite hard red winter wheat population. *Mol. Breed.* 39, 94. doi: 10.1007/s11032-019-0999-y

Tamura, K., Stecher, G., and Kumar, S. (2021). MEGA11: molecular evolutionary genetics analysis version 11. *Mol. Biol. Evol.* 38, 3022–3027. doi: 10.1093/molbev/msab120

Thomas, J., Fox, S., McCallum, B., Fetch, T., Gilbert, J., Menzies, J., et al. (2013). Vesper hard red spring wheat. *Can. J. Plant Sci.* 93, 315–321. doi: 10.4141/cjps2012-233

Tuberosa, R., Salvi, S., Sanguineti, M. C., Landi, P., Maccaferri, M., and Conti, S. (2002). Mapping QTLs regulating morpho-physiological traits and yield: Case studies, shortcomings and perspectives in drought-stressed maize. *Ann. Bot-london* 89, 941–963. doi: 10.1093/aob/mcf134

Uffelmann, E., Huang, Q. Q., Munung, N. S., de Vries, J., Okada, Y., Martin, A. R., et al. (2021). Genome-wide association studies. *Nat. Rev. Methods Primers* 1, 59. doi: 10.1038/s43586-021-00056-9

Valverde-Bogantes, E., Bianchini, A., Herr, J. R., Rose, D. J., Wegulo, S. N., and Hallen-Adams, H. E. (2020). Recent population changes of Fusarium head blight pathogens: drivers and implications. *Can. J. Plant Pathol.* 42, 315–329. doi: 10.1080/07060661.2019.1680442

Venske, E., dos Santos, R. S., Farias, D., Rother, V., da Maia, L. C., Pegoraro, C., et al. (2019). Meta-analysis of the QTLome of Fusarium head blight resistance in bread wheat: Refining the current puzzle. *Front. Plant Sci.* 10, 727. doi: 10.3389/fpls.2019.00727

Verma, S. S., de Andrade, M., Tromp, G., Kuivaniemi, H., Pugh, E., Namjou-Khales, B., et al. (2014). Imputation and quality control steps for combining multiple genome-wide datasets. *Front. Genet.* 5, 370. doi: 10.3389/fgene.2014.00370

Voorrips, R. E. (2002). MapChart: Software for the graphical presentation of linkage maps and QTLs. *J. Hered* 93, 77–78. doi: 10.1093/jhered/93.1.77

Waalwijk, C., Kastelein, P., de Vries, I., Kerényi, Z., van der Lee, T., Hesselink, T., et al. (2003). Major changes in *Fusarium* spp. in wheat in the Netherlands. *Eur. J. Plant Pathol.* 109, 743–754. doi: 10.1023/A:1026086510156

Wang, S., Dvorkin, D., and Da, Y. (2012). SNPEVG: a graphical tool for GWAS graphing with mouse clicks. *BMC Bioinf.* 13, 1–6. doi: 10.1186/1471-2105-13-S5-S1

Wang, J., Wan, X., Crossa, J., Crouch, J., Weng, J., Zhai, H., et al. (2006). QTL mapping of grain length in rice (Oryza sativa L.) using chromosome segment substitution lines. *Genet. Res.* 88, 93–104. doi: 10.1017/S0016672306008408

Wang, S., Wong, D., Forrest, K., Allen, A., Chao, S., Huang, B. E., et al. (2014). Characterization of polyploid wheat genomic diversity using a high-density 90,000 single nucleotide polymorphism array. *Plant Biotechnol. J.* 12, 787–796. doi: 10.1111/pbi.12183

Wang, S., Xie, F., and Xu, S. (2022). Estimating genetic variance contributed by a quantitative trait locus: A random model approach. *PloS Comput. Biol.* 18, e1009923. doi: 10.1371/journal.pcbi.1009923

Wiśniewska, H., Surma, M., Krystkowiak, K., Adamski, T., Kuczyńska, A., Ogrodowicz, P., et al. (2016). Simultaneous selection for yield-related traits and susceptibility to Fusarium head blight in spring wheat RIL population. *Breed. Sci.* 66, 281–292. doi: 10.1270/jsbbs.66.281

Wilhelm, E. P., Turner, A. S., and Laurie, D. A. (2009). Photoperiod insensitive *Ppd-A1a* mutations in tetraploid wheat (*Triticum durum* Desf.). *Theor. Appl. Genet.* 118, 285–294. doi: 10.1007/s00122-008-0898-9

Worland, A. J., Börner, A., Korzun, V., Li, W. M., Petrovíc, S., and Sayers, E. J. (1998). The influence of photoperiod genes on the adaptability of European winter wheats. *Euphytica* 100, 385–394. doi: 10.1023/A:1018327700985

Wu, L., Zhang, Y., He, Y., Jiang, P., Zhang, X., and Ma, H. (2019). Genome-wide association mapping of resistance to Fusarium head blight spread and deoxynivalenol accumulation in Chinese elite wheat germplasm. *Phytopathology* 109, 1208–1216. doi: 10.1094/PHYTO-12-18-0484-R

Xu, X. M., Nicholson, P., Thomsett, M. A., Simpson, D., Cooke, B. M., Doohan, F. M., et al. (2008). Relationship between the fungal complex causing fusarium head blight of wheat and environmental conditions. *Phytopathology* 98, 69–78. doi: 10.1094/PHYTO-98-1-0069

Xu, X. M., Parry, D. W., Nicholson, P., Thomsett, M. A., Simpson, D., Edwards, S. G., et al. (2005). Predominance and association of pathogenic fungi causing Fusarium ear blightin wheat in four European countries. *Eur. J. Plant Pathol.* 112, 143–154. doi: 10.1007/s10658-005-2446-7

Xue, A. G., Chen, Y., Seifert, K., Guo, W., Blackwell, B. A., Harris, L. J., et al. (2019). Prevalence of Fusarium species causing head blight of spring wheat, barley and oat in Ontario during 2001–2017. *Can. J. Plant Pathol.* 41, 392–402. doi: 10.1080/07060661.2019.1582560

Xue, S., Xu, F., Tang, M., Zhou, Y., Li, G., An, X., et al. (2011). Precise mapping Fhb5, a major QTL conditioning resistance to Fusarium infection in bread wheat (Triticum aestivum L.). *Theor. Appl. Genet.* 123, 1055–1063. doi: 10.1007/s00122-011-1647-z

Yan, Z., Chen, W., van der Lee, T., Waalwijk, C., van Diepeningen, A. D., Feng, J., et al. (2022). Evaluation of fusarium head blight resistance in 410 chinese wheat cultivars selected for their climate conditions and ecological niche using natural infection across three distinct experimental sites. *Front. Plant Sci.* 13, 916282. doi: 10.3389/fpls.2022.916282

Yan, Z., Zhang, H., van der Lee, T. A. J., Waalwijk, C., van Diepeningen, A. D., Deng, Y., et al. (2020). Resistance to Fusarium head blight and mycotoxin accumulation among 129 wheat cultivars from different ecological regions in China. *World Mycotoxin J.* 13, 189–200. doi: 10.3920/WMJ2019.2501

Yang, Z., Gilbert, J., Fedak, G., and Somers, D. J. (2005). Genetic characterization of QTL associated with resistance to Fusarium head blight in a doubled-haploid spring wheat population. *Genome* 48, 187–196. doi: 10.1139/g04-104

Yi, X., Cheng, J., Jiang, Z., Hu, W., Bie, T., Gao, D., et al. (2018). Genetic analysis of Fusarium head blight resistance in CIMMYT bread wheat line C615 using traditional and conditional QTL mapping. *Front. Plant Sci.* 9, 573. doi: 10.3389/fpls.2018.00573

Yong-Fang, W., Chi, Y., and Jun-Liang, Y. (1997). Sources of resistance to head scab in Triticum. *Euphytica* 94, 31–36. doi: 10.1023/A:1002982005541

Zhang, Q. J., Axtman, J. E., Faris, J. D., Chao, S. M., Zhang, Z. C., Friesen, T. L., et al. (2014). Identification and molecular mapping of quantitative trait loci for Fusarium head blight resistance in emmer and durum wheat using a single nucleotide polymorphism-based linkage map. *Mol. Breed.* 34, 1677–1687. doi: 10.1007/s11032-014-0180-6

Zhang, W., Boyle, K., Brule-Babel, A., Fedak, G., Gao, P., Djama, Z. R., et al. (2021). Evaluation of genomic prediction for Fusarium head blight resistance with a multi-parental population. *Biology* 10, 756. doi: 10.3390/biology10080756

Zhang, W., Boyle, K., Brûlé-Babel, A. L., Fedak, G., Gao, P., Robleh Djama, Z., et al. (2020b). Genetic characterization of multiple components contributing to Fusarium head blight resistance of FL62R1, a Canadian bread wheat developed using systemic breeding. *Front. Plant Sci.* 11, 580833. doi: 10.3389/fpls.2020.580833

Zhang, W., Francis, T., Gao, P., Boyle, K., Jiang, F., Eudes, F., et al. (2018). Genetic characterization of type II Fusarium head blight resistance derived from transgressive segregation in a cross between Eastern and Western Canadian spring wheat. *Mol. Breed.* 38, 13. doi: 10.1007/s11032-017-0761-2

Zhang, L., Li, H., Meng, L., and Wang, J. (2020a). Ordering of high-density markers by the k-Optimal algorithm for the traveling-salesman problem. *Crop J.* 8, 701–712. doi: 10.1016/j.cj.2020.03.005

Zhao, M., Leng, Y., Chao, S., Xu, S. S., and Zhong, S. (2018a). Molecular mapping of QTL for Fusarium head blight resistance introgressed into durum wheat. *Theor. Appl. Genet.* 131, 1939–1951. doi: 10.1007/s00122-018-3124-4

Zhao, M., Wang, G., Leng, Y., Wanjugi, H., Xi, P., Grosz, M. D., et al. (2018b). Molecular mapping of fusarium head blight resistance in the spring wheat line nd2710. *Phytopathology* 108, 972–979. doi: 10.1094/PHYTO-12-17-0392-R

Zhu, Z., Hao, Y., Mergoum, M., Bai, G., Humphreys, G., Cloutier, S., et al. (2019). Breeding wheat for resistance to Fusarium head blight in the Global North: China, USA, and Canada. *Crop J.* 7, 730–738. doi: 10.1016/j.cj.2019.06.003

Zhu, T., Wang, L., Rimbert, H., Rodriguez, J. C., Deal, K. R., De Oliveira, R., et al. (2021a). Optical maps refine the bread wheat Triticum aestivum cv. Chinese Spring genome assembly. *Plant J.* 107, 303–314. doi: 10.1111/tpj.15289

Zhu, Z., Xu, X., Fu, L., Wang, F., Dong, Y., Fang, Z., et al. (2021b). Molecular mapping of quantitative trait loci for fusarium head blight resistance in a doubled haploid population of Chinese bread wheat. *Plant Dis.* 105, 1339–1345. doi: 10.1094/PDIS-06-20-1186-RE

Zuvich, R. L., Armstrong, L. L., Bielinski, S. J., Bradford, Y., Carlson, C. S., Crawford, D. C., et al. (2011). Pitfalls of merging GWAS data: lessons learned in the eMERGE network and quality control procedures to maintain high data quality. *Genet. Epidemiol.* 35, 887–898. doi: 10.1002/gepi.20639

frontiers | Frontiers in Microbiology

TYPE Original Research
PUBLISHED 25 August 2023
DOI 10.3389/fmicb.2023.1234724

OPEN ACCESS

EDITED BY
Inmaculada Larena,
Instituto Nacional de Investigación y Tecnología Agraria y Alimentaria (INIA-CSIC), Spain

REVIEWED BY
Luca Roscini,
University of Perugia, Italy
Nelson Sigfrido Torres,
University of Texas at San Antonio, United States

*CORRESPONDENCE
Hokyoung Son
✉ hogongi7@snu.ac.kr
Kyunghun Min
✉ mymin117@snu.ac.kr

†These authors have contributed equally to this work and share first authorship

RECEIVED 22 June 2023
ACCEPTED 26 July 2023
PUBLISHED 25 August 2023

CITATION
Choi S, Yang JW, Kim J-E, Jeon H, Shin S, Wui D, Kim LS, Kim BJ, Son H and Min K (2023) Infectivity and stress tolerance traits affect community assembly of plant pathogenic fungi.
Front. Microbiol. 14:1234724.
doi: 10.3389/fmicb.2023.1234724

Infectivity and stress tolerance traits affect community assembly of plant pathogenic fungi

Soyoung Choi[1†], Jung Wook Yang[2†], Jung-Eun Kim[3], Hosung Jeon[1], Soobin Shin[1], Dayoun Wui[1], Lee Seul Kim[1], Byung Joo Kim[2], Hokyoung Son[1,4]* and Kyunghun Min[1]*

[1]Department of Agricultural Biotechnology, Seoul National University, Seoul, Republic of Korea, [2]Crop Cultivation and Environment Research Division, National Institute of Crop Science, Rural Development Administration, Suwon, Republic of Korea, [3]Research Institute of Climate Change and Agriculture, National Institute of Horticultural and Herbal Science, Rural Development Administration, Jeju, Republic of Korea, [4]Research Institute of Agriculture and Life Sciences, Seoul National University, Seoul, Republic of Korea

Understanding how ecological communities assemble is an urgent research priority. In this study, we used a community ecology approach to examine how ecological and evolutionary processes shape biodiversity patterns of plant pathogenic fungi, *Fusarium graminearum* and *F. asiaticum*. High-throughput screening revealed that the isolates had a wide range of phenotypic variation in stress tolerance traits. Net Relatedness Index (NRI) and Nearest Taxon Index (NTI) values were computed based on stress-tolerant distance matrices. Certain local regions exhibited positive values of NRI and NTI, indicating phenotypic clustering within the fungal communities. Competition assays of the pooled strains were conducted to investigate the cause of clustering. During stress conditions and wheat colonization, only a few strains dominated the fungal communities, resulting in reduced diversity. Overall, our findings support the modern coexistence theory that abiotic stress and competition lead to phenotypic similarities among coexisting organisms by excluding large, low-competitive clades. We suggest that agricultural environments and competition for host infection lead to locally clustered communities of plant pathogenic fungi in the field.

KEYWORDS

***Fusarium graminearum*, *Fusarium asiaticum*, community assembly, high-throughput screening, competition assay**

1. Introduction

A fundamental objective of ecology is to understand the mechanisms that mediate the assembly of natural communities (Stephen Brewer, 2000). There are various theories on how the assembly of a community occurs, and it is still a subject of debate (Webb et al., 2002; Mayfield and Levine, 2010; Goberna et al., 2014; Salazar et al., 2016; Sommer et al., 2017). Current theory predicts that the assembly of a community at the local level is determined by two primary ecological processes: the interaction between a species and its abiotic environment, and interactions among the species themselves (Gotzenberger et al., 2012). Fungi typically co-occur with evolutionarily related organisms more often than expected by chance, a process that results in clustering (Pellissier et al., 2014; Mykra et al., 2016; Chen et al., 2017). Clustering is a common pattern in ecological communities, in which species tend to co-occur with their evolutionary relatives more frequently than expected by chance. Classical community theory suggests that clustering results from the selection of taxa that share similar ecological traits (e.g., stress

tolerance and morphology), allowing them to persist in a specific environment (Webb et al., 2002). These traits may be conserved across phylogenetic lineages, leading to related taxa clustering. Under the traditional framework, biotic interactions, particularly competition, drive the co-existence of organisms that are phenotypically distant, resulting in overdispersed patterns. This results from the competitive exclusion of ecologically similar organisms based on their niche similarities (Webb et al., 2002). Modern coexistence theory (Mayfield and Levine, 2010) has refined this view, arguing that competition can generate both phenotypic clustering when it operates through environmentally mediated differences in competitive abilities among entire clades. We postulate that this mechanism may operate in plant-pathogenic fungal communities, which are typically under environmental stresses and competition for host infections.

Fusarium graminearum and *F. asiaticum* are plant pathogenic fungi that cause Fusarium head blight (FHB) diseases in small grain cereals such as wheat, barley, and rice (van der Lee et al., 2015). In addition to the yield loss, they produce trichothecene mycotoxins, such as nivalenol (NIV), deoxynivalenol (DON), 15-acetyldeoxynivalenol (15-ADON), and 3-acetyldeoxynivalenol (3-ADON), as well as zearalenone (Desjardins, 2006). Mycotoxins threaten food security by causing toxicosis in livestock and humans, leading to economic losses and health risks. *F. graminearum* and *F. asiaticum* are closely related species that belong to *Fusarium graminearum* species complex (FGSC). A comparison of genome structure and gene content revealed a 93% overlap between the two species, which are also morphologically indistinguishable (O'Donnell et al., 2004). *F. asiaticum* was identified as the major species causing FHB outbreaks in cereal crops in the southern region of the Republic of Korea (Lee J. et al., 2009; Ahn et al., 2022). In terms of life cycle, both species are primarily soil-borne and overwinter as mycelia or spores in plant debris (Trail, 2009). In soil and plant debris, they are exposed to various environmental stresses such as water stress, oxidative stress, and agricultural chemical stress. They can infect crops at any stage of growth, but typically infect the heads of cereal plants during the flowering stage. Both species produce masses of spores that are spread by wind and rain, facilitating the spread of the disease to neighboring plants. The success of the fungal pathogens depends on their ability to successfully infect and spread within host plants. Another important factor in determining the success of the pathogens is their ability to persist as saprophytes on the dead plant debris long after the crop has been removed (Min et al., 2012). These factors can have a significant impact on the fungal community. Population genomics analyses of *F. graminearum* have been conducted, revealing a high level of genetic diversity and extensive recombination within the population (Talas and McDonald 2015; Talas et al., 2016).

In 2021, a FHB outbreak occurred in the southern region of the Republic of Korea (Kim, 2021; Supplementary Note S1). To determine the population structure of *F. graminearum* and *F. asiaticum*, 205 strains were isolated from diseased cereals crops at 18 sites. Stress tolerance of the strains was compared in 11 different conditions, using a high-throughput screening approach. Our competition assays revealed that the diversity of the fungal community decreased under chemical stress and host infection. In conclusion, we found that the selection for infectivity and stress tolerance traits leads to phenotypic clustering of fungal communities. These findings shed light on the mechanism driving the clustering of plant-pathogenic fungal communities and provide insights into the dynamics of plant-fungi interactions.

2. Materials and methods

2.1. *Fusarium graminearum* species complex isolation

FGSC isolates were collected from different cereal fields in the southern region of the Republic of Korea in 2021. Cereal crops (barley, wheat, oat, and rice) with FHB symptoms were sampled from fields located in 18 cities/counties and 4 provinces (Figure 1A and Supplementary Data S1). The infected seeds were surface sterilized with 1% sodium hypochlorite and 70% ethanol solution. The seeds were placed onto potato dextrose agar (PDA, BD Difco, Franklin Lakes, New Jersey) plates and incubated for 3 days at 25°C. We isolated 205 FGSC strains based on morphological characteristics, such as colony pigmentation. Fungal strains were grown on PDA and stored in 20% glycerol solution at −80°C.

2.2. PCR amplification and sequencing, and phylogenetic analyses

Fungal isolates were cultured in liquid complete medium for 3 days at 25°C. Genomic DNA was extracted from lyophilized mycelia powder using a conventional Cetyltrimethylammonium Bromide (CTAB) method (Leslie and Summerell, 2006). The *TEF-1α* region was amplified by PCR using ExTaq polymerase in accordance with the manual (Takara Bio, Otsu, Japan). The EF-2 and FusF oligonucleotide pair was used for *TEF-1α* amplification (Supplementary Table S1). The oligonucleotides were synthesized at a commercial synthesis facility (Bioneer, Daejeon, Republic of Korea). The PCR products were purified using a commercial Kit (Intron, Seongnam, Republic of Korea) and submitted to the Bioneer PCR sequencing service. The oligonucleotide used for sequencing were the same as those used for amplification. The trimmed DNA sequences were BLAST-searched against the NCBI GenBank database for species identification (Supplementary Data S1, S2).

To determine the trichothecene chemotypes, we subjected the FGSC isolates to PCR using two primer sets. One set amplified the trichothecene 15-O-acetyltransferase (*TRI3*) gene, and the other set amplified the trichothecene efflux pump (*TRI12*) gene (Ward et al., 2002). Each set of primers include one common primer and three chemotype-specific primers for NIV, 3-ADON, and 15-ADON trichothecene chemotype, respectively (Supplementary Table S1). The amplified products were loaded onto 1.5% (w/v) agarose gel. The trichothecene chemotypes were predicted from the gel images based on the band size.

The *TEF-1α* sequences were used for the phylogenetic analysis of *F. graminearum* and *F. asiaticum*. Reference sequences of *F. graminearum* (NRRL 5883, NRRL 6394, NRRL 13383, NRRL 28063, NRRL 28336, NRRL 28439, and NRRL 29169), *F. asiaticum* (NRRL 6101, NRRL 13818, NRRL 26156, and NRRL 28720), and *F. pseudograminearum* strains (NRRL 28062, NRRL 28065, NRRL 28334, and NRRL 28338) were obtained from NCBI PopSet[1] (O'Donnell et al., 2000). The DNA sequences were aligned using the

1 https://ncbi.nlm.nih.gov/popset/12003438

10.3389/fmicb.2023.1234724

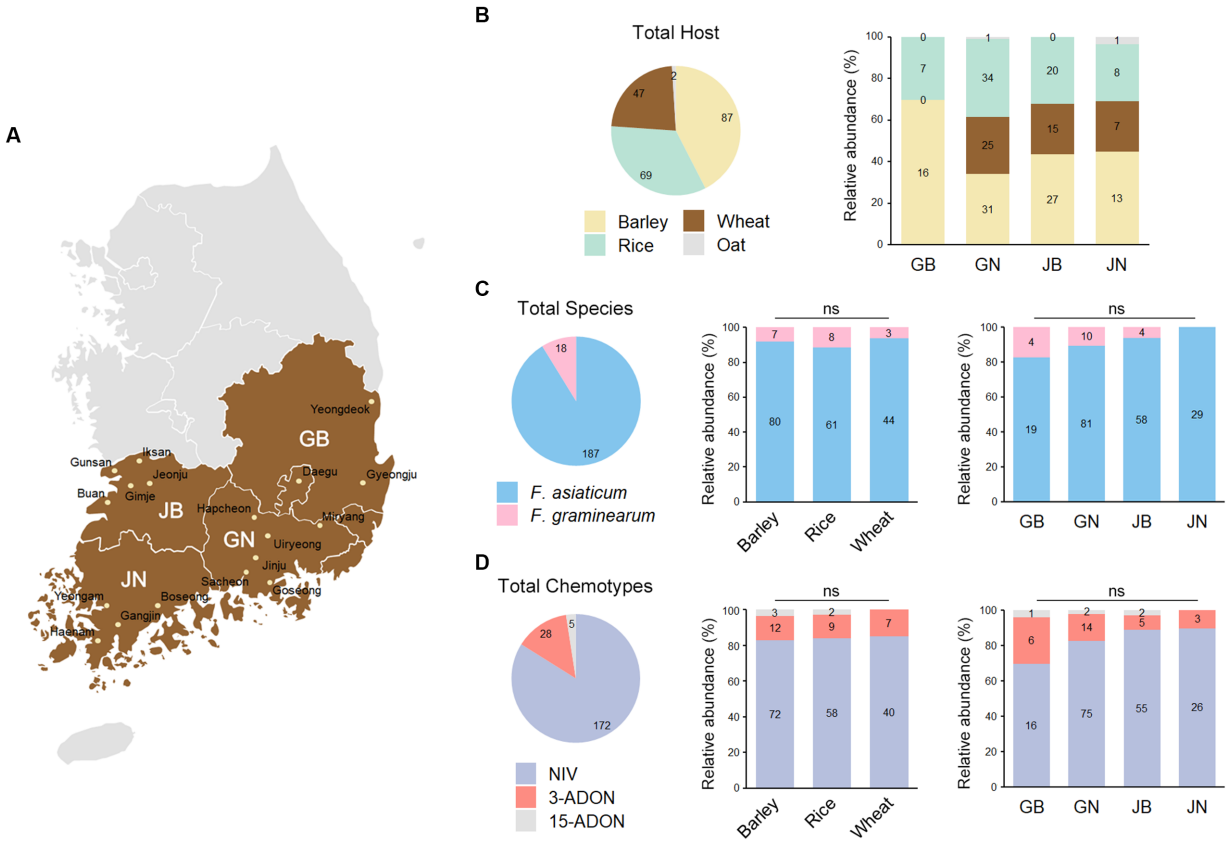

FIGURE 1
The distribution of *Fusarium graminearum* and *F. asiaticum* isolates in southern region of the Republic of Korea. **(A)** Map of the Republic of Korea indicating the 18 sampling sites in 4 southern provinces. GB, Gyeongsangbuk-do; GN, Gyeongsangnam-do; JB, Jeollabuk-do; JN, Jeollanam-do. **(B)** The pie chart illustrates the number of strains that have been isolated from the indicated hosts. The bar charts on the right show the percentage of hosts from the marked provinces, with the actual number of the hosts labeled inside the bars. **(C)** *F. asiaticum* represents 91% of the field isolates while *F. graminearum* accounts for the remaining 9%. The bar charts on the right show the percentage of *F. asiaticum* and *F. graminearum* strains isolated from the marked hosts or provinces, with the actual number of strains labeled inside the bars. There was no significant (ns) correlation observed between species and either host or location. **(D)** NIV chemotype represents 84% of the field isolates while DON chemotypes count for the remaining 16. There was not a significant correlation between chemotype and either host or location. NIV, nivalenol; 3-ADON, 3-acetyldeoxynivalenol; 15-ADON, 15-acetyldeoxynivalenol.

Geneious Prime software and used to construct phylogenetic trees (Biomatters, Auckland, New Zealand). Maximum Likelihood analysis was performed utilizing the General Time Reversible model with Invariant sites and Gamma distribution (GTR + I + G). This model was selected due to its comprehensive approach, accounting for base substitution rates, invariant sites, and rate variations among sites (Abadi et al., 2019). The robustness of the obtained tree was evaluated by bootstrap analysis with 1,000 replicates (Pattengale et al., 2010).

2.3. High-throughput phenotypic screening

For conidia production, the fungal strains were incubated in carboxymethylcellulose medium (Cappellini and Peterson, 1965) for 7 days at 25°C in a shaking incubator at 0.314 rcf. The conidia were filtered through Miracloth (Millipore, Burlington, MA, United States) and resuspended in liquid complete medium to give 1×10^5 conidia mL^{-1}. We mixed 100 µL of conidia suspension with an equal volume of complete media supplemented with different chemicals on 96-well plates. Final concentration of chemicals in the cultures were 0.31 mM hydrogen peroxide, 1 M sorbitol, 1 M sodium chloride, 0.1 mg mL^{-1} sodium dodecyl sulfate, 0.05 µg mL^{-1} fludioxonil, 125 µg mL^{-1} iprodione, 0.625 µg mL^{-1} tebuconazole, 2 µg mL^{-1} tunicamycin, 1.25 mM dithiothreitol, 23.5 µL mL^{-1} hydrogen chloride (pH 2), and 5.3 µL mL^{-1} sodium hydroxide (pH 12). The cultures on the 96-well plates were incubated for 60 h at 25°C in plastic containers to prevent evaporation. There were two replicates for each condition. The OD_{600} value was measured every 12 h using a microplate reader a Synergy HTX microplate reader (BioTek, Winooski, VT, United States). The OD_{600} values at 48 h was used to compare stress tolerance. The absorbance of the medium alone was subtracted and the resulting values were averaged. To compare the growth of the strains under different stress conditions, the growth in complete medium was used as a reference point and the growth in stress conditions was normalized accordingly. The resulting values were used to calculate the Log2 fold difference from the average growth for heatmap analysis. Data analysis was performed using R software (version 4.1.2). A heatmap was created to visualize the data matrix using the "heatmap.2" function from the "gplots" package. For the hierarchical clustering,

we utilized the "pvclust" function from the "pvclust" package in R (Suzuki and Shimodaira, 2006). The dendrogram was created based on the Euclidean distances between variables and was cut into clusters using the average linkage method. To assess the robustness of the clusters, the "pvclust" function calculated AU (Approximately Unbiased) *p*-values for hierarchical clustering via multiscale bootstrap resampling. We performed 30,000 bootstrap replicates to assess the uncertainty in our hierarchical cluster analysis.

2.4. Structure analysis of fungal communities

We analyzed the structure of fungal communities using Picante R package (Kembel et al., 2010). The community phylogenetic and phenotypic over/underdispersion was quantified using NRI and NTI (Salazar et al., 2016). NRI measures the extent to which taxa within a community are closely related to each other than would be expected by chance. NTI measures the extent to which the phylogenetic distance between the closest relatives of co-occurring taxa is greater or smaller than expected by chance. Positive values of NTI and NRI indicate that similar taxa (phylogenetically and phenotypically) co-occur more than expected by chance; negative values indicate that similar taxa are not likely to co-occur; values near 0 indicate random distribution. The randomization to generate null communities was done by shuffling phylogeny and stress tolerance dendrogram taxa labels in order to calculate the standardized effect sizes for NRI and NTI (abundance weighted model, $n = 1{,}000$ per community; Picante package).

2.5. Competition assays for infectivity and stress tolerance

We selected field isolates that exhibited different stress tolerance patterns; SY6, SY16, SY22, SY32, SY98, SY144, SY147, and SY175. The fungal isolates were grown in liquid complete medium for 72 h at 25°C in a shaking incubator at 0.314 rcf. For conidia production, the mycelia were harvested, spread on yeast malt agar plates, and then incubated for 7 days at 25°C under near-UV light (wavelength, 352 nm; Sankyo Denki). The conidia were collected with sterile water, filtered through Miracloth (Millipore), and washed with water again. The conidia were resuspended in a sterile 15% glycerol solution to yield 2×10^6 conidia mL^{-1}. The conidia suspension is stored at −80°C until it is ready to be used.

For competition assay for infectivity, the point inoculation method (Lee S. H. et al., 2009) was employed using the wheat cultivar Geumgang. Frozen stocks of conidia suspension were thawed and pooled. The pooled conidia were spin down and resuspended in sterile water to make 1×10^6 conidia mL^{-1}. Ten microliters of conidia suspension were injected into the center spikelet of a wheat head at early anthesis. All inoculations were repeated at least 15 times, and the wheat heads were covered with plastic bags for 3 days to maintain humidity conditions. At day 7 and day 14, the samples were harvested, lyophilized, and ground into small particles using a grinder. We used Lysing Matrix S with a Fastprep-24TM 5G instrument (MP biomedicals, Irvine, CA, United States) to lyse cells for the preparation of fungal DNA extraction. Fungal DNA was extracted by using CTAB method (Leslie and Summerell, 2006). The assay was repeated two times.

For competition assay in stress condition, frozen stocks of conidia suspension were thawed and pooled. Two microliters of the conidia suspension were inoculated into 200 µL complete media supplemented with different chemicals on 96-well plates. The chemicals and their concentrations were same as described above. The cultures in the 96-well plates were incubated for 4 days at 25°C in plastic containers to prevent evaporation. To extract fungal DNA, the mycelia were harvested and resuspended in a lysis buffer (2% Triton X-100, 1% SDS, 0.1 M NaCl, 10 mM Tris-Cl, 1 mM EDTA and pH 8.0). We used 0.5 mm Zirconia/Silica beads (BioSpec Products, Bartlesville, OK, United States) with a Fastprep-24TM 5G instrument (MP biomedicals) to lyse cells. The fungal DNA was extracted with a mixture of phenol: chloroform: isoamyl alcohol (25: 24: 1). The assay was repeated two times.

To create an inoculum standard, we inoculated 2 µL of individual conidia stock into a separate well containing 200 µL of complete medium. The cultures on the 96-well plates were incubated for 2 days at 25°C. The fungal cultures were pooled, and DNA was extracted as described above. The extracted fungal DNA was used as an inoculum standard prior to competitive assay.

2.6. Estimation of relative abundance of fungal isolates

The relative abundance of each strain in competitive assays was determined by analyzing the relative proportions of their DNA variants (Carr et al., 2009; Seroussi, 2021). The *TEF-1α* sequence was selected because each isolate has a unique single-nucleotide sequence variant (SNV) in the region (Supplementary Figure S3 and Supplementary Data S2). First, The *TEF-1α* region was amplified from the fungal DNA using FgEF-F and FgEF-R primers which are specific to FGSC (Supplementary Table S1). The PCR products were purified and submitted to Bioneer for Sanger sequencing. The *TEF-1α* region was sequenced using two forward primers (FusF and FgEF-F2) and two reverse primers (FgEF-R and FgEF-R2). Relative copy number information of a unique single-nucleotide sequence variant was extracted from the sequencing chromatograms. We calculated the occurrence ratio of SNVs from sequence trace files using the SnapGene software (Dotmatics, Boston, MA, United States). The values of the same condition were averaged. Experiments comparing 8 strains resulted in 8 occurrence ratios of SNV for the pooled inoculum (*I*) and the samples (*S*). Finally, *S*/*I* was calculated for each stress condition and wheat infection; these are presented in Supplementary Data S3.

3. Results

3.1. Isolation of *F. graminearum* and *F. asiaticum* strains in cereal fields

To determine the population structure of *F. graminearum* and *F. asiaticum*, we isolated 205 strains from diseased cereals crops in 18 sites in southern provinces of the Republic of Korea (Figure 1A and Supplementary Data S1). The samples were from barley (42%), rice (34%), wheat (23%), and oat (1%) (Figure 1B). Sequences of the translation elongation factor-1 α (*TEF-1α*) gene were analyzed for species identification. *F. asiaticum* represents 91% of the isolates while

F. graminearum accounts for the remaining 9% (Figure 1C). We constructed a phylogenetic tree of the fungal strains based on the *TEF-1α* sequences inferred by maximum-likelihood analysis (Supplementary Figure S1). The phylogenetic analysis with reference strains validated the species identification. A chi-square test was performed to compare the species compositions in different hosts and locations. Surprisingly, the results showed that there was no significant difference in species compositions between hosts and locations ($p > 0.1$). Trichothecene genotypes of the 205 isolates were determined using multiple PCR targeting the *TRI3* and *TRI12* genes (Starkey et al., 2007). Based on trichothecene genotypes, the *F. asiaticum* and *F. graminearum* strains were divided into three chemotype groups: NIV, 3-ADON, and 15-ADON. The predominance of the NIV chemotype in our study is consistent with findings from the previous studies (Lee J. et al., 2009; Ahn et al., 2022; Figure 1C). However, chi-square test showed that there was no significant difference in chemotype compositions between hosts and locations ($p > 0.1$) (Figure 1D). These results contrast to the previous hypothesis that the species and trichothecene chemotypes have host preference (Lee et al., 2010; Xu et al., 2021; Ahn et al., 2022).

3.2. High-throughput screening revealed phenotypic diversity of *F. graminearum* and *F. asiaticum* isolates

We performed a high-throughput screening for chemical stress tolerance. Specifically, we grew fungal strains in complete media supplemented with 11 different chemicals on 96-well plates and compared stress tolerance by measuring the OD_{600} (optical density at the 600 nm wavelength) of the cultures. *F. graminearum* and *F. asiaticum* isolates showed a wide range of variation in stress tolerance (Figure 2 and Supplementary Data S1). Based on their stress tolerance pattern, the strains were classified into 14 groups. Distinct stress tolerance patterns were observed in each group. For instance, strains in group 9 exhibited tolerances to fungicides such as iprodione, fludioxonil, and tebuconazole. Groups 9 and 14 were tolerant to sodium dodecyl sulfate (SDS), while other groups were sensitive to SDS. In an acidic condition (pH 2), groups 12 and 14 were tolerated but other groups displayed strong sensitivity. Interestingly, *F. graminearum* strains had similar phenotypes and were categorized into group 14. *F. asiaticum* strains, despite being the same species, exhibited greater diversity and were classified into multiple groups. Correlation coefficients were calculated to determine the relationships among the 11 stress tolerance traits (Supplementary Figure S2). A strong positive correlation ($R = 0.78$) was observed between dithiothreitol and hydrogen peroxide tolerances. Additionally, the tolerance to osmotic stress induced by 1 M sorbitol showed a weak correlation ($R = 0.66$) with either hydrogen peroxide or sodium chloride.

3.3. Phenotypic clustering of *F. graminearum* and *F. asiaticum* communities

Structure analysis of the fungal communities revealed that fungal strains are more closely related in certain local regions (Figure 3). Net Relatedness Index (NRI) and Nearest Taxon Index (NTI) values were calculated based on stress tolerant distance matrices (Kembel et al., 2010; Salazar et al., 2016). The NRI values indicate that Gyeongsangbuk-do (GB) and Gyeongsangnam-do (GN) showed phenotypic clustering ($NRI > 0$), while Jeollabuk-do (JB) and Jeollanam-do (JN) showed overdispersion ($NRI < 0$) (Figure 3A). Similar trends were observed in the NTI values. Examining the local sites, we found that *F. graminearum* and *F. asiaticum* communities were clustered in most sites (Figures 3B,C). Furthermore, the fungal communities in all GB and GN sites exhibited phenotypic clustering based on stress tolerance ($NRI > 0$ and $NTI > 0$). In contrast, JB and JN displayed diverse fungal community structures (Figure 3C). GB and GN, which are geographically close, are often grouped as Gyeongsang-do (G), while JB and JN, also geographically close, belong to Jeolla-do (J). These two regions are separated by high mountains and have distinct climates. Jeolla-do (J) experiences higher annual precipitation and more winter snow compared to Gyeongsang-do (G) (Administration, 2022). It is likely that these geographical and climate differences contribute to the observed variations in fungal community structures (Backhouse, 2014; Scala et al., 2016; Xu et al., 2021; Wang et al., 2022).

3.4. The diversity of the fungal community decreased under chemical stress and host infection

To investigate the cause of clustering, competition assays were conducted under chemical stress and host infection (Figure 4A). A pooled inoculum of eight field isolates, each possessing distinct stress tolerance traits, was injected into wheat heads, resulting in typical symptoms of FHB (Figure 4B). DNA was extracted from infected wheat heads harvested at days 7 and 14, and the *TEF-1α* region was sequenced. The relative abundance of fungal strains during wheat infection was estimated from the sequencing chromatograms (Figures 4A,C). Interestingly, *F. asiaticum* SY16 (NIV type) emerged as the dominant strain, while *F. graminearum* SY175 (DON type) showed a decrease in abundance. Inverse Simpson and Shannon indices dropped on days 7 and 14, indicating a sharp decline in the diversity of the fungal community during wheat infection (Figure 4D). This suggests that competition in the host results in overrepresentation of infectivity traits leading to clustered communities. In parallel, the pooled inoculum was grown in various stress conditions such as oxidative stress, osmotic stress, cell wall stress, fungicide stress, ER stress, and pH stress, resulting in diverse abundance patterns across different stress conditions (Figure 4E). For example, *F. graminearum* SY175 showed tolerance in SDS and pH 2 when grown in single culture (Figure 2 and Supplementary Data S1). When grown in mixed cultures under the same stress conditions, this strain was more competitive and became predominant (Figure 4E). *F. asiaticum* SY16 showed a highly competitive ability in the mixed cultures when grown in complete medium and stress conditions. This observation is consistent with the high infectivity of *F. asiaticum* SY16 in wheat heads (Figure 4C). To assess the impact of stress on fungal diversity, we calculated the Inverse Simpson and Shannon indices for each stress condition. The results showed that the diversity indices in stress conditions were significantly lower than in the initial inoculum (Figure 4F). This suggests that exposure to stress leads to an overrepresentation of stress-tolerant traits, reducing the diversity in

10.3389/fmicb.2023.1234724

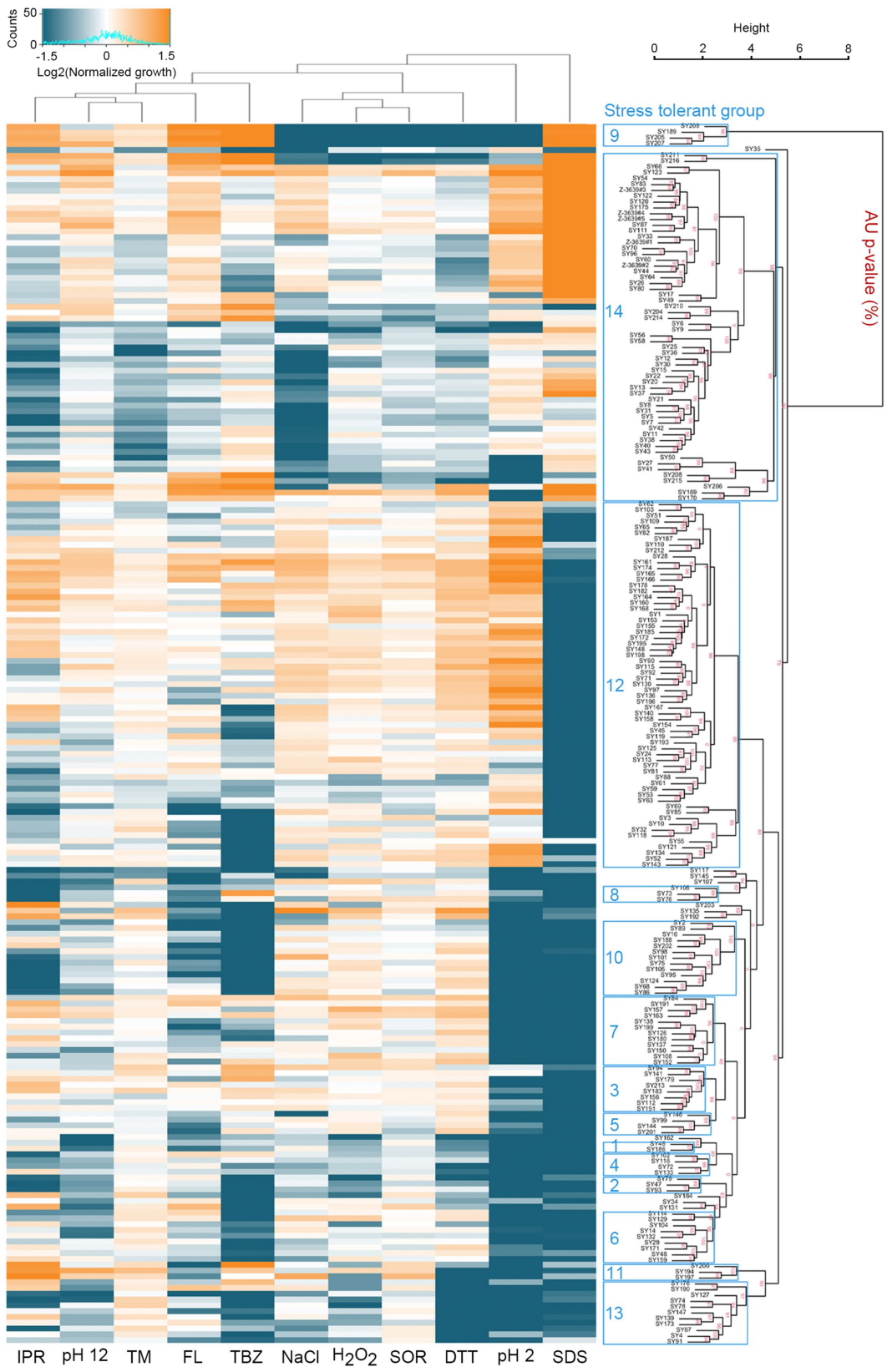

FIGURE 2
High-throughput phenotypic screening reveals intraspecific variation in stress tolerance. *F. graminearum* and *F. asiaticum* strains were grown on complete media (CM) on 96-well plates. Various chemicals were added to CM to assays their effects on growth by oxidative [0.31 mM hydrogen peroxide (H_2O_2)], osmotic [1 M sorbitol (SOR) or 1 M NaCl], cell wall [0.1 mg mL^{-1} sodium dodecyl sulfate (SDS)], fungicide [0.05 μg mL^{-1} fludioxonil (FL), 125 μg mL^{-1} iprodione (IPR), or 0.625 μg mL^{-1} tebuconazole (TBZ)], ER [2 μg mL^{-1} tunicamycin (TM) or 1.25 mM dithiothreitol (DTT)], and acidic (pH 2) or alkaline (pH 12) pH stresses. Each stress condition had two replicate wells per chemical. The cultures in the 96-well plates were incubated for 48 h at

(Continued)

FIGURE 2 (Continued)
25°C and the OD_{600} value was measured. To compare the growth of the strains under different stress conditions, the growth in CM was used as a reference point and the growth in stress conditions was normalized accordingly. The resulting values were used to calculate the Log2 fold difference from the average growth for heatmap analysis. Supplementary Data S1 contains the values that were used to generate the heatmap. Growth under different stress conditions is shown in a heatmap where orange indicates above-average growth and green-blue indicates below-average growth. Hierarchical clustering of the fungal strains was performed based on their stress tolerance pattern (Suzuki and Shimodaira, 2006). Approximately unbiased (AU) *p*-values for each stress tolerant group were calculated using bootstrap resampling techniques (30,000 replicates). Clusters with AU $p > 95\%$ are highlighted by blue rectangles, indicating strong support from the data.

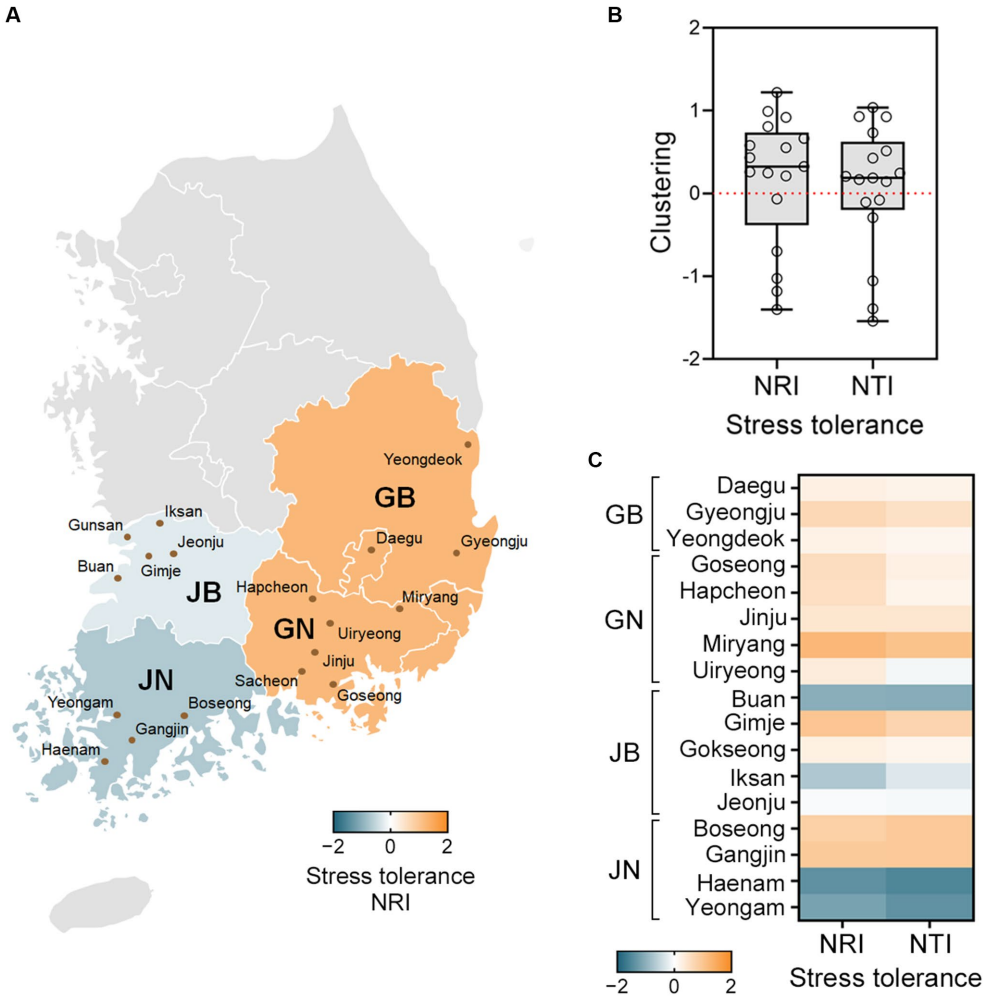

FIGURE 3
Communities of *F. graminearum* and *F. asiaticum* exhibit phenotypic clustering in certain local regions. Net Relatedness Index (NRI) and Nearest Taxon Index (NTI) values were calculated based on distance matrices of the stress tolerant groups. **(A)** The NRI and NTI values above 0 indicate clustering (orange) and values below 0 indicate overdispersion (green-blue). The NRI values for each province are shown in a heatmap. GB and GN showed phenotypic clustering, while JB and JN showed overdispersion. GB, Gyeongsangbuk-do; GN, Gyeongsangnam-do; JB, Jeollabuk-do; JN, Jeollanam-do. **(B)** Local tests for phenotypic structure of the fungal strains. The NRI and NTI values are represented using a box and whisker plot, with the box covering 50% of the data, the vertical bars showing the full data range, and the middle box line indicating the group median. **(C)** The NRI and NTI values for each site are shown in a heatmap. In both the GB and GN provinces, all sites exhibited NRI and NTI values above 0 (orange), indicating phenotypic clustering. The NRI and NTI values varied in the JB and JN provinces, and some sites exhibited overdispersion (green-blue).

the pool. Overall, our lab experiments demonstrated that fungal diversity decreased in both wheat infection and stress conditions.

4. Discussion

The findings of our study provide evidence supporting the idea that infectivity and stress tolerance traits are significant drivers of clustering in communities of plant pathogenic fungi. High-throughput screening revealed that the *F. graminearum* and *F. asiaticum* isolates had a wide range of phenotypes. We also observed interesting patterns of phenotypic clustering in the local sites. In competition assays, a few strains were able to dominate the fungal communities, leading to decreased diversity in the pool. This phenomenon was particularly evident in the case of wheat infection, where a *F. asiaticum* single strain became predominant in the middle of the disease's progression.

10.3389/fmicb.2023.1234724

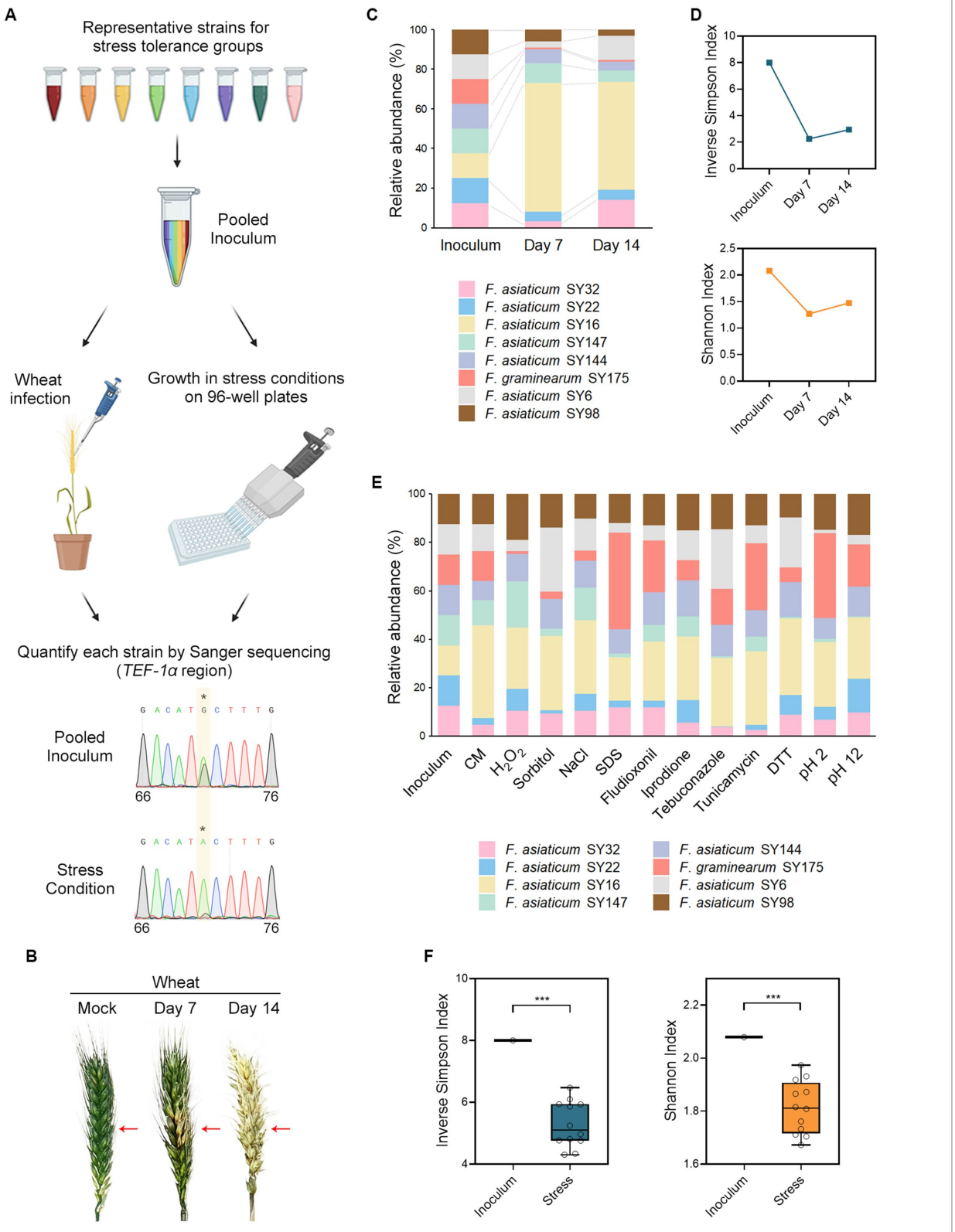

FIGURE 4
Wheat infection and exposure to chemical stresses decrease the diversity of the fungal community. **(A)** Experimental scheme of competition assays for infectivity and stress tolerance. We selected *F. graminearum* and *F. asiaticum* strains that represent different stress tolerance patterns; SY6, SY16, SY22, SY32, SY98, SY144, SY147, and SY175. Equal amounts of freshly harvested conidia of each strain were mixed and the resulting mixtures were used to inoculate wheat heads by injection or grow under stress conditions in 96-well plates. Fungal DNA was isolated from the wheat heads or 96-well cultures for sequencing. The *TEF-1α* region was amplified from the fungal DNA and sequenced using Sanger sequencing. Relative copy number information of a unique single-nucleotide sequence variant was extracted from the sequencing chromatograms. For example, SY147 has an A to G variant at nucleotide position 71 that was unique to the strain. The A to G ratio decreased from 0.417 in the pooled inoculum to 0.078 in a certain stress

(Continued)

FIGURE 4 (Continued)

condition, indicating 82% reduction in the relative abundance of the strain. **(B)** The disease symptoms of infected wheat heads. The pooled inoculum was injected into the center spikelet of a wheat head at early anthesis. As a mock control, the wheat head was inoculated with sterile water. The injection point is indicated by the red arrows. Photographs were taken on days 7 and 14 to monitor the development of the disease. **(C)** Relative abundance of the fungal strains during the wheat infection. The colors in the graph represent the pooled strains, which were equal in abundance in the inoculum. On day 7, *F. asiaticum* SY16 emerged as the dominant strain, while *F. graminearum* SY175 decreased in abundance. **(D)** Based on the relative abundance of fungal strains, we calculated the inverse Simpson and Shannon indices. The decrease in these alpha diversity indices on days 7 and 14 suggests a sharp decline in the diversity of the fungal community during wheat infection. **(E)** The abundance patterns of fungal strains varied across different stress conditions. Each bar in the graph shows the strain composition of a particular stress condition 4 days after inoculation. The different colors in the graph represent the pooled strains, which had equal abundance in the inoculum. CM, complete medium only; H_2O_2, hydrogen peroxide; NaCl, sodium chloride; SDS, sodium dodecyl sulfate; DTT, dithiothreitol. **(F)** The Inverse Simpson and Shannon indices were determined for each stress condition based on the relative abundance of fungal strains, and the results are presented using box and whisker plots. The box spans the interquartile range, the vertical lines show the full range of data, and the middle line within the box represents the median value. The presence of asterisks indicates a significant decline in the average alpha diversity indices compared to the initial inoculum ($p < 0.001$), implying that the diversity of the fungal community decreased in stress conditions.

These observations fit well with the modern coexistence theory (Mayfield and Levine, 2010) that competition operates by competitive ability differences, leading to the exclusion of distantly related taxa and thus to phenotypic clustering. Abiotic filtering also results in the overrepresentation of environmental tolerance traits leading to phenotypically clustered (related) communities. Based on this theory, we propose a mechanism by which both abiotic and biotic filtering have shaped the communities of *F. graminearum* and *F. asiaticum* (Figure 5). *F. asiaticum* was the dominant species in the field, whereas *F. graminearum* was less abundant. The geographical distribution of these two species was related to the climate, with *F. graminearum* predominant in the cold temperate region and *F. asiaticum* in the warm temperate region of East Asia (Suga et al., 2008; Lee et al., 2010; Wang et al., 2022). This pattern is consistent with a previous observation that climate plays a significant role in shaping the distribution of various *Fusarium* species responsible for FHB globally (Backhouse, 2014; Xu et al., 2021). By infecting the host plant, the plant pathogens gain access to resources and outcompete other microorganisms that lack the ability to infect plants. Biotic filtering, resulting from competition for host infection, leads to the overrepresentation of infectivity-related traits, generating phenotypic clustering. Our study demonstrated that competition between *Fusarium* strains for infection and colonization of host plants resulted in the predominance of a highly infectious strain (Figure 4C). Previous greenhouse and field studies on other plant pathogenic fungi, has underscored the significant role the host plays in determining the outcome of such competitions (Sommerhalder et al., 2011; Zhan and McDonald, 2013; Bernasconi et al., 2022). Wang et al. showed that a single wheat head in the field is colonized by a single dominant species: *F. graminearum* or *F. asiaticum* (Wang et al., 2022). Similarly, most wheat heads with FHB in Europe were colonized by a single *Fusarium* species: *Fusarium graminearum* or *Fusarium culmorum* (Klix et al., 2008). The use of monoculture and crop rotation resulted in the homogeneous distribution of host plants, which increased the competition between *Fusarium* strains and selected for few strains with the ability to infect a wide range of crop plants. As a result, agricultural intensification resulted in locally clustered communities of plant pathogenic fungi in the field.

Large-scale phenotyping has been implemented to assess the phenotypic variations of many field isolates (Talas et al., 2016; Dutta et al., 2021). However, the filamentous growth of these fungi makes it difficult to use the high-throughput approach. Measuring the radius of a colony on agar plates is often laborious and does not provide a quantitative measure of growth. In this study, we utilized the high-throughput approach that developed to efficiently examine the tolerance of the yeast-like fungi to various stressors, including antifungal agents (Siles et al., 2013; Caplan et al., 2020; Aguiar-Cervera et al., 2021; Du Bois et al., 2022). To achieve this, a suspension conidia (asexual spores) was used to inoculate liquid media on 96-well plates. This method allowed for easy control of the inoculum size and scalability of experiments. By using small volumes of media for 96-well cultures, toxic chemical usage was reduced, and quantitative measurement of growth as OD using a plate reader saved time and reduced human bias. However, it should be noted that chemicals with colors could not be used due to their interference with OD readings, presenting a potential limitation. Our approach can be used for the identification of antifungal resistant strains in the field and for screening mutant libraries in various stress conditions. We believe our high-throughput screening approach will be a valuable toolkit for study of filamentous fungi.

One interesting observation from our high-throughput screening was that stress tolerance traits had a wide range of phenotypic variation *F. asiaticum* (Figure 3A). Similarly, global strains of the fungal wheat pathogen *Zymoseptoria tritici* showed a high degree of phenotypic diversity across all measured traits. This indicates rapid and divergent evolution of these traits among related taxa (Goberna et al., 2014). This rapid evolution of stress tolerance traits may be due to genome plasticity, which many pathogenic fungi use to adapt to environmental and host stress (Covo, 2020; Bussotti et al., 2021; Min et al., 2021; Smith et al., 2022). For instances, in the human pathogen *Candida albicans*, genetic changes and aneuploidy are frequently detected, and are known to contribute to antifungal resistance, stress tolerance, and virulence (Legrand et al., 2019; Min et al., 2021; Smith et al., 2022). In the context of *Fusarium graminearum*, population genomics analyses have revealed a high level of genetic diversity and evidence of extensive recombination within the population (Talas and McDonald, 2015; Talas et al., 2016). These findings underscore the dynamic nature of pathogenic fungal genomes and their inherent capacity to adapt and evolve in response to environmental and host-induced stresses. This diversity and plasticity potentially play a crucial role in their ability to cause disease and thrive in various environments, thereby posing significant challenges to disease management strategies.

In conclusion, we propose a model for *Fusarium* community assembly (Figure 5). Our analysis of community structure reveals

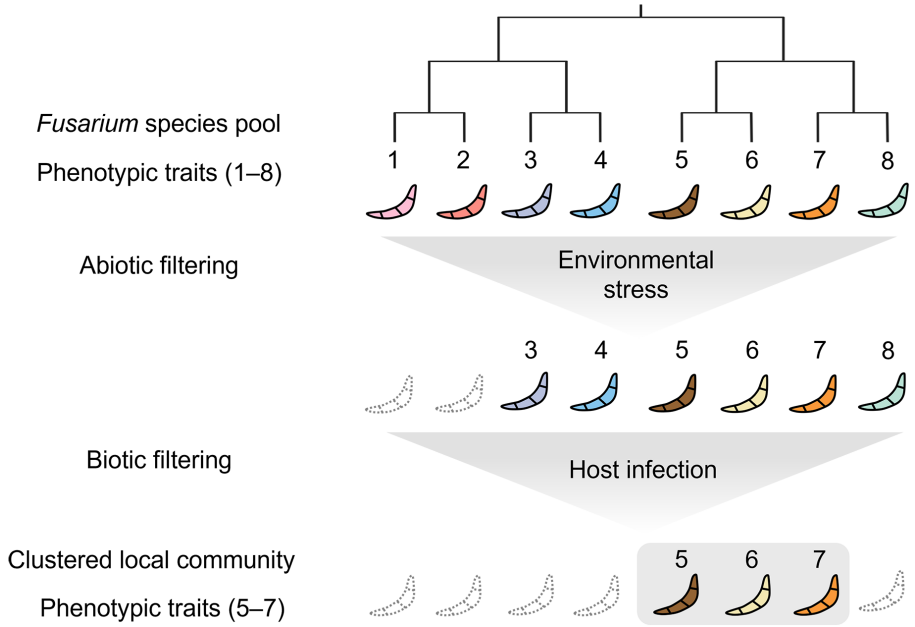

FIGURE 5
Conceptual representation of the clustering model tested for *F. graminearum* and *F. asiaticum* strains of the Republic of Korea. Fungal strains from the Republic of Korea *Fusarium* species pool are subjected to an abiotic filter that selects for strains with tolerances to various environmental stresses, such as desiccation, harsh temperature, and agrochemicals. The selected strains then segregate into local communities according to local biotic filters, such as host infection, which leads to a clustered phenotypic structure. As a result, the local communities have fewer phenotypic traits and reduced phylogenetic diversity. In summary, abiotic stresses and biotic interactions generate phenotypic and phylogenetic clustering in the plant pathogenic fungi.

that *F. graminearum* and *F. asiaticum* evolve stress tolerance traits rapidly and divergently. However, abiotic and biotic filtering result in overrepresentation of certain traits, leading to phenotypically clustered communities. These findings have important implications for understanding the dynamics of fungal communities in agriculture. By highlighting the role of infectivity and stress tolerance traits in driving clustering, our study provides insights into the factors that shape the structure and composition of pathogenic fungi communities. Future studies focusing on the genetic basis of these traits using high-throughput screening and multi-omics approaches will further elucidate the molecular mechanisms underlying community assembly in pathogenic fungi.

Data availability statement

The data presented in the study are deposited in the NCBI repository, accession numbers from OR348436 to OR348639.

Author contributions

SC, JWY, HS, and KM conceived and designed the experiments. SC, JWY, HJ, SS, DW, LSK, and KM conducted the experiments. HS and KM supervised the experiments. SC and KM performed statistical analysis and interpreted the data. SC, JWY, HS, and KM wrote and edited the manuscript. All authors read and approved the final manuscript.

Funding

This work was supported by the National Research Foundation of Korea (2022R1I1A1A01065138 and 2021R1C1C1004200) and the project PJ015741022023 of National Institute of Crop Science, Rural Development Administration, Republic of Korea.

Conflict of interest

The authors declare that the research was conducted in the absence of any commercial or financial relationships that could be construed as a potential conflict of interest.

Publisher's note

All claims expressed in this article are solely those of the authors and do not necessarily represent those of their affiliated organizations, or those of the publisher, the editors and the reviewers. Any product that may be evaluated in this article, or claim that may be made by its manufacturer, is not guaranteed or endorsed by the publisher.

Supplementary material

The Supplementary material for this article can be found online at: https://www.frontiersin.org/articles/10.3389/fmicb.2023.1234724/full#supplementary-material

References

Abadi, S., Azouri, D., Pupko, T., and Mayrose, I. (2019). Model selection may not be a mandatory step for phylogeny reconstruction. *Nat. Commun.* 10:934. doi: 10.1038/s41467-019-08822-w

Administration, K. M. (2022). *Climatological normals*. Available at: https://data.kma.go.kr/normals/index.do

Aguiar-Cervera, J. E., Delneri, D., and Severn, O. (2021). A high-throughput screening method for the discovery of *Saccharomyces and non-Saccharomyces* yeasts with potential in the brewing industry. *Eng. Biol.* 5, 72–80. doi: 10.1049/enb2.12013

Ahn, S., Kim, M., Lim, J. Y., Choi, G. J., and Seo, J. A. (2022). Characterization of *Fusarium asiaticum* and *F. graminearum* isolates from gramineous weeds in the proximity of rice fields in Korea. *Plant Pathol.* 71, 1164–1173. doi: 10.1111/ppa.13541

Backhouse, D. (2014). Global distribution of *Fusarium graminearum*, *F-asiaticum* and *F-boothii* from wheat in relation to climate. *Eur. J. Plant Pathol.* 139, 161–173. doi: 10.1007/s10658-013-0374-5

Bernasconi, A., Alassimone, J., McDonald, B. A., and Sanchez-Vallet, A. (2022). Asexual reproductive potential trumps virulence as a predictor of competitive ability in mixed infections. *Environ. Microbiol.* 24, 4369–4381. doi: 10.1111/1462-2920.16018

Bussotti, G., Piel, L., Pescher, P., Domagalska, M. A., Rajan, K. S., Cohen-Chalamish, S., et al. (2021). Genome instability drives epistatic adaptation in the human pathogen *Leishmania*. *Proc. Natl. Acad. Sci. U. S. A.* 118:e2113744118. doi: 10.1073/pnas.2113744118

Caplan, T., Lorente-Macias, A., Stogios, P. J., Evdokimova, E., Hyde, S., Wellington, M. A., et al. (2020). Overcoming fungal Echinocandin resistance through inhibition of the non-essential stress kinase Yck2. *Cell Chem. Biol.* 27, 269–282.e5. doi: 10.1016/j.chembiol.2019.12.008

Cappellini, R. A., and Peterson, J. L. (1965). Macroconidium formation in submerged cultures by a non-sporulating strain of *Gibberella Zeae*. *Mycologia* 57, 962–966. doi: 10.1080/00275514.1965.12018285

Carr, I. M., Robinson, J. I., Dimitriou, R., Markham, A. F., Morgan, A. W., and Bonthron, D. T. (2009). Inferring relative proportions of DNA variants from sequencing electropherograms. *Bioinformatics* 25, 3244–3250. doi: 10.1093/bioinformatics/btp583

Chen, Y. L., Xu, Z. W., Xu, T. L., Veresoglou, S. D., Yang, G. W., and Chen, B. D. (2017). Nitrogen deposition and precipitation induced phylogenetic clustering of arbuscular mycorrhizal fungal communities. *Soil Biol. Biochem.* 115, 233–242. doi: 10.1016/j.soilbio.2017.08.024

Covo, S. (2020). Genomic instability in fungal plant pathogens. *Genes* 11:421. doi: 10.3390/genes11040421

Desjardins, A. E. (2006). "Fusarium mycotoxins: chemistry, genetics, and biology", St. Paul, MN, APS Press.

Du Bois, A. C., Xue, A., Pham, C., Revie, N. M., Meyer, K. J., Yashiroda, Y., et al. (2022). High-throughput chemical screen identifies a 2,5-disubstituted pyridine as an inhibitor of *Candida albicans* Erg11. *mSphere* 7:e0007522. doi: 10.1128/msphere.00075-22

Dutta, A., Hartmann, F. E., Francisco, C. S., McDonald, B. A., and Croll, D. (2021). Mapping the adaptive landscape of a major agricultural pathogen reveals evolutionary constraints across heterogeneous environments. *ISME J.* 15, 1402–1419. doi: 10.1038/s41396-020-00859-w

Goberna, M., Navarro-Cano, J. A., Valiente-Banuet, A., Garcia, C., and Verdu, M. (2014). Abiotic stress tolerance and competition-related traits underlie phylogenetic clustering in soil bacterial communities. *Ecol. Lett.* 17, 1191–1201. doi: 10.1111/ele.12341

Gotzenberger, L., de Bello, F., Brathen, K. A., Davison, J., Dubuis, A., Guisan, A., et al. (2012). Ecological assembly rules in plant communities--approaches, patterns and prospects. *Biol. Rev. Camb. Philos. Soc.* 87, 111–127. doi: 10.1111/j.1469-185X.2011.00187.x

Kembel, S. W., Cowan, P. D., Helmus, M. R., Cornwell, W. K., Morlon, H., Ackerly, D. D., et al. (2010). Picante: R tools for integrating phylogenies and ecology. *Bioinformatics* 26, 1463–1464. doi: 10.1093/bioinformatics/btq166

Kim, J. H. (2021). Press release: prevention of *Fusarium* head blight, important before and after harvest. Available at: https://www.rda.go.kr:2360/board/board.do?boardId=farmprminfo&prgId=day_farmprminfoEntry&currPage=1&dataNo=100000771605&mode=updateCnt&searchSDate=&searchEDate=&searchOrgDeptKey=org&searchOrgDeptVal=&searchKey=subject&searchVal=%EB%B6%89%EC%9D%80%EA%B3%B0%ED%8C%A1%EC%9D%B4%EB%B3%91.

Klix, M. B., Beyer, M., and Verreet, J. A. (2008). Effects of cultivar, agronomic practices, geographic location, and meteorological conditions on the composition of selected *Fusarium* species on wheat heads. *Can. J. Plant Pathol.* 30, 46–57. doi: 10.1080/07060660809507495

Lee, J., Chang, I. Y., Kim, H., Yun, S. H., Leslie, J. F., and Lee, Y. W. (2009). Genetic diversity and fitness of *Fusarium graminearum* populations from rice in Korea. *Appl. Environ. Microbiol.* 75, 3289–3295. doi: 10.1128/AEM.02287-08

Lee, S. H., Han, Y. K., Yun, S. H., and Lee, Y. W. (2009). Roles of the glyoxylate and methylcitrate cycles in sexual development and virulence in the cereal pathogen *Gibberella zeae*. *Eukaryot. Cell* 8, 1155–1164. doi: 10.1128/EC.00335-08

Lee, S. H., Lee, J., Nam, Y. J., Lee, S., Ryu, J. G., and Lee, T. (2010). Population structure of *Fusarium graminearum* from maize and rice in 2009 in Korea. *Plant Pathol. J.* 26, 321–327. doi: 10.5423/PPJ.2010.26.4.321

Legrand, M., Jaitly, P., Feri, A., d'Enfert, C., and Sanyal, K. (2019). *Candida albicans*: an emerging yeast model to study eukaryotic genome plasticity. *Trends Genet.* 35, 292–307. doi: 10.1016/j.tig.2019.01.005

Leslie, J. F., and Summerell, B. A. (2006). The *Fusarium* laboratory manual, Blackwell Pub, Ames, IA.

Mayfield, M. M., and Levine, J. M. (2010). Opposing effects of competitive exclusion on the phylogenetic structure of communities. *Ecol. Lett.* 13, 1085–1093. doi: 10.1111/j.1461-0248.2010.01509.x

Min, K., Jannace, T. F., Si, H., Veeramah, K. R., Haley, J. D., and Konopka, J. B. (2021). Integrative multi-omics profiling reveals cAMP-independent mechanisms regulating hyphal morphogenesis in *Candida albicans*. *PLoS Pathog.* 17:e1009861. doi: 10.1371/journal.ppat.1009861

Min, K., Son, H., Lee, J., Choi, G. J., Kim, J. C., and Lee, Y. W. (2012). Peroxisome function is required for virulence and survival of *Fusarium graminearum*. *Mol. Plant-Microbe Interact.* 25, 1617–1627. doi: 10.1094/MPMI-06-12-0149-R

Mykra, H., Tolkkinen, M., Markkola, A. M., Pirttila, A. M., and Muotka, T. (2016). Phylogenetic clustering of fungal communities in human-disturbed streams. *Ecosphere* 7:e01316. doi: 10.1002/ecs2.1316

O'Donnell, K., Kistler, H. C., Tacke, B. K., and Casper, H. H. (2000). Gene genealogies reveal global phylogeographic structure and reproductive isolation among lineages of *Fusarium graminearum*, the fungus causing wheat scab. *Proc. Natl. Acad. Sci. U.S. A.* 97, 7905–7910. doi: 10.1073/pnas.130193297

O'Donnell, K., Ward, T. J., Geiser, D. M., Corby Kistler, H., and Aoki, T. (2004). Genealogical concordance between the mating type locus and seven other nuclear genes supports formal recognition of nine phylogenetically distinct species within the *Fusarium graminearum* clade. *Fungal Genet. Biol.* 41, 600–623. doi: 10.1016/j.fgb.2004.03.003

Pattengale, N. D., Alipour, M., Bininda-Emonds, O. R., Moret, B. M., and Stamatakis, A. (2010). How many bootstrap replicates are necessary? *J. Comput. Biol.* 17, 337–354. doi: 10.1089/cmb.2009.0179

Pellissier, L., Niculita-Hirzel, H., Dubuis, A., Pagni, M., Guex, N., Ndiribe, C., et al. (2014). Soil fungal communities of grasslands are environmentally structured at a regional scale in the Alps. *Mol. Ecol.* 23, 4274–4290. doi: 10.1111/mec.12854

Salazar, D., Jaramillo, M. A., and Marquis, R. J. (2016). Chemical similarity and local community assembly in the species rich tropical genus Piper. *Ecology* 97, 3176–3183. doi: 10.1002/ecy.1536

Scala, V., Aureli, G., Cesarano, G., Incerti, G., Fanelli, C., Scala, F., et al. (2016). Climate, soil management, and cultivar affect fusarium head blight incidence and deoxynivalenol accumulation in durum wheat of southern Italy. *Front. Microbiol.* 7:1014. doi: 10.3389/fmicb.2016.01014

Seroussi, E. (2021). Estimating copy-number proportions: the comeback of sanger sequencing. *Genes* 12:283. doi: 10.3390/genes12020283

Siles, S. A., Srinivasan, A., Pierce, C. G., Lopez-Ribot, J. L., and Ramasubramanian, A. K. (2013). High-throughput screening of a collection of known pharmacologically active small compounds for identification of *Candida albicans* biofilm inhibitors. *Antimicrob. Agents Chemother.* 57, 3681–3687. doi: 10.1128/AAC.00680-13

Smith, A. C., Morran, L. T., and Hickman, M. A. (2022). Host defense mechanisms induce genome instability leading to rapid evolution in an opportunistic fungal pathogen. *Infect. Immun.* 90:e0032821. doi: 10.1128/iai.00328-21

Sommer, B., Sampayo, E. M., Beger, M., Harrison, P. L., Babcock, R. C., and Pandolfi, J. M. (2017). Local and regional controls of phylogenetic structure at the high-latitude range limits of corals. *Proc. Biol. Sci.* 284:20170915. doi: 10.1098/rspb.2017.0915

Sommerhalder, R. J., McDonald, B. A., Mascher, F., and Zhan, J. (2011). Effect of hosts on competition among clones and evidence of differential selection between pathogenic and saprophytic phases in experimental populations of the wheat pathogen *Phaeosphaeria nodorum*. *BMC Evol. Biol.* 11:188. doi: 10.1186/1471-2148-11-188

Starkey, D. E., Ward, T. J., Aoki, T., Gale, L. R., Kistler, H. C., Geiser, D. M., et al. (2007). Global molecular surveillance reveals novel fusarium head blight species and trichothecene toxin diversity. *Fungal Genet. Biol.* 44, 1191–1204. doi: 10.1016/j.fgb.2007.03.001

Stephen Brewer, J. (2000). Ecological Assembly Rules: Perspectives, Advances, Retreats. Cambridge: Cambridge University Press.

Suga, H., Karugia, G. W., Ward, T., Gale, L. R., Tomimura, K., Nakajima, T., et al. (2008). Molecular characterization of the *Fusarium graminearum* species complex in Japan. *Phytopathology* 98, 159–166. doi: 10.1094/PHYTO-98-2-0159

Suzuki, R., and Shimodaira, H. (2006). Pvclust: an R package for assessing the uncertainty in hierarchical clustering. *Bioinformatics* 22, 1540–1542. doi: 10.1093/bioinformatics/btl117

Talas, F., Kalih, R., Miedaner, T., and McDonald, B. A. (2016). Genome-wide association study identifies novel candidate genes for aggressiveness, deoxynivalenol production, and

azole sensitivity in natural field populations of *Fusarium graminearum*. *Mol. Plant Microbe Interact.* 29, 417–430. doi: 10.1094/MPMI-09-15-0218-R

Talas, F., and McDonald, B. A. (2015). Genome-wide analysis of *Fusarium graminearum* field populations reveals hotspots of recombination. *BMC Genomics* 16:996. doi: 10.1094/MPMI-09-15-0218-R

Trail, F. (2009). For blighted waves of grain: *Fusarium graminearum* in the postgenomics era. *Plant Physiol.* 149, 103–110. doi: 10.1104/pp.108.129684

van der Lee, T., Zhang, H., van Diepeningen, A., and Waalwijk, C. (2015). Biogeography of *Fusarium graminearum* species complex and chemotypes: a review. *Food Addit. Contam. Chem. Anal. Control Expo. Risk Assess.* 32, 453–460. doi: 10.1080/19440049.2014.984244

Wang, Q., Song, R., Fan, S., Coleman, J. J., Xu, X., and Hu, X. (2022). Diversity of *Fusarium* community assembly shapes mycotoxin accumulation of diseased wheat heads. *Mol. Ecol.* 32, 2504–2518. doi: 10.1111/mec.16618

Ward, T. J., Bielawski, J. P., Kistler, H. C., Sullivan, E., and O'Donnell, K. (2002). Ancestral polymorphism and adaptive evolution in the trichothecene mycotoxin gene cluster of phytopathogenic *Fusarium*. *Proc. Natl. Acad. Sci. U. S. A.* 99, 9278–9283. doi: 10.1073/pnas.142307199

Webb, C. O., Ackerly, D. D., McPeek, M. A., and Donoghue, M. J. (2002). Phylogenies and community ecology. *Annu. Rev. Ecol. Evol. Syst.* 33, 475–505. doi: 10.1146/annurev.ecolsys.33.010802.150448

Xu, F., Liu, W., Song, Y. L., Zhou, Y. L., Xu, X. M., Yang, G. Q., et al. (2021). The distribution of *Fusarium graminearum* and *Fusarium asiaticum* causing fusarium head blight of wheat in relation to climate and cropping system. *Plant Dis.* 105, 2830–2835. doi: 10.1094/PDIS-01-21-0013-RE

Zhan, J., and McDonald, B. A. (2013). Field-based experimental evolution of three cereal pathogens using a mark- release-recapture strategy. *Plant Pathol.* 62, 106–114. doi: 10.1111/ppa.12130

frontiers | Frontiers in Plant Science

TYPE Original Research
PUBLISHED 24 October 2023
DOI 10.3389/fpls.2023.1289959

OPEN ACCESS

EDITED BY
Mahyar Mirmajlessi,
Ghent University, Belgium

REVIEWED BY
Ali Chenari Bouket,
Agricultural Research, Education and Extension Organization, Tabriz, Iran
Elsherbiny A. Elsherbiny,
Mansoura University, Egypt

*CORRESPONDENCE
Jianghui Xie
xiejianghui@itbb.org.cn
Wei Wang
wangwei@itbb.org.cn
Yong-Zhong Liu
liuyongzhong@mail.hzau.edu.cn

†These authors contributed equally to this work

RECEIVED 06 September 2023
ACCEPTED 29 September 2023
PUBLISHED 24 October 2023

CITATION
Long W, Chen Y, Wei Y, Feng J, Zhou D, Cai B, Qi D, Zhang M, Zhao Y, Li K, Liu Y-Z, Wang W and Xie J (2023) A newly isolated *Trichoderma Parareesei* N4-3 exhibiting a biocontrol potential for banana fusarium wilt by Hyperparasitism.
Front. Plant Sci. 14:1289959.
doi: 10.3389/fpls.2023.1289959

A newly isolated *Trichoderma Parareesei* N4-3 exhibiting a biocontrol potential for banana fusarium wilt by Hyperparasitism

Weiqiang Long[1,2†], Yufeng Chen[1†], Yongzan Wei[1], Junting Feng[1], Dengbo Zhou[1], Bingyu Cai[1], Dengfeng Qi[1], Miaoyi Zhang[1], Yankun Zhao[1], Kai Li[1], Yong-Zhong Liu[2*], Wei Wang[1,2*] and Jianghui Xie[1,2*]

[1]National Key Laboratory of Tropical Crop Breeding, Institute of Tropical Bioscience and Biotechnology, Chinese Academy of Tropical Agricultural Sciences, Haikou, Hainan, China, [2]National Key Laboratory for Germplasm Innovation and Utilization of Horticultural Crops, College of Horticulture and Forestry Sciences, Huazhong Agricultural University, Wuhan, Hubei, China

Banana Fusarium wilt caused by *Fusarium oxysporum* f. sp. *cubense* tropical race4 (*Foc* TR4) is one of the most destructive soil-borne fungal diseases and currently threatens banana production around the world. Until now, there is lack of an effective method to control banana Fusarium wilt. Therefore, it is urgent to find an effective and eco-friendly strategy against the fungal disease. In this study, a strain of *Trichoderma* sp. N4-3 was isolated newly from the rhizosphere soil of banana plants. The isolate was identified as *Trichoderma parareesei* through analysis of *TEF1* and *RPB2* genes as well as morphological characterization. *In vitro* antagonistic assay demonstrated that strain N4-3 had a broad-spectrum antifungal activity against ten selected phytopathogenic fungi. Especially, it demonstrated a strong antifungal activity against *Foc* TR4. The results of the dual culture assay indicated that strain N4-3 could grow rapidly during the pre-growth period, occupy the growth space, and secrete a series of cell wall-degrading enzymes upon interaction with *Foc* TR4. These enzymes contributed to the mycelial and spore destruction of the pathogenic fungus by hyperparasitism. Additionally, the sequenced genome proved that strain N4-3 contained 21 genes encoding chitinase and 26 genes encoding β-1,3-glucanase. The electron microscopy results showed that theses cell wall-degrading enzymes disrupted the mycelial, spore, and cell ultrastructure of *Foc* TR4. A pot experiment revealed that addition of strain N4-3 significantly reduced the amount of *Foc* TR4 in the rhizosphere soil of bananas at 60 days post inoculation. The disease index was decreased by 45.00% and the fresh weight was increased by 63.74% in comparison to the control. Hence, *Trichoderma parareesei* N4-3 will be a promising biological control agents for the management of plant fungal diseases.

KEYWORDS

banana fusarium wilt, biological control, *Trichoderma*, enzyme, hyperparasitism

Introduction

Banana is the important staple and cash crops in tropical and subtropical regions. About 500 million people depend on bananas as a staple food in the world (Lozano-Durán et al., 2022). Meanwhile global banana exports have been largely on an upward trend. The world banana trade reached $28.963 billion US dollars in 2022 (Zou and Fan, 2022). The domestication and asexual reproduction techniques of most seedless edible banana varieties limit the genetic variation of bananas, ultimately leading to their susceptibility to pests and diseases (Perrier et al., 2011).

Banana Fusarium wilt, caused by *Fusarium oxysporum* f. sp. *cubense* (*Foc*), is the most destructive and threatening soil-borne fungal disease in banana production (Chen et al., 2022). The causal agent is subdivided into four subspecies depending on the infected banana species (Dita et al., 2018). One of these pathogenic fungi named *Fusarium oxysporum* f. sp. *cubense* tropical race 4 (*Foc* TR4) can infect almost all banana varieties (Dita et al., 2018; García-Bastidas, 2019). Notably, *Foc* TR4 spores are able to tolerate harsh environmental conditions and survive in soil for more than 20 years (Qi et al., 2021). They are capable of spreading on non-host species by soil, irrigation or agricultural equipment (Ploetz, 2015a). To date, there are no commercially available banana varieties that are resistant to *Foc* TR4. In addition, *Foc* TR4 is insensitive to some fungicides and long-term application of chemical pesticides caused a bad pollution on soil ecology (Cannon et al., 2022). In contrast, microbial fungicides have the ability to control pathogenic fungi and do not damage soil ecology. Therefore, the application of microorganisms to control pathogenic fungi has good prospects.

Trichoderma spp. present in soil and plants are diverse and easy to pure cultivation (Guo et al., 2019; Savani et al., 2021). *Trichoderma* species are fast-growing fungus that compete with pathogenic fungi for nutrition and living space, thereby limiting the growth of pathogenic fungi. They can parasitize the hyphae of pathogenic fungi and produce cell wall-degrading enzymes, ultimately leading to the death of the pathogenic fungi. Additionally, *Trichoderma* can also inhibit the growth of plant pathogens by producing secondary metabolites and volatile organic compounds that have antagonistic activity (Harni et al., 2020; Lv et al., 2023). For instance, the active metabolite gliotoxin, isolated from the culture broth of *Trichoderma virens* HZA14, was found to completely inhibit the growth of *Phytophthora capici* mycelium when added to PDA at a concentration of 5.0 μg/mL (Tomah et al., 2020). Rajani et al. found that *Trichoderma longibrachiatum* MK751759 can produce volatile organic compounds to inhibit the growth of *Sclerotium rolfsii CSR* (Rajani et al., 2021). In addition, *Trichoderma* has been shown to stimulate systemic induced resistance in host plants (Mukherjee et al., 2013; Sood et al., 2020). Although a large number of studies on *Trichoderma* have been reported (Tomah et al., 2020; Díaz-Gutiérrez et al., 2021; Tamizi et al., 2022), the inhibitory mechanism of different *Trichoderma* on pathogens still needs to be elucidated. Therefore, it is necessary to isolate *Trichoderma* strains with high antagonistic activity and characterize their antagonistic mechanism.

In this study, an antagonistic strain N4-3 against *Foc* TR4 was isolated from banana plantation soil. Morphological identification and multigene association analysis were used to determine its taxonomic characteristics. We further evaluated its broad-spectrum antifungal activity against various plant pathogenic fungi. The hyperparasitism of strain N4-3 was confirmed by observing the dual culture region using scanning electron microscopy. In order to elucidate the antifungal mechanism of strain N3-4, the cell wall-degrading enzymes secreted by the isolate were extracted and identified. And further testing was conducted to investigate the effects of enzymes on the mycelium, spores, and cellular ultrastructure of the pathogenic fungus. Genomic analysis revealed the presence of a large number of genes encoding chitinases and β-1,3-glucanase in the genome of strain N4-3. A pot experiment was carried out to further investigate the biocontrol efficiency of strain N4-3 against *Foc* TR4. The results will provide additional selection for agricultural biocontrol agents and biofertilizers.

Materials and methods

Isolation of *Trichoderma* spp.

Soil samples was collected from rhizosphere of a banana plantation without symptom of banana fusarium wilt for more than ten years in Lingao County, Hainan Province, China (19°45'3 "N, 109°55'17 "E). The collected samples were transported to the laboratory in a sterile plastic bag and stored at 4°C. *Trichoderma* were isolated from soil samples by a gradient dilution method (Rahman et al., 2023). Briefly, 5 g of fresh soil was added to 45 mL of sterile distilled water, incubated at 28°C with shaking at 180 r/min for 30 min, and then diluted with sterile water to 10^{-1}~10^{-3}. 100 μL of diluted soil suspension was poured onto the Rose Bengal Agar (RBA) (5.0 g peptone, 10.0 g glucose, 1.0 g dipotassium hydro gen phosphate, 0.5 g magnesium sulfate, 0.033 g Bengal Red, 0.1 g chloramphenicol, 20.0 g agar in one liter water) was spread on the plate using an applicator. Subsequently, the plates were placed at 28°C and incubated for 3-5 days. Single colony on the selection medium was transferred to the potato dextrose agar medium (PDA) for purification. The purified strains were stored at 4°C for the following study.

Antifungal activity screening of *Trichoderma* against *Foc* TR4

The isolate with the highest antifungal activity against *Foc* TR4 was screened by a dual culture method (Tian et al., 2016). Mycelial discs (5 mm in diameter) of *Trichoderma* were placed on the edge of PDA plates and the same size mycelial discs of *Foc* TR4 were placed on the opposite side. A mycelial disc of *Foc* TR4 alone was used as a control. Plates were incubated at 28°C for 7 days. The radius of *Foc* TR 4 colonies on the dual culture plates was determined. The inhibition rate (MI) was calculated using the following equation: $MI = [(R_1-R_2)/R_1] \times 100$, where R_1 and R_2 represented the radius of *Foc* TR4 colonies in the control and the treatment groups, respectively.

Based on inhibition rate against *Foc* TR4, an isolate, labeled as strain N4-3, with strong antifungal activity was selected for the following study.

Morphological, physiological and biochemical characteristics of strain N4-3

Mycelial discs of strain N4-3 from actively growing colonies were placed on PDA plates, incubated at 28°C for 48-72 h. Morphological characteristics of mycelium and spores were observed using biomicroscope (CellcutPlus, MMI, Germany) and scanning electron microscope (SEM, SIGMA Field Emission Scanning Electron Microscope). The physiological and biochemical parameters of strain N4-3 were determined, including resistance to pH and utilization of carbon and nitrogen sources (Wei et al., 2020).

Phylogenetic analysis

DNA from fresh mycelium was extracted using the Fungal Genome Rapid Extraction Kit (Aidlab, China). The primers for RNA polymerase II subunit (rpb2) were fRPB2-5f (GAYGAYMGWGATCAYTTYGG) and fRPB2-7cr (CCCATRGCTTGTYYRCCCAT). The primers for translation elongation factor 1 α(tef1) were EF1 (ATGGGTAAGG ARGACAAGAC) and EF2 (GGARGTACCAGTSATCATGTT) (Liu et al., 1999; Kothe et al., 2016; Cai and Druzhinina, 2021). The amplified PCR products were sequenced using a Sanger-based automated sequencer (Applied Biosystems). Sequences were edited by DNAMAN. Reference sequences were analyzed by nucleotide BLAST searches in the GenBank database (Supplementary Table 1). Phylogenetic trees were constructed by using two locus combinations of the *TEF1* and *RPB2* datasets. The gene sequences were aligned with MAFFT and the generated sequences were edited by Gblocks to remove ambiguously aligned positions and divergent regions prior to phylogenetic analysis. Two locus data were pooled and analyzed using the maximum likelihood method in MEGA Version 7.0.

Sequencing and annotation of the strain N4-3 genome

Genomic DNA was extracted from strain N4-3. Libraries were constructed using the Hieff NGS® MaxUp II DNA Library Preparation Kit for Illumina® and quantified using the Thermo Qubit 4.0 Fluorescence Quantification Instrument Q33226 (ThermoFisher). Sequencing was performed on the Illumina High-Throughput Sequencing Platform (HiSeq). Quality of raw sequencing data was assayed by FastQC. Sequence correction was performed using PrInSeS-G to correct for editing errors and insertion deletion of small fragments during splicing. Genetic components such as genes, tRNAs, rRNAs were predicted using GeneMark, etc. The repetitive sequences were identified using Repeat Masker (Koren et al., 2017). CRISPR prediction analysis was performed using CRT. Gene protein sequences were aligned with multiple databases such as CDD, KOG, COG, NR, NT, PFAM, Swissprot and TrEMBL. GO and KEGG annotation was analyzed according to the previous methods (Wei et al., 2020).

Determination of the broad-spectrum antifungal activity of strain N4-3

To evaluate the broad-spectrum antifungal activity of strain N4-3, ten phytopathogenic fungi were selected including *C. gloeosporioides* (ATCC 58222), *C. gloeosporioides* (ATCC16330), *C. fragariae* (ATCC 58718), *C. lunata* (ATCC 42011), *F. graminearum Sehw* (ATCC MYA-4620), *C. musae* (ATCC 96167), *F. oxysporum f.* sp. *cucumerinum* (ATCC 204378), *C. acutatum* (ATCC56815), *C. gloeosporioides* (ATCC MY A-456), and *C. fallax* (ATCC 38579). A 5 mm mycelial discs of *Trichoderma* were placed on the edge of PDA plates. The same size discs of various pathogenic fungi were placed on the opposite side. The pathogenic mycelial discs alone were used as a control. All experiments were repeated in triplicate.

Interaction observation between strain N4-3 and *Foc* TR4

The dynamics of strain N4-3 and *Foc* TR4 interactions was observed using a dual culture method (Damodaran et al., 2020). The discs were punched at the colonial edge of *Trichoderma* and *Foc* TR4, respectively, and placed on the PDA plates at 28°C for incubation. The growth was recorded at 12 h intervals. After successful fungal superparasitism on the pathogen, the dual culture areas were observed using the UItra-depth-of-field Three-dimensional Microscope system (VHX-600, Kerns). Mycelial region of *Foc* TR4 on the dual culture plate were selected and fixed in 2.5% of glutaraldehyde for 12 h. The samples were dehydrated with a gradient ethanol (30, 50, 70, 80, 90, 95, 100%) for 2-3 min each time. The samples were freeze-dried, and then observed by scanning electron microscopy (SEM).

Determination of antifungal activity of extracts and volatile organic compounds of strain N4-3

The metabolites of strain N4-3 were extracted according to Zhang et al. (Zhang et al., 2021). Briefly, strain N4-3 was incubated in PDB at 28°C and 180 r/min for 7 days. The culture broth was mixed with an equal volume of anhydrous ethanol and shaken at 150 rpm for 3 days. After filtration through the Whatman No.1 filter, the extract was evaporated using a rotary evaporator. The dried extracts were dissolved into saturated solution using sterile water. The extracts solution was used to test antimicrobial activity by an agar diffusion method.

Antifungal activity of volatile organic compounds produced by strain N4-3 was tested according to Rajani et al. (Rajani et al., 2021).

Mycelial discs (5 mm in diameter) of strain N4-3 and *Foc* TR4 were picked from the edge of colonies and placed on two separate plates containing PDA. The two plates were placed against each other. To prevent cross-contamination, a sterile cellophane layer was added between the two petri dishes. Only mycelial discs of *Foc* TR4 were used as a control. The inhibition rate was measured and calculated after 7 days.

Crude enzyme solution extraction of strain N4-3

Strain N4-3 was incubated in the PDB medium at 28°C and 180 r/min with shaking for 7 days. The culture solution was filtered through filter paper to collect the filtrate. 100 mL of the filtrate was then added to a 250 mL conical flask. Ammonium sulfate was added to prepare a mixed solution with varying saturations (10%, 20%, 30%, 40%, 50%, 60%, 70%, 80%, 90% and 100%) and left overnight at 4°C (Xu et al., 2022). At least three replicates of each experiment were performed. The mixture was then centrifuged at 10,000 r/min for 10 min at 4°C, and the supernatant was discarded. The precipitates were suspended in 2 mL of phosphate buffer (pH 7.2-7.4) to obtain crude enzyme solution for chitinase and β-1,3-glucanase.

Inhibition efficiency of crude enzyme solution on mycelial growth of *Foc* TR4

The crude enzyme solution was freeze-dried to powder. Different concentrations (400, 200, 100, 50 and 25 mg/mL) of crude enzyme were prepared using PBS. Inhibition efficiency was tested as described by Mohiddin et al. (2021). After filtering through a membrane to remove bacteria, 200 µL of the crude enzyme solution were evenly poured to the PDA medium and inoculated with *Foc* TR4 mycelial blocks. The crude enzyme solution after high-temperature inactivation was used as a control. At least three replicates were set for each concentration. The inhibition efficiency was calculated by measuring the colony diameter after 5 days. A toxicity regression equation was established as a linear regression using a least squares method. The EC_{50} value was calculated from the toxicity regression equation (Wei et al., 2020).

Inhibition of crude enzyme solution on spore germination of *Foc* TR 4

The germination rate of *Foc* TR4 spores was measured as the description of Li et al. (2021) with a minor modification. Firstly, 20 µL of spore suspension (1.0×10^6 CFU/mL) was mixed with an equal volume of crude enzyme solution at a final concentration of $1\times$ EC_{50}. The mixture was then added to a concave slide. The same concentration of heat-inactivated crude enzyme solution was used as a control. The spores were incubated at 28°C for 24 h, and 100 spores on each slide were observed using a light microscope. The spore germination rate was used to evaluate the inhibition efficiency. All experiments were performed in triplicates.

Effect of crude enzyme solution on the growth of *Foc* TR4 mycelia

The mycelial discs of *Foc* TR4 were inoculated in the center of the PDA plate, and four sterilized coverslips were placed equidistantly around the plate. The plate was incubated at 28°C until the mycelia of *Foc* TR4 covering the whole coverslips. Subsequently, 100 µL of crude enzyme solution ($1\times EC_{50}$) filtered through a syringe filter and covered with mycelia on the coverslips. The plates were gently shaken to ensure that the enzyme solution covered the entire slide. Two coverslips per plate were treated with the crude enzyme solution. Other two coverslips were treated with the same concentration of heat-inactivated crude enzyme solution as a control. After one day of incubation, the morphological changes of the mycelia were observed under a light microscope.

Effect of crude enzyme solution on spore morphology of *Foc* TR4

To prepare a spore suspension of *Foc* TR4, 100 µL of spore suspension (1.0×10^6 CFU/mL) was pipetted onto a coverslip, followed by the addition of 100 µL of crude enzyme solution ($2 \times EC_{50}$) (Chen et al., 2018). The same concentration of heat-inactivated crude enzyme solution was used as a control. The spores were incubated at 28°C for 24 h. After fixation, changes of spore morphology were observed using SEM.

Effect of crude enzyme solution on the ultrastructure of *Foc* TR4 cells

Mycelial discs were inoculated at the center of PDA plates. After two days at 28°C, the peripheral mycelia of colonies were treated with a crude enzyme solution ($1 \times EC_{50}$). The control group was treated with the same concentration of heat-inactivated crude enzyme solution. After one day of incubation, samples were prepared according to Yun et al. (2021). The ultrastructure of *Foc* TR4 cells was observed with using a transmission electron microscope (TEM, JEM-1400Flash, Hitachi, Ltd., Tokyo, Japan).

Pot experiment

Banana seedlings (*Musa acuminata* L. AAA genotype cv. Cavendish) with the height of 8-10 cm were transplanted into plastic pots (8 cm × 8 cm) containing 1000 g of sterilized soil. The plants were then placed in a greenhouse at 28°C and a relative humidity of 70-80%. *Foc* TR4 expressing the GFP gene (GFP-*Foc* TR4) was provided by the Institute of Environment and Plant Protection, Chinese Academy of Tropical Agricultural Sciences,

Haikou, China. Three treatments were set, including Blank (sterile water), Control (positive control, inoculated with GFP-*Foc* TR4) and Treatment (1.0×10^7 CFU/mL of strain N4-3 fermentation broth and 1.0×10^7 CFU/mL of GFP-*Foc* TR4). 100 mL of mixture was added to the roots of banana seedlings (Jing et al., 2020). Banana seedlings were treated at 7 days intervals. Roots were selected at 60 days post inoculation (dpi) and sections were made using a manual method (Jing et al., 2020). *Foc* TR4 infection was observed with a laser scanning confocal microscope (ZEISS, LSM800, Germany). The maximum photosynthetic efficiency, relative chlorophyll content, leaf area, leaf thickness, stem thickness, plant height, fresh weight and index of photosynthetic system II were also measured. Inter-root soil was collected for *Foc* TR4 quantification as our previous description (Chen et al., 2018). The number of *Foc* TR4 colony-forming units (CFU/g) was determined using the inter-root soil suspension gradient dilution method. Each experiment was replicated in triplicate. Ten plants were used in each replication.

Statistical analysis

The data were analyzed using the SPSS software (Version 23.0). All experiments were performed in triplicate. Significant difference ($p < 0.05$) was determined using the Duncan's multiple extreme difference test. The results obtained from three independent experiments were expressed as a mean ± standard deviation.

Results

Isolation and screening of *Trichoderma* spp.

To screen *Trichoderma* spp. exhibiting antifungal activity against *Foc* TR4, the rhizosphere soil was selected from banana plantations without disease symptom for ten years. A double incubation experiment was performed. Nine members of *Trichoderma* spp. were obtained and incubated with *Foc* TR4 at 28°C for 7 days. The colonial radius of *Foc* TR4 was measured in both the treatment and control groups (Figure 1A). The inhibition efficiency of each strain was calculated. The results showed that strain N4-3 exhibited the highest inhibition activity at 72.37 ± 1.67%, whereas N1-4 displayed the lowest inhibition efficiency at 37.29 ± 2.98%. The inhibition rate of strain N4-3 was significantly higher than that of other strains (Figure 1B). Therefore, strain N4-3 was selected for the following experiment.

Identification of strain N4-3

After 48 h of growth on the PDA medium, strain N4-3 exhibited abundant aerial mycelia. The conidiophores were densely packed and appeared white or green in color (Figure 2A). The conidia were ellipsoidal in shape and grew along the main axis, with terminal thick-walled conidia that were globose to subglobose in shape (Figure 2A). Strain N4-3 produced a yellow pigment on the PDA medium (Supplementary Figure 1C). The results of physiological and biochemical tests indicated that strain N4-3 exhibited tolerance to pH ranging from 5 to 9. Additionally, strain N4-3 demonstrated the ability to utilize all 16 tested carbon sources. Among the tested nitrogen sources, strain N4-3 could utilize eight sources, except for L-arginine (Supplementary Table 2).

The sequencing of PCR products was assembled using DNAMAN software. After alignment using MAFFT and editing with Gblocks, the length of *tef1* and *rpb2* were 1127 bp and 1074 bp, respectively. To analyze the evolutionary relationship of strain N4-3, *tef1* and *rpb2* were used for constructing the phylogenetic tree by alignment of the selected 25 type strains. The results revealed that strain N4-3 clustered with *Trichoderma parareesei* CP55_3, forming a distinct evolutionary branch with 87% of ML-BS (Figure 2B).

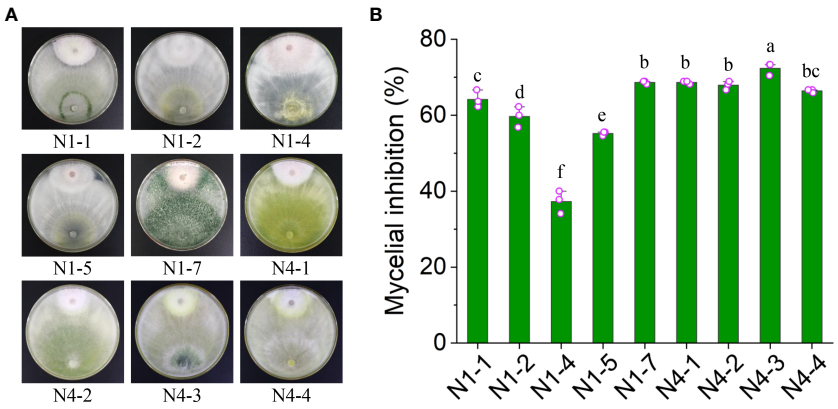

FIGURE 1
Inhibition efficiency of nine isolated fungi against *Foc* TR4. **(A)** Dual culture of nine fungal strains with *Foc* TR4. **(B)** Inhibition efficiency of nine fungal strains against *Foc* TR4. Different lowercase letters represented the significant difference (P<0.05).

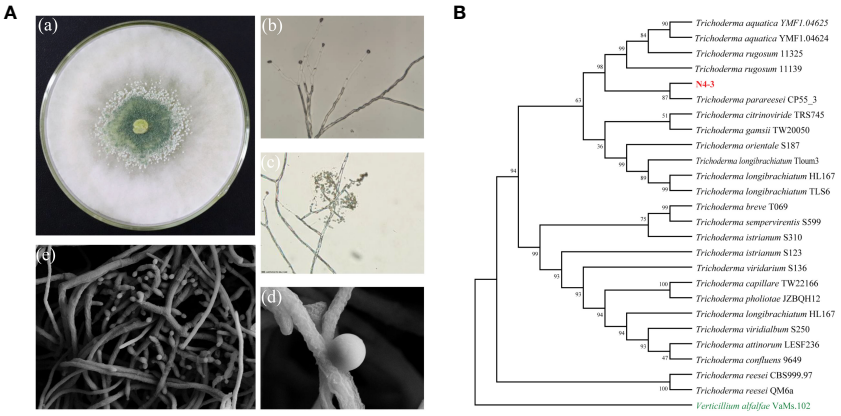

FIGURE 2
Morphological observations and phylogenetic analysis of strain N4-3. **(A)** Morphological observation of strain N4-3. a.Morphological characterization of N4-3 grown on top of potato dextrose agar medium, b-c. Morphological characteristics of spores and hyphae of N4-3 were observed using a biomicroscope, d-e Morphological characteristics of spores and hyphae of N4-3 were observed using a scanning electron microscope. **(B)** Phylogenetic tree generated by maximum likelihood analysis based on the tandem sequence alignment of two genes (*tef1* and *rpb2*).

Combining with the morphological characteristics, strain N4-3 was identified as *Trichoderma parareesei*.

Genome assembly and annotation

By sequencing and assembling, the genome size of strain N4-3 was 32,339,192 bp. The GC content was 54% and repetitive sequences accounted for 2.08%. A total of 9,271 genes were predicted for the strain N4-3 genome, with an average sequence length of 1,522 bp (Figure 3A; Supplementary Table 3). Among these genes, 6,320 (68.17%), 4,806 (51.84%), and 3261 (35.17%) were annotated using GO, KOG and KEGG, respectively (Supplementary Table 4). The annotated genes were classified according to the GO terms in the three categories of Biological Process, Cellular Component and Molecular Function, (Figure 3B). In KOG, the pathways with high number of annotated genes were translation, ribosome structure and biogenesis (6.39%), followed by

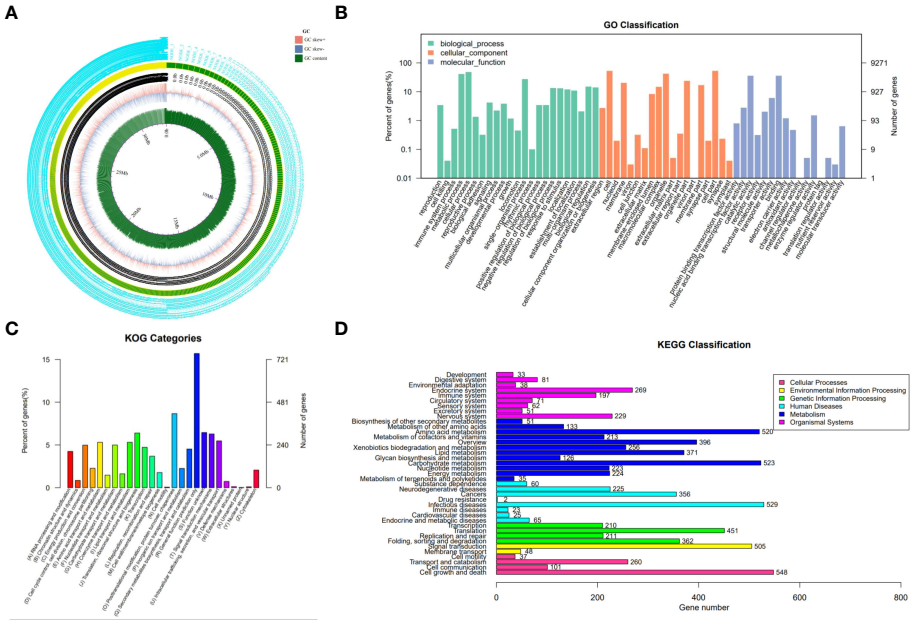

FIGURE 3
Genomic information of strain N4-3 and functional annotation of predicted genes. **(A)** Gene circle map of strain N4-3. **(B)** Histogram of GO annotation. The horizontal axis was the secondary classification of GO and the vertical axis was the number of genes. Different colors represented different orthologs. **(C)** Histogram of KOG classification. Each color on the horizontal axis represented a functional classification of KOG and the vertical axis was the number of genes. **(D)** Classification of KEGG Pathway. The vertical axis was the name of the metabolic pathway and the vertical axis was the number of genes.

amino acid transport and metabolism (5.31%) and energy production and transformation (4.97%) (Figure 3C). The metabolic pathways of KEGG were classified based on the linkage between KO and pathway. The pathways were divided into five branches: cellular processes, environmental information processing, genetic information pathways, metabolism and organismal systems (Figure 3D).

Strain N4-3 exhibiting the broad-spectrum antifungal activity

Ten phytopathogenic fungi were selected to test the broad-spectrum antagonistic potential of strain N4-3. The antifungal activity was measured after one week of dual incubation. Strain N4-3 exhibited different inhibition ability against different pathogenic fungi (Figure 4). By constrast, strain N4-3 had a strong inhibitory activity on the mycelial growth of *C. lunata* (ATCC 42011), *C. acutatum* (ATCC56815) and *C. fallax* (ATCC 38579), resulting in a reduction in colony growth diameters of 75.45 ± 0.91, 75.45 ± 0.91, and 75.17 ± 3.33, respectively. The least inhibitory activity was observed against *C. gloeosporioides* (ATCC MYA-456), with a reduction in colony growth diameter of 64.40 ± 3.58 (Figure 4). These results indicated that strain N4-3 possessed a broad-spectrum antagonistic ability against phytopathogenic fungi.

Interaction of strain N4-3 with *Foc* TR4

We further detected the dynamic interaction between strain N4-3 and *Foc* TR4. Observation was recorded at 12-hour intervals during the dual incubation. The results showed that two strains started to come into contact at 48 h and show inhibition circles at 60 h (Figure 5A). Numerous distinct clusters of green *Trichoderma* spores appeared in the colony area of *Foc* TR4 on 10th day. The parasitic area was observed using a stereomicroscope. Mycelia and spores of strain N4-3 attached to the mycelia of *Foc* TR4, resulting in the lysis of the pathogenic fungal mycelia (Figure 5B). Additionally, a large number of *Trichoderma* spores were observed in the pathogenic area, and gaps were also found in the pathogenic fungal mycelia and spores (Figure 5B). Therefore, strain N4-3 was able to destroy the complete structure of mycelia and spores of *Foc* TR4.

Determination of antifungal components of strain N4-3

The dual culture assay approved that strain N4-3 was able to inhibit the growth of *Foc* TR4. To identify the active components with antagonistic activity, the experiment was set to determine the antagonistic activity of crude extracts of strain N4-3 and the inhibitory efficiency of volatile organic compounds against *Foc* TR4. However, no antagonistic activity of both strain N4-3 fermentation products and volatile organic compounds was detected (Supplementary Figure 1A, Figure 1B). We speculated that strain N4-3 may inhibit the growth of *Foc* TR4 by secreting enzymes with antagonistic activity. The crude enzymes were extracted using the ammonium sulfate precipitation method. Considering that the cell wall components of pathogenic fungi primarily consist of chitin and glucan (Adams, 2004; Jones et al., 2014), the activities of chitinase and β-1,3-glucanase were determined in crude enzyme solutions. The results showed that both chitinase and β-1,3-glucanase activities in the crude enzyme solution exhibited an increasing trend and then decreasing with the increase of ammonium sulfate saturation. The maximal activities were detected in the crude enzyme solution extracted with 30% of saturation of ammonium sulfate (Figure 6A).

To test the inhibition activity of crude enzymes against *Foc* TR4, the inhibition efficiency was determined. The results showed that the inhibition rate increased along with the increase of crude enzyme concentrations. When the concentration reached 400 mg/mL, the inhibition rate of the pathogenic mycelia was 39.96 ± 1.57% (Figure 6B). The EC_{50} value was 496.94 mg/mL using the toxicity regression equation. Furthermore, the effect of crude enzymes on spore germination of Foc TR4 was investigated. The germination rate of spores after treatment with EC_{50} of crude enzyme solution was only 9.98 ± 0.23% in comparison to 87.30 ± 2.03% of the control group. Additionally, the tube length of the germinated spores treated with crude enzymes was only 14.2 μm, while that in the control group reached 67.93 μm (Figure 6C). Therefore,

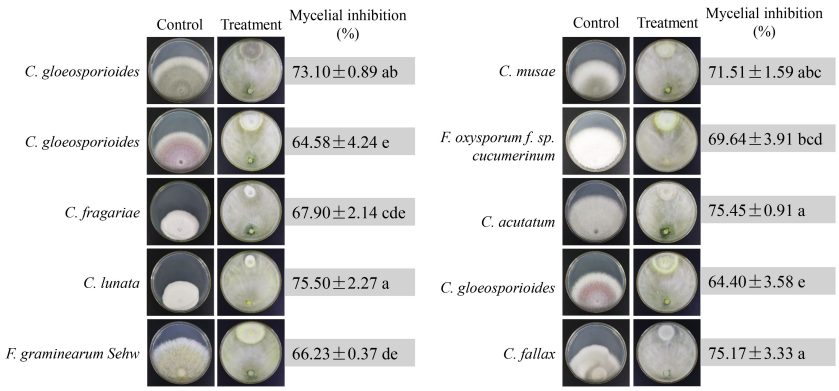

FIGURE 4
Broad-spectrum inhibition efficiency test of N4-3 against 10 phytopathogenic fungi. Data are expressed as mean ± standard deviation. Different lowercase letters indicate significant differences at $P < 0.05$ in Duncan's multiple range test.

10.3389/fpls.2023.1289959

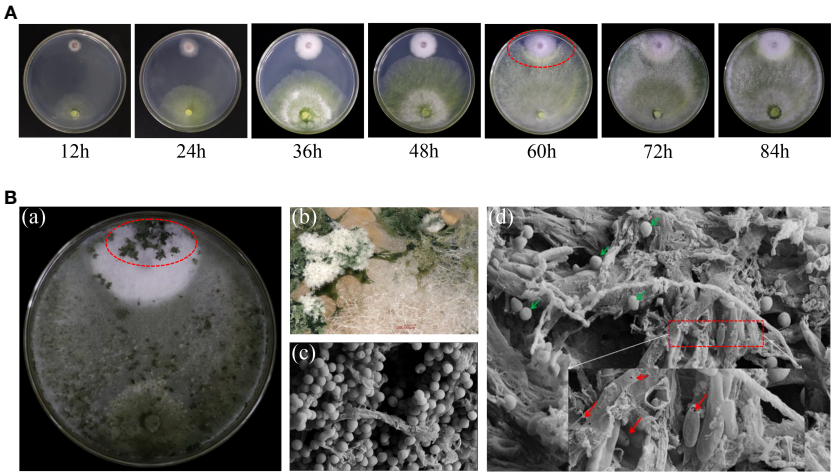

FIGURE 5
Interaction of strain N4-3 with *Foc* TR4. **(A)** Dynamic process of the interaction between strain N4-3 and *Foc* TR4. The red elliptical region indicated the appearance of the inhibition circle. **(B)** Dual culture of strain N4-3 and *Foc* TR4 was carried out for 10 days (a). Spore clusters of strain N4-3 appeared in the *Foc* TR4 colony area (b). The dual culture area was observed using SEM (c-d). The green arrow showed the spores of strain N4-3 and the red arrow showed the mycelia and spores of *Foc* TR4.

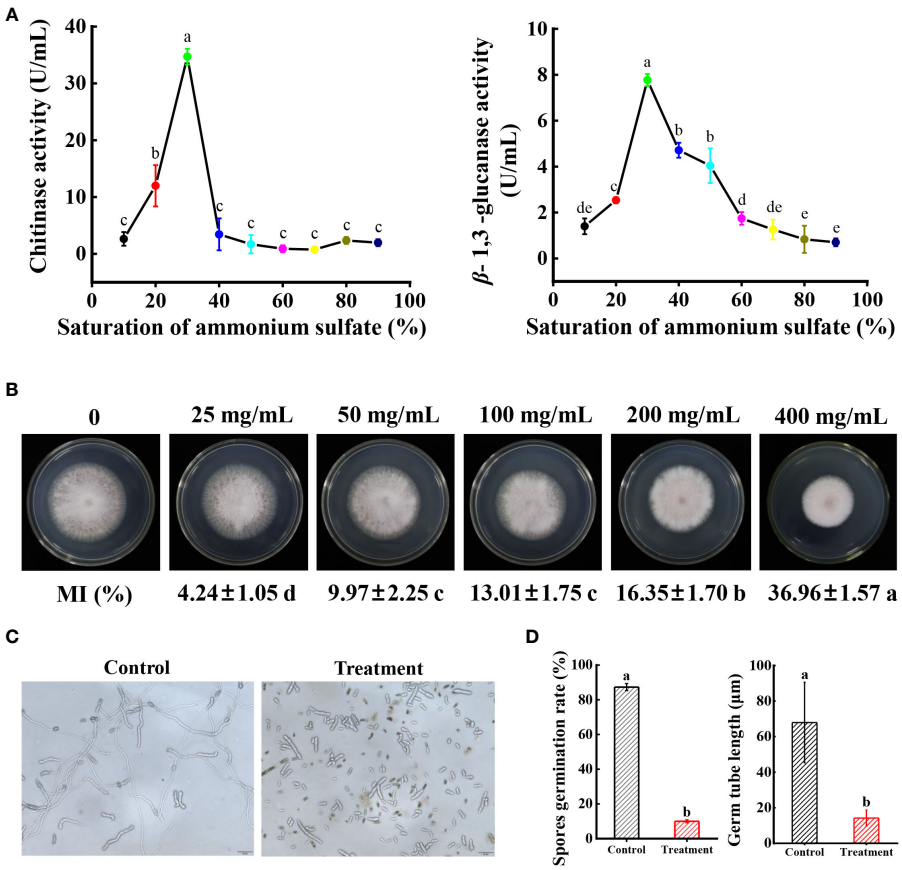

FIGURE 6
Determination of *Foc* TR4 antagonism efficiency of crude enzyme solution. **(A)** Determination of chitinase activity and *β*-1,3-glucanase activity in crude enzyme solutions extracted with different saturations of ammonium sulfate. **(B)** Inhibition efficiency of *Foc* TR4 by different concentrations of crude enzyme solution. Data are expressed as mean ± standard deviation. **(C)** Spores were treated with EC_{50} crude enzyme solution, incubated for 1 day, and then observed under a biological microscope. **(D)** Statistical analysis of spore germination rate and spore budding tube length. Different lowercase letters indicate significant differences at $P < 0.05$ in Duncan's multiple range test.

crude enzyme solution not only significantly reduced the germination rate of spores, but also inhibited the length of spore germination tubes.

Crude enzyme solution destroying the ultrastructure of *Foc* TR4 cells

We further evaluate whether crude enzyme solution had a disruptive effect on the morphological structure of *Foc* TR4. In the control group, the mycelial and spore morphology of the pathogenic fungi remained intact and had a smooth surface. SEM was used to observe the morphological changes of the *Foc* TR4 spores. After treatment with1×EC_{50} of crude enzymes, the mycelia of *Foc* TR4 was broken (Figure 7). The spores exhibited significant deformation and fragmentation, with leakage of cell contents. These observations were consistent with the results obtained from dual cultures (Figures 5B, 7). SEM analysis also demonstrated intact cell walls in the normal growth of *Foc* TR4 mycelia. By contrast, cell wall of the treated group became thinner and defective. A number of intracellular vesicles and collapse of organelles were observed in *Foc* TR4 after treatment with crude enzyme solution (Figure 7). These results suggested that the enzymes secreted by strain N4-3 possessed antifungal activity, ultimately leading to deformation, cell wall degradation, organelle collapse and leakage of cell contents of *Foc* TR4.

Strain N4-3 improving the resistance to *Foc* TR4 and plant growth of banana seedlings

To assess the biocontrol efficiency of strain N4-3, a pot cultivation experiment was conducted. At 60 dpi, symptoms of leaf yellowing and wilting were observed in the control plants, while no obvious disease symptom was detected in the banana plants treated with strain N4-3. Comparing with the control group, the disease index decreased from 62.50 ± 6.78% to 17.50 ± 3.12% after strain N4-3 treatment. The biocontrol efficiency was 72.00% (Figures 8A, 8B). Infection of GFP-*Foc* TR4 on banana roots was observed using the laser scanning confocal microscopy. The results showed a strong green fluorescence was observed in the banana

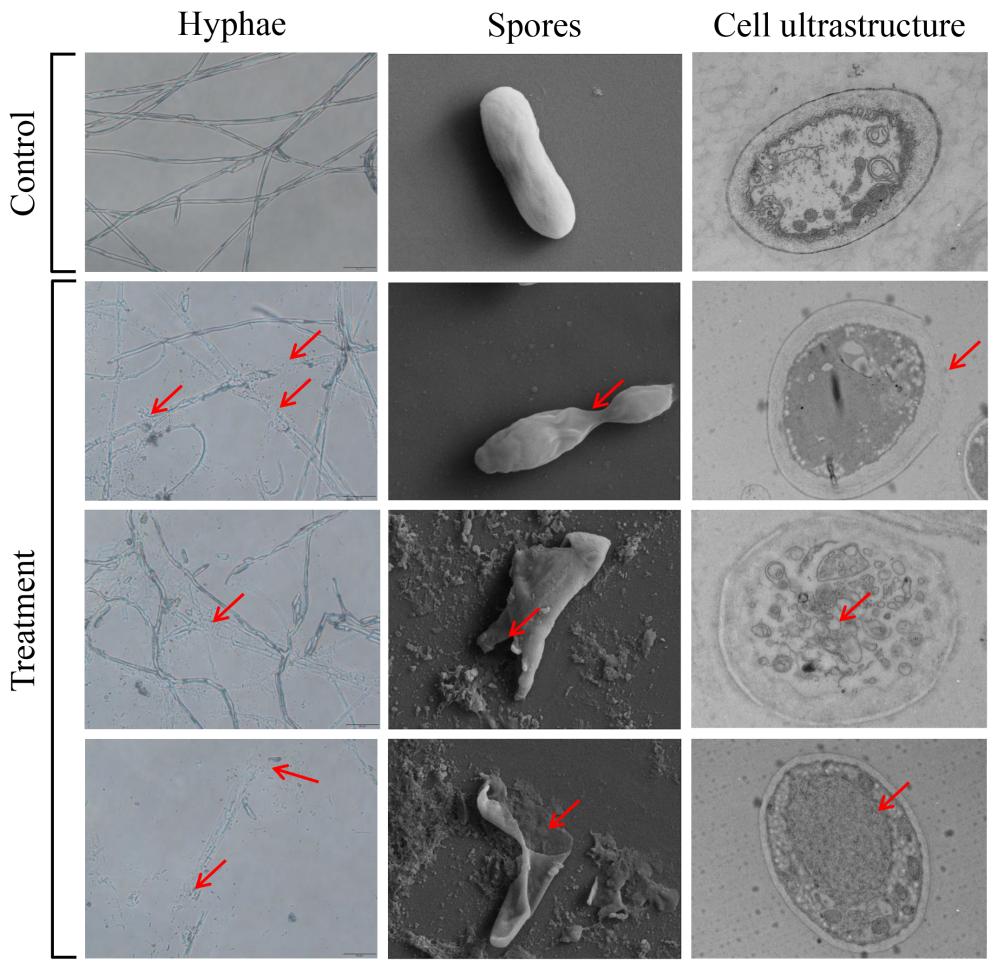

FIGURE 7
Effect of crude enzyme solution at EC_{50} concentration on *Foc* TR4 mycelium, spores and cell structure. The red arrow points to where it differs from the control.

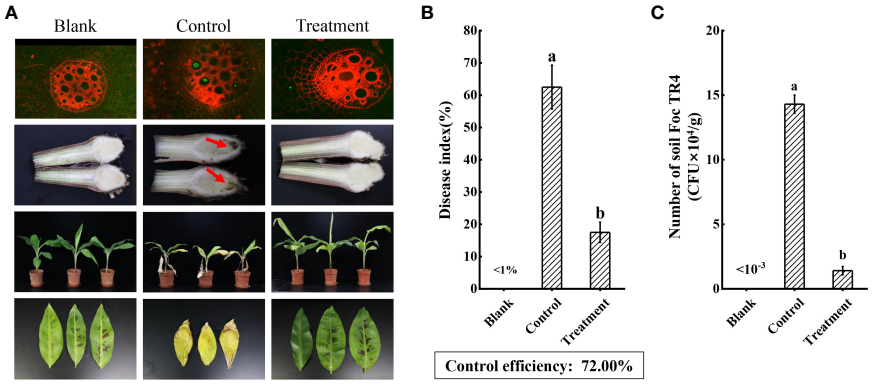

FIGURE 8
Evaluating the biocontrol effect of strain N4-3. **(A)** Growth status of banana plants in the blank (H_2O), control (*Foc* TR4) and treatment (strain N4-3 + *Foc* TR4) at 60 dpi. The arrow indicated the site of *Foc* TR4 infection. **(B)** Statistical analysis of disease indices. **(C)** Statistical quantification of *Foc* TR4 in the rhizosphere soil of banana. The experiments were repeated three times. Different lowercase letters indicated a significant difference at the level of $P<0.05$.

roots of the control group, while no obvious signal was detected in the treated group. Additionally, the roots of the control group exhibited black decayed symptom due to *Foc* TR4 infection (Figure 8A). Statistical analysis showed that the number of pathogens in the rhizosphere soil was 1.43×10^5 CFU/g in the control group, while the rhizosphere soil inoculated with strain N4-3 contained 1.41×10^4 CFU/g (Figure 8C). These results indicated that application of strain N4-3 effectively reduced the number of pathogenic fungi in the rhizosphere soil, leading to a silght symptom of *Foc* TR4 infection.

Furthermore, several agronomic characteristics of banana plants were measured. At 60 dpi, the SPAD in the banana leaves of the treated group (52.12 ± 5.33) was higher than that of the control (26.88 ± 7.51) and the blank group (34.79 ± 6.22) (Figure 9A). Although there was no significant increase in leaf thickness between the control group (1.09 ± 0.08 mm) and the blank group (1.18 ± 0.11 mm) (Figure 9C), the leaf area after strain N4-3 application was 1.75-fold than that of the blank group (138.69 cm^2) (Figure 9B). Moreover, the maximum photosynthetic efficiency of the leaves was also measured using the chlorophyll fluorometer. The maximum photosynthetic efficiency was 0.81 in the treated group, 0.77 in the blank group and 0.74 in control group (Supplementary Figure 2). These results indicated that strain N4-3 can improve photosynthesis in banana plants. Additionally, the fresh weight of the banana plants was obviously improved by strain N4-3. Compared to fresh weight in the blank group (89.90 ± 5.31 g) and the control group (64.76 ± 19.13 g) (Figure 9D), a significant increase was found in the treatment group (106.03 ± 6.40 g). Similar changes were observed in plant height and stem thickness (Figures 9E, 9F). Hence, strain N4-3 not only improved the resistance of banana plants to *Foc* TR4, but also enhanced photosynthetic capacity and plant growth.

Discussion

Banana Fusarium wilt caused by *Foc* TR4 is a serious disease that limits the banana industry (Kubicek et al., 2014). After successful infection of *Foc* TR4, it produces several harmful substances such as fusarium acid and beauverin, eventually leading to wilting or death of banana plants. Long-term application of chemicals can cause damage to local soil ecology (Ploetz, 2015b). Beneficial microorganisms originating from the natural environment are recognized as an important component of sustainable agriculture (Singh et al., 2020; Woo et al., 2022). Therefore, isolation and screening of beneficial microorganisms is key for the selection of biocontrol agent.

Trichoderma sp. is a widely utilized beneficial microorganism that exhibits a fast growth in diverse environments (Damodaran et al., 2020; Savani et al., 2021). *Trichoderma* sp. directly employs in antagonistic and competitive mechanisms to inhibit the growth of pathogenic fungi and induce systemic resistance in plants (Druzhinina et al., 2011). In our study, we aim to screen and identify one *Trichoderma* that exhibit antagonistic activity against *Foc* TR4. To isolate *Trichoderma* strains, soil samples were selected from banana plantations without disease symptom for ten years. Nine *Trichoderma* strains were isolated using the RBA medium (Figure 1A). By evaluating the antagonistic efficiency against *Foc* TR4, strain N4-3 had the highest antagonistic activity (Figure 1B). Its broad-spectrum antifungal activity was also found by a dual culture test (Figure 4). To further identify the strain, ML analysis based on *tef1* and *rpb2* was performed. The analysis showed that strain N4-3 clustered with *Trichoderma parareesei* CP55-3 (Figure 2B). The morphological characteristics of strain N4-3 supported the result (Atanasova et al., 2010). The previous by comparison of ITS sequences was normally used to identify the fungal species, but numerous fungal sister species cannot be distinguished using this method. Multiple gene sequences are concatenated to increase the number of effective informative loci, which can increase the accuracy of species identification (Heled and Drummond, 2009).

Trichoderma parareesei was mainly distributed in the pantropical climatic zone. It was an asexual variant of *Trichoderma reesei*. The previous study showed *Trichoderma parareesei* exhibited high parasitism and wide ecological

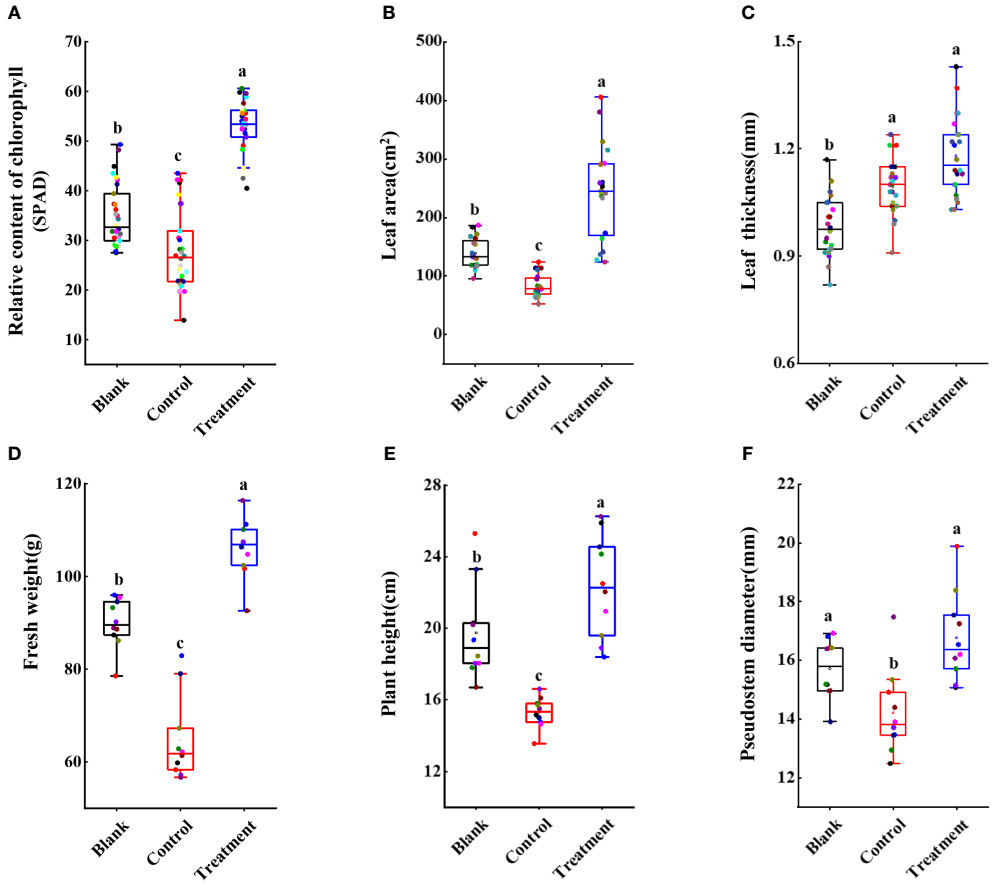

FIGURE 9
Statistical analysis of agronomic traits of banana seedlings. **(A)** Relative content of chlorophyll. **(B)** Leaf area (cm^2). **(C)** Leaf thickness (mm). **(D)** Fresh weight (g). **(E)** Plant height (cm). **(F)** Pseudostem diameter (mm). Different lowercase letters indicate significant differences at the level of $p<0.05$.

adaptability (Herrera-Estrella et al., 2010). The rhizosphere of plants was one of the most common ecological niches for the genus *Trichoderma*. *Trichoderma parareesei* could utilize sucrose secreted by plant roots and form symbiotic interactions (Rubio et al., 2014). *Trichoderma parareesei* promoted the tolerance of *Brassica napus* L. to salt and drought by abscisic acid and ethylene singalling pathways (Poveda, 2020). Moreover, *Trichoderma* spp. could inhibit the growth of pathogenic fungi by secreting antibiotics and volatile organic compounds (Harni et al., 2020). Here, we also found that strain N4-3 exhibited a remarkable ability to inhibit the growth of *Foc* TR4 mycelia. Further experiments revealed that the metabolites and volatile organic compounds produced by *Trichoderma parareesei* N4-3 had no inhibitory actitvity on *Foc* TR4 (Supplementary Figure 1). By analysis, the formation of the inhibition zone may be attributed to the cell wall-degrading enzyme secreted by strain N4-3. The results were supported by that cellular structure of *Foc* TR4 was disrupted after treatment with the crude enzyme solution, resulting in the inhibition of spore germination and mycelial growth.

To further identify the important enzymes, the whole genome of strain N4-3 was sequenced. The annotation results revealed that 221 glycoside hydrolase genes were found in the genome of strain N4-3 (Supplementary Figure 3A). Among these, the GH18 family was responsible for the production of chitinases. β-1,3-glucanases synthesized by the GH16, GH55, GH64, and GH81 families played a role in degrading cell wall of pathogenic fungi (Gruber and Seidl-Seiboth, 2012). By alignment, there were 21 genes for chitinases and 26 genes for β-1,3-glucanases (Supplementary Figure 3B). This result suggested that *Trichoderma parareesei* N4-3 had the ability to secrete a large amount of cell wall-degrading enzymes to inhibit *Foc* TR4. Therefore, strain N4-3 growed rapidly to occupy the growth space and destroy the mycelia and spores of the pathogenic fungus by the production of a series of cell wall-degrading enzymes. This is a typical hyperparasitic phenomenon of *Trichoderma* (Gruber and Seidl-Seiboth, 2012).

Additionally, the abundance of *Foc* TR4 in the rhizospheric soil of banana plants after application of strain N4-3 was much lower than that in the control group (Figure 8C). The previous study showed that the density of pathogenic fungi was correlated with plant disease, and these fungi need to reach a certain concentration before disease appearance in plants (Zhang et al., 2021). Therefore, *Trichoderma parareesei* N4-3 could reduce the disease likelihood by inhibiting the growth of *Foc* TR4 in banana roots. Furthermore, the addition of strain N4-3 significantly increased the leaf area, relative chlorophyll content, and photosynthetic efficiency, thereby improving the resistance of plants to *Foc* TR4. Similar studies

supported that beneficial microorganisms can indirectly enhance plant resistance to pathogenic fungi by promoting plant growth (Chen et al., 2020). Therefore, strain N4-3 could inhibit the growth of *Foc* TR4 through ecological niche competition and secretion of cell wall-degrading enzymes, thereby reducing the number of pathogenic fungi in the rhizospheric soil. Moreover, strain N4-3 also promoted the growth of banana plants to improve the disease resistance.

Conclusion

In this study, *Trichoderma parareesei* N4-3 with a broad-spectrum antifungal activity was isolated and identified from banana plantation soil. *In vitro* experiments demonstrated that strain N4-3 could adhere to the surface of *Foc* TR4 hyphae. The production of chitinase and β-1,3-glucanase disintegrated hyphae and spores of pathogenic fungi. These enzymes degraded the cell wall, thereby disrupting the cellular structure and ultrastructure of the pathogenic fungi. The number of genes encoding chitinases and β-1,3-glucanase were identified in the genome of strain N4-3. In pot experiment, strain N4-3 significantly decreased the population of *Foc* TR4 in the rhizosphere of banana plants, leading to a reduction in the disease index. Therefore, *Trichoderma parareesei* N4-3 exhibited a great potential as a biocontrol agent to manage *Foc* TR4.

Data availability statement

The original contributions presented in the study are publicly available. This data can be found here: rpb2 and tef1 sequences to GeneBank, BankIt2753675 rpb2 OR687153, BankIt2754798 tef1 OR687154, genomic data to NCBI, PRJNA1025137.

Author contributions

WL: Conceptualization, Data curation, Investigation, Methodology, Writing – original draft, Formal Analysis, Software, Writing – review & editing. YC: Conceptualization, Data curation, Funding acquisition, Investigation, Methodology, Writing – review & editing, Software, Supervision, Writing – original draft. YW: Formal Analysis, Software, Visualization, Writing – review & editing. JF: Formal Analysis, Software, Visualization, Writing – original draft. DZ: Formal Analysis, Project administration, Software, Visualization, Writing – review & editing. BC: Formal Analysis, Software, Visualization, Writing – review & editing. DQ: Resources, Software, Validation, Writing – review & editing. MZ: Resources, Validation, Writing – review & editing. YZ: Resources, Validation, Writing – review & editing. KL: Resources, Validation, Writing – review & editing. YL: Conceptualization, Investigation, Project administration, Supervision, Writing – review & editing. WW: Funding acquisition, Investigation, Project administration, Supervision, Writing – review & editing. JX: Funding acquisition, Investigation, Project administration, Supervision, Writing – review & editing.

Funding

The author(s) declare financial support was received for the research, authorship, and/or publication of this article. This work was supported by the Natural Science Foundation of Hainan (321MS084, 322MS126, 323QN277, 323RC541, 321QN312), the Central Public-interest Scientific Institution Basal Research Fund (1630052022006, CATASCXTD202308), the project of National Key Laboratory for Tropical Crop Breeding (NKLTCB202306), the National Natural Science Foundation of China (31770476, U22A20487) and the China Agriculture Research System (CARS-31).

Acknowledgments

The authors thank Zhufeng Gao for her technical assistance in the experiment.

Conflict of interest

The authors declare that the research was conducted in the absence of any commercial or financial relationships that could be construed as a potential conflict of interest.

Publisher's note

Supplementary material

The Supplementary Material for this article can be found online at: https://www.frontiersin.org/articles/10.3389/fpls.2023.1289959/full#supplementary-material

References

Adams, D. J. (2004). Fungal cell wall chitinases and glucanases. *Microbiology* 150 (7), 2029–2035. doi: 10.1099/mic.0.26980-0

Atanasova, L., Jaklitsch, W. M., Komoní-Zelazowska, M., Kubicek, C. P., and Druzhinina, I. S. (2010). Clonal species *Trichoderma parareesei* sp. nov. likely resembles the ancestor of the cellulase producer *Hypocrea jecorina/T. reesei*. *Appl. Environ. Microb.* 76 (21), 7259–7267. doi: 10.1128/aem.01184-10

Cai, F., and Druzhinina, I. S. (2021). In honor of John Bissett: authoritative guidelines on molecular identification of *Trichoderma*. *Fungal Divers.* 107 (1), 1–69. doi: 10.1007/s13225-020-00464-4

Cannon, S., Kay, W., Kilaru, S., Schuster, M., Gurr, S. J., and Steinberg, G. (2022). Multi-site fungicides suppress banana Panama disease, caused by *Fusarium oxysporum* f. sp. *cubense* Tropical Race 4. *PLoS Pathog.* 18 (10). doi: 10.1371/journal.ppat.1010860

Chen, L., Wang, X., Ma, Q., Bian, L., Liu, X., Xu, Y., et al. (2020). *Bacillus velezensis* CLA178-induced systemic resistance of Rosa multiflora against grown gall disease. *Front. Microbiol.* 11. doi: 10.3389/fmicb.2020.587667

Chen, Y., Wei, Y., Cai, B., Zhou, D., Qi, D., Zhang, M., et al. (2022). Discovery of niphimycin C from *Streptomyces yongxingensis* sp. nov. as a promising agrochemical fungicide for controlling banana Fusarium wilt by destroying the mitochondrial structure and function. *J. Agr. Food Chem.* 70 (40), 12784–12795. doi: 10.1021/acs.jafc.2c02810

Chen, Y., Zhou, D., Qi, D., Gao, Z., Xie, J., and Luo, Y. (2018). Growth promotion and disease suppression ability of a *Streptomyces* sp. CB-75 from banana rhizosphere soil. *Front. Microbiol.* 8. doi: 10.3389/fmicb.2017.02704

Damodaran, T., Rajan, S., Muthukumar, M., Ram, G., Yadav, K., Kumar, S., et al. (2020). Biological management of banana fusarium wilt caused by *Fusarium oxysporum f.* sp. cubense Tropical Race 4 using antagonistic fungal isolate CSR-T-3 (*Trichoderma reesei*). *Front. Microbiol.* 11. doi: 10.3389/fmicb.2020.595845

Díaz-Gutiérrez, C., Arroyave, C., Llugany, M., Poschenrieder, C., Martos, S., and Peláez, C. (2021). *Trichoderma asperellum* as a preventive and curative agent to control Fusarium wilt in Stevia rebaudiana. *Biol. Control* 155. doi: 10.1016/j.biocontrol.2021.104537

Dita, M., Barquero, M., Heck, D., Mizubuti, E. S. G., and Staver, C. P. (2018). Fusarium wilt of banana: current knowledge on epidemiology and research needs toward sustainable disease management. *Front. Plant Sci.* 9. doi: 10.3389/fpls.2018.01468

Druzhinina, I. S., Seidl-Seiboth, V., Herrera-Estrella, A., Horwitz, B. A., Kenerley, C. M., Monte, E., et al. (2011). *Trichoderma*: the genomics of opportunistic success. *Nat. Rev. Microbiol.* 9 (10), 749–759. doi: 10.1038/nrmicro2637

García-Bastidas, F. A. (2019). *'Panama disease in banana: Spread, screens and genes* (Doctor of Philosophy, Wageningen University, Wageningen). doi: 10.18174/467427

Gruber, S., and Seidl-Seiboth, V. (2012). Self versus non-self: fungal cell wall degradation in *Trichoderma*. *Microbiol-Sgm* 158 (1), 26–34. doi: 10.1099/mic.0.052613-0

Guo, Y., Ghirardo, A., Weber, B., Schnitzler, J.-P., Benz, J. P., and Rosenkranz, M. (2019). *Trichoderma* Species differ in their volatile profiles and in antagonism toward ectomycorrhiza laccaria bicolor. *Front. Microbiol.* 10. doi: 10.3389/fmicb.2019.00891

Harni, R., Amaria, W., and Mahsunah, A. H. (2020). Effect of secondary metabolites of *Trichoderma* spp. in inhibiting Phytophthora palmivora growth in cacao (*Theobroma cacao L.*). *IOP Conf. Ser.: Earth Environ. Sci.* 468 (1). doi: 10.1088/1755-1315/468/1/012049

Heled, J., and Drummond, A. J. (2009). Bayesian inference of species trees from multilocus data. *Mol. Biol. Evol.* 27 (3), 570–580. doi: 10.1093/molbev/msp274

Herrera-Estrella, A., Druzhinina, I. S., Komoń-Zelazowska, M., Atanasova, L., Seidl, V., and Kubicek, C. P. (2010). Evolution and ecophysiology of the industrial producer *Hypocrea jecorina (Anamorph Trichoderma reesei)* and a new sympatric agamospecies related to it. *PLoS One* 5 (2). doi: 10.1371/journal.pone.0009191

Jing, T., Zhou, D., Zhang, M., Yun, T., Qi, D., Wei, Y., et al. (2020). Newly isolated *Streptomyces* sp. JBS5-6 as a potential biocontrol agent to control banana Fusarium wilt: genome sequencing and secondary metabolite cluster profiles. *Front. Microbiol.* 11. doi: 10.3389/fmicb.2020.602591

Jones, L., Riaz, S., Morales-Cruz, A., Amrine, K. C. H., McGuire, B., Gubler, W. D., et al. (2014). Adaptive genomic structural variation in the grape powdery mildew pathogen, Erysiphe necator. *BMC Genomics* 15 (1), 1081. doi: 10.1186/1471-2164-15-1081

Koren, S., Walenz, B. P., Berlin, K., Miller, J. R., Bergman, N. H., and Phillippy, A. M. (2017). Canu: scalable and accurate long-read assembly *via* adaptive k-mer weighting and repeat separation. *Genome Res.* 27 (5), 722–736. doi: 10.1101/gr.215087.116

Kothe, E., Jiang, Y., Wang, J.-L., Chen, J., Mao, L.-J., Feng, X.-X., et al. (2016). *Trichoderma* biodiversity of agricultural fields in east China reveals a gradient distribution of species. *PLoS One* 11 (8). doi: 10.1371/journal.pone.0160613

Kubicek, C. P., Starr, T. L., and Glass, N. L. (2014). Plant cell wall–degrading enzymes and their secretion in plant-pathogenic fungi. *Annu. Rev. Phytopathol.* 52 (1), 427–451. doi: 10.1146/annurev-phyto-102313-045831

Li, X., Zhang, M., Qi, D., Zhou, D., Qi, C., Li, C., et al. (2021). Biocontrol ability and mechanism of a broad-spectrum antifungal strain *Bacillus safensis* sp. QN1NO-4 against strawberry anthracnose caused by colletotrichum fragariae. *Front. Microbiol.* 12. doi: 10.3389/fmicb.2021.735732

Liu, Y. J., Whelen, S., and Hall, B. D. (1999). Phylogenetic relationships among ascomycetes: evidence from an RNA polymerse II subunit. *Mol. Biol. Evol.* 16 (12), 1799–1808. doi: 10.1093/oxfordjournals.molbev.a026092

Lozano-Durán, R., van Westerhoven, A. C., Meijer, H. J. G., Seidl, M. F., and Kema, G. H. J. (2022). Uncontained spread of Fusarium wilt of banana threatens African food security. *PLoS Pathog.* 18 (9). doi: 10.1371/journal.ppat.1010769

Lv, D., Zhang, W., Meng, X., and Liu, W. (2023). A novel fusion transcription factor drives high cellulase and xylanase production on glucose in *Trichoderma reesei*. *Bioresource Technol.* 370. doi: 10.1016/j.biortech.2022.128520

Mohiddin, F. A., Padder, S. A., Bhat, A. H., Ahanger, M. A., Shikari, A. B., Wani, S. H., et al. (2021). Phylogeny and optimization of *Trichoderma harzianum* for chitinase production: evaluation of their antifungal behaviour against the prominent soil borne phyto-pathogens of temperate India. *Microorganisms* 9 (9) 1962. doi: 10.3390/microorganisms9091962

Mukherjee, P. K., Horwitz, B. A., Herrera-Estrella, A., Schmoll, M., and Kenerley, C. M. (2013). *Trichoderma* research in the genome era. *Annu. Rev. Phytopathol.* 51 (1), 105–129. doi: 10.1146/annurev-phyto-082712-102353

Perrier, X., De Langhe, E., Donohue, M., Lentfer, C., Vrydaghs, L., Bakry, F., et al. (2011). Multidisciplinary perspectives on banana (*Musa* spp.) domestication. *Proc. Natl. Acad. Sci. U.S.A.* 108 (28), 11311–11318. doi: 10.1073/pnas.1102001108

Ploetz, R. C. (2015a). Fusarium wilt of banana. *Phytopathology* 105 (12), 1512–1521. doi: 10.1094/phyto-04-15-0101-rvw

Ploetz, R. C. (2015b). Management of Fusarium wilt of banana: A review with special reference to tropical race 4. *Crop Prot.* 73, 7–15. doi: 10.1016/j.cropro.2015.01.007

Poveda, J. (2020). *Trichoderma parareesei* favors the tolerance of rapeseed (*Brassica napus L.*) to salinity and drought due to a chorismate mutase. *Agronomy* 10 (1). doi: 10.3390/agronomy10010118

Qi, D., Zou, L., Zhou, D., Zhang, M., Wei, Y., Zhang, L., et al. (2021). Identification and antifungal mechanism of a novel actinobacterium *Streptomyces huiliensis* sp. nov. against *Fusarium oxysporum f.* sp. cubense tropical race 4 of banana. *Front. Microbiol.* 12. doi: 10.3389/fmicb.2021.722661

Rahman, M., Borah, S. M., Borah, P. K., Bora, P., Sarmah, B. K., Lal, M. K., et al. (2023). Deciphering the antimicrobial activity of multifaceted rhizospheric biocontrol agents of solanaceous crops viz., *Trichoderma harzianum* MC2, and *Trichoderma harzianum* NBG. *Front. Plant Sci.* 14. doi: 10.3389/fpls.2023.1141506

Rajani, P., Rajasekaran, C., Vasanthakumari, M. M., Olsson, S. B., Ravikanth, G., and Uma Shaanker, R. (2021). Inhibition of plant pathogenic fungi by endophytic *Trichoderma* spp. through mycoparasitism and volatile organic compounds. *Microbiol. Res.* 242. doi: 10.1016/j.micres.2020.126595

Rubio, M. B., Quijada, N. M., Pérez, E., Domínguez, S., Monte, E., and Hermosa, R. (2014). Identifying beneficial qualities of *Trichoderma parareesei* for plants. *Appl. Environ. Microb.* 80 (6), 1864–1873. doi: 10.1128/aem.03375-13

Savani, A.k., Bhattacharyya, A., Boro, R. C., Dinesh, K., and Jc, N. S. (2021). Exemplifying endophytes of banana (*Musa paradisiaca*) for their potential role in growth stimulation and management of *Fusarium oxysporum f. sp* cubense causing Panama wilt. *Folia Microbiol.* 66 (3), 317–330. doi: 10.1007/s12223-021-00853-5

Singh, B. K., Trivedi, P., Egidi, E., Macdonald, C. A., and Delgado-Baquerizo, M. (2020). Crop microbiome and sustainable agriculture. *Nat. Rev. Microbiol.* 18 (11), 601–602. doi: 10.1038/s41579-020-00446-y

Sood, M., Kapoor, D., Kumar, V., Sheteiwy, M. S., Ramakrishnan, M., Landi, M., et al. (2020). Trichoderma: The "Secrets" of a multitalented biocontrol agent. *Plants* 9 (6), 762. doi: 10.3390/plants9060762

Tamizi, A.-A., Mat-Amin, N., Weaver, J. A., Olumakaiye, R. T., Akbar, M. A., Jin, S., et al. (2022). Genome sequencing and analysis of *Trichoderma (Hypocreaceae)* isolates exhibiting antagonistic activity against the papaya dieback pathogen, Erwinia mallotivora. *J. Fungi* 8 (3), 246. doi: 10.3390/jof8030246

Tian, Y., Tan, Y., Liu, N., Yan, Z., Liao, Y., Chen, J., et al. (2016). Detoxification of deoxynivalenol *via* glycosylation represents novel insights on antagonistic activities of *Trichoderma* when confronted with Fusarium graminearum. *Toxins* 8 (11), 335. doi: 10.3390/toxins8110335

Tomah, A. A., Abd Alamer, I. S., Li, B., and Zhang, J.-Z. (2020). A new species of *Trichoderma* and gliotoxin role: A new observation in enhancing biocontrol potential of *T. virens* against Phytophthora capsici on chili pepper. *Biol. Control* 145. doi: 10.1016/j.biocontrol.2020.104261

Wei, Y., Zhao, Y., Zhou, D., Qi, D., Li, K., Tang, W., et al. (2020). A newly isolated *Streptomyces* sp. YYS-7 with a broad-spectrum antifungal activity improves the banana plant resistance to *Fusarium oxysporum f.* sp. *cubense* tropical race 4. *Front. Microbiol.* 11. doi: 10.3389/fmicb.2020.01712

Woo, S. L., Hermosa, R., Lorito, M., and Monte, E. (2022). *Trichoderma*: a multipurpose, plant-beneficial microorganism for eco-sustainable agriculture. *Nat. Rev. Microbiol.* 21 (5), 312–326. doi: 10.1038/s41579-022-00819-5

Xu, Q. Q., Zhu, G. W., Zhao, Z. L., Tao, X. T., Li, Z. Y., Hao, Z. B., et al. (2022). Separation, purification and characterization of chitinase of the endophytic bacterium *Bacillus thuringiensis* Bt028 isolated from sour orange. *Sci. Technol. Food Industry* 43 (11), 159–166. doi: 10.13386/j.issn1002-0306.2021100184

Yun, T., Zhang, M., Zhou, D., Jing, T., Zang, X., Qi, D., et al. (2021). Anti-Foc TR4 activity of a newly isolated *Streptomyces* sp. 5-10 from a medicinal plant (*Curculigo capitulata). Front. Microbiol.* 11. doi: 10.3389/fmicb.2020.610698

Zhang, Z., Li, J., Zhang, Z., Liu, Y., and Wei, Y. (2021). Tomato endophytic bacteria composition and mechanism of suppressiveness of wilt disease (*Fusarium oxysporum*). *Front. Microbiol.* 12. doi: 10.3389/fmicb.2021.731764

Zou, D. M., and Fan, Q. (2022). Present situation of globle banana production and trade and prospect for banana industry. *Guangdong Agric. Sci.* 49 (7), 131–140.. doi: 10.16768/j.issn.1004-874X.2022.07.017

frontiers | Frontiers in Plant Science

TYPE Original Research
PUBLISHED 23 November 2023
DOI 10.3389/fpls.2023.1272136

OPEN ACCESS

EDITED BY
Inmaculada Larena,
Instituto Nacional de Investigación y Tecnología Agraria y Alimentaria (INIA-CSIC), Spain

REVIEWED BY
Malkhan Singh Gurjar,
Indian Agricultural Research Institute (ICAR), India
Rupam Kapoor,
University of Delhi, India

*CORRESPONDENCE
Kurt Heungens
kurt.heungens@ilvo.vlaanderen.be

RECEIVED 03 August 2023
ACCEPTED 01 November 2023
PUBLISHED 23 November 2023

CITATION
Mestdagh H, Van Poucke K, Haegeman A, Dockx T, Vandevelde I, Dendauw E, Decombel A, Höfte M and Heungens K (2023) Detection of *Fusarium oxysporum* f.sp. *lactucae* race 1 and 4 via race-specific real-time PCR and target enrichment. *Front. Plant Sci.* 14:1272136. doi: 10.3389/fpls.2023.1272136

Detection of *Fusarium oxysporum* f.sp. *lactucae* race 1 and 4 via race-specific real-time PCR and target enrichment

Hanna Mestdagh[1,2], Kris Van Poucke[1], Annelies Haegeman[1], Tinne Dockx[3], Isabel Vandevelde[3], Ellen Dendauw[4], An Decombel[5], Monica Höfte[2] and Kurt Heungens[1]*

[1]Flanders Research Institute for Agriculture, Fisheries and Food (ILVO), Plant Sciences Unit, Merelbeke, Belgium, [2]Department of Plants and Crops, Faculty of Bioscience Engineering, Ghent University, Gent, Belgium, [3]Research Station for Vegetable Production (PSKW), Sint-Katelijne-Waver, Belgium, [4]Vegetable Research Centre (PCG), Kruishoutem, Belgium, [5]Inagro, Rumbeke-Beitem, Belgium

Fusarium oxysporum f.sp. *lactucae* (Fol) causes a vascular disease in lettuce that results in significant yield losses. Race-specific and sensitive real-time PCR assays were developed for Fol races 1 and 4, which are prevalent in Europe. Using genotyping-by-sequencing, unique DNA loci specific to each race were identified and subsequently used for the design of primers and hydrolysis probes. Two assays per race were developed to ensure specificity. The two assays of each race could be run in duplex format, while still giving a sensitivity of 100 fg genomic DNA for all assays. Sample preparation methods were developed for plant tissue, soil, and surfaces, with an extra enrichment step when additional sensitivity was required. By controlling the incubation conditions during the enrichment step, the real-time PCR signal could be matched to the number of spore equivalents in the original sample. When enriching naturally infested soil, down to six conidiospore equivalents L^{-1} soil could be detected. As enrichment ensures sensitive detection and focuses on living Fol propagules, it facilitates the evaluation of control measures. The developed detection methods for soil and surfaces were applied to samples from commercial lettuce farms and confirmed the prevalence of Fol race 4 in Belgium. Monitoring of soil disinfestation events revealed that despite a dramatic decrease in quantity, the pathogen could still be detected either immediately after sheet steaming or after harvesting the first new crop. The detection method for plant tissue was successfully used to quantify Fol in lettuce inoculated with race 1, race 4 or a combination of both. Under the temperature conditions used, race 4 was more aggressive than race 1, as reflected in larger amounts of DNA of race 4 detected in the roots. These newly developed assays are a promising tool for epidemiological research as well as for the evaluation of control measures.

KEYWORDS

Fusarium wilt, *Lactuca sativa* L., genotyping-by-sequencing, real-time PCR, soilborne pathogen

1 Introduction

Fusarium oxysporum f.sp. *lactucae* (Fol) is a soilborne fungal pathogen that causes vascular wilt in lettuce (*Lactuca sativa* L.), one of the most economically important leafy vegetables in Europe. The pathogen, first reported in Japan (Matuo and Motohashi, 1967) is divided into four races, of which race 1 is the most widespread. In Europe, race 1 was first discovered in 2001 in Italy (Garibaldi et al., 2002), then in Portugal (Pasquali et al., 2007), France (Gilardi et al., 2017b), Spain (Guerrero et al., 2020), Norway (Herrero et al., 2021), Belgium (Claerbout et al., 2023), Greece (Tziros and Karaoglanidis, 2023) and Ireland (van Amsterdam et al., 2023). Since 2015, a new race (race 4) has emerged as a serious threat to lettuce production in several European countries. Fol race 4 was first identified in the Netherlands (Gilardi et al., 2017). Since then, its presence has been documented in Belgium (Claerbout et al., 2018), Ireland and England (Taylor et al., 2019), Italy (Gilardi et al., 2019), and Spain (Gálvez et al., 2023). Race 2 has only been reported in Japan and race 3 in only Taiwan and Japan (Fujinaga et al., 2001; Fujinaga et al., 2003; Lin et al., 2014).

Fusarium wilt is a big problem for soil-grown lettuce. Infestation can cause significant yield losses and reduce the quality of the lettuce heads. The disease is characterized by vascular discoloration, chlorosis of the leaves, stunted growth, and wilting of the plant. The fungus can survive in the soil for several years in the form of chlamydospores carried along with crop residues (Scott et al., 2012). The persistence of Fol in soil poses significant management challenges as restrictions on the use of soil fumigants make it difficult to reduce the Fol inoculum in soil (Gullino et al., 2021). The pathogen can spread via infested soil on equipment as well as via infected seed (Garibaldi et al., 2004a; Claerbout et al., 2023). The use of resistant lettuce cultivars can be an effective control method against the disease, but currently no commercially viable resistant lettuce varieties are available.

Before the emergence of Fol, high intensity soil-based lettuce production in greenhouses was the most common cultivation method in Belgium, yielding up to five crops annually. The dramatic impact of Fol has led to research into the diversity and biology of the pathogen. Between 2015 and 2018, 78 *Fusarium* isolates were collected from symptomatic butterhead lettuce plants in Belgian commercial greenhouses (Claerbout et al., 2023). Using genotyping as well as inoculation experiments on differential cultivars, it was determined that 91% of the isolates belonged to race 4 while only 6% of the isolates belonged to race 1. The prevalence of race 4 in Belgium can be explained by the higher virulence of race 4 at soil temperatures below 18°C (Gilardi et al., 2021) which are typical for northwest Europe.

Monitoring the pathogen requires race-specific and sensitive detection techniques. Traditional methods for Fol detection are time-consuming, laborious, and may lead to false-negative results. Therefore, the development of a reliable and sensitive molecular detection method for Fol races 1 and 4 is needed to assess the prevalence and distribution of these races in lettuce production fields as well as to evaluate potential control methods. Existing detection assays for *Fusarium oxysporum* f.sp. *lactucae* races 1 and 4 include a LAMP assay (Franco Ortega et al., 2018) but this does not discriminate between the two races and it is only semi-quantitative. Conventional PCR assays have suboptimal specificity and sensitivity (Gilardi et al., 2017a; Pasquali et al., 2007). Recently, a real-time PCR assay for Fol race 1 has been developed, but not for race 4 (Sanna et al., 2022).

In this study, we aimed to develop sensitive and specific molecular detection methods for Fol race 1 and race 4 and to apply these techniques to a variety of samples such as soil, surfaces of equipment and containers, and plant tissue. The first objective was to use genotyping-by-sequencing (GBS) to identify candidate loci for race-specific primers and hydrolysis probes and to test the resulting qPCR assays for specificity and sensitivity. GBS is a high-throughput sequencing technique that can be used to distinguish the closely related race 1 and race 4, as these races cannot be discriminated based on the sequence of commonly used barcoding loci such as the intergenic spacer region (IGS) and the translation elongation factor 1-α (*tef1*) (Gilardi et al., 2017a). GBS reduces genome complexity with the use of restriction enzymes and can identify approximately 10 000 DNA loci in *Fusarium* species using a double digest with *Pst*I and *Hpa*II (Van Poucke et al., 2021; Claerbout et al., 2023). The second objective was to optimize sample processing in order to increase sensitivity. The third objective was to validate the detection method on plant tissue, on greenhouse soil, and on equipment surfaces by collecting samples at commercial lettuce farms and analyzing them using these optimized methods.

2 Materials and methods

2.1 Fungal isolates and DNA extraction

Isolates used in this study and their origin are listed in Table 1. The *Fusarium* cultures were stored at −80°C in 50% glycerol. To obtain genomic DNA, the isolates were grown in potato dextrose broth (Becton Dickinson) during one week at room temperature. The mycelium was dried on sterile filter paper and collected in microcentrifuge tubes. The samples were crushed to a fine powder using liquid nitrogen, sterile stainless steel beads (5 mm diameter) and a mixer mill (MM 400, Retsch). Genomic DNA was extracted using the Nucleospin Plant II kit (Macherey-Nagel) with PL1 as extraction buffer and eluted in 50 µl TE buffer. DNA concentrations were measured using the Quantus Fluorometer (Promega). DNA samples were stored at -20°C.

2.2 Inoculum production

To produce conidiospore suspensions of Fol races 1 and 4, the isolates were grown for one week at room temperature on potato dextrose agar (PDA). Sterile water (5 mL) was added to each plate and the colony was scraped with a sterile Drigalski spatula. The suspension was filtered through a 250 µm mesh filter to remove hyphal fragments. A haemocytometer was used to determine the spore concentration and the desired concentrations were obtained by diluting with sterile water. The viability of the inoculum was determined by plating dilution series onto PDA plates.

10.3389/fpls.2023.1272136

TABLE 1 Details of isolates used in this study.

Species (and race)	Isolate code	Host or substrate	Geographic origin	Source
Fusarium oxysporum f.sp.				
lactucae race 1	Fus1.39	*Lactuca sativa*	Belgium	(Claerbout et al., 2023)
lactucae race 1	Fus1.59	*Lactuca sativa*	Belgium	(Claerbout et al., 2023)
lactucae race 1	Fus1.60	*Lactuca sativa*	Belgium	(Claerbout et al., 2023)
lactucae race 1	Fus6.01	*Lactuca sativa*	Japan	(Claerbout et al., 2023)
lactucae race 1	244120	*Lactuca sativa*	Japan	NARO Genebank
lactucae race 4	Fus1.01	*Lactuca sativa*	Belgium	(Claerbout et al., 2023)
lactucae race 4	Fus1.02	*Lactuca sativa*	Belgium	(Claerbout et al., 2023)
lactucae race 4	Fus1.33	*Lactuca sativa*	Belgium	(Claerbout et al., 2023)
lactucae race 4	Fus1.34	*Lactuca sativa*	Belgium	(Claerbout et al., 2023)
lactucae race 4	Fus1.56	*Lactuca sativa*	Belgium	(Claerbout et al., 2023)
lactucae race 4	Fus1.58	*Lactuca sativa*	Belgium	(Claerbout et al., 2023)
lactucae race 4	Fus1.62	*Lactuca sativa*	Belgium	(Claerbout et al., 2023)
lactucae race 2	244121	*Lactuca sativa*	Japan	NARO Genebank
lactucae race 3	244122	*Lactuca sativa*	Japan	NARO Genebank
lactucae race 3	744085	naturally infested soil	Japan	NARO Genebank
lactucae race 3	744086	naturally infested soil	Japan	NARO Genebank
asparagi	CBS 143081	*Asparagus*	the Netherlands	Westerdijk Institute
cepea	CBS 148.25	*Allium cepa*	unknown	Westerdijk Institute
conglutinans	CBS 186.53	*Brassica oleracea*	USA	Westerdijk Institute
lilli	CBS 130322	*Lilium*	USA	Westerdijk Institute
melonis	CBS 420.90	*Cucumis melo*	Israel	Westerdijk Institute
opuntiarum	CBS 743.79	*Zygocactus truncatus*	Germany	Westerdijk Institute
phaseoli	CBS 935.73	*Phaseolus*	USA	Westerdijk Institute
rhois	CBS 220.49	*Rhus typhina*	unknown	Westerdijk Institute
tulipae	CBS 242.59	*Tulipa*	Germany	Westerdijk Institute
vasinfectum	CBS 116615	*Gossipium hirsutum*	Ivory Coast	Westerdijk Institute
cyclaminis	DSMZ 62315	*Cyclamen*	unknown	unknown
Other species				
Fusarium curvatum	CBS 247.61	*Matthiola incana*	Germany	Westerdijk Institute
Fusarium solani	D/20/2673	*Lactuca sativa*	Belgium	ILVO
Fusarium poae	MY2	unknown	Belgium	ILVO
Fusarium avenaceum	MY3	unknown	Belgium	PCF
Fusarium nirenbergiae	CBS 130303	*Solanum lycopersicum*	USA	Westerdijk Institute
Phytophthora ramorum		unknown	unknown	ILVO
Trichoderma asperellum		unknown	unknown	ILVO
Penicillium brevicompactum	MY27	air	Belgium	ILVO
Aspergillus westerdijkiae	MY13	*Capsicum annuum*	Belgium	PSKW
Plectosphaerella plurivora	MY61	*Lactuca sativa*	Belgium	ILVO

(Continued)

TABLE 1 Continued

Species (and race)	Isolate code	Host or substrate	Geographic origin	Source
Botrytis cinerea	PCF895	*Fragaria* x *ananassa*	Belgium	(Debode et al., 2013)
Olpidium sp.	6	*Lactuca sativa*	Belgium	ILVO
Verticillium dahliae	10	unknown	Belgium	ILVO
Sclerotinia minor	27	unknown	Belgium	ILVO
Cladosporium halotolerans	MY28	unknown	unknown	ILVO
Pythium sp.	D/20/0242A	unknown	unknown	ILVO
Rhizoctonia solani		unknown	unknown	ILVO

Chlamydospores were produced following the protocol of Smith and Snyder (1971), adapted as described in Claerbout et al. (2023). In brief, air-dried sandy loam soil was autoclaved on two consecutive days. The soil (200 g) was inoculated with a microconidia suspension (10 mL, 10^6 spores mL^{-1}) and incubated at 23°C in the dark for a minimum of four weeks. The lid of the jar was closed loosely to allow drying of the soil. Before use, inoculum density was checked by dilution plating of the soil on PDA.

2.3 Design of race-specific real-time PCR assays for *Fusarium oxysporum* f.sp. *lactucae* races 1 and 4

Primers and corresponding hydrolysis probes were designed using Oligo Analyzer based on race-specific loci identified via genotyping-by-sequencing (GBS) as conducted by Claerbout et al. (2023) following the method of Van Poucke et al. (2021). During GBS, 81 *Fusarium oxysporum* f.sp. *lactucae* isolates were sequenced as well as 10 other *formae speciales* of *F. oxysporum* and two other *Fusarium* species. Unique DNA loci specific to either race 1 or race 4 were selected from the approximately 10 000 DNA loci (30 – 300 bp) sequenced for both races, based on the absence of the loci in the other *formae speciales* of *F. oxysporum* and other *Fusarium* species that were included in the GBS run. This was done using a custom-made Perl script (see data availability statement). For each race, candidate primer pairs were manually selected for 20 of these unique loci and risk for primer dimer formation was verified with OligoAnalyzer 1.1.2. Real-time PCR was first performed using Sybr Green with the selected primer pairs. The reaction mixture (20 µl) contained 1x PowerUp SYBR Green Master Mix (Applied Biosystems, Belgium), 300 nM of both primers and 100 pg genomic DNA. Amplification was performed using a Quantstudio Real-Time PCR system (Applied Biosystems) at 95°C for 10 min, followed by 40 cycles of 95°C for 15 s and 60°C for 1 min. A melting curve stage was added by heating to 95°C, cooling to 60°C, and slowly heating to 95°C in steps of 0.1°C/s. No-template controls (NTC) for each primer set were analyzed. The best performing primer sets were selected and tested for race-specificity. Fol race 4 isolates were analyzed with the Fol race 1 assays and Fol race 1 isolates were analyzed with the Fol race 4 assays. Hydrolysis probes were developed for primer sets with sufficient specificity. For both race 1 and race 4 of Fol, two primer sets with corresponding probes were developed. For each race, the corresponding two primer sets with probes were run in duplex format, after having shown that there was no significant difference versus running them in simplex format. The probes from the two assays of the same race were labeled with a different fluorochrome. Primer and probe sequences are shown in Table 2.

Real-time PCR with the hydrolysis probes was performed in 20 µl reactions. These contained 10 µl of 2x GoTaq qPCR Master Mix (Promega), 300 nM of the two forward and reverse primers, 50 nM of the two corresponding probes and 2 µl of DNA extract. During real-time PCR optimization, other primer/probe concentrations were evaluated (300/50, 600/50, 900/50, 300/100, 600/100 and 900/100 nM), of which 300/50 nM was finally selected. Amplification was performed using a CFX96 Touch system (Bio-Rad) at 95°C for 10 min, followed by 40 cycles of 95°C for 15 s and 60°C for 1 min. In every run, a 10-fold dilution series of race 1 and race 4 genomic DNA (0.01 to 10 ng per qPCR reaction) was included to enable quantification of DNA. No-template controls and a negative control (the other race) were also included. Each sample was run in duplicate.

2.4 Specificity and sensitivity of the race-specific real-time PCR assays

Specificity of the real-time PCR assays was further tested using DNA from four *Fusarium oxysporum* f.sp. *lactucae* race 1 isolates, one race 2 isolate, three race 3 isolates and seven race 4 isolates. Eleven other *F. oxysporum* isolates, four other *Fusarium* spp. and 12 isolates of other fungi or oomycetes were also tested (Table 1). Genomic DNA was analyzed with the newly developed real-time PCR assays (100 to 250 pg genomic DNA was added). Fus1.39 and Fus1.01 were added as positive control for the race 1 and race 4 assays, respectively.

Sensitivity of the real-time PCR assays was determined via analysis of DNA dilution series. The standard curves were generated using genomic DNA extracted from mycelia of Fus1.39 (race 1) and Fus1.01 (race 4). A ten-fold dilution series (100 ng to 100 fg per qPCR reaction) of the extracted DNA was analyzed with the real-time PCR assays.

Conidiospore standard curves were developed by producing conidiospore inoculum from Fol races 1 (Fus1.39) and 4 (Fus1.01)

10.3389/fpls.2023.1272136

TABLE 2 Details of the primers and probes for the new *Fusarium oxysporum* f.sp. *lactucae* race-specific qPCR assays.

Assay	Primer/probe name	Sequence (5′ to 3′)	Amplicon size (bp)
Fol1a	Fol1a-F	TGTACCCTGATAATCCTGGTAC	142
	Fol1a-R	AGCTTGACTCTATCGTTGTCGA	
	Fol1a-P	(6-FAM)CCAGCAGGCTGAAGGATGCTTTGTA(QSY-7)	
Fol1b	Fol1b-F	CAGCATTGCCCTTTCAAGTTCA	179
	Fol1b-R	CGAGCTGCTTTAGTATTGGTGT	
	Fol1b-P	(VIC)ACCAGATTGCACCGAATTCCCTCGC(QSY-7)	
Fol4a	Fol4a-F	ACAATGACACCATGTGAGGTAC	223
	Fol4a-R	TTGTGTACGATCATGTGGACCA	
	Fol4a-P	(6-FAM)CGACTGCATTGGCAACCTGTGAC(QSY-7)	
Fol4b	Fol4b-F	GACGCCTTTCAACTTCATGCTT	195
	Fol4b-R	CCTAGATGCGTTCAAATGCTCT	
	Fol4b-P	(VIC)TGCAACGCTGGGAGAACCTTGTC(QSY-7)	

as described above. A dilution series was made from $10^{4.4}$ to $10^{6.9}$ spores per tube. After centrifugation (18 000 g, 5 min), the supernatant was removed and DNA was extracted with the Nucleospin Plant II kit (Macherey-Nagel) with PL1 as extraction buffer and 50 µl TE elution buffer. The genomic DNA of a range of 10^3 to $10^{5.5}$ conidiospores per qPCR reaction was analyzed with the real-time PCR assays.

2.5 Quantification of Fol in plant tissue

To analyze the quantity of Fol in plant tissue, plant parts were placed in aluminum foil bags, flash frozen in liquid nitrogen, and kept at -20°C until further processing. The plant tissue was again placed in liquid nitrogen, removed from the aluminum bag, weighed, and added to a plastic maceration bag (Bioreba). Half the weight of the plant tissue was added in mL sterile Tris-HCl buffer (100 nM, pH 8) (e.g., 0.5 mL buffer was added to 1 g root tissue). A Bioreba homogenizer (hand model) was used to crush the tissue in the maceration bags until the plant structure was no longer visible. The suspension was collected on the opposite side of the fine-meshed gauze, quantified, and a subsample (2 mL) was taken if the resulting volume was more than 2 mL. This (sub)sample was centrifuged for 5 min at 18 000 g and the supernatant was removed. The pellets were stored at -20°C until DNA extraction. The samples were crushed into a fine powder using liquid nitrogen, sterile stainless steel beads (5 mm diameter), and a mixer mill (MM 400, Retsch). DNA extraction was performed using the Nucleospin Plant II kit (Macherey-Nagel) with PL1 as extraction buffer and elution in 50 µl TE buffer. The DNA samples were stored at -20°C. Real-time PCR was performed, and the quantity of DNA in the roots was converted to conidiospore equivalents per mg root by using DNA and conidiospore standard curves.

To validate the real-time PCR assays for plant samples, we analyzed butterhead lettuce that was artificially inoculated with Fol races 1 and 4. Lettuce seeds of the cultivar 'Cosmopolia', which is susceptible to both Fol races 1 and 4, were surface sterilized for 30 s in 1% NaOCl and washed three times with sterile water. After sterilization, the seeds were sown in sterilized potting soil (universal type 1 structural at 56% moisture content, Snebbout N.V., Belgium) and incubated in a growth chamber at 18°C (16h/8h day/night). Sterilization of the potting soil was conducted on two consecutive days for 1 h at 121°C and 103.4 kPa. After two weeks, the lettuce seedlings were transplanted in pots with either 110 g sterile potting soil (control) or with 110 g sterile potting soil artificially infested with Fol race 1 (Fus1.39), Fol race 4 (Fus1.01), or a combination of both races. As inoculum, six-week-old chlamydospores (100 cfu g^{-1} potting soil) were used. For the pots with both races combined, 100 cfu g^{-1} potting soil of each race was added, mainly to see if there was an additive effect or whether competition occurred between the two races. Transplanted lettuce seedlings were incubated at 24°C (16h/8h day/night). Each treatment had eight replicates. After three weeks the wilting symptoms were scored on a scale from 0 to 4 following the disease scale developed by Claerbout et al. (2023). The disease index (DI) for each treatment was calculated as follows: $DI_{0-100} = \frac{\sum N_{plants} * Rating\ \ scale_{0-4} * 100}{Total\ \ N_{recorded\ \ plants} * 4}$. The roots were washed, weighed and the vascular discoloration was scored on a scale of 0 to 4 as indicated in Figure 1. Disease Index (DI) was calculated for the vascular discoloration of the roots following the same equation as for the wilting symptoms. The root tissue was surface-disinfested for 1 min with ethanol (70%), and 1 min with NaOCl (1%) and subsequently washed three times with sterile, distilled water. After superficial drying of the roots, they were processed for quantification of Fol1 and Fol4 as described above. Prior to maceration in the Bioreba bags, the roots were pooled to increase the total weight. The eight roots from the treatment with Fol race 1 were pooled into two groups of four roots each based on their wilting symptoms, weight and vascular discoloration. The eight roots for the three other treatments (control, Fol race 4 and the combination of both races) were pooled into one group each.

FIGURE 1
Disease scale (0-4) to score vascular discoloration of lettuce roots caused by Fol, 0 = no discoloration, 1 = light vascular discoloration, 2 = clear vascular discoloration, 3 = dark vascular discoloration, 4 = roots completely discolored and rotten.

2.6 Quantification of Fol in soil via target enrichment

For soil samples, an enrichment step was added to increase the sensitivity of the assays and target living propagules. This was done by incubating the samples in the semi-selective *Fusarium* medium of Komada (1975).

Greenhouse soil samples were kept at 4°C for a maximum of three days until processing. Before subsampling, the soil samples were mixed thoroughly. A soil suspension was made by diluting 100 mL of soil to 500 mL with sterile water. The suspension was thoroughly shaken before adding 10 mL to each of two 50 mL centrifuge tubes. These tubes were centrifuged (5000 g, 15 min) and supernatant was removed. The soil samples were subsequently resuspended to 10 mL with Komada medium. The samples were incubated for 48 h at 25 ˚C and 110 rpm. The tubes were set at an inclination of 20 degrees (relative to the horizontal axis). After 48 h, two subsamples of 1 mL were taken from the tubes and added to sterile 2 mL microcentrifuge tubes. These subsamples were centrifuged (18 000 g, 5 min) and the supernatant was removed. The subsamples were stored at -20°C until DNA extraction.

DNA extraction was done using the Powersoil Pro kit (Qiagen) with 50 µl elution buffer (C6). A mixer mill (MM 400, Retsch) was used for homogenization and lysis (25 Hz, twice 5 min, with inversion of the adapters in between). The DNA samples were stored at -20°C. The real-time PCR assays were used to detect and quantify Fol race 1 and race 4 in the DNA from the soil samples. We first developed a standard curve using spiked conidiospore dilution series in soil. A linear standard curve was developed that correlates the number of spores before enrichment with the DNA quantity after enrichment. By including a target DNA standard curve during real-time PCR analysis of a sample, the DNA concentration after enrichment could be calculated and this concentration was used to calculate back to the initial number of conidiospore equivalents. In addition, enrichment of soil with conidiospores was compared to enrichment of soil with chlamydospores. Soil artificially infested with chlamydospores was prepared as described above and inoculum density was checked by dilution plating of the soil on PDA. The soil was diluted with sterilized soil to a series of inoculum densities and subsequently enriched before DNA extraction and real-time PCR.

Possible interference of non-targets with the Fol race 1 and 4 assays during enrichment in soil was investigated. Chlamydospores of Fol races 1 and 4 (Fus1.39 and Fus1.01) were prepared as described above and 100 cfu of each race were added per gram of potting soil either separately or simultaneously. The three soil treatments were enriched as described above before DNA extraction and real-time PCR analysis.

2.7 Quantification of Fol on surfaces via target enrichment

Similar to the soil samples, an enrichment step was added for swab samples (from surfaces). Swab samples were kept at 4°C for a maximum of 3 days until processing. The swabs were transferred to or kept in a sterile 12 mL centrifuge tube after sampling and 5 mL Komada medium was added before incubation. The tubes were incubated horizontally for 48 h at 25 ˚C and 110 rpm. After 48 h the swabs were trimmed with sterile scissors and transferred to 2 mL microcentrifuge tubes with 1.5 mL of the corresponding suspension. All tubes were centrifuged (18 000 g, 5 min) and the supernatant was removed. The subsamples were stored at -20°C until DNA extraction.

DNA was extracted from the swab samples using the Nucleospin Plant II kit (Macherey-Nagel) with PL1 as extraction buffer and 50 µl TE buffer. For each swab, 200 mg zirconium beads were added with the extraction buffer and RNase. The swabs were bead-beaten at 30 Hz for 1 min using a mixer mill (400 MM, Retsch), followed by 10 min incubation at 65°C and 1400 rpm. This step was repeated three times before following the rest of the protocol from the manufacturer. The DNA samples were stored at -20°C. The real-time PCR assays were used to detect and quantify Fol race 1 and race 4 in the DNA from the swab samples. A standard curve was developed by using a spiked conidiospore dilution series on swabs. The linear standard curve correlates the number of conidiospores before enrichment with the DNA quantity after enrichment. During real-time PCR analysis of a sample, a target

DNA standard curve was included, and the DNA concentration after enrichment could be calculated. This concentration was used to calculate back to the initial number of conidiospore equivalents.

2.8 Sampling and analysis of naturally infested soil and surfaces at lettuce farms

To determine if the real-time PCR assays can be used to quantify the pathogen in naturally infested soil and on infested surfaces, samples were obtained from commercial lettuce growers. Fol inoculum levels in the soil were monitored at two lettuce growers who performed soil disinfestation by sheet steaming. Soil samples were taken before and after disinfestation and after one subsequent crop of butterhead lettuce. Greenhouse compartments were sampled along an X-pattern with a core borer (Ø3 cm, 0-30 cm deep). The soil was mixed thoroughly before taking two subsamples for enrichment. Three compartments were sampled at farm 1 and two compartments at farm 2. At farm 2, an additional soil sample was taken with the core borer from a spot where more disease symptoms were observed. Samples were taken from the same locations on each of the three time points.

To validate the method on surfaces that may be infested with Fol, various samples were taken at five other commercial lettuce farms. Swabs were used to sample the surface of cultivators and planters. These swabs were taken from parts that came in contact with the soil. Four to five spots without any adhering soil were swabbed (25 cm^2 in total). Any residual soil left on the machines was also sampled, mixed and two subsamples were taken for enrichment. Greenhouse soil at these five farms was sampled as described above.

After enrichment and DNA extraction of all samples, real-time PCR analysis was performed as described above with the assays for Fol races 1 and 4. The Fol inoculum was quantified by including a DNA standard curve during real-time PCR and by using the developed standard curves that correlate the number of conidiospores before enrichment to the DNA concentration after enrichment. Numbers were then expressed in relevant units, i.e., conidiospore equivalents L^{-1} soil and conidiospore equivalents m^{-2} surface area.

2.9 Data analysis

Cycle threshold (Cq) values for each real-time PCR reaction were automatically determined using the CFX Maestro Software (version 5.0.021.0616) for reactions analyzed by the CFX96 Touch system (Bio-Rad). The Quantstudio Design & Analysis (version 1.5.1) was used to determine the Cq values for reactions analyzed by the Quantstudio Real-Time PCR system (Applied Biosystems). The PCR efficiency of each real-time PCR assay was calculated from the slopes of the genomic DNA standard curves as follows: $efficiency\ (\%) = 10^{\frac{1}{slope}} - 1$.

Statistical analysis was performed with R (version 4.2.3) and R studio (version 2023.03.0) at a confidence level of $\alpha = 0.05$. Ordinal data of wilting symptoms and root vascular discoloration was analyzed with the nonparametric Wilcoxon rank sum test. For the comparison of lettuce head and root weights between treatments, the distribution of the data was analyzed with Levene's test (homogeneity of variances) and the Shapiro-Wilk test (normality). When the assumptions were fulfilled, a one-way analysis of variance (ANOVA) was performed, followed by Tukey's multiple comparison test. When the assumptions were not met, the nonparametric Wilcoxon rank sum test was used. The ability to multiplex the real-time PCR assays and the possible interference of non-targets with Fol during enrichment in soil was analyzed with the two-samples T-test when the assumptions were met.

3 Results

3.1 Development of race-specific real-time PCR assays

PCR primers and hydrolysis probes specific to Fol race 1 and race 4 were developed. For each race, two primer sets and corresponding probes were selected to run in duplex. The four isolates of Fol race 1 (Fus1.39, Fus1.59, Fus1.60 and Fus6.01) were each amplified with the race 1 assays, while no amplification occurred with the race 4 isolates. In total, 100 pg DNA (Fus1.01) corresponded to a (average ± stdev) Cq of 27.61 ± 0.20 for assay 1a and 29.30 ± 0.27 for assay 1b. With the race 4 assays, isolates from both race 4 subgroups as mentioned in Claerbout et al. (2023) (Fus1.01, Fus1.02, Fus1.33, Fus1.34, Fus1.56, Fus1.58 and Fus1.62) were amplified. One hundred pg DNA (Fus1.39) corresponded to a (average ± stdev) Cq of 28.67 ± 0.50 for assay 4a and 27.87 ± 0.13 for assay 4b. The Fol race 4 specific assays did not amplify DNA from race 1 isolates. The Fol race 1 and race 4 assays showed no amplification of Fol race 2 and race 3 isolates, 11 F. *oxysporum* isolates from other *formae speciales*, four isolates from other *Fusarium* species and 12 isolates of other fungi and oomycetes.

Table 3 shows the features of the standard curves generated with DNA (dilution series of 100 fg to 100 ng per qPCR reaction) from mycelium and microconidia (a range of 10^3 to $10^{5.5}$ conidiospores per qPCR reaction). A reliable threshold for all assays was set at a Cq of 38. As the spore samples were analyzed in the same qPCR run as the genomic DNA, the quantity of DNA could be converted to conidiospore equivalents using the combined equations: $number\ of\ conidiospore\ equivalents = 1E(\frac{\log(amount\ of\ DNA\ (pg))+1.358}{0.957})$ for the combined assays of race 1 and $number\ of\ conidiospore\ equivalents = 1E(\frac{\log(amount\ of\ DNA\ (pg))+1.463}{0.967})$ for the combined assays of race 4.

The ability to multiplex the two assays for each race was checked by comparing the multiplex analysis of target DNA against an analysis in which the two assays were run separately. The Fol1a and Fol1b assays detected 100.3% and 99.5% of the target (Fus1.39, 10 ng), respectively, when run in multiplex versus in singleplex format ($p = 0.55$ and $p = 0.21$). For Fol race 4 (Fus1.01, 10 ng), this was 99.0% and 99.4% for the Fol4a and Fol4b assays, respectively ($p = 0.16$ and $p = 0.13$). Similar results were obtained at 1 ng.

3.2 Quantification of Fol in plant samples

Consistent with the results of Claerbout et al. (2023), Fol race 4 (Fus1.01) was more aggressive on butterhead lettuce cv.

10.3389/fpls.2023.1272136

TABLE 3 Standard curve features of the race-specific real time PCR assays for Fol race 1 and race 4 with DNA obtained from either mycelium or microconidia. Standard curves are in the format Cq = slope × log (X) + intercept with X either fg gDNA used per qPCR reaction or the number of conidiospores from which the extracted DNA was used in the qPCR reaction.

Description of X	Assay	Isolate	Standard curve features			Efficiency (%)	100 fg (average Cq± stdev)	csp eq at Cq=38
			slope	intercept	R^2			
gDNA from mycelium	1a	Fus1.39 (race 1)	-3.524	34.68	0.9992	92.2	38.21±0.11	N/A
	1b	Fus1.39 (race 1)	-3.392	36.11	0.9970	97.2	38.78±0.53	N/A
	4a	Fus1.01 (race 4)	-3.458	35.53	0.9990	94.6	38.83±0.92	N/A
	4b	Fus1.01 (race 4)	-3.389	34.61	0.9965	97.3	37.18±0.72	N/A
Microconidia	1a	Fus1.39 (race 1)	-3.310	40.21	0.9788	100.5	N/A	0.67
	1b	Fus1.39 (race 1)	-3.157	40.10	0.9768	107.4	N/A	0.67
	4a	Fus1.01 (race 4)	-3.112	40.18	0.9666	109.6	N/A	0.70
	4b	Fus1.01 (race 4)	-3.142	40.83	0.9674	108.1	N/A	0.90

csp eq, conidiospore equivalents.
N/A, not applicable.

'Cosmopolia' than Fol race 1 (Fus1.39) (Figure 2). The race 4 isolate produced more severe wilting symptoms, more vascular discoloration and a lower head and root weight. In the combination treatment, the observed additive effect in disease symptoms indicated absence of competition between the races.

The real-time PCR analysis of the roots confirmed the difference in aggressiveness between the two races, showing differences in conidiospore equivalents mg^{-1} root between the two treatments. The roots from the treatment with Fol race 1 were pooled into two groups prior to maceration. The group with lower disease severity resulted in 111 conidiospore equivalents mg^{-1} root and the other group in 674 conidiospore equivalents mg^{-1} root, resulting in a mean of 393 conidiospore equivalents mg^{-1} root. The assays allowed detection of both races in the combination treatment.

3.3 Quantification of Fol in soil samples

Figure 3 shows the standard curves that relate the inoculum densities in soil before enrichment to the Cq values after enrichment for both Fol race 1 and race 4. No differences were obtained between soils inoculated either separately or simultaneously with race 1 and 4 ($p = 0.34$ for Fol race 1 and $p = 0.40$ for Fol race 4).

To validate if the real-time PCR assays can be used for determining pathogen levels in naturally infested soil, samples were obtained from two commercial lettuce growers that performed soil disinfestation (Table 4). Within and between farms, large differences were observed in the number of conidiospore equivalents L^{-1} soil. At farm 1, no detection occurred in any of the soil samples after disinfestation, while detection occurred in two of the three compartments after the first crop of lettuce. One compartment at farm 2 showed a signal of Fol immediately after disinfestation, corresponding with a reduction of 88.4%. After one crop of lettuce, detection occurred in all soil samples.

Table 5 shows the results of the analysis of regular soil samples and soil and swab samples taken from machinery at five other commercial lettuce farms. Soil from Farms 3 to 6 produced a Fol race 4 signal while soil from Farm 7 produced a Fol race 1 signal; the latter also corresponded with the highest number of conidiospore equivalents observed (4.8 log levels). At three farms, residual soil was found on the cultivator. All of these soil samples produced a Fol race 4 signal. The same farms had adhering soil on the planting machines with Fol race 4 detection at two of the three farms.

3.4 Quantification of Fol in surface samples

Figure 4 shows the quantification after enrichment of spiked conidiospores of Fol races 1 and 4 on swabs, via real-time PCR. Coefficients of determination ranged from 0.929 to 0.999. To validate this method, surface samples were taken at lettuce growers (Table 5). Swabs were used to sample surfaces from the cultivator and planter at four lettuce farms. Fol race 4 was detected on one of the four sampled cultivators and on two of the four planting machines.

10.3389/fpls.2023.1272136

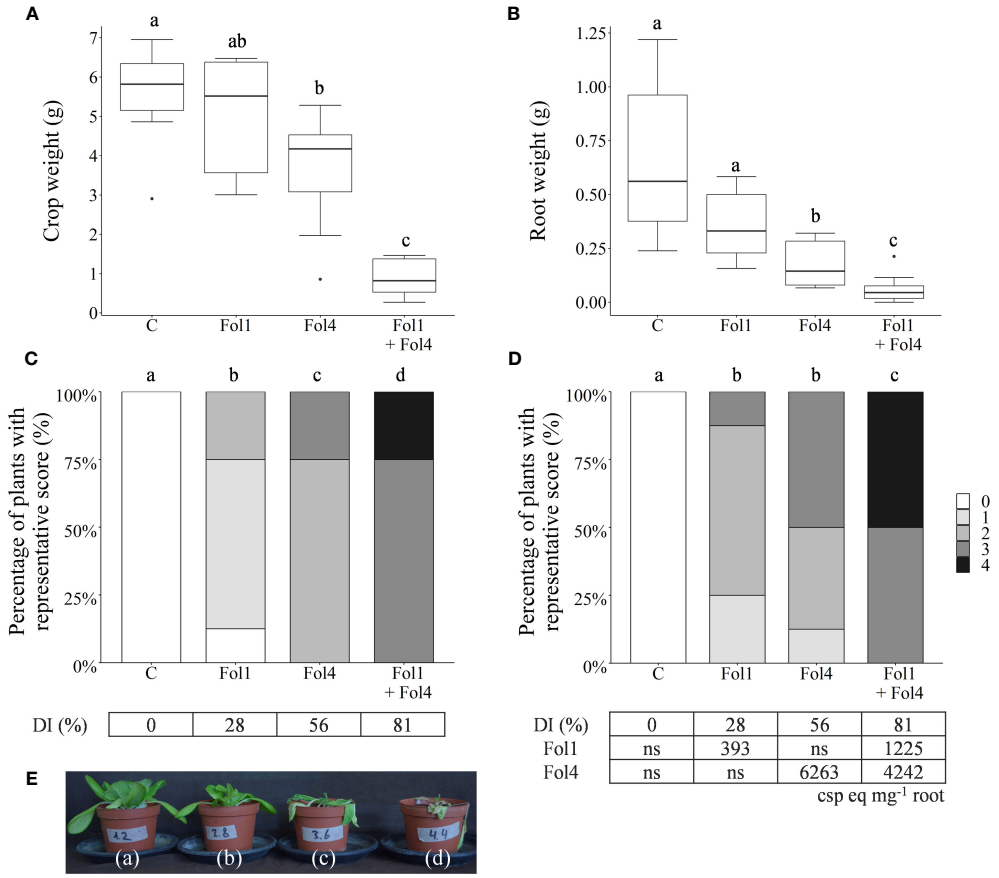

FIGURE 2
Aggressiveness of Fol race 1, Fol race 4 and the combination of both races on the susceptible butterhead lettuce cv. 'Cosmopolia'. Inoculation was performed by adding chlamydospores (100 cfu g^{-1} soil) to sterile potting soil. For the combination treatment, 100 cfu g^{-1} soil of both races was added. Lettuce seedlings were transplanted into the inoculated soil and kept at 24°C. After three weeks the plants were analyzed by weighing the head **(A)** and root **(B)** (Tukey's Test and Wilcoxon Rank Sum test, n = 8). Disease severity caused by Fol was assessed by scoring the wilting symptoms **(C)** and the vascular discoloration of the lettuce roots **(D)** (Wilcoxon Rank Sum test, n = 8). Conidiospore equivalents mg^{-1} root of Fol race 1 and race 4 for each treatment were quantified with real-time PCR. **(E)** Representative plants for each treatment: control (a), inoculated with Fol race 1 (b), with Fol race 4 (c) and with the combination of both races (d). Different letters in the graphs indicate statistical differences. In parts **(A)** and **(B)**, boxes represent data range (except outliers) and error bars represent the 95% confidence interval. DI, disease index; csp eq, conidiospore equivalents; ns, no signal.

4 Discussion

Within the present study, race-specific real-time PCR assays were successfully developed for *Fusarium oxysporum* f.sp. *lactucae* race 1 and race 4. Race-specific primers and corresponding hydrolysis probes were based on loci identified with genotyping-by-sequencing. Differentiation between Fol race 1 and race 4 isolates cannot be made based on *tef1*, *cmdA* and *rpb2*, but the genetic differentiation between the two races is clear when using the higher resolution GBS technique (Claerbout et al., 2023). Here the two most suitable candidate assays for each race were combined in duplex format as a protection against the possible presence of one of the loci in an unknown non-target organism. Specificity of these real-time PCR assays was confirmed based on a representative collection of pathogens, including Fol races 2 and 3, as well as a number of other fungi that could be present in the same niche. The DNA standard curves of the developed assays showed high efficiencies and high coefficients of determination. The sensitivity of the assays (100 fg genomic DNA) is comparable to that of the real-time PCR assay for Fol race 1 from Sanna et al. (2022).

The introduction of an enrichment step in the sample preparation method results in a sensitive detection method. Without enrichment of a soil sample, the detection limit of the real-time PCR assays (100 fg) would theoretically correspond to a detection limit in the soil of approximately 6000 conidiospore equivalents L^{-1} soil, while the lowest detection in naturally infested soil in this study was six conidiospore equivalents L^{-1} soil. This demonstrated the need for the enrichment technique. Another advantage of this sample preparation method is its focus on living (or at least non-dormant) and thus potentially infective fungal propagules, which represents a better risk assessment. A critical point is the potential variation in growth between enrichments of replicate samples. Based on the results presented, the variation among replicate samples analyzed at the same time was acceptable, but care should be taken in the comparison of samples analyzed at different time points: minor deviations in the growth response of the chlamydospores, e.g. as a result of additional storage time, could create differences in spore equivalents due to activity rather than a difference in number. Depending on the

10.3389/fpls.2023.1272136

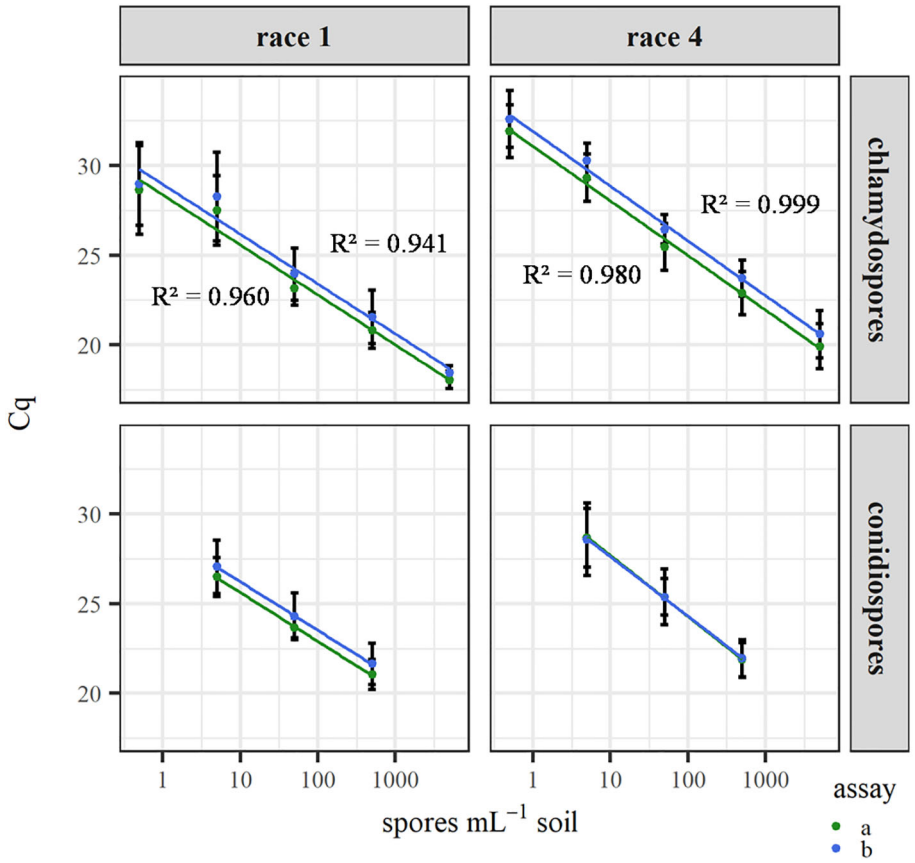

FIGURE 3
Real-time PCR quantification after enrichment of dilution series of conidiospores and chlamydospores in soil. Soil with conidiospores was prepared by inoculation with 5, 50 and 500 conidiospores mL^{-1} soil. Soil with chlamydospores was prepared as described in the text and diluted by adding sterile potting soil to obtain 0.5, 5, 50, 500 and 5000 chlamydospores mL^{-1} soil. Error bars represent standard deviation from 12, 11, 5 and 8 replicate enrichments (in soil) for Fol race 1 chlamydospores, Fol race 4 chlamydospores, Fol race 1 conidiospores and Fol race 4 conidiospores, respectively. Coefficients of determination (R^2) for the conidiospore standard curves were at least 0.999 with all assays for both races.

research objective, more enrichment replicates could be included and attention could be paid to the simultaneous enrichment of the samples to minimize this variation. Besides soil and surface samples, the enrichment method could also be applied to lettuce seed (data not shown). High sensitivity is required in obtaining a proper detection method for Fol in seed as few contaminated seeds in a large seed lot can disseminate the pathogen (Garibaldi et al., 2004a; Gordon and Koike, 2015). Sensitive assays to detect Fol in seed already exist but are not race-specific (Mbofung and Pryor, 2010; Franco Ortega et al., 2018).

TABLE 4 Real-time PCR-mediated quantification of Fol race 4 in soil samples from two commercial lettuce growers who performed soil disinfestation (sheet steaming).

Farm	Location within farm	conidiospore equivalents L^{-1} soil[a]					
		Before disinfestation		After disinfestation		After 1st crop of lettuce	
		A	B	A	B	A	B
1	Compartment 1	1722	4716	ns	ns	7.1	ns
	Compartment 2	273	312	ns	ns	ns	ns
	Compartment 3	27	301	ns	ns	16.9	3104
2	Compartment 1	8748	3141	702	675	34.8	13
	Compartment 2	18 045	35 457	ns	ns	203	27
	Spot 1	51 526	49 885	ns	ns	4401	4147

ns, no signal.
[a]Soil samples were mixed thoroughly before taking two subsamples for enrichment (A and B).

10.3389/fpls.2023.1272136

TABLE 5 Real-time PCR-mediated quantification of Fol in different types of soil samples and in swabs from commercial lettuce growers.

Farm	greenhouse		cultivator			planter		
	soil[c] (csp eq L^{-1})		soil[c] (csp eq L^{-1})		swab (csp eq m^{-2})	soil[c] (csp eq L^{-1})		swab (csp eq m^{-2})
	A	B	A	B		A	B	
3[a]	1094	24 497	329	1114	ns	948	33	4.4
4[a]	36	5.6	19	12	1.2	ns	ns	1.2
5[a]	15 328	6057	/	/	ns	/	/	ns
6[a]	4085	3236	29 887	17 172	ns	24 469	43 402	ns
7[b]	32 086	69 300	/	/	/	/	/	/

ns, no signal; / = no sample was taken; csp eq, conidiospore equivalents.
[a]Detection occurred only with the Fol race 4 assays.
[b]Detection occurred only with the Fol race 1 assays.
[c]Soil samples were mixed thoroughly before taking two subsamples for enrichment (A and B).

The detection and quantification of Fol race 4 in soil samples from two commercial lettuce growers who performed soil disinfestation indicate that the real-time PCR assays are a potential tool for assessment of soil inoculum levels. At one farm these inoculum levels ranged from 27 to 4716 conidiospore equivalents L^{-1} soil before disinfestation to no detection in any of the compartments after disinfestation, proving that sheet steaming can be an effective method in reducing the Fol soil population. However, after one subsequent crop of lettuce, detection occurred at two of the three compartments ranging from 7 to 3104 conidiospore equivalents L^{-1} soil, indicating that Fol was still present but was either not detected or had been reintroduced after steaming. The first hypothesis seems more likely when taking into consideration the results of the second farm, which still showed some detection in one of the two sampled compartments immediately after disinfestation. Non-detection can be the result of presence under the detection limit of the used assays or the sampling method. Soil was taken up to a depth of 30 cm, thus it is also possible the pathogen survived in deeper layers. At the second farm, a specific spot was sampled where more disease symptoms were observed. As expected, more conidiospore equivalents were detected in this soil sample relative to the overall soil sample of the two compartments. The new detection methods allowed evaluation of disinfection methods and demonstrated that the effect of sheet steaming is clearly temporary. Even low numbers of remaining pathogen in the soil will increase in the host and lead to accumulation of Fol soil inoculum levels because lettuce roots are incorporated in the soil after harvest.

Further evaluation of the race-specific real-time PCR assays was conducted by collecting soil samples from five additional commercial lettuce farms. This resulted in Fol race 4 detection at four farms and Fol race 1 detection on one farm. Additionally, soil

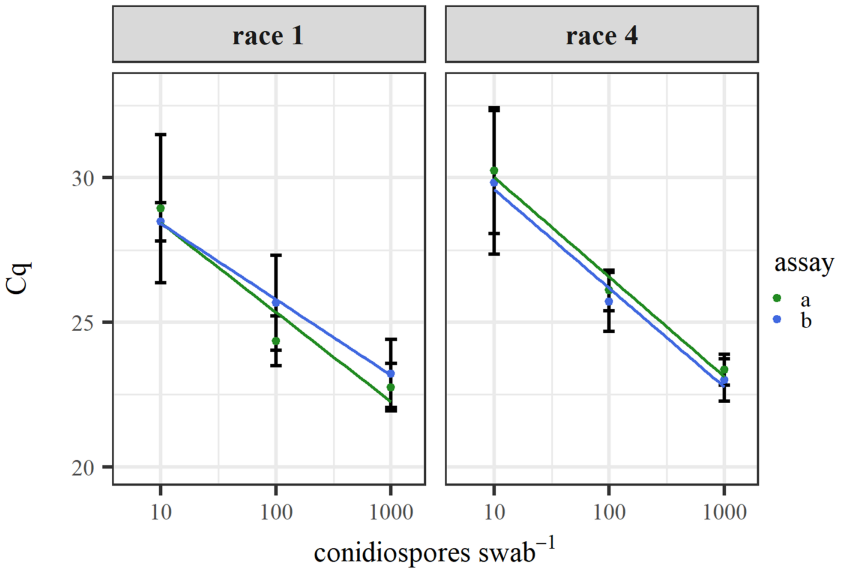

FIGURE 4
Real-time PCR mediated quantification of Fol race 1 and race 4 after enrichment of a dilution series of conidiospores spiked on swabs. Error bars represent standard deviation from five replicates.

adhering to cultivators and planters was obtained, leading to the detection of Fol in five out of the six sampled machines. This demonstrates the importance of machinery in the spread of the pathogen. Furthermore, even on swabbed surfaces devoid of any adherent soil on four cultivators and four planters, Fol was detected in three cases, albeit at low levels. These results highlight the importance of not only rinsing off soil but also implementing disinfection measures for the equipment in order to effectively mitigate the spread of the pathogen. The race-specificity of the assays allowed us to confirm that most farms seem to be affected by Fol race 4 and not Fol race 1. As mentioned before, the greater pathogenic importance and prevalence of Fol race 4 in western Europe is probably due to the lower soil temperatures during most of the production year. Knowledge of the race present at a given farm or farm compartment also has implications for the choice of cultivars, as newly released commercially viable cultivars will initially have resistance to either race 1 or race 4 but not both.

The use of the race-specific real-time PCR assays for detection of Fol in plant tissue was validated by conducting a plant experiment with both races 1 and 4. Fol race 4 was more aggressive on butterhead lettuce cv. 'Cosmopolia' than Fol race 1, confirming results of Claerbout et al. (2023). This also showed in the results of the real-time PCR analysis of the roots, as more conidiospore equivalents mg^{-1} root were detected in the treatment with Fol race 4. Comparing the two separate treatments where race 1 or race 4 was inoculated with the combined treatment did not result in any sign of competition between the two races.

The developed real-time PCR assays and the optimized sample preparation method can be used for risk assessment of Fol. In doing this, multiple influencing factors should be considered, such as the sampling method. This method is important because Fol is not uniformly distributed in the soil, as evidenced by spots with higher inoculum (and corresponding disease) levels. This was the case at lettuce farm 2, as higher concentrations occurred in a specific spot in the greenhouse where more disease symptoms were noted. Associating risk of disease to observed inoculum levels may also be difficult under field conditions for other reasons than the patchy distribution, as dose response is affected by several other factors such as temperature, cultivar, nutrient status and the microbiome (Garibaldi et al., 2004b; Scott et al., 2009; Okubara et al., 2013; Veresoglou et al., 2013).

Risk assessment can also be performed by using the real-time PCR assays for the detection of Fol in (semi) resistant cultivars and potential other crops for crop rotation. While these crops may not show *Fusarium* symptoms, their xylem vessels might harbor considerable amounts of Fol (Scott et al., 2014). By comparing the quantities of Fol races 1 and 4 in non-symptomatic crops to the amount of Fol in roots of susceptible lettuce cultivars, the risk of inoculum build-up can now be assessed.

5 Conclusions and future perspectives

This study provides sensitive and race-specific real-time PCR detection methods for Fol races 1 and 4. Race-specific targets for these assays could be identified via genotyping-by-sequencing (GBS). The combination of duplicate assays per race protects against possible future specificity issues. An enrichment method is needed for cases where added sensitivity is crucial or where the focus is on the detection of living propagules. We demonstrated the applicability of the assays in complex matrices such as root tissue and soil. The molecular detection methods and optimized sample preparation provide easy tools for race identification, which should contribute to better disease management practices and ultimately reduce the economic losses caused by this pathogen.

The assays can now be used to study the spread of the pathogen as well as to evaluate the effect of control measures such as different soil disinfestation methods and the use of new resistant varieties and alternative crops. The added sensitivity obtained with the enrichment method could be applied to examine the risk of introduction or spread of the pathogen via seeds or irrigation water. This study provides the first quantitative data on the presence of Fol in greenhouse soil. It can now be extended to an in-depth study of the two- and three dimensional distribution of the pathogen in greenhouse soils. Assays with in-field applicability, such as LAMP and RPA, could be developed based on the same race-specific loci.

Data availability statement

The original contributions presented in the study are included in the article/supplementary material. Further inquiries can be directed to the corresponding author. More information on the GBS data processing as well as all scripts can be found on https://gitlab.ilvo.be/genomics/GBS/GBS_Fol4 or on Zenodo with DOI 10.5281/zenodo.8175922.

Author contributions

HM: Conceptualization, Writing – review & editing, Formal Analysis, Investigation, Methodology, Validation, Visualization, Writing – original draft. KV: Investigation, Methodology, Writing – review & editing. AH: Formal Analysis, Software, Writing – review & editing. TD: Conceptualization, Project administration, Resources, Writing – review & editing. IV: Conceptualization, Funding acquisition, Project administration, Supervision, Writing – review & editing. ED: Project administration, Resources, Writing – review & editing. AD: Conceptualization, Funding acquisition, Project administration, Resources, Writing – review & editing. MH: Conceptualization, Funding acquisition, Project administration, Supervision, Writing – review & editing. KH: Conceptualization, Funding acquisition, Project administration, Supervision, Writing – review & editing.

Funding

The author(s) declare financial support was received for the research, authorship, and/or publication of this article. This research was funded by grant no. HBC.2018.2200 from the 'Flanders Innovation & Entrepreneurship (VLAIO)'.

Acknowledgments

We are grateful to Rijk Zwaan (the Netherlands) for providing the lettuce seeds for the plant experiment. We thank Fran Focquet for her technical assistance. We thank Miriam Levenson for English language editing.

Conflict of interest

The authors declare that the research was conducted in the absence of any commercial or financial relationships that could be construed as a potential conflict of interest.

The author(s) declared that they were an editorial board member of Frontiers, at the time of submission. This had no impact on the peer review process and the final decision.

Publisher's note

References

Claerbout, J., Van Poucke, K., Mestdagh, H., Delaere, I., Vandevelde, I., Venneman, S., et al. (2023). *Fusarium* isolates from Belgium causing wilt in lettuce show genetic and pathogenic diversity. *Plant Pathol.* 72, 593–609. doi: 10.1111/ppa.13668

Claerbout, J., Venneman, S., Vandevelde, I., Decombel, A., Bleyaert, P., Volckaert, A., et al. (2018). First report of *Fusarium oxysporum* f. sp. *lactucae* race 4 on lettuce in Belgium. *Plant Dis.* 102, 1037. doi: 10.1094/PDIS-10-17-1627-PDN

Debode, J., Van Hemelrijck, W., Creemers, P., and Maes, M. (2013). Effect of fungicides on epiphytic yeasts associated with strawberry. *Microbiologyopen* 2, 482–491. doi: 10.1002/MBO3.85

Franco Ortega, S., Tomlinson, J., Gilardi, G., Spadaro, D., Gullino, M. L., Garibaldi, A., et al. (2018). Rapid detection of *Fusarium oxysporum* f. sp. *lactucae* on soil, lettuce seeds and plants using loop-mediated isothermal amplification. *Plant Pathol.* 67, 1462–1473. doi: 10.1111/ppa.12855

Fujinaga, M., Ogiso, H., Tsuchiya, N., and Saito, H. (2001). Physiological Specialization of *Fusarium oxysporum* f. sp. *lactucae*, a Causal Organism of Fusarium Root Rot of Crisp Head Lettuce in Japan. *J. G. Plant Path.* 67, 205–206. doi: 10.1007/pl00013012

Fujinaga, M., Ogiso, H., Tuchiya, N., Saito, H., Yamanaka, S., Nozue, M., et al. (2003). Race 3, a new race of *Fusarium oxysporum* f. sp. *lactucae* determined by a differential system with commercial cultivars. *J. G. Plant Path.* 69, 23–28. doi: 10.1007/s10327-002-0009-8

Gálvez, L., Brizuela, A. M., Garcés, I., Cainarca, J. S., and Palmero, D. (2023). First Report of *Fusarium oxysporum* f. sp. *lactucae* Race 4 Causing Lettuce Wilt in 2 Spain. *Plant Dis.* 107 (8), 2549. doi: 10.1094/PDIS-10-17-1627

Garibaldi, A., Gilardi, G., and Gullino, M. L. (2002). First report of *fusarium oxysporum* on lettuce in Europe. *Plant Dis.* 86, 1052. doi: 10.1094/PDIS.2002.86.9.1052B

Garibaldi, A., Gilardi, G., and Gullino, M. L. (2004a). Seed Transmission of Fusarium oxysporum f.sp. *lactucae*. *Phytoparasitica* 32, 61–65. doi: 10.1007/BF02980861

Garibaldi, A., Gilardi, G., and Gullino, M. L. (2004b). Varietal resistance of lettuce to Fusarium oxysporum f. sp. *lactucae*. *Crop Prot.* 23, 845–851. doi: 10.1016/j.cropro.2004.01.005

Gilardi, G., Franco Ortega, S., van Rijswick, P. C. J., Ortu, G., Gullino, M. L., and Garibaldi, A. (2017a). A new race of *Fusarium oxysporum* f. sp. *lactucae* of lettuce. *Plant Pathol.* 66, 677–688. doi: 10.1111/ppa.12616

Gilardi, G., Garibaldi, A., Matic, S., Senatore, M. T., Pipponzi, S., Prodi, A., et al. (2019). First Report of *Fusarium oxysporum* f. sp. *lactucae* Race 4 on Lettuce in Italy. *Plant Dis.* 103 (10), 2680. doi: 10.1094/PDIS-05-19-0902-PDN

Gilardi, G., Pons, C., Gard, B., Franco Ortega, S., and Gullino, M. L. (2017b). Presence of *Fusarium* Wilt, Incited by *Fusarium oxysporum* f.sp. lactucae, on Lettuce in France. *Plant Dis.* 101, 1053. doi: 10.1094/PDIS-12-16-1815-PDN

Gilardi, G., Vasileiadou, A., Garibaldi, A., and Gullino, M. L. (2021). Low temperatures favour *Fusarium* wilt development by race 4 of *Fusarium oxysporum* f. sp. *lactucae*. *J. Plant Path* 103, 973–979. doi: 10.1007/S42161-021-00859-5/TABLES/5

Gordon, T. R., and Koike, S. T. (2015). Management of *Fusarium* wilt of lettuce. *Crop Prot* 73, 45–49. doi: 10.1016/j.cropro.2015.01.011

Guerrero, M. M., Martínez, M. C., León, M., Armengol, J., and Monserrat, A. (2020). First Report of *Fusarium* Wilt of Lettuce Caused by *Fusarium oxysporum* f. sp. *lactucae* Race 1 in Spain. *Plant Dis.* 104, 1858–1858. doi: 10.1094/PDIS-10-19-2143-PDN

Gullino, M. L., Gilardi, G., and Garibaldi, A. (2021). Ready-to-eat salad crops: A plant pathogen's heaven. *Plant Dis.* 103 (9), 2153–2170. doi: 10.1094/PDIS-03-19-0472-FE

Herrero, M. L., Nagy, N. E., and Solheim, H. (2021). First Report of *Fusarium oxysporum* f. sp. *lactucae* Race 1 Causing *Fusarium* Wilt of Lettuce in Norway. *Plant Dis.* 105, 2239. doi: 10.1094/pdis-01-21-0134-pdn

Komada, H. (1975). Development of a selective medium for quantitative isolation of *Fusarium oxysporum* from natural soil. *Rev. Plant Prot. Res.* 8, 114–124.

Lin, Y. H., Lai, P. J., Chang, T. H., Wan, Y. L., Huang, J. W., Huang, J. H., et al. (2014). Genetic diversity and identification of race 3 of *Fusarium oxysporum* f. sp. *lactucae* in Taiwan. *Eur. J. Plant Pathol.* 140, 721–733. doi: 10.1007/s10658-014-0493-7

Matuo, T., and Motohashi, S. (1967). On *Fusarium oxysporum* f. sp. *lactucae* n. f. causing root rot of lettuce. *Trans. Mater. Res. Soc Jpn* 32, 13–15.

Mbofung, G. C. Y., and Pryor, B. M. (2010). A PCR-based assay for detection of *Fusarium oxysporum* f. sp. *lactucae* in lettuce seed. *Plant Dis.* 94, 860–866. doi: 10.1094/PDIS-94-7-0860

Okubara, P. A., Harrison, L. A., Gatch, E. W., Vandemark, G., Schroeder, K. L., and du Toit, L. J. (2013). Development and evaluation of a TaqMan real-time PCR assay for *Fusarium oxysporum* f. sp. *spinaciae*. *Plant Dis.* 97, 927–937. doi: 10.1094/PDIS-03-12-0317-RE

Pasquali, M., Dematheis, F., Gullino, M. L., and Garibaldi, A. (2007). Identification of race 1 of *Fusarium oxysporum* f. sp. *lactucae* on lettuce by inter-retrotransposon sequence-characterized amplified region technique. *Phytopathology* 97, 987–996. doi: 10.1094/PHYTO-97-8-0987

Sanna, M., Gilardi, G., Gullino, M. L., and Mezzalama, M. (2022). A fast approach to discard false negative susceptible lettuce genotypes to *Fusarium oxysporum* f.sp. *lactucae* race 1. *J. Phytopathol.* 170, 635–642. doi: 10.1111/JPH.13128

Scott, J. C., Gordon, T. R., Kirkpatrick, S. C., Koike, S. T., Matheron, M. E., Ochoa, O. E., et al. (2012). Crop rotation and genetic resistance reduce risk of damage from *Fusarium* wilt in lettuce. *Calif. Agric. (Berkeley)* 66, 20–24. doi: 10.3733/ca.v066n01p20

Scott, J. C., Gordon, T. R., Shaw, D. V., and Koike, S. T. (2009). Effect of Temperature on Severity of *Fusarium* Wilt of Lettuce Caused by *Fusarium oxysporum* f. sp. *lactucae*. *Plant Dis.* 94, 13–17. doi: 10.1094/PDIS-94-1-0013

Scott, J. C., Mcroberts, D. N., and Gordon, T. R. (2014). Colonization of lettuce cultivars and rotation crops by *Fusarium oxysporum* f. sp. *lactucae*, the cause of *Fusarium* wilt of lettuce. *Plant Pathol.* 63, 548–553. doi: 10.1111/ppa.12135

Smith, S. N., and Snyder, W. C. (1971). Relationship of inoculum density and soil types to severity of *fusarium* wilt of sweet potato. *Phytopathology* 61, 1049–1051. doi: 10.1094/Phyto-61-1049

Taylor, A., Jackson, A. C., and Clarkson, J. P. (2019). First Report of *Fusarium oxysporum* f. sp. *lactucae* Race 4 Causing Lettuce Wilt in England and Ireland. *Plant Dis.* 103 (5), 1033. doi: 10.1094/PDIS-10-18-1858-PDN

Tziros, G. T., and Karaoglanidis, G. S. (2023). Identification of *Fusarium oxysporum* f. sp. *lactucae* Race 1 as the Causal Agent of Lettuce *Fusarium* Wilt in Greece, Commercial Cultivars' Susceptibility, and Temporal Expression of Defense-Related Genes. *Microorganisms* 11, 1082. doi: 10.3390/MICROORGANISMS11041082

van Amsterdam, S., Jenkins, S., and Clarkson, J. (2023). First report of *Fusarium oxysporum* f. sp. *lactucae* Race 1 causing lettuce wilt in Northern Ireland. *Plant Dis.* 107 (8), 2524. doi: 10.1094/PDIS-01-23-0196-PDN

Van Poucke, K., Haegeman, A., Goedefroit, T., Focquet, F., Leus, L., Jung, M. H., et al. (2021). Unravelling hybridization in *Phytophthora* using phylogenomics and genome size estimation. *IMA Fungus* 12 (1), 16. doi: 10.1186/s43008-021-00068-w

Veresoglou, S. D., Barto, E. K., Menexes, G., and Rillig, M. C. (2013). Fertilization affects severity of disease caused by fungal plant pathogens. *Plant Pathol.* 62, 961–969. doi: 10.1111/ppa.12014

frontiers | Frontiers in Microbiology

TYPE Original Research
PUBLISHED 01 December 2023
DOI 10.3389/fmicb.2023.1257437

OPEN ACCESS

EDITED BY
Mahyar Mirmajlessi,
Ghent University, Belgium

REVIEWED BY
Abhijeet Shankar Kashyap,
National Bureau of Agriculturally Important Microorganisms (ICAR), India
Jihua Wang,
Guangdong Academy of Agricultural Sciences, China

*CORRESPONDENCE
Tijiang Shan
✉ tjshan@scau.edu.cn
Ping Ding
✉ dingping@gzucm.edu.cn

RECEIVED 12 July 2023
ACCEPTED 25 October 2023
PUBLISHED 01 December 2023

CITATION
Chen Z, Han P, Che X, Luo Z, Chen Z, Chen J, Shan T and Ding P (2023) Biocontrol fungi induced stem-base rot disease resistance of *Morinda officinalis* How revealed by transcriptome analysis.
Front. Microbiol. 14:1257437.
doi: 10.3389/fmicb.2023.1257437

Biocontrol fungi induced stem-base rot disease resistance of *Morinda officinalis* How revealed by transcriptome analysis

Zien Chen[1], Panpan Han[1], Xiaoying Che[1], Zhenhua Luo[1], Zeyu Chen[1], Jinfang Chen[1], Tijiang Shan[2]* and Ping Ding[1]*

[1]College of Traditional Chinese Medicine, Guangzhou University of Chinese Medicine, Guangzhou, China, [2]College of Forestry and Landscape Architecture, South China Agricultural University, Guangzhou, China

Introduction: *Morinda officinalis* How (MO) is a Rubiaceae plant, and its medicinal part is dried root, which is one of the "Four Southern Medicines" in China. At present, the plant MO breed seedlings mainly by cutting methods. Long-term asexual propagation makes pathogenic fungi accumulate in MO, leading to stem-base rot, which is caused by *Fusarium oxysporum* (Fon).

Methods: In this study, we used *Trichoderma harzianum* and *Pestalotiopsis* sp. as biocontrol fungi to investigate their antagonistic ability to Fon through in vitro antagonism and pot experiments, and combined with transcriptome sequencing to explore the mechanism of biocontrol.

Results: The results showed that both *Trichoderma harzianum* and *Pestalotiopsis* sp. could inhibit the growth of Fon. In addition, *Trichoderma harzianum* and *Pestalotiopsis* sp. could also enhance the basic immunity to Fon by increasing the activities of defensive enzymes such as POD and SOD, chlorophyll content, soluble sugar content, and oligosaccharide content of MO. The mechanism of biological control of stem-base rot of MO was discussed by transcriptome technology. MO was treated with two treatments, root irrigation with biocontrol fungi or inoculation with Fon after root irrigation with biocontrol fungi. Transcriptome sequencing revealed that nearly 11,188 differentially expressed genes (DEGs) were involved in the process of inducing MO systemic resistance to Fon by biocontrol fungi. Meanwhile, Gene Ontology (GO) classification and Kyoto Encyclopedia of Genes and Genomes (KEGG) pathway enrichment, as well as transcription factor (TFs) prediction showed that there were significant differences in the expression levels of MO roots under different treatments. Also, the genes of the "MAPK signaling pathway" and "plant hormone signaling pathway" were analyzed, in which the ERFs gene of the ethylene signal transduction pathway participated in the metabolism of glycosyl compounds. It is speculated that the ethylene signal may participate in the immune response of the sugar signal to the infection of Fon. After qRT-PCR verification of 10 DEGs related to the ethylene signal transduction pathway, the expression trend is consistent with the results of transcriptome sequencing, which proves the reliability of transcriptome sequencing.

Discussion: In conclusion, this study preliminarily identified the molecular mechanism of the biological control of MO stem-base rot and provided a scientific basis for further research on the prevention and control mechanism of MO stem-base rot.

KEYWORDS

***Morinda officinalis* How, stem-base rot disease, *Fusarium oxysporum*, biological control, induced resistance, transcriptome analysis**

1 Introduction

Morinda officinalis How (MO) is a plant of the Rubiaceae family, with the medicinal part of dried root, which has the effects of tonifying kidney yang, strengthening bones and muscles, and expelling wind and dampness (National Pharmacopoeia Committee, 2020). It is one of the famous "Four Southern Herbal Medicines" in China. MO is mainly produced in Guangdong, Fujian, Guangxi, Hainan, and other provinces in China, among which Deqing County of Guangdong is an authentic producing area (Cai et al., 2021). According to morphology, MO can be divided into large leaf species, middle leaf species, small leaf species, and wild species, etc. (Zhang et al., 2016). From the previous study of our research group, it was found that the small leaf species MO had stronger resistance to stem-base rot. At present, MO seedlings are mainly propagated by cutting, and long-term asexual propagation leads to the accumulation of pathogenic fungi. And MO is a perennial plant, with the extension of planting years, stem-base rot often occurs. MO stem-base rot is also known as MO *Fusarium* wilt, and the pathogenic fungus is *Fusarium oxysporum* (Fon) (Orr and Nelson, 2018). The disease is commonly seen in wheat, corn, and other crops, and a few in medicinal plants such as atractylodes and codonopsis (Jevtić et al., 2019; Qi et al., 2021; Shen et al., 2021; Wang et al., 2022). The symptoms of the disease first appeared in the stem base. In the early stage, the cortex of the stem base showed reddish-brown spots, which expanded into severe disease spots in the late stage, showing water stains. Subsequently, the vascular bundle became violet-brown, and the cortex of the stem base began to rot and deteriorate, with white mycelium visible (McNally et al., 2018; Castillo et al., 2022). The disease can cause serious quality damage and yield loss during MO production. Therefore, it is valuable and urgent to find effective and environmentally friendly methods to reduce the damage caused by Fon to MO production.

Biological control mainly uses antagonistic fungi, bacteria, actinomyces, and other antagonistic bacteria as well as plant-derived active substances, biocontrol microorganisms, or mixed with organic fertilizers. Because of its environment-friendly characteristics, it has a good application prospect in agriculture (Sharma, 2023). The biological control of stem-base rot is mainly through the antagonism of some microorganisms to induce systemic disease resistance in plants (Zhou et al., 2021). At present, more antagonistic microorganisms have been studied, including *Streptomyces*, *Bacillus*, and *Trichoderma harzianum* (Dor et al., 2007). *Trichoderma harzianum* is a common biological control fungus, which can inhibit the growth of pathogenic fungi through heavy parasitism and its active components also have antagonistic effects, even better than chemical reagents (Yassin et al., 2021). In addition, Kumar et al. (2021) found that *Trichoderma* sp. can activate antioxidant mechanisms in plants, such as peroxidase, polyphenol oxidase, superoxide dismutase, catalase, and ascorbic acid. Moreover, the potential ability of *Trichoderma* sp. as a biocontrol agent against various plant diseases has also been studied (Asad, 2022). In addition to the biocontrol fungi listed above, many other species can be used as biocontrol agents to control stem-base rot. Most species of *Pestalotiopsis* sp. have been studied as plant pathogenic fungi for more than a century, until the 1990s, when endophytic *Pestalotiopsis* sp. was first reported (Steyaert, 1953; Mordue, 1985; Strobel et al., 1997; Photita et al., 2001). However, whether endophytic *Pestalotiopsis* sp. can antagonize the pathogen has not been reported, and it can be further studied.

The effects of biocontrol fungi on pathogens are usually multiple inhibition mechanisms, which are coordinated and integrated to achieve the purpose. Biocontrol fungi can be divided into two mechanisms, including direct inhibition mechanism and indirect inhibition mechanism. The direct mechanism can be divided into hyperparasitism, competition, antagonism, and lysis, the indirect mechanisms include induction and growth promotion. In the common microecological environment, biocontrol fungi compete with pathogens for limited space and nutrition resources through rapid propagation and growth, which is called competition. Sa et al. (2021) found that *Bacillus subtilis* N6-34 could colonize rhizosphere soil and poplar plants and inhibit the growth of pathogens. In addition, biocontrol fungi directly or indirectly inhibit the growth of pathogens by secreting metabolites and antibacterial substances. Swain et al. (2008) studied the interaction between *Bacillus subtilis* CM1 and CM3 and Fon by scanning electron microscopy and found that the chitin and β-1, 3-glucanase produced by CM1 and CM3 distorted the mycelium of Fon. The important defense mechanisms of plant resistance mediated by microorganisms include systemic acquired resistance (SAR) and induced systemic resistance (ISR) (Narware et al., 2023). Many effective biocontrol fungi can induce ISR, and some related research results have been reported in recent years. For example, the *Pseudomonas fluorescen*t WCS417r-mediated ISR antagonize various plant pathogens in Arabidopsis by activating the JA signaling pathway (Pieterse et al., 1998). Recent studies have shown that ISR is also one of the important mechanisms of biological control of Fon. According to the report, *Trichoderma gamsii* can induce ISR against Fon by different pathways (Stefania et al., 2020). Therefore, further analysis of ISR induced by biocontrol fungi is of great significance for the biological control of stem-base rot.

At present, chemical control is mainly used to control stem-base rot in MO, which can easily cause environmental pollution. In this study, we identified two efficient biocontrol fungi *Trichoderma harzianum* and *Pestalotiopsis* sp. which can be used for Fon control in MO. The results showed that biocontrol fungi could inhibit the growth of Fon *in vitro*. In addition, biocontrol fungi can enhance the immunity of plants to Fon by raising the activity of defensive enzymes, the content of chlorophyll, and the content of soluble sugar, and also affect the content of MO oligosaccharide. To explore the control mechanism of biocontrol fungi, transcriptome sequencing was used for analysis. A total of 921,532 unigenes were identified in MO, and transcriptome analysis showed that there were more than 10,000 DEGs in biocontrol fungi against Fon. These genes were annotated and enriched for GO functions and KEGG pathways, as well as predicted TFs, and validated using real-time PCR (qRT-PCR). The results showed that the expression levels of MO roots were significantly different after different biocontrol fungi treatments. We also analyzed the MAPK signaling pathway and plant hormone signaling pathway and related genes involved in the control process. In conclusion, this study aims to understand the mechanism of systemic resistance of MO to Fon induced by biocontrol fungi from the molecular level, providing a scientific basis for further analysis of the biocontrol mechanism.

2 Materials and methods

2.1 Plant material, fungi, and growth condition

Morinda officinalis used in this experiment came from Deqing County, Guangdong, China, and was detoxified by tissue culture. When the tissue culture seedlings were rooted and transplanted into sterile nutrient soil for 6 months.

Fusarium oxysporum (ON454550) and *Trichoderma harzianum* (ON454551) were isolated from the root of *Morinda officinalis* and identified and preserved by our research group. And a strain of *Pestalotiopsis* sp. (OR608750)with antibacterial activity proposed by the College of Forestry and Landscape Architecture, South China Agricultural University. The pathogens and biocontrol fungi were cultured on potato dextrose agar (PDA) medium at 25°C under dark conditions for 5 days. The microconidia suspension of the pathogens and biocontrol fungi used in greenhouse experiments was prepared as described by Sabry et al. (2022).

2.2 Effects of biocontrol fungi on fungal antagonism and hyphal growth

To evaluate the biocontrol potential of *Trichoderma harzianum* and *Pestalotiopsis* sp., we evaluated the effect of fungal antagonism and hyphal growth. For the fungal antagonism, we used the flat antagonism experiment on the PDA medium *in vitro*. The six-millimeter plugs from 5-day-old cultures of the pathogens and biocontrol fungi were inoculated on both ends of the PDA culture medium plate, and the distance between biocontrol fungi and pathogens was 5 cm. After incubation at 28°C for 7 days, the colonies' diameters of pathogens were determined. The experiment was repeated three times with only pathogenic bacteria inoculated as control. The inhibition rate was calculated according to the following formula: inhibition rate (%) = [(colonies' diameter of the control group–colonies' diameter of treatment group)/colonies' diameter of control group] × 100% (Zhang et al., 2021).

The effect of biocontrol fungi on the hyphal growth of pathogens was detected according to the method of Kong et al. (2022) with minor modifications. Spreading a 1 mm thick PDA culture medium on a sterile glass slide, the six-millimeter plugs from 5-day-old cultures of the pathogens and biocontrol fungi were inoculated on both ends of the glass slide, 2 cm apart. Each treatment was repeated 3 times, cultured at 28°C for 24 ~ 36 h, observed by a microscope (Olympus Microscope BX43F), and photographed after biocontrol fungi contacted with Fon hyphae.

2.3 Experimental design in greenhouse

To evaluate the biocontrol effect of biocontrol fungi on MO stem-base rot, a greenhouse experiment was carried out in this study. Six months after transplanting tissue culture seedlings of MO into sterile nutrient tanks, plants were treated with 100 mL single biocontrol fungus or combined biocontrol fungi (1×10^6 conidia /ml, T, P, TP), and sterile water was used as a mock control (NF). After 24 h, each treated plant was inoculated with 100 mL Fon spore suspension (1×10^6 conidia/ml, FT, FP, FTP), and Fon alone was used as a control (F). Disease index (DI) was recorded and photographed 30 days after inoculation, and the roots of MO were harvested for RNA sequencing and determination of oligosaccharide content. In addition, the leaves of MO at different time points were harvested for the determination of physiological and biochemical indexes.

2.4 Determination of physiological and biochemical indexes and oligosaccharide content

At harvest, we analyzed the activity of plant defense-related enzymes (SOD and POD), chlorophyll content, and soluble sugars during the process of biocontrol fungi triggering ISR to stem-base rot in MO. The above physiological and biochemical indicators were determined by using the corresponding detection kit, namely "The SOD detection kit" and "The POD detection kit" (Nanjing Jiancheng Biological Engineering Institute, Nanjing, China), "The Chlorophyll content test kit" (Leagene, Beijing, China) and "The Soluble sugar content detection kit" (Solarbio, Beijing, China) according to the manufacturer's instructions. The oligosaccharide content was determined according to the method of Liu et al. (2022).

2.5 RNA extraction, library construction, and RNA sequencing

Total RNA was extracted by Total RNA Extractor (Trizol) (Sangon Biotech, Shanghai, China) according to the manufacturer's instructions. The concentration of RNA was measured by Qubit2.0 (Thermo Fisher Scientific, United States), and the integrity of RNA and genomic contamination were detected by agarose gel.

A total of 24 samples were used for library construction in this study. Of these, 12 samples were obtained from MO treated with *Trichoderma harzianum* or *Pestalotiopsis* sp. alone (T, P), *Trichoderma harzianum* mixed with *Pestalotiopsis* sp. (TP), and sterile water treatment (NF). The other 12 samples were pretreated with the above biocontrol fungi for 24 h and then challenged with Fon (FT, FP, FTP, F). All samples were taken from at least 5 MO roots and stored in a −80°C refrigerator. The total RNA of each sample was isolated by the above method.

The library was constructed using the qualified total RNA above. The first-strand cDNA was synthesized by the 1st Strand Synthesis Reaction Buffer (Sangon Biotech, Shanghai, China), and the second cDNA strand was synthesized immediately after the reaction. After the terminal was repaired and the sequencing joint was connected, the junction product was purified and fragment size was sorted by magnetic beads. Finally, PCR amplification was performed with 2 × Super Canace™ High-Fidelity Mix and Primer mix reagent (YEASEN, Shanghai, China). Library amplification products were purified using Hieff NGS™ DNA Selection Beads (0.9×, Beads: DNA = 1:1) (YEASEN, Shanghai, China). The library was detected by agarose gel electrophoresis, and the recovered DNA was accurately quantified by a Qubit DNA detection kit (YEASEN, Shanghai, China). Illumina sequencing was carried out in the Shanghai Sangon Biotech, China, and performed using the Illumina MiSeq™ platform according to the manufacturer's instructions (Illumina, United States).

2.6 *De novo* assembly, functional annotation, and differentially expressed genes analysis

The raw image data files obtained from Illumina Miseq™ were converted into raw sequenced reads by CASAVA Base Calling analysis, which contained the sequence information of the reads and the corresponding sequencing quality information. The raw data quality values and other information were counted, and the sequencing data quality of the samples was evaluated visually by using FastQC. Raw data from sequencing, which contains low-quality sequences with junctions. To ensure the quality of information analysis, the raw data must be filtered to obtain clean data. In this study, clean data *de novo* was assembled into transcripts using Trinity, and sequencing data were assembled into transcripts through three steps: Inchworm, Chrysalis, and Butterfly.

The transcript obtained by Trinity assembly was deredundant, and the longest transcript in each transcript cluster was taken as Unigene, which was used as the reference sequence for subsequent analysis. The Unigene was compared with CDD, KOG, COG, NR, NT, PFAM, and GO databases using Blast alignment software, and the KEGG database was compared using KAAS alignment software to obtain the annotation information of Unigene.

All Unigene was compared with the reference sequence, and the comparison results were calculated by RSeQC. Then, according to the comparison results and the annotation file of the reference genome, the read count data was standardized by TMM, and then the difference analysis was conducted by DEGseq. In order to get a significant difference of gene will filter is set to: qValue <0.05, and the difference between multiples | FoldChange | > 2. Then all DEGs were subjected to GO and KEGG functional enrichment analysis, and when the corrected *p*-value (Qvalue) < 0.05, the function was considered to be significantly enriched. In addition, to identify all transcription factors (TFs) in the root of MO, all Unigene was compared to the plant transcription factor database for TFs prediction.

2.7 Validation of DEGs by qRT-PCR

To confirm the transcriptome data, 10 DEGs related to the ethylene signaling pathway were randomly selected and verified (Supplementary Table S1). The total RNA of the sample was reverse transcribed using the Color Reverse Transcription Kit (with gDNA Remover) (EZBioscience, Beijing, China). qRT-PCR was conducted on Qtower3 Real-Time PCR Instrument (Jena, Germany) by using the 2 × Color SYBR qPCR Master Mix (ROX2 puls) (EZBioscience, Beijing, China). The reaction was performed under the following conditions: 95°C for 8 min, followed by 40 cycles of 95°C for 10 s, and 60°C for 30 s. The actin gene of MO was employed as the internal standard. All the gene information and PCR primers used in our study are shown in Supplementary Table S1.

2.8 Statistical analysis

All bioassays and experiments were performed three times with 5 seedlings treated each time. Significant differences between means were compared using the LSD test (Fisher's protected most significant difference test) at $P \geqq 0.05$. *p*-value < 0.05 was considered statistically significant. All data were analyzed by analysis of variance using SPSS 20.0 (SPSS Inc., Chicago, IL).

3 Results

3.1 Antagonistic effect of biocontrol fungi *in vitro*

Through antagonistic experiments, the results showed that *Trichoderma harzianum* and *Pestalotiopsis* sp. have antagonistic activity against Fon *in vitro* (Figure 1A). The inhibition rate of *Trichoderma harzianum* against Fon was 58.30% ($p = 0.000$), and the inhibition rate of *Pestalotiopsis* sp. against Fon was 33.81% ($p = 0.000$) (Supplementary Table S2). Through microscope observation, it was found that in the process of antagonizing Fon, the biocontrol fungi first recognized Fon, then parasitically parasitized on Fon mycelia by way of entanglement or attachment, and finally penetrated and dissolved Fon mycelia (Figure 1B).

3.2 Effect of biocontrol fungi in greenhouse experiment

Based on the above results, we found that *Trichoderma harzianum* and *Pestalotiopsis* sp. have the potential to control MO stem base rot. To test this hypothesis, we conducted a greenhouse experiment. After 30 days of inoculation with Fon, the disease symptoms of the control group were obvious, while the stem-base rot symptoms of MO treated with biocontrol fungi were significantly reduced. Among them, the combined treatment of *Trichoderma harzianum* and *Pestalotiopsis* sp. had the most obvious effect, with a control effect of 46.67% ($p = 0.000$), while the control effect of biocontrol fungus alone was 36.36% ($p = 0.010$) (Figure 2A; Supplementary Table S3). In addition, we also found that the degree of vascular browning after biocontrol fungi treatment was significantly lower than that in the control group, indicating that biocontrol fungi could effectively delay the infection process of Fon (Figure 2B).

3.3 Determination of physiological and biochemical indexes and oligosaccharide content

The SOD activity and POD activity after each biocontrol treatment were significantly higher than that of the control group and showed a trend of first increasing and then decreasing as time went by (Figures 3A,B). These results indicated that the disease resistance of Mo was enhanced by using biocontrol fungi. The chlorophyll content of MO after biocontrol treatment was higher than that of the control group, but lower than that of the normal group (Figure 3C). With the change of time, except for *the Trichoderma harzianum* treatment group, the total chlorophyll content of other biocontrol fungi treatments had little change, while the total chlorophyll content of *the Trichoderma harzianum* treatment group would increase as time went by. The soluble sugar content of the biocontrol treatment was higher than that of the control group and showed a trend of increasing first and then decreasing as time went by Figure 3D. Compared with the normal group, the oligosaccharide content in the control group increased.

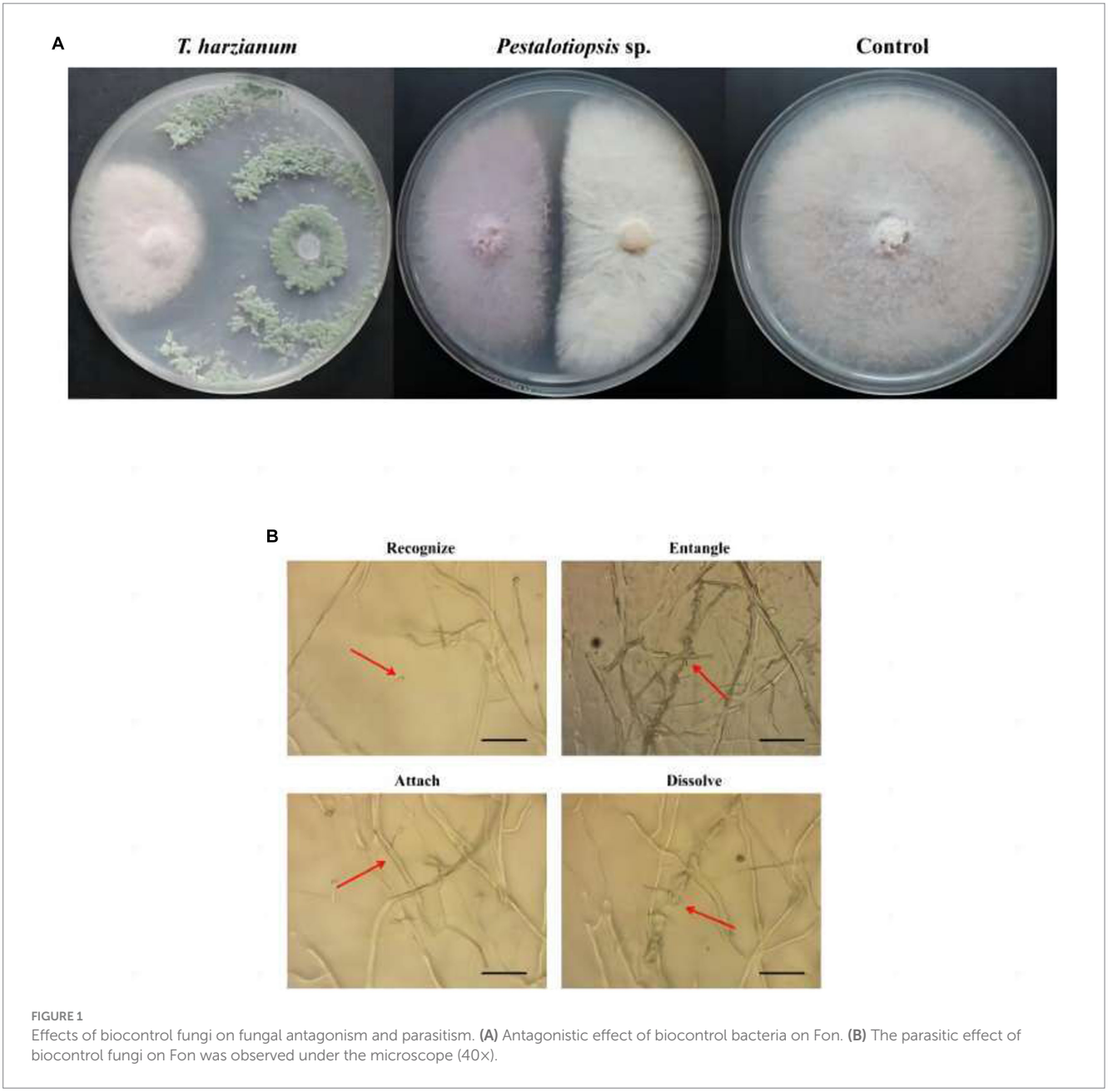

FIGURE 1
Effects of biocontrol fungi on fungal antagonism and parasitism. **(A)** Antagonistic effect of biocontrol bacteria on Fon. **(B)** The parasitic effect of biocontrol fungi on Fon was observed under the microscope (40×).

Compared with the control group, the contents of 1-ketose and nystose in each biocontrol treatment group were decreased, while the contents of fructose and glucose were increased, which was consistent with the results of soluble sugar content (Supplementary Table S4).

3.4 Transcriptome sequence and assembly

The quality and concentration of all RNA samples were tested by Qubit2.0. The RNA quality of all samples was high, with an OD value above 2.0. The samples with unqualified concentration and quality were re-extracted to ensure that all samples met the requirements of the transcriptome sequencing library.

A total of 583,671 million raw reads were obtained by high-throughput sequencing, and filtering of the raw data resulted in 522,375 million clean reads, representing 90% of the raw reads. The Q20 bases ranged from 97.79 to 98.46%, Q30 ranged from 92.82 to 94.68, and the GC amount ranged from 46.36 to 57.52%, indicating that the sequencing accuracy is high and can meet the requirements of subsequent analysis (Supplementary Table S5). The 1,390,679 transcripts obtained from the trinity assembly yielded 921,532 unigenes with an average length of 461.48 bp and N50 of 547 bp, and the length distribution of these unigenes is shown in Figures 4A,B. The longest transcript in each transcript cluster was used as the reference sequence for subsequent analyses. From the principal component analysis (PCA) it can be seen that the distribution of the samples in each group is more clustered, indicating that there is less variation within the samples, whereas analyzing the variation between groups shows that the control group is more dispersed from the rest of the component samples with significant differences (Figure 4C).

The similarity of Unigenes sequences was compared with seven public databases (CDD, KOG, COG, NR, NT, PFAM, and

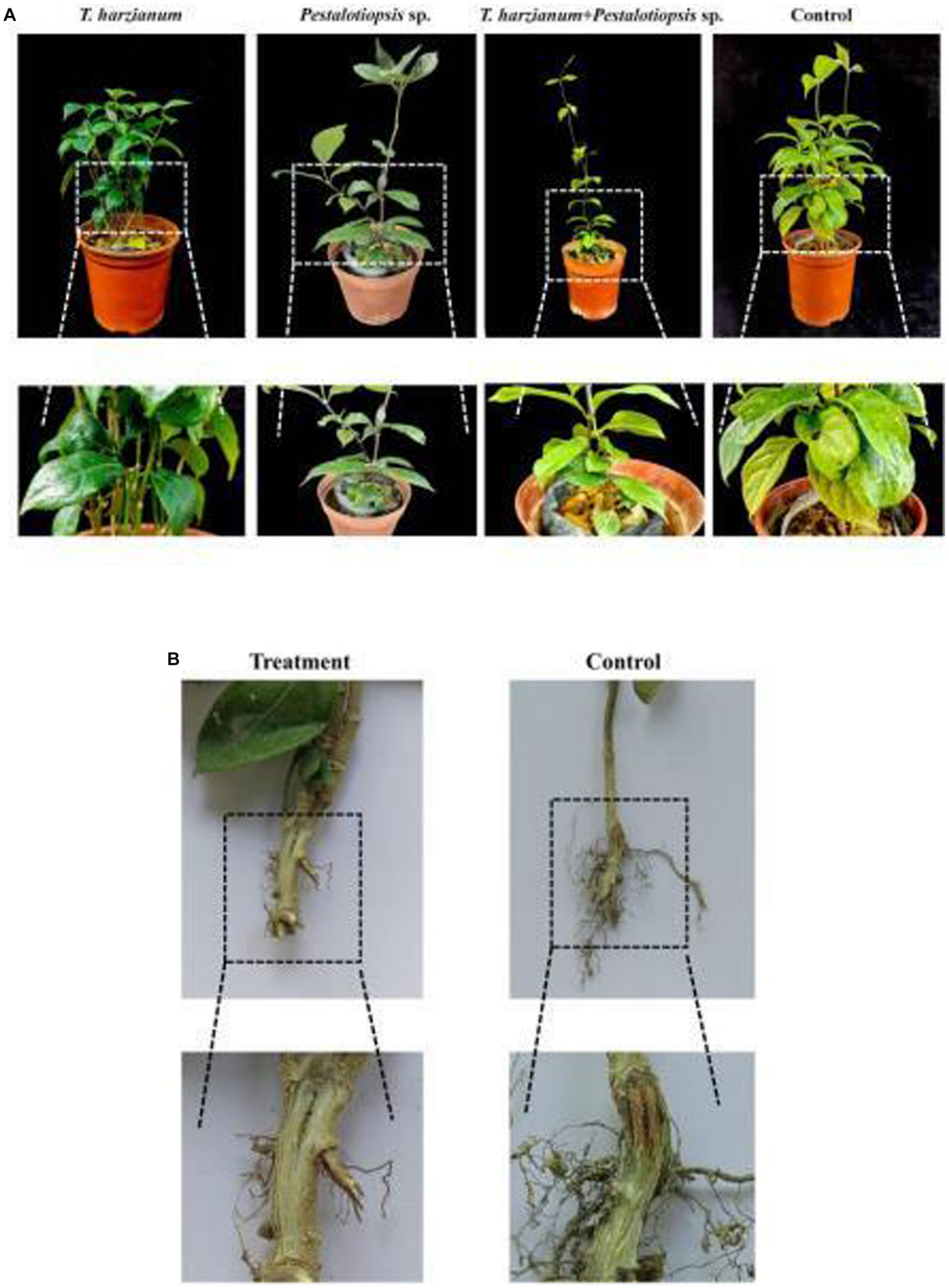

FIGURE 2
Greenhouse experiment with different bacterial treatments. **(A)** Symptoms of stem-base rot in different treatments of MO plants 30d after inoculation with Fon in a greenhouse experiment. **(B)** Degree of vascular browning in the base-stem of MO after biocontrol fungi treatment.

GO) using blast (E-value≤10^{-5}). The unigenes sequences were aligned to the KEGG database using the KAAS software. A total of 921,532 Unigenes were obtained annotated, of these, 176,943 (19.2%) were annotated to the CDD database, 204,656 (22.21%) were annotated to the PFAM database, 191,958 (20.83%) were annotated to the KEGG database, 228,126 (24.76%) were annotated to the KOG database, 268,497 (29.14%) were annotated to the GO database, 417,346 (45.29%) were annotated to the NR

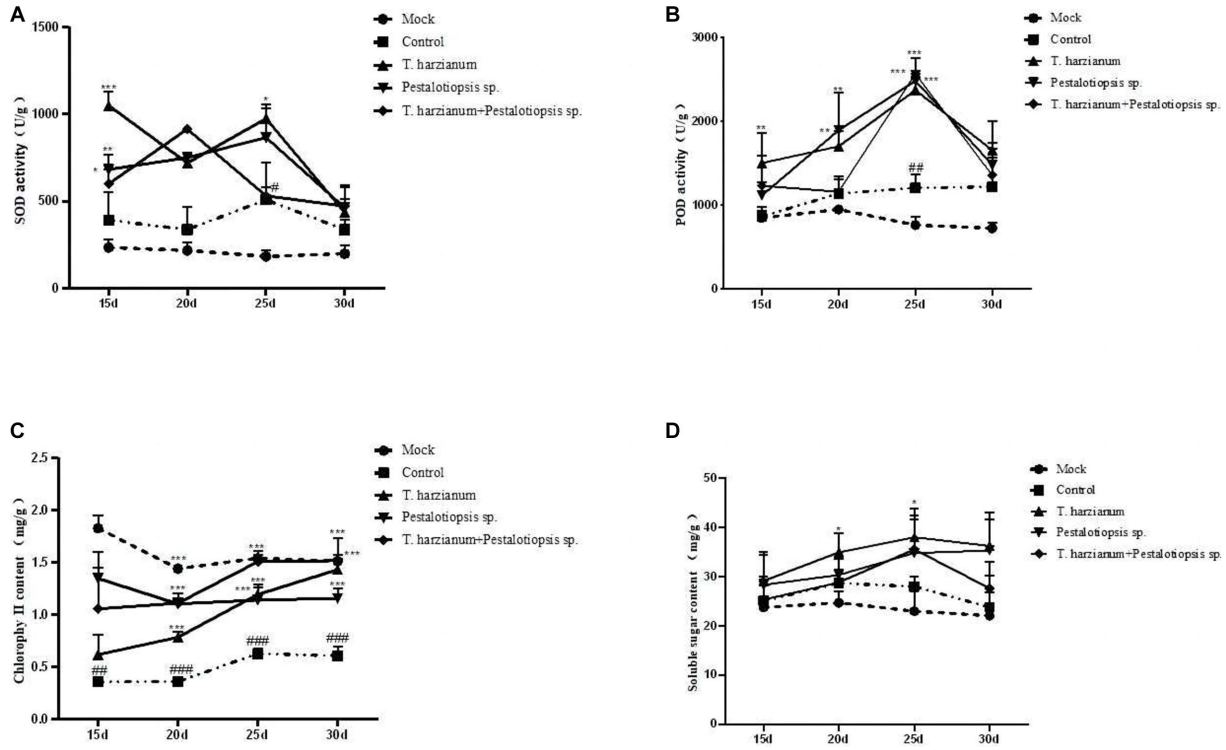

FIGURE 3
Effects of biocontrol fungi on physiological and biochemical indexes of MO which was pretreated with biocontrol fungi and challenged with Fon. **(A,B)** The activities of defense-related enzymes (SOD and POD) in the leaves of MO. **(C)** The content of chlorophyll in the leaves of MO. **(D)** The content of soluble sugar in the leaves of MO.

database, 47,654 (5.17%) were annotated in the NT database (Supplementary Table S6).

3.5 DEGs analysis and functional annotation of different biocontrol fungi treatments

Based on the above sequencing data, two control groups were established to study the control mechanism of different biocontrol bacteria on stem-base rot of MO. In one group, only treated with biocontrol fungi and compared with the sample treated with sterile water. The other group was inoculated with the pathogen Fon after being pretreated with biocontrol fungi for 24 h and compared with the sample inoculated with Fon after sterile water treatment. It was observed that the expression levels of a large number of genes in the root of MO were changed whether the biocontrol fungi were treated alone or pretreated before inoculation with pathogenic bacteria (Figures 5A,B). According to the qValue <0.05 multiples and differences | FoldChange | > 2 conditions of screening DEGs analysis, according to the results by the Figures 5C–H, in the group of only treated with biocontrol fungi, 715 DEGs (65 up-regulated genes, 650 down-regulated genes) were detected in the *Trichoderma harzianum* treatment group, 619 DEGs (552 up-regulated genes, 67 down-regulated genes) were detected in the *Pestalotiopsis* sp. treatment group, and 105 DEGs (24 up-regulated genes, 81 genes downregulated) were detected in the co-treatment group with *Trichoderma harzianum* and *Pestalotiopsis* sp. In the samples pretreated with biocontrol bacteria, 2,332 DEGs (1,509 up-regulated genes, 823 down-regulated genes) were detected in the *Trichoderma harziamum* group, and 4,745 DEGs (3,822 up-regulated genes, 923 down-regulated genes) were detected in the *Pestalotiopsis* sp. group. A total of 2,672 DEGs (1960 up-regulated genes, 712 down-regulated genes) were detected in the co-treatment group of *Trichoderma harzianum* and *Pestalotiopsis* sp.

The selected DEGs were compared with the GO database for functional annotation. The GO database was divided into 3 categories, including "biological process," "cellular component" and "molecular function," which were further divided into 68 sub-categories. The results showed that compared with mock treatment or Fon inoculation alone, the most DEGs were annotated to the "cellular process," "metabolic process" and "cell component organization or biogenesis" in the category of "biological process" in the libraries constructed from MO treated with biocontrol fungi alone or pretreated with biocontrol fungi and then inoculated with Fon. In the category of "cell component," the number of DEGs annotated as "cell components," "cells" and "organelles" was the most, while the number of DEGs annotated as "binding" and "catalytic activity" in the category of "molecular functions" was the most (Supplementary Figure S1). These results indicate that the physiological and biochemical functions of MO can be changed by biocontrol bacteria in the process of stem-base rot control.

The selected DEGs were compared with the KEGG database to analyze the metabolic pathways in MO. According to the results (Supplementary Figure S2), KEGG pathways are divided into five categories, namely "cell process," "environmental information processing," "genetic information processing," "metabolic pathway"

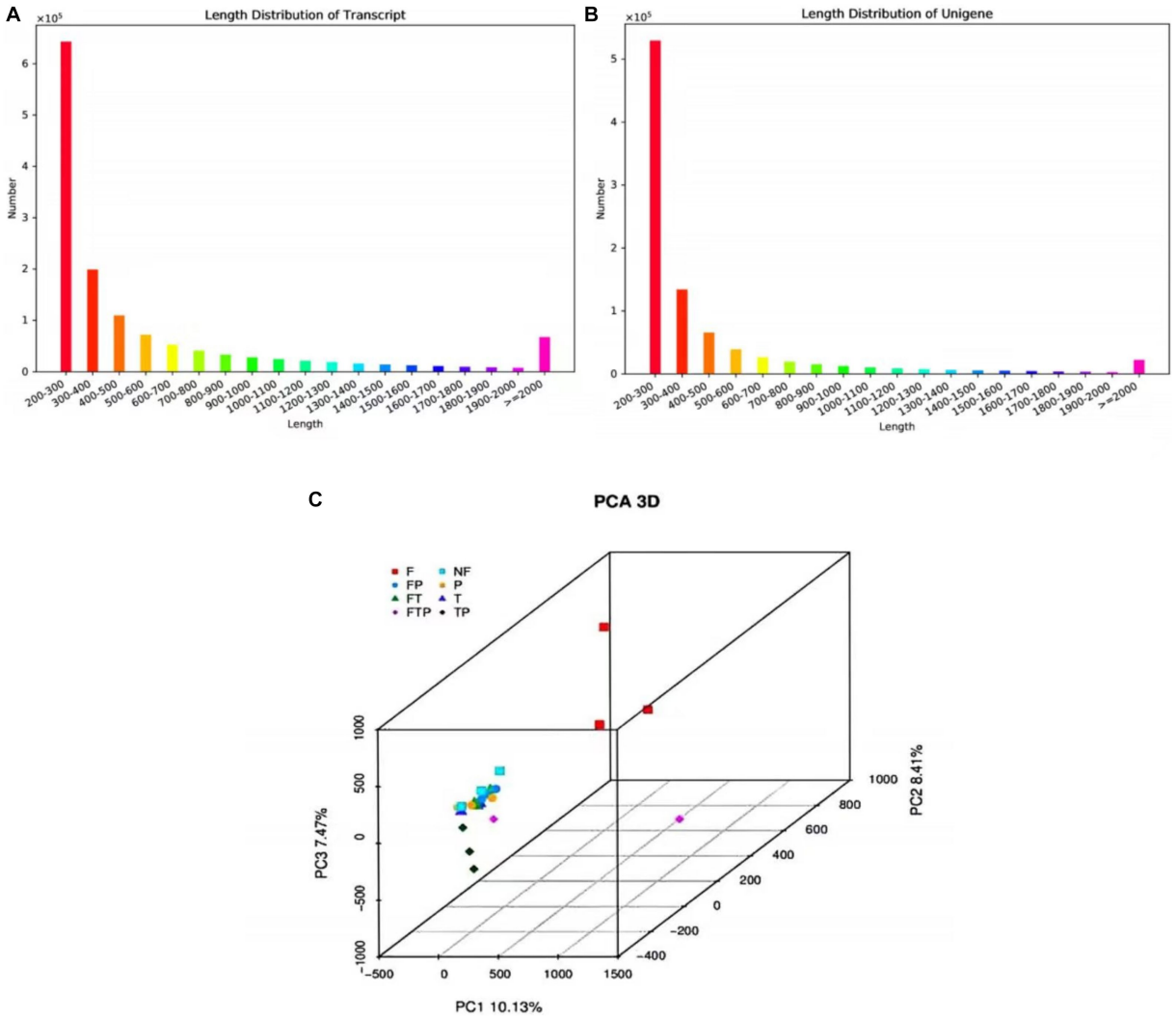

FIGURE 4
The sequence length distribution plot and principal component analysis. **(A)** Transcript sequence length cumulative distribution. **(B)** Unigene sequence length cumulative distribution. The horizontal axis is the length interval, and the vertical axis is the number of sequences in the interval. **(C)** Principal component analysis.

and "organic system." The five categories could be further divided into 33 sub-categories, which were mainly annotated in the "transport and catabolism," "signal transduction," "translation," "folding and explanation," "carbohydrate metabolism," and "energy metabolism" pathway. The above analysis of the KEGG metabolic pathway may lay a foundation for the study of the biological control mechanism of MO stem-base rot.

3.6 GO function and pathway enrichment analysis for DEGs

GO functional enrichment analysis of DEGs in the group treated with biocontrol fungi alone showed that the functions of DEGs enriched by different biocontrol treatments were also different (Supplementary Figure S3). When treated with *Trichoderma harzianum* alone, DEGs were obviously enriched in the "oxidation reduction process," "antibiotic metabolism process" and "cell response to oxidative stress." When treated with *Pestalotiopsis* sp. alone, DEGs were significantly enriched in the "endoplasmic reticulum subcompartment," "epigenuclear membrane-endoplasmic reticulum network," and "cytoplasmic stress granules." After *Trichoderma harzianum* and *Pestalotiopsis* sp. were treated together, only the "mitochondrial respiratory chain supercomplex" function of cell group classification was significantly enriched in DEGs, which may be related to the low amount of DEGs in this treatment.

GO function enrichment analysis of DEGs in the biocontrol pretreatment group showed that DEGs after biocontrol pretreatment was significantly enriched in different functions (Figure 6). After pretreatment by *Trichoderma harzianum*, DEGs were significantly enriched in the "multicellular biological process," "multicellular biological development," "multicellular biological reproduction process," "cytoplasmic ribosome," "ribosome" and "molecular structural activity." After pretreatment by *Pestalotiopsis* sp., DEGs were significantly enriched in "polysaccharide catabolic process," "reaction to acidic chemicals," "reaction to inorganic substances," "extracellular

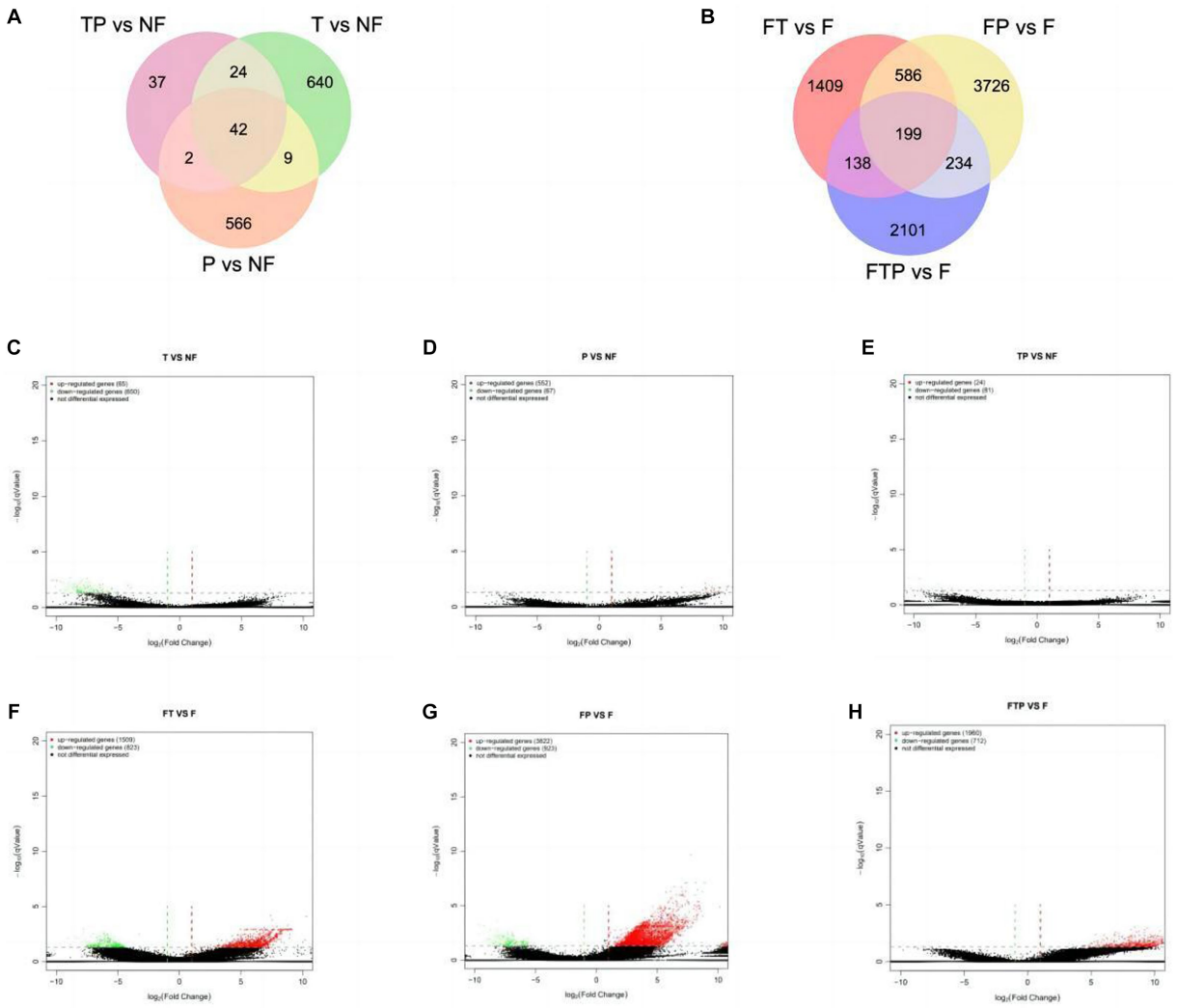

FIGURE 5
Classification of differentially expressed genes (DEGS) in the root of MO in response to different biocontrol fungi treatment or in combination with Fon inoculation. **(A)** Venn diagram of DEGs identified in the root of MO treated with biocontrol fungi alone. **(B)** Venn diagram of DEGs identified in the root of MO pretreated with biocontrol fungi and challenged with Fon. **(C–E)** Volcanic map of DEGs identified in the root of MO treated with biocontrol fungi alone. **(F–H)** Volcanic map of DEGs identified in the root of MO pretreated with biocontrol fungi and challenged with Fon. The horizontal axis is the fold-change (log (B/A)) value of gene expression difference between different groups, and the vertical axis is the pValue of the statistical significance of gene expression change. The smaller the pValue and the larger the –log (pValue), the more significant the difference. Red indicates up-regulated genes, green indicates down-regulated genes, and black indicates non-differential bases.

region," "cytoplasmic desmata," "hydrolase activity, hydrolyzed O-linked glycosyl compounds", "Hydrolase activity, acting on glycosyl bonds" function. After co-treatment with *Trichoderma harzian*um and *Pestalotiopsis* sp., DEGs significantly enriched "cytoplasmic translation," "antibiotic catabolic process," "organic nitrogen compound biosynthesis process," "fungus-type cell wall," "ribosome," "structural components of ribosomes," "formate dehydrogenase (NAD+) activity" and "structural molecular activity."

By analyzing the enrichment of DEGs in the KEGG pathway of the group treated with biocontrol fungi alone, the results showed that the top 30 KEGG pathways of DEGs under different biocontrol bacteria treatments were different (Supplementary Figure S4). The DEGs of the group treated with *Trichoderma harzian*um alone could be enriched into the "MAPK signal pathway," "P53 signal pathway," "cGMP-PKG signal pathway," "carbon metabolism," etc. The DEGs of the group treated with *Pestalotiopsis* sp. alone could be enriched into "MAPK signal pathway," "starch and sucrose metabolism," "fatty acid metabolism," etc. DEGs in the co-treatment group of *Trichoderma harzian*um and *Pestalotiopsis* sp. could be enriched to "MAPK signaling pathway," "phenylpropane synthesis pathway," "carbon metabolism" and "tyrosine metabolism." All the above three treatments can enrich MAPK signaling pathways related to plant immunity and carbohydrate metabolism, indicating that the basic immunity of plants can be improved after biocontrol bacteria alone treatment.

Enrichment in the KEGG pathway of DEGs pretreated with biocontrol fungi showed that the KEGG pathway related to plant immunity was significantly enriched in each group (Figure 7). In *the Trichoderma harzian*um pretreatment group, DEGs were significantly enriched in the "phenylpropane synthesis pathway" and "mutual

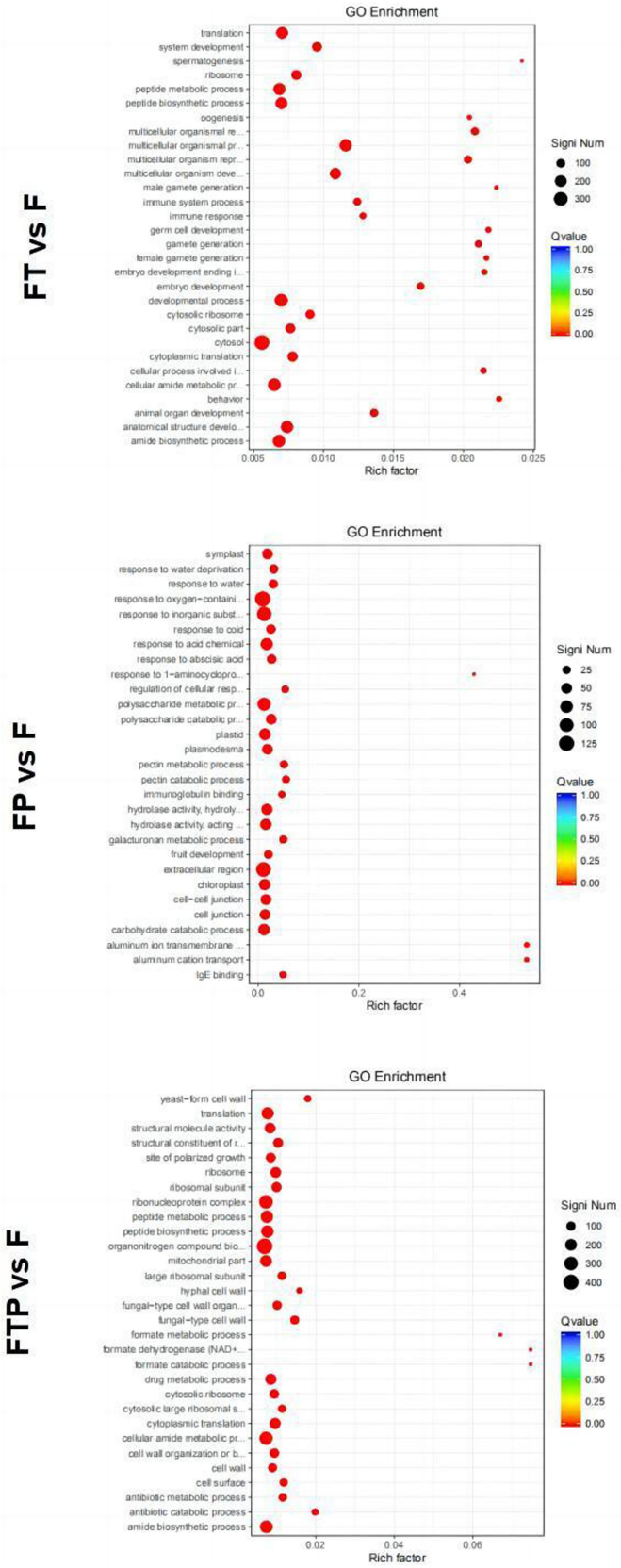

FIGURE 6
Significant enrichment GO function scatter diagram of DEGs. Significant enrichment GO function of DEGs in the comparisons of MO pretreated with biocontrol fungi and then inoculated with Fon. The vertical axis represents the functional annotation information, and the horizontal axis represents the Rich factor corresponding to the function (the number of differentially annotated genes for the function divided by the number of genes annotated for the

(Continued)

FIGURE 6 (Continued)
function). The size of the Qvalue is represented by the color of the point, where the smaller the Qvalue, the redder the color. The number of differential genes included under each function is represented by the size of the dots. (Only select the top 30 GO with the highest enrichment degree to draw).

conversion of pentose and glucuronic acid," while in *the Pestalotiopsis* sp. pretreatment group, DEGs were significantly enriched in "MAPK signal pathway," "phenylpropane synthesis pathway," "plant hormone signal transduction" and "plant-pathogen interaction." In the pretreatment group of *Trichoderma harzianum* and *Pestalotiopsis* sp., DEGs were significantly enriched in "MAPK signaling pathway," "pentose and glucuronic acid interconversion" and "carbon metabolism." In general, although the signal pathways of DEGs enrichment after pretreatment of different biocontrol bacteria are not consistent, all the above pathways can play an important role in the process of biological control.

3.7 Prediction of transcription factors during biocontrol fungi against Fon

Transcription factors play an important role in plant growth and development, hormone signal transduction, leaf senescence, and plant disease resistance. In order to explore which transcription factors are related to the mechanism of biological control of stem-based rot, the transcriptome sequence of the root of MO was compared and analyzed with the plant transcription factor database (PlnTFDB2) (Figure 8). The results showed that a total of 2,017 genes were aligned to PlnTFDB2, and the aligned transcription factors could be divided into 53 categories, including transcription factors related to plant disease resistance, such as WRKY, MYB, bZIP, AP2, and NAC, and transcription factors related to plant hormone signal transduction, such as ARF, BZIP, ERF, and MYB transcription factors were differentially expressed significantly when the biocontrol agents were used alone, while bZIP, ERF, and C2H2 transcription factors were significantly differentially expressed after pretreatment with the biocontrol agents.

3.8 Gene expression level validation by qRT-PCR

To confirm the reliability of the RNA-seq data, 10 DEGs related to the ethylene signaling pathway were randomly selected for the qRT-PCR validation analysis. The results showed that after the biocontrol fungi were treated separately, the five DEGs of TRINITY_DN488910_c0_g1, TRINITY_DN529234_c1_g1, TRINITY_DN520737_c0_g2, TRINITY_DN520737_c0_g1, and TRINITY_DN505197_c1_g1 were all significantly down-regulated. TRINITY_DN537446_c0_g4 and TRINITY_DN533749_c2_g3 were up-regulated significantly, but the expression trend of some genes was inconsistent after different treatments. The TRINITY_DN532960_c2_g1 gene was up-regulated after *Trichoderma harzianum* alone treatment, but it was down-regulated significantly after the other treatments. The gene of TRINITY_DN519710_c1_g1 was down-regulated after co-treatment with *Trichoderma harzianum* and *Pestalotiopsis* sp., and all other treatments were significantly up-regulated, while the gene of TRINITY_DN517401_c2_g1 was up-regulated after treated with *Pestalotiopsis* sp. alone, and all the other treatments were significantly down-regulated (Supplementary Figure S5A). After biocontrol fungi pretreatment, the expression trends of the 10 DEGs in each group were consistent, and all the DEGs were significantly up-regulated after *Trichoderma harzianum* pretreatment, and down-regulated after *Pestalotiopsis* sp. pretreatment, but all the DEGs were up-regulated after the co-pretreatment with two biocontrol fungi (Supplementary Figure S5B). Although the qRT-PCR-verified DEGs expression levels were not consistent with transcriptome sequencing, the expression trends were consistent with transcriptome sequencing. These differences can be due to variable shearing, sample handling, and data analysis. There may be multiple transcripts in a gene, and the differential trend of each transcript may be inconsistent. If qRT-PCR verifies a specific transcript and transcriptome sequencing yields gene-level expression, there may be cases where expression levels are inconsistent, but expression trends are consistent.

4 Discussion

MO stem-base rot first appeared in 1979, researchers found MO stem-base, roots, and seeds can be infected with stem-base rot (Cheng and Xu, 1979). MO stem-base rot is caused by Fon and can lead to rot and deterioration of the stem-base. At present, the control of this disease mainly relies on chemical control, but the control effect is not ideal. It has been reported that some biocontrol bacteria can antagonize stem-base rot bacteria and induce systemic disease resistance in crops. For example, Hou et al. (2022) obtained a stain of *streptomyces sclerous* SM3-7 from the rhizosphere soil of corn, which showed good potted control against stem-base rot. Chen et al. (2022) found that the co-culture of *Trichoderma verticillium* HB20111 and *Trichoderma harzianum* TW21990 had a synergistic effect, and the control effect on stem rot at the wheat seedling stage was significantly higher than that of a single strain. However, biocontrol agents have seldom been used to control the stem-base rot of MO. In this study, we report for the first time that *Trichoderma harzianum* and *Pestalotiopsis* sp. can be used as biocontrol fungi against the stem-base rot of MO, and the control effect is better when they are used together (Figure 2).

In a common microecological environment, biocontrol bacteria compete with pathogenic bacteria for limited space and nutritional resources through rapid propagation and growth, thus limiting the growth of pathogenic bacteria, which is called competition. For example, Zheng et al. (2023) found that biocontrol bacteria *Penicillium oxalicum* QZ8 and *Trichoderma asperellum* QZ2 inhibit the growth of Fon through spatial competition. In addition to the competitive effect, biocontrol bacteria also identify plant pathogens, carry out entanglement and adsorption on pathogenic bacteria, and dissolve the mycelia of pathogenic bacteria, so as to parasitize in pathogenic bacteria and obtain the nutrients of pathogenic bacteria for growth and reproduction. For example, Harman et al. (2004) found that *Trichoderma* produces a series of enzymes to degrade the cell wall of *Fusarium*, and completes the process of hyperparasitism to *Fusarium* through recognition, contact, entrench, penetration, and parasitism. In

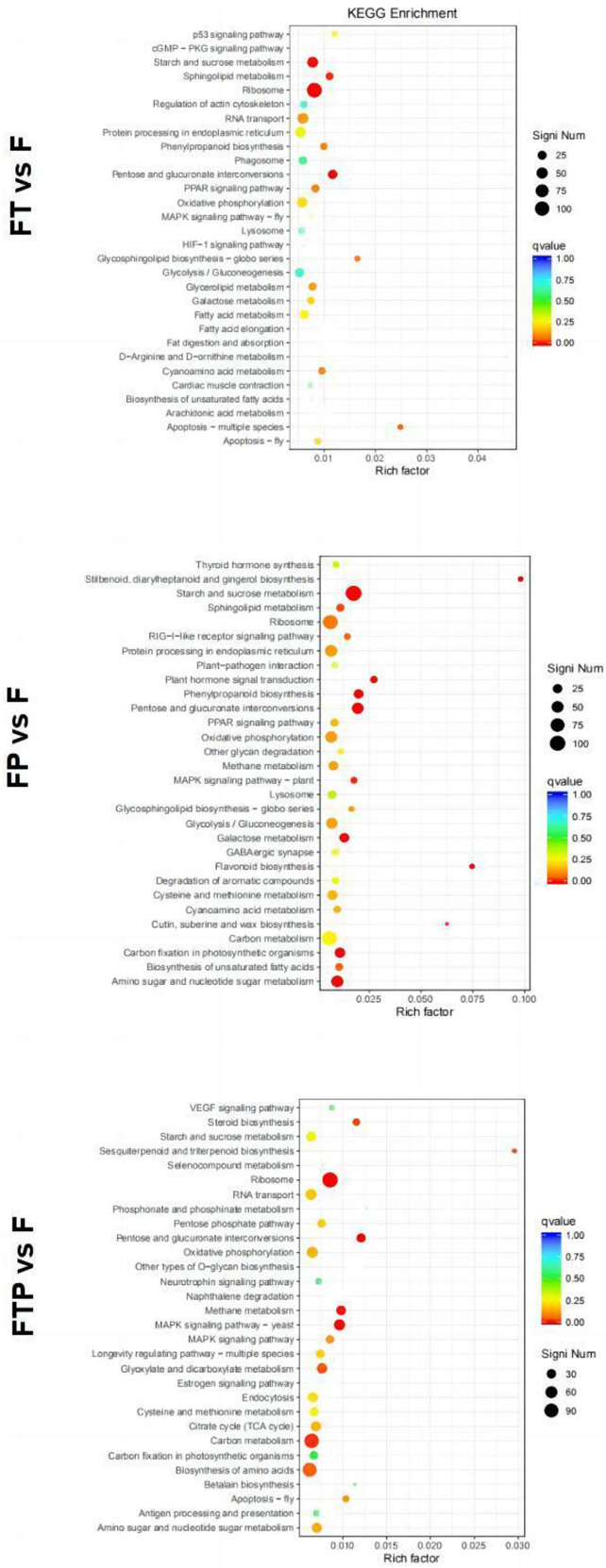

FIGURE 7
Significant enrichment KEGG pathway scatter diagram of DEGs. Significant enrichment KEGG pathway of DEGs in the comparisons of MO pretreated with biocontrol fungi and then inoculated with Fon. The vertical axis represents the functional annotation information, and the horizontal axis represents the Rich factor corresponding to the function (the number of differentially annotated genes for the function divided by the number of

(Continued)

FIGURE 7 (Continued)
genes annotated for the function). The size of the Qvalue is represented by the color of the point, where the smaller the Qvalue, the redder the color. The number of differential genes included under each function is represented by the size of the dots. (Only select the top 30 KEGG with the highest enrichment degree to draw).

our study, both *Trichoderma harzianum* and *Pestalotiopsis* sp. showed different degrees of resistance to the stem-base rot pathogen Fon, and parasitic on pathogenic bacteria mycelia through identification, entanglement or attachment, and finally penetrating and dissolving pathogenic bacteria mycelia (Figure 1). In recent years, there have been many reports that biocontrol bacteria can cause ISR, including those that may cause ISR in *Fusarium*. Sakineh et al. (2019) reported that the use of *S. enissocaesilis* strains IC10 and *S. rochei* strains Y28, or after the application of plant, hormones can induce ISR to Fon. Besides, some non-pathogenic fungi like *Fusarium moniliforme* can also induce ISR against Fon (Patil et al., 2011). In our study, the activities of defense-related enzymes (POD and SOD), chlorophyll content, and soluble sugar content were determined. The results showed that, compared with the control treatment, biocontrol fungi could improve the activity of defense-related enzymes, chlorophyll content, and soluble sugar content. However, the levels of 1-ketose and nystose in MO were decreased, and the levels of fructose and glucose were increased (Figure 3; Supplementary Table S4; Kashyap et al., 2021).

At present, high-throughput transcriptome sequencing technology has been widely used to study the interaction mechanism between plants and pathogens, and a large number of functional genes related to plant disease resistance have been mined, revealing the pathogenesis of pathogenic bacteria and the molecular mechanism of plant disease resistance. However, there have been no reports on the mechanism of preventing and controlling MO stem-base rot from the transcriptome level (Xu et al., 2020). In this study, we identified tens of thousands of genes that function on ISR to Fon from biocontrol fungi in MO. By treating biological control fungi alone or pretreating them before inoculation with Fon, the expression of a large number of genes in MO can be altered or modified (Figure 4; Supplementary Tables S5, S6), suggesting that biological control fungi can induce systemic resistance to Fon by altering the transcription level of MO genes. Furthermore, through our data analysis, we found that many genes are involved in regulating this regulatory process. TFs play essential roles in the immune response of plants to various stresses (Fu et al., 2019; Li et al., 2021). The transcription factors involved in stress response mainly include NAC, WRKY, bHLH, MYB, and AP2/ERF (Garg et al., 2014; Aditya and Aryadeep, 2017; Peng et al., 2021). WRKY has been shown to play an important role in plant response to pathogens. Some WRKYs play a positive regulatory role in plant defense against pathogen stress. For example, in chrysanthemums, CmWRKY15 plays a positive regulatory role in chrysanthemum resistance to stem rust by influencing the SA signaling pathway (Bi et al., 2021). In addition, some MYB factors can also enhance plant resistance to pathogens by regulating the SA pathway (Seo and Park, 2010). Besides, it has been shown that ERF proteins regulate ET/JA or SA-mediated signaling pathways in plants, resulting in moderate disease resistance responses (Liang et al., 2008). In our study, based on RNA sequencing data, we identified many TFs involved in the systemic resistance process of MO to Fon induced by biocontrol fungi, including WRKY, MYB, bZIP, ARF, and ERF, etc. (Figure 8). Among them, WRKY transcription factors are able to respond to the MAPK signaling pathway, while ERFs transcription factors are able to respond to the ethylene signaling pathway, which together regulate downstream defense-related genes.

Studies have shown that the MAPK signaling pathway plays a crucial role in promoting and protecting plant growth when plants are subjected to environmental stress (Bi and Zhou, 2017). The response of the MAPK signaling pathway to plant diseases is mainly divided into three parts, including pathogen invasion, pathogen attack, and plant hormone. After pretreatment by biocontrol bacteria, DEGs are significantly enriched in the MAPK signaling pathway. As can be seen from Supplementary Figure S6A, related DEGs in this pathway are up-regulated, including WRKY transcription factor 33(TRINITY_DN531732_c5_g3), disease-related protein 1 (PR1, TRINITY_DN536232_c0_g2), ethylene non-sensitive protein 3 (EIN3, TRINITY_DN542286_c4_g5) and alkaline endochitinase B (Chi B, TRINITY_DN526230_c1_g3, TRINITY_DN526230_c1_g2). WRKY transcription factors play an important role in plant defense against stem basal rot, and one of the important mechanisms is to regulate the downstream defense-related genes together with the MAPK signaling pathway. MAPK phosphorylates or dephosphorylates WRKY transcription factors, thereby altering the function and activity of WRKY transcription factors, which in turn regulate the expression of downstream defense-related genes. For example, in *Arabidopsis thaliana*, MPK3 and MPK6 can phosphorylate WRKY33 and increase its affinity for W-box elements, thereby promoting the expression of their target genes, such as genes involved in plant secondary metabolic pathways, such as PAD3 and CYP71A13, as well as genes involved in plant antimicrobial pathways, such as PDF1.2 and PR4. The expression of these genes enhances plant resistance to stem basal rot pathogens (Eckardt, 2011; Sheikh et al., 2016). In summary, WRKY transcription factors and the MAPK signaling pathway regulate plant resistance to stem-base rot through synergistic actions.

Hormone-regulated genes play a crucial role in plant growth and development as well as in responding to biotic stresses (Pieterse et al., 2012). Among them, SA, JA, and ethylene are known to be key phytohormones in response to biotic stresses (Lazebnik et al., 2014). In this study, this signaling pathway was activated when treated with biocontrol fungi, mainly involving hormone signaling of auxin, gibberellin, abscisic acid, ethylene, JA, and SA (Supplementary Figure S6B). In the ethylene signaling pathway, the EIN3 protein (TRINITY_DN542286_c4_g5) was up-regulated to promote the transcription of ethylene response genes. Ethylene is an important phytohormone that induces the expression of disease resistance-related genes when plants are infested with pathogenic bacteria, thereby increasing plant disease resistance. The ethylene signaling pathway has been extensively studied and some of the key enzymes and transcription factors have been identified. Ethylene signaling is mainly composed of ethylene receptors, CTR1, EIN2, EIN3/EIL1, etc., which constitute a negative feedback regulatory network to maintain the balance of ethylene signaling, they can sense ethylene signals and transmit them to downstream transcription factors such as ERFs (Zhao et al., 2021). The ERFs gene family is a class of plant-specific transcription factors that bind to ethylene-responsive elements (EREs) and regulate gene expression downstream of ethylene

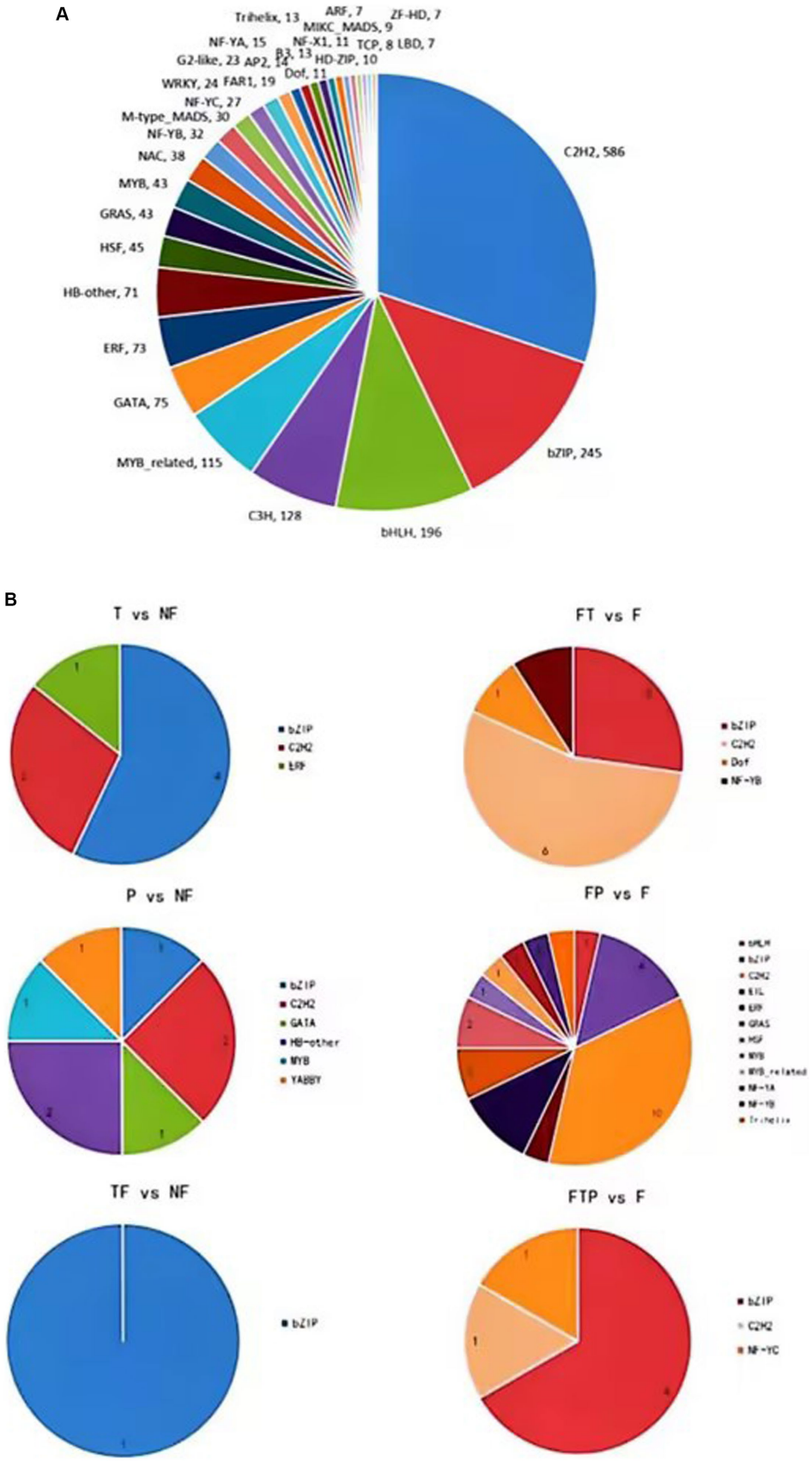

FIGURE 8
Transcription factors (TFs) prediction of DEGs. **(A)** Prediction of TFs in MO unigenes sequence. **(B)** Prediction of TFs of DEGs in biocontrol fungi treatment.

signaling, which can regulate biological processes such as glucose metabolism, cell wall degradation, pigment synthesis, and aroma synthesis (Zhou et al., 2022). Studies have shown that the ethylene and sugar signaling play important roles in regulating plant growth and development and in response to stress (Etzler, 1998; Shi et al., 2019). In this study, we found that the infection of Fon into the root of MO can lead to differential enrichment of glucose-related metabolic pathways. Ethylene receptor, ERFs, EIN3, ein2 et al. genes are annotated into glycosyl compound metabolic processes (GO: 1901657) and sugar-mediated signaling pathways (GO: 0010182). Therefore, the ethylene signaling may mediate the co-involvement of the sugar signaling in the immune response of MO to Fon infection. These results suggest that the ethylene signaling pathway in MO play an important role in biocontrol fungi triggering plant immunity to Fon.

Overall, the *in vitro* antagonistic results showed that *Trichoderma harzianum* and *Pestalotiopsis* sp. Inhibited Fon. Combined with the results of the greenhouse experiments, it was verified that both fungi could be used as biocontrol fungi to control MO stem-base rot, and the detection of physiological and biochemical indexes reflected that a variety of metabolic processes and functions in the plant changed after the use of the two biocontrol fungi, such as increasing the activity of antioxidant enzymes, chlorophyll content, and soluble sugars, which reflected that biocontrol fungi could promote the response of MO to Fon stress from the side. Continuing to explore the biocontrol mechanism by transcriptome sequencing, the results showed that *Trichoderma harzianum* and *Pestalotiopsis* sp. could affect the gene expression of MO and regulate the signal transduction and phytohormone pathways related to Fon resistance, such as the MAPK signaling pathway and the ethylene signaling pathway, which could improve the disease resistance and growth of MO.

Data availability statement

The data presented in the study are deposited in the NCBI repository, accession number PRJNA1043455.

Author contributions

ZiC: Writing – original draft, Writing – review & editing. PH: Writing – review & editing. ZL: Writing – review & editing. ZeC: Writing – review & editing. JC: Writing – review & editing. XC: Writing – review & editing. TS: Writing – review & editing. PD: Writing – review & editing.

Funding

The author(s) declare financial support was received for the research, authorship, and/or publication of this article. This research was supported by Guangzhou Key R&D Project (No. 202206010010), Guangdong Provincial Rural Revitalization Strategy Special Project (No. 2021KJ268), and Guangdong Agricultural Science and Technology Innovation and Promotion Project (No. 2022KJ142).

Acknowledgments

We would like to thank associate researcher Tijiang Shan (South China Agricultural University, Guangzhou, China) for providing us with *Pestalotiopsis* sp.

Conflict of interest

The authors declare that the research was conducted in the absence of any commercial or financial relationships that could be construed as a potential conflict of interest.

Publisher's note

Supplementary material

The Supplementary material for this article can be found online at: https://www.frontiersin.org/articles/10.3389/fmicb.2023.1257437/full#supplementary-material

References

Aditya, B., and Aryadeep, R. (2017). Epigenetic regulation during salinity and drought stress in plants: histone modifications and DNA methylation. *Plant Gene* 11, 199–204. doi: 10.1016/j.plgene.2017.05.011

Asad, S. A. (2022). Mechanisms of action and biocontrol potential of Trichoderma against fungal plant diseases – a review. *Ecol. Complex.* 49:100978. doi: 10.1016/j.ecocom.2021.100978

Bi, M. M., Li, X. Y., Yan, X., Liu, D., Gao, G., Zhu, P. F., et al. (2021). Chrysanthemum WRKY15-1 promotes resistance to Puccinia horiana Henn. via the salicylic acid signaling pathway. *Hortic. Res.* 8:6. doi: 10.1038/s41438-020-00436-4

Bi, G., and Zhou, J. M. (2017). Map kinase signaling pathways: a hub of plant-microbe interactions. *Cell Host Microbe* 21, 270–273. doi: 10.1016/j.chom.2017.02.004

Cai, M. M., Liu, M. Y., Yang, L., Feng, C., and Ding, P. (2021). Research progress of Morinda officinalis germplasm resources and quality evaluation. *Chin. Herb. Med.* 44, 1008–1013. doi: 10.13863/j.issn1001-4454.2021.04.044

Castillo, S. Y., Rodríguez, M. C., González, L. F., Franky, Z. L., Adriana, M. Y., Camilo, M. H., et al. (2022). Ganoderma zonatum is the causal agent of basal stem rot in oil palm in Colombia. *J. Fungi* 8:230. doi: 10.3390/jof8030230

Chen, K., Sui, L. N., Yang, K., Zhao, Z. J., Hu, J. D., and Li, J. S. (2022). Co-culture and fermentation of two Trichoderma strains to improve the control effect of stem base rot in wheat seedling stage. *Acta Phytopathol. Sin.* 52, 425–433. doi: 10.13926/j.cnki.apps.000759

Cheng, R. Y., and Xu, J. J. (1979). Identification of pathogenic bacteria on stem base rot of Euphorbia officinalis. *Bull. Subtrop. Bot.* 2, 28–30.

Dor, E., Evidente, A., Amalfitano, C., Agrelli, D., and Hershenhorn, J. (2007). The influence of growth conditions on biomass, toxins and pathogenicity of Fusarium oxysporumf. Sp. orthoceras, a potential agent for broomrape biocontrol. *Weed Res.* 47, 345–352. doi: 10.1111/j.1365-3180.2007.00567.x

Eckardt, N. A. (2011). Induction of phytoalexin biosynthesis: WRKY33 is a target of MAPK signaling. *Plant Cell* 23:1190. doi: 10.1105/tpc.111.230413

Etzler, M. E. (1998). Oligosaccharide signaling of plant cells. *Journal of Cellular Biochemistry*. 72, 123–128.

Fu, Y., Mason, A. S., Zhang, Y. F., Lin, B. G., Xiao, M. L., Fu, D. H., et al. (2019). MicroRNA-mRNA expression profiles and their potential role in cadmium stress response in *Brassica napus*. *BMC Plant Biol.* 19:570. doi: 10.1186/s12870-019-2189-9

Garg, R., Verma, M., Agrawal, S., Shankar, R., Majee, M., and Jain, M. (2014). Deep transcriptome sequencing of wild halophyte rice, Porteresia coarctata, provides novel insights into the salinity and submergence tolerance factors. *DNA Res.* 21, 69–84. doi: 10.1093/dnares/dst042

Harman, G. E., Howell, C. R., Viterbo, A., Chet, I., and Lorito, M. (2004). Trichoderma species--opportunistic, avirulent plant symbionts. *Nat Rev Microbiol.* 2, 43–56. doi: 10.1038/nrmicro797

Hou, X. Y., Wu, H. X., Zhang, J., Huang, P., Yao, J. A., and Yu, D. Y. (2022). Identification of an antagonistic strain of Streptomyces SM3-7 and its control effect on maize stem base rot. *Chin. J. Biol. Control* 38, 1526–1533. doi: 10.16409/j.cnki.2095-039x.2022.08.004

Jevtić, R., Stošić, N., Župunski, V., Lalošević, M., and Orbović, B. (2019). Variability of Stem-Base infestation and coexistence of fusarium spp. causing crown rot of winter wheat in Serbia. *Plant Pathol. J.* 35, 553–563. doi: 10.5423/PPJ.OA.02.2019.0038

Kashyap, A. S., Manzar, N., Rajawat, M. V. S., Kesharwani, A. K., Singh, R. P., Dubey, S. C., et al. (2021). Screening and biocontrol potential of Rhizobacteria native to Gangetic Plains and hilly regions to induce systemic resistance and promote plant growth in Chilli against bacterial wilt disease. *Plan. Theory* 10:2125. doi: 10.3390/plants10102125

Kong, W. L., Chen, X., Sun, H., Sun, X. R., and Wu, X. Q. (2022). Identification of two fungal pathogens responsible for *Liriodendron chinense* × tulipifera black spot and screening of Trichoderma sp. for the disease control. *Plant Dis.* 106, 2172–2181. doi: 10.1094/PDIS-06-21-1266-RE

Kumar, S., Shukla, V., Dubey, M. K., and Upadhyay, R. S. (2021). Activation of defense response in common bean against stem rot disease triggered by Trichoderma erinaceum and Trichoderma viridae. J. *Basic Microbiol.* 61, 910–922. doi: 10.1002/jobm.202000749

Lazebnik, J., Frago, E., Dicke, M., and Van Loon, J. J. A. (2014). Phytohormone mediation of interactions between herbivores and plant pathogens. *J. Chem. Ecol.* 40, 730–741. doi: 10.1007/s10886-014-0480-7

Li, Y. Y., Wang, L., Sun, G. W., Li, X. H., Chen, Z. G., Feng, J., et al. (2021). Digital gene expression analysis of the response to *Ralstonia solanacearum* between resistant and susceptible tobacco varieties. *Sci. Rep.* 11:3887. doi: 10.1038/s41598-021-82576-8

Liang, H., Lu, Y., Liu, H., Wang, F., Xin, Z., and Zhang, Z. (2008). A novel activator-type ERF of *Thinopyrum intermedium*, TiERF1, positively regulates defence responses. *J. Exp. Bot.* 59, 3111–3120. doi: 10.1093/jxb/ern165

Liu, M. Y., Luo, Z. H., Chen, Z. E., Qin, Y. R., Liu, Q. Y., Ding, P., et al. (2022). Quality markers for processed products of Morinda officinalis How based on the oligosaccharides-spectrum-effect. *J. Pharm. Biomed. Anal.* 208:114403. doi: 10.1016/j.jpba.2021.114403

McNally, R. R., Curland, R. D., Webster, B. T., Robinson, A. P., and Ishimaru, C. A. (2018). First report of stem rot on potato caused by *Dickeya chrysanthemi* in Minnesota. *Plant Dis.* 102:238. doi: 10.1094/PDIS-07-17-0966-PDN

Mordue, J. E. M. (1985). An unusual species of Pestalotiopsis: P. Steyaertii sp. nov. *Trans. Br. Mycol. Soc.* 85, 378–380. doi: 10.1016/S0007-1536(85)80210-2

Narware, J., Singh, S. P., Manzar, N., and Kashyap, A. S. (2023). Biogenic synthesis, characterization, and evaluation of synthesized nanoparticles against the pathogenic fungus Alternaria solani. *Front. Microbiol.* 14:1159251. doi: 10.3389/fmicb.2023.1159251

National Pharmacopoeia Committee (2020), *Chinese pharmacopoeia*, China Medical Science and Technology Press, Beijing, pp. 84–85.

Orr, R., and Nelson, P. N. (2018). Impacts of soil abiotic attributes on fusarium wilt, focusing on bananas. *Appl. Soil Ecol.* 132, 20–33. doi: 10.1016/j.apsoil.2018.06.019

Patil, S., Sriram, S., Savitha, M. J., and Arulmani, N. (2011). Induced systemic resistance in tomato by non-pathogenic fusarium species for the management of fusarium wilt. *Arch. Phytopathol. Plant Protect.* 44, 1621–1634. doi: 10.1080/03235408.2010.526774

Peng, T., Wang, Y. Q., Yang, T., Wang, F. S., Luo, J., and Zhang, Y. L. (2021). Physiological and biochemical responses, and comparative transcriptome profiling of two Angelica sinensis cultivars under enhanced ultraviolet-B radiation. *Front. Plant Sci.* 12:8054087. doi: 10.3389/fpls.2021.805407

Photita, W., Lumyong, S., Lumyong, P., and Hyde, K. D. (2001). Endophytic fungi of wild banana (*Musa acuminata*) at Doi Suthep Pui National Park, Thailand. *Mycol. Res.* 105, 1508–1513. doi: 10.1017/S0953756201004968

Pieterse, C. M., van Wees, S. C., van Pelt, J. A., Knoester, M., Laan, R., Gerrits, H., et al. (1998). A novel signaling pathway controlling induced systemic resistance in Arabidopsis. *Plant Cell* 10, 1571–1580. doi: 10.1105/tpc.10.9.1571

Pieterse, C. M. J., Dieuwertje, V. D. D., Christos, Z., Antonio, L. R., and Van Wees, S. C. M. (2012). Hormonal modulation of plant immunity. *Annu. Rev. Cell Dev. Biol.* 28, 489–521. doi: 10.1146/annurev-cellbio-092910-154055

Qi, Y. H., Li, M. Q., Cao, S. F., Jiang, J. J., Li, X. P., Li, Q. Q., et al. (2021). Identification of fusarium codonopsis stem base rot disease and its sensitivity to fungicides. *J. Agric.* 11, 74–78. doi: 10.11923/j.issn.2095-4050.cjas2020-0052

Sa, R. B., Zhang, J. L., Sun, J. Z., and Gao, Y. X. (2021). Colonization characteristics of poplar fungal disease biocontrol Bacteria N6-34 and the inhibitory effect on pathogenic fungi by real-time fluorescence quantitative PCR detection. *Curr. Microbiol.* 78, 2916–2925. doi: 10.1007/s00284-021-02529-2

Sabry, S., Ali, A. Z., Abdel-Kader, D. A., and Abou-Zaid, M. I. (2022). Histopathological and biochemical aspects of grafted and non-grafted cucumber infected with stem rot caused by fusarium spp. *Saudi J. Biol. Sci.* 29, 1770–1780. doi: 10.1016/j.sjbs.2021.10.053

Sakineh, A., Naser, S., Akram, S., and Masoud, S. (2019). Streptomyces strains induce resistance to fusarium oxysporum f. sp. lycopersici race 3 in tomato through different molecular mechanisms. *Front. Microbiol.* 10:1505. doi: 10.3389/fmicb.2019.01505

Seo, P. J., and Park, C. M. (2010). MYB96-mediated abscisic acid signals induce pathogen resistance response by promoting salicylic acid biosynthesis in Arabidopsis. *New Phytol.* 186, 471–483. doi: 10.1111/j.1469-8137.2010.03183.x

Sharma, P. K. (2023). Screening microbial inoculants and their interventions for cross kingdom management of wilt disease of solanaceous crop-a step towards sustainable agriculture. *Front. Microbiol.* 14:1174532. doi: 10.3389/fmicb.2023.1174532

Sheikh, A. H., Lippold, L. E., Pecher, P., Hoehenwarter, W., Sinha, A. K., and Scheel, D. (2016). Regulation of WRKY46 transcription factor function by mitogen-activated protein kinases in *Arabidopsis thaliana*. *Front. Plant Sci.* 7:61. doi: 10.3389/fpls.2016.00061

Shen, G. S., Yu, S. J., Guo, N., Zhou, X. L., and Bian, Q. (2021). Research progress on control of maize stem base rot. *Pesticide* 60, 235–238. doi: 10.16820/j.cnki.1006-0413.2021.04.002

Shi, Q. L., Li, Z. F., Dong, Y. B., and Li, Y. L. (2019). Research progress on plant ethylene signal transduction pathway and its related genes. *Current Biotechnology.* 9,449–454. doi: 10.19586/j.2095-2341.2019.0080

Stefania, G., Roberta, P., and Stefano, C. (2020). Selected isolates of Trichoderma gamsii induce different pathways of systemic resistance in maize upon fusarium verticillioides challenge. *Microbiol. Res.* 233:126406. doi: 10.1016/j.micres.2019.126406

Steyaert, R. L. (1953). New and old species of Pestalotiopsis. *Trans. Br. Mycol. Soc.* 36, 81–89. doi: 10.1016/S0007-1536(53)80052-5

Strobel, G. A., Hess, W. M., Li, J. Y., Ford, E., Sears, J., Sidhu, R. S., et al. (1997). Pestalotiopsis guepinii, a taxol-producing endophyte of the Wollemipine, Wollemia nobilis. *Aust. J. Bot.* 45, 1073–1082. doi: 10.1071/BT96094

Swain, M. R., Ray, R. C., and Nautiyal, C. S. (2008). Biocontrol efficacy of *Bacillus subtilis* strains isolated from cow dung against postharvest yam (*Dioscorea rotundata* L.) pathogens. *Curr. Microbiol.* 57, 407–411. doi: 10.1007/s00284-008-9213-x

Wang, F., Li, X. M., Gao, S. X., Wen, Y., Qin, Y. H., and Liu, Y. X. (2022). Identification and selection of pathogens from stem base rot of Atractylodes atractylodes in Henan. *Chin. J. Plant Pathol.*, 1–13. doi: 10.13926/j.cnki.apps.001011

Xu, T. S., Liu, T. G., Liu, B., Chen, W. Q., and Gao, L. (2020). Transcriptome sequencing and its application in the study of plant pathogens, plant and fungus interaction. *Plant Prot.* 46, 13–17. doi: 10.16688/j.zwbh.2019358

Yassin, M. T., Mostafa, A. A. F., Al-Askar, A. A., Sayed, S. R. M., and Rady, A. M. (2021). Antagonistic activity of Trichoderma harzianum and Trichoderma viride strains against some fusarial pathogens causing stalk rot disease of maize, in vitro. *J. King Saud Univ. Sci.* 33:101363. doi: 10.1016/j.jksus.2021.101363

Zhang, R. J., Li, Q., Qu, M. H., Gao, J. L., Ma, W. T., Liu, W. X., et al. (2016). Investigation on germplasm resources of Morinda officinalis. *Chin. J. Mod. Tradit. Chin. Med.* 18, 482–487. doi: 10.13313/j.issn.1673-4890.2016.4.020

Zhang, C. Y., Wang, W. W., Xue, M., Liu, Z., Zhang, Q. M., Hou, J. M., et al. (2021). The combination of a biocontrol agent Trichoderma asperellum SC012 and Hymexazol reduces the effective fungicide dose to control fusarium wilt in cowpea. *J. Fungi* 7:685. doi: 10.3390/jof7090685

Zhao, H., Yin, C. C., Ma, B., Chen, S. Y., and Zhang, J. S. (2021). Ethylene signaling in rice and Arabidopsis: new regulators and mechanisms. *J. Integr. Plant Biol.* 63, 102–125. doi: 10.1111/jipb.13028

Zheng, M. Q., Jiang, R. Q., Fang, W., Chen, J. Y., Zhao, M. L., Si, J. P., et al. (2023). Inhibitory effects of three biocontrol strains on pathogenic bacteria of Polygonum floriculata root rot. *China J. Chin. Mater. Med.* 48, 1212–1217. doi: 10.19540/j.carol carroll nki CJCMM. 20221203.102

Zhou, J. L., Feng, Z. L., Wei, F., Zhao, L. H., Zhou, Y. L., Zhou, Y., et al. (2021). Effect and mechanism of endophytic bacteria YUPP-10 and its secreted protein CGTase on cotton fusarium wilt. *China Agric. Sci.* 54, 3691–3701. doi: 10.3864/j.issn.0578-1752.2021.17.011

Zhou, J. G., Mu, Q., Wang, X. Y., Zhang, J., Yu, H. Z., Huang, T. Z., et al. (2022). Multilayered synergistic regulation of phytoalexin biosynthesis by ethylene, jasmonate, and MAPK signaling pathways in Arabidopsis. *Plant Cell* 34, 3066–3087. doi: 10.1093/plcell/koac139

frontiers | Frontiers in Plant Science

TYPE Review
PUBLISHED 04 December 2023
DOI 10.3389/fpls.2023.1228749

OPEN ACCESS

EDITED BY
Inmaculada Larena,
Instituto Nacional de Investigación y Tecnología Agraria y Alimentaria (INIA-CSIC), Spain

REVIEWED BY
Belen Guijarro,
Instituto Nacional de Investigación y Tecnología Agroalimentaria (INIA), Spain
Carmen Gómez-Lama Cabanás,
Spanish National Research Council (CSIC), Spain

*CORRESPONDENCE
Daniel Muller
daniel.muller@univ-lyon1.fr

RECEIVED 25 May 2023
ACCEPTED 10 November 2023
PUBLISHED 04 December 2023

CITATION
Todorović I, Moënne-Loccoz Y, Raičević V, Jovičić-Petrović J and Muller D (2023) Microbial diversity in soils suppressive to *Fusarium* diseases.
Front. Plant Sci. 14:1228749.
doi: 10.3389/fpls.2023.1228749

Microbial diversity in soils suppressive to *Fusarium* diseases

Irena Todorović [1,2], Yvan Moënne-Loccoz [1], Vera Raičević [2], Jelena Jovičić-Petrović [2] and Daniel Muller [1*]

[1]Université Claude Bernard Lyon 1, CNRS, INRAE, VetAgro Sup, UMR5557 Ecologie Microbienne, Villeurbanne, France, [2]University of Belgrade, Faculty of Agriculture, Belgrade, Serbia

Fusarium species are cosmopolitan soil phytopathogens from the division *Ascomycota*, which produce mycotoxins and cause significant economic losses of crop plants. However, soils suppressive to *Fusarium* diseases are known to occur, and recent knowledge on microbial diversity in these soils has shed new lights on phytoprotection effects. In this review, we synthesize current knowledge on soils suppressive to *Fusarium* diseases and the role of their rhizosphere microbiota in phytoprotection. This is an important issue, as disease does not develop significantly in suppressive soils even though pathogenic *Fusarium* and susceptible host plant are present, and weather conditions are suitable for disease. Soils suppressive to *Fusarium* diseases are documented in different regions of the world. They contain biocontrol microorganisms, which act by inducing plants' resistance to the pathogen, competing with or inhibiting the pathogen, or parasitizing the pathogen. In particular, some of the *Bacillus*, *Pseudomonas*, *Paenibacillus* and *Streptomyces* species are involved in plant protection from *Fusarium* diseases. Besides specific bacterial populations involved in disease suppression, next-generation sequencing and ecological networks have largely contributed to the understanding of microbial communities in soils suppressive or not to *Fusarium* diseases, revealing different microbial community patterns and differences for a notable number of taxa, according to the *Fusarium* pathosystem, the host plant and the origin of the soil. Agricultural practices can significantly influence soil suppressiveness to *Fusarium* diseases by influencing soil microbiota ecology. Research on microbial modes of action and diversity in suppressive soils should help guide the development of effective farming practices for *Fusarium* disease management in sustainable agriculture.

KEYWORDS

deoxynivalenol, nivalenol, zearalenone, *Fusarium* head blight, induced systemic resistance, lipopolysaccharides

Abbreviations: DON, Deoxynivalenol; NIV, Nivalenol; ZEA, Zearalenone; FHB, Fusarium Head Blight; ISR, Induced Systemic Resistance; LPS, Lipopolysaccharides; FOL, *F. oxysporum* f. sp. *lycopersici*; PR, Pathogenesis-Related; VOC, Volatile Organic Compound; BEA, beauvericin; ENN, enniatins.

1 Introduction

The fungal genus *Fusarium* encompasses several plant-pathogenic species, which are among the most destructive phytopathogens world-wide, causing diseases on many agricultural crops (Burgess and Bryden, 2012). They are ubiquitous in parts of the world where cereals and other crops are grown and they produce a wide variety of mycotoxins, which may be present in feed and food products (Babadoost, 2018; Moretti et al., 2018; Chen et al., 2019). Consumption of products that are contaminated with mycotoxins may cause acute or chronic effects in both animals and humans, and could result in immune-suppressive or carcinogenic effects (Jard et al., 2011). By producing mycotoxins and by inducing necrosis and wilting in plants, *Fusarium* fungi are causing huge economic losses of cereal crops throughout the world (Khan et al., 2017). Their broad distribution has been attributed to their ability to develop on different substrates and plant species, and to produce spores that enable efficient propagation (Desjardins, 2006; Arie, 2019). They are typical soil-borne microorganisms, routinely found in plant-associated fungal communities (Reyes Gaige et al., 2020).

Efficient management of plant diseases caused by *Fusarium* is important to limit crop losses and to reduce mycotoxin production in alimentary products (Babadoost, 2018). Because mycotoxin synthesis can occur not only after harvesting but also before, one of the best ways to reduce its presence in food and feed products is to prevent its formation in the crop (Jard et al., 2011). Over the years, different methods, such as the use of resistant cultivars and chemical fungicides, have been undertaken in order to control or prevent crop diseases (Willocquet et al., 2021). In spite of that, *Fusarium* continues to cause huge crop losses, up to 70% in South America, 54% in the United States and 50% in Europe in the case of Fusarium head blight (FHB) disease of wheat (Scott et al., 2021).

Alternative control methods, based on plant-protection effects of beneficial microorganisms, have also been investigated (Janvier et al., 2007; Nguyen et al., 2018). Farming practices greatly influence these effects by shaping the rhizosphere microbial community (Campos et al., 2016), stimulating the activity of beneficial rhizosphere microorganisms and restricting the activity of soil-borne *Fusarium* pathogens (Janvier et al., 2007). Indeed, crop rotation, tillage and addition of organic amendments may provide some control of soil-borne pathogens, through different microbial direct and indirect mechanisms (Janvier et al., 2007). The effect of plant-protecting soil microbiota on plant health is of particular interest in the case of disease-suppressive soils, which were defined by Baker and Cook (1974) as "soils in which the pathogen does not establish or persist, establishes but causes little or no damage, or establishes and causes disease for a while but thereafter the disease is less important, although the pathogen may persist in the soil". Suppressive soils represent a reservoir of beneficial microorganisms, which may confer effective plant protection against various soil-borne diseases (Gómez Expósito et al., 2017). This biocontrol potential of suppressive soils is of great importance when considering phytopathogens like *Fusarium* spp., which are causing increasing damage to crops in the on-going climate change context (Babadoost, 2018). Insight into the time and space microbial dynamics of soils suppressive to *Fusarium* diseases, together with the understanding of microbial modes of action and agricultural practices applied, is needed in order to develop safe, effective, and stable tools for disease management (Gómez Expósito et al., 2017).

By selecting their rhizosphere microbiome (Tkacz et al., 2015; Gruet et al., 2023), plants may contribute themselves to suppressiveness (Almario et al., 2014; Gómez Expósito et al., 2017). Soil represents the richest known reservoir of microbial biodiversity (Curtis et al., 2002; Wang et al., 2016) and displays several compartments, i.e. the bulk soil containing microorganisms that are not affected by the roots, the rhizosphere where soil microorganisms are under the influence of roots (and roots exudates), the rhizoplane with root-adhering microorganisms, and the endosphere for root tissues colonized by microorganisms (Sánchez-Cañizares et al., 2017). The rhizosphere and rhizoplane harbor an abundant community of bacteria, archaea, oomycetes and fungi, whose individual members can have beneficial, deleterious or neutral effects on the plant. The collective genome of this microbial community is larger than that of the plant itself, and is often referred to as the plant's second genome (Berendsen et al., 2012). Thus, this alliance of the plant and its associated microorganisms represents a holobiont, which has interdependent, fine-tuned and complex functioning (Berendsen et al., 2012; Vandenkoornhuyse et al., 2015; Sánchez-Cañizares et al., 2017). In this system, the plant is a key player, as nearly 40% of all photosynthates are released directly by roots into the rhizosphere, serving as a fuel for microbial communities, thus recruiting and shaping this microbiome (Berendsen et al., 2012; Tkacz and Poole, 2015). These photosynthates are conditioned by the plant genotype, developmental stage, metabolism, immune system and its ability to exudate (Sánchez-Cañizares et al., 2017). In this context, suppressiveness will depend on microbiome diversity and functioning.

This review deals with recent knowledge on soils suppressive to *Fusarium* diseases, which sheds new lights on molecular and ecological mechanisms underpinning phytoprotection effects and highlights the importance of microbial diversity in the functioning of these suppressive soils. To this end, we summarize current knowledge on *Fusarium* taxonomy and ecology, and their mechanisms of plant infection. In addition, we review our understanding of biocontrol agents against *Fusarium* and their modes of action. Finally, we focus on soils suppressive to *Fusarium* diseases and the importance of farming and environmental factors modulating suppressiveness, with an emphasis on the particularities of the different *Fusarium* pathosystems.

2 *Fusarium* phytopathogens and plant diseases

2.1 *Fusarium* ecology

Fusarium species occur in soils, but they can also grow in and on living and dead plants (Laraba et al., 2021) and animals (Xia et al., 2019), with the ability to live as parasites or saprophytes

(Smith, 2007; Summerell, 2019). Some can also be found in caves (Bastian et al., 2010) or in man-made water systems (Sautour et al., 2012). *Fusarium* species are mostly known as phytopathogens, but some of them have been evidenced as contaminants in industrial processes, indoor environments, or pharmaceutical and food products (Abdel-Azeem et al., 2019), whereas others behave as opportunistic human/animal pathogens (Al-Hatmi et al., 2019; da Silva Santos et al., 2020) or are fungicolous (Torbati et al., 2021).

Focusing on plant-interacting *Fusarium* species, their saprophytic potential enables them to survive the winter in the crop debris, in the form of mycelium or spores that serve as plant-infecting propagules in the spring (Figure 1A) (Leslie and Summerell, 2006). *Fusarium* species vary in reproduction strategies, and they produce sexual spores as well as three types of asexual spores, i.e. (i) microconidia, which are typically produced under all environmental conditions, (ii) macroconidia, which are often found on the surface of diseased plants, and (iii) chlamydospores (survival structures), which are thick walled and produced from macroconidia or older mycelium (Ajmal et al., 2023). More than 80% of *Fusarium* species propagate using asexual spores, but not all of them produce all three types of spores, while sexual reproduction can involve self-fertility or out-crossing (Rana et al., 2017). Additionally, some species produce sclerotia, which promote survival in soil (Leslie and Summerell, 2006).

Fusarium shows climatic preferences, as *F. oxysporum*, *F. solani*, *F. verticillioides* (formerly *F. moniliforme*), *F. tricinctum, F. fujikuroi, F. pseudograminearum* and *F. graminearum* are found worldwide, *F. culmorum and F. avenaceum* in temperate regions, whereas some species occur in tropical or cool regions (Backhouse and Burgess, 2002; Babadoost, 2018; Senatore et al., 2021). The growth of each *Fusarium* species is largely determined by abiotic environmental conditions, notably temperature and humidity (Table S1) (Xu, 2003; Crous et al., 2021). However, other environmental factors, such as soil characteristics, cropping systems, agricultural practices and other human activities may influence the diversity of *Fusarium* in soils (Abdel-Azeem et al., 2019; Pfordt et al., 2020; Wang et al., 2020; Du et al., 2022).

2.2 Taxonomy of *Fusarium* spp.

The *Fusarium* genus exhibits high level of variability in terms of morphological, physiological and ecological properties, which represents a difficulty in establishing a consistent taxonomy of these species (Burgess et al., 1996). An additional difficulty for classification is the existence of both asexual (anamorph) and sexual (teleomorph) phases in their life cycle (Summerell, 2019). Based on the most widely used classification, the anamorph state of the genus *Fusarium* is classified in the family *Nectriaceae*, order *Hypocreales* and division *Ascomycota* (Crous et al., 2021). Several teleomorphs have been related to *Fusarium* species, but not all *Fusarium* species have a known sexual state in their life cycle (Munkvold, 2017). Most of these teleomorphs are in the genus *Gibberella*, including the economically important pathogens, such as *G. zeae* (anamorph *F. verticillioides*) and *G. moniliformis* (anamorph *F. verticillioides*) (Keszthelyi et al., 2007). Other *Fusarium* teleomorphs are members of the genera *Albonectria*, *Neocosmospora* or *Haematonectria*. Teleomorphs are usually not observed in the field, but rather under lab conditions. The dual anamorph-teleomorph nomenclature for fungi has now been abolished, and the name *Fusarium* has been retained for these fungi (Geiser et al., 2013).

The genus *Fusarium* is currently composed of 23 species complexes and at least 69 well-individualized species. *Fusarium* species complexes are groups of closely-related species with the same morphology, which are strongly supported from a phylogenetic perspective (O'Donnell et al., 2013; O'Donnell et al., 2015; Summerell, 2019; Xia et al., 2019; Laraba et al., 2021; Senatore et al., 2021; Yilmaz et al., 2021), as shown in Figure 2. Within a

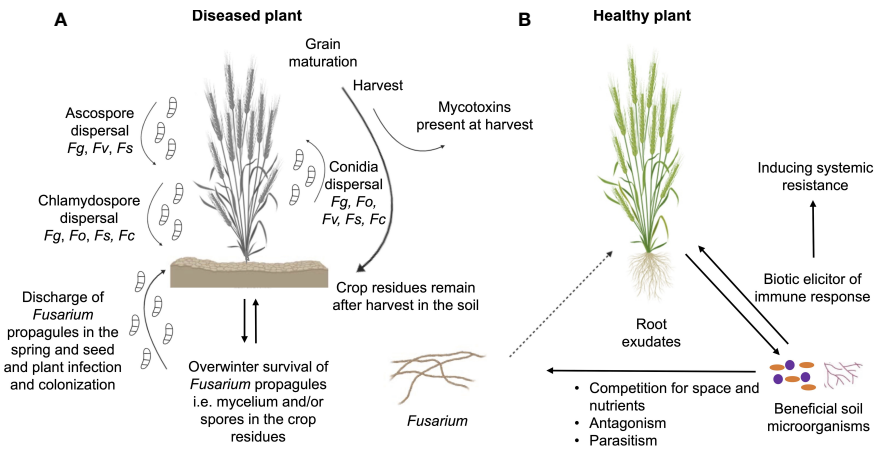

FIGURE 1
Interactions of *Fusarium* species with plant and other microbiota members. **(A)** Life cycle of *Fusarium* species and their mechanism of plant infection by producing three types of spores: ascospores, conidia and chlamydospores. *Fg, F graminearum*; *Fo, F oxysporum*; *Fs, F solani*; *Fc, F culmorum*; *Fv, F verticillioides*. **(B)** Dynamic interactions between beneficial soil microorganisms, plant and phytopathogenic *Fusarium* species.

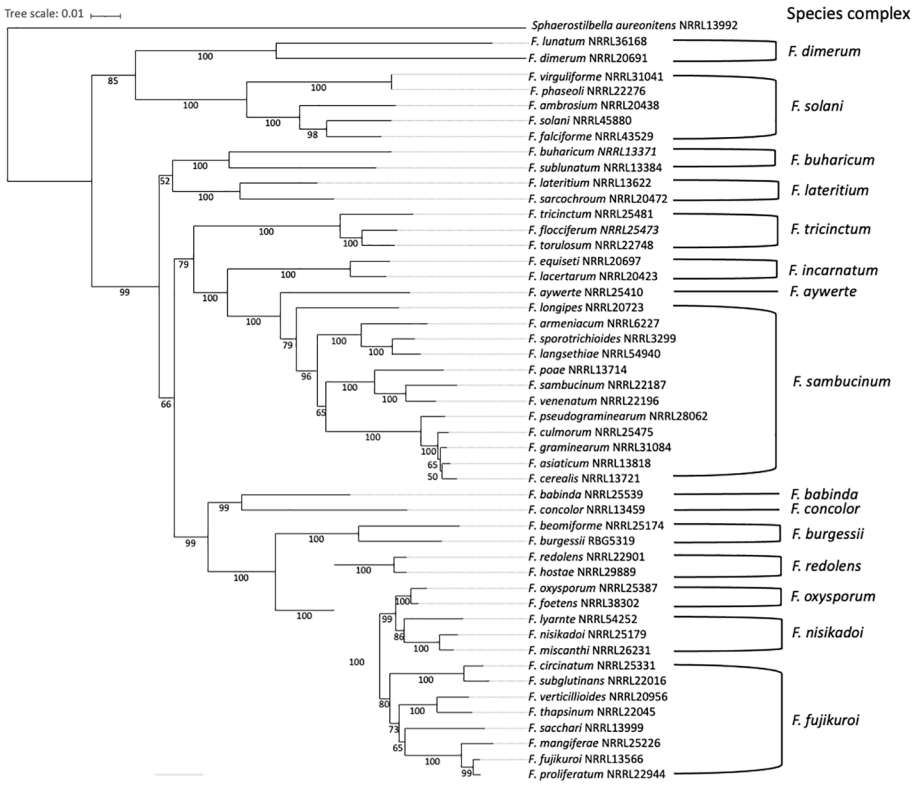

FIGURE 2
Phylogenetic relationship between pathogenic *Fusarium* species and 15 different species complexes. The distance-method tree (1000 bootstrap replicates) was inferred from the *rpb1* (RNA Polymerase 1) data set, using the SeaView multiplatform (Gouy et al., 2010). The tree was visualized using iTol (Letunic and Bork, 2021). *Sphaerostilbella aureonitens* NRRL 13992 was used as an outgroup. Species complexes delimitation is based on the phylogeny published in Summerell (2019).

given *Fusarium* species, certain strains may be pathogenic while others are not (Fuchs et al., 1997; De Lamo and Takken, 2020; Constantin et al., 2021). However, most phytopathogenic species belong to the *F. fujikuroi*, *F. sambucinum*, *F. oxysporum, F. tricinctum* or *F. solani* species complexes (O'Donnell et al., 2013; Senatore et al., 2021). Furthermore, *Fusarium* species capable of infecting a wide range of plants are classified into different *formae speciales*, based on the host plant they can infect (Edel-Hermann and Lecomte, 2019; Coleman, 2016). Currently, there are 106 well-described *F. oxysporum formae speciales* (Edel-Hermann and Lecomte, 2019) and 12 well-described *F. solani formae speciales* (Šišić et al., 2018).

Over the past 100 years, the taxonomy of *Fusarium* has undergone many changes, but most classification procedures have been based on the size and shape of the macroconidia, the presence or absence of microconidia and chlamydospores, and the structure of the conidiophores (Ristić, 2012). Identification of *Fusarium* species based on morphological characteristics also included observations of colony pigmentation and type of aerial mycelium (Crous et al., 2021). The standard method now used to identify *Fusarium* isolates to a species level is to sequence one (or more) of the following genes: translocation elongation factor-1α (*tef-1α*), RNA polymerase 1 and 2 (*rpb1* and *rpb2*), β-tubulin (*tub*), histone (*his*), ATP citrate lyase (*acl1*) or calmodulin (*CaM*) (Herron et al., 2015; Summerell, 2019; Crous et al., 2021; Laraba et al., 2021; Yilmaz et al., 2021). The *tef-1α* gene is a first-choice marker as it has good resolution power for the majority of *Fusarium* species, while sequencing the gene *rpb2* allows differentiation of close species. The other genetic markers mentioned have variable resolution power and are often used together with *tef-1α* or *rpb2* (Crous et al., 2021). The internal transcribed spacer regions of the ribosomal gene (*ITS*), which are common barcodes to identify fungi, are not recommended for *Fusarium* identification, as they are not sufficiently informative for a significant number of *Fusarium* species (Summerell, 2019).

2.3 Mechanisms of *Fusarium* infection, symptoms and etiology

Before infecting the host plant tissues, soil-borne pathogens may grow in the rhizosphere or on the host as saprophytes, managing to escape the rhizosphere battlefield (Raaijmakers et al., 2009). The outcome is directly influenced by host and microbial defense mechanisms, at the level of the holobiont (Berendsen et al., 2012; Vandenkoornhuyse et al., 2015). During their life cycle, plants are exposed to numerous phytopathogens, and they have developed different adaptive strategies. Upon pathogen attack, both composition and quantity of root metabolites may change (Rolfe et al., 2019), which can be useful for direct defense against the pathogens (Rizaludin et al., 2021), for signaling the impending

threat to the neighboring plants (Pélissier et al., 2021), or for recruiting beneficial microorganisms with biocontrol capabilities. The latter phenomenon is referred to as the 'a cry for help' strategy (Rizaludin et al., 2021).

If the pathogen manages to escape from the rhizosphere battlefield, the infection cycle can proceed. Plant infection by *Fusarium* occurs in a few successive stages (Figure 1A), which differs according to *Fusarium* species. Seeds infected with *Fusarium* in the previous season can also serve as disease initiators (Jiménez-Díaz et al., 2015). *F. graminearum* grows saprophytically on crop debris, which is the overwintering reservoir of the pathogen (Brown et al., 2010). The fungus may infect roots and cause damage to the collar (Ares et al., 2004). During the crop anthesis and under warm and humid weather conditions, asexual conidia, sexual ascospores or chlamydospores are dispersed by rain or wind and reach the outer anthers and outer glumes of the plant. After spore germination, hyphae penetrate the host plant through the cracked anthers, followed by inter- and intracellular mycelial growth, resulting in damage to host tissues and especially head blight disease (Brown et al., 2010). Unlike *F. graminearum*, *F. culmorum* produces only asexual conidia and chlamydospores, which are also dispersed by rain and wind, reaching plant heads and infecting the ears during the anthesis. Subsequently, conidia germinate on the lemma and palea, followed by inter- and intracellular mycelial growth (Wagacha and Muthomi, 2007). In contrast, the infection cycle of *F. oxysporum* begins when mycelia, germinating asexual conidia or chlamydspores enter the healthy plant through the root tip, lateral roots or root wounds. The fungus progresses intracellularly, entering the xylem sap flow and being transported to the aerial parts of the plant where it forms infection structures. The infection structures that form close the vascular vessels, disrupt nutrient translocation, leading to stomatal closure, leaf wilting and plant death (Banerjee and Mittra, 2018; Redkar et al., 2022a; Redkar et al., 2022b). In the case of *F. verticillioides*, infection starts when mycelia, asexual conidia or sexual ascospores are carried inside the seed or on the seed surface and later develop inside the growing plant, moving from the roots up to the maize kernels (Oren et al., 2003; Gai et al., 2018). Sometimes, the fungus colonizes and grows along the veins of the plant root, while sometimes it manages to penetrate the plant cells and form internal hyphae, therefore causing damage (Lei et al., 2011; Blacutt et al., 2018). Finally, for *F. solani*, the attachment of mycelia, asexual conidia, sexual ascospores or chlamydospores to the susceptible host is the first step in disease development, after which the fungus enters the host through stomata or the epidermis. Following penetration, *F. solani* is able to spread through the xylem, ultimately causing wilting of the host plant (Coleman, 2016).

It is reported that mycotoxins play a key role in pathogenesis, and that the aggressiveness of *Fusarium* depends on its toxin-producing capacity (Mesterházy, 2002; Xia et al., 2019; Laraba et al., 2021; Senatore et al., 2021; Yilmaz et al., 2021). Several mycotoxins are produced by *Fusarium* species, including the trichothecenes deoxynivalenol (DON) and nivalenol (NIV), zearalenone (ZEA), the cyclodepsipeptides beauvericin (BEA) and enniatins (ENN), and fusaric acid (Wagacha and Muthomi, 2007; Munkvold et al., 2021). The biosynthesis of these toxins is encoded by the *tri*, *pks, bea* and *fus* genes, respectively (Dhanti et al., 2017). However, not every species has the ability of producing all of the abovementioned mycotoxins. For example, DON and NIV are commonly produced by *F. graminearum* and *F. culmorum*, while ZEA and fusaric acid are often produced by some members of the *F. sambucinum* species complex (i.e. *F. graminearum*, *F. culmorum*), the *F. fujikuroi* complex (*F. verticillioides*) and the *F. incarnatum-equiseti* complex (Nešić et al., 2014; Munkvold et al., 2021), and BEA and ENN are produced by certain *F. oxysporum* and members of the *F. tricinctum* species complex (Munkvold et al., 2021; Senatore et al., 2021). DON production by *F. graminearum* is reported to be essential for disease development in wheat spikes (Cuzick et al., 2008). Spikes treated with DON or NIV led to yield losses even in the absence of the pathogen, indicating a strong negative effect of these trichothecenes on wheat growth (Ittu et al., 1995). In addition to DON, fusaric acid is also a virulence factor involved in programmed cell death (López-Díaz et al., 2018). It was shown that alkaline pH and low nitrogen and iron availabilities lead to increased fusaric acid production in *F. oxysporum* (Palmieri et al., 2023). Besides mycotoxins, there are other metabolites produced by *Fusarium* species that play a role in disease pathogenesis. Deletion of the *F. graminearum* gene cluster responsible for the synthesis of fusaoctaxin A abolished the fungal ability to colonize wheat coleoptiles (Jia et al., 2019). Extracellular lipases secreted by *F. graminearum* affected the plant's defense responses by inhibiting callose synthase activity (Blümke et al., 2014).

Diseases caused by *Fusarium* species include blights, wilts and rots of various crops in natural environments and in agroecosystems (Nelson et al., 1994; Ma et al., 2013). Fusarium Head Blight (FHB) or 'scab' is a disease caused primarily by the *F. graminearum* species complex. It is the fourth-ranked fungal phytopathogen in term of economic importance (Dean et al., 2012; Legrand et al., 2017), causing yield losses of 20% to 70% (Bai and Shaner, 1994). *F. graminearum* is responsible for kernel damage and mycotoxin production (Ma et al., 2013) in cereals like wheat, barley, rice and oats (Goswami and Kistler, 2004). Typical symptoms of FHB begin soon after flowering, as diseased spikelets gradually bleach, leading to bleaching of the entire head. After this stage, black spherical structures called perithecia may appear on the surface of diseased spikelets. Later, as the disease becomes more severe, the fungus begins to attack the kernels inside the head, causing them to wrinkle and shrink (Schmale and Bergstrom, 2003). FHB can also be caused by *F. culmorum*, which is dominant in cooler regions of Europe (Wagacha and Muthomi, 2007). Vascular wilt is responsible for severe losses in crops such as melon, tomato, cotton, bean and banana. It is caused by *Fusarium oxysporum*, the fifth most economically important fungal phytopathogen (Michielse and Rep, 2009; Dean et al., 2012; Husaini et al., 2018). Symptoms of vascular wilt are first observed on the older leaves, as they begin to droop, followed by defoliation and yellowing of the younger leaves and eventually, plant death (Britannica, 2017; Redkar et al., 2022a). Root, stem and foot rots of various non-grain host plants are often caused by *Fusarium solani*, and the disease symptoms depend on the host plant and the particular *forma specialis* (Voigt, 2002; Coleman, 2016). However, typical symptoms of root, stem and foot rots include brown lesions on the affected plant organs. *Fusarium verticillioides* causes ear and stalk rot in hosts such as maize, sorghum and rice (Murillo-Williams and Munkvold, 2008; Dastjerdi and Karlovsky, 2015), whereas *F. graminearum* is responsible for causing *Fusarium* ear and stalk rot in maize

(Goswami and Kistler, 2004). *Fusarium* ear rot is characterized by discoloration of single or multiple kernels in different areas of the ear, while early signs of stalk rot include lodging and discoloration of the stem.

3 Biocontrol agents against *Fusarium* and their modes of action

Plant-beneficial microorganisms present in the rhizosphere may protect plants from *Fusarium* pathogens, through different modes of action including (i) induction of resistance in the plant, (ii) competition with the pathogens for space and nutrients, (iii) amensalism based on the production of different metabolites or lytic enzymes, or (iv) parasitism (Figure 1B) (Nguvo and Gao, 2019; Morimura et al., 2020). Some of them are also able to inhibit mycotoxin synthesis or to enhance their detoxification (Legrand et al., 2017; Morimura et al., 2020). Certain biocontrol microorganisms have multiple modes of action, which may be expressed simultaneously or sequentially (Legrand et al., 2017).

3.1 Induced systemic resistance

Induced Systemic Resistance (ISR) is the phenomenon whereby a plant, once appropriately stimulated by biological or chemical inducers, exhibits enhanced resistance when challenged by a pathogen (Walters et al., 2013). ISR involves (i) the plant perception of inducing signals, (ii) signal transduction by plant tissues, and (iii) expression of plant mechanisms inhibiting penetration of the pathogen into the host tissues (Magotra et al., 2016). A wide variety of microorganisms, including the bacteria *Pseudomonas, Bacillus, Streptomyces* and the fungi *Trichoderma* and non-pathogenic *F. oxysporum* can induce ISR (Fuchs et al., 1997; Choudhary et al., 2007; Zhao et al., 2014; Galletti et al., 2020) in plants against *Fusarium* (Table 1). ISR in the plant-*Fusarium* system is based on microbial induction of the activity of various defense-related enzymes in plants, such as chitinase (Amer et al., 2014), lipoxygenase (Aydi Ben Abdallah et al., 2017), polyphenol oxidase (Akram et al., 2013), peroxidase, phenylalanine ammonia-lyase (Zhao et al., 2012), β-1,3-glucanase, catalase (Sundaramoorthy et al., 2012), and also the accumulation of phytoalexins, defense metabolites against fungi (Kuć, 1995). Cyclic lipopeptide antibiotics, e.g. fusaricidin (Li and Chen, 2019) and external cell components, e.g. lipopolysaccharides (LPS) (Leeman et al., 1995) can also trigger ISR. Some biocontrol agents can lead to ISR in different plant species, while other biocontrol agents show plant species specificity, suggesting specific recognition between microorganisms and receptors on the root surface (Choudhary et al., 2007).

Bacillus amyloliquefaciens subsp. *plantarum* strain SV65 was assessed on tomato plants infected or not with *F. oxysporum* f. sp.

TABLE 1 Biocontrol agents, plant-*Fusarium* systems and ISR mechanisms.

Biocontrol agent	Plant	Pathogen	Mechanism	Reference
Bacillus amyloliquefaciens	Tomato	*F. oxysporum*	Induction of genes coding for lipoxygenase or pathogenesis-related (PR) proteins, i.e. acidic protein PR-1 and PR-3 chitinases	Aydi Ben Abdallah et al., 2017
Bacillus thuringiensis	Tomato	*F. oxysporum*	Increase in polyphenol oxidase, phenyl ammonia lyase and peroxidase in plant	Akram et al., 2013
Bacillus megaterium	Tomato	*F. oxysporum*	Induction of chitinase, β-1,3-glucanase, peroxidase and polyphenol oxidase activities in plant	Amer et al., 2014
Bacillus subtilis	Tomato	*F. oxysporum*	Increased activities of phenylalanine ammonia-lyase, polyphenol oxidase, and peroxidase enzymes in plant	Akram et al., 2015
Bacillus subtilis and *Pseudomonas protegens* (in combination and alone)	Chilli	*F. solani*	Increased activities of peroxidase, polyphenol oxidase, phenylalanine ammonia lyase, β-1,3-glucanase, chitinase enzymes and phenol compounds involved in the synthesis of phytoalexins	Sundaramoorthy et al., 2012
Bacillus sp., *Brevibacillus brevis* and *Mesorhizobium ciceri* (in combination)	Chickpea	*F. oxysporum*	Increase in peroxidase, polyphenol oxidase, phenylalanine ammonia lyase, phenols and total proteins in plants	Kumari and Khanna, 2019
Brevibacillus parabrevis	Cumin	*F. oxysporum*	Increase in peroxidase and polyphenol oxidase in plants	Abo-Elyousr et al., 2022
Burkholderia gladioli	Saffron	*F. oxysporum*	Increased levels of endogenous jasmonic acid (JA) and expression of JA-regulated and plant defense genes	Ahmad et al., 2022
Pseudomonas aeruginosa	Tomato	*F. oxysporum*	Bacterial production of 3-hydroxy-5-methoxy benzene methanol	Fatima and Anjum, 2017
Pseudomonas simiae	Tomato	*F. oxysporum*	Bacterial production of lipopolysaccharides	Duijff et al., 1997

(Continued)

TABLE 1 Continued

Biocontrol agent	Plant	Pathogen	Mechanism	Reference
Pseudomonas defensor	Radish	*F. oxysporum*	Bacterial production of lipopolysaccharides	Leeman et al., 1995
Paenibacillus polymyxa	Cucumber	*F. oxysporum*	Bacterial production of fusaricidin, which induces ISR via salicylic acid	Li and Chen, 2019
P. fluorescens	Barley	*F. culmorum*	Changed transcript levels of lipid transfer proteins and protease inhibitors	Petti et al., 2010
Streptomyces enissocaesilis	Tomato	*F. oxysporum*	Increased catalase activity in plant	Abbasi et al., 2019
Streptomyces rochei	Tomato	*F. oxysporum*	Increased catalase and peroxidase activity in plant	Abbasi et al., 2019
Streptomyces bikiniensis	Cucumber	*F. oxysporum*	Increased activities of peroxidase, phenylalanine ammonia-lyase, and β-1,3-glucanase in plant	Zhao et al., 2012
Trichoderma gamsii	Maize	*F. verticillioides*	Enhanced transcript levels of ISR marker genes	Galletti et al., 2020
Trichoderma longibrachiatum	Onion	*F. oxysporum*	Accumulation of 25 stress-response metabolites	Abdelrahman et al., 2016
Non-pathogenic *Fusarium oxysporum*	Tomato	*F. oxysporum*	Increased activities of chitinase, β-1,3-glucanase and β-1,4-glucosidase	Fuchs et al., 1997

lycopersici (FOL). The expression of genes coding for lipoxygenase or pathogenesis-related (PR) proteins, i.e. acidic protein PR-1 and PR-3 chitinases was induced by *B. amyloliquefaciens* subsp. *plantarum* SV65 in both FOL-inoculated and uninoculated plants, suggesting its ability to induce ISR (Aydi Ben Abdallah et al., 2017). Inoculation of chilli plants with *Bacillus subtilis* EPCO16 and EPC5 and *P. protegens* Pf1, separately or in combination, induced ISR, with enhanced phytoalexin activities, and protected plants against *F. solani* (Sundaramoorthy et al., 2012). Inoculation of chickpea plants with a combination of *Bacillus* sp., *Brevibacillus brevis* and *Mesorhizobium ciceri* lead to the accumulation of peroxidase, polyphenol oxidase, phenylalanine ammonia lyase and phenols in plants as well as resistance to *F. oxysporum* (Kumari and Khanna, 2019). *Paenibacillus polymyxa* WLY78 controls Fusarium wilt, caused by *Fusarium oxysporum* f. sp. *cucumerinum*, through the production of fusaricidin, which can induce ISR in cucumber via the salicylic acid pathway (Li and Chen, 2019). Tomato showed increased catalase and peroxidase activities when treated with either *Streptomyces* sp. IC10 and Y28, or with Y28 alone, respectively, outlining a strain-specific ISR in tomato against Fusarium wilt mediated by FOL (Abbasi et al., 2019). *Streptomyces bikiniensis* increased the activities of peroxidase, phenylalanine ammonia-lyase and β-1,3-glucanase in cucumber leaves (Zhao et al., 2012). Nonpathogenic *Fusarium oxysporum* Fo47 can triger induced resistance to FOL and protects tomato from Fusarium wilt (Fuchs et al., 1999). *Trichoderma gamsii* IMO5 increased transcript levels of ISR-marker genes *ZmLOX10*, *ZmAOS* and *ZmHPL* in maize leaves, thereby protecting the plant from the pink ear rot pathogen *F. verticillioides* (Galletti et al., 2020).

An important determinant of biocontrol efficacy is the population density of ISR-triggering microorganisms. For example, ~10^5 CFU of *Pseudomonas defensor* (ex *fluorescens*) WCS374 per g of root are required for significant suppression of Fusarium wilt of radish (Raaijmakers et al., 1995). Another important feature of ISR in plants is that its effects are not only expressed at the site of induction but also in plant parts that are distant from the site of induction (Pieterse et al., 2014). For example, root-colonizing *Pseudomonas simiae* (ex *fluorescens*) WCS417r induced resistance in carnation, with phytoalexin accumulation in stems, and protected shoots from *F. oxysporum* (Van Peer et al., 1991). Priming of barley heads with *P. fluorescens* MKB158 led to changes in the levels of 1203 transcripts (including some involved in host defense responses), upon inoculation with pathogenic *F. culmorum* (Petti et al., 2010).

3.2 Competition for space and nutrients

In the case of competition, biocontrol of pathogens occurs when another microorganism is able to colonize the environment faster and use nutrient sources more efficiently than the pathogen itself, especially under limited conditions (Maheshwari et al., 2013; Legrand et al., 2017). Bacteria and fungi have the ability to compete with *Fusarium*, but the underlying mechanism of competition is sometimes unclear. For example, competition between non-pathogenic *F. oxysporum* strains and pathogenic *F. oxysporum* has been described, reducing disease incidence (Eparvier and Alabouvette, 1994; Fuchs et al., 1999). Similarly, a non-aflatoxigenic *Aspergillus flavus* strain was found to outcompete a mycotoxin-producing *F. verticillioides* during colonization of maize (Reis et al., 2020). Competition may involve bacteria such as *Pseudomonas capeferrum* (ex *putida*) strain WCS358, which suppresses Fusarium wilt of radish (Lemanceau et al., 1993).

In some cases, traits involved in competition have been identified. In *P. putida* (Trevisan) Migula isolate Corvallis,

competition for root colonization entails plant's production of agglutinin, and *P. putida* mutants lacking the ability to agglutinate with this plant glycoprotein showed reduced levels of rhizosphere colonization and suppression of Fusarium wilt of cucumber (Tari and Anderson, 1988). *P. capeferrum* WCS358 suppresses Fusarium wilt of radish by competing for iron through the production of its pseudobactin siderophore (Lemanceau et al., 1993). In addition to bacteria, the fungus *Trichoderma asperellum* strain T34 can control the disease caused by *F. oxysporum* f. sp. *lycopersici* on tomato plants by competing for iron (Segarra et al., 2010).

3.3 Amensalism based on antibiosis or lytic enzymes

Another important microbial mechanism to suppress plant pathogens is the secretion of inhibitors by beneficial microorganisms. They include anti-fungal secondary metabolites, sometimes termed antibiotics (e.g. fengycin, iturin, surfactin (Chen et al., 2018), fusaricidin and polymyxin (Zalila-Kolsi et al., 2016)), as well as Volatile Organic Compounds (VOCs; Zaim et al., 2016; Legrand et al., 2017) (Table 2). Extracellular lytic enzymes such as cellulase, chitinase, pectinase, xylanase (Khan et al., 2018), protease and glucanase (Saravanakumar et al., 2017), can also interfere with *Fusarium* growth or activity.

Bacillota representatives (formerly *Firmicutes*), i.e. *Bacillus* and *Brevibacillus* species are highlighted in several studies as candidates for *Fusarium* biocontrol through production of anti-fungal metabolites (Palazzini et al., 2007; Zhao et al., 2014; Chen et al., 2018; Johnson et al., 2020). *Bacillus subtilis* SG6 has the ability to produce fengycins and surfactins acting against *F. graminearum* (Zhao et al., 2014), whereas *Bacillus velezensis* LM2303 exhibited strong inhibition of *F. graminearum* and significantly reduced FHB severity under field conditions (Chen et al., 2018). Genome mining of *B. velezensis* LM2303 identified 13 biosynthetic gene clusters encoding secondary metabolites and chemical analysis confirmed their presence. These metabolites included three antifungal metabolites (fengycin B, iturin A, and surfactin A) and eight antibacterial metabolites (surfactin A, butirosin, plantazolicin and hydrolyzed plantazolicin, kijanimicin, bacilysin, difficidin, bacillaene A and bacillaene B, 7-o-malonyl macrolactin A and 7-o-succinyl macrolactin A) (Chen et al., 2018). *Brevibacillus fortis* NRS-1210 produces edeine, a compound with antimicrobial activity, which inhibits chlamydospore germination and conidia growth in *F. oxysporum* f. sp. *cepae* (Johnson et al., 2020). *Pseudomonadota* representatives (formerly *Proteobacteria*) are also known for disturbing *Fusarium* growth or activity. Thin layer chromatography analysis showed that *Gluconacetobacter diazotrophicus* produces pyoluteorin, which is involved in the suppression of *F. oxysporum* (Logeshwarn et al., 2011), while *Burkholderia* sp. HQB-1 produces phenazine-1-carboxylic acid, which is efficient at controlling Fusarium wilt of banana, caused by *F. oxysporum* f. sp. *cubense* (Xu et al., 2020). *Pseudomonas* sp. EM85 was successful in suppressing disease caused by *F. verticillioides* and *F. graminearum*, by producing antifungal antibiotics and fluorescent pigments (Pal et al., 2001). Besides bacteria, *Trichoderma* fungi synthesize a number of secondary metabolites such as pyrones (which completely inhibit spore germination of *F. oxysporum*), koningins (which affect the growth of *F. oxysporum*) and viridin (which prevents the germination of spores of *F. caeruleum*) (Reino et al., 2008).

VOCs have recently received more attention, as they can enable interactions between organisms in the soil ecosystem through both

TABLE 2 Biocontrol agents, plant-*Fusarium* systems and biocontrol enzymes and metabolites.

Biocontrol agents	*Fusarium* pathogens	Biocontrol enzymes and metabolites	References
Bacillus subtilis	*F. oxysporum* *F. graminearum*	Cellulase, chitinase, pectinase, xylanase, protease, fengycins and surfactins	Zhao et al., 2014; Zalila-Kolsi et al., 2016; Khan et al., 2018
Bacillus velezensis	*F. graminearum* *F. culmorum*	Fengycin B, iturin A, surfactin A and siderophores	Chen et al., 2018; Adeniji et al., 2019
Bacillus pumilus	*F. oxysporum*	Chitinolytic enzymes and antibiotic surfactin	Agarwal et al., 2017
Bacillus amyloliquefaciens	*F. graminearum*	Iturin and surfactin	Zalila-Kolsi et al., 2016
Brevibacillus fortis	*F. oxysporum*	Edeine	Johnson et al., 2020
Brevibacillus reuszeri	*F. oxysporum*	Chitinolytic enzymes	Masri et al., 2021
Burkholderia sp.	*F. oxysporum*	Phenazine-1-carboxylic acid	Xu et al., 2020
Chryseobacterium sp.	*F. solani*	VOCs	Tyc et al., 2015
Gluconacetobacter diazotrophicus	*F. oxysporum*	Antibiotic (pyoluteorin) and VOCs	Logeshwarn et al., 2011
Kosakonia arachidis	*F. verticillioides* *F. oxysporum*	Chitinase, protease, cellulase and endoglucanase	Singh et al., 2021
Lysobacter antibioticus	*F. graminearum*	VOCs	Kim et al., 2019
Paenibacillus polymyxa	*F. graminearum* *F. oxysporum*	Fusaricidin, polymyxin and VOCs	Raza et al., 2015; Zalila-Kolsi et al., 2016
Pseudomonas sp.	*F. verticillioides* *F. graminearum*	Antifungal antibiotics and fluorescent pigments	Pal et al., 2001
Streptomyces spp.	*F. oxysporum*	Antibiotic compounds, lipopeptin A and lipopeptin B	Cuesta et al., 2012; Wang et al., 2023
Trichoderma sp.	*F. oxysporum* *F. caeruleum*	Pyrones, koningins and viridins	Reino et al., 2008

water and air phases (De Boer et al., 2019). *Paenibacillus polymyxa* WR-2 produced VOCs when cultivated in the presence of organic fertilizer and root exudates. Among them, benzothiazole, benzaldehyde, undecanal, dodecanal, hexadecanal, 2-tridecanone and phenol inhibited mycelial growth and spore germination of *F. oxysporum* f. sp. *niveum* (Raza et al., 2015). *Chryseobacterium* sp. AD48 inhibited growth of *F. solani* through the production of VOCs (Tyc et al., 2015). VOCs produced by *Lysobacter antibioticus* HS124 enhanced mycelial development, but they also reduced sporulation and spore germination of *F. graminearum* at the same time (Kim et al., 2019). In addition, testing the antagonistic mechanisms of *Aspergillus pseudocaelatus* and *T. gamsii* revealed the presence of the VOCs 2,3,4-trimethoxyphenylethylamine, 3-methoxy-2-(1-methylethyl)-5-(2-methylpropyl) pyrazine, (Z)-9-octadecenamide, pyrrolo [1,2-a] pyrazine-1,4-dione, hexahydro-3-(2-methylpropyl)-, thieno [2,3-c] pyridine-3-carboxamide,4,5,6,7-tetrahydro-2-amino-6-methyl- and hexadecanamide, which have an inhibitory activity against *F. solani* (Zohair et al., 2018).

Regarding extracellular lytic enzymes, *B. subtilis* 30VD-1 inhibited FOL by producing cellulase, chitinase, pectinase, xylanase and protease (Khan et al., 2018), while *Bacillus pumilus* synthesized a chitinolytic enzyme that reduced severity of disease caused by *F. oxysporum* on buckwheat under gnotobiotic conditions (Agarwal et al., 2017). *Brevibacillus reuszeri* affected the growth of *F. oxysporum* by producing chitinolytic enzymes (Masri et al., 2021). *Kosakonia arachidis* EF1 produced different cell-wall degrading enzymes, such as chitinases, proteases, cellulases and endoglucanases, which inhibited growth of *F. verticillioides* and *F. oxysporum* f. sp. *cubense*. Scanning electron microscopy revealed broken fungal mycelia surface and hyphae fragmentation when pathogens were grown in the presence of *K. arachidis* EF1 (Singh et al., 2021).

3.4 Parasitism

Mycoparasitism is an ancient lifestyle, during which one fungus parasitizes another fungus (Kubicek et al., 2011). It involves direct physical contact with the host mycelium (Pal and McSpadden Gardener, 2006), secretion of cell wall-degrading enzymes and subsequent hyphal penetration (Viterbo et al., 2002). Mycoparasitic relationships can be biotrophic, where the host remains alive and the mycoparasitic fungus obtains nutrients from the mycelium of its partner, or necrotrophic, where the parasite contacts and penetrates the host, resulting in the death of the host and allowing the mycoparasite to use the remains of the host as a nutrient source (Jeffries, 1995). Several species of fungi are mycoparasitic, of which *Trichoderma* is the best described. Contact between the mycoparasitic fungi *Gliocladium roseum*, *Penicillium frequentans*, *T. atroviride*, *T. longibrachiatum* or *T. harzianum* and their phytopathogenic targets *F. culmorum*, *F. graminearum* and *F. nivale* triggers the formation of various mycoparasitic structures, such as hooks and pincers, which lead to cell disruption in the phytopathogens (Pisi et al., 2001). When *T. asperellum* and *T. harzianum* were grown in the presence of *F. solani* cell wall, they secreted several cell wall-degrading enzymes, such as β-1,3-glucanase, *N*-acetylglucosaminidases, chitinase, acid phosphatase, acid proteases and alginate lyase (Qualhato et al., 2013), and similarly, *Clonostachys rosea* produced chitinase and β-1,3-glucanase in the presence of *F. oxysporum* cell wall (Chatterton and Punja, 2009). *Sphaerodes mycoparasitica* is a biotrophic fungus that parasitizes *F. avenaceum*, *F. oxysporum* and *F. graminearum* hyphae and forms hooks as parasitic structures (Vujanović and Goh, 2009). However, the direct contribution of mycoparasitism to biological control is difficult to quantify as mycoparasitic fungi typically exhibit a number of different biocontrol mechanisms (Pal and McSpadden Gardener, 2006).

3.5 Inhibition and detoxification of mycotoxins

Biocontrol research often focuses on pathogen inhibition, and effects on mycotoxin synthesis or detoxification are often neglected (Pellan et al., 2020). It can be expected that *Fusarium* inhibition will diminish mycotoxin synthesis, but one comprehensive study found that *B. amyloliquefaciens* FZB42 inhibited *F. graminearum* but at the same time stimulated biosynthesis of DON toxin (Gu et al., 2017). Conversely, DON production of *F. graminearum* (on wheat kernels) was reduced by more than 80% with *B. amyloliquefaciens* WPS4-1 and WPP9 (Shi et al., 2014), and *Paenibacillus polymyxa* W1-14-3 and C1-8-b (He et al., 2009), whereas *Pseudomonas* strains MKB158 and MKB249 significantly reduced DON production in *F. culmorum*-infected wheat seeds (Khan and Doohan, 2009). *Pseudomonas* sp. MKB158 lowered expression of the gene coding for trichodiene synthase (an enzyme involved in the production of trichothecene mycotoxins in *Fusarium*) by 33%, in wheat treated with *F. culmorum* (Khan et al., 2006). DON production in both *F. graminearum* and *F. verticillioides* was also inhibited by the fungus *T. asperellum* TV1 and the oomycete *Pythium oligandrum* M1/ATCC (Pellan et al., 2020). Other mycotoxins may be targeted, as *Trichoderma harzianum* Q710613, *T. atroviride* Q710251 and *T. asperellum* Q710682 decreased ZEA production in a dual-culture assay with *F. graminearum* (Tian et al., 2018), and *Streptomyces* sp. XY006 lowered the synthesis of fusaric acid in *Fusarium oxysporum* f. sp. *cubense* (Wang et al., 2023).

4 Soils suppressive to *Fusarium* diseases

4.1 General suppressiveness

Soils that are suppressive to soil-borne diseases have been known for more than 70 years (Vasudeva and Roy, 1950), and disease suppression is associated primarily with the activity of beneficial microorganisms (Schlatter et al., 2017). These microorganisms interact with phytopathogens, thus affecting their survival, development or infection of the plant (Weller et al., 2002; Raaijmakers et al., 2009). Two types of soil suppressiveness have been described, i.e. general (microbial community-based) suppressiveness and specific (microbial population-based)

suppressiveness (Schlatter et al., 2017). General suppressiveness is dependent on the entire soil microbial biomass, which causes pathogen inhibition through various mechanisms, especially competition and the microbial release of inhibitors (Garbeva et al., 2011; De Boer et al., 2019), and it cannot be transferred experimentally between the soils (Weller et al., 2002). Hence, all soils may present some level of general suppressiveness to soil-borne diseases, and this level depends on soil type, agricultural practices and total microbial activity (Janvier et al., 2007; Raaijmakers et al., 2009).

General suppressiveness typically results in the inability of the pathogen to survive and proliferate in soil, and is termed fungistasis in the case of fungal phytopathogens. Fungistasis can affect *Fusarium* pathogens (De Boer et al., 2019; Legrand et al., 2019), but its significance in relation to different *Fusarium* species or *formae speciales* needs clarification. Legrand et al. (2019) determined the soil fungistasis status of 31 wheat fields in the case of *F. graminearum*, highlighting higher bacterial diversity, a higher prevalence of *Pseudomonas* and *Bacillus* species and a denser network of co-occurring bacterial taxa in soils with fungistasis. It suggests the importance of cooperations within diversified bacterial communities (including with antagonistic taxa) to control *F. graminearum* in soil (Legrand et al., 2019). Accordingly, both bacterial and fungal communities differed between Fusarium wilt-diseased soils vs healthy (presumably suppressive) soils taken from from eight countries and grown with different crop plants (Yuan et al., 2020).

4.2 Specific suppressiveness to *Fusarium* diseases

Besides general suppressiveness, there is also specific suppression to certain diseases, which relies on the activity of a few plant-protecting microbial groups (Weller et al., 2007; Almario et al., 2014; Mousa and Raizada, 2016). Specific suppressiveness may be conferred to non-suppressive soils (i.e. conducive soils) by inoculating them with 0.1% - 10% of suppressive soil (Garbeva et al., 2004; Raaijmakers et al., 2009). Although abiotic factors, such as soil physicochemical properties, may contribute to the control of a given pathogen, specific suppressiveness is essentially a phenomenon mediated by beneficial soil microorganisms, since sterilization processes convert suppressive into conducive soils (Garbeva et al., 2004). It is expected that specific suppressiveness entails the contribution of a few plant-protecting microbial groups (Weller et al., 2007), but microbial community comparison of suppressive vs conducive soils may evidence significant differences for a large number of taxa (Kyselková et al., 2009; Legrand et al., 2019; Ossowicki et al., 2020; Yuan et al., 2020; Lv et al., 2023).

The phenomenon of disease suppressiveness has been described for many soil-borne fungal pathogens, including *Gaeumannomyces graminis* var. *tritici* (Shipton et al., 1973; Weller et al., 2007; Schlatter et al., 2017), *Thievalopsis basicola* (Stutz et al., 1986; Almario et al., 2014) and *Rhizoctonia solani* (Mendes et al., 2011; Schlatter et al., 2017). It is also well established in the case of several *Fusarium* pathogenic species (Table 3), such as *F. culmorum* on wheat (in the Netherlands and Germany; Ossowicki et al., 2020) and barley (in Denmark; Rasmussen et al., 2002), *F. oxysporum* f. sp. *albedinis* on palm tree (in Marocco; Rouxel and Sedra, 1989), *F. oxysporum* f. sp. *batatas* on sweet potato (in California; Smith and Snyder, 1971), *F. oxysporum* f. sp. *cubense* on banana (in India, Indonesia, China, Gran Canaria island and several Central America states; Stotzky and Torrence Martin, 1963; Domínguez et al., 1996; Shen et al., 2015b; Wang et al., 2019; Nisrina et al., 2021; Yadav et al., 2021; Fan et al., 2023), *F. oxysporum* f. sp. *cucumerinum* on cucumber (in California; Sneh et al., 1984) and cape gooseberry (in Colombia; Bautista et al., 2023), *F. oxysporum* f. sp. *dianthi* on carnation (in Italy; Garibaldi et al., 1983), *F. oxysporum* f. sp. *fragariae* on strawberry (in Korea; Cha et al., 2016), *F. oxysporum* f. sp. *lini* on flax (in Italy, California; Kloepper et al., 1980; Tamietti and Pramotton, 1990), *F. oxysporum* f. sp. *lycopersici* on tomato (in France, Italy; Tamietti and Alabouvette, 1986; Tamietti et al., 1993) and wheat (in Italy; Tamietti and Matta, 1984), *F. oxysporum* f. sp.

TABLE 3 List of locations with soils suppressive to *Fusarium* diseases known to date, with a pathosystem, disease and the underlying suppression mechanism.

Pathogen	Disease	Country	Suppression mechanism	References
F. culmorum	Seedling blight of barley	Denmark	Soil microbiota that has a more efficient cellulolytic activity	Rasmussen et al., 2002
F. culmorum	*F. culmorum* disease in wheat	Netherlands and Germany	No specific taxa, but a guild of bacteria working together	Ossowicki et al., 2020
F. graminearum	No disease supression tested, only fungistasis	Britanny, France	*Pseudomonas* and *Bacillus*	Legrand et al., 2019
F. graminearum Fg1	Wheat damping-off	Serbia	Under progress	Todorović et al., unpublished data
F. oxysporum f. sp. *albedinis*	Bayoud vascular wilt of palm tree	Marocco	Competition with soil microbiota	Rouxel and Sedra, 1989
F. oxysporum f. sp. *melonis*	Fusarium wilt of watermelon	Châteaurenard, France	Competition with soil microbiota including non-pathogenic *Fusarium*	Louvet et al., 1976; Alabouvette et al., 1985

(Continued)

TABLE 3 Continued

Pathogen	Disease	Country	Suppression mechanism	References
F. oxysporum f. sp. *fragariae*	Fusarium wilt of strawberry	Korea	*Streptomyces*, wilt-suppressive soil that was developed through monoculture	Cha et al., 2016
F. oxysporum f. sp. *dianthi*	Vascular wilting disease of carnations	Albenga, Italy	Competition with other *Fusarium*	Garibaldi et al., 1983
F. oxysporum f. sp. *batatas*	Fusarium wilt on sweet potato	California, USA	No data	Smith and Snyder, 1971
F. oxysporum f. sp. *cubense*	Fusarium wilt of banana disease	Ayodhya district, India	*Bacillus licheniformis* producing anti-fungal secondary metabolites	Yadav et al., 2021
F. oxysporum f. sp. *cubense*	Fusarium wilt of banana disease	Gran Canaria, Spain	Sodium in soil	Domínguez et al., 1996
F. oxysporum f. sp. *cubense*	Fusarium wilt of banana disease	Indonesia	*Pseudomonas* and *Burkholderia*	Nisrina et al., 2021
F. oxysporum f. sp. *cubense*	Fusarium wilt of banana disease	Honduras, Costa Rica, Panama and Guatemala	Clay mineralogy, presence of montmorillonite-type clay in suppressive soil	Stotzky and Torrence Martin, 1963
F. oxysporum f. sp. *cubense*	Fusarium wilt of banana disease	Hainan, China	*Pseudomonas* inducing jasmonate and salicylic acid pathways and shared core microbiome in suppressive soils	Shen et al., 2015b; Zhou et al., 2019; Shen et al., 2022; Lv et al., 2023; Wang et al., 2023
F. oxysporum f. sp. *cubense*	Fusarium wilt of banana disease	Yunnan, China	*Bacillus* and *Sphingomonas* negatively correlated to *F. oxysporum*. *B. velezensis* strain YN1910 presented biocontrol properties	Fan et al., 2023
F. oxysporum f. sp. *cucumerinum*	Fusarium wilt of cape gooseberry	Colombia	Higher prevalence of certain bacterial taxa	Bautista et al., 2023
F. oxysporum f. sp. *physalis*	Fusarium wilt of cucumber	California, USA	*Pseudomonas* siderophores and lytic bacteria	Sneh et al., 1984
F. oxysporum f. sp. *lini*	Fusarium wilt of flax	California, USA	*Pseudomonas* siderophores	Kloepper et al., 1980
F. oxysporum f. sp. *lini*	Fusarium wilt of flax	Carmagnola and Santena, Italy	Competition with other *Fusarium*	Tamietti and Pramotton, 1990
F. oxysporum f. sp. *lycopersici*	Fusarium wilt of tomato	Noirmoutier, France	Non-pathogenic *F. oxysporum*	Tamietti and Alabouvette, 1986
F. oxysporum f. sp. *lycopersici*	Fusarium wilt of wheat	Albenga, Italy	Non-pathogenic *F. oxysporum* inducing plant defense	Tamietti and Matta, 1984
F. oxysporum f. sp. *lycopersici*	Fusarium wilt of tomato	Albenga, Italy	Non-pathogenic *F. oxysporum* inducing plant defense	Tamietti et al., 1993
F. oxysporum f. sp. *niveum*	Fusarium wilt of watermelon	Florida, USA	Wilt-suppressive soil that was developed through monoculture	Larkin et al., 1993
F. oxysporum f. sp. *radicis-cucumerinum*	Cucumber crown and root rot	Israel	Suppressiveness induced by mixing sandy soil with wild rocket (*Diplotaxis tenuifolia*) debris under field conditions	Klein et al., 2013
F. udum Butl.	Wilt of pigeon-pea	Dehli, India	Soil microbiota	Vasudeva and Roy, 1950

melonis on melon (in France; Louvet et al., 1976), *F. oxysporum* f. sp. *niveum* on watermelon (in Florida; Larkin et al., 1993), *F. oxysporum* f. sp. *radicis-cucumerinum* on cucumber (in Israel; Klein et al., 2013), *F. udum* on pigeon-pea (in India; Vasudeva and Roy, 1950), and *F. graminearum* on wheat (in Serbia; Todorović et al., unpublished data). Therefore, unlike with other pathogenic taxa, suppressiveness is documented across a wide range of *Fusarium* pathosystems. It also appears that suppressiveness to *Fusarium* diseases occurs in numerous parts of the world (Figure 3).

4.3 Natural and induced specific suppressiveness to *Fusarium* diseases

Specific suppressiveness is sometimes an intrinsic property of the soil and persists over years, despite changing ecological conditions related to crop rotation. This natural/long-term suppressiveness is well documented for several pathosystems, for instance in Swiss soils suppressive to tobacco black root rot (*T. basicola*) near Morens (Stutz et al., 1986). Suppressive and

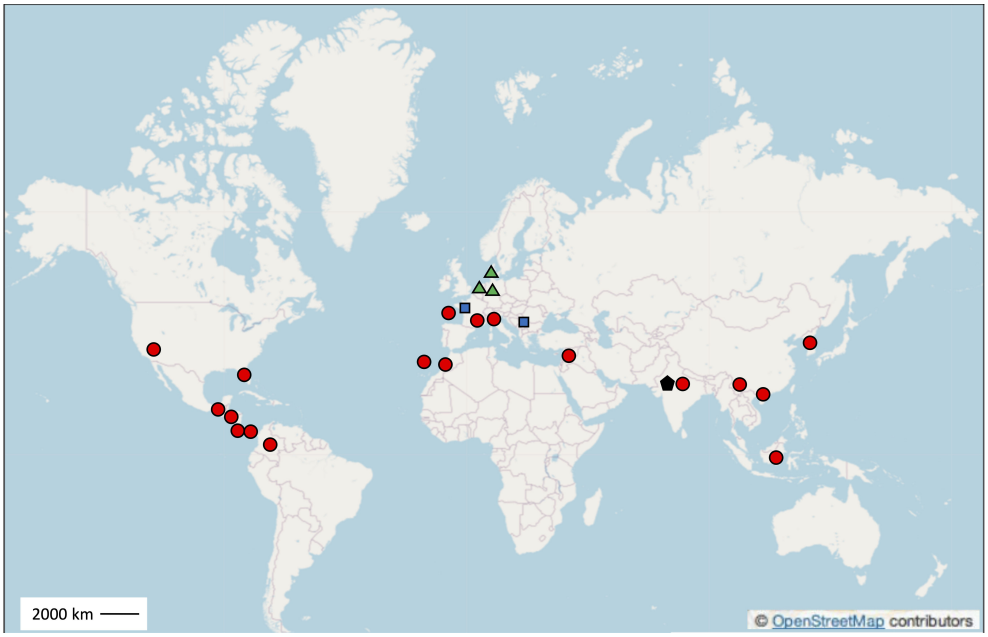

FIGURE 3
Geographic locations of the main field sites with soils documented to be suppressive to *Fusarium* diseases, in Europe including France (Noirmoutier Island, Châteaurenard in Southeast France, and Brittany), Denmark, The Netherlands, Germany, Italy (Albenga, Carmagnola, and Santena), Gran Canaria Island (Spain, located in the Atlantic Ocean), and Serbia, in North America (California and Florida), Central America (Honduras, Costa Rica, Panama, and Guatemala), South America (Colombia), Asia (Korea, China, India, Israel, and Indonesia), and Africa (Morocco). Each location is marked with the corresponding pathogen: *F. oxysporum* (indicated by a red dot), *F. culmorum* (green triangle), *F. graminearum* (blue square), and *F. udum* (black pentagon).

conducive soils may be located at small geographic distances in the landscape, and differences in plant disease incidence between neighbouring fields that share similar climatic conditions and agronomic practices are attributed by the differences in the resident microbiota in these soils (Almario et al., 2014). Natural suppressiveness has also been extensively studied in the case of *Fusarium* diseases, in particular with the Fusarium wilt suppressive soils of Salinas Valley (California) or Châteaurenard (France). In these soils, Fusarium wilt disease remains minor despite the long history of cultivation of different crops, and the introduction of small amount of these soils to sterilized suppressive soil or conducive soil significantly decreased Fusarium wilt disease incidence (Scher and Baker, 1980; Alabouvette, 1986). In both locations, the small level of disease in plants cannot be attributed to the absence of *Fusarium* in the soil, but rather to plant protection by the soil microbiota (Sneh et al., 1984; Alabouvette et al., 1985; Siegel-Hertz et al., 2018), as found in later investigations (Bautista et al., 2023).

Specific disease suppressiveness can also result from particular farming practices leading to the built-up of a plant-protecting microbiota. Often, this takes place following crop monoculture, typically after early disease outbreak, and is examplified by take-all decline of wheat (Weller et al., 2002; Sanguin et al., 2009) and barley (Schreiner et al., 2010). Induced suppressiveness is initiated and maintained by monoculture, in the presence of the pathogen *Gaeumannomyces graminis* var. *tritici* (Weller et al., 2002). Soil suppressiveness to *Fusarium* diseases is usually natural, but cases of induced suppressiveness are also documented. Thus, soils found in Hainan island (China) that were grown for years with banana in confontration with pathogenic *F. oxysporum* displayed rhizosphere enrichment in microbial taxa conferring protection from banana wilt (termed banana Panama disease) (Shen et al., 2022), watermelon monoculture in Florida induced suppressiveness to wilt caused by *F. oxysporum* f. sp. *niveum* (Larkin et al., 1993), and 15 years of strawberry monoculture in Korea triggered suppressiveness to wilt caused by *F. oxysporum* f. sp. *fragariae* (Cha et al., 2016). Soil addition of wild rocket residues resulted in suppressiveness to cucumber crown and root rot (*F. oxysporum* f. sp. *radicis-cucumerinum*) in Israel (Klein et al., 2013), whereas suppressiveness to Fusarium wilt can also be induced by microbial biofertilizer inoculants reshaping the soil microbiome (Xiong et al., 2017). Thus, organic fertilizer containing *B. amyloliquefaciens* W19 enhanced levels of indigenous *Pseudomonas* spp. and provided suppression of Fusarium wilt of banana (Tao et al., 2020). The combined action of *B. amyloliquefaciens* W19 and *Pseudomonas* spp. is thought to cause a decrease in *Fusarium* density in the root zone of banana. Organic fertilizers inoculated with *Erythrobacter* sp. YH-07 controlled Fusarium wilt in tomato, as a direct result of the bacteria and indirectly by altering the composition of the microbial community (Tang et al., 2023). Organic fertilizer amended with *Bacillus* and *Trichoderma* resulted in an increase in indigenous *Lysobacter* spp., thus indirectly inducing suppression of Fusarium wilt of vanilla (Xiong et al., 2017).

5 The microbiome of soils suppressive to *Fusarium* diseases

5.1 Biocontrol microorganisms in soils suppressive to *Fusarium* diseases

Many biocontrol strains originate from suppressive soils, and they were investigated as a mean to understand disease suppressiveness. In the case of *Fusarium* diseases, examples include *Pseudomonas* sp. Q2-87 (*P. corrugata* subgroup) (Weller et al., 2007), isolated from wheat in take-all decline soils but that protects tomato from *F. oxysporum* f. sp. *radicis-lycopersici*, *Pseudomonas* sp. C7 (*P. corrugata* subgroup) (Lemanceau and Alabouvette, 1991) isolated from soil suppressive to Fusarium wilt of tomato, and non-pathogenic *F. oxysporum* strains Fo47 (Fuchs et al., 1997; Duijff et al., 1998; Fuchs et al., 1999), CAV 255 (Sajeena et al., 2020) and Ro-3 (Bubici et al., 2019). Based on the biocontrol traits thus identified, the corresponding microbial functional groups have been characterized in suppressive vs conducive soils, using isolate collections, molecular fingerprints or sequencing. Fluorescent *Pseudomonas* bacteria, especially those producing the antifungal metabolite 2,4-diacetylphloroglucinol, have been extensively targeted in take-all-decline soils (Cook and Rovira, 1976; Weller et al., 2002; Weller et al., 2007) and soils suppressive to black root rot (Stutz et al., 1986; Laville et al., 1992; Kyselková and Moënne-Loccoz, 2012), whereas studies on soils suppressive to *R. solani* diseases have focused on *Pseudomonas* spp. producing antifungal lipopeptides (Mendes et al., 2011), *Streptomyces* spp. producing volatile metabolites (Cordovez et al., 2015) and *Paraburkholderia graminis* producing sulfurous volatile compounds (Carrión et al., 2018). In the case of soils suppressive to *Fusarium* diseases, competition with pathogenic *Fusarium* species is considered important, involving the entire soil microbiota or more specifically non-pathogenic *Fusarium* strains in Châteaurenard soils (Louvet et al., 1976; Alabouvette, 1986), or fluorescent *Pseudomonas* (iron competition; Scher and Baker, 1980; Sneh et al., 1984) in soils of Salinas Valley (California) or Châteaurenard (France). The role of extracellular lytic enzymes can be significant, as soil microbiota may protect barley from *Fusarium culmorum* via a more efficient cellulolytic activity than the pathogen, which consequently is outcompeted for nutrients (Rasmussen et al., 2002). Suppressiveness may result in part from chitinolytic effects of the soil microbiota against the pathogen, based on inhibition of *Fusarium* fungi by chitinases *in vitro* and effective protection of plant by chitinase-producing inoculants (Veliz et al., 2017). Other modes of action evidenced include the production of antifungal secondary metabolites in wilt-suppressive soils, such as a new thiopeptide by *Streptomyces* (Cha et al., 2016) and phenazines by *Pseudomonas* spp. (Mazurier et al., 2009), and immunity stimulation in banana (induction of the jasmonate and salicylic acid pathways) by fluorescent *Pseudomonas* (Lv et al., 2023).

5.2 Microbial diversity in soils suppressive to *Fusarium* diseases

Specific disease suppressiveness is attributed to the contribution of a few plant-benefical populations, but comparison of suppressive vs conducive soils has evidenced differences in the occurrence or prevalence of multiple taxa, in the case of suppressiveness to take all (Sanguin et al., 2009; Schreiner et al., 2010; Chng et al., 2015), black root rot (Kyselková et al., 2009), *R. solani*-mediated damping-off (Mendes et al., 2011), or potato common scab (Rosenzweig et al., 2012). Similar findings were made with soils suppressive to *Fusarium* diseases. No single phylum was uniquely associated with *F. oxysporum* wilt suppressiveness in Korean soils, even though *Actinomycetota* (formerly *Actinobacteria*) was identified as the most prevalent bacterial taxa colonizing strawberry in suppressive soils (Cha et al., 2016). Likewise, the bacterial genera *Devosia*, *Flavobacterium* and *Pseudomonas* were more abundant (and the pathogen less abundant) in Chinese soils suppressive to banana wilt than in conducive soils, and *Pseudomonas* inoculants isolated from suppressive could control the disease (Lv et al., 2023). Compared with conducive soil, Fusarium wilt suppressive soil from Châteaurenard displayed higher relative abundance of *Adhaeribacter*, *Arthrobacter, Amycolatopsis*, *Geobacter, Massilia*, *Microvirga*, *Paenibacillus*, *Rhizobium*, *Rhizobacter*, *Rubrobacter* and *Stenotrophomonas* (but not *Pseudomonas*) (Siegel-Hertz et al., 2018). However, differences were also found in the fungal community, with several fungal genera (*Acremonium*, *Ceratobasidium*, *Chaetomium*, *Cladosporium*, *Clonostachys*, *Mortierella*, *Penicillium*, *Scytalidium*, *Verticillium*, but also *Fusarium*) detected exclusively in the wilt suppressive soil (Siegel-Hertz et al., 2018). Data also pointed to a greater degree of microbial complexity in suppressive soils, with particular co-occurrence networks of taxa (Bakker et al., 2014; Lv et al., 2023). In German and Dutch soils, co-occurrence networks showed that the suppressive soil microbiota involves a guild of bacteria that probably function together, and in two of the suppressive soils this guild is dominated by *Acidobacteriota* (formerly *Acidobacteria*) (Ossowicki et al., 2020).

Many studies focused on a few, geographically-close soils, which does not provide a global view on the importance of microbial diversity. However, two studies have considered geographically diverse agricultural soils suppressive to Fusarium wilt. Various Chinese soils suppressive to banana wilt mediated by *F. oxysporum* were shown to share a common core microbiota, specific to suppressive soils, which included the genus *Pseudomonas* (Shen et al., 2022). In a wider range of soils from the Netherlands and Germany, soils suppressive to *F. culmorum*-mediated wilt of wheat did not display a specific bacterial species that correlated with suppressiveness (Ossowicki et al., 2020). There was no relation either with soil physicochemical composition (i.e. soil type, pH, contents in C, N, or bioavailable Fe, K, Mg, P) or field

history, yet suppressiveness was microbial in nature, as sterilizing suppressive soils made them become conducive. This suggests that each suppressive soil may harbor its own set of phytobeneficial bacteria, supporting the notion of functional redundancy between microbiomes, meaning that different microbiomes may share common functionalities despite taxonomic differences in the microbial actors involved (Lemanceau et al., 2017). Taken together, this might be explained by the fact that protection of wheat from *F. culmorum*-mediated wilt corresponds to a case of natural suppressiveness (Ossowicki et al., 2020), where biogeographic patterns are probably important, whereas soils suppressive to Fusarium wilt of banana are induced by monoculture (Wang et al., 2019; Shen et al., 2022), with convergent effects resulting from similar banana recruitment across different soil types.

To go beyond individual analyses considered separately, we re-analyzed sequence data from five investigations comparing disease-suppressive and conducive soils of cultivated plants (flax, watermelon, bananas, and wheat) infected by different *Fusarium* species (*F. oxysporum* or *F. culmorum*). At the level of bacterial phyla, fluctuations among Châteaurenard (flax-*F. oxysporum*; Siegel-Hertz et al., 2018), Hainan (banana-*F. oxysporum*; Shen et al., 2022) (Figure S1A) and Dutch/German (wheat-*F. culmorum*; Ossowicki et al., 2020) (Figure S1B) suppressive soils were important, as were those among their conducive counterparts, and the comparison between suppressive and conducive soils at these locations was not fruitful. In another study, fluctuations among other Hainan (banana-*F. oxysporum*; Zhou et al., 2019) suppressive or conducive soils were of less magnitude, but again the comparison was not insightful (Figure S1B). In contrast, Jiangsu (watermelon-*F. oxysporum*; Wang et al., 2015) suppressive soils displayed a higher relative abundance of *Acidobacteriota* and *Pseudomonadota* than in conducive soils (Figure S1B), but this property was not relevant when considering the other locations/plant species/*Fusarium* species. Based on heatmap comparisons (Figure S2), the main finding was the lower prevalence of the *Bacillota* phylum in the Jiangsu (watermelon-*F. oxysporum*) suppressive vs conducive soils, which was restricted to the case of these soils.

At the level of bacterial genera, the comparison of Châteaurenard (flax-*F. oxysporum*), Hainan (banana-*F. oxysporum*) or Dutch/German (wheat-*F. culmorum*) soils did not lead to the identification of indicator taxa (Figures 4, S3), but at Jiangsu (watermelon-*F. oxysporum*) the genera *Bacillus*, *Dongia*, *Rhodoplanes* and *Terrimonas* were less prevalent and the genera *Ferruginibacter, Flavobacterium, Pseudomonas* and *Sphingomonas* more prevalent in suppressive soils than in conducive soils (Figure S3A). Therefore, the comparison between suppressive and conducive soils was sometimes meaningful at the local scale, but typically not when considering a wider range of geographic or biological (plant and *Fusarium* species) conditions together. In other words, the information available so far points that suppressiveness to *Fusarium* diseases relies on microbial selection processes by roots that depend on local conditions, i.e. probably related to microbial biogeography, soil type, plant species, *Fusarium* genotype and most likely other local factors as well.

6 Variability and management of soil suppressiveness to *Fusarium* diseases

6.1 Environmental factors influencing soil suppressiveness to *Fusarium* diseases

Environmental conditions in soil may influence *Fusarium* autecology, the composition and activity of the soil microbial community, the tripartite interactions between this microbiota, *Fusarium* pathogens and the plant, and ultimately the level of disease suppressiveness (Marshall and Alexander, 1960; Amir and Alabouvette, 1993; Mazzola, 2002; Czembor et al., 2015). Key environmental factors in this regard include soil physicochemical properties and weather conditions (Weber and Kita, 2010).

Early work on the suppressiveness of soils to vascular Fusarium diseases drew attention to the positive role of certain abiotic factors and, in particular, montmorillonite-type clays (Stover, 1956; Stotzky and Torrence Martin, 1963). In addition, higher clay contents may contribute to reduced infestation by *Fusarium* (Kurek and Jaroszuk-Ściseł, 2003; Deltour et al., 2017), by altering oxygen diffusion, pH buffering and nutrient availability (Orr and Nelson, 2018). Höper et al. (1995) showed that the level of suppressiveness to Fusarium wilt of flax increased in soils amended with montmorillonite, kaolinite or illite at pH 7. A negative correlation between soil pH and *Fusarium* disease severity was reported in experiments with flax (Senechkin et al., 2014), strawberry (Fang et al., 2012) and banana (Shen et al., 2015a). However, the correlation between pH and Fusarium wilt incidence was positive in studies on banana (Peng et al., 1999) and watermelon (Cao et al., 2016). Certain experiments acidified soil originally at pH 8.0 (Peng et al., 1999) or 7.4 (Cao et al., 2016), whereas others limed an acidic soil (Fang et al., 2012; Senechkin et al., 2014; Shen et al., 2015a). Inconsistencies may relate to the complexity of pH effects on *Fusarium* pathogens and diseases, and possible interactions with soil properties, *Fusarium* and plant genotypes, or other experimental conditions. In addition, soil suppressiveness to Fusarium wilt necessitates sufficient levels of nitrogen, as disease incidence negatively correlates with the NH_4^+ and NO_3^- contents in the soil (Li et al., 2016; Meng et al., 2019). Moreover, the addition of calcium to the soils suppressed Fusarium wilt in several soil type × plant conditions (Spiegel et al., 1987; Peng et al., 1999; Gatch and du Toit, 2017). In Brittany, *F. graminearum* growth positively correlated with manganese and iron contents in the soil (Legrand et al., 2019). A positive correlation was found between hemicellulose concentration and suppression of Fusarium wilt in tomato and carnation (Castaño et al., 2011), as well as cellulose concentration and suppression of Fusarium seedling blight of barley (Rasmussen et al., 2002). This is attributed to the activity of cellulolytic microorganisms that limit *Fusarium* growth, as lower organic matter content (following decomposition) would reduce resources supporting this microbiota and disease suppression (Orr and Nelson, 2018).

Climatic conditions, notably temperature and precipitation may strongly affect the incidence of *Fusarium* diseases (Orr and Nelson, 2018). Phytopathogenic species *F. oxysporum*, *F. solani*, *F. verticillioides*, *F. graminearum* and *F. culmorum* develop best

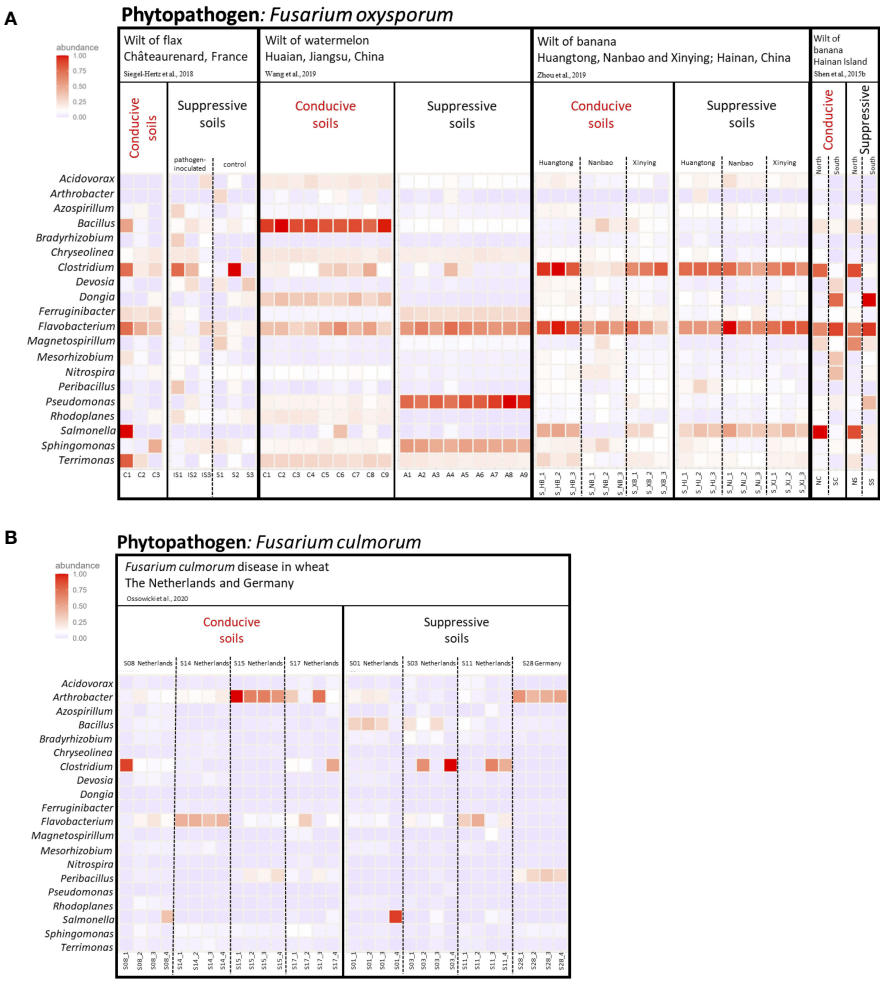

FIGURE 4
Heatmap of the major bacterial genera detected in the rhizosphere of plants grown in soils suppressive or conducive to different *Fusarium* diseases, based on analysis (File S1) of selected studies (Shen et al., 2015b; Siegel-Hertz et al., 2018; Wang et al., 2019; Zhou et al., 2019; Ossowicki et al., 2020). **(A)** The 20 most abundant genera in soils conducive or suppressive to diseases caused by *Fusarium oxysporum*. In Siegel-Hertz et al. (2018), suppressive soils were assessed after *Fusarium* inoculation or without. **(B)** The 20 most abundant genera in soils conducive or suppressive to diseases caused by *Fusarium culmorum*. The color intensity in each cell indicates the relative abundance (%) of a genus in each study for each plant type. When relevant, dotted lines are used to separate pathogen-inoculated samples from non-inoculated samples (in Châteaurenard) or samples from different fields. More details on individual conditions are available in Table S2.

under humid conditions, at water activity above 0.86 (Table S1) (Thrane, 2014). Severity of Fusarium wilt in lettuce (Scott et al., 2009; Ferrocino et al., 2013) and FHB in wheat was positively correlated with soil temperature (Xu et al., 2007; Nazari et al., 2018). For example, Fusarium wilt incidence significantly increased when lettuce was grown at 22-26°C instead of 18-22°C (Ferrocino et al., 2013). Similarly, in both conducive and suppressive soils, severity of Fusarium wilt of banana was significantly increased when temperature was raised from 24°C to 34°C (Peng et al., 1999).

6.2 Farming practices and the management of soil suppressiveness to *Fusarium* diseases

As many other soil-inhabiting pathogenic fungi, the *Fusarium* spp. can overwinter as mycelium in plant debris or dormant structures in the soil, which leads to cause the initial infection of plants in the following season (Nelson et al., 1994; Janvier et al., 2007; Leplat et al., 2013; Xu et al., 2021). Therefore, cultural practices removing the primary inoculum of the pathogen from overwintering soils are useful to prevent future infection (Voigt, 2002). However, farming practices also influence soil suppressiveness by shaping the rhizosphere microbial community (Campos et al., 2016) and stimulating the activity of beneficial rhizosphere microorganisms (Janvier et al., 2007). In this context, various agricultural practices, such as crop rotation/monocropping, tillage, organic amendments and fertilisers, are important to consider to develop suppressiveness-based control methods in farm fields (Janvier et al., 2007; Fu et al., 2016).

Except in the few cases where monoculture induces suppressiveness to *Fusarium* diseases (Larkin et al., 1993; Shen et al., 2022), cropping systems based on rotation of different plant species result in reduced survival of soil-borne pathogen propagules

over the short term (Winter et al., 2014). Crop rotation may reduce severity and incidence of diseases caused by *Fusarium* spp. (Wang et al., 2015; Khemir et al., 2020). For example, compared with the tomato monoculture, soil management under wheat - tomato rotation changes soil microbial composition by increasing the abundance of microbial taxa such as *Bacillus*, *Paenibacillus*, *Pseudomonas*, *Streptomyces*, *Aspergillus*, *Penicillium* and *Mortierella*, which may control Fusarium wilt of tomato (De Corato et al., 2020). Reduced incidence of *F. pseudograminearum* and *F. culmorum* in the soils under cereal – legumes rotation management may be due to the non-host character of the legumes (Evans et al., 2010). However, not all crop rotations lead to reduced disease pressure (Ranzi et al., 2017). In the case of the FHB, it was advocated to rotate wheat and corn with crops like soybean, until it was shown that *F. graminearum* can also cause disease in soybean, as it has a wide range of hosts (Marburger et al., 2015). This suggests that there is no common rule regarding the relationship between crop rotation and *Fusarium* disease incidence.

Crop residues of high cellulose content promoted the activity of beneficial cellulolytic microorganisms and limited the development of *Fusarium culmorum* (Rasmussen et al., 2002), as organic amendments represent a favorable environment for beneficial microorganisms that are able to combat phytopathogenic *Fusarium* species (Maher et al., 2008; Cuesta et al., 2012). Accordingly, organic amendments like animal manure, solid wastes and different composts are often used to improve soil health by delivering nutrients to the soil and also by stimulating beneficial microbiota (Fu et al., 2016; Mousa and Raizada, 2016). Thus, soils with added organic amendments exhibited inhibitory effects against *F. verticillioides* by reducing the production of a fungal pigment and sporulation, consequently disabling fungal spread (Nguyen et al., 2018). Addition of vermicompost reduced tomato infection by *F. oxysporum* f. sp. *lycopersici* (Szczech, 1999) and mulched straw contributed to the suppression of seedling blight caused by *F. culmorum* (Knudsen et al., 1999). Soils supplemented with coffee residue compost or rapeseed meal exhibited suppressiveness to *F. oxysporum*-mediated wilt, and microorganisms isolated from supplemented soils inhibited *F. oxysporum* growth on agar plates (Mitsuboshi et al., 2018). Carbon addition to soil influenced the soil microbiome, enhancing *Fusarium*-inhibitory populations from the *Streptomyces* genus (Dundore-Arias et al., 2020). However, increasing organic matter content may promote *Fusarium* survival in certain (rare) cases. One study tested the effects of 18 composts (made from different mixtures of manure, domestic biowaste and green waste) on Fusarium wilt disease suppression, caused by *F. oxysporum* f. sp. *lini*, and it was shown that only one compost did not positively affect the disease suppression (Termorshuizen et al., 2006). The efficiency of organic amendments in controlling plant diseases is determined by the pathosystem, the application rate, the kind of amendment and the level of maturity of composts or disintegration phase of crop residues (Janvier et al., 2007).

Tillage, which is one factor influencing organic matter decomposition, appears to have contrasting effects on soil suppressiveness. Under conventional tillage, tillage depth appears to play a crucial role in soil survival of *Fusarium*, such that the deeper the tillage, the lower the abundance of *Fusarium* species (Steinkellner and Langer, 2004). This can be partly explained by the fact that the pathogen is displaced from its niche, reducing its ability to survive (Bailey and Lazarovits, 2003), and the rate of decomposition of buried residues is faster than at the soil surface (Leplat et al., 2013). The carbon released during these decomposition processes increases the activity of the soil microbiota, thereby improving the overall functioning of the soil (Bailey and Lazarovits, 2003). Under conservation tillage, surface residues persist and can act as a long-term source of inoculum for plant infection by *F. verticillioides*, *F. proliferatum* and *F. subglutinans*, as they can colonise crop residues and produce overwintering spores that often survive the period when plants are absent from the agrosystem (Bockus and Shroyer, 1998; Cotten and Munkvold, 1998; Pereyra et al., 2004). This is consistent with results suggesting that conservation tillage and leaving crop residues *in situ* increase *Fusarium* abundance (Govaerts et al., 2008; Wang et al., 2020). For example, spores of *Fusarium* species could be recovered from plant residues more than two years after harvest (Pereyra et al., 2004). In certain cases, lower occurrence of plant infection by *F. culmorum*, *F. equiseti* (Weber et al., 2001) and *F. pseudograminearum* (Theron et al., 2023) was found under conservation tillage compared with conventional tillage. These contrasting results might be due to differences in environmental factors, cropping patterns and soil types, which could modulate interactions between soil conditions, *Fusarium* ecology and plant physiology (Sturz and Carter, 1995). The use of simplified tillage practices was proposed to reduce *F. culmorum* abundance, by mixing crop residues with the topsoil layer to promote the growth of beneficial straw-decomposing microorganisms (Weber and Kita, 2010).

Different fertilizers have different effects on phytopathogenic *Fusarium* spp. On one hand, the development of FHB caused by *F. culmorum* and *F. graminearum* increased with inorganic nitrogen fertilization (Lemmens et al., 2004), and on the other hand, nitrite could reduce the population of *F. oxysporum* (Löffler et al., 1986). Besides, higher doses of nitrogen may contribute to higher accumulation of *Fusarium* mycotoxins (Podolska et al., 2017). The addition of phosphorus fertilizer, in the form of P_2O_5, significantly reduced *Fusarium*-caused wilting in chickpea, lentil and lupine, in both greenhouse and field conditions (Elhassan et al., 2010). Organic fertilizers can lead to an increase in indigenous microbial populations, thus contributing to suppression of Fusarium wilt disease (Montalba et al., 2010; Raza et al., 2015). When grown with the addition of organic N fertilizer, highbush blueberry exhibited increased tolerance to *F. solani*, in parallel to increased soil microbial activity and mycorrhizal colonization (Montalba et al., 2010).

7 Conclusion and outlook

Disease-suppressiveness of soils is a useful model to understand microbial phytoprotection and develop sustainable plant protection strategies for soils devoid of this property. In this review, we

summarized the current knowledge on *Fusarium* phytopathogens, the available control methods and soils suppressive to *Fusarium* diseases, with the underlying mechanisms involved in the suppression. On one hand, extensive information is available on environmental and microbial properties responsible for suppressiveness to *Fusarium* diseases. One prominent feature is the diversity of *Fusarium*-based pathosystems for which suppressive soils are documented, in terms of *Fusarium* species (often *F. oxysporum*, but not only), host plants (both monocots and dicots), types of disease (often wilt, but not only), geographic locations of soil and farming conditions, and types of suppressiveness (i.e. natural suppressiveness to *Fusarium* diseases, but also monoculture-induced suppressiveness as well as fungistasis towards *Fusarium* pathogens). This diversity is paralleled by differences in microbiota composition and diversity associated with disease control in the different cases of suppressiveness. On the other hand, despite the fact that soils suppressive to *Fusarium* diseases have been studied for decades, they are still poorly understood in terms of microbiota functioning, and knowledge remains fragmented.

On this basis, additional research is needed to integrate further the scientific approaches used to decipher suppressiveness to *Fusarium* diseases. First, by combining complementary assessment methodology with current next-generation sequencing and ecological networks research, and incorporating experimental strategies to manipulate and transplant rhizosphere microbiome (or single microorganisms) of plants grown in suppressive soils to those in conducive soils to go beyond correlative work, as started recently (Ye et al., 2020; Jiang et al., 2022). Second, by extending the range of soil conditions investigated, and develop meta-analyses to estimate key microbiota differences between suppressive and conducive soils, as pioneered by Yuan et al. (2020). Third, by considering a wider range of biological actors, including beneficial fungi (often neglected), soil fauna (likely to influence microbial communities, *Fusarium* vectorisation, and plant health; e.g. Dita et al., 2018; Wagner et al., 2022). Fourth, by taking into account plant genetics, behavior and physiological responses to *Fusarium* pathogens (e.g. Liu et al., 2019). Therefore, there is a need for a more multidisciplinary approach to understand microbiota functioning in soils suppressive to *Fusarium* diseases.

Author contributions

All authors contributed to the writing of this review article and approved the submitted version.

Funding

IT was funded by a grant from the Ministry of Youth and Sports, Belgrade, Serbia (grant numbers 670-00-573/1/372/2019-04, 670-00-2590/1/304/2020-04, 670-00-2551/1/298/2021-04 and 670-00-1/1/317/2022-01) and grants from Campus France (grant numbers 964308G, 972203C and 103939T). This research was also funded through the 2018-2019 BiodivERsA joint call for research proposals, under the BiodivERsA3 ERA-Net COFUND programme, and with the funding organization ANR (Paris) (project SuppressSOIL ANR-19-EBI3-0007), as well as by The Ministry of Education, Science, and Technological Development of the Republic of Serbia (grant number 451-03-47/2023-01/200116).

Acknowledgments

We are grateful to Danis Abrouk (iBio) for help with retrieving metabarcoding sequences from various articles and comparative analyses.

Conflict of interest

The authors declare that the research was conducted in the absence of any commercial or financial relationships that could be construed as a potential conflict of interest.

Publisher's note

Supplementary material

The Supplementary Material for this article can be found online at: https://www.frontiersin.org/articles/10.3389/fpls.2023.1228749/full#supplementary-material

References

Abbasi, S., Safaie, N., Sadeghi, A., and Shamsbakhsh, M. (2019). *Streptomyces* strains induce resistance to *Fusarium oxysporum* f. sp. *lycopersici* Race 3 in tomato through different molecular mechanisms. *Front. Microbiol.* 10. doi: 10.3389/fmicb.2019.01505

Abdel-Azeem, A. M., Abdel-Azeem, M. A., Darwish, A. G., Nafady, N. A., and Ibrahim, N. A. (2019). "*Fusarium*: Biodiversity, ecological significances, and industrial applications," in *Recent Advancement in White Biotechnology Through Fungi: Volume 1: Diversity and Enzymes Perspectives Fungal Biology*. Eds. A. N. Yadav, S. Mishra, S. Singh and A. Gupta (Cham: Springer International Publishing), 201–261. doi: 10.1007/978-3-030-10480-1_6

Abdelrahman, M., Abdel-Motaal, F., El-Sayed, M., Jogaiah, S., Shigyo, M., Ito, S., et al. (2016). Dissection of *Trichoderma longibrachiatum* - induced defense in onion (*Allium cepa* L.) against *Fusarium oxysporum* f. sp. *cepa* by target metabolite profiling. *Plant Sci.* 246, 128–138. doi: 10.1016/j.plantsci.2016.02.008

Abo-Elyousr, K. A. M., Saad, M. M., Al-Qurashi, A. D., Ibrahim, O. H. M., and Mousa, M. A. A. (2022). Management of cumin wilt caused by *Fusarium oxysporum* using native endophytic bacteria. *Agronomy* 12, 1–14. doi: 10.3390/agronomy12102510

Adeniji, A. A., Aremu, O. S., and Babalola, O. O. (2019). Selecting lipopeptide-producing, *Fusarium*-suppressing *Bacillus* spp.: Metabolomic and genomic probing of *Bacillus velezensis* NWUMFkBS10.5. *MicrobiologyOpen* 8 (6), e00742. doi: 10.1002/mbo3.742

Agarwal, M., Dheeman, S., Dubey, R. C., Kumar, P., Maheshwari, D. K., and Bajpai, V. K. (2017). Differential antagonistic responses of *Bacillus pumilus* MSUA3 against *Rhizoctonia solani* and *Fusarium oxysporum* causing fungal diseases in *Fagopyrum esculentum* Moench. *Microbiol. Res.* 205, 40–47. doi: 10.1016/j.micres.2017.08.012

Ahmad, T., Bashir, A., Farooq, S., and Riyaz-Ul-Hassan, S. (2022). *Burkholderia gladioli* E39CS3, an endophyte of *Crocus sativus* Linn., induces host resistance against corm-rot caused by *Fusarium oxysporum*. *J. Appl. Microbiol.* 132, 495–508. doi: 10.1111/jam.15190

Ajmal, M., Hussain, A., Ali, A., Chen, H., and Lin, H. (2023). Strategies for controlling the sporulation in *Fusarium* spp. *J. Fungi.* 9, 10. doi: 10.3390/jof9010010

Akram, W., Anjum, T., and Ali, B. (2015). Searching ISR determinant/s from *Bacillus subtilis* IAGS174 against *Fusarium* wilt of tomato. *BioControl* 60, 271–280. doi: 10.1007/s10526-014-9636-1

Akram, W., Mahboob, A., and Javed, A. A. (2013). *Bacillus thuringiensis strain* 199 can induce systemic resistance in tomato against *Fusarium* wilt. *Eur. J. Microbiol. Immunol.* 3, 275–280. doi: 10.1556/EuJMI.3.2013.4.7

Alabouvette, C. (1986). Fusarium-wilt suppressive soils from the Châteaurenard region : review of a 10-year study. *Agronomie* 6 (3), 273–284. doi: 10.1051/agro:19860307

Alabouvette, C., Couteaudier, Y., Louvet, J., Bremeersch, P., Richard, P., and Soulas, M.-L. (1985). Recherches sur la resistance des sols aux maladies. XI. Etude comparative du comportement des *Fusarium* spp. dans un sol résistant et un sol sensible aux fusarioses vasculaires enrichis en glucose. *Agronomie* 5, 63–68. doi: 10.1051/agro:19850109

Al-Hatmi, A. M., de Hoog, G. S., and Meis, J. F. (2019). Multiresistant *Fusarium* pathogens on plants and humans: solutions in (from) the antifungal pipeline? *Infect. Drug Resist.* 12, 3727–3737. doi: 10.2147/IDR.S180912

Almario, J., Muller, D., Défago, G., and Moënne-Loccoz, Y. (2014). Rhizosphere ecology and phytoprotection in soils naturally suppressive to Thielaviopsis black root rot of tobacco. *Environ. Microbiol.* 16, 1949–1960. doi: 10.1111/1462-2920.12459

Amer, M. A., El-Samra, I. A., Abou-El-Seoud, I. I., El-Abd, S. M., and Shawertamimi, N. K. (2014). Induced systemic resistance in tomato plants against Fusarium wilt disease using biotic inducers. *Middle East J. Agric. Res.* 3 (4), 1090–1103.

Amir, H., and Alabouvette, C. (1993). Involvement of soil abiotic factors in the mechanisms of soil suppressiveness to Fusarium wilts. *Soil Biol. Biochem.* 25, 157–164. doi: 10.1016/0038-0717(93)90022-4

Ares, J. L. A., Ferro, R. C. A., Ramirez, L. C., and González, J. M. (2004). *Fusarium graminearum* Schwabe, a maize root and stalk rot pathogen isolated from lodged plants in Northwest Spain. *Span. J. Agric. Res.* 2, 249–252. doi: 10.5424/sjar/2004022-82

Arie, T. (2019). *Fusarium* diseases of cultivated plants, control, diagnosis, and molecular and genetic studies. *J. Pestic. Sci.* 44, 275–281. doi: 10.1584/jpestics.J19-03

Aydi Ben Abdallah, R., Stedel, C., Garagounis, C., Nefzi, A., Jabnoun-Khiareddine, H., Papadopoulou, K. K., et al. (2017). Involvement of lipopeptide antibiotics and chitinase genes and induction of host defense in suppression of Fusarium wilt by endophytic Bacillus spp. in tomato. *Crop Prot.* 99, 45–58. doi: 10.1016/j.cropro.2017.05.008

Babadoost, M. (2018). "*Fusarium*: Historical and continued importance," in *Fusarium—Plant Diseases, Pathogen Diversity, Genetic Diversity, Resistance and Molecular Markers*. Ed. T. Askun (London, UK: Intech Open), 13–24. doi: 10.5772/intechopen.74147

Backhouse, D., and Burgess, L. W. (2002). Climatic analysis of the distribution of *Fusarium graminearum*, *F. pseudograminearum* and *F. culmorum* on cereals in Australia. *Australas. Plant Pathol.* 31, 321–327. doi: 10.1071/AP02026

Bai, G., and Shaner, G. (1994). Scab of wheat: Prospects for control. *Plant Dis.* 78, 760–766. doi: 10.1094/PD-78-0760

Bailey, K. L., and Lazarovits, G. (2003). Suppressing soil-borne diseases with residue management and organic amendments. *Soil Tillage Res.* 72, 169–180. doi: 10.1016/S0167-1987(03)00086-2

Baker, K. F., and Cook, R. J. (1974). Biological control of plant pathogens. *St. Paul: Am. Phytopathol. Soc* 433.

Bakker, M. G., Schlatter, D. C., Otto-Hanson, L., and Kinkel, L. L. (2014). Diffuse symbioses: roles of plant–plant, plant–microbe and microbe–microbe interactions in structuring the soil microbiome. *Mol. Ecol.* 23, 1571–1583. doi: 10.1111/mec.12571

Banerjee, A., and Mittra, B. (2018). Morphological modification in wheat seedlings infected by *Fusarium oxysporum*. *Eur. J. Plant Pathol.* 152, 521–524. doi: 10.1007/s10658-018-1470-3

Bastian, F., Jurado, V., Nováková, A., Alabouvette, C., and Saiz-Jimenez, C. (2010). The microbiology of Lascaux cave. *Microbiol. Read. Engl.* 156, 644–652. doi: 10.1099/mic.0.036160-0

Bautista, D., García, D., Dávila, L., Caro-Quintero, A., Cotes, A. M., González, A., et al. (2023). Studying the microbiome of suppressive soils against vascular wilt, caused by *Fusarium oxysporum* in cape gooseberry (*Physalis Peruviana*). *Environ. Microbiol. Rep.* 15, 1–12. doi: 10.1111/1758-2229.13195

Berendsen, R. L., Pieterse, C. M. J., and Bakker, P. A. H. M. (2012). The rhizosphere microbiome and plant health. *Trends Plant Sci.* 17, 478–486. doi: 10.1016/j.tplants.2012.04.001

Blacutt, A. A., Gold, S. E., Voss, K. A., Gao, M., and Glenn, A. E. (2018). *Fusarium verticillioides*: Advancements in understanding the toxicity, virulence, and niche adaptations of a model mycotoxigenic pathogen of maize. *Phytopathology* 108, 312–326. doi: 10.1094/PHYTO-06-17-0203-RVW

Blümke, A., Falter, C., Herrfurth, C., Sode, B., Bode, R., Schäfer, W., et al. (2014). Secreted fungal effector lipase releases free fatty acids to inhibit innate immunity-related callose formation during wheat head infection. *Plant Physiol.* 165, 346–358. doi: 10.1104/pp.114.236737

Bockus, W. W., and Shroyer, J. P. (1998). The impact of reduced tillage on soilborne plant pathogens. *Annu. Rev. Phytopathol.* 36, 485–500. doi: 10.1146/annurev.phyto.36.1.485

Britannica, The Editors of Encyclopaedia (2017) *Fusarium wilt*. Available at: https://www.britannica.com/science/fusarium-wilt (Accessed June 15 2022).

Brown, N. A., Urban, M., van de Meene, A. M. L., and Hammond-Kosack, K. E. (2010). The infection biology of *Fusarium graminearum*: Defining the pathways of spikelet to spikelet colonisation in wheat ears. *Fungal Biol.* 114, 555–571. doi: 10.1016/j.funbio.2010.04.006

Bubici, G., Kaushal, M., Prigigallo, M. I., Gómez-Lama Cabanás, C., and Mercado-Blanco, J. (2019). Biological control agents against Fusarium wilt of banana. *Front. Microbiol.* 10, 616. doi: 10.3389/fmicb.2019.00616

Burgess, L. W., and Bryden, W. L. (2012). *Fusarium*: A ubiquitous fungus of global importance. *Microbiol. Aust.* 33, 22–25. doi: 10.1071/MA12022

Burgess, L. W. B., Summerell, A., Backhouse, D., Benyon, F., and Lević, J. (1996). Biodiversity and population studies in *Fusarium*. *Sydowia* 48, 1–11.

Campos, S. B., Lisboa, B. B., Camargo, F. A. O., Bayer, C., Sczyrba, A., Dirksen, P., et al. (2016). Soil suppressiveness and its relations with the microbial community in a Brazilian subtropical agroecosystem under different management systems. *Soil Biol. Biochem.* 96, 191–197. doi: 10.1016/j.soilbio.2016.02.010

Cao, Y., Wang, J., Wu, H., Yan, S., Guo, D., Wang, G., et al. (2016). Soil chemical and microbial responses to biogas slurry amendment and its effect on Fusarium wilt suppression. *Appl. Soil Ecol.* 107, 116–123. doi: 10.1016/j.apsoil.2016.05.010

Carrión, V. J., Cordovez, V., Tyc, O., Etalo, D. W., de Bruijn, I., de Jager, V. C. L., et al. (2018). Involvement of *Burkholderiaceae* and sulfurous volatiles in disease-suppressive soils. *ISME J.* 12, 2307–2321. doi: 10.1038/s41396-018-0186-x

Castaño, R., Borrero, C., and Avilés, M. (2011). Organic matter fractions by SP-MAS 13C NMR and microbial communities involved in the suppression of Fusarium wilt in organic growth media. *Biol. Control.* 58, 286–293. doi: 10.1016/j.biocontrol.2011.05.011

Cha, J.-Y., Han, S., Hong, H.-J., Cho, H., Kim, D., Kwon, Y., et al. (2016). Microbial and biochemical basis of a Fusarium wilt-suppressive soil. *ISME J.* 10, 119–129. doi: 10.1038/ismej.2015.95

Chatterton, S., and Punja, Z. K. (2009). Chitinase and beta-1,3-glucanase enzyme production by the mycoparasite *Clonostachys rosea* f. *catenulata* against fungal plant pathogens. *Can. J. Microbiol.* 55, 356–367. doi: 10.1139/w08-156

Chen, L., Heng, J., Qin, S., and Bian, K. (2018). A comprehensive understanding of the biocontrol potential of *Bacillus velezensis* LM2303 against Fusarium head blight. *PloS One* 13 (6), e0198560. doi: 10.1371/journal.pone.0198560

Chen, Y., Kistler, H. C., and Ma, Z. (2019). *Fusarium graminearum* trichothecene mycotoxins: Biosynthesis, regulation, and management. *Annu. Rev. Phytopathol.* 57, 15–39. doi: 10.1146/annurev-phyto-082718-100318

Chng, S., Cromey, M. G., Dodd, S. L., Stewart, A., Butler, R. C., and Jaspers, M. V. (2015). Take-all decline in New Zealand wheat soils and the microorganisms associated with the potential mechanisms of disease suppression. *Plant Soil.* 397, 239–259. doi: 10.1007/s11104-015-2620-4

Choudhary, D. K., Prakash, A., and Johri, B. N. (2007). Induced systemic resistance (ISR) in plants: mechanism of action. *Indian J. Microbiol.* 47, 289–297. doi: 10.1007/s12088-007-0054-2

Coleman, J. J. (2016). The *Fusarium solani* species complex: ubiquitous pathogens of agricultural importance. *Mol. Plant Pathol.* 17, 146–158. doi: 10.1111/mpp.12289

Constantin, M. E., Fokkens, L., de Sain, M., Takken, F. L., and Rep, M. (2021). Number of candidate effector genes in accessory genomes differentiates pathogenic from endophytic *Fusarium oxysporum* strains. *Front. Plant Sci.* 12, 761740. doi: 10.3389/fpls.2021.761740

Cook, R. J., and Rovira, A. D. (1976). The role of bacteria in the biological control of *Gaeumannomyces graminis* by suppressive soils. *Soil Biol. Biochem.* 8, 269–273. doi: 10.1016/0038-0717(76)90056-0

Cordovez, V., Carrion, V. J., Etalo, D. W., Mumm, R., Zhu, H., van Wezel, G. P., et al. (2015). Diversity and functions of volatile organic compounds produced by *Streptomyces* from a disease-suppressive soil. *Front. Microbiol.* 6. doi: 10.3389/fmicb.2015.01081

Cotten, T. K., and Munkvold, G. P. (1998).). Survival of *Fusarium moniliforme*, *F. proliferatum*, and *F. subglutinans* in maize stalk residue. *Phytopathology* 88, 550–555. doi: 10.1094/PHYTO.1998.88.6.550

Crous, P. W., Lombard, L., Sandoval-Denis, M., Seifert, K. A., Schroers, H. J., Chaverri, P., et al. (2021). *Fusarium*: more than a node or a foot-shaped basal cell. *Stud. Mycol.* 98, 100116. doi: 10.1016/j.simyco.2021.100116

Cuesta, G., García-de-la-Fuente, R., Abad, M., and Fornes, F. (2012). Isolation and identification of actinomycetes from a compost-amended soil with potential as biocontrol agents. *J. Environ. Manage.* 95, S280–S284. doi: 10.1016/j.jenvman.2010.11.023

Curtis, T. P., Sloan, W. T., and Scannell, J. W. (2002). Estimating prokaryotic diversity and its limits. *Proc. Natl. Acad. Sci. U. S. A.* 99, 10494–10499. doi: 10.1073/pnas.142680199

Cuzick, A., Urban, M., and Hammond-Kosack, K. (2008). *Fusarium graminearum* gene deletion mutants map1 and tri5 reveal similarities and differences in the pathogenicity requirements to cause disease on *Arabidopsis* and wheat floral tissue. *New Phytol.* 177, 990–1000. doi: 10.1111/j.1469-8137.2007.02333.x

Czembor, E., Stępień, Ł., and Waśkiewicz, A. (2015). Effect of environmental factors on *Fusarium* species and associated mycotoxins in maize grain grown in Poland. *PloS One* 10, e0133644. doi: 10.1371/journal.pone.0133644

da Silva Santos, A. C., Diniz, A. G., Tiago, P. V., and de Oliveira, N. T. (2020). Entomopathogenic *Fusarium* species: a review of their potential for the biological control of insects, implications and prospects. *Fungal Biol. Rev.* 34, 41–57. doi: 10.1016/j.fbr.2019.12.002

Dastjerdi, R., and Karlovsky, P. (2015). Systemic infection of maize, sorghum, rice, and beet seedlings with fumonisin-producing and non-producing *Fusarium verticillioides* strains. *Plant Pathol. J.* 31, 334–342. doi: 10.5423/PPJ.OA.05.2015.0088

Dean, R., Van Kan, J. A. L., Pretorius, Z. A., Hammond-Kosack, K. E., Di Pietro, A., Spanu, P. D., et al. (2012). The top 10 fungal pathogens in molecular plant pathology. *Mol. Plant Pathol.* 13 (4), 414–430. doi: 10.1111/j.1364-3703.2011.00783.x

De Boer, W., Li, X., Meisner, A., and Garbeva, P. (2019). Pathogen suppression by microbial volatile organic compounds in soils. *FEMS Microbiol. Ecol.* 95 (8), fiz105. doi: 10.1093/femsec/fiz105

De Corato, U., Patruno, L., Avella, N., Salimbeni, R., Lacolla, G., Cucci, G., et al. (2020). Soil management under tomato-wheat rotation increases the suppressive response against Fusarium wilt and tomato shoot growth by changing the microbial composition and chemical parameters. *Appl. Soil Ecol.* 154, 103601. doi: 10.1016/j.apsoil.2020.103601

De Lamo, F. J., and Takken, F. L. (2020). Biocontrol by *Fusarium oxysporum* using endophyte-mediated resistance. *Front. Plant Sci.* 11, 37. doi: 10.3389/fpls.2020.00037

Deltour, P., Franca, S. C., Pereira, O. L., Cardoso, I., De Neve, S., Debode, J., et al. (2017). Disease suppressiveness to Fusarium wilt of banana in an agroforestry system: influence of soil characteristics and plant community. *Agric. Ecosyst. Environ.* 239, 173–181. doi: 10.1016/j.agee.2017.01.018

Desjardins, A. E. (2006). *Fusarium mycotoxins: chemistry, genetics, and biology* (St Paul, MN, USA: APS Press).

Dhanti, K. R., Widiastuti, A., and Joko, T. (2017). "Detection of mycotoxin-encoding genes in *Fusarium* spp. isolated from maize kernels in Indonesia," in *Proceeding of the 1st International Conference on Tropical Agriculture*, Cham (Switzerland: Springer International Publishing). doi: 10.1007/978-3-319-60363-6_11

Dita, M., Barquero, M., Heck, D., Mizubuti, E. S. G., and Staver, C. P. (2018). Fusarium wilt of banana: Current knowledge on epidemiology and research needs toward sustainable disease management. *Front. Plant Sci.* 9. doi: 10.3389/fpls.2018.01468

Domínguez, J., Negrín, M. A., and Rodríguez, C. M. (1996). Soil chemical characteristics in relation to Fusarium wilts in banana crops of Gran Canaria Island (Spain). *Commun. Soil Sci. Plant Anal.* 27, 2649–2662. doi: 10.1080/00103629609369729

Du, S., Trivedi, P., Wei, Z., Feng, J., Hu, H. W., Bi, L., et al. (2022). The proportion of soil-borne fungal pathogens increases with elevated organic carbon in agricultural soils. *mSystems* 7, e01337–e01321. doi: 10.1128/msystems.01337-21

Duijff, B. J., Gianinazzi-Pearson, V., and Lemanceau, P. (1997). Involvement of the outer membrane lipopolysaccharides in the endophytic colonization of tomato roots by biocontrol *Pseudomonas fluorescens* strain WCS417r. *New Phytol.* 135, 325–334. doi: 10.1046/j.1469-8137.1997.00646.x

Duijff, B. J., Pouhair, D., Olivain, C., Alabouvette, C., and Lemanceau, P. (1998). Implication of systemic induced resistance in the suppression of Fusarium wilt of tomato by *Pseudomonas fluorescens* WCS417r and by nonpathogenic *Fusarium oxysporum* Fo47. *Eur. J. Plant Pathol.* 104, 903–910. doi: 10.1023/A:1008626212305

Dundore-Arias, J. P., Castle, S. C., Felice, L., Dill-Macky, R., and Kinkel, L. L. (2020). Carbon amendments influence composition and functional capacities of indigenous soil microbiomes. *Front. Mol. Biosci.* 6. doi: 10.3389/fmolb.2019.00151

Edel-Hermann, V., and Lecomte, C. (2019). Current status of *Fusarium oxysporum formae speciales* and races. *Phytopathology* 109 (4), 512–530. doi: 10.1094/PHYTO-08-18-0320-RVW

Elhassan, A., El-Tilib, A., H.S., I., and Awadelkarim, A. (2010). Effect of phosphorus fertilizer treatments on incidence of Fusarium root-rot/wilt disease complex, and on yield components of lupine, chickpea and lentil crops. *Arab Univ. J. Agric. Sci.* 18, 193–202. doi: 10.21608/ajs.2010.14989

Eparvier, A., and Alabouvette, C. (1994). Use of ELISA and GUS-transformed strains to study competition between pathogenic and non-pathogenic *Fusarium oxysporum* for root colonization. *Biocontrol Sci. Technol.* 4, 35–47. doi: 10.1080/09583159409355310

Evans, M. L., Hollaway, G. J., Dennis, J. I., Correll, R., and Wallwork, H. (2010). Crop sequence as a tool for managing populations of *Fusarium pseudograminearum* and *F. culmorum* in South-Eastern Australia. *Australas. Plant Pathol.* 39, 376–382. doi: 10.1071/AP09092

Fan, H., He, P., Xu, S., Li, S., Wang, Y., Zhang, W., et al. (2023). Banana disease-suppressive soil drives *Bacillus* assembled to defense Fusarium wilt of banana. *Front. Microbiol.* 14, 1211301. doi: 10.3389/fmicb.2023.1211301

Fang, X., You, M. P., and Barbetti, M. J. (2012). Reduced severity and impact of Fusarium wilt on strawberry by manipulation of soil pH, soil organic amendments and crop rotation. *Eur. J. Plant Pathol.* 134, 619–629. doi: 10.1007/s10658-012-0042-1

Fatima, S., and Anjum, T. (2017). Identification of a potential ISR determinant from *Pseudomonas aeruginosa* PM12 against Fusarium wilt in tomato. *Front. Plant Sci.* 8. doi: 10.3389/fpls.2017.00848

Ferrocino, I., Chitarra, W., Pugliese, M., Gilardi, G., Gullino, M. L., and Garibaldi, A. (2013). Effect of elevated atmospheric CO_2 and temperature on disease severity of *Fusarium oxysporum* f.sp. *lactucae* on lettuce plants. *Appl. Soil Ecol.* 72, 1–6. doi: 10.1016/j.apsoil.2013.05.015

Fu, L., Ruan, Y., Tao, C., Li, R., and Shen, Q. (2016). Continous application of bioorganic fertilizer induced resilient culturable bacteria community associated with banana Fusarium wilt suppression. *Sci. Rep.* 6, 27731. doi: 10.1038/srep27731

Fuchs, J.-G., Moënne-Loccoz, Y., and Défago, G. (1997). Nonpathogenic *Fusarium oxysporum* strain Fo47 induces resistance to Fusarium wilt in tomato. *Plant Dis.* 81, 492–496. doi: 10.1094/PDIS.1997.81.5.492

Fuchs, J.-G., Moënne-Loccoz, Y., and Défago, G. (1999). Ability of nonpathogenic *Fusarium oxysporum* Fo47 to protect tomato against Fusarium wilt. *Biol. Control.* 14, 105–110. doi: 10.1006/bcon.1998.0664

Gai, X., Dong, H., Wang, S., Liu, B., Zhang, Z., Li, X., et al. (2018). Infection cycle of maize stalk rot and ear rot caused by *Fusarium verticillioides*. *PloS One* 13, e0201588. doi: 10.1371/journal.pone.0201588

Galletti, S., Paris, R., and Cianchetta, S. (2020). Selected isolates of *Trichoderma gamsii* induce different pathways of systemic resistance in maize upon *Fusarium verticillioides* challenge. *Microbiol. Res.* 233, 126406. doi: 10.1016/j.micres.2019.126406

Garbeva, P., Hol, W. H. G., Termorshuizen, A. J., Kowalchuk, G. A., and de Boer, W. (2011). Fungistasis and general soil biostasis – A new synthesis. *Soil Biol. Biochem.* 43, 469–477. doi: 10.1016/j.soilbio.2010.11.020

Garbeva, P., van Veen, J. A., and van Elsas, J. D. (2004). Microbial diversity in soil: selection microbial populations by plant and soil type and implications for disease suppressiveness. *Annu. Rev. Phytopathol.* 42, 243–270. doi: 10.1146/annurev.phyto.42.012604.135455

Garibaldi, A., Dalla, G. C., Della, G. C., and D'Aquila, F. (1983). Osservazioni su terreni repressivi nei confronti di *Fusarium oxysporum* f. sp. *dianthi* (Prill. et Del.) Snyd. et Hans. *Riv. Ortoflorofrutticoltura Ital.* 67, 251–259.

Gatch, E. W., and du Toit, L. J. (2017). Limestone-mediated suppression of Fusarium wilt in spinach seed crops. *Plant Dis.* 101, 81–94. doi: 10.1094/PDIS-04-16-0423-RE

Geiser, D. M., Aoki, T., Bacon, C. W., Baker, S. E., Bhattacharyya, M. K., Brandt, M. E., et al. (2013). One fungus, one name: Defining the genus *Fusarium* in a scientifically robust way that preserves longstanding use. *Phytopathology* 103, 400–408. doi: 10.1094/PHYTO-07-12-0150-LE

Gómez Expósito, R., de Bruijn, I., Postma, J., and Raaijmakers, J. M. (2017). Current insights into the role of rhizosphere bacteria in disease suppressive soils. *Front. Microbiol.* 8. doi: 10.3389/fmicb.2017.02529

Goswami, R. S., and Kistler, H. C. (2004). Heading for disaster: *Fusarium graminearum* on cereal crops. *Mol. Plant Pathol.* 5, 515–525. doi: 10.1111/j.1364-3703.2004.00252.x

Gouy, M., Guindon, S., and Gascuel, O. (2010). SeaView version 4: A multiplatform graphical user interface for sequence alignment and phylogenetic tree building. *Mol. Biol. Evol.* 27, 221–224. doi: 10.1093/molbev/msp259

Govaerts, B., Mezzalama, M., Sayre, K. D., Crossa, J., Lichter, K., Troch, V., et al. (2008). Long-term consequences of tillage, residue management, and crop rotation on selected soil micro-flora groups in the subtropical highlands. *Appl. Soil Ecol.* 38, 197–210. doi: 10.1016/j.apsoil.2007.10.009

Gruet, C., Alaoui, M., Gerin, F., Prigent-Combaret, C., Börner, A., Muller, D., et al. (2023). Genomic content of wheat has a higher influence than plant domestication status on the ability to interact with *Pseudomonas* plant growth-promoting rhizobacteria. *Plant Cell Environ.* 46, 3933–3948. doi: 10.1111/pce.14698

Gu, Q., Yang, Y., Yuan, Q., Shi, G., Wu, L., Lou, Z., et al. (2017). Bacillomycin D produced by *Bacillus amyloliquefaciens* is involved in the antagonistic interaction with the plant-pathogenic fungus *Fusarium graminearum*. *Appl. Environ. Microbiol.* 83, e01075–e01017. doi: 10.1128/AEM.01075-17

He, J., Boland, G. J., and Zhou, T. (2009). Concurrent selection for microbial suppression of *Fusarium graminearum*, Fusarium head blight and deoxynivalenol in wheat. *J. Appl. Microbiol.* 106, 1805–1817. doi: 10.1111/j.1365-2672.2009.04147.x

Herron, D. A., Wingfield, M. J., Wingfield, B. D., Rodas, C. A., Marincowitz, S., and Steenkamp, E. T. (2015). Novel taxa in the *Fusarium fujikuroi* species complex from *Pinus* spp. *Stud. Mycol.* 80, 131–150. doi: 10.1016/j.simyco.2014.12.001

Höper, H., Steinberg, C., and Alabouvette, C. (1995). Involvement of clay type and pH in the mechanisms of soil suppressiveness to Fusarium wilt of flax. *Soil Biol. Biochem.* 27, 955–967. doi: 10.1016/0038-0717(94)00238-V

Husaini, A. M., Sakina, A., and Cambay, S. R. (2018). Host-pathogen interaction in *Fusarium oxysporum* infections: Where do we stand? *Mol. Plant-Microbe Interact.* 31, 889–898. doi: 10.1094/MPMI-12-17-0302-CR

Ittu, M., Hagima, I., Moraru, I., and Raducanu, F. (1995). Reaction of some wheat and triticale genotypes to toxins, culture filtrates and cultures of *Fusarium. In vivo* screening and the relation between results obtained in *vivo* and in *vitro*. *Theor. Appl. Genet.* 27 (1), 1–13.

Janvier, C., Villeneuve, F., Alabouvette, C., Edel-Hermann, V., Mateille, T., and Steinberg, C. (2007). Soil health through soil disease suppression: Which strategy from descriptors to indicators? *Soil Biol. Biochem.* 39, 1–23. doi: 10.1016/j.soilbio.2006.07.001

Jard, G., Liboz, T., Mathieu, F., Guyonvarch, A., and Lebrihi, A. (2011). Review of mycotoxin reduction in food and feed: From prevention in the field to detoxification by adsorption or transformation. *Food Addit. Contam.* 28, 1590–1609. doi: 10.1080/19440049.2011.595377

Jeffries, P. (1995). Biology and ecology of mycoparasitism. *Can. J. Bot.* 73, 1284–1290. doi: 10.1139/b95-389

Jia, L.-J., Tang, H.-Y., Wang, W.-Q., Yuan, T.-L., Wei, W.-Q., Pang, B., et al. (2019). A linear nonribosomal octapeptide from *Fusarium graminearum* facilitates cell-to-cell invasion of wheat. *Nat. Commun.* 10, 922. doi: 10.1038/s41467-019-08726-9

Jiang, G., Zhang, Y., Gan, G., Li, W., Wan, W., Jiang, Y., et al. (2022). Exploring rhizo-microbiome transplants as a tool for protective plant-microbiome manipulation. *ISME Commun.* 2, 1–10. doi: 10.1038/s43705-022-00094-8

Jiménez-Díaz, R. M., Castillo, P., Jiménez-Gasco, M., del, M., Landa, B. B., and Navas-Cortés, J. A. (2015). Fusarium wilt of chickpeas: Biology, ecology and management. *Crop Prot.* 73, 16–27. doi: 10.1016/j.cropro.2015.02.023

Johnson, E. T., Bowman, M. J., and Dunlap, C. A. (2020). *Brevibacillus fortis* NRS-1210 produces edeines that inhibit the in *vitro* growth of conidia and chlamydospores of the onion pathogen *Fusarium oxysporum* f. sp. *cepae*. *Antonie Van Leeuwenhoek.* 113, 973–987. doi: 10.1007/s10482-020-01404-7

Keszthelyi, A., Jeney, A., Kerényi, Z., Mendes, O., Waalwijk, C., and Hornok, L. (2007). Tagging target genes of the MAT1-2-1 transcription factor in *Fusarium verticillioides* (*Gibberella fujikuroi* MP-A). *Antonie Van Leeuwenhoek* 91, 373–391. doi: 10.1007/s10482-006-9123-5

Khan, M. R., and Doohan, F. M. (2009). Bacterium-mediated control of Fusarium Head Blight disease of wheat and barley and associated mycotoxin contamination of grain. *Biol. Control.* 48, 42–47. doi: 10.1016/j.biocontrol.2008.08.015

Khan, M. R., Fischer, S., Egan, D., and Doohan, F. M. (2006). Biological control of Fusarium seedling blight disease of wheat and barley. *Phytopathology* 96, 386–394. doi: 10.1094/PHYTO-96-0386

Khan, N., Martínez-Hidalgo, P., Ice, T. A., Maymon, M., Humm, E. A., Nejat, N., et al. (2018). Antifungal activity of *Bacillus* species against *Fusarium* and analysis of the potential mechanisms used in biocontrol. *Front. Microbiol.* 9, 2363. doi: 10.3389/fmicb.2018.02363

Khan, N., Maymon, M., and Hirsch, A. (2017). Combating *Fusarium* infection using *Bacillus*-based antimicrobials. *Microorganisms* 5, 75. doi: 10.3390/microorganisms5040075

Khemir, E., Samira, C., Moretti, A., Gharbi, M. S., Allagui, M. B., and Gargouri, S. (2020). Impacts of previous crops on inoculum of *Fusarium culmorum* in soil, and development of foot and root rot of durum wheat in Tunisia. *Phytopathol. Mediterr.* 59, 187–201. doi: 10.36253/phyto-10827

Kim, Y.-T., Monkhung, S., Lee, Y. S., and Kim, K. Y. (2019). Effects of *Lysobacter antibioticus* HS124, an effective biocontrol agent against *Fusarium graminearum*, on crown rot disease and growth promotion of wheat. *Can. J. Microbiol.* 65, 904–912. doi: 10.1139/cjm-2019-0285

Klein, E., Ofek, M., Katan, J., Minz, D., and Gamliel, A. (2013). Soil suppressiveness to *Fusarium* disease: Shifts in root microbiome associated with reduction of pathogen root colonization. *Phytopathology* 103, 23–33. doi: 10.1094/PHYTO-12-11-0349

Kloepper, J. W., Leong, J., Teintze, M., and Schroth, M. N. (1980). *Pseudomonas* siderophores: A mechanism explaining disease-suppressive soils. *Curr. Microbiol.* 4, 317–320. doi: 10.1007/BF02602840

Knudsen, I. M. B., Debosz, K., Hockenhull, J., Jensen, D. F., and Elmholt, S. (1999). Suppressiveness of organically and conventionally managed soils towards brown foot rot of barley. *Appl. Soil Ecol.* 12, 61–72. doi: 10.1016/s0929-1393(98)00156-5

Kubicek, C. P., Herrera-Estrella, A., Seidl-Seiboth, V., Martinez, D. A., Druzhinina, I. S., Thon, M., et al. (2011). Comparative genome sequence analysis underscores mycoparasitism as the ancestral life style of *Trichoderma*. *Genome Biol.* 12, 1–15. doi: 10.1186/gb-2011-12-4-r40

Kuć, J. (1995). "Induced systemic resistance — an overview," in *Induced Resistance to Disease in Plants*. Eds. R. Hammerschmidt and J. Kuć (Dordrecht: Springer Netherlands), 169–175. doi: 10.1007/978-94-015-8420-3_8

Kumari, P., and Khanna, V. (2019). Seed bacterization stimulated resistance in chickpea against *Fusarium oxysporum* f. sp. *ciceris*. *Indian Phytopathol.* 72, 689–697. doi: 10.1007/s42360-019-00163-4

Kurek, E., and Jaroszuk-Ściseł, J. (2003). Rye (*Secale cereale*) growth promotion by *Pseudomonas fluorescens* strains and their interactions with *Fusarium culmorum* under various soil conditions. *Biol. Control.* 26, 48–56. doi: 10.1016/S1049-9644(02)00115-9

Kyselková, M., Kopecký, J., Frapolli, M., Défago, G., Ságová-Marečková, M., Grundmann, G., et al. (2009). Comparison of rhizobacterial community composition in soil suppressive or conducive to tobacco black root rot disease. *ISME J.* 3, 1127–1138. doi: 10.1038/ismej.2009.61

Kyselková, M., and Moënne-Loccoz, Y. (2012). "*Pseudomonas* and other microbes in disease-suppressive soils," in *Organic Fertilisation, Soil Quality and Human Health Sustainable Agriculture Reviews*. Ed. E. Lichtfouse (Dordrecht: Springer Netherlands), 93–140. doi: 10.1007/978-94-007-4113-3_5

Laraba, I., McCormick, S. P., Vaughan, M. M., Geiser, D. M., and O'Donnell, K. (2021). Phylogenetic diversity, trichothecene potential, and pathogenicity within *Fusarium sambucinum* species complex. *PloS One* 16, e0245037. doi: 10.1371/journal.pone.0245037

Larkin, R. P., Hopkins, D. L., and Martin, F. N. (1993). Ecology of *Fusarium oxysporum* f. sp. *niveum* in soils suppressive and conducive to Fusarium wilt of watermelon. *Phytopathology* 83, 1105–1116. doi: 10.1094/Phyto-83-1105

Laville, J., Voisard, C., Keel, C., Maurhofer, M., Défago, G., and Haas, D. (1992). Global control in *Pseudomonas fluorescens* mediating antibiotic synthesis and suppression of black root rot of tobacco. *Proc. Natl. Acad. Sci. U. S. A.* 89, 1562–1566. doi: 10.1073/pnas.89.5.1562

Leeman, M., van Pelt, J. A., Den Ouden, F. M., Heinsbroek, M., Bakker, P. A. H. M., and Schippers, B. (1995). Induction of systemic resistance against Fusarium wilt of radish by lipopolysaccharides of *Pseudomonas fluorescens*. *Phytopathology* 85, 1021–1027. doi: 10.1094/Phyto-85-1021

Legrand, F., Chen, W., Cobo-Díaz, J. F., Picot, A., and Le Floch, G. (2019). Co-occurrence analysis reveal that biotic and abiotic factors influence soil fungistasis against *Fusarium graminearum*. *FEMS Microbiol. Ecol.* 95, fiz056. doi: 10.1093/femsec/fiz056

Legrand, F., Picot, A., Cobo-Díaz, J. F., Chen, W., and Le Floch, G. (2017). Challenges facing the biological control strategies for the management of Fusarium Head Blight of cereals caused by *F. graminearum*. *Biol. Control.* 113, 26–38. doi: 10.1016/j.biocontrol.2017.06.011

Lei, W., Xiao-Ming, W., Rong-Qi, X., and Hong-Jie, L. (2011). Root infection and systematic colonization of DsRed-labeled *Fusarium verticillioides* in maize. *Acta Agron. Sin.* 37, 793–802. doi: 10.1016/S1875-2780(11)60023-0

Lemanceau, P., and Alabouvette, C. (1991). Biological control of *Fusarium* diseases by fluorescent *Pseudomonas* and non-pathogenic *Fusarium*. *Crop Prot.* 10, 279–286. doi: 10.1016/0261-2194(91)90006-D

Lemanceau, P., Bakker, P., de Kogel, W., Alabouvette, C., and Schippers, B. (1993). Antagonistic effect of nonpathogenic *Fusarium oxysporum* Fo47 and pseudobactin 358 upon pathogenic *Fusarium oxysporum* f. sp. *dianthi*. *Appl. Environ. Microbiol.* 59, 74–82. doi: 10.1128/AEM.59.1.74-82.1993

Lemanceau, P., Blouin, M., Muller, D., and Moënne-Loccoz, Y. (2017). Let the core microbiota be functional. *Trends Plant Sci.* 22, 583–595. doi: 10.1016/j.tplants.2017.04.008

Lemmens, M., Haim, K., Lew, H., and Ruckenbauer, P. (2004). The effect of nitrogen fertilization on Fusarium head blight development and deoxynivalenol contamination in wheat. *J. Phytopathol.* 152, 1–8. doi: 10.1046/j.1439-0434.2003.00791.x

Leplat, J., Friberg, H., Abid, M., and Steinberg, C. (2013). Survival of *Fusarium graminearum*, the causal agent of Fusarium head blight. A review. *Agron. Sustain. Dev.* 33, 97–111. doi: 10.1007/s13593-012-0098-5

Leslie, J. F., and Summerell, B. A. (2006). *The Fusarium laboratory manual* (Ames: John Wiley and Sons). doi: 10.1002/9780470278376

Letunic, I., and Bork, P. (2021). Interactive Tree Of Life (iTOL) v5: an online tool for phylogenetic tree display and annotation. *Nucleic Acids Res.* 49, W293–W296. doi: 10.1093/nar/gkab301

Li, Y., and Chen, S. (2019). Fusaricidin produced by *Paenibacillus polymyxa* WLY78 induces systemic resistance against Fusarium wilt of cucumber. *Int. J. Mol. Sci.* 20, 1–19. doi: 10.3390/ijms20205240

Li, R., Shen, Z., Sun, L., Zhang, R., Fu, L., Deng, X., et al. (2016). Novel soil fumigation method for suppressing cucumber Fusarium wilt disease associated with soil microflora alterations. *Appl. Soil Ecol.* 101, 28–36. doi: 10.1016/j.apsoil.2016.01.004

Liu, Y., Zhu, A., Tan, H., Cao, L., and Zhang, R. (2019). Engineering banana endosphere microbiome to improve Fusarium wilt resistance in banana. *Microbiome* 7, 74. doi: 10.1186/s40168-019-0690-x

Löffler, H. J. M., Cohen, E. B., Oolbekkink, G. T., and Schippers, B. (1986). Nitrite as a factor in the decline of *Fusarium oxysporum* f. sp. *dianthi* in soil supplemented with urea or ammonium chloride. *Neth. J. Plant Pathol.* 92, 153–162. doi: 10.1007/BF01999797

Logeshwarn, P., Thangaraju, M., and Kandaiah, R. (2011). Antagonistic potential of *Gluconacetobacter diazotrophicus* against *Fusarium oxysporum* in sweet potato (*Ipomea batatus*). *Arch. Phytopathol. Plant Prot.* 44, 216–223. doi: 10.1080/03235400902952707

López-Díaz, C., Rahjoo, V., Sulyok, M., Ghionna, V., Martín-Vicente, A., Capilla, J., et al. (2018). Fusaric acid contributes to virulence of *Fusarium oxysporum* on plant and mammalian hosts. *Mol. Plant Pathol.* 19, 440–453. doi: 10.1111/mpp.12536

Louvet, J., Rouxel, F., and Alabouvette, C. (1976). Recherches sur la resistance des sols aux maladies. I. Mise en evidence de la nature microbiobiologique de la résistance d'un sol au developpement de la fusariose vasculaire du melon. *Ann. Phytopathol.* 8, 425–436.

Lv, N., Tao, C., Ou, Y., Wang, J., Deng, X., Liu, H., et al. (2023). Root-associated antagonistic Pseudomonas spp. contribute to soil suppressiveness against banana Fusarium wilt disease of banana. *Microbiol. Spectr.* 11 (2), e0352522. doi: 10.1128/spectrum.03525-22

Ma, L.-J., Geiser, D. M., Proctor, R. H., Rooney, A. P., O'Donnell, K., Trail, F., et al. (2013). *Fusarium* pathogenomics. *Annu. Rev. Microbiol.* 67, 399–416. doi: 10.1146/annurev-micro-092412-155650

Magotra, S., Trakroo, D., Ganjoo, S., and Vakhlu, J. (2016). "*Bacillus*-mediated-Induced Systemic Resistance (ISR) against Fusarium corm rot," in *Microbial-mediated Induced Systemic Resistance in Plants*. Eds. D. K. Choudhary and A. Varma (Singapore: Springer International Publishing), 15–22. doi: 10.1007/978-981-10-0388-2_2

Maher, M., Prasad, M., and Raviv, M. (2008). "Organic soilless media components", in *Soilless culture, theory and practice*. Ed. L. Raviv (Amsterdam: Elsevier), 459–504. doi: 10.1016/B978-044452975-6.50013-7

Maheshwari, D. K., Saraf, M., and Aeron, A. (2013). *Bacteria in agrobiology: Disease management* (Berlin: Springer International Publishing). doi: 10.1007/978-3-642-33639-3

Marburger, D. A., Venkateshwaran, M., Conley, S. P., Esker, P. D., Lauer, J. G., and Ané, J. M. (2015). Crop rotation and management effect on *Fusarium* spp. populations. *Crop Sci.* 55, 365–376. doi: 10.2135/cropsci2014.03.0199

Marshall, K. C., and Alexander, M. (1960). Competition between soil bacteria and *Fusarium*. *Plant Soil.* 12, 143–153. doi: 10.1007/BF01377367

Masri, M., Sukmawaty, E., and Amir, A. A. (2021). Antifungal activity of chitinolytic bacteria *Lysinibacillus fusiformis* and *Brevibacillus reuszeri* against the fungal pathogens *Rhizoctonia solani* and *Fusarium oxysporum*. *Microbiol. Indones.* 15, 135–138. doi: 10.5454/mi.15.4.3

Mazurier, S., Corberand, T., Lemanceau, P., and Raaijmakers, J. M. (2009). Phenazine antibiotics produced by fluorescent pseudomonads contribute to natural soil suppressiveness to Fusarium wilt. *ISME J.* 3, 977–991. doi: 10.1038/ismej.2009.33

Mazzola, M. (2002). Mechanisms of natural soil suppressiveness to soilborne diseases. *Antonie Van Leeuwenhoek.* 81, 557–564. doi: 10.1023/A:1020557523557

Mendes, R., Kruijt, M., de Bruijn, I., Dekkers, E., van der Voort, M., Schneider, J. H. M., et al. (2011). Deciphering the rhizosphere microbiome for disease-suppressive bacteria. *Science* 332, 1097–1100. doi: 10.1126/science.1203980

Meng, T., Wang, Q., Abbasi, P., and Ma, Y. (2019). Deciphering differences in the chemical and microbial characteristics of healthy and Fusarium wilt-infected watermelon rhizosphere soils. *Appl. Microbiol. Biotechnol.* 103, 1497–1509. doi: 10.1007/s00253-018-9564-6

Mesterházy, Á. (2002). Role of deoxynivalenol in aggressiveness of *Fusarium graminearum* and *F. culmorum* and in resistance to Fusarium Head Blight. *Eur. J. Plant Pathol.* 108, 675–684. doi: 10.1023/A:1020631114063

Michielse, C. B., and Rep, M. (2009). Pathogen profile update: *Fusarium oxysporum*. *Mol. Plant Pathol.* 10, 311–324. doi: 10.1111/j.1364-3703.2009.00538.x

Mitsuboshi, M., Kioka, Y., Noguchi, K., and Asakawa, S. (2018). Evaluation of suppressiveness of soils exhibiting soil-borne disease suppression after long-term application of organic amendments by the co-cultivation method of pathogenic *Fusarium oxysporum* and indigenous soil microorganisms. *Microbes Environ.* 33, 58–65. doi: 10.1264/jsme2.ME17072

Montalba, R., Arriagada, C., Alvear, M., and Zúñiga, G. E. (2010). Effects of conventional and organic nitrogen fertilizers on soil microbial activity, mycorrhizal colonization, leaf antioxidant content, and Fusarium wilt in highbush blueberry (*Vaccinium corymbosum* L.). *Sci. Hortic.* 125, 775–778. doi: 10.1016/j.scienta.2010.04.046

Moretti, A., Pascale, M., and Logrieco, A. F. (2018). Mycotoxin risks under a climate change scenario in Europe. *Trends Food Sci. Technol.* 84, 38–40. doi: 10.1016/j.tifs.2018.03.008

Morimura, H., Ito, M., Yoshida, S., Koitabashi, M., Tsushima, S., Camagna, M., et al. (2020). *In vitro* assessment of biocontrol effects on Fusarium head blight and deoxynivalenol (DON) accumulation by DON-degrading bacteria. *Toxins* 12 (6), 399. doi: 10.3390/toxins12060399

Mousa, W. K., and Raizada, M. N. (2016). Natural disease control in cereal grains. *Encycl. Food Grains.* 4, 257–263. doi: 10.1016/B978-0-12-394437-5.00206-0

Munkvold, G. P. (2017). "*Fusarium* species and their associated mycotoxins," in *Mycotoxigenic fungi*. Eds. A. Moretti and A. Susca (New York, NY: Humana Press), 51–106.

Munkvold, G. P., Proctor, R. H., and Moretti, A. (2021). Mycotoxin production in *Fusarium* according to contemporary species concepts. *Annu. Rev. Phytopathol. 59* 373–402. doi: 10.1146/annurev-phyto-020620-102825

Murillo-Williams, A., and Munkvold, G. P. (2008). Systemic infection by *Fusarium verticillioides* in maize plants grown under three temperature regimes. *Plant Dis.* 92, 1695–1700. doi: 10.1094/PDIS-92-12-1695

Nazari, L., Pattori, E., Manstretta, V., Terzi, V., Morcia, C., Somma, S., et al. (2018). Effect of temperature on growth, wheat head infection, and nivalenol production by *Fusarium poae*. *Food Microbiol.* 76, 83–90. doi: 10.1016/j.fm.2018.04.015

Nelson, P. E., Dignani, M. C., and Anaissie, E. J. (1994). Taxonomy, biology, and clinical aspects of *Fusarium* species. *Clin. Microbiol. Rev.* 7, 479–504. doi: 10.1128/CMR.7.4.479

Nešić, K., Ivanović, S., and Nešić, V. (2014). Fusarial toxins: secondary metabolites of *Fusarium* fungi. *Rev. Environ. Contam. Toxicol.* 228, 101–120. doi: 10.1007/978-3-319-01619-1_5

Nguvo, K. J., and Gao, X. (2019). Weapons hidden underneath: biocontrol agents and their potentials to activate plant induced systemic resistance in controlling crop *Fusarium* diseases. *J. Plant Dis. Prot.* 126, 177–190. doi: 10.1007/s41348-019-00222-y

Nguyen, P.-A., Strub, C., Durand, N., Alter, P., Fontana, A., and Schorr-Galindo, S. (2018). Biocontrol of *Fusarium verticillioides* using organic amendments and their actinomycete isolates. *Biol. Control.* 118, 55–66. doi: 10.1016/j.biocontrol.2017.12.006

Nisrina, L., Effendi, Y., and Pancoro, A. (2021). Revealing the role of Plant Growth Promoting Rhizobacteria in suppressive soils against *Fusarium oxysporum* f.sp. *cubense* based on metagenomic analysis. *Heliyon* 7, e07636. doi: 10.1016/j.heliyon.2021.e07636

O'Donnell, K., Rooney, A. P., Proctor, R. H., Brown, D. W., McCormick, S. P., Ward, T. J., et al. (2013). Phylogenetic analyses of *RPB1* and *RPB2* support a middle Cretaceous origin for a clade comprising all agriculturally and medically important fusaria. *Fungal Genet. Biol.* 52, 20–31. doi: 10.1016/j.fgb.2012.12.004

O'Donnell, K., Ward, T. J., Robert, V. A. R. G., Crous, P. W., Geiser, D. M., and Kang, S. (2015). DNA sequence-based identification of *Fusarium*: current status and future directions. *Phytoparasitica* 43, 583–595. doi: 10.1007/s12600-015-0484-z

Oren, L., Ezrati, S., Cohen, D., and Sharon, A. (2003). Early Events in the *Fusarium verticillioides* - maize interaction characterized by using a green fluorescent protein-expressing transgenic isolate. *Appl. Environ. Microbiol.* 69, 1695–1701. doi: 10.1128/AEM.69.3.1695-1701.2003

Orr, R., and Nelson, P. N. (2018). Impacts of soil abiotic attributes on Fusarium wilt, focusing on bananas. *Appl. Soil Ecol.* 132, 20–33. doi: 10.1016/j.apsoil.2018.06.019

Ossowicki, A., Tracanna, V., Petrus, M. L. C., van Wezel, G., Raaijmakers, J. M., Medema, M. H., et al. (2020). Microbial and volatile profiling of soils suppressive to *Fusarium culmorum* of wheat. *Proc. Biol. Sci.* 287, 20192527. doi: 10.1098/rspb.2019.2527

Pal, K. K., and McSpadden Gardener, B. (2006). Biological control of plant pathogens. *Plant Health Instruct.* 2, 1117–1142. doi: 10.1094/PHI-A-2006-1117-02

Pal, K. K., Tilak, K. V. B. R., Saxena, A. K., Dey, R., and Singh, C. S. (2001). Suppression of maize root diseases caused by *Macrophomina phaseolina*, *Fusarium moniliforme* and *Fusarium graminearum* by plant growth promoting rhizobacteria. *Microbiol. Res.* 156, 209–223. doi: 10.1078/0944-5013-00103

Palazzini, J. M., Ramirez, M. L., Torres, A. M., and Chulze, S. N. (2007). Potential biocontrol agents for Fusarium head blight and deoxynivalenol production in wheat. *Crop Prot.* 26, 1702–1710. doi: 10.1016/j.cropro.2007.03.004

Palmieri, D., Segorbe, D., López-Berges, M. S., De Curtis, F., Lima, G., Di Pietro, A., et al. (2023). Alkaline pH, low iron availability, poor nitrogen sources and CWI MAPK signaling are associated with increased fusaric acid production in *Fusarium oxysporum*. *Toxins* 15 (1), 50. doi: 10.3390/toxins15010050

Pélissier, R., Violle, C., and Morel, J.-B. (2021). Plant immunity: Good fences make good neighbors? *Curr. Opin. Plant Biol.* 62, 102045. doi: 10.1016/j.pbi.2021.102045

Pellan, L., Durand, N., Martinez, V., Fontana, A., Schorr-Galindo, S., and Strub, C. (2020). Commercial biocontrol agents reveal contrasting comportments against two mycotoxigenic fungi in cereals: *Fusarium graminearum* and *Fusarium verticillioides*. *Toxins* 12, 152. doi: 10.3390/toxins12030152

Peng, H. X., Sivasithamparam, K., and Turner, D. W. (1999). Chlamydospore germination and Fusarium wilt of banana plantlets in suppressive and conducive soils are affected by physical and chemical factors. *Soil Biol. Biochem.* 31, 1363–1374. doi: 10.1016/S0038-0717(99)00045-0

Pereyra, S. A., Dill-Macky, R., and Sims, A. L. (2004). Survival and inoculum production of *Gibberella zeae* in wheat residue. *Plant Dis.* 88, 724–730. doi: 10.1094/PDIS.2004.88.7.724

Petti, C., Khan, M., and Doohan, F. (2010). Lipid transfer proteins and protease inhibitors as key factors in the priming of barley responses to Fusarium head blight disease by a biocontrol strain of *Pseudomonas fluorescens*. *Funct. Integr. Genomics* 10, 619–627. doi: 10.1007/s10142-010-0177-0

Pfordt, A., Ramos Romero, L., Schiwek, S., Karlovsky, P., and von Tiedemann, A. (2020). Impact of environmental conditions and agronomic practices on the prevalence of *Fusarium* species associated with ear-and stalk rot in maize. *Pathogens* 9, 236. doi: 10.3390/pathogens9030236

Pieterse, C. M. J., Zamioudis, C., Berendsen, R. L., Weller, D. M., Van Wees, S. C. M., and Bakker, P. A. H. M. (2014). Induced systemic resistance by beneficial microbes. *Annu. Rev. Phytopathol.* 52, 347–375. doi: 10.1146/annurev-phyto-082712-102340

Pisi, A., Cesari, A., Zakrisson, E., Filippini, G., Roberti, R., and Mantovani, W. (2001). SEM investigation about hyphal relationships between some antagonistic fungi against *Fusarium* spp. foot rot pathogen of wheat. *Phytopathol. Mediterr.* 40, 37–44. doi: 10.14601/PHYTOPATHOL_MEDITERR-1588

Podolska, G., Bryła, M., Sułek, A., Waśkiewicz, A., Szymczyk, K., and Jędrzejczak, R. (2017). Influence of the cultivar and nitrogen fertilisation level on the mycotoxin contamination in winter wheat. *Qual. Assur. Saf. Crops Foods.* 9, 451–461. doi: 10.3920/QAS2016.1064

Qualhato, T. F., Lopes, F. A. C., Steindorff, A. S., Brandão, R. S., Jesuino, R. S. A., and Ulhoa, C. J. (2013). Mycoparasitism studies of *Trichoderma* species against three phytopathogenic fungi: evaluation of antagonism and hydrolytic enzyme production. *Biotechnol. Lett.* 35, 1461–1468. doi: 10.1007/s10529-013-1225-3

Raaijmakers, J., Leeman, M., van Oorschot, M., van der Sluis, I., Schippers, B., and Bakker, P. (1995). Dose-response relationships in biological control of Fusarium wilt of radish by *Pseudomonas* spp. *Phytopathology* 85, 1075–1081. doi: 10.1094/Phyto-85-1075

Raaijmakers, J. M., Paulitz, T. C., Steinberg, C., Alabouvette, C., and Moënne-Loccoz, Y. (2009). The rhizosphere: a playground and battlefield for soilborne pathogens and beneficial microorganisms. *Plant Soil.* 321, 341–361. doi: 10.1007/s11104-008-9568-6

Rana, A., Sahgal, M., and Johri, B. N. (2017). "*Fusarium oxysporum*: genomics, diversity and plant–host interaction," in *Developments in Fungal Biology and Applied Mycology*. Eds. T. Satyanarayana, S. Deshmukh and B. Johri (Singapore: Springer International Publishing), 159–199. doi: 10.1007/978-981-10-4768-8_10

Ranzi, C., Camera, J. N., and Deuner, C. C. (2017). Influence of continuous cropping on corn and soybean pathogens. *Summa Phytopathol.* 43, 14–19. doi: 10.1590/0100-5405/2150

Rasmussen, P. H., Knudsen, I. M. B., Elmholt, S., and Jensen, D. F. (2002). Relationship between soil cellulolytic activity and suppression of seedling blight of barley in arable soils. *Appl. Soil Ecol.* 19, 91–96. doi: 10.1016/S0929-1393(01)00177-9

Raza, W., Yuan, J., Ling, N., Huang, Q., and Shen, Q. (2015). Production of volatile organic compounds by an antagonistic strain *Paenibacillus polymyxa* WR-2 in the presence of root exudates and organic fertilizer and their antifungal activity against *Fusarium oxysporum* f. sp. *niveum*. *Biol. Control.* 80, 89–95. doi: 10.1016/j.biocontrol.2014.09.004

Redkar, A., Gimenez Ibanez, S., Sabale, M., Zechmann, B., Solano, R., and Di Pietro, A. (2022a). *Marchantia polymorpha* model reveals conserved infection mechanisms in the vascular wilt fungal pathogen *Fusarium oxysporum*. *New Phytol.* 234, 227–241. doi: 10.1111/nph.17909

Redkar, A., Sabale, M., Zuccaro, A., and Di Pietro, A. (2022b). Determinants of endophytic and pathogenic lifestyle in root colonizing fungi. *Curr. Opin. Plant Biol.* 67, 102226. doi: 10.1016/j.pbi.2022.102226

Reino, J. L., Guerrero, R. F., Hernández-Galán, R., and Collado, I. G. (2008). Secondary metabolites from species of the biocontrol agent *Trichoderma*. *Phytochem. Rev.* 7, 89–123. doi: 10.1007/s11101-006-9032-2

Reis, T. A., Oliveira, T. D., Zorzete, P., Faria, P., and Corrêa, B. (2020). A non-toxigenic *Aspergillus flavus* strain prevents the spreading of *Fusarium verticillioides* and fumonisins in maize. *Toxicon* 181, 6–8. doi: 10.1016/j.toxicon.2020.04.091

Reyes Gaige, A., Todd, T., and Stack, J. P. (2020). Interspecific competition for colonization of maize plants between *Fusarium proliferatum* and *Fusarium verticillioides*. *Plant Dis.* 104, 2102–2110. doi: 10.1094/PDIS-09-19-1964-RE

Ristić, D. (2012). *Characterization of Fusarium species pathogen for sorghum [Sorghum bicolor (L.) Moench] in Serbia and genotype susceptibility. [dissertation]* (Belgrade: University of Belgrade, Faculty of Agriculture). doi: 10.2298/BG20121008RISTIC

Rizaludin, M. S., Stopnisek, N., Raaijmakers, J. M., and Garbeva, P. (2021). The chemistry of stress: Understanding the 'cry for help' of plant roots. *Metabolites* 11, 357. doi: 10.3390/metabo11060357

Rolfe, S. A., Griffiths, J., and Ton, J. (2019). Crying out for help with root exudates: adaptive mechanisms by which stressed plants assemble health-promoting soil microbiomes. *Curr. Opin. Microbiol.* 49, 73–82. doi: 10.1016/j.mib.2019.10.003

Rosenzweig, N., Tiedje, J. M., Quensen, J. F., Meng, Q., and Hao, J. J. (2012). Microbial communities associated with potato common scab-suppressive soil determined by pyrosequencing analyses. *Plant Dis.* 96, 718–725. doi: 10.1094/PDIS-07-11-0571

Rouxel, F., and Sedra, H. (1989). Resistance des sols aux maladies. Mise en evidence de la resistance d'un sol de la palmeraie de Marrakech aux fusarioses vasculaires. *Al Awamia.* 66, 35–54.

Sajeena, A., Nair, D. S., and Sreepavan, K. (2020). Non-pathogenic *Fusarium oxysporum* as a biocontrol agent. *Indian Phytopathol.* 73, 177–183. doi: 10.1007/s42360-020-00226-x

Sánchez-Cañizares, C., Jorrín, B., Poole, P. S., and Tkacz, A. (2017). Understanding the holobiont: the interdependence of plants and their microbiome. *Curr. Opin. Microbiol.* 38, 188–196. doi: 10.1016/j.mib.2017.07.001

Sanguin, H., Sarniguet, A., Gazengel, K., Moënne-Loccoz, Y., and Grundmann, G. L. (2009). Rhizosphere bacterial communities associated with disease suppressiveness stages of take-all decline in wheat monoculture. *New Phytol.* 184, 694–707. doi: 10.1111/j.1469-8137.2009.03010.x

Saravanakumar, K., Li, Y., Yu, C., Wang, Q.-Q., Wang, M., Sun, J., et al. (2017). Effect of *Trichoderma harzianum* on maize rhizosphere microbiome and biocontrol of Fusarium stalk rot. *Sci. Rep.* 7, 1771. doi: 10.1038/s41598-017-01680-w

Sautour, M., Edel-Hermann, V., Steinberg, C., Sixt, N., Laurent, J., Dalle, F., et al. (2012). *Fusarium* species recovered from the water distribution system of a French university hospital. *Int. J. Hyg. Environ. Health* 215, 286–292. doi: 10.1016/j.ijheh.2011.11.003

Scher, F. M., and Baker, R. (1980). Mechanism of biological control in a *Fusarium*-suppressive soil. *Phytopathology* 70, 412–417. doi: 10.1094/Phyto-70-412

Schlatter, D., Kinkel, L., Thomashow, L., Weller, D., and Paulitz, T. (2017). Disease suppressive soils: New insights from the soil microbiome. *Phytopathology* 107, 1284–1297. doi: 10.1094/PHYTO-03-17-0111-RVW

Schmale, D. G., and Bergstrom, G. C. (2003). *Fusarium* head blight in wheat. *Plant Health Instr.* doi: 10.1094/PHI-I-2003-0612-01

Schreiner, K., Hagn, A., Kyselková, M., Moënne-Loccoz, Y., Welzl, G., Munch, J. C., et al. (2010). Comparison of barley succession and take-all disease as environmental factors shaping the rhizobacterial community during take-all decline. *Appl. Environ. Microbiol.* 76, 4703–4712. doi: 10.1128/AEM.00481-10

Scott, J. C., Gordon, T. R., Shaw, D. V., and Koike, S. T. (2009). Effect of temperature on severity of Fusarium wilt of lettuce caused by *Fusarium oxysporum* f. sp. *lactucae*. *Plant Dis.* 94, 13–17. doi: 10.1094/PDIS-94-1-0013

Scott, P., Strange, R., Korsten, L., and Gullino, M. L. (2021). *Plant Diseases and Food Security in the 21st Century* (The Netherlands: Springer International Publishing).

Segarra, G., Casanova, E., Avilés, M., and Trillas, I. (2010). *Trichoderma asperellum* strain T34 controls Fusarium wilt disease in tomato plants in soilless culture through competition for iron. *Microb. Ecol.* 59, 141–149. doi: 10.1007/s00248-009-9545-5

Senatore, M. T., Ward, T. J., Cappelletti, E., Beccari, G., McCormick, S. P., Busman, M., et al. (2021). Species diversity and mycotoxin production by members of the Fusarium tricinctum species complex associated with Fusarium head blight of wheat and barley in Italy. *J. Food Microbiol.* 358, 109298. doi: 10.1016/j.ijfoodmicro.2021.109298

Senechkin, I. V., van Overbeek, L. S., and van Bruggen, A. H. C. (2014). Greater Fusarium wilt suppression after complex than after simple organic amendments as affected by soil pH, total carbon and ammonia-oxidizing bacteria. *Appl. Soil Ecol.* 73, 148–155. doi: 10.1016/j.apsoil.2013.09.003

Shen, Z., Ruan, Y., Wang, B., Zhong, S., Su, L., Li, R., et al. (2015a). Effect of biofertilizer for suppressing Fusarium wilt disease of banana as well as enhancing microbial and chemical properties of soil under greenhouse trial. *Appl. Soil Ecol.* 93, 111–119. doi: 10.1016/j.apsoil.2015.04.013

Shen, Z., Ruan, Y., Xue, C., Zhong, S., Li, R., and Shen, Q. (2015b). Soils naturally suppressive to banana Fusarium wilt disease harbor unique bacterial communities. *Plant Soil.* 393, 21–33. doi: 10.1007/s11104-015-2474-9

Shen, Z., Thomashow, L. S., Ou, Y., Tao, C., Wang, J., Xiong, W., et al. (2022). Shared core microbiome and functionality of key taxa suppressive to banana Fusarium wilt. *Research* 2022, 9818073. doi: 10.34133/2022/9818073

Shi, C., Yan, P., Li, J., Wu, H., Li, Q., and Guan, S. (2014). Biocontrol of *Fusarium graminearum* growth and deoxynivalenol production in wheat kernels with bacterial antagonists. *Int. J. Environ. Res. Public. Health* 11, 1094–1105. doi: 10.3390/ijerph110101094

Shipton, P. J., Cook, R. J., and Sitton, J. W. (1973). Occurrence and transfer of a biological factor in soil that suppresses take-all of wheat in Eastern Washington. *Phytopathology* 63, 511–517. doi: 10.1094/Phyto-63-511

Siegel-Hertz, K., Edel-Hermann, V., Chapelle, E., Terrat, S., Raaijmakers, J. M., and Steinberg, C. (2018). Comparative microbiome analysis of a Fusarium wilt suppressive soil and a Fusarium wilt conducive soil from the Châteaurenard region. *Front. Microbiol.* 9, 568. doi: 10.3389/fmicb.2018.00568

Singh, R. K., Singh, P., Guo, D.-J., Sharma, A., Li, D.-P., Li, X., et al. (2021). Root-derived endophytic diazotrophic bacteria *Pantoea cypripedii* AF1 and *Kosakonia arachidis* EF1 promote nitrogen assimilation and growth in sugarcane. *Front. Microbiol.* 12. doi: 10.3389/fmicb.2021.774707

Šišić, A., Baćanović-Šišić, J., Al-Hatmi, A. M. S., Karlovsky, P., Ahmed, S. A., Maier, W., et al. (2018). The "*forma specialis*" issue in *Fusarium*: A case study in *Fusarium solani* f. sp. pisi. *Sci. Rep.* 8, 1252. doi: 10.1038/s41598-018-19779-z

Smith, S. N. (2007). An overview of ecological and habitat aspects in the genus *Fusarium* with special emphasis on the soil-borne pathogenic forms. *Plant Pathol. Bull.* 16, 97–120.

Smith, S. N., and Snyder, W. C. (1971). Relationship of inoculum density and soil types to severity of Fusarium wilt of sweet potato. *Phytopathology* 61, 1049–1051. doi: 10.1094/Phyto-61-1049

Sneh, B., Dupler, M., Elad, Y., and Baker, R. (1984). Chlamydospore germination of *Fusarium oxysporum* f. sp. *cucumerinum* as affected by fluorescent and lytic bacteria from a Fusarium-suppressive soil. *Phytopathology* 74 (9), 1115–1124. doi: 10.1094/PHYTO-74-1115

Spiegel, Y., Netzer, D., and Kafkafi, U. (1987). The role of calcium nutrition on Fusarium-wilt syndrome in muskmelon. *J. Phytopathol.* 118, 220–226. doi: 10.1111/j.1439-0434.1987.tb00451.x

Steinkellner, S., and Langer, I. (2004). Impact of tillage on the incidence of *Fusarium* spp. in soil. *Plant Soil.* 267, 13–22. doi: 10.1007/s11104-005-2574-z

Stotzky, G., and Torrence Martin, R. (1963). Soil mineralogy in relation to the spread of Fusarium wilt of banana in Central America. *Plant Soil.* 18, 317–337. doi: 10.1007/BF01347232

Stover, R. H. (1956). Studies on Fusarium wilt of bananas: I. The behavior of *F. oxysporum* f. *cubense* in different soils. *Can. J. Bot.* 34, 927–942. doi: 10.1139/b56-073

Sturz, A. V., and Carter, M. R. (1995). Conservation tillage systems, fungal complexes and disease development in soybean and barley rhizospheres in Prince Edward Island. *Soil Tillage Res.* 34, 225–238. doi: 10.1016/0167-1987(95)00469-9

Stutz, E. W., Défago, G., and Kern, H. (1986). Naturally occurring fluorescent pseudomonads involved in suppression of black root rot of tobacco. *Phytopathology* 76, 181–185. doi: 10.1094/Phyto-76-181

Summerell, B. A. (2019). Resolving *Fusarium*: Current status of the genus. *Annu. Rev. Phytopathol.* 57, 323–339. doi: 10.1146/annurev-phyto-082718-100204

Sundaramoorthy, S., Raguchander, T., Ragupathi, N., and Samiyappan, R. (2012). Combinatorial effect of endophytic and plant growth promoting rhizobacteria against wilt disease of *Capsicum annum* L. caused by *Fusarium solani*. *Biol. Control.* 60, 59–67. doi: 10.1016/j.biocontrol.2011.10.002

Szczech, M. M. (1999). Suppressiveness of vermicompost against Fusarium wilt of tomato. *J. Phytopathol.* 147, 155–161. doi: 10.1046/j.1439-0434.1999.147003155.x

Tamietti, G., and Alabouvette, C. (1986). Résistance des sols aux maladies : XIII - Rôle des *Fusarium oxysporum* non pathogènes dans les mécanismes de résistance d'un sol de Noirmoutier aux fusarioses vasculaires. *Agronomie* 6, 541–548. doi: 10.1051/agro:19860606

Tamietti, G., Ferraris, L., Matta, A., and Abbattista Gentile, I. (1993). Physiological responses of tomato plants grown in Fusarium suppressive soil. *J. Phytopathol.* 138, 66–76. doi: 10.1111/j.1439-0434.1993.tb01361.x

Tamietti, G., and Matta, A. (1984). "*Fusarium lycopersici*-suppressive properties in the soil of Albenga (Italy): preliminary observations," in *Proc. 6th Congr. Union Phytopathol*, Mediterr, Cairo. 129–131.

Tamietti, G., and Pramotton, R. (1990). La réceptivité des sols aux fusarioses vasculaires : rapports entre résistance et microflore autochtone avec référence particulière aux *Fusarium* non pathogènes. *Agronomie* 10, 69–76. doi: 10.1051/agro:19900109

Tang, T., Sun, X., Liu, Q., Dong, Y., and Zha, M. (2023). Treatment with organic manure inoculated with a biocontrol agent induces soil bacterial communities to inhibit tomato Fusarium wilt disease. *Front. Microbiol.* 13, 1006878. doi: 10.3389/fmicb.2022.1006878

Tao, C., Li, R., Xiong, W., Shen, Z., Liu, S., Wang, B., et al. (2020). Bio-organic fertilizers stimulate indigenous soil *Pseudomonas* populations to enhance plant disease suppression. *Microbiome* 8, 137. doi: 10.1186/s40168-020-00892-z

Tari, P. H., and Anderson, A. J. (1988). Fusarium wilt suppression and agglutinability of *Pseudomonas putida*. *Appl. Environ. Microbiol.* 54, 2037–2041. doi: 10.1128/aem.54.8.2037-2041.1988

Termorshuizen, A. J., van Rijn, E., van der Gaag, D. J., Alabouvette, C., Chen, Y., Lagerlöf, J., et al. (2006). Suppressiveness of 18 composts against 7 pathosystems: Variability in pathogen response. *Soil Biol. Biochem.* 38, 2461–2477. doi: 10.1016/j.soilbio.2006.03.002

Theron, J. S., Johannes van Coller, G., Rose, L. J., Labuschagne, J., and Swanepoel, P. A. (2023). The effect of crop rotation and tillage practice on Fusarium crown rot and agronomic parameters of wheat in South Africa. *Crop Prot.* 166, 106175. doi: 10.1016/j.cropro.2022.106175

Thrane, U. (2014). "Fusarium," in *Encyclopedia of Food Microbiology*. Eds. C. A. Batt and M. L. Tortorello (Amsterdam, The Netherlands: Elsevier), 76–81. doi: 10.1016/B978-0-12-384730-0.00141-5

Tian, Y., Tan, Y., Yan, Z., Liao, Y., Chen, J., de Boevre, M., et al. (2018). Antagonistic and detoxification potentials of *Trichoderma* isolates for control of zearalenone (ZEN) producing *Fusarium graminearum*. *Front. Microbiol.* 8. doi: 10.3389/fmicb.2017.02710

Tkacz, A., Cheema, J., Chandra, G., Grant, A., and Poole, P. S. (2015). Stability and succession of the rhizosphere microbiota depends upon plant type and soil composition. *ISME J.* 9, 2349–2359. doi: 10.1038/ismej.2015.41

Tkacz, A., and Poole, P. S. (2015). Role of root microbiota in plant productivity. *J. Exp. Bot.* 66, 2167–2175. doi: 10.1093/jxb/erv157

Torbati, M., Arzanlou, M., and da Silva Santos, A. C. (2021). Fungicolous *Fusarium* species: Ecology, diversity, isolation, and identification. *Curr. Microbiol.* 78, 2850–2859. doi: 10.1007/s00284-021-02584-9

Tyc, O., Zweers, H., de Boer, W., and Garbeva, P. (2015). Volatiles in inter-specific bacterial interactions. *Front. Microbiol.* 6, 1412. doi: 10.3389/fmicb.2015.01412

Vandenkoornhuyse, P., Quaiser, A., Duhamel, M., Le Van, A., and Dufresne, A. (2015). The importance of the microbiome of the plant holobiont. *New Phytol.* 206, 1196–1206. doi: 10.1111/nph.13312

Van Peer, R., Niemann, G. J., and Schippers, B. (1991). Induced resistance and phytoalexin accumulation in biological control of Fusarium wilt of carnation by *Pseudomonas* sp. strain WCS417r. *Phytopathology* 81, 728–734. doi: 10.1094/Phyto-81-728

Vasudeva, R. S., and Roy, T. C. (1950). The effect of associated soil microflora on *Fusarium udum* Butl., the fungus causing wilt of pigeon-pea (*Cajanus cajan* (L.) Millsp.). *Ann. Appl. Biol.* 37, 169–178. doi: 10.1111/j.1744-7348.1950.tb01037.x

Veliz, E. A., Martínez-Hidalgo, P., and Hirsch, A. M. (2017). Chitinase-producing bacteria and their role in biocontrol. *AIMS Microbiol.* 3, 689. doi: 10.3934/microbiol.2017.3.689

Viterbo, A., Ramot, O., Chernin, L., and Chet, I. (2002). Significance of lytic enzymes from *Trichoderma* spp. in the biocontrol of fungal plant pathogens. *Antonie Van Leeuwenhoek.* 81, 549–556. doi: 10.1023/a:1020553421740

Voigt, K. (2002). "Management of *Fusarium* diseases," in *Agricultural Applications*. Ed. F. Kempken (Berlin, Heidelberg: Springer Berlin Heidelberg), 217–242. doi: 10.1007/978-3-662-03059-2_12

Vujanović, V., and Goh, Y. K. (2009). *Sphaerodes mycoparasitica* sp. nov., a new biotrophic mycoparasite on *Fusarium avenaceum*, *F. graminearum* and *F. oxysporum*. *Mycol. Res.* 113, 1172–1180. doi: 10.1016/j.mycres.2009.07.018

Wagacha, J. M., and Muthomi, J. W. (2007). *Fusarium culmorum*: Infection process, mechanisms of mycotoxin production and their role in pathogenesis in wheat. *Crop Prot.* 26, 877–885. doi: 10.1016/j.cropro.2006.09.003

Wagner, T. A., Duke, S. E., Davie, S. M., Magill, C., and Liu, J. (2022). Interaction of Fusarium wilt race 4 with root-knot nematode increases disease severity in cotton. *Plant Dis.* 106, 2558–2562. doi: 10.1094/PDIS-12-21-2725-SC

Walters, D. R., Ratsep, J., and Havis, N. D. (2013). Controlling crop diseases using induced resistance: challenges for the future. *J. Exp. Bot.* 64, 1263–1280. doi: 10.1093/jxb/ert026

Wang, X., Du, Z., Chen, C., Guo, S., Mao, Q., Wu, W., et al. (2023). Antifungal effects and biocontrol potential of lipopeptide-producing *Streptomyces* against banana Fusarium wilt fungus *Fusarium oxysporum* f. sp. *cubense*. *Front. Microbiol.* 14, 1177393. doi: 10.3389/fmicb.2023.1177393

Wang, T., Hao, Y., Zhu, M., Yu, S., Ran, W., Xue, C., et al. (2019). Characterizing differences in microbial community composition and function between Fusarium wilt diseased and healthy soils under watermelon cultivation. *Plant Soil* 438, 421–433. doi: 10.1007/s11104-019-04037-6

Wang, H., Li, X., Li, X., Wang, J., Li, X., Guo, Q., et al. (2020). Long-term no-tillage and different residue amounts alter soil microbial community composition and increase the risk of maize root rot in Northeast China. *Soil Tillage Res.* 196, 104452. doi: 10.1016/j.still.2019.104452

Wang, B., Li, R., Ruan, Y., Ou, Y., Zhao, Y., and Shen, Q. (2015). Pineapple–banana rotation reduced the amount of *Fusarium oxysporum* more than maize–banana rotation mainly through modulating fungal communities. *Soil Biol. Biochem.* 86, 77–86. doi: 10.1016/j.soilbio.2015.02.021

Wang, J.-T., Zheng, Y.-M., Hu, H.-W., Li, J., Zhang, L.-M., Chen, B.-D., et al. (2016). Coupling of soil prokaryotic diversity and plant diversity across latitudinal forest ecosystems. *Sci. Rep.* 6 (1), 19561. doi: 10.1038/srep19561

Weber, R., Hrynczuk, B., Runowska-Hrynczuk, B., and Kita, W. (2001). Influence of the mode of tillage on diseases of culm base in some winter wheat varieties, oats and spring wheat. *J. Phytopathol.* 149, 185–188. doi: 10.1046/j.1439-0434.2001.00592.x

Weber, R., and Kita, W. (2010). Effects of tillage system and forecrop type on frequency of *Fusarium culmorum* and *F. avenaceum* occurrence on culm base of some winter wheat (*Triticum aestivum* L.) cultivars. *Acta Agrobot.* 63, 121–128. doi: 10.5586/aa.2010.014

Weller, D. M., Landa, B. B., Mavrodi, O. V., Schroeder, K. L., de la Fuente, L., Blouin Bankhead, S., et al. (2007). Role of 2,4-diacetylphloroglucinol-producing fluorescent Pseudomonas spp. in the defense of plant roots. *Plant Biol. Stuttg. Ger.* 9, 4–20. doi: 10.1055/s-2006-924473

Weller, D. M., Raaijmakers, J. M., McSpadden Gardener, B. B., and Thomashow, L. S. (2002). Microbial populations responsible for specific soil suppressiveness to plant pathogens. *Annu. Rev. Phytopathol.* 40, 309–348. doi: 10.1146/annurev.phyto.40.030402.110010

Willocquet, L., Meza, W. R., Dumont, B., Klocke, B., Feike, T., Kersebaum, K. C., et al. (2021). An outlook on wheat health in Europe from a network of field experiments. *Crop Prot.* 139, 105335. doi: 10.1016/j.cropro.2020.105335

Winter, M., de Mol, F., and von Tiedemann, A. (2014). Cropping systems with maize and oilseed rape for energy production may reduce the risk of stem base diseases in wheat. *Field Crops Res.* 156, 249–257. doi: 10.1016/j.fcr.2013.10.009

Xia, J. W., Sandoval-Denis, M., Crous, P. W., Zhang, X. G., and Lombard, L. (2019). Numbers to names-restyling the *Fusarium incarnatum-equiseti* species complex. *Persoonia* 43, 186–221. doi: 10.3767/persoonia.2019.43.05

Xiong, W., Guo, S., Jousset, A., Zhao, Q., Wu, H., Li, R., et al. (2017). Bio-fertilizer application induces soil suppressiveness against Fusarium wilt disease by reshaping the soil microbiome. *Soil Biol. Biochem.* 114, 238–247. doi: 10.1016/j.soilbio.2017.07.016

Xu, X. (2003). Effects of environmental conditions on the development of Fusarium Ear Blight. *Eur. J. Plant Pathol.* 109, 683–689. doi: 10.1023/A:1026022223359

Xu, F., Liu, W., Song, Y., Zhou, Y., Xu, X., Yang, G., et al. (2021). The distribution of *Fusarium graminearum* and *Fusarium asiaticum* causing Fusarium head blight of wheat in relation to climate and cropping system. *Plant Dis.* 105, 2830–2835. doi: 10.1094/PDIS-01-21-0013-RE

Xu, X.-M., Monger, W., Ritieni, A., and Nicholson, P. (2007). Effect of temperature and duration of wetness during initial infection periods on disease development, fungal biomass and mycotoxin concentrations on wheat inoculated with single, or combinations of *Fusarium* species. *Plant Pathol.* 56, 943–956. doi: 10.1111/j.1365-3059.2007.01650.x

Xu, Z., Wang, M., Du, J., Huang, T., Liu, J., Dong, T., et al. (2020). Isolation of Burkholderia sp. HQB-1, a promising biocontrol bacteria to protect banana against Fusarium wilt through phenazine-1-carboxylic acid secretion. *Front. Microbiol.* 11, 605152. doi: 10.3389/fmicb.2020.605152

Yadav, K., Damodaran, T., Dutt, K., Singh, A., Muthukumar, M., Rajan, S., et al. (2021). Effective biocontrol of banana Fusarium wilt tropical race 4 by a *Bacillus* rhizobacteria strain with antagonistic secondary metabolites. *Rhizosphere* 18, 100341. doi: 10.1016/j.rhisph.2021.100341

Ye, X., Li, Z., Luo, X., Wang, W., Li, Y., Li, R., et al. (2020). A predatory myxobacterium controls cucumber Fusarium wilt by regulating the soil microbial community. *Microbiome* 8 (49), 1–17. doi: 10.1186/s40168-020-00824-x

Yilmaz, N., Sandoval-Denis, M., Lombard, L., Visagie, C. M., Wingfield, B. D., and Crous, P. W. (2021). Redefining species limits in the *Fusarium fujikuroi* species complex. *Persoonia* 46, 129–162. doi: 10.3767/persoonia.2021.46.05

Yuan, J., Wen, T., Zhang, H., Zhao, M., Penton, C. R., Thomashow, L. S., et al. (2020). Predicting disease occurrence with high accuracy based on soil macroecological patterns of Fusarium wilt. *ISME J.* 14 (12), 2936–2950. doi: 10.1038/s41396-020-0720-5

Zaim, S., Belabid, L., Bayaa, B., and Bekkar, A. A. (2016). "Biological control of chickpea Fusarium wilts using rhizobacteria PGPR," in *Microbial-mediated Induced Systemic Resistance in Plants*. Eds. D. Choudhary and A. Varma (Singapore: Springer Nature), 147–162.

Zalila-Kolsi, I., Ben Mahmoud, A., Ali, H., Sellami, S., Nasfi, Z., Tounsi, S., et al. (2016). Antagonist effects of Bacillus spp. strains against *Fusarium graminearum* for protection of durum wheat (*Triticum turgidum* L. subsp. *durum*). *Microbiol. Res.* 192, 148–158. doi: 10.1016/j.micres.2016.06.012

Zhao, S., Du, C.-M., and Tian, C.-Y. (2012). Suppression of *Fusarium oxysporum* and induced resistance of plants involved in the biocontrol of cucumber Fusarium wilt by *Streptomyces bikiniensis* HD-087. *World J. Microbiol. Biotechnol.* 28, 2919–2927. doi: 10.1007/s11274-012-1102-6

Zhao, Y., Selvaraj, J., Xing, F., Zhou, L., Wang, Y., Song, H., et al. (2014). Antagonistic action of *Bacillus subtilis* strain SG6 on *Fusarium graminearum*. *PloS One* 9, e92486. doi: 10.1371/journal.pone.0092486

Zhou, D., Jing, T., Chen, Y., Wang, F., Qi, D., Feng, R., et al. (2019). Deciphering microbial diversity associated with Fusarium wilt-diseased and disease-free banana rhizosphere soil. *BMC Microbiol.* 19, 1–13. doi: 10.1186/s12866-019-1531-6

Zohair, M. M., El-Beih, A. A., Sadik, M. W., Hamed, E. R., and Sedik, M. Z. (2018). Promising biocontrol agents isolated from medicinal plants rhizosphere against root-rot fungi. *Biocatal. Agric. Biotechnol.* 15, 11–18. doi: 10.1016/j.bcab.2018.04.015

frontiers | Frontiers in Microbiology

TYPE Original Research
PUBLISHED 01 February 2024
DOI 10.3389/fmicb.2023.1265265

OPEN ACCESS

EDITED BY
Mahyar Mirmajlessi,
Ghent University, Belgium

REVIEWED BY
Arindam Ghatak,
University of Vienna, Austria
Arshi Jamil,
Aligarh Muslim University, India

*CORRESPONDENCE
Karma L. Bhutia
klbhutia@rpcau.ac.in
Akbar Hossain
akbarhossainwrc@gmail.com

RECEIVED 22 July 2023
ACCEPTED 30 October 2023
PUBLISHED 01 February 2024

CITATION
Bhutia KL, Ahmad M, Kisku A, Sudhan R, Bhutia ND, Sharma V, Prasad BD, Thudi M, Obročník O, Bárek V, Brestic M, Skalicky M, Gaber A and Hossain A (2024) Shoot transcriptome revealed widespread differential expression and potential molecular mechanisms of chickpea (*Cicer arietinum* L.) against *Fusarium* wilt. *Front. Microbiol.* 14:1265265. doi: 10.3389/fmicb.2023.1265265

Shoot transcriptome revealed widespread differential expression and potential molecular mechanisms of chickpea (*Cicer arietinum* L.) against *Fusarium* wilt

Karma L. Bhutia[1]*, Mahtab Ahmad[1], Anima Kisku[1], R. A. Sudhan[1], Nangsol D. Bhutia[2], V. K. Sharma[1], Bishun Deo Prasad[1], Mahendar Thudi[1], Oliver Obročník[3], Viliam Bárek[3], Marian Brestic[4,5], Milan Skalicky[5], Ahmed Gaber[6] and Akbar Hossain[7]*

[1]Department of Agricultural Biotechnology and Molecular Biology, CBS&H, Dr. Rajendra Prasad Central Agricultural University, Pusa, Bihar, India, [2]College of Horticulture and Forestry, Central Agricultural University (Imphal), Pasighat, Arunachal Pradesh, India, [3]Department of Water Resources and Environmental Engineering, Faculty of Horticulture and Landscape Engineering, Slovak University of Agriculture, Nitra, Slovakia, [4]Institute of Plant and Environmental Sciences, Slovak University of Agriculture, Nitra, Slovakia, [5]Department of Botany and Plant Physiology, Faculty of Agrobiology, Food, and Natural Resources, Czech University of Life Sciences Prague, Prague, Czechia, [6]Department of Biology, College of Science, Taif University, Taif, Saudi Arabia, [7]Division of Soil Science, Bangladesh Wheat and Maize Research Institute, Dinajpur, Bangladesh

Introduction: The yield of chickpea is severely hampered by infection wilt caused by several races of *Fusarium oxysporum* f. sp. *ciceris (Foc).*

Methods: To understand the underlying molecular mechanisms of resistance against *Foc4 Fusarium* wilt, RNA sequencing-based shoot transcriptome data of two contrasting chickpea genotypes, namely KWR 108 (resistant) and GL 13001 (susceptible), were generated and analyzed.

Results and Discussion: The shoot transcriptome data showed 1,103 and 1,221 significant DEGs in chickpea genotypes KWR 108 and GL 13001, respectively. Among these, 495 and 608 genes were significantly down and up-regulated in genotypes KWR 108, and 427 and 794 genes were significantly down and up-regulated in genotype GL 13001. The gene ontology (GO) analysis of significant DEGs was performed and the GO of the top 50 DEGs in two contrasting chickpea genotypes showed the highest cellular components as membrane and nucleus, and molecular functions including nucleotide binding, metal ion binding, transferase, kinase, and oxidoreductase activity involved in biological processes such as phosphorylation, oxidation–reduction, cell redox homeostasis process, and DNA repair. Compared to the susceptible genotype which showed significant up-regulation of genes involved in processes like DNA repair, the significantly up-regulated DEGs of the resistant genotypes were involved in processes like energy metabolism and environmental adaptation, particularly host-pathogen interaction. This indicates an efficient utilization of environmental adaptation pathways, energy homeostasis, and stable DNA molecules as the strategy to cope with *Fusarium* wilt infection in chickpea. The findings of the study will be useful in targeting the genes in designing gene-based markers for association mapping with the traits of interest in chickpea under *Fusarium* wilt which could be efficiently utilized in marker-assisted breeding of chickpea, particularly against *Foc4 Fusarium* wilt.

KEYWORDS

chickpea, *Fusarium* wilt, RNA sequencing, transcriptome, environmental adaptation, energy metabolism

1. Introduction

Chickpea (*Cicer arietinum* L) is a protein and nutrient-enriched pulse crops, cultivated in different parts of the world, with an area of about 15 million hectares (Mha) and an annual production of 16 million tons (MT; FAOSTAT, 2023). India contributes more than 75% of the world's chickpea production (around 12 MT @ 1,192 kg ha^{-1}) in an area of around 10 Mha (Indiastat, 2023). The demand for protein and other nutrient-dense foods like pulses is increasing to meet the food and nutritional security of the growing world population. However, the area and production of chickpea have only increased marginally in the past few decades. One of the reasons for the antagonistic production and productivity of chickpea is *Fusarium* wilt disease, caused by *Fusarium oxysporum* f. sp. *ciceris (Foc)*. *Fusarium* wilt is a devastating biotic stress that causes up to 100% yield loss in chickpea (Jendoubi et al., 2017) if the proper disease management practices are not followed.

The *Fusarium* wilt disease is very difficult to manage by conventional methods like the application of fungicides, crop rotation, etc., as the nature of the pathogen is soil- and seed-borne and it can survive in the soil for up to 6 years without a host (Haware et al., 1996). However, most of the time, farmers' preference is higher yield over disease resistance. Several high-yielding varieties that are preferred by farmers are susceptible to *Fusarium* wilt. Hence, the cultivation of wilt-resistant varieties of chickpea is the best way to overcome yield and production losses. Cultivation of one resistant variety over a long time in the same field may also lead to a breakdown of the resistance mechanism by pathogens, as many of these mechanisms are controlled by one major gene or oligogenes (Adugna, 2004). The different races of this pathogen cause wilt disease and other related symptoms in chickpea across chickpea-growing countries. The wilting symptom in chickpea is caused by specific races of this pathogen, namely 1A, 2, 3, 4, 5, and 6 (Jendoubi et al., 2017).

Therefore, understanding the molecular mechanisms behind the resistance to *Fusarium* wilt is a positive step toward the development of chickpea genotypes with better yield and quality, along with resistance to diseases. To understand the underlying molecular mechanisms in chickpea plants for resistance against *Fusarium* wilt, various approaches, including "omics" tools, are being utilized, such as cDNA-RAPD and cDNA-AFLP techniques (Gupta et al., 2009), small RNA sequencing to identify microRNAs (Kohli et al., 2014), genome-wide transcriptome profiling (Sharma et al., 2016), and a long SAGE transcriptome approach to understanding host-pathogen interaction (Upasani et al., 2017). Similarly, studies on root transcriptome, marker-trait association, marker-based DNA profiling, and race-specific marker development against several races of *Foc* were conducted (Yadava et al., 2023) and these reported several underlying genes and pathways involved in host-pathogen interaction and resistance mechanisms. However, most of these studies were conducted with races 1, 2, 3, and 5 of *Foc* and with different genotypic backgrounds of the chickpea.

Considering the above burning issues, the present study was conducted with two contrasting genotypes of chickpea (one highly resistant and one highly susceptible) against *Foc4,* aiming to reveal the important molecular pathways that are associated with *Fusarium* wilt resistance and the genes involved in it. The identified genes could be targeted to design candidate gene-based markers to be utilized in marker-trait association (MTA) studies. The MTA studies will enable us to understand how these genes are directly or indirectly imparting resistance against *Fusarium* wilt via different traits; that information will ultimately help to develop chickpea genotypes by using marker-assisted breeding, particularly against *Foc4*.

2. Materials and methods

2.1. Experimental details

Two chickpea genotypes, namely KWR 108 and GL 13001, were selected for the study as these two varieties were reported to be highly contrasting in response to *Fusarium* wilt (Kumar et al., 2019), particularly to *Foc4*. The experiment was conducted in the *Fusarium* wilt sick plot of TCA, Dholi farm (a designated plot for chickpea *Fusarium* wilt pathological trials from the All India Co-ordinated Research Projects on Chickpea located at TCA-Dholi under the Department of Agricultural Biotechnology and Molecular Biology, CBS&H, Dr. Rajendra Prasad Central Agricultural University, Pusa (Samastipur) 848,125, Bihar, India). *F. oxysporum* isolates were collected from the field of TCA, Dholi and identified as *Foc4* (Sharma et al., 2014). Among these chickpea genotypes, KWR 108 was reported as highly resistant and GL 13001 was reported as a highly susceptible genotype against *Fusarium* wilt (Kumar et al., 2019). The seeds of KWR 108 and GL 13001 genotypes were procured from the ICAR-Indian Institute of Pulse Research, Kanpur, Uttar Pradesh, India. Seeds of both genotypes were sown in a grow bag filled with a mixture of autoclaved soil and compost at a ratio of 6:4. For each genotype, two seeds were sown in each grow bag. After germination, only one plant bag^{-1} was maintained for 25 days after sowing. Then plants of both genotypes were divided into two groups, namely control and treatment, which had three biological replicates. All the field experiments were carried out under the net house condition during rabi season 2021–2022, and the molecular works were carried out at the Functional Genomics Laboratory of the Department of Agricultural Biotechnology and Molecular Biology (25.98°N latitude and 85.67°E longitude and 52 m altitude from mean sea level), College of Basic Sciences and Humanities, Dr. Rajendra Prasad Central Agricultural University, Pusa 848,125, Bihar, India during the year 2021–2022.

2.2. Treatment of plants with *Fusarium oxysporum* f. sp. *ciceris* culture

For infecting the plants, broth culture was prepared from the pure culture plates of *Foc4* (pure culture was derived from the wilt-infected chickpea plant grown at the wilt sick plot of TCA, Dholi). Small-size inoculums (0.5 cm^2) from the pure culture plate were inoculated in broth culture media (Potato Dextrose Broth) with the help of a forcep. The broth culture was incubated at 26°C and 150 rpm in a rotary agitator for 7 days. For inducing wilt infection in the treatment group of plants, the broth culture was thoroughly mixed using a pipette, and 2 mL of the solution was added to each plant at the root zone with the help of a pipette. To further ensure the infection of plants in treatment groups, soil collected from the *Fusarium* wilt sick plot of TCA Dholi was filled on the top of the grow bags (treatment), followed by light irrigation. Symptoms appeared in the susceptible genotypes within

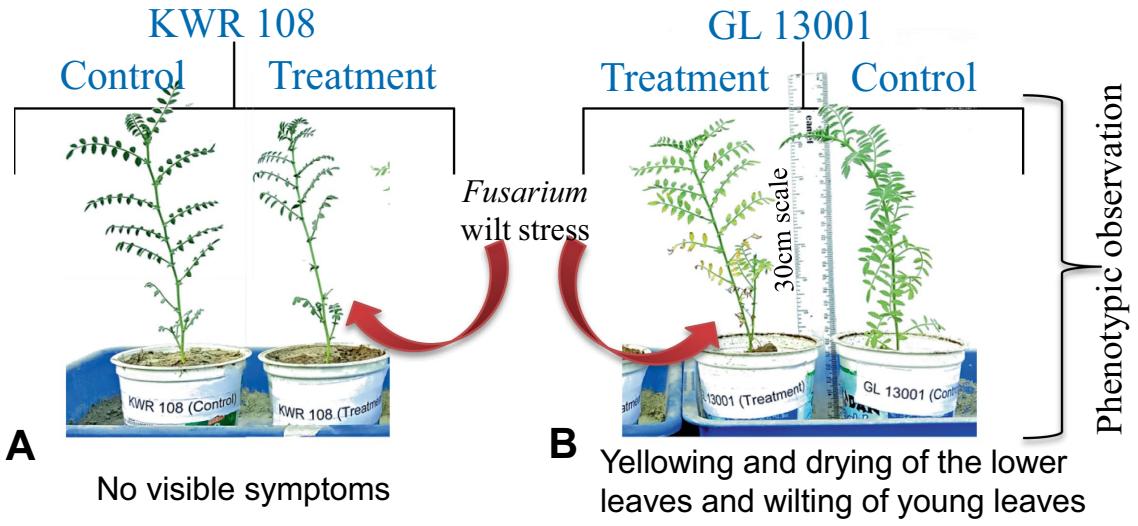

FIGURE 1
Phenotypic observations of **(A)** No visible symptoms in genotype KWR 108 and **(B)** Yellowing and drying of lower leaves and wilting of young leaves in genotype GL 13001 due to the infection of *F. oxysporum* as compared to control.

8–10 days of the treatment (Figures 1A,B). The plant leaf samples were collected after 10 days of treatment for transcriptome sequencing.

2.3. RNA isolation and preparation of library for transcriptome sequencing

The leaf samples were collected from control and treated plants of both the genotypes in three biological replicates and immediately dipped in the 2 mL micro-centrifuge tubes filled with RNA stabilizer solution (G-Biosciences) and outsourced for RNA isolation and transcriptome sequencing at Unigenome, Ahmedabad, Gujarat, India-380015. The leaf samples from three biological replicates were bulked together for RNA isolation. RNA was isolated by using the Alexgen Total RNA kit. RNA quality and quantity were analyzed using 1% agarose gel and Qubit® 4.0 fluorometer, respectively. The NEBNext® Ultra™ RNA Library Prep Kit for Illumina NEB #E 7770 was used for paired-end sequencing library preparation. The mRNA enrichment was performed as per the user manual and mRNA was first fragmented, followed by cDNA synthesis and repairing of ends and adenylation of 3′ end. Subsequently, the adapter was ligated at the fragmented ends and PCR amplification was performed for selective enrichment of adapter ligated DNA fragments. The adapter-based selectively enriched amplified fragments/libraries were analyzed on TapeStation 4,150 (Agilent using RNA ScreenTape® as per manufacturer's instructions). The average size of libraries was observed to be 331 bp, 363 bp for GL 13001 (control and treatment) and 353 bp and 344 bp for KWR 108 (Control and Treatment), respectively. The final library was pooled with other samples, denatured, and loaded onto the flow cell. On the flow cell, cluster generation and sequencing were performed using the Illumina Novaseq 6,000 platform to generate 2 × 150 bp paired-end (PE) reads. Data were filtered to remove the adapter and low-quality reads. The raw transcriptome sequencing data obtained from both genotypes under control and *F. oxysporum* f. sp. *ciceris*-treated plants with two technical replicates were submitted to the SRA (Sequence Read Archive) database of NCBI (accessed on 20 October 2023).[1]

2.4. Reference genome-based transcript mapping, assembly, and further bioinformatics works

From the NCBI database (accessed on 20 October 2023),[2] the reference genome of *Cicer arietinum* (GCA_000331145.1_ASM33114v1) and reference genome annotation GTF file were downloaded. Subsequently, by using STAR (v2.7.10a) aligner, reference genome-based assembly of transcripts was performed first by separately mapping high-quality (HQ) clean reads of control and treatment samples of GL 13001 and KWR 108 on the reference genome, respectively. The STAR Genome-Generate mode option was used to carry out indexing of the reference genome. Then the input reads, in FASTQ format, along with the indexed reference genome generated in the previous step, were given to the STAR aligner. To identify the positions of the origin of the reads, the STAR aligner created the alignment in BAM format for each sample through reference genome-guided mapping of the HQ reads followed by assembly of transcripts using StringTie (v2.2.1). After the assembly of transcripts by StringTie, the quantification of assembled transcripts was performed. The quantification of the assembled transcripts was done in order of most highly abundant transcripts to less abundant by using the network flow algorithm. The annotation of assembled transcripts was performed using the GFF annotation file of reference genome having "known" gene exon structures followed by quantification of the expression of known genes. Simultaneously, to

1 https://submit.ncbi.nlm.nih.gov/subs/sra/SUB12177877/
2 https://www.ncbi.nlm.nih.gov/genome/?term=Chickpea

merge the gene structure found in all four samples, the assembled transcripts of all four samples were passed to StringTie's merge function to avoid assembly of only a partial version of any of the transcripts in the initial StringTie run.

2.5. Identification of novel transcripts and novel isoforms of transcripts

The reference GTF file and the string-tie merged GTF file were taken and the GFF compare utility was run to check or identify if there were any novel transcripts or novel isoforms of transcripts were present in the merge sample. Novel transcripts were then identified using a method described by Gleeson et al. (2022). The transcripts that did not have any available information in the annotation file of the reference genome were considered novel transcripts.

2.6. Differential gene expression analysis

Using the SringTie merge function, a consensus set of transcripts was derived by merging the structures of all the genes found in all four samples and simultaneously estimating the abundances of the merged transcripts in the four samples. The read count information that was obtained from the files generated by StringTie was extracted by using prepDE.py, a Python program (Gill and Dhillon, 2022). The edgeR package (Robinson et al., 2010) was then used to calculate differential gene expression (DEGs) by taking read count results of a Python program prepDE.py as input.

2.7. Gene ontology and KEGG enrichment pathway analysis

Gene ontology (GO) analysis was done to identify the distribution of significant differentially expressed genes (DEGs) into three major domains, i.e., cellular component, molecular function, and biological process. GO term was assigned to each significant differentially expressed transcript using Blas2GOcli 1.4. KAAS (KEGG automatic annotation server; Moriya et al., 2007) was used for ortholog identification and mapping of significant differentially expressed transcripts to the biological pathways. The criteria used to identify significantly down and up-regulated transcripts were log2FC > 0 and q value<0.05 (means significantly up-regulated), and log2FC < 0 and q value <0.05 (means significantly down-regulated). Using BLASTX with a threshold bit-score value of 60 (default), significant differentially expressed transcripts were compared against the KEGG database. A Heatmap of DEGs was generated for 25 highly significant down and up-regulated genes (a total top 50 transcripts) based on q value (i.e., least q value).

2.8. Identification of genes encoding differentially expressed transcripts

The reference of the genome-based transcript identification revealed that many of the transcripts showed differential expression under *Fusarium* wilt infections, which are the transcript fragments encoding the same proteins. Further analysis was conducted using the NCBI gene database. However, the protein IDs of the transcripts revealed that several proteins were the products/isoforms of the same genes. Using the sorting option available in MS Excel, the transcripts encoded by the same genes were sorted together to finally get the exact numbers of genes showing differential expression under *Fusarium* wilt stress in chickpea.

2.9. Primer design and real-time PCR analysis

From the RNA sequencing data, 15 genes that showed significant differential expression in the resistant genotype, i.e., KWR 108, were selected for real-time PCR verification of the RNA sequencing results. Primer Blast Program, available at NCBI database (accessed on 20 October 2023),[3] was used for designing primers with CDS of 15 selected genes and CDS of Glucose-6-Phosphate Dehydrogenase (G6PD) gene as internal control (Reddy et al., 2016). RNA was extracted by using RNA isolation kit (Qiagen) from control and treatment plants of KWR 108 and cDNA was synthesized from RNA using the cDNA synthesis kit following the manufacturer's protocol (Himedia, HiGenoMB). The gene expression analysis was done by using the cDNA template and 2× AB HS SYBR Green qPCR Mix (Thermo Scientific) in a qRT-PCR (Stratagene Mx3000P, Agilent). The details of real-time PCR primers specific to the ERF transcription factor family used in the experiment are listed in Table 1.

2.10. Data analysis and graphing

Sample comparison was made for GL 13001 (control vs. treatment) and KWR 108 (control vs. treatment), respectively, for differential expression analysis. The analyses were performed in the edge R package to identify differentially expressed genes. Reads per million mapped reads or Counts per million mapped reads for both control and treatment samples, LogCPM (Log10 of CPM value), Log2Fold Change [the logarithm (base 2) of the fold change], pval (value of p for the statistical significance of this change), FDR [FDR adjusted value of p (q-value)], and the criteria used to identify significantly down and up-regulated transcripts were log2FC > 0 (means up-regulated), log2FC > 0 and q value<0.05 (means significantly up-regulated), log2FC < 0 (means down-regulated), log2FC < 0 and q value <0.05 (means significantly down-regulated). In real-time PCR analysis, the mean and standard deviation were calculated based on three pieces of biological replicated data and, using the Livak method (Schmittgen and Livak, 2008), the relative gene expression was calculated with G6PD as the internal reference gene. The rest of the data statistics and graphing were performed using MS Excel. The reliability of the RNAseq data was confirmed by comparing the expression data of selected genes using a linear regression model in Excel.

3 https://www.ncbi.nlm.nih.gov/tools/primer-blast/

3. Results

3.1. Transcriptome data generation, transcript mapping, and assembly

In the present investigation, the total reads obtained from four samples, i.e., GL 13001 (control and treatment) and KWR 108 (control and treatment), ranged from 33.19 million reads in GL 13001-Control to 42.43 million reads in KWR 108-Treatment (Table 2).

The QC passed reads were then subjected to reference-based transcript assembly. The genome size for *Cicer arietinum* is 531 Mb. There are a total of 30,236 genes and 220,289 CDS as per the GFF file of the NCBI chickpea reference genome. The transcript assembly was performed by mapping clean reads of control and treatment samples of GL 13001 and KWR 108 on the reference genome using STAR (v 2.7.10a). The mapping statistics of HQ reads against the reference genome are presented in Table 3.

The number of assembled transcripts varied from 36,081 to 39,186 with an average transcript size of 2003.40 bp and 1992.60 bp in control and treated GL 1300, respectively. Similarly, the number of assembled transcripts ranged from 37,496 and 37,304 with an average transcript size of 2005.90 bp and 1984.60 bp in control and treated KWR 108

TABLE 1 List of qRT PCR primers specific to selected genes that showed significant up-regulation in KWR 108 in shoot transcriptome data for validation of RNA sequencing-based shoot transcriptome data.

Sl. no.	ERF gene Id	Forward primer sequence	Reverse primer sequence	Expt. A. size (bp)
1.	LOC101488294	ACACTCGTCAAGTTGCTGCT	TGAGGGTCCTTGAGAAGAAGG	98
2.	LOC101489178	CCAACGCCAACAACCTCAAC	GCCTTCTTCTAACCCCTCGG	90
3.	LOC101490960	GTCCTTGGGGGAAATACGCA	GCAGCTTCTTCAGCTGTTTGG	94
4.	LOC101494217	TCCGAAACCGGAGGTGATTG	TTTCCCCACGGTCTTTGTCT	90
5.	LOC101495836	AGTTCAGAGGCGTAAGGCAG	CCGCCGTGTTAAAAGTTCCG	102
6.	LOC101496212	GGAAATTCGCGGCGGAGATA	AAGCAAGTGCTGCTGCTTCA	93
7.	LOC101501427	ATACTGCGCTTAGCGTTGGT	CGCTCATAATCCACGACGGA	106
8.	LOC101502122	CGCTGAGATTCGTCTCCCTC	CTTAAAAGCTTCGCGGTCGT	100
9.	LOC101502737	CAGCAGAGATTCGTGACCCA	ACATCATAAGCACGTGCAGC	91
10.	LOC101504196	TCTGTCTCCGGTGGAGTTCA	ACAACGGTGGAGGTTCGTTT	106
11.	LOC101505842	GAAGATTGATACCGTTTCTGGAG	GCTGTCTGTTGTACTTCTTCCAC	110
12.	LOC101508871	CGCTTCCTCTGTTTCCTGGT	GAAGGTGGTAAACCCGACCC	100
13.	LOC101512924	AGAAGGCCATGGGGGAAATG	TAGCAGCTTCCTCAGCAGTG	100
14.	LOC101515629	GGTCAAGGAAGAACCTCAACCT	GCCCATTTTCCCCAAGGTCT	93
15.	LOC105852724	CTGCTTCCTCCTCCTCCTCT	CGGGTCGGGTGACTCATAAC	107
16.	G6PD	GCAATTTGCAACACCTTAGTGG	GTGGTTGAACAACTTCAGCGT	83

Expt. A. size (bp) is the expected amplicon size (base pair).

TABLE 2 The transcriptome data statistics (A) for clean data after removal of the adapter and low-quality bases.

Sample name	Total reads (R1 + R2)	Total bases (R1 + R2)	Total data (~Gb)
GL 13001 (Control)	33,192,474	4,94,41,97,791	4.94
GL 13001 (Treatment)	37,251,762	5,55,45,96,976	5.55
KWR 108 (Control)	35,184,976	5,24,08,35,996	5.24
KWR 108 (Treatment)	42,432,918	6,30,99,29,526	6.31

R1 and R2, two technical replicates; Gb, Gigabase.

TABLE 3 Highlights of mapping statistics high-quality reads derived from shoot transcriptome mapped to chickpea reference genome using STAR aligner.

Sample name	Total reads	Mapped reads (no.)	Mapped read (%)	Uniquely mapped reads (no.)	Uniquely mapped reads (no.)
GL 13001 (Control)	33,192,474	29,327,660	88.36	27,482,244	82.80
GL 13001 (Treatment)	37,251,762	35,757,750	95.99	33,881,974	90.95
KWR 108 (Control)	35,184,976	33,512,528	95.25	32,497,028	92.36
KWR 108 (Treatment)	42,432,918	40,655,068	95.81	23,111,318	54.47

TABLE 4 The statistics of merged transcripts (generated by the combination of all four samples as well as reference genome) and individual transcript assembly using StringTie assembly and merge function.

Sample name	Assembled transcripts (no.)	Total assembled (bp)	Mean transcript size (bp)	Max transcript size (bp)
Merged	51,353	9,74,67,567	1,898	33,235
GL 13001 (Control)	36,081	7,22,83,697	2,003.40	33,235
GL 13001 (Treatment)	39,186	7,80,82,916	1,992.60	33,235
KWR 108 (Control)	37,496	7,52,13,757	2,005.90	33,235
KWR 108 (Treatment)	37,304	7,40,32,603	1,984.60	33,235

TABLE 5 The statistics of transcripts showing differential expression.

Transcripts combinations	Total transcripts	Down-regulated	Up-regulated	Significant-down-regulated	Significant-up-regulated	Total significant transcripts
GL 13001 (Treatment vs. Control)	32,430	15,428	17,002	2,835	4,669	7,504
KWR 108 (Treatment vs. Control)	31,038	15,789	15,249	3,139	3,559	6,698

The statistics of calculating up and down-regulated genes were log2FC > 0 (up-regulated), log2FC < 0 (Down-regulated), log2FC > 0 and q value < 005 (significantly up-regulated) and log2FC < 0 and q value < 0.05 (significantly down-regulated).

leaves samples, respectively. Simultaneously, StringTie's merge resulted in several transcripts assembled as 51,353 with an average transcript size of 1898 bp in merge data (Table 4).

StringTie's merge function was used because individually in some of the samples, transcripts might only be partially covered by reads, leading to the assembly of only a partial version of those transcripts in the initial StringTie run. Thus, the set of transcripts that are consistent in all four samples was created to be compared in the subsequent steps using the merge step.

3.2. Novel transcripts and novel isoform transcripts identified

A total of 4,111 novel transcript isoforms corresponding to or encoded by 2,918 genes were identified as potential novel isoforms. Interestingly, 167 novel transcripts in KWR 108 and 170 novel transcripts in GL 13001, which were not available in the annotation file of the reference genome, were identified. The detailed list of novel transcripts and novel isoform transcripts identified are enlisted in Supplementary raw data file S1.

3.3. Identification of differentially expressed transcripts

Large numbers of transcripts were shown to be differentially expressed as revealed by differential expression analysis using edgeR software. Simultaneously, 7,504 and 6,698 transcripts were found to be significantly differentially expressed in GL 13001 and KWR 108, respectively (Table 5).

By transforming the data onto A (mean average) and M (log ratio) scales, the differences between measurements taken in control and treatment samples were visualized in MA plot. Simultaneously, a volcano plot that arranges differentially expressed transcripts along dimensions of statistical as well as biological significance was obtained from the edgeR software (Figures 2A–D). Similarly, the heatmap of 25 highly significant down and up-regulated genes (total 50 transcripts) based on q-value (i.e., least q value) and transcripts with proper annotations generated for both the genotypes are represented in Figures 2G,H.

3.4. Validation of RNAseq-based transcriptome data using a real-time PCR

The reliability of sequencing data was confirmed by real-time-based expression analysis of 15 selected genes that showed significant up-regulation in the resistant genotype under *Fusarium* wilt infection as revealed by RNAseq data. Similar to RNA sequencing results, the real-time PCR data of 15 selected genes showed significant differential expression of the genotype KWR 108 (Figure 2E). The linear regression analysis of RNAseq and real-time PCR-based expression data also showed significant similarity ($R^2 = 0.871$), which confirmed that the RNAseq data were reliable for further analysis (Figure 2F).

3.5. Reference genome-based transcript identification

Identification of genes encoding differentially expressed transcripts revealed that, in GL 13001, 427 genes were significantly down-regulated and 794 were significantly up-regulated (Supplementary raw data file S2). Similarly, in KWR 108, 495 genes were significantly down-regulated and 608 genes were significantly up-regulated (Supplementary raw data file S2). When the genes that showed significant differential expression were compared between two genotypes, i.e., GL 13001 and KWR 108, it was revealed that 81 genes

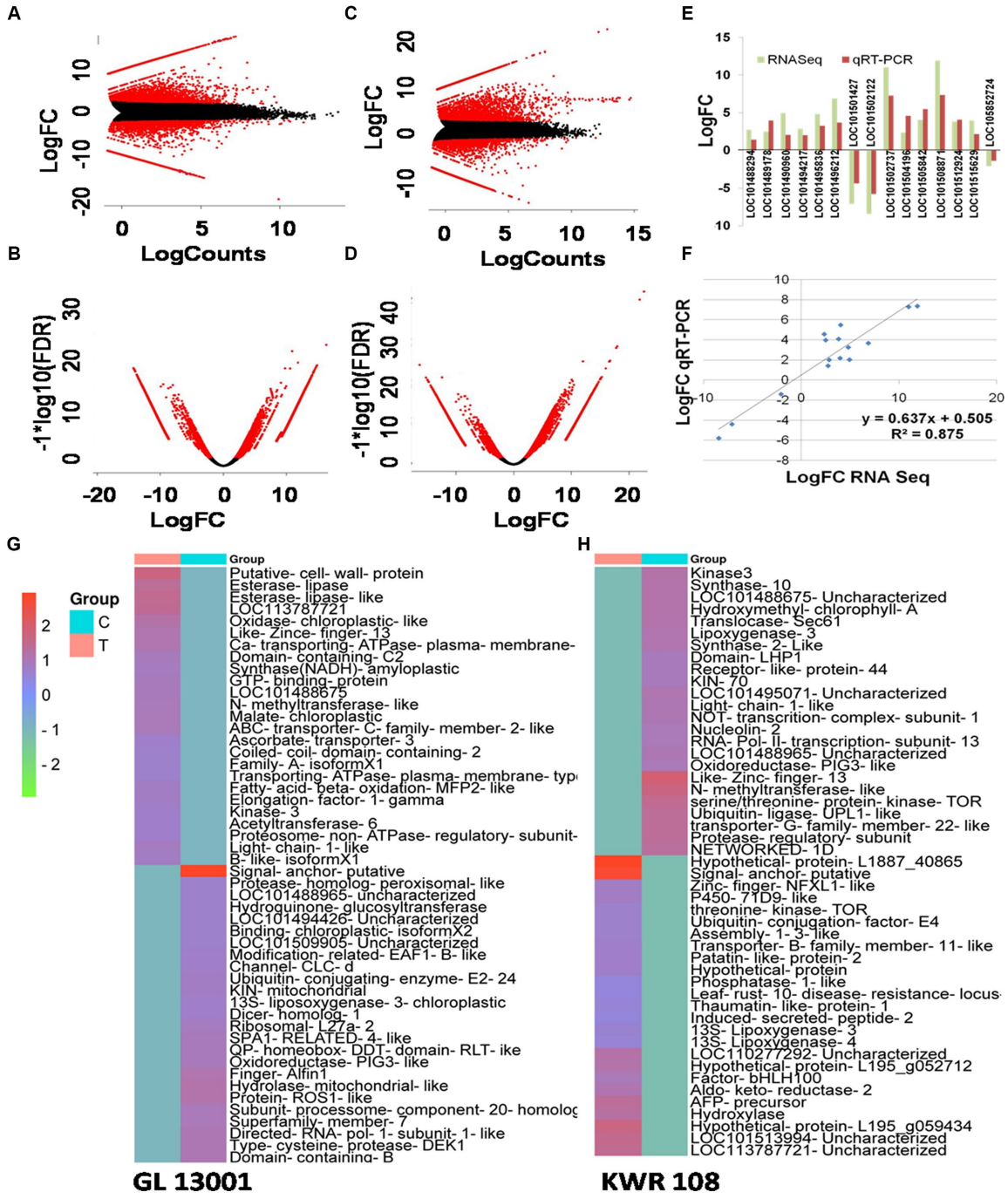

FIGURE 2
MA plot and volcano plot showing differentially expressed transcripts in treatment vs. control combination in GL 13001 **(A,B)** and KWR 108 **(C,D)**. Red corresponds to transcripts with adjusted *p* value/*q* value <0.05. Validation of RNA-Seq data by qRT-PCR by using primers specific to 15 genes which in RNA-Seq result showed significant differential expression in KWR 108 **(E,F)**. The heatmap of 25 highly significant down and up-regulated transcripts based on *q* value (i.e., least *q* value) in GL 13001 **(G)** and KWR 108 **(H)**. The color coding ranges from red to green, where shades of red represent high transcript expression and shades of green represent low transcript expression. T means treatment sample and C means control sample.

were down-regulated and 211 genes were up-regulated in both the genotypes. Ninety-one and 172 genes showed significant down-regulation and up-regulation only in GL 13001 and 93 and 97 genes showed significant down-regulation and up-regulation only in KWR 108, respectively. Similarly, 111 genes were significantly up-regulated in GL 13001 but significantly down-regulated in KWR 108 and 50 genes were significantly down-regulated in GL 13001 but significantly up-regulated in KWR 108.

3.6. Gene ontology enrichment analysis

The GO enrichment analysis of significant differentially expressed genes (DEGs) summarized the genes into three main GO categories, namely cellular component, molecular function, and biological process (Supplementary raw data file S2). The GO enrichment results of the top 50 significantly up-regulated and down-regulated genes in two genotypes are represented as pie charts (Figure 3).

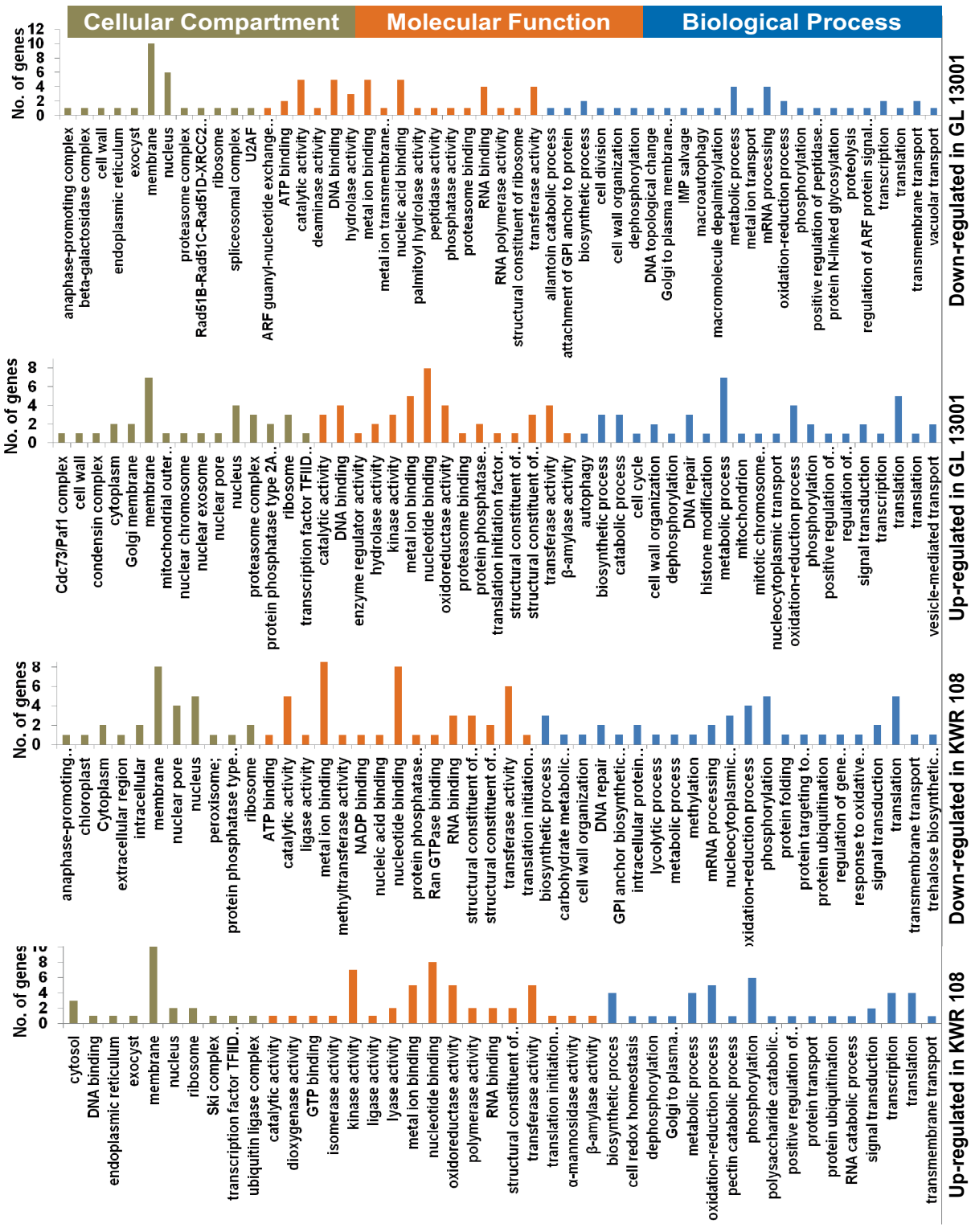

FIGURE 3
Gene ontology (GO) enrichment graphs of the top 50 up and 50 down-regulated genes in KWR 108 and GL 13001. Moss green color bar represents Cellular Compartments, Orange color bar represents Molecular functions, and Blue color bar represents biological processes in which the top 50 DEGs are involved.

The GO enrichment results of the top 50 significantly up and down-regulated genes revealed that the proteins encoded by most of these genes are the components of the membrane and nucleus. The products of most of the top 50 genes down-regulated in GL 13001 have nucleotide binding, catalytic, metal ion binding, transferase, and hydrolase activity involved in biological processes like metabolic processes, mRNA processing, DNA repair, oxidation–reduction process, and macroautophagy. Apart from membrane and nucleus,

many of the proteins encoded by the top 50 genes up-regulated in GL 13001 are the components of proteasome and ribosome having nucleotide binding, catalytic, metal ion binding, oxidoreductase, and transferase activity involved in biological processes like metabolic processes, translation, DNA repair, and oxidation–reduction process.

Similar to the GO terms of the top 50 genes significantly up and down-regulated in GL 13001, the GO terms of the top 50 genes down-regulated in KWR 108 showed the highest cellular component as membrane and nucleus and molecular functions as nucleotide binding, metal ion binding, transferase, catalytic, and nuclear pore activities. However, the GO terms of the top 50 genes up-regulated in KWR 108 revealed that, apart from membrane and nucleus, the products of the genes are the components of ribosome and cytosol having molecular functions such as kinase activity, oxidoreductase activity, nucleotide binding, transferase, and metal ion binding activities involved in biological processes such as phosphorylation, oxidation–reduction process, metabolic and biosynthetic process, and cell redox homeostasis (Figure 3).

3.7. Pathways involving differentially expressed genes

KEGG enrichment analysis of the significant DEGs identified in both the genotypes of chickpea was performed to estimate the numbers of significant DEGs involved in different KEGG pathway levels. It revealed that, in the susceptible genotype, i.e., GL 13001, the number of significantly up-regulated genes involved in different pathways such as DNA replication and DNA repair, cell motility, lipid metabolism, carbohydrate metabolism, and DNA degradation is significantly higher than in KWR 108. Whereas the number of DEGs specifically involved in energy metabolism and environmental adaptation pathways are significantly higher in KWR 108 than in GL 13001 (Figure 4A). The same genes that were up-regulated in GL 13001 but down-regulated in KWR 108 were observed to be higher in most of the pathways; more specifically, the genes involved in cell motility and membrane transport were significantly up-regulated only in GL 13001 (Figure 4B). However, the same genes involved in carbohydrate metabolism were up-regulated in resistant genotype KWR 108 but down-regulated in susceptible genotype GL 13001 (Figure 4B).

4. Discussion

In the present study, transcriptome dissection was done to understand the probable molecular mechanisms imparting the ability to tolerate *Fusarium* wilt in the chickpea genotype, particularly in the genome background of KWR 108, a highly resistant variety screened at TCA-Dholi, Bihar, India (Kumar et al., 2019). The comparative analysis of the transcriptome data generated from susceptible genotypes GL 13001 and resistant variety KWR 108 was performed to identify the pathways and genes involved that are showing differential expression under *Fusarium* wilt stress. Compared to the susceptible genotypes, higher numbers of genes belonging to the pathways involved in environmental adaptation and energy metabolism showed highly significant up-regulation in resistant genotype KWR 108 and, along with genes involved in several other processes, more genes belonging to DNA repair mechanisms showed significant up-regulation in susceptible genotype GL13001 (Figure 4A).

4.1. Significant up-regulation of genes involved in DNA repair mechanism in susceptible genotype

In our present study, a comparison between the shoot transcriptome of KWR 108 and GL 13001 showed a significantly higher number of genes involved in DNA repair mechanisms were up-regulated in GL 13001, a susceptible genotype (Figure 4A). Although, under normal circumstances, DNA damage can be thought of as a frequent occurrence, it is likely to occur even more in response to several stress conditions (Nisa et al., 2019) either directly or indirectly due to increased level of reactive oxygen species (ROS; Szurman-Zubrzycka et al., 2023). The resistant or tolerant plants protect the DNA from damage by activating enzymatic and non-enzymatic antioxidant machinery (Moradbeygi et al., 2020). In the present study, the significantly up-regulated genes related to DNA repair mechanism in susceptible genotypes are crossover junction endonuclease EME1, DNA excision repair protein ERCC-1 & 4, DNA mismatch repair protein MLH3, DNA repair and recombination protein RAD54 and RAD54-like protein, DNA repair protein REV1, DNA-3-methyladenine glycosylase I, flap endonuclease-1, telomere length regulation protein, UV excision repair protein RAD23, and WD repeat-containing protein 48. This suggests that DNA replication and other similar processes of DNA synthesis are more stable in resistant genotypes as compared to susceptible genotypes under *Fusarium* wilt stress condition.

4.2. Significant up-regulation of environmental adaptations genes in the resistant genotype

The genes specifically belonging to environmental adaptation pathways are significantly up-regulated in the resistant genotype. The environmental adaptation genes basically encode for the proteins or enzymes involved in plant-pathogen interaction upon infection. In the present study, the significantly up-regulated environmental adaptation genes in KWR 108 were calcium-dependent protein kinase (CDPK), pathogenesis-related genes transcriptional activator (Pti5 & Pti6), calmodulin (CaM), calmodulin-like proteins (CML), cyclic nucleotide-gated channel (CNGC), mitochondrial translation elongation factor Tu (TUFM), chitin elicitor receptor kinase 1 (CERK1), enhanced disease susceptibility 1 protein (EDS1), disease resistance protein (RPM1/RPS3), mitogen-activated protein kinase 3 (MPK3), mitogen-activated protein kinase 4 (MPK4), mitogen-activated protein kinase kinase 4/5 (MKK4_5), pathogenesis-related protein 1 (PR1), and WRKY transcription factor 33 (WRKY33). The important roles and involvement of environmental adaptation genes like CDPK (Asano et al., 2012; Baba et al., 2019; Wu et al., 2021), Pti5 & Pti6 (Yang et al., 2020; Wang Y. et al., 2021; Sun et al., 2022), CaM, and CML (Zeng et al., 2015; Ranty et al., 2016) in several biotic and abiotic stress responses have been extensively studied and reported. The plant accumulates Ca^{+} upon experiencing stress as a secondary

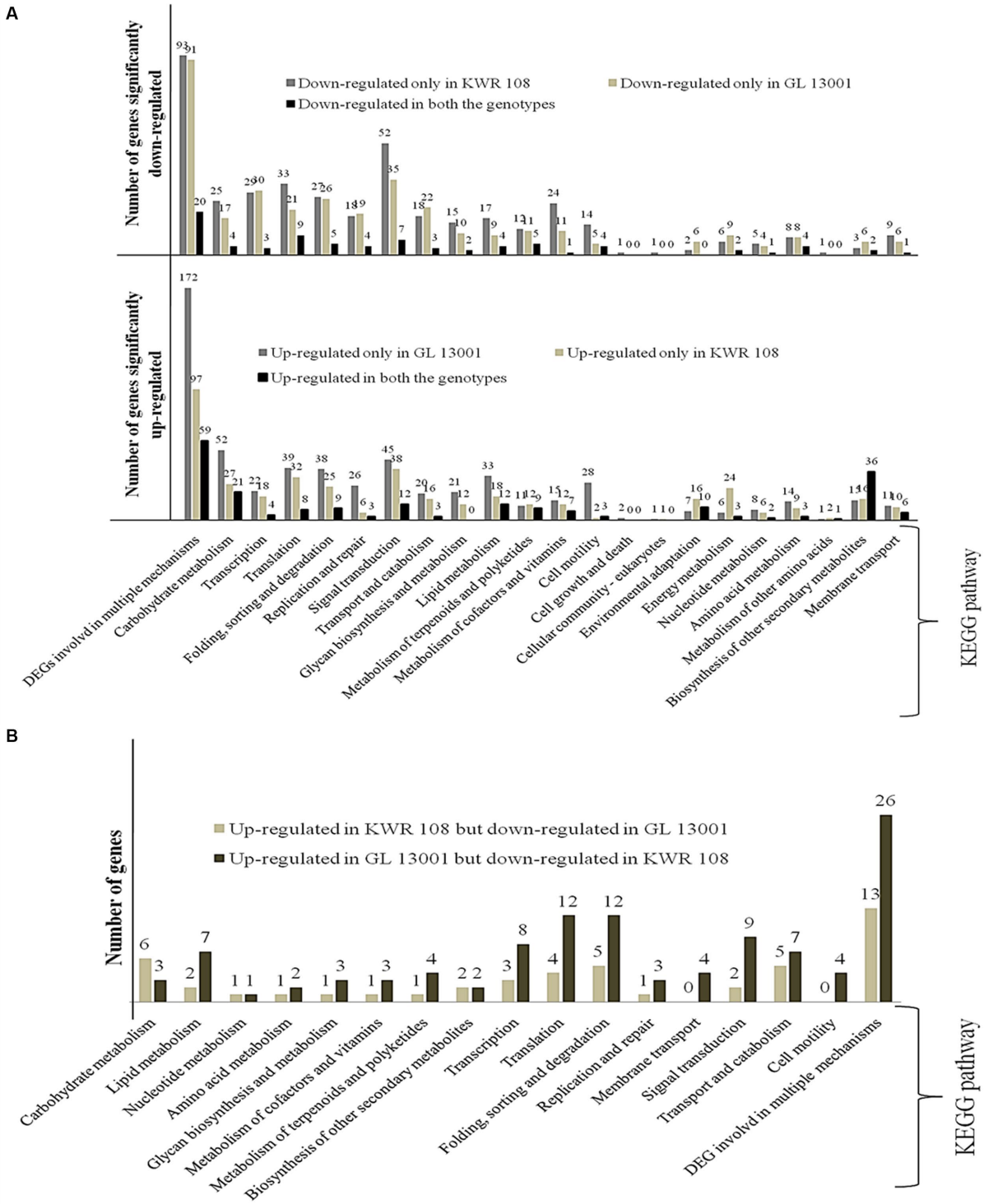

FIGURE 4
KEGG enrichment/Pathway analysis results **(A)** genes significantly up-regulated and down-regulated in two genotypes of chickpea, i.e., KWR 108 and GL 13001 and **(B)** genes significantly up-regulated in KWR 108 but down-regulated in GL 13001 and vice versa. 'Y' axis represents the number of significant DEGs.

messenger to modulate the cellular processes (Luan, 2009). CNGC, which showed significant up-regulation under *Fusarium* wilt in the present study, is mostly localized to the plasma membrane and acts as ligand-gated cation channels (Chin et al., 2009) for the accumulation of Ca^{+} in the cell during stress. Several reports suggested the potential role of CNGC in plant disease resistance through hypersensitive response (Clough et al., 2000; Ahn, 2007; Keisa et al., 2011; Ma and Berkowitz, 2011; Guo et al., 2018; Peng et al., 2019; Dietrich et al., 2020; Chakraborty et al., 2021; Zhao et al., 2021). Mitochondrial translation elongation factor Tu

(TUFM) is a mitochondrial protein encoded by the nuclear genome that potently inhibits RLR (RIG-I-like receptors) signaling and promotes autophagy during a pathogen infection, particularly viruses (Lei, 2011; Wu et al., 2022). In the study, TUFM showed significant up-regulation in *Fusarium* wilt-resistant genotype KWR 108, suggesting its potential role in imparting resistance against fungal pathogens and other stresses as reported in crops like maize (Rao et al., 2004) and soybean (Yin et al., 2009). Chitin, which is an essential unit of fungal cell walls including chickpea wilt, causes *F. oxysporum* to act as an elicitor of plant immunity (Gong et al., 2020). Chitin elicitor receptor kinase 1 (CERK1), which showed significant up-regulation in resistant genotypes in the present study, is a heterotrimeric complex (Gigli-Bisceglia and Testerink, 2021) required for the perception of chitin and subsequent activation of the chitin-responsive cellular processes as well as for triggering the innate immunity of the plants against abiotic stress (Espinoza et al., 2017). CERK1 mutant (cerk1) plants showed increased susceptibility to fungal pathogens like *Erisiphe cichoracearum, Alternaria brassicicola*, and *Blumeria graminis* (Gigli-Bisceglia and Testerink, 2021), indicating its vital role in perceiving pathogen signals and subsequent induction of defense mechanism in resistant plants. The enhanced disease susceptibility 1 (EDS1) gene, which showed significant upregulation in KWR 108 in the present study, encodes a lipase-like protein that has been reported to be essential for resistance against biotrophic pathogens (Ochsenbein et al., 2006). In plants, it is basically required by Toll/Interleukin-1 receptor (TIR) domain of NLR (nucleotide-binding leucine-rich repeat) immune receptors (Johanndrees et al., 2023) and for inducing expression of PR (pathogen-related) proteins through the salicylic acid (SA) pathway against several pathogens (Yan et al., 2016; Bhandari et al., 2019; Neubauer et al., 2020). Likewise, RPM1/RPS3 (disease resistance protein), which in the present study showed significant up-regulation in the resistant genotype, is basically a CC-NBS-LRR protein that was first identified as a protein in Arabidopsis essential for resistance mechanism against *P syringae pv. Maculicola*. It was later reported to have roles in resistance against diseases caused by other pathogens like *Puccinia striiformis f.* sp. *tritici* through hypersensitive response and Ca^{+} concentration dynamics (Grant et al., 2000; Wang et al., 2020). In the present study, mitogen-activated protein kinases (MAPK) such as MPK3, MPK4, and MKK4_5 showed significant up-regulation in resistant genotypes that are basically involved in intracellular responses (Sinha et al., 2011). In plants, MAPKs are reported to induce stress tolerance (Lin et al., 2021) including biotic stresses (Zhang and Zhang, 2022) through JA (Jasmonic acid) and SA signaling pathways (Jagodzik et al., 2018). The SA signaling in plants under stress including fungal infection induces the expression of defense proteins like PR1 (pathogenesis-related protein 1; Almeida-Silva and Venancio, 2022; Anuradha et al., 2022). Antifungal and several other antimicrobial activities of PR1 have been well-reviewed and reported (Kattupalli et al., 2021; Almeida-Silva and Venancio, 2022; Anuradha et al., 2022; Pečenková et al., 2022). Similar to all these reports, in the present study also, PR1 genes showed significant up-regulation in chickpea under *Fusarium* wilt stress, confirming its role as a defense mechanism against *Fusarium* wilt disease. Likewise, in plant defense responses, an important oxidoreductase enzyme is peroxidase, which is involved in cell wall modifications and the generation of reactive oxygen species (ROS; Chang et al., 2021). Xue et al. (2017) reported that, in common bean, the peroxidase gene PvPOX1 enhanced resistance against *Fusarium* wilt. In the present study, a large number of peroxidase genes up-regulated in KWR 108, but none in GL 13001, suggesting its role in resistance against *Fusarium* wilt in chickpea also. Similarly, WRKY33, an important member of WRKY transcription factor family in plants, showed significant up-regulation in the resistant genotype. The role of WRKY transcription factor has been studied extensively and it plays a role in responses to several stimuli irrespective of physiological, biotic, or abiotic stress (Phukan et al., 2016; Cheng et al., 2021).

4.3. Significant up-regulation of energy metabolism genes in the resistant genotype

The important metabolites involved in redox homeostasis of plant cells are nicotinamide adenine dinucleotide (NAD) and its other derivatives, which are mostly nucleotide coenzymes (Kapoor et al., 2015). The redox state of NAD, i.e., NAD (P)+/NAD(P)H (ratio of oxidized to reduced form) in the cell plays an important role as a signal to ameliorate the bridge between cellular metabolic state and gene expression under various conditions, including biotic and abiotic stress condition (Kapoor et al., 2015), and are vital for homeostasis of cellular energy in plant cells under stress condition for optimum growth and development. In the present study, genes related to NAD (P)H, such as NADH-dependent glutamate synthase, NAD(P)H-quinone oxidoreductase subunit 4, NADH dehydrogenase (ubiquinone) Fe-S protein, NADH:quinone reductase, and NADH–ubiquinone oxidoreductase, showed significant up-regulation in resistant genotypes, confirming its role in energy homeostasis in plants under stress conditions. Other than NADH-related genes, shoot transcriptome data of resistant genotypes in the present study also showed significant up-regulation of other genes involved in energy metabolism, such as phosphoenolpyruvate carboxylase (Wang et al., 2016; Waseem and Ahmad, 2019), alcohol dehydrogenase (Su et al., 2020), alanine transaminase (Bashar et al., 2020), ATP citrate (pro-S)-lyase (Liu F. et al., 2022), ATPase (Li J. et al., 2022; Li Y. et al., 2022), carbonic anhydrase (Rudenko et al., 2021), cytochrome c, cytochrome c oxidase (Guerra-Castellano et al., 2018; Analin et al., 2020), fructose-bisphosphate aldolase (Lv et al., 2017; Cai et al., 2022), malate dehydrogenase (Song et al., 2022), 6-phosphofructokinase 1 (Wang H. et al., 2021), photosystem II P680 reaction center D1 protein (Landi and Guidi, 2022), phosphoserine aminotransferase (Wang et al., 2022), pyruvate-orthophosphate dikinase (Yadav et al., 2020), and serine O-acetyltransferase (Mulet et al., 2004; Liu D. et al., 2022), and their molecular mechanism and role in energy homeostasis in different crops is well reviewed. It indicates that the significant up-regulation of the genes involved in energy metabolism in KWR 108 might have helped it to cope with *Fusarium* wilt stress by maintaining energy homeostasis in cells under stress conditions.

The genes particularly involved in environmental adaptation, energy metabolism, and others which showed significant up-regulation in wilt-resistant genotypes will be a target for designing gene-based markers for marker-trait association studies. The marker-trait association study, especially for the traits attributing to wilt resistance and yield under wilt infection, will be our next target to check whether these up-regulated genes

have any roles in imparting resistance against *Fusarium* wilt through some desirable phenotypic traits or whether there are no roles in phenotypic traits of chickpea under wilt. If these gene-based marker/s are found to be robustly associated with *Fusarium* wilt-resistant traits, then they could be utilized in marker-assisted breeding to develop a wilt-resistant high-yielding variety of chickpea.

5. Conclusion

The present study was conducted to gain insight into the molecular mechanism imparting resistance against *Fusarium* wilt infection in chickpea using an RNA sequencing-based shoot transcriptome approach. The shoot transcriptome data derived from two contrasting genotypes of chickpea, namely KWR 108 (wilt resistant variety) and GL 13001 (wilt susceptible variety), revealed that the resistant genotype efficiently maintains the energy homeostasis in the cell under stress conditions by up-regulating the large sets of genes responsible for maintaining the cellular energy homeostasis. The up-regulation of significant numbers of genes involved in environmental adaptation, particularly host-pathogen interaction in resistant genotypes, suggests that the resistant genotypes efficiently deploy the defense mechanism starting from perceiving and transduction of pathogen signal to activation and implementation of the defense-related mechanism. Similarly, the susceptible genotype showed significant up-regulation of genes involved in several mechanisms, including the DNA repair mechanism, thus it can be perceived that the DNA molecules of the susceptible genotype were more unstable and damaged than the DNA molecules of the resistant genotype, which showed optimum growth under *Fusarium* wilt stress. Therefore, it can be concluded that efficient energy metabolism, activation of environmental adaptation mechanisms, and DNA stability were key to resistance against *Fusarium* wilt infection in chickpea genotypes.

Data availability statement

The datasets presented in this study can be found in online repositories. The names of the repository/repositories and accession number(s) can be found in the article/Supplementary material.

Author contributions

KB: Conceptualization, Data curation, Formal analysis, Funding acquisition, Investigation, Methodology, Project administration, Resources, Software, Supervision, Validation, Visualization, Writing – original draft. MA: Conceptualization, Funding acquisition, Investigation, Methodology, Resources, Supervision, Validation, Visualization, Writing – original draft. AK: Conceptualization, Investigation, Methodology, Resources, Supervision, Validation, Visualization, Writing – original draft. RS: Investigation, Methodology, Validation, Visualization, Writing – original draft. NB: Methodology, Software, Validation, Visualization, Writing – original draft. VS: Investigation, Methodology, Validation, Visualization, Writing – original draft. BP: Methodology, Software, Validation, Visualization, Writing – original draft. MT: Investigation, Methodology, Validation, Visualization, Writing – original draft. OO: Data curation, Formal analysis, Funding acquisition, Software, Writing - review & editing. VB: Data curation, Formal analysis, Funding acquisition, Software, Writing – review & editing. MB: Data curation, Formal analysis, Funding acquisition, Software, Writing – review & editing. MS: Data curation, Formal analysis, Funding acquisition, Software, Writing – review & editing. AG: Data curation, Formal analysis, Funding acquisition, Software, Writing – review & editing. AH: Data curation, Formal analysis, Funding acquisition, Software, Writing – review & editing.

Funding

The author(s) declare financial support was received for the research, authorship, and/or publication of this article. This experiment was funded by the Science and Engineering Research Board (SERB), DST-Government of India (Project Id No. EEQ/2020/000535). The study was also financially supported by the Slovak Research and Development Agency under contract no. APVV-15-0562, APVV-20-0071 and Science grant agency under contract no. VEGA-1/0300/22. The study received funding from the Deanship of Scientific Research, Taif University.

Acknowledgments

The authors are thankful to the Slovak Research and Development Agency for supporting the study. The researchers would also like to acknowledge the Deanship of Scientific Research, Taif University, Taif, Saudi Arabia for funding this work.

Conflict of interest

The authors declare that the research was conducted in the absence of any commercial or financial relationships that could be construed as a potential conflict of interest.

Publisher's note

Supplementary material

The Supplementary material for this article can be found online at: https://www.frontiersin.org/articles/10.3389/fmicb.2023.1265265/full#supplementary-material

References

Adugna, A. (2004). Alternate approaches in deploying genes for disease resistance in crop plants. *Asian J. Plant Sci.* 3, 618–623. doi: 10.3923/ajps.2004.618.623

Ahn, I. P. (2007). Disturbance of the Ca^{2+}/calmodulin-dependent signalling pathway is responsible for the resistance of Arabidopsis dnd1 against *Pectobacterium carotovorum* infection. *Mol. Plant Pathol.* 8, 747–759. doi: 10.1111/j.1364-3703.2007.00428.x

Almeida-Silva, F., and Venancio, T. M. (2022). Pathogenesis-related protein 1 (PR-1) genes in soybean: genome-wide identification, structural analysis and expression profiling under multiple biotic and abiotic stresses. *Gene* 809:146013. doi: 10.1016/j.gene.2021.146013

Analin, B., Mohanan, A., Bakka, K., and Challabathula, D. (2020). Cytochrome oxidase and alternative oxidase pathways of mitochondrial electron transport chain are important for the photosynthetic performance of pea plants under salinity stress conditions. *Plant Physiol. Biochem.* 154, 248–259. doi: 10.1016/j.plaphy.2020.05.022

Anuradha, C., Chandrasekar, A., Backiyarani, S., Thangavelu, R., Giribabu, P., and Uma, S. (2022). Genome-wide analysis of pathogenesis-related protein 1 (PR-1) gene family from Musa spp. and its role in defense response during stresses. *Gene* 821:146334. doi: 10.1016/j.gene.2022.146334

Asano, T., Hayashi, N., Kikuchi, S., and Ohsugi, R. (2012). CDPK-mediated abiotic stress signaling. *Plant Signal. Behav.* 7, 817–821. doi: 10.4161/psb.20351

Baba, A. I., Rigó, G., Andrási, N., Tietz, O., Palme, K., Szabados, L., et al. (2019). "Striving towards abiotic stresses: role of the plant CDPK superfamily members" in *International climate protection*. eds. M. Palocz-Andresen, D. Szalay, A. Gosztom, L. Sípos and T. Taligás (Cham: Springer), 99–105.

Bashar, K. K., Tareq, M. Z., and Islam, M. S. (2020). Unlocking the mystery of plants' survival capability under waterlogging stress. *Plant Sci. Today* 7, 142–153. doi: 10.14719/pst.2020.7.2.663

Bhandari, D. D., Lapin, D., Kracher, B., von Born, P., Bautor, J., Niefind, K., et al. (2019). An EDS1 heterodimer signalling surface enforces timely reprogramming of immunity genes in Arabidopsis. *Nat. Commun.* 10:772. doi: 10.1038/s41467-019-08783-0

Cai, B., Ning, Y., Li, Q., Li, Q., and Ai, X. (2022). Effects of the chloroplast fructose-1, 6-bisphosphate aldolase gene on growth and low-temperature tolerance of tomato. *Int. J. Mol. Sci.* 23:728. doi: 10.3390/ijms23020728

Chakraborty, S., Toyota, M., Moeder, W., Chin, K., Fortuna, A., Champigny, M., et al. (2021). CYCLIC NUCLEOTIDE-GATED ION CHANNEL 2 modulates auxin homeostasis and signaling. *Plant Physiol.* 187, 1690–1703. doi: 10.1093/plphys/kiab332

Chang, Y., Sun, F., Sun, S., Wang, L., Wu, J., and Zhu, Z. (2021). Transcriptome analysis of resistance to *Fusarium* wilt in mung bean (*Vigna radiata* L.). *Front. Plant Sci.* 12:1213. doi: 10.3389/fpls.2021.679629

Cheng, Z., Luan, Y., Meng, J., Sun, J., Tao, J., and Zhao, D. (2021). WRKY transcription factor response to high-temperature stress. *Plan. Theory* 10:2211. doi: 10.3390/plants10102211

Chin, K., Moeder, W., and Yoshioka, K. (2009). Biological roles of cyclic-nucleotide-gated ion channels in plants: what we know and don't know about this 20-member ion channel family. *Botany* 87, 668–677. doi: 10.1139/B08-147

Clough, S. J., Fengler, K. A., Yu, I. C., Lippok, B., Smith, R. K., and Bent, A. F. Jr. (2000). The Arabidopsis dnd1 "defense, no death" gene encodes a mutated cyclic nucleotide-gated ion channel. *Proc. Natl. Acad. Sci.* 97, 9323–9328. doi: 10.1073/pnas.15000569

Dietrich, P., Moeder, W., and Yoshioka, K. (2020). Plant cyclic nucleotide-gated channels: new insights on their functions and regulation. *Plant Physiol.* 184, 27–38. doi: 10.1104/pp.20.00425

Espinoza, C., Liang, Y., and Stacey, G. (2017). Chitin receptor CERK 1 links salt stress and chitin-triggered innate immunity in Arabidopsis. *Plant J.* 89, 984–995. doi: 10.1111/tpj.13437

FAOSTAT. (2023). World Chickpea production in 2020–21, UN FAO, Corporate Statistical Database. Available at: https://www.fao.org/faostat/en/#data/QCL/visualize. Retrieved on 5 January 2023.

Gigli-Bisceglia, N., and Testerink, C. (2021). Fighting salt or enemies: shared perception and signaling strategies. *Curr. Opin. Plant Biol.* 64:102120. doi: 10.1016/j.pbi.2021.102120

Gill, N., and Dhillon, B. (2022). "RNA-seq data analysis for differential expression" in *Fusarium wilt. Methods in molecular biology*. ed. J. Coleman, vol. *2391* (New York, NY: Humana)

Gleeson, J., Leger, A., Prawer, Y. D., Lane, T. A., Harrison, P. J., Haerty, W., et al. (2022). Accurate expression quantification from nanopore direct RNA sequencing with NanoCount. *Nucleic Acids Res.* 50:e19. doi: 10.1093/nar/gkab1129

Gong, B. Q., Wang, F. Z., and Li, J. F. (2020). Hide-and-seek: chitin-triggered plant immunity and fungal counterstrategies. *Trends Plant Sci.* 25, 805–816. doi: 10.1016/j.tplants.2020.03.006

Grant, M., Brown, I., Adams, S., Knight, M., Ainslie, A., and Mansfield, J. (2000). The RPM1 plant disease resistance gene facilitates a rapid and sustained increase in cytosolic calcium that is necessary for the oxidative burst and hypersensitive cell death. *Plant J.* 23, 441–450. doi: 10.1046/j.1365-313x.2000.00804.x

Guerra-Castellano, A., Díaz-Quintana, A., Pérez-Mejías, G., Elena-Real, C. A., González-Arzola, K., García-Mauriño, S. M., et al. (2018). Oxidative stress is tightly regulated by cytochrome c phosphorylation and respirasome factors in mitochondria. *Proc. Natl. Acad. Sci.* 115, 7955–7960. doi: 10.1073/pnas.1806833115

Guo, J., Islam, M. A., Lin, H., Ji, C., Duan, Y., Liu, P., et al. (2018). Genome-wide identification of cyclic nucleotide-gated ion channel gene family in wheat and functional analyses of TaCNGC14 and TaCNGC16. *Front. Plant Sci.* 9:18. doi: 10.3389/fpls.2018.00018

Gupta, S., Chakraborti, D., Rangi, R. K., Basu, D., and Das, S. (2009). A molecular insight into the early events of chickpea (*Cicer arietinum*) and *Fusarium oxysporum* f. sp. *ciceri* (race 1) interaction through cDNA-AFLP analysis. *Phytopathology* 99, 1245–1257. doi: 10.1094/PHYTO-99-11-1245

Haware, M. P., Nene, Y. L., and Natarajan, M. (1996). Survival of *Fusarium oxysporum* f. sp. *ciceri* in the soil in the absence of chickpea. *Phytopathol. Mediterr.* 35, 9–12.

Indiastat. (2023). India Chickpea production in 2020–21. Available at: https://www.indiastat.com/data/agriculture. Retrieved on 5 January 2023.

Jagodzik, P., Tajdel-Zielinska, M., Ciesla, A., Marczak, M., and Ludwikow, A. (2018). Mitogen-activated protein kinase cascades in plant hormone signaling. *Front. Plant Sci.* 9:1387. doi: 10.3389/fpls.2018.01387

Jendoubi, W., Bouhadida, M., Boukteb, A., Béji, M., and Kharrat, M. (2017). *Fusarium* wilt affecting chickpea crop. *Agriculture* 7:23. doi: 10.3390/agriculture7030023

Johanndrees, O., Baggs, E. L., Uhlmann, C., Locci, F., Läßle, H. L., Melkonian, K., et al. (2023). Variation in plant toll/Interleukin-1 receptor domain protein dependence on ENHANCED DISEASE SUSCEPTIBILITY 1. *Plant Physiol.* 191, 626–642. doi: 10.1093/plphys/kiac480

Kapoor, D., Sharma, R., Handa, N., Kaur, H., Rattan, A., Yadav, P., et al. (2015). Redox homeostasis in plants under abiotic stress: role of electron carriers, energy metabolism mediators and proteinaceous thiols. *Front. Environ. Sci.* 3:13. doi: 10.3389/fenvs.2015.00013

Kattupalli, D., Srinivasan, A., and Soniya, E. V. (2021). A genome-wide analysis of pathogenesis-related Protein-1 (PR-1) genes from *Piper nigrum* reveals its critical role during Phytophthora capsici infection. *Gene* 12:1007. doi: 10.3390/genes12071007

Keisa, A., Kanberga-Silina, K., Nakurte, I., Kunga, L., and Rostoks, N. (2011). Differential disease resistance response in the barley necrotic mutant nec1. *BMC Plant Biol.* 11:66. doi: 10.1186/1471-2229-11-66

Kohli, D., Joshi, G., Deokar, A. A., Bhardwaj, A. R., Agarwal, M., Katiyar-Agarwal, S., et al. (2014). Identification and characterization of wilt and salt stress-responsive microRNAs in chickpea through high-throughput sequencing. *PLoS One* 9:e108851. doi: 10.1371/journal.pone.0108851

Kumar, S., Sahni, S., and Kumar, B. (2019). Screening of chickpea genotypes for resistance against *Fusarium* wilt. *Current J. App. Sci. Technol.* 38, 1–6. doi: 10.9734/CJAST/2019/v38i630409

Landi, M., and Guidi, L. (2022). Effects of abiotic stress on photosystem II proteins. *Photosynthetica* 61, 148–156. doi: 10.32615/ps.2022.043

Lei, Y. (2011). *Biochemical and functional characterization of the mitochondrial immune Signaling protein complex*. A dissertation submitted to the faculty of the University of North Carolina at Chapel Hill in partial fulfillment of the requirements for the degree of Doctor of Philosophy in the Curriculum of Oral Biology, School of Dentistry. doi: 10.17615/sr3j-8s02

Li, J., Guo, Y., and Yang, Y. (2022). The molecular mechanism of plasma membrane H+-ATPases in plant responses to abiotic stress. *J. Genetics Genomics.* 49, 715–725. doi: 10.1016/j.jgg.2022.05.007

Li, Y., Zeng, H., Xu, F., Yan, F., and Xu, W. (2022). H^+-ATPases in plant growth and stress responses. *Annu. Rev. Plant Biol.* 73, 495–521. doi: 10.1146/annurev-arplant-102820-114551

Lin, L., Wu, J., Jiang, M., and Wang, Y. (2021). Plant mitogen-activated protein kinase cascades in environmental stresses. *Int. J. Mol. Sci.* 22:1543. doi: 10.3390/ijms22041543

Liu, D., Li, M., Guo, T., Lu, J., Xie, Y., Hao, Y., et al. (2022). Functional characterization of the serine acetyltransferase family genes uncovers the diversification and conservation of cysteine biosynthesis in tomato. *Front. Plant Sci.* 13:913856. doi: 10.3389/fpls.2022.913856

Liu, F., Ma, Z., Cai, S., Dai, L., Gao, J., and Zhou, B. (2022). ATP-citrate lyase B (ACLB) negatively affects cell death and resistance to verticillium wilt. *BMC Plant Biol.* 22:443. doi: 10.1186/s12870-022-03834-z

Luan, S. (2009). The CBL-CIPK network in plant calcium signaling. *Trends Plant Sci.* 14, 37–42. doi: 10.1016/j.tplants.2008.10.005

Lv, G. Y., Guo, X. G., Xie, L. P., Xie, C. G., Zhang, X. H., Yang, Y., et al. (2017). Molecular characterization, gene evolution, and expression analysis of the fructose-1, 6-bisphosphate aldolase (FBA) gene family in wheat (*Triticum aestivum* L.). *Front. Plant Sci.* 8:1030. doi: 10.3389/fpls.2017.01030

Ma, W., and Berkowitz, G. A. (2011). Ca^{2+} conduction by plant cyclic nucleotide gated channels and associated signaling components in pathogen defense signal transduction cascades. *New Phytol.* 190, 566–572. doi: 10.1111/j.1469-8137.2010.03577.x

Moradbeygi, H., Jamei, R., Heidari, R., and Darvishzadeh, R. (2020). Investigating the enzymatic and non-enzymatic antioxidant defense by applying iron oxide nanoparticles

in *Dracocephalum moldavica* L. plant under salinity stress. *Sci. Hortic.* 272:109537. doi: 10.1016/j.scienta.2020.109537

Moriya, Y., Itoh, M., Okuda, S., Yoshizawa, A. C., and Kanehisa, M. (2007). KAAS: an automatic genome annotation and pathway reconstruction server. *Nucleic Acids Res.* 35, W182–W185. doi: 10.1093/nar/gkm321

Mulet, J. M., Alemany, B., Ros, R., Calvete, J. J., and Serrano, R. (2004). Expression of a plant serine O-acetyltransferase in *Saccharomyces cerevisiae* confers osmotic tolerance and creates an alternative pathway for cysteine biosynthesis. *Yeast* 21, 303–312. doi: 10.1002/yea.1076

Neubauer, M., Serrano, I., Rodibaugh, N., Bhandari, D. D., Bautor, J., Parker, J. E., et al. (2020). Arabidopsis EDR1 protein kinase regulates the association of EDS1 and PAD4 to inhibit cell death. *Mol. Plant-Microbe Interact.* 33, 693–703. doi: 10.1094/MPMI-12-19-0339-R

Nisa, M. U., Huang, Y., Benhamed, M., and Raynaud, C. (2019). The plant DNA damage response: signaling pathways leading to growth inhibition and putative role in response to stress conditions. *Front. Plant Sci.* 10:653. doi: 10.3389/fpls.2019.00653

Ochsenbein, C., Przybyla, D., Danon, A., Landgraf, F., Göbel, C., Imboden, A., et al. (2006). The role of EDS1 (enhanced disease susceptibility) during singlet oxygen-mediated stress responses of Arabidopsis. *Plant J.* 47, 445–456. doi: 10.1111/j.1365-313X.2006.02793.x

Pečenková, T., Pejchar, P., Moravec, T., Drs, M., Haluška, S., Šantrůček, J., et al. (2022). Immunity functions of Arabidopsis pathogenesis-related 1 are coupled but not confined to its C-terminus processing and trafficking. *Mol. Plant Pathol.* 23, 664–678. doi: 10.1111/mpp.13187

Peng, X., Zhang, X., Li, B., and Zhao, L. (2019). Cyclic nucleotide-gated ion channel 6 mediates thermotolerance in Arabidopsis seedlings by regulating nitric oxide production via cytosolic calcium ions. *BMC Plant Biol.* 19, 368–313. doi: 10.1186/s12870-019-1974-9

Phukan, U. J., Jeena, G. S., and Shukla, R. K. (2016). WRKY transcription factors: molecular regulation and stress responses in plants. *Front. Plant Sci.* 7:760. doi: 10.3389/fpls.2016.00760

Ranty, B., Aldon, D., Cotelle, V., Galaud, J. P., Thuleau, P., and Mazars, C. (2016). Calcium sensors as key hubs in plant responses to biotic and abiotic stresses. *Front. Plant Sci.* 7:327. doi: 10.3389/fpls.2016.00327

Rao, D., Momcilovic, I., Kobayashi, S., Callegari, E., and Ristic, Z. (2004). Chaperone activity of recombinant maize chloroplast protein synthesis elongation factor, EF-Tu. *Eur. J. Biochem.* 271, 3684–3692. doi: 10.1111/j.1432-1033.2004.04309.x

Reddy, D. S., Bhatnagar-Mathur, P., Reddy, P. S., Sri Cindhuri, K., Sivaji Ganesh, A., and Sharma, K. K. (2016). Identification and validation of reference genes and their impact on normalized gene expression studies across cultivated and wild cicer species. *PLoS One* 11:e0148451. doi: 10.1371/journal.pone.0148451

Robinson, M. D., McCarthy, D. J., and Smyth, G. K. (2010). edgeR: a Bioconductor package for differential expression analysis of digital gene expression data. *Bioinformatics* 26, 139–140. doi: 10.1093/bioinformatics/btp616

Rudenko, N. N., Borisova-Mubarakshina, M. M., Ignatova, L. K., Fedorchuk, T. P., Nadeeva-Zhurikova, E. M., and Ivanov, B. N. (2021). Role of plant carbonic anhydrases under stress conditions. *Plant Stress Physiol.* 4, 301–325. doi: 10.5772/intechopen.91971

Schmittgen, T. D., and Livak, K. J. (2008). Analyzing real-time PCR data by the comparative C T method. *Nat. Protoc.* 3, 1101–1108. doi: 10.1038/nprot.2008.73

Sharma, M., Nagavardhini, A., Thudi, M., Ghosh, R., Pande, S., and Varshney, R. K. (2014). Development of DArT markers and assessment of diversity in *Fusarium oxysporum* f. sp. *ciceris*, wilt pathogen of chickpea (*Cicer arietinum* L.). *BMC Genomics* 15, 454–414. doi: 10.1186/1471-2164-15-454

Sharma, M., Sengupta, A., Ghosh, R., Agarwal, G., Tarafdar, A., Nagavardhini, A., et al. (2016). Genome wide transcriptome profiling of *Fusarium oxysporum* f sp. *ciceris* conidial germination reveals new insights into infection-related genes. *Sci. Rep.* 6, 1–11. doi: 10.1038/srep37353

Sinha, A. K., Jaggi, M., Raghuram, B., and Tuteja, N. (2011). Mitogen-activated protein kinase signaling in plants under abiotic stress. *Plant Signal. Behav.* 6, 196–203. doi: 10.4161/psb.6.2.14701

Song, J., Zou, X., Liu, P., Cardoso, J. A., Schultze-Kraft, R., Liu, G., et al. (2022). Differential expressions and enzymatic properties of malate dehydrogenases in response to nutrient and metal stresses in *Stylosanthes guianensis*. *Plant Physiol. Biochem.* 170, 325–337. doi: 10.1016/j.plaphy.2021.12.012

Su, W., Ren, Y., Wang, D., Su, Y., Feng, J., Zhang, C., et al. (2020). The alcohol dehydrogenase gene family in sugarcane and its involvement in cold stress regulation. *BMC Genomics* 21, 521–517. doi: 10.1186/s12864-020-06929-9

Sun, M., Qiu, L., Liu, Y., Zhang, H., Zhang, Y., Qin, Y., et al. (2022). Pto interaction proteins: critical regulators in plant development and stress response. *Front. Plant Sci.* 13:774229. doi: 10.3389/fpls.2022.774229

Szurman-Zubrzycka, M., Jędrzejek, P., and Szarejko, I. (2023). How do plants cope with DNA damage? A concise review on the DDR pathway in plants. *Int. J. Mol. Sci.* 24:2404. doi: 10.3390/ijms24032404

Upasani, M. L., Limaye, B. M., Gurjar, G. S., Kasibhatla, S. M., Joshi, R. R., Kadoo, N. Y., et al. (2017). Chickpea-*Fusarium oxysporum* interaction transcriptome reveals differential modulation of plant defense strategies. *Sci. Rep.* 7, 1–12. doi: 10.1038/s41598-017-07114-x

Wang, Y., Feng, G., Zhang, Z., Liu, Y., Ma, Y., Wang, Y., et al. (2021). Overexpression of Pti4, Pti5, and Pti6 in tomato promote plant defense and fruit ripening. *Plant Sci.* 302:110702. doi: 10.1016/j.plantsci.2020.110702

Wang, L., Li, S., Sun, L., Tong, Y., Yang, L., Zhu, Y., et al. (2022). Over-expression of phosphoserine aminotransferase-encoding gene (AtPSAT1) prompts starch accumulation in *L. turionifera* under nitrogen starvation. *Int. J. Mol. Sci.* 23:11563. doi: 10.3390/ijms231911563

Wang, J., Tian, W., Tao, F., Wang, J., Shang, H., Chen, X., et al. (2020). TaRPM1 positively regulates wheat high-temperature seedling-plant resistance to *Puccinia striiformis* f. sp. *tritici*. Frontiers. *Plant Sci.* 10:1679. doi: 10.3389/fpls.2019.01679

Wang, H., Zhao, P., Shen, X., Xia, Z., Zhou, X., Chen, X., et al. (2021). Genome-wide survey of the phosphofructokinase family in cassava and functional characterization in response to oxygen-deficient stress. *BMC Plant Biol.* 21, 376–315. doi: 10.1186/s12870-021-03139-7

Wang, N., Zhong, X., Cong, Y., Wang, T., Yang, S., Li, Y., et al. (2016). Genome-wide analysis of phosphoenolpyruvate carboxylase gene family and their response to abiotic stresses in soybean. *Sci. Rep.* 6, 1–14. doi: 10.1038/srep38448

Waseem, M., and Ahmad, F. (2019). The phosphoenolpyruvate carboxylase gene family identification and expression analysis under abiotic and phytohormone stresses in *Solanum lycopersicum* L. *Gene* 690, 11–20. doi: 10.1016/j.gene.2018.12.033

Wu, W., Luo, X., and Ren, M. (2022). Clearance or hijack: universal interplay mechanisms between viruses and host autophagy from plants to animals. *Front. Cell. Infect. Microbiol.* 11:1345. doi: 10.3389/fcimb.2021.786348

Wu, Y., Zhang, L., Zhou, J., Zhang, X., Feng, Z., Wei, F., et al. (2021). Calcium-dependent protein kinase GhCDPK28 was identified and involved in verticillium wilt resistance in cotton. *Front. Plant Sci.* 12:772649. doi: 10.3389/fpls.2021.772649

Xue, R., Wu, X., Wang, Y., Zhuang, Y., Chen, J., Wu, J., et al. (2017). Hairy root transgene expression analysis of a secretory peroxidase (PvPOX1) from common bean infected by *Fusarium* wilt. *Plant Sci.* 260, 1–7. doi: 10.1016/j.plantsci.2017.03.011

Yadav, S., Rathore, M. S., and Mishra, A. (2020). The pyruvate-phosphate dikinase (C4-SmPPDK) gene from *Suaeda monoica* enhances photosynthesis, carbon assimilation, and abiotic stress tolerance in a C_3 plant under elevated CO_2 conditions. *Front. Plant Sci.* 11:345. doi: 10.3389/fpls.2020.00345

Yadava, Y. K., Chaudhary, P., Yadav, S., Rizvi, A. H., Kumar, T., Srivastava, R., et al. (2023). Genetic mapping of quantitative trait loci associated with drought tolerance in chickpea (*Cicer arietinum* L.). *Sci. Rep.* 13:17623. doi: 10.1038/s41598-023-44990-y

Yan, Z., Xingfen, W., Wei, R., Jun, Y., and Zhiying, M. (2016). Island cotton enhanced disease susceptibility 1 gene encoding a lipase-like protein plays a crucial role in response to *verticillium dahliae* by regulating the SA level and H_2O_2 accumulation. *Front. Plant Sci.* 7:1830. doi: 10.3389/fpls.2016.01830

Yang, X., Chen, L., Yang, Y., Guo, X., Chen, G., Xiong, X., et al. (2020). Transcriptome analysis reveals that exogenous ethylene activates immune and defense responses in a high late blight resistant potato genotype. *Sci. Rep.* 10, 21294–21314. doi: 10.1038/s41598-020-78027-5

Yin, G., Sun, H., Xin, X., Qin, G., Liang, Z., and Jing, X. (2009). Mitochondrial damage in the soybean seed axis during imbibition at chilling temperatures. *Plant Cell Physiol.* 50, 1305–1318. doi: 10.1093/pcp/pcp074

Zeng, H., Xu, L., Singh, A., Wang, H., Du, L., and Poovaiah, B. W. (2015). Involvement of calmodulin and calmodulin-like proteins in plant responses to abiotic stresses. *Front. Plant Sci.* 6:600. doi: 10.3389/fpls.2015.00600

Zhang, M., and Zhang, S. (2022). Mitogen-activated protein kinase cascades in plant signaling. *J. Integr. Plant Biol.* 64, 301–341. doi: 10.1111/jipb.13215

Zhao, C., Tang, Y., Wang, J., Zeng, Y., Sun, H., Zheng, Z., et al. (2021). A mis-regulated cyclic nucleotide-gated channel mediates cytosolic calcium elevation and activates immunity in Arabidopsis. *New Phytol.* 230, 1078–1094. doi: 10.1111/nph.17218

frontiers | Frontiers in Microbiology

TYPE Original Research
PUBLISHED 27 March 2024
DOI 10.3389/fmicb.2024.1371336

OPEN ACCESS

EDITED BY
Mahyar Mirmajlessi,
Ghent University, Belgium

REVIEWED BY
Francesco Lops,
University of Foggia, Italy
Kuldeep Singh Jadon,
Indian Council of Agricultural Research (ICAR), India

*CORRESPONDENCE
Huacai Fan
✉ hcfan325@126.com
Si-Jun Zheng
✉ sijunzheng63@163.com

RECEIVED 16 January 2024
ACCEPTED 08 March 2024
PUBLISHED 27 March 2024

CITATION
Zhou Y, Yang L, Xu S, Li S, Zeng L, Shang H, Li X, Fan H and Zheng S-J (2024) Biological control of the native endophytic fungus *Pochonia chlamydosporia* from the root nodule of *Dolichos lablab* on Fusarium wilt of banana TR4. *Front. Microbiol.* 15:1371336. doi: 10.3389/fmicb.2024.1371336

Biological control of the native endophytic fungus *Pochonia chlamydosporia* from the root nodule of *Dolichos lablab* on Fusarium wilt of banana TR4

Yunfan Zhou[1,2], Limei Yang[1], Shengtao Xu[1], Shu Li[1], Li Zeng[1], Hui Shang[1], Xundong Li[1], Huacai Fan[1]* and Si-Jun Zheng[1,3]*

[1]Yunnan Key Laboratory of Green Prevention and Control of Agricultural Transboundary Pests, The Ministry of Agriculture and Rural Affairs International Joint Research Center for Agriculture, The Ministry of Agriculture and Rural Affairs Key Laboratory for Prevention and Control of Biological Invasions, Agricultural Environment and Resource Research Institute, Yunnan Academy of Agricultural Sciences, Kunming, Yunnan, China, [2]Resource Plant Research Institute, Yunnan University, Kunming, Yunnan, China, [3]Bioversity International, Kunming, Yunnan, China

Fusarium wilt of banana caused by *Fusarium oxysporum* f. sp. *cubense*, Tropical Race 4 (TR4) is a soil-borne disease, and it is devastating. At present, the biological control using antagonistic microorganisms to mitigate TR4 is one of the best strategies as a safe and green way. Yunnan has abundant and diverse microbial resources. Using the dual-culture method, the antagonistic endophytic fungi against TR4 were isolated and screened from the root nodule of *Dolichos lablab*. The effect of the highest antagonistic activity strain on the morphology of the TR4 mycelium was observed using the scanning electron microscope. According to morphological characteristics and sequence analysis, the strain was identified. The biocontrol effect and plant growth promotion were investigated by greenhouse pot experiment. Using the confocal laser scanning microscope and the real-time fluorescence quantitative PCR, the dynamics of TR4 infestation and the TR4 content in banana plant roots and corms would also be detected. In this study, 18 native endophytic fungi were isolated from a root nodule sample of *Dolichos lablab* in the mulch for banana fields in Yuxi, Yunnan Province, China. The YNF2217 strain showed a high antagonistic activity against TR4 in plate confrontation experiments, and the inhibition rate of YNF2217 is 77.63%. After TR4 culture with YNF2217 for 7 days in plate confrontation experiments, the morphology of the TR4 mycelium appeared deformed and swollen when observed under a scanning electron microscope. According to morphological characteristics and sequence analysis, the strain YNF2217 was identified as *Pochonia chlamydosporia*. In the greenhouse pot experiment, the biocontrol effect of YNF2217 fermentation solution on TR4 was 70.97% and 96.87% on banana plant leaves and corms, respectively. Furthermore, YNF2217 significantly promoted the growth of banana plants, such as plant height, leaf length, leaf width, leaf number, pseudostem girth, and both the aboveground and underground fresh weight. Observations of TR4 infestation dynamics in banana roots and corms, along with real-time fluorescence quantitative PCR, verified that YNF2217 inoculation could significantly reduce the TR4 content. Therefore, YNF2217 as *P. chlamydosporia*, which was found first time in China and reported here, is expected to be an important new fungal resource for the green control of Fusarium wilt of banana in the future.

KEYWORDS

Foc TR4, endogenous rhizobia, *Pochonia chlamydosporia*, biocontrol, *Dolichos lablab*

1 Introduction

The banana (*Musa* spp.) is the most important fruit in tropical and subtropical regions, and it is also one of the most traded fruits in the world (Luo et al., 2023). However, in recent years, the banana industry has been restricted by various pests and diseases, among which Fusarium wilt of banana (FWB) is the most widespread and serious disease. FWB, also known as Panama disease or banana yellow leaf disease, is a destructive fungal soil-borne disease caused by *Fusarium oxysporum* f. sp. *cubense*, with Tropical Race 4 (TR4) infestation being particularly severe (Thukkaram et al., 2020; Yadav et al., 2021). The chlamydospores of this pathogen can survive in the soil for more than several decades, making control efforts challenging (Fu et al., 2016). Given the serious threats posed by FWB, effective prevention and control methods for the development of the banana industry around the world have become crucial. At present, soil fumigation, strategic crop rotation (Li et al., 2020), selection and breeding of varieties which are disease-resistant varieties (Xu et al., 2017; Huang et al., 2023), application of chemicals (Guo et al., 2013), biological control (Wang et al., 2013), and other methods are used to restrain FWB in China and other countries. However, the chlamydospores of FWB can persist in the soil for many years, limiting the effectiveness of crop rotation control. Additionally, planting disease-resistant varieties has the disadvantages of unstable yield and poor fruit flavor (Sunisha et al., 2020); and long-term chemical application will not only make the pathogen resistant but also cause environmental pollution. In recent years, application of biological strains has become the focus of FWB control because of its advantages of economic efficiency, green environmental protection. The results of the experiment reveal that biological strains can decrease TR4 while having no effect on the banana quality or the yield (Fu et al., 2017). However, the biocontrol effects of some biological strains in field experiments are not ideal; therefore, a large number of antagonistic strains that are more efficient and have adapted to the local ecological growth conditions must still be screened. At present, the strains that have been screened and have good antagonistic effects in previous studies, such as *Pseudomonas* (Li et al., 2021), *Bacillus* (Huang et al., 2017), *Trichoderma* (Qin et al., 2017), and *Streptomyces* (Zhang et al., 2021). Fan et al. (2021) screened and obtained the biocontrol bacteria *Bacillus amyloliquefaciens* YN0904 and *B. subtilis* YN1419, which were identified by our research team in the previous study. The biocontrol effects in the pot experiment were 82.6% and 85.6%. Additionally, two biocontrol bacteria could promote banana plant growth significantly (Fan et al., 2021). We also isolated *B. velezensis* strain YN1910 which had a significant control effect (78.43–81.76%) on FWB (Fan et al., 2023).

To further explore the native biocontrol resources that have a high biocontrol effect on TR4 other than *Bacillus* species, the root nodule of *Dolichos lablab* in the mulch of banana fields in Yuxi, Yunnan, China was selected to screen endophytic antagonist fungal strains in this study. The prevention and control experiment would be carried out in the greenhouse. Using the confocal laser scanning microscope and the real-time fluorescence quantitative PCR, the dynamics of TR4 infestation and the TR4 content in banana plant roots and corms would also be detected. The objective of this study is to evaluate the biocontrol potential of isolated microbes and to provide new and high-quality native biocontrol agents for control of Fusarium wilt of banana in the field.

2 Materials and methods

2.1 Isolation and screening of the antagonistic endophytic fungus against TR4

In January 2022, root nodules of *Dolichos lablab* were collected from the mulch of banana fields with Fusarium wilt of banana symptoms in Yuanjiang County (102°15′13″ E; 23°59′21″ N; altitude 895 m), Yuxi City, Yunnan Province, China. The root nodules of *Dolichos lablab* were washed with sterile water, which were then dried naturally indoors. Under aseptic conditions, the roots were sterilized with 75% ethanol and were cut into small pieces with a sterilized blade. After being washed 2–3 times in sterile water, the small pieces were immersed in 75% ethanol to be soaked for 30–60 s and then into 0.1% mercury chloride for 30–60 s. Next, the small pieces were washed again 2–3 times with sterile water before grinding out the sap. The endophytic fungi were obtained on the Rose Bengal medium (Rose Bengal medium: Peptone 5 g, Glucose 10 g, KH_2PO_4 1 g, $MgSO_4{\cdot}7H_2O$ 0.5 g, Agar 20 g, Chloramphenicol 0.1 g) using spread plate and streak plate methods. All treatments were repeated 3 times and cultured at 28°C for 72 h. Then, the colonies with different morphologies were purified for 2–3 times. Finally, when the mycelium produced spores, with the help of single-spore isolation method, the single spore was cultured on the PDA medium (PDA medium: Glucose 20 g, Agar 15 g, Potato 200 g, ddH_2O 1000 mL, pH 7), and the strain was stored at −80°C with 50% sterile glycerol for later use.

The isolated and preserved antagonistic endophytic fungi were selected based on the primary screening and secondary screening methodologies (Fan et al., 2021). They were then cultured at 28°C for 7 days. The inhibition rate was calculated using the cross method, measuring the diameter of the TR4 colonies. The computational formula is as follows:

Inhibition rate (%) = (TR4 colony diameter of control group – TR4 colony diameter of treated group)/TR4 colony diameter of control group ×100.

2.2 Effect of the antagonistic endophytic fungus on the morphology of the TR4 mycelium

Using the dual-culture method, the strain TR4 (15–1) was isolated, identified, and preserved by the Banana Research Group, Agricultural Environment and Resource Research Institute, Yunnan Academy of Agricultural Sciences (Zhang et al., 2018). It was then cultured with the antagonistic endophytic fungus for 7 days at 28°C. A fresh TR4 mycelium near the antagonistic strains was selected and transferred to a temporary slide with a sterilized toothpick. The effect of the antagonistic fungus on mycelia growth of TR4 was observed using the scanning electron microscope (ZEISS Sigma 300, Germany), and the fresh TR4 mycelium cultured alone was used as the control.

2.3 Identification of the antagonistic endophytic fungus

2.3.1 Morphological observation of the antagonistic endophytic fungus

The antagonistic endophytic fungus was inoculated on the PDA to culture for 7 days at 28°C. The morphology and color of the colony were observed and recorded. The morphology of the mycelium and spore was observed using a scanning electron microscope (ZEISS Sigma 300, Germany).

2.3.2 Molecular identification of the antagonistic endophytic fungus

First, the antagonistic endophytic fungus was inoculated on the PDA at 28°C, and it was cultured for 7 days. The DNA of the antagonistic endophytic fungus was extracted using the TSINGKE plant DNA extraction kit (universal type) and part of the ITS gene sequence of the antagonistic endophytic fungus was amplified by PCR using the primers ITS1/ITS4 (5′-TCCGT AGGTGAACCTGCGG-3′/ 5′-TCCTCCGCTTATTGATATGC-3′) (Chen et al., 2021), which was synthesized by Beijing Qingke Xinye Biotechnology Co., LTD. Next, the results of PCR amplification products were compared using BLAST on the NCBI website. An ITS phylogenetic tree was constructed by adopting the adjacent method with MEGA11 software.

2.4 Greenhouse pot experiment

In this study, the experiment was conducted in greenhouse (temperature is 25–35 °C, humidity is 50–80%) from May to October 2022. The Brazilian cultivar (*Musa* spp. AAA) was used in the pot experiment, and the transplanting substrate was supplied by Yunnan Yuxi Leshi Technology Co., Ltd. Banana plantlets of the same plant height and size with 4–5 leaves were transplanted into a plastic pot measuring 11 cm in diameter and 12 cm in height. Through the greenhouse pot experiment, the infection process of green fluorescent protein-TR4 (GFP-TR4) (Zhang et al., 2018) was observed using the confocal laser scanning microscope (Lecia TCS-SP, Wetzlar, Germany). In addition, the real-time fluorescence quantitative PCR was used to detect the content of TR4 in banana roots and corms derived from different treatments and time points, so as to further verify the effect of the antagonistic endophytic fungus on the biocontrol of banana Fusarium wilt.

2.4.1 Preparation of the antagonistic endophytic fungus and TR4 and GFP-TR4 fermentation broth

First, the antagonistic endophytic fungus and the pathogens TR4 and GFP-TR4 (Zhang et al., 2018) were activated on the PDA medium at 28°C for 7 days, and the mycelium was picked and inoculated in the PDB medium. After shaking them at 28°C and 150 r/min for 7 days, the spore suspension was filtered through 4-layer sterile gauze. The 1×10^6 cfu/mL antagonistic endophytic fungus and TR4 and GFP-TR4 fermentation broth were obtained by diluting the spore suspension with sterile water.

TABLE 1 Pot experiment treatment.

Treatment	Description in details
I	Blank PDB culture solution (CK)
II	Antagonistic endophytic fungus fermentation broth
III	Blank PDB culture solution + TR4 spore broth (TR4)
IV	Antagonistic endophytic fungus fermentation broth + TR4 spore broth
V	Blank PDB culture solution + GFP-TR4 spore broth (GFP-TR4)
VI	Antagonistic endophytic fungus fermentation broth + GFP-TR4 spore broth

2.4.2 Experiment design and method

The pot experiment included six treatments, with each treatment repeated three times. Treatment I involved 18 banana plants in each replicate, totaling 54 banana plants (12 plants were used as control to observe the infection process of TR4 in the roots and corms at 4 time points). Treatment II involved 10 banana plants in each replicate. Treatments III and IV involved 14 banana plants in each replicate respectively (12 plants were used to detect the TR4 content in the roots and corms after TR4 invasion at 4 time points). Treatments V and VI involved 4 banana plants in each replicate.

Treatment I drenched the blank PDB (PDB medium: Glucose 20 g, Potato 200 g, ddH_2O 1000 mL, pH 7) culture solution alone. Treatment II drenched the antagonistic endophytic fungus fermentation broth alone. Treatment III drenched TR4 spore broth and blank PDB culture solution. Treatment IV drenched the TR4 spore broth and the antagonistic endophytic fungus fermentation broth. Treatment V: drenched GFP-TR4 spore broth + blank PDB culture solution. Treatment VI drenched the GFP-TR4 spore broth and the antagonistic endophytic fungus fermentation broth (Table 1). Through treatments I and II, the plant growth promotion effect of the antagonistic endophytic fungus could be calculated. Through treatments III and IV, the biocontrol effect of antagonistic endophytic fungus could be calculated. Through treatments I, III, and IV, the TR4 content in the roots and corms after TR4 invasion was detected. Through treatments I, V, and VI, the infection process of TR4 in the roots and corms was observed.

At 4 time points after inoculation with TR4, the DNA extracted from different banana roots and corms was subjected to real-time fluorescence quantitative PCR. At 4 time points after inoculation with GFP-TR4, the roots and corms of banana plants were selected and sliced to observe GFP-TR4 infection using the confocal laser microscope based on the protocol outlined by Zhou et al. (2023).

2.4.3 Investigation of biocontrol effect

After 45 days of GFP-TR4 inoculation, the biocontrol effect of the antagonistic endophytic fungus was investigated. The McKinney index (McKinney, 1923) for both leaves and corms was recorded following the protocol outlined by Fan et al. (2021), and the biocontrol effect of each treatment was calculated. The classification for disease index was shown in Supplementary Table S1.

McKinney index (%) = $\sum$ (number of disease plants at all levels × relative representative value)/(total number of investigated plants × highest representative value) ×100.

Control effect (%) = (CK disease index - treatment disease index)/CK disease index ×100.

2.4.4 Investigation of plant growth promotion effect

To evaluate the plant growth promotion effect, the plant height, leaf length, leaf width, leaf number, pseudostem girth, and fresh weight of both aboveground and underground parts of banana plants were measured and recorded for treatments I and II. Two time points on day 1 of inoculating the antagonistic endophytic fungus and on day 45 after inoculating with TR4 were taken for measurements and recordings.

The measurement of plant height, leaf number, and pseudostem girth was taken as outlined by Fan et al. (2021). The length and width of the first expanded leaves were also measured. The fresh weight of the aboveground portion was recorded from the base of the corm, 1 cm above the ground level, and the fresh weight of the underground portion was recorded from other parts of plant after removing the aboveground part.

2.4.5 Observation of TR4 infection process in roots and corms of banana plants

To monitor the infection process of TR4 in the roots and corms of banana plants, samples of these plant parts were taken, and their tissues sectioned at 1 day, 7 days, 14 days, and 45 days after inoculating with GFP-TR4. The treatment without inoculated TR4 was used as a control. The control and treated samples of roots and corms at 4 time points were repeated three times.

The roots and corms of banana plants were washed with sterile water and sterilized with 75 % ethanol by dipping and rinsing in sterile water for 3 times. Finally, the sterilized filter paper was used to absorb surface moisture. After that, the banana roots and corms were sectioned with an ultrathin blade along the horizontal and vertical directions. Then, the sectioned tissues were placed on a glass slide, dripped with sterile water, and covered with another glass slide. The sectioned tissues were stored at 4°C in a refrigerator for observation. The excitation wavelength of GFP-TR4 fluorescence is 488:500 nm−560 nm, and the excitation wavelength of plant cell wall spontaneous fluorescence is 561:570 nm−670 nm.

2.4.6 Real-time fluorescence quantitative PCR for detection of TR4 content

To detect TR4 content changes in banana roots and corms after TR4 infection, on 1 day, 7 days,14 days and 45 days after inoculating GFP-TR4, the banana roots and corms were sampled for extracting plant tissue DNA (Zhou et al., 2023). The treatment without inoculated TR4 was used as the control. The control and samples of roots and corms at 4 time points were collected and each time point was repeated three times. Using the real-time fluorescence quantitative measurement, the number of genomic quantification of gene copy was carried out. Additionally, a specific protocol and a method were referred from Zhou et al. (2023) and a standard curve was established for data analysis (efficiency, 90%−110%; correlation coefficient, R2 > 0.99).

TABLE 2 The antagonistic activity of the strain YNF2217 against TR4.

Strain	TR4 colony diameter (cm)	Inhibition rate (%)
YNF2217+TR4	1.98 ± 0.03b	77.63 ± 0.3
TR4	8.87 ± 0.03a	

2.5 Data analysis

All data were analyzed and processed using Excel 2003 and SPSS 10.0 software. One-way ANOVA was employed to calculate the difference in the mean value of each treatment. The mean value is recorded as "mean ± standard error (S.E.)." Duncan's new complex range method was employed to examine the significance of the difference among all treatments ($P < 0.05$).

3 Results

3.1 Isolation and screening of antagonistic endophytic fungus

Eighteen endophytic fungi were isolated from a root nodule sample of *Dolichos lablab* in the mulch for banana fields in Yuxi, Yunnan Province, China. After primary screening, three endophytic fungi were screened, which exhibited antagonistic activities against TR4. The secondary screening results showed that one isolate has a high antagonistic activity and is named as YNF2217. The average diameter of the TR4 mycelium was 1.98 cm, and the inhibition rate was 77.63% (Table 2; Figure 1).

3.2 Effect of the antagonistic strain YNF2217 on the TR4 mycelium morphology

After TR4 was dual-cultured with the antagonistic strain YNF2217 for 7 days at 28°C. It was discovered using the scanning electron microscope that all of the TR4 mycelium was deformed and swollen and that the interior protoplasm was concentrated and aggregated (Figure 2A). However, the mycelium of theTR4 control was of normal smoothness, uniform thickness, and natural extension, and the interior protoplasm was normal (Figure 2B).

3.3 Identification of the antagonistic strain YNF2217

3.3.1 Morphological characteristics of the antagonistic strain YNF2217

The strain YNF2217 was cultured on the PDA medium at 28°C for 7 days, the colony appeared milky white and cottony. The margin of the colony was anomalous and the colony itself was of prostrate growth. The aerial mycelium was well developed and dense (Figure 3A). Meanwhile, conidiophores were observed

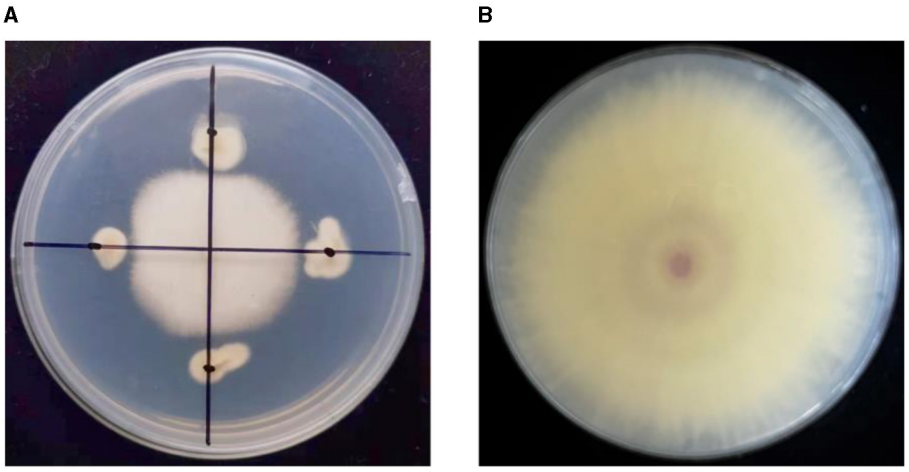

FIGURE 1
The antagonistic effect of the strain YNF2217 on TR4. **(A)** The antagonistic effect of the strain YNF2217 on TR4. **(B)** TR4 (CK).

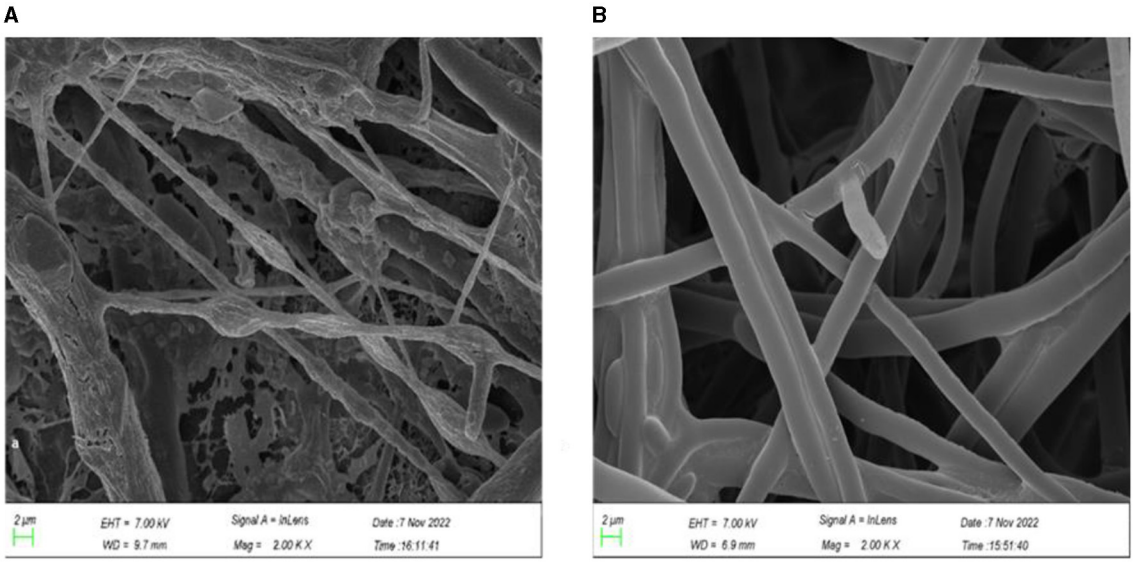

FIGURE 2
The effect of strain YNF2217 on the TR4 mycelium morphology. **(A)** The TR4 mycelium morphology under the scanning electron microscope after 7 days of YNF2217+TR4 culture. **(B)** The morphology of the TR4 mycelium under the scanning electron microscope after 7 days of TR4 culture.

growing on the top or lateral branches of the mycelium through the scanning electron microscope (SEM). The conidium was individually clustered on the top of the conidiophore, and the surface of the conidium was raised and appeared like verrucae (Figure 3B).

3.3.2 Molecular identification of the antagonistic strain YNF2217

Using the genome DNA of the strain YNF2217 as a template and ITS4/ITS5 as a primer, PCR amplification sequencing was performed. The ITS gene segment of YNF2217 was 1420 base pairs (bp). The ITS sequence of YNF2217 (GenBank Accession OQ586031) was compared with sequences in GenBank, and a phylogenetic tree of the sequence was constructed using MEGA 11.0 (Figure 4). It was indicated that the similarity between the sequence of YNF2217 and *Pochonia chlamydosporia* (MW760774, MH424139, OP799677) was 100%. According to the combined morphology and molecular identification methods described above, the antagonistic strain YNF2217 was identified as *Pochonia chlamydosporia*.

3.4 Pot experiment of the antagonistic strain YNF2217

3.4.1 Biocontrol effect of the antagonistic strain YNF2217

After drenching the antagonistic strain YNF2217 fermentation broth and the GFP-TR4 spore broth into banana plants

10.3389/fmicb.2024.1371336

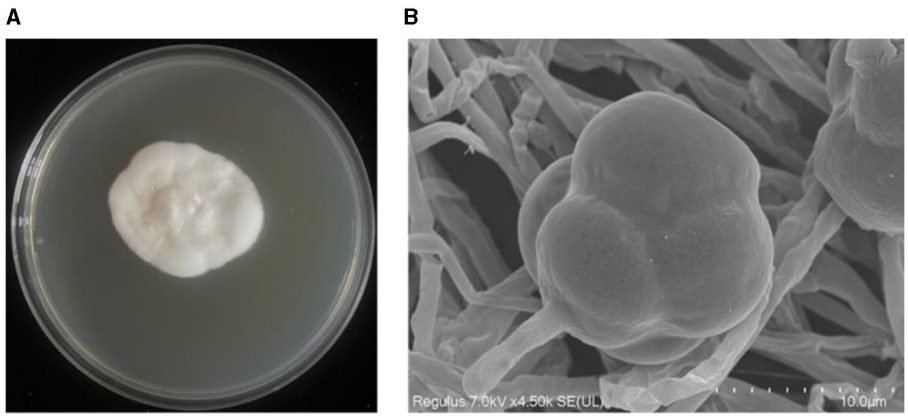

FIGURE 3
Morphological characteristics of the strain YNF2217. **(A)** The morphology of YNF2217 cultured on the PDA medium for 7 days. **(B)** The morphology of the mycelium and the conidium under the scanning electron microscope after 7 days of YNF2217 culture.

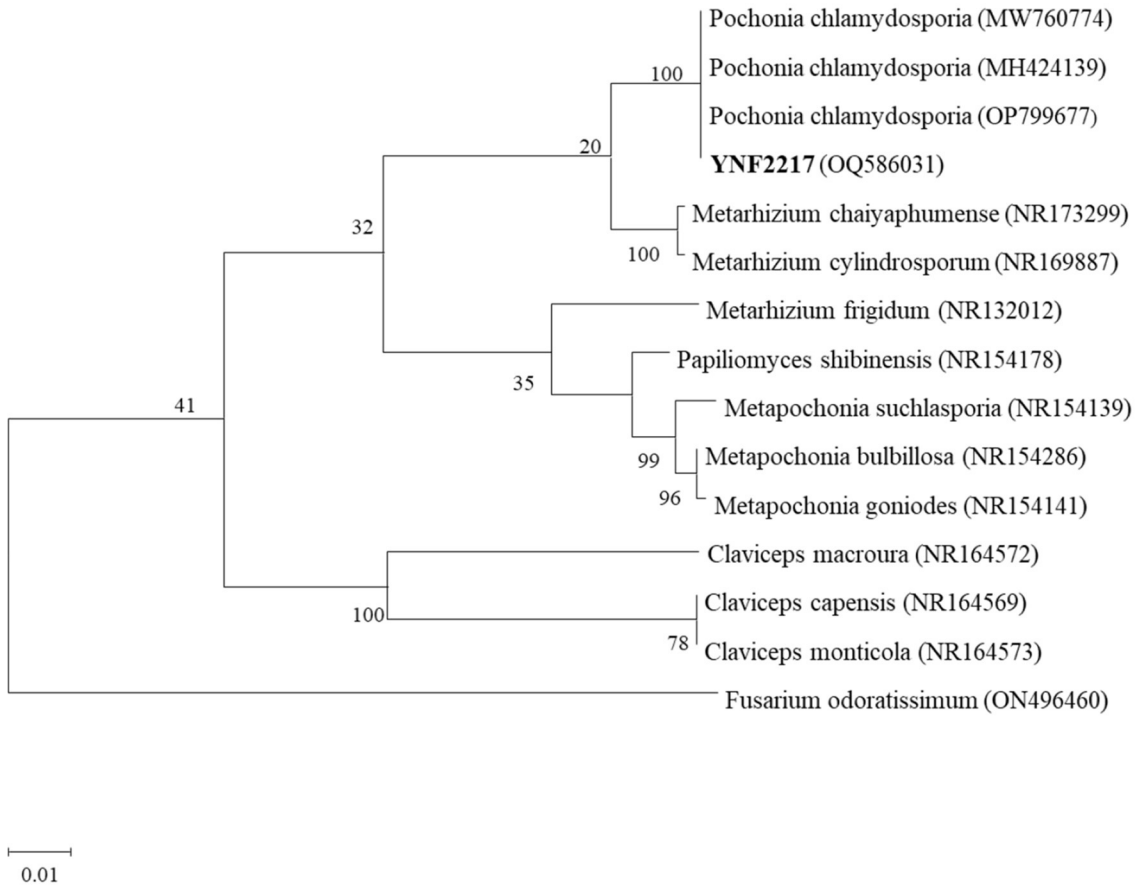

FIGURE 4
A gene phylogenetic tree of YNF2217.

for 45 days, the leaves appeared wilted and yellow, and the plants grew slowly in treatment III, which were only inoculated with TR4 (Figure 5). However, in the treatment IV of TR4+YNF2217, the most leaves remained healthy, the plants grew well and taller than those in treatment III. Additionally, after dissecting the corms, the corms inoculated with the YNF2217 were hardly invaded by the TR4 mycelium, and only a few brownish-black parts of corms were visible. However, many corms only inoculated with TR4 were brownish-black.

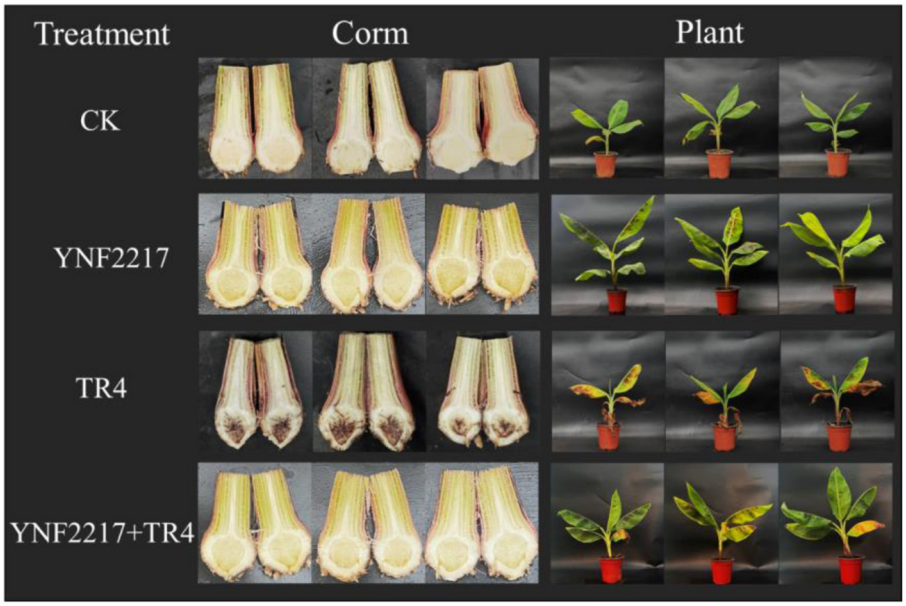

FIGURE 5
Biocontrol and plant growth promotion effects of the antagonistic strain YNF2217.

The disease index of the leaves and corms of banana plants in treatments III and IV was calculated 45 days after inoculation. In the treatment IV of TR4+YNF2217, the results showed that the disease index was 19.17 ± 0.83 in leaves and 2.50 ± 1.44 in corms. In the treatment III of TR4, the disease index was 66.67 ± 3.63 in leaves and 77.50 ± 4.33 in corms. In the treatment IV (YNF2217+TR4), the disease index of the leaves and the corms was significantly lower than that in treatment III (CK+TR4). According to the calculation, the biocontrol effect of the antagonistic strain YNF2217 was 70.97% in leaves and 96.87% in corms (Table 3).

TABLE 3 Control effect of the antagonistic strain YNF2217 on TR4.

Treatment	Disease index		Control effect	
	Corm	Leaf	Corm	Leaf
YNF2217+TR4	2.50 ± 1.44b	19.17 ± 0.83b	96.87 ± 1.86	70.97 ± 2.67
TR4	77.50 ± 4.33a	66.67 ± 3.63a		

3.4.2 Plant-promoting effect of the antagonistic strain YNF2217

After 45 days of inoculated YNF2217, plant growth parameters in all 4 treatments were measured (Table 4). The banana plant height (20.97 ± 0.76 cm), pseudostem girth (20.86 ± 0.61 mm), fresh weight of the aboveground (58.64 ± 3.03 g) and fresh weight of the underground (45.85 ± 2.45 g) of the antagonistic strain treated were significantly higher than the control (CK) (17.65 ± 0.59 cm, 16.83± 0.44 mm and 33.90± 1.57 g, 27.80± 0.96 g, respectively). Moreover, the leaf length (CK: 21.45 ± 0.50 cm, YNF2217: 25.29 ± 0.75 cm), leaf width (CK: 11.00 ± 0.36 cm; YNF2217:12.45 ± 0.32 cm), and leaf number (CK: 4.73 ± 0.16; YNF2217: 6.13 ± 0.17) were significantly high. The results revealed that the antagonistic strain, YNF2217, had significant growth-promoting effects on banana plants (Table 4 and Supplementary Figures S1–S7). Furthermore, the antagonistic strain, YNF2217, also significantly promoted plant growth even in the presence of TR4 inoculation.

3.4.3 Monitoring TR4 infection in roots and corms

The GFP-TR4 strain was used to monitor its infection process in treatments V and VI. After 1 day and 7 days of inoculating GFP-TR4, in the treatment VI (YNF2217+GFP-TR4), there were no detection of traces of the GFP-TR4 mycelium in the roots and corms. However, in the treatment V of only inoculating GFP-TR4, the mycelium was found in both roots and corms. Furthermore, after 14 days and 45 days of inoculating GFP-TR4, a small amount of the TR4 mycelium were found in the roots and corms treated with the antagonistic strain, YNF2217, while a large amount of the TR4 mycelium were present in both the roots and corms inoculating with GFP-TR4 (Figures 6, 7).

3.4.4 TR4 measurement using real-time fluorescence quantitative PCR

Real-time fluorescence quantitative PCR was employed to quantify the TR4 content in roots and corms on day 1, day 7, day 14, and day 45 after TR4 inoculation. The result is shown in Figure 8, in 4 different time points, and the content of TR4 in roots after TR4 inoculation ranged from 4.41 × 10^5 copies/g to 54.28 × 10^5

10.3389/fmicb.2024.1371336

TABLE 4 Growth promotion effect of the antagonistic strain YNF2217 on banana plants.

Treatment	Plant height	Leaf length	Leaf width	Leaf number	Pseudostem girth	Fresh weight of the aboveground	Fresh weight of the underground
CK	17.65 ± 0.59c	21.45 ± 0.50b	11.00 ± 0.36b	4.73 ± 0.16b	16.83 ± 0.44b	33.90 ± 1.57b	27.80 ± 0.96b
YNF2217	20.97 ± 0.76a	25.29 ± 0.75a	12.45 ± 0.32a	6.13 ± 0.17a	20.86 ± 0.61a	58.64 ± 3.03a	45.85 ± 2.45a
TR4	15.30 ± 1.90d	20.68 ± 0.38b	10.24 ± 0.35b	3.30 ± 0.17c	15.25 ± 0.31c	32.77 ± 1.44b	21.50 ± 0.68c
YNF2217+TR4	19.20 ± 1.31b	24.47 ± 0.40a	10.80 ± 0.30b	4.60 ± 0.10b	17.91 ± 0.31b	53.03 ± 1.96a	41.97 ± 1.14a

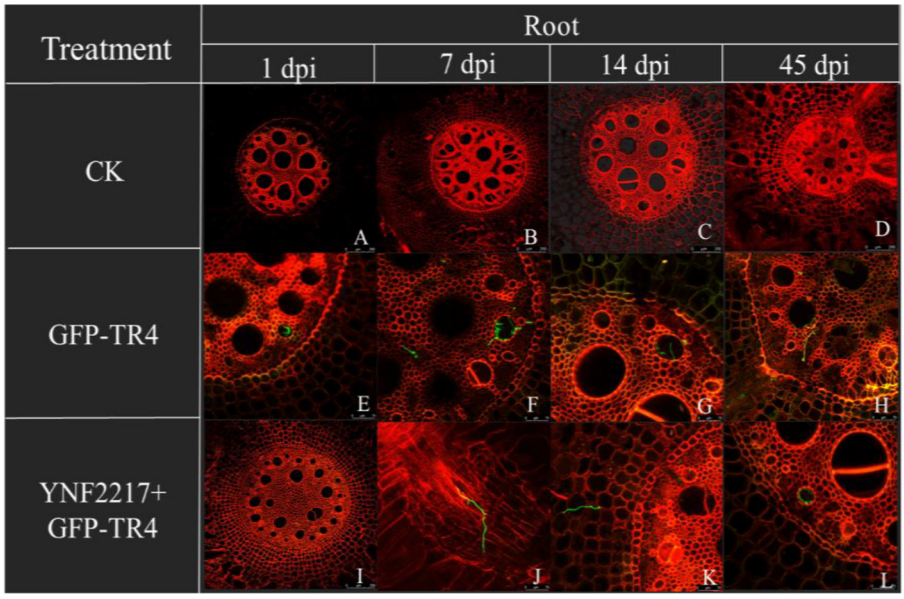

FIGURE 6
Infection process of GFP-TR4 in the roots of banana (1 dpi, 7 dpi, 14 dpi, 45 dpi). Bar = 250 mm in A, B, C, D, and I; Bar = 75 mm in E, F, G, and H.

copies/g. While, in the YNF2217 +TR4 treatment, it ranged from 0.70 × 10^5 copies/g to 17.02 × 10^5 copies/g. For all 4 time points, the content of TR4 in corms after TR4 inoculation ranged from 1.11 × 10^5 copies/g to 27.61 × 10^5 copies/g. However, in the YNF2217 +TR4 treatment, it ranged from 0.83 × 10^5 copies/g to 9.43 × 10^5 copies/g.

In roots, the content of TR4 treated with YNF2217+ TR4 was significantly lower than that of inoculation only with TR4 in all 4 time points. In corms, on day 7, day 14, and day 45, the content of TR4 treated with YNF2217+ TR4 was significantly lower than that of corms inoculated only with TR4. These results indicate that the TR4 content both in roots and corms was significantly reduced when treated with YNF2217+TR4, compared to inoculation with TR4 alone.

4 Discussion

Native strains have the ability to amplify the positive effects of biocontrol strains (Chong et al., 2023). Compared to exogenous strains, native strains have the advantages of the survival rate, reproduction rate, and stress resistance (Gan et al., 2024). Although various biocontrol strains have been developed and utilized at present, biocontrol strains are easily influenced by the environment and other soil microbial communities (Wang et al., 2023). Therefore, it is imperative to screen for local, unique, and adaptable biocontrol strains that can thrive in local ecological environments and are resistant to FWB. In this study, an antagonistic endophytic fungus, YNF2217, was isolated from the mulch in banana fields in Yuxi, Yunnan, China. Antagonistic activity screening and greenhouse pot experiments confirmed that the strain YNF2217 had high biocontrol effect on banana Fusarium wilt. The inhibition rate of YNF2217 was 77.63%. According to the morphology and molecular identification, the antagonistic strain YNF2217 was *Pochonia chlamydosporia*. In the greenhouse pot experiment, the biocontrol effect of the strain YNF2217 on the leaves and corms of banana plants was 70.97% and 96.87%, respectively. It is proved that YNF2217 had a significant biocontrol effect on the banana Fusarium wilt. In addition, various characteristics of banana plants was measured, including plant height, leaf length, leaf width, leaf number, pseudostem girth, and fresh weight both in the aboveground and belowground parts. The results showed that the strain YNF2217 had significant growth-promoting effects on banana plants. Furthermore, the results from monitoring the infection process of GFP-TR4 in roots and corms indicated that the GFP-TR4 mycelium in plants inoculated with YNF2217+TR4 was

10.3389/fmicb.2024.1371336

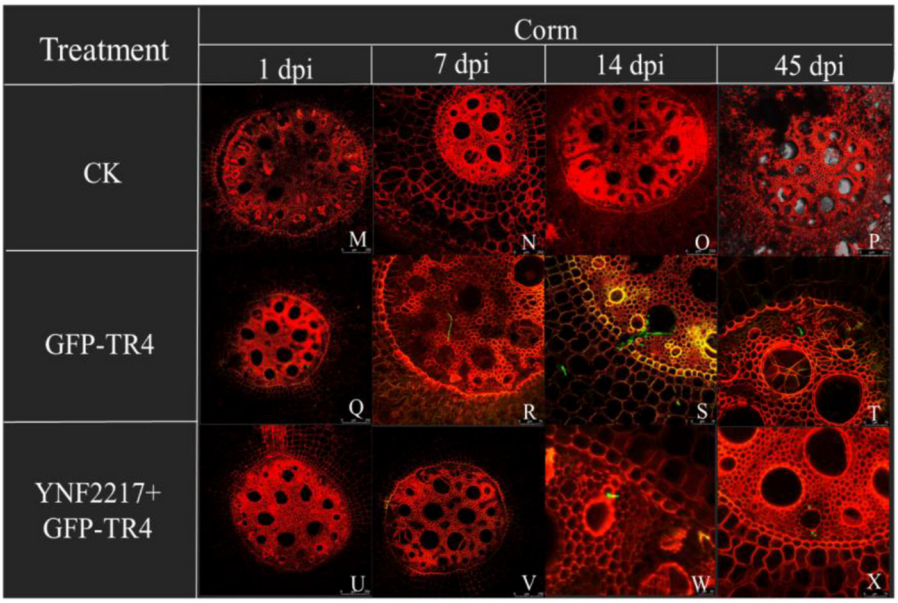

FIGURE 7
Infection process of GFP-TR4 in the corms of a banana (1 dpi, 7 dpi, 14 dpi, 45 dpi). Bar = 250 mm in M, N, O, P, Q, R, U, and V; Bar = 75 mm in R, S, T, W, and X.

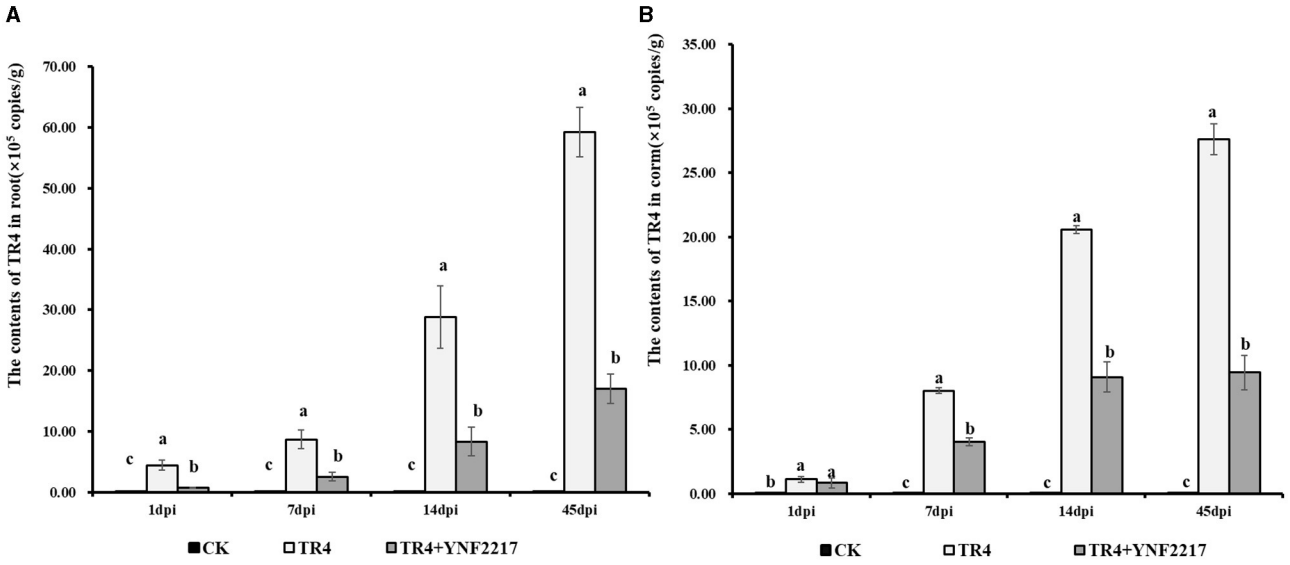

FIGURE 8
The content of TR4 in banana plants at 4 time points. **(A)** The content of TR4 in banana roots at 4 time points. **(B)** The content of TR4 in banana corms at 4 time points. The data were expressed as mean ± standard error, $P < 0.05$ was considered indicative of a significant difference, and different letters indicated significant differences.

lower than that in the treatment of only inoculated with TR4 on day 1, day 7, day 14, and day 45 after TR4 inoculation. Additionally, the real-time fluorescence quantitative PCR detection results also indicated that the content of TR4 in the roots inoculated with YNF2217+TR4 was significantly lower than that in the treatment of only inoculated with TR4. On day 7, day 14, and day 45, the content of TR4 in corms inoculated with YNF2217+TR4 was also significantly lower than that in the treatment of only inoculated with TR4. Therefore, it was confirmed that this fungal strain YNF2217 had a significant biocontrol effect on FWB.

It was reported that *P. chlamydosporia* exists in the microbial population of the banana planting region (Ciancio et al., 2022). The expression of related resistance genes such as *PIN II*, *PR1*, and lipoxygenase (*LOX*) in the host leaf was also reported after *P. chlamydosporia* was used to treat banana plants (Tolba et al., 2021). However, there is no study linking *P. chlamydosporia* to FWB. In

this study, the biocontrol effect of *P. chlamydosporia* YNF2217 on FWB was first reported in China. Therefore, this strain will be an important biocontrol strain resource for the green control of FWB. YNF2217 could be used as an additional and new biocontrol strain resource along with the previously discovered strains such as *Pseudomonas* (Xie et al., 2023), *Bacillus* (Fan et al., 2021, 2023; Duan et al., 2023), *Trichoderma* (Thukkaram et al., 2020) and *Streptomyces* (Lu et al., 2022). The prevention and control mechanisms of biocontrol fungi mainly include competition (Alwathnani et al., 2012), mycoparasitism (Amira et al., 2017), antibiosis (Vinale et al., 2014), induced resistance (Chemical et al., 2012), growth promotion (López-Bucio et al., 2015), and synergistic antagonism (Schulz et al., 2013). The active resistance of plants includes resistant genes involved and induced resistance, and induced systemic resistance is usually systematic, broad-spectrum, and non-specific (Stéphane et al., 2005). The manifestation of induced resistance includes the expression and accumulation of PR protein and antibacterial enzymes in plants. PR protein is an important component of disease and pest resistance in plants and often has antifungal and insecticidal activities (Muthukrishnan et al., 2001). Jiang had discovered that the related resistance marker genes such as *PR-1*, *PR-2*, and *PR-5* increased expression levels after *Nigrospora* sp. inoculation into the rhizosphere of wheat (Jiang, 2016). Tijerino et al. (2011), by analyzing the genomes of three *Trichoderma* species and using high-throughput gene knockout techniques, reported that a large number of genes related to secondary metabolism were discovered, and the genes *Tbtri5* and *Tri5* for *Trichoderma* synthase were obtained. Therefore, YNF2217 is expected to have great application prospects in the biological control of FWB.

P. chlamydosporia is a type of nematophagous fungus, with the ability to parasitize root-node nematodes and cyst nematode eggs. It is now widely used in the control of both animal and plant nematodes (Zhu et al., 2017). *P. chlamydosporia* serves as an effective ingredient in commercial fungicides and biological agents of plant parasitic nematodes. Moreover, its liquid culture is simple and cost-effective (Uthoff et al., 2024). Ghahremani et al. had reported that *P. chlamydosporia* is the common antagonistic fungus of vegetable root-node nematodes (Ghahremani et al., 2022). Zavala et al. (2017) discovered that *P. chlamydosporia* not only controls nematode diseases but also promotes the growth of plants, it was found that *P. chlamydosporia* promoted plant growth and improved the yield through the jasmonate signaling pathway. *P. chlamydosporia* also has a good preventive effect on animal parasitic diseases. Tábata et al. (2023) found that *P. chlamydosporia* can be parasitic in nematode eggs so as to reduce the degree of gastrointestinal nematodes in horses. Stoupa et al. (2020) found that the combined application of *Arthrobotrys cladodes* with *P. chlamydosporia* could effectively reduce the infection degree of cattle gastrointestinal nematode larvae. The greenhouse experiment results from Fu et al. (2014) showed that, when nematodes and TR4 infected bananas simultaneously, the disease index of FWB was higher than that when nematodes were not present. Yin et al. (2021) conducted experiments in banana plantations, and the results also indicate that the incidence rate of FWB was positively correlated with the disease index of root-node nematodes. So the results indicated that the control of root-knot nematodes could reduce the incidence rate of FWB. Therefore, YNF2217 as the nematophagous fungus is expected to have a better biocontrol effect on FWB when applied in the field in the future. *P. chlamydosporia* could directly inhibit TR4 and root-knot nematodes (Silva et al., 2017), and that most probably reduces the wounds of banana plants by its nematophagous nature. Furthermore, the transmission route of *Fusarium oxysporum* f. sp. *cubense* is reduced, thereby decreasing the occurrence of FWB.

The control effect of a biocontrol strain in soil-borne diseases mainly depends on its successful colonization in the soil or rhizosphere, competing with pathogens for nutrients and ecological sites, while also secreting antibacterial substances into the soil (Liu et al., 2023). As a result, under the premise of effective colonization of biocontrol strains, those that have better control effects are preferred. Lin et al. (2018) performed the transcriptome analysis of *P. chlamydosporia* and revealed its parasitism capacity on egg parasitoids, which is the main mechanism for controlling plant nematode diseases. Larriba et al. (2015) performed an analysis of barley roots after *P. chlamydosporia* colonization by transcriptome changes and found that growth-promoting genes were upregulated and plant immune-responsible genes were induced. In this study, YNF2217, identified as the native endophytic fungus *P. chlamydosporia* from the root nodule of *Dolichos lablab*, demonstrated its very promising potential application in FWB management. Based on previous studies on the relevant mechanisms of *P. chlamydosporia*, we expect that YNF2217 would have similar features as other *P. chlamydosporia*. Furthermore, the exact biocontrol mechanism and its field control effect of YNF2217 will be conducted in next research. Additionally, efforts will be made to develop the biocontrol formulation with YNF2217 for application in the management of FWB in the future.

Data availability statement

The datasets presented in this study can be found in online repositories. The names of the repository/repositories and accession number(s) can be found in the article/Supplementary material.

Author contributions

YZ: Conceptualization, Data curation, Formal analysis, Investigation, Methodology, Software, Validation, Visualization, Writing—original draft, Writing—review & editing. LY: Data curation, Investigation, Methodology, Software, Validation, Visualization, Writing—review & editing. SX: Data curation, Investigation, Methodology, Resources, Validation, Visualization, Writing—review & editing. SL: Data curation, Investigation, Methodology, Software, Validation, Visualization, Writing—review & editing. LZ: Data curation, Investigation, Resources, Validation, Writing—review & editing. HS: Data curation, Investigation, Methodology, Validation, Writing—review & editing. XL: Formal analysis, Investigation, Methodology, Resources, Validation, Writing—review & editing. HF: Conceptualization, Funding acquisition, Investigation, Project administration, Resources,

Supervision, Visualization, Writing—review & editing. S-JZ: Conceptualization, Funding acquisition, Methodology, Project administration, Resources, Supervision, Validation, Visualization, Writing—review & editing.

Funding

The author(s) declare that financial support was received for the research, authorship, and/or publication of this article. This study was funded by the earmarked fund for CARS (CARS-31); Yunnan Province Joint Special Project for Agricultural Basic Research (202301BD070001–048); Yunnan Province Technology Innovation and Talent Training object Huacai Fan (202405AD350068); Yunling Scholar Programme of Yunnan Provincial Government (YNWR-YLXZ-2018–018); partially funded by IAEA CRP D23033 - An Integrative Approach to Enhance Disease Resistance Against Fusarium Wilt (Foc TR4) in Banana – Phase II.

Acknowledgments

We are grateful to Guang-Dong Zhou for providing technical guidance during the experiments.

Conflict of interest

The authors declare that the research was conducted in the absence of any commercial or financial relationships that could be construed as a potential conflict of interest.

Publisher's note

Supplementary material

The Supplementary Material for this article can be found online at: https://www.frontiersin.org/articles/10.3389/fmicb.2024.1371336/full#supplementary-material

References

Alwathnani, H. A., Perveen, K., Tahmaz, R., and Alhaqbani, S. (2012). Evaluation of biological control potential of locally isolated antagonist fungi against *Fusarium oxysporum* under *in vitro* and pot conditions. *Afr. J. Microbiol. Res.* 6, 312–319. doi: 10.5897/AJMR11.1367

Amira, M. B., Lopez, D., Mohamed, A. T., Khouaja, A., Chaar, H., Fumanal, B., et al. (2017). Beneficial effect of Trichoderma harzianum strain Ths97 in biocontrolling *Fusarium solani* causal agent of root rot disease in olive trees. *Biol. Control* 110, 70–78. doi: 10.1016/j.biocontrol.2017.04.008

Chemical, Biological Process Development Group, P. N. N. L., Richland, W. A., U. S. A., Institute of Sciences of Food Production, N. R. C., Bari, Italy., Washington State University, T.-C., Richland, W. A., U. S. A., Institute of Sciences of Food Production, N. R. C., Bari, Italy, Biotechnology, A., et al. (2012). Phylogenomic analysis of polyketide synthase-encoding genes in Trichoderma. *Microbiology* 158, 147–154. doi: 10.1099/mic.0.053462-0

Chen, Y., Yan, D., Han, K., Ma, C., Gao, Z., Bao, X., et al. (2021). Occurrence of necrosis of balloon flower (*Platycodon grandiflorus*) caused by *Nigrospora sphaerica* in China. *Plant Dis.* 106:1–14. doi: 10.1094/PDIS-05-21-0960-PDN

Chong, L., Zhaohui, J., Shilin, M., Xin, L., Jinchi, Z., Christoph, M., et al. (2023). Plant and native microorganisms amplify the positive effects of microbial inoculant. *Microorganisms* 11, 570–570. doi: 10.3390/microorganisms11030570

Ciancio, A., Rosso, L. C., Lopez-Cepero, J., and Colagiero, M. (2022). Rhizosphere 16S-ITS metabarcoding profiles in banana crops are affected by nematodes, cultivation, and local climatic variations. *Front. Microbiol.* 13:855110. doi: 10.3389/fmicb.2022.855110

Duan, Y., Pang, Z., Yin, S., Xiao, W., Hu, H., Xie, J., et al. (2023). Screening and analysis of antifungal strains bacillus subtilis JF-4 and B. amylum JF-5 for the biological control of fusarium wilt of banana. *J. Fungi* 9:886. doi: 10.3390/jof9090886

Fan, H., He, P., Xu, S., Li, S., Wang, Y., Zhang, W., et al. (2023). Banana disease-suppressive soil drives Bacillus assembled to defense Fusarium wilt of banana. *Front. Microbiol.* 14:1211301. doi: 10.3389/fmicb.2023.1211301

Fan, H., Li, S., Zeng, L., He, P., Xu, S., Bai, T., et al. (2021). Biological control of *Fusarium oxysporum* F. sp. cubense tropical race 4 using natively isolated *Bacillus* spp. YN0904 and YN1419. *J. Fungi* 7:795. doi: 10.3390/jof7100795

Fu, L., Penton, C. R., Ruan, Y., Shen, Z., Xue, C., Li, R., et al. (2017). Inducing the rhizosphere microbiome by biofertilizer application to suppress banana Fusarium wilt disease. *Soil Biol. Biochem.* 104, 39–48. doi: 10.1016/j.soilbio.2016.10.008

Fu, L., Ruan, Y., Tao, C., Li, R., and Shen, Q. (2016). Continous application of bioorganic fertilizer induced resilient culturable bacteria community associated with banana Fusarium wilt suppression. *Sci. Rep.* 6:27731. doi: 10.1038/srep27731

Fu, M., Xiao, T., Wu, F., Zeng, X., and Chen, M. (2014). Determination of virulence of *Meloidogyne incognita*, *Radopholus similis* and *Fusarium oxysporum* f. sp. cubense race 4 on banana. *Guangdong Agric. Sci.* 41, 56–60. doi: 10.16768/j.issn.1004-874x.2014.01.021

Gan, L., Dai, Y., Liu, X., Lan, C., and Yang, X. (2024). Screening and control efficacies of highly effective antagonistic native bacteria against banana Fusarium wilt. *J. Northwest A&F Univ.* 6, 1–11. doi: 10.13207/j.cnki.jnwafu.2024.06.010

Ghahremani, Z., Escudero, N., Marín, I., Sanz, A., García, S., Expósito, A., et al. (2022). *Pochonia chlamydosporia* is the most prevalent fungal species responsible for meloidogyne suppression in sustainable vegetable production systems. *Sustainability* 14:16941. doi: 10.3390/su142416941

Guo, L., Yang, L., Peng, J., Wang, G., Liang, C., Liu, L., et al. (2013). Evaluation of control affection of fungicides on fusarium wilt of banana. *Chin. Agric. Sci. Bullet.* 29, 188–192.

Huang, J., Zhang, F., Pang, Y., Huang, Q., and Tang, S. (2017). Inhibition of banana Fusarium wilt by two biocontrol agents. *Microbiol. China* 44, 835–844. doi: 10.13344/j.microbiol.china.160370

Huang, S., Zhou, W., Wei, L., Wei, D., Li, C., Qin, L., et al. (2023). A new banana cultivar'guijiao 9'with resistance to fusarium wilt *Acta Horticulturae Sinica* 50, 45–46. doi: 10.16420/j.issn.0513-353x.2023-0303

Jiang, H. (2016). The antagonistic fungi HPFJ3-induced wheat's resistance to take-all disease and its mechanism. *J. Lishui Univ.* 38, 60–67.

Larriba, E., Jaime, M. D., Nislow, C., and Martín-Nieto, J. (2015). Endophytic colonization of barley (*Hordeum vulgare*) roots by the nematophagous fungus *Pochonia chlamydosporia* reveals plant growth promotion and a general defense and stress transcriptomic response. *J. Plant Res.* 12, 1–19. doi: 10.1007/s10265-015-0731-x

Li, S., Yang, L., Xiao, X., Hu, J., Zhang, H., Shen, N., et al. (2021). Screening, identification and biocontrol effect of antagonistic bacteria against banana Fusarium wilt. *J. Southern Agric.* 52, 1826–1834.

Li, Z., Wang, T., He, C., Cheng, K., Zeng, R., Song, Y., et al. (2020). Control of panama disease of banana by intercropping with Chinese chive (*Allium tuberosum* Rottler): cultivar differences. *BMC Plant Biol.* 20:432. doi: 10.1186/s12870-020-02640-9

Lin, R., Qin, F., Shen, B., Shi, Q., Liu, C., Zhang, X., et al. (2018). Genome and secretome analysis of Pochonia chlamydosporia provide new insight into egg-parasitic mechanisms. *Springer Nature* 1:169. doi: 10.1038/s41598-018-19169-5

Liu, Y., Lai, J., Sun, X., Wei, S., Zeng, H., Chen, C., et al. (2023). Research progress in the mechanism of rhizosphere micro-ecology in regulating the occurrence of clubroot disease in Chinese cabbage. *Microbiol. China* 22, 1–21. doi: 10.13344/j.microbiol.china.230587

López-Bucio, J., Pelagio-Flores, R., and Herrera-Estrella, A. (2015). Trichoderma as biostimulant: exploiting the multilevel properties of a plant beneficial fungus. *Sci. Hortic.* 196, 109–123. doi: 10.1016/j.scienta.2015.08.043

Lu, Z., Ziyu, L., Yong, W., Jiaqi, Z., Shujie, W., Yating, H., et al. (2022). Biocontrol potential of endophytic streptomyces malaysiensis 8ZJF-21 from medicinal plant against banana fusarium wilt caused by *Fusarium oxysporum* f. sp. cubense Tropical Race 4and#13. *Frontiers in Plant Science* 13, 874819–874819. doi: 10.3389/fpls.2022.874819

Luo, M., Chen, Y., Huang, Q., Huang, Z., Song, H., Dong, Z., et al. (2023). Trichoderma koningiopsis Tk905: an efficient biocontrol, induced resistance agent against banana Fusarium wilt disease and a potential plant-growth-promoting fungus. *Front. Microbiol.* 14:1301062. doi: 10.3389/fmicb.2023.1301062

McKinney, H. H.. (1923). *Influence of soil temperature and moisture on infection of wheat seedlings by Helminthosporium sativum.*

Muthukrishnan, S., Liang, G. H., Trick, H. N., and Gill, B. S. (2001). Pathogenesis-related proteins and their genes in cereals. *Plant Cell Tissue Organ Cult.* 64, 93–114. doi: 10.1023/A:1010763506802

Qin, L., Guo, C., Huang, S., Li, C., Wei, L., Wei, S., et al. (2017). Growth-promoting effects of *Trichoderma asperellum* strain PZ6 on banana and its indoor control effect against banana fusarium wilt. *J. Southern Agric.* 48, 277–283.

Schulz, M., Marocco, A., Tabaglio, V., Macias, F. A., and Molinillo, J. M. G. (2013). Benzoxazinoids in rye allelopathy - from discovery to application in sustainable weed control and organic farming. *J. Chem. Ecol.* 39:235. doi: 10.1007/s10886-013-0235-x

Silva, S. D., Carneiro, R., Faria, M., Souza, D. A., Monnerat, R. G., Lopes, R. B., et al. (2017). Evaluation of *Pochonia chlamydosporia* and *Purpureocillium lilacinum* for suppression of meloidogyne enterolobii on tomato and banana. *J. Nematol.* 49, 77–85. doi: 10.21307/jofnem-2017-047

Stéphane, C., Brion, D., Jerzy, N., Christophe, C., and Ait, B. E. (2005). Use of plant growth-promoting bacteria for biocontrol of plant diseases: principles, mechanisms of action, and future prospects. *Appl. Environ. Microbiol.* 71, 4951–4959. doi: 10.1128/AEM.71.9.4951-4959.2005

Stoupa, V. Í., Castro, O. I. D., Kanadani, C. A., and Victor, A. J. (2020). Arthrobotrys cladodes and Pochonia chlamydosporia: nematicidal effects of single and combined use after passage through cattle gastrointestinal tract. *Exp. Parasitol.* 218, 108005–108005. doi: 10.1016/j.exppara.2020.108005

Sunisha, C., Sowmya, H. D., Usharani, T. R., Umesha, M., Gopalkrishna, H. R., Saxena, A., et al. (2020). Deployment of stacked antimicrobial genes in banana for stable tolerance against *Fusarium oxysporum* f.sp. cubense through genetic transformation. *Mol. Biotechnol.* 62, 8–17. doi: 10.1007/s12033-019-00219-w

Tábata, A. C., Mateus, O. M., Isabela, A. C., Giordani, M. F., Gabriel, J. G., Sara, C. P., et al. (2023). Biological control of gastrointestinal nematodes in horses fed with grass in association with nematophagus fungi Duddingtonia flagrans and Pochonia chlamydosporia. *Biol. Control* 182: 105219. doi: 10.1016/j.biocontrol.2023.105219

Thukkaram, D., Shailendra, R., Manoharan, M., Gopal, R., Kavita, Y., Sandeep, K., et al. (2020). Biological management of banana fusarium wilt caused by *Fusarium oxysporum* f. sp. cubense tropical race 4 using antagonistic fungal isolate CSR-T-3 (*Trichoderma reesei*)and#13. *Front. Microbiol.* 11: 595845. doi: 10.3389/fmicb.2020.595845

Tijerino, A., Hermosa, R., Cardoza, R. E., Moraga, J., Malmierca, M. G., Aleu, J., et al. (2011). Overexpression of the *Trichoderma brevicompactum* tri5 Gene: effect on the expression of the trichodermin biosynthetic genes and on tomato seedlings. *Toxins* 3, 1220–1232. doi: 10.3390/toxins3091220

Tolba, S. R. T., Rosso, L. C., Pentimone, I., Colagiero, M., Moustafa, M. M. A., Elshawaf, I. I. S., et al. (2021). Root endophytism by pochonia chlamydosporia affects defense-gene expression in leaves of monocot and dicot hosts under multiple biotic interactions. *Plants* 10:718. doi: 10.3390/plants10040718

Uthoff, J., Schönwandt, D. J., Dietz, K. J., and Patel, A. (2024). Development of a seed treatment withpochonia chlamydosporiafor biocontrol application. *Agriculture* 14:10138. doi: 10.3390/agriculture14010138

Vinale, F., Manganiello, G., Nigro, M., Mazzei, P., Piccolo, A., Pascale, A., et al. (2014). A novel fungal metabolite with beneficial properties for agricultural applications. *Molecules* 19, 9760–9772. doi: 10.3390/molecules19079760

Wang, B., Yuan, J., Zhang, J., Shen, Z., Zhang, M., Li, R., et al. (2013). Effects of novel bioorganic fertilizer produced by Bacillus amyloliquefaciens W19 on antagonism of Fusarium wilt of banana. *Biol. Fertility Soils* 49, 435–446. doi: 10.1007/s00374-012-0739-5

Wang, E., Wu, Y., Liang, B., Huang, Y., Li, Y., Zhang, R., et al. (2023). Screening, identification and growth conditions research of an antagonistic strain against tomato fusarium wilt. *J. Qingdao Agric. Univ.* 40, 174–181.

Xie, J., Singh, P., Qi, Y., Singh, R. K., Qin, Q., Jin, C., et al. (2023). *Pseudomonas aeruginosa* strain 91: a multifaceted biocontrol agent against banana fusarium wilt. *J. Fungi* 9:1047. doi: 10.3390/jof9111047

Xu, L., Zhang, X., Li, H., Chen, B., Huang, B., Chen, W., et al. (2017). The breeding of new banana varieties 'Nan Tian huang' for resistance to fusarium wilt. *Chin. J. Trop. Crops* 38, 998–1004.

Yadav, K., Damodaran, T., Dutt, K., Singh, A., Muthukumar, M., Rajan, S., et al. (2021). Effective biocontrol of banana fusarium wilt tropical race 4 by a bacillus rhizobacteria strain with antagonistic secondary metabolites. *Rhizosphere* 18:100341. doi: 10.1016/j.rhisph.2021.100341

Yin, K., Zheng, S. J., Li, X., Yang, B., Li, Y., Huang, Y., et al. (2021). Preliminary study on the correlation between root knot nematode damage and banana wilt disease. *South China Fruits* 50, 71–78. doi: 10.13938/j.issn.1007-1431.20200268

Zavala, G. E. A., Rodríguez, C. E., Escudero, N., Aranda, M. A., Martínez, L. A., Ramírez, L. M., et al. (2017). *Arabidopsis thaliana* root colonization by the nematophagous fungus Pochonia chlamydosporia is modulated by jasmonate signaling and leads to accelerated flowering and improved yield. *The New Phytol.* 213, 351–364. doi: 10.1111/nph.14106

Zhang, H., Wang, W., Zhou, D., Yun, T., Chen, Y., Xie, J., et al. (2021). Solation and identification of Actionmycetes JRGG-11 and its antagonistc mechanism against banana fusarium wilt. *South China Fruits* 50, 1–8. doi: 10.13938/j.issn.1007-1431.20210174

Zhang, L., Yuan, T., Wang, Y., Zhang, D., Bai, T., Xu, S., et al. (2018). Identification and evaluation of resistance to *Fusarium oxysporum* f. sp. cubense tropical race 4 in *Musa acuminata* Pahang. *Euphytica* 214, 1–12. doi: 10.1007/s10681-018-2185-4

Zhou, G. D., He, P., Tian, L., Xu, S., Yang, B., Liu, L., et al. (2023). Disentangling the resistant mechanism of Fusarium wilt TR4 interactions with different cultivars and its elicitor application. *Front. Plant Sci.* 14:1145837. doi: 10.3389/fpls.2023.1145837

Zhu, X., Xu, K., Wang, X., Liang, M., Zhang, W., Yang, X., et al. (2017). Growth characteristics of a nematode-trapping fungus-*Pochonia chlamydosporia* ARSEF3539. *Anim. Husb. Feed Sci.* 38, 1–4. doi: 10.16003/j.cnki.issn1672-5190.2017.04.001

frontiers | Frontiers in Plant Science

TYPE Original Research
PUBLISHED 30 May 2024
DOI 10.3389/fpls.2024.1383914

OPEN ACCESS

EDITED BY
Inmaculada Larena,
Instituto Nacional de Investigación y Tecnología Agraria y Alimentaria (INIA-CSIC), Spain

REVIEWED BY
Kang Zhang,
Chinese Academy of Agricultural Sciences, China
Jose M. Diaz-Minguez,
University of Salamanca, Spain

*CORRESPONDENCE
Maria Samsonova
m.samsonova@spbstu.ru

†These authors have contributed equally to this work

RECEIVED 08 February 2024
ACCEPTED 16 May 2024
PUBLISHED 30 May 2024

CITATION
Logachev A, Kanapin A, Rozhmina T, Stanin V, Bankin M, Samsonova A, Orlova E and Samsonova M (2024) Pangenomics of flax fungal parasite *Fusarium oxysporum* f. sp. *lini*. *Front. Plant Sci.* 15:1383914. doi: 10.3389/fpls.2024.1383914

Pangenomics of flax fungal parasite *Fusarium oxysporum* f. sp. *lini*

Anton Logachev[1†], Alexander Kanapin[2†], Tatyana Rozhmina[3], Vladislav Stanin[1], Mikhail Bankin[1], Anastasia Samsonova[2], Ekaterina Orlova[1] and Maria Samsonova[1*]

[1]Mathematical Biology and Bioinformatics Laboratory, Peter the Great St.Petersburg Polytechnic University, Saint Petersburg, Russia, [2]Center for Computational Biology, Peter the Great St. Petersburg Polytechnic University, Saint Petersburg, Russia, [3]Flax Institute, Federal Research Center for Bast Fiber Crops, Torzhok, Russia

To assess the genomic diversity of *Fusarium oxysporum* f. sp. *lini* strains and compile a comprehensive gene repertoire, we constructed a pangenome using 13 isolates from four different clonal lineages, each exhibiting distinct levels of virulence. Syntenic analyses of two selected genomes revealed significant chromosomal rearrangements unique to each genome. A comprehensive examination of both core and accessory pangenome content and diversity points at an open genome state. Additionally, Gene Ontology (GO) enrichment analysis indicated that non-core pangenome genes are associated with pathogen recognition and immune signaling. Furthermore, the *Folini* pansecterome, encompassing secreted proteins critical for fungal pathogenicity, primarily consists of three functional classes: effector proteins, CAZYmes, and proteases. These three classes account for approximately 3.5% of the pangenome. Each functional class within the pansecterome was meticulously annotated and characterized with respect to pangenome category distribution, PFAM domain frequency, and strain virulence assessment. This analysis revealed that highly virulent isolates have specific types of PFAM domains that are exclusive to them. Upon examining the repertoire of *SIX* genes known for virulence in other formae speciales, it was found that all isolates had a similar gene content except for two, which lacked *SIX* genes entirely.

KEYWORDS

Fusarium wilt, flax, pangenome, *Fusarium oxysporum*, virulence, effectors, *SIX* genes

1 Introduction

Fusarium wilt of flax is a disease that affects many areas worldwide, caused by a specific type of *Fusarium oxysporum* Schlecht., a fungus in the Ascomycota phylum (Gordon, 2017; Zhang and Ma, 2017). This special form (i.e., forma specialis, f. sp.) of *Fusarium oxysporum* is known to infect only flax (Baayen et al., 2000).

Flax is an excellent source of oil and fiber. Oilseed flax is rich in unsaturated fatty acids, lignins, easily digestible proteins, dietary fiber, vitamins, and minerals. It is also used in the production of paints, resins, printing inks, varnishes, and linoleum. Fiber flax varieties are used as the base material to produce textiles and composites. The Fusarium wilt causes substantial economic damage, as it leads to a reduction in both seed productivity and fiber quality (Kommedahl et al., 1970; Dean et al., 2012; Kumar et al., 2014; Rozhmina et al., 2022).

Fusarium oxysporum displays several peculiar features that distinguish it from the other *Fusarium* species. Indeed, the phenomenon of sexual reproduction has not yet been observed in *Fusarium oxysporum* despite the presence of the conserved mating-type genes (either *MAT1–1* or *MAT1–2*) that are typical of sexual species (Yun et al., 2000). On top of this, *Fusarium oxysporum* exhibits a polymorphic lifestyle that varies across genotypes from soil saprophytes to endophytic strains and to specialized parasites capable of infecting plants, as well as animals, including humans (Dean et al., 2012). The lifestyle is mainly set by genetics, however switching between different lifestyles may result from a loss of dispensable chromosomes or be triggered by parasexual processes.

Phytopathogenic *Fusarium oxysporum* strains are usually found in soil as saprophytes. Nonetheless, when environmental conditions are right, they infect plants by penetrating roots and by colonizing vascular tissues (Gordon, 2017). Strains with the same host range are grouped in a forma specialis. Most *Fusarium oxysporum* special forms are restricted to a single plant species, yet some may infect several species, which are either close relatives or at least belong to one family (Kistler, 1997; O'Donnell et al., 1998; Edel-Hermann and Lecomte, 2019). To date, around 100 forms of *Fusarium oxysporum* (Dean et al., 2012) have been identified, with *Fusarium oxysporum* f. sp *lini* (*Folini*) being one of them. The strains of *Folini* have been separated into several clades, implying that its pathogenicity is of a clonal origin (Samsonova et al., 2021).

Recently it has been shown that in *Fusarium oxysporum* strains the estimated genome size varies from 54 Mb to 77 Mb, while the number of chromosomes ranges from 9 to 20 (Ma et al., 2010; Fokkens et al., 2020; Kanapin et al., 2020; Wang et al., 2020). Importantly, all sequenced *Fusarium oxysporum* chromosomes, even those assembled with the Hi-C data (Fokkens et al., 2020; Wang et al., 2020), are predicted pseudomolecules. Only in a handful of them the concordance with physical chromosomes was examined (Ayukawa et al., 2018). The predicted gene count in different *Fusarium oxysporum* genomes vary between 13K and 18K, with the average number of predicted gene models being 17K. Yet, mapping transcriptome sequencing data to *F. oxysporum* f. sp. *lycopersici* genome assembly, built with LRS technology data, predicted 50% more gene models (Sun et al., 2022)

Comparative synteny analysis reveals that *Fusarium oxysporum* genome has a complex structure encompassing conservative (i.e., conservative or core chromosomes) and variable parts (i.e., dispensable or accessory chromosomes). The latter is lineage-specific, meaning that it either exhibits poor syntenic alignment with other *Fusarium oxysporum* genomes from distinct lineages (Ma et al., 2010; Williams et al., 2016; Armitage et al., 2018) or does not align to them at all. The dispensable genome has a low density of genes and a high abundance of transposons. It has a high number of variants and undergoes rapid evolutionary changes. On the other hand, conservative chromosomes have a higher gene density, a lower density of repetitive regions and SNPs. Also, they contain a larger number of genes related to primary metabolism (Armitage et al., 2018; Yang et al., 2020).

The majority of well-studied *Fusarium oxysporum* genomes are characterized with 11 conservative chromosomes, with the number of dispensable chromosomes ranging between 1 and 8 (Kanapin et al., 2020; Wang et al., 2020; Samsonova et al., 2021). Remarkably, the dispensable chromosomes may dissipate with little consequence to the fungus's survival, but with a measurable detrimental effect on its virulence. Upon re-acquisition of such chromosomes, the virulence of the fungus is likely to increase (Ma et al., 2010). These dispensable chromosomes, also referred to as pathogenic-specific chromosomes, contain specific effector genes that are essential for the successive suppression of the host plant immunity (Armitage et al., 2018). The pathogenic-specific chromosomes were found in several special forms including ff. spp. *lycopersici*, *cepae*, *radicis-cucmerineum* and *fragariae* (van Dam et al., 2017; Li et al., 2020a; Henry et al., 2021; Sakane et al., 2023). Notably, the horizontal transfer of the whole chromosome or its part into a non-pathogenic strain Fo47 have been registered previously for ff. spp. *lycopersici* and *radicis-cucumerinum* (Ma et al., 2010; Vlaardingerbroek et al., 2016; van Dam et al., 2017; Li et al., 2020a, Li et al., 2020b). The resulting transformed strains can induce the same disease symptoms as the donor strains on the corresponding host plants. The *Folini* strain MI39 has 11 conservative and 4 dispensable chromosomes, among which chromosomes 12, 13 or 15 are potentially pathogenic-specific chromosomes due to the presence of *SIX* genes encoding specific effectors. However, a focused experiment is required to validate this fact (Kanapin et al., 2020; Samsonova et al., 2021).

The set of genes in the dispensable parts of the individual *Fusarium oxysporum* genomes varies significantly between ff. spp (Plissonneau et al., 2017; Jangir et al., 2021; Sabahi et al., 2021), clonal lineages and surprisingly also within a single f. sp (de Sain and Rep, 2015; van Dam et al., 2016), probably due to their polyphyletic origin (Zhang and Ma, 2017). Capturing the whole set of genes either of *Fusarium oxysporum* or a single f. sp. within *Fusarium oxysporum* is of paramount importance for understanding the mechanisms underlying genome evolution and plasticity, especially for addressing various questions regarding parasite's adaptation to the host plant, as key determinants of pathogenicity are often functionally redundant and are encoded by genes not shared among all lineages or ff. spp (van Dam et al., 2018; Guallar et al., 2022)

Pangenome research (Badet and Croll, 2020; Badet et al., 2020; Alouane et al., 2021), which refers to the characterization of the complete set of genes of a species or an infra-species taxa, is crucial for pinpointing the virulence factors of fungal isolates. We conducted an analysis of the pangenome of 13 *Folini* isolates that belong to 4 clonal lineages with varying virulence. Our study mainly focused on the functional diversity and content of the pansecretome, a collection of secreted proteins that are crucial for the fungus's pathogenicity. Notably, our findings indicate that strongly and moderately virulent strains have a different range of PFAM domains in non-core pansecretome groups.

Our research has revealed that all *Folini* strains have the same set of *SIX* genes, with the exception of two strains that had no *SIX* genes at all. This suggests that various fungal isolates possess different virulence factors to counteract plant defense mechanisms, and that while the presence of *SIX* genes is likely a contributing factor to strain virulence, it is not the only factor at play.

2 Material and methods

2.1 *Folini* strains virulence and VCG

The *Folini* strains under investigation were provided by the Federal Crop Research Institute, city of Torzhok, Tver' region, Russia. Their virulence was assessed under greenhouse conditions using reference cultivars (Tost 3, Tvertza, A-29) with contrasting susceptibility to Fusarium wilt. Mitcherlich vessels were filled with healthy soil by 2/3 of the height. Next, a pure fungal culture was introduced into each vessel (40 grams per vessel), covered with soil and abundantly watered. The seeds of a reference cultivar were sown on the fifth – sixth day after the inoculation.

The pure culture inoculum of a strain was prepared by growing it on the beer-wort agar-agar medium with subsequent incubation on the oat grain substrate (the grain-to-water ratio of 1 to 1.75). After three, maximum four, weeks' time, once the substrate had been completely colonized and the macro and microconidia had formed, the pathogen was introduced into the soil.

The severity of the disease in a reference cultivar was evaluated during harvest after the onset of the phase of early yellow ripeness. The DSS (Disease Severity Score) grades ranged from 0 to 3, where 0 stands for a healthy plant, 1 indicates a partial plant browning or stem browning from one side, 2 matches a fully browned plant with bolls, and, finally, 3 corresponds to a fully browned plant that collapses before the formation of bolls. Based on these grades the disease severity index (DSI) was calculated according to the formula generally accepted in the phytopathology field:

$$DSI = \frac{\sum ab}{AK}\ 100\%$$

where a - is the number of plants with the same DSS; b – is the estimated DSS; A is the total number of plants and K is the highest DSS grade (i.e., grade 3). A strain was considered strongly virulent, if DSI value exceeds 50%, moderately virulent, if the DSI value is in the range from 20% to 50%, and, finally, weakly virulent in those cases, where the DSI ≤ 20%. Three flax cultivars representing contrasted disease susceptibility groups, namely highly resistant A-29, moderately resistant Tvertza and the highly susceptible Tost3 were used to classify *Folini* strains into strong, moderate and weakly virulent groups.

Vegetative Compatibility groups are determined in accordance with the adapted method first introduced by Puhalla (Puhalla, 1985). The modifications are as follows: to recover nitrogen-nonutilizing (*nit*) mutants we used PDA supplemented with potassium chlorate (15 g/l) and sucrose (20 g/l) as a chlorate-containing medium.

2.2 Genome sequencing, assembly and analysis

Fusarium oxysporum strains F200, F365, F418 were grown in Chapek broth medium (30 g/l sucrose, 2 g/l sodium nitrate, 1 g/l potassium monohydrogen phosphate, 0.5 g/l magnesium sulfate, 0.5 g/l potassium chloride, 0.01 g/l ferrous sulfate). DNA was extracted with NucleoSpin Plant II (Macherey-Nagel, Germany) with the addition of RNAse A. DNA sequencing of the F418 genome was conducted at BGI (Hong Kong, China), with 100x coverage by PacBio RS II System and 30x coverage by Illumina HighSeq. Both the remaining 2 isolates i.e., F200 and F365 were sequenced with 30x coverage using Illumina HighSeq (paired-end reads, 150 bp). Hybrid assembly of the F418 genome was performed in three steps: (1) the initial assembly of PacBio contigs was performed with Canu package (v. 1.4) using the default settings (Koren et al., 2017); (2) further polishing and correction of the assembly was done with Pilon software (v. 1.23) (Walker et al., 2014) using sequencing reads generated by Illumina HighSeq; (3) the guided chromosome-level assembly was constructed with MI39 reference genome using RagTag program (version 2.1) (Alonge et al., 2022).

An assembly of genomes sequenced with short reads (Illumina) only includes two steps: contigs assembly with abyss-pe program from the ABYSS package (version 2.1.5) (Simpson et al., 2009), and reference-guided assembly using MI39 reference genome. To ensure the uniformity of data processing the genomes of previously published strains F329, F324, F282, and F287 (Kanapin et al., 2020) were reassembled with RagTag package (Alonge et al., 2022). Besides the genomes of the strains sequenced in (Dvorianinova et al., 2021) (i.e., F456, F476, F482, F483, F525) and newly sequenced strains F200 and F365 were constructed with abyss-pe and RagTag using MI39 as a reference. The quality of every genome assembly was assessed with the QUAST program (version 5.0.2) (Gurevich et al., 2013). Short reads of 12 *Folini* strains were aligned to the MI39 reference genome using bwa-mem (Li and Durbin, 2009) with default parameters.

To accomplish gene prediction and functional annotation of the proteins, we used BUSCO (v 4.0.4) (Seppey et al., 2019) with parameters "–augustus" and "-l hypocreales_odb10", respectively. Variant calling for the alignments was completed with NGSEP version 4.0 (Tello et al., 2022) Synteny analysis was done using Satsuma2 program (Grabherr et al., 2010).

Protein orthogroups were identified with silix software (version 1.3.0) (Miele et al., 2011), where the minimum percent of identity to accept blast hits for building families has been set to 0.8. The pangenome accumulation curves were plotted using R vegan package's specaccum function (Oksanen et al., 2018)

Candidate secreted proteins were identified in three steps. First, secretory signal peptides were predicted using signalP tool (version 5.0) (Nielsen et al., 2019). Then, the TMHMM (v2.0) program was used to keep proteins without a transmembrane domain or with a single transmembrane domain in the N-terminal signal peptide (Krogh et al., 2001). Lastly, PredGPI was applied to remove sequences containing GPI (glycosylphosphatidylinositol) anchors (Pierleoni et al., 2008). Subsequently, the secretomes were screened for CAZymes using a stand-alone version of DBCan2 suite (Zheng et al., 2023) and for effector genes using EffectorP software (version 3.0) (Sperschneider and Dodds, 2022). *SIX* genes were not accounted for in the BUSCO program's prediction, leading to their inclusion in the final count. Putative peptidases and peptidase inhibitors were predicted using the MEROPS database (Rawlings et al., 2017).

2.3 Phylogenetic analysis

For the purposes of phylogenetic analysis, EF-1α gene sequences were selected from 53 strains. These include 13 *Folini* genomes from this study, 20 strains of *Folini* available from the NCBI repositories, and 19 strains of different *F. oxysporum* ff. spp. and *F. solani, F. graminearum, F. verticelloides*, and *F. avenaceum* were used as an outgroup (Supplementary Table S1). First, the sequences were aligned with CLC Sequence Viewer tool (http://www.qiagenbioinformatics.com). Next, the maximum likelihood phylogeny tree was constructed with the Tamura-Nei model using 1000 bootstrap replicates, as implemented in the IQ-TREE tool (Minh et al., 2020).

A phylogenetic analysis of *SIX* genes was done using sequences from 13 *Folini* strains and other special forms of *F. oxysporum* (Supplementary Table S2). All the sequences were obtained from the NCBI database (https://www.ncbi.nlm.nih.gov/nucleotide/) and aligned with the aforementioned the CLC Sequence Viewer. Again, a consensus tree was built using IQ-TREE (Minh et al., 2020) with bootstrap support (1000 replicates). The following substitution models for each of the trees constructed were in use: *SIX1* -TNe+G4, *SIX7* - K2P+I, *SIX10* - K2P+G4, *SIX12* - K2P, *SIX13* - K2P.

The whole-genome SNP-based phylogeny (as identified in the 12 *Folini* genomes) was inferred by MEGAX software (version 10.1.8) (Tamura et al., 2021), where the MI39 genome served as a reference.

2.4 RNA isolation and differential gene expression analysis

Seedlings of the Fusarium wilt-resistant flax cultivar Atalante, as well as the seedlings of the susceptible cultivar LM98, were infected with the fungus strain MI39. RNA isolation from infected and uninfected plants was performed in three independent replicates on days 3 and 5 post-inoculation. Thus, RNA was obtained from 21 samples in total, where each sample includes material collected from three to five roots. Total RNA from infected roots was isolated using the RNeasy Mini Kit (QIAGEN, Germany). The isolated transcripts were sequenced on the DNBSEQ platform at the Beijing Genome Institute (BGI) (paired-end, 100 bp reads). The resulting data was filtered using SOAPnuke (Chen et al., 2017). To assess read abundance for reference transcriptomes of both flax (GCA_000224295.2) and *Folini* (MI39 strain) (Bray et al., 2016) the Kalisto tool (v.0.44.0) with bootstrap support for 100 samples and a k-mer length of 31 nucleotides was applied. Further downstream analysis was conducted using the sleuth package (version 0.30.1) (Pimentel et al., 2016). Transcripts characterized with low coverage values (i.e., 5 reads in either half or more than half of the samples undergoing the comparison) were filtered out and excluded from further consideration.

2.5 Analysis of the *SIX* genes

Fusarium cultures were grown in Chapek Broth medium for a week in a shaker incubator at 25°C and 100 rpm. Then mycelia were concentrated and rinsed twice in sterile water by centrifugation (3200 rpm) for as long as 15 min at 4°C. Next, the washed mycelia were collected, placed into mortars and dried in a thermostat at 32°C for 24 hours. The product was then powdered with sterile pestles. To extract DNA from the mycelial powder, we used DNeasy Plant Mini Kit (Qiagen) in accordance with the manufacturer's recommendations. DNA quality was assessed by Qubit 4.0 fluorimeter (Thermo Fisher Scientific) and electrophoresis in 1% agarose gel with subsequent visualization by GelDoc system (Bio-Rad). Finally, we ran PCRs with specific oligonucleotide primers (Supplementary Table S3) to evaluate expression levels of *SIX1 — SIX 14* genes in each strain. Likewise, PCR products were documented by electrophoresis in 1% agarose gel using the GelDoc system (Bio-Rad).

Nucleotide sequences of genes *SIX1, SIX7, SIX10, SIX12* and *SIX13* were extracted from Genbank. Homologous loci in *Folini* genomes were identified with the blast+ tool. The resulting homology regions were analyzed with the MIT GENSCAN web server (Burge and Karlin, 1998) and the FindORF tool from the NCBI web server. The predicted polypeptides were aligned to the homologous regions to visualize introns with CLC Sequence Viewer (QIAGEN Aarhus).

3 Results

3.1 *Folini* strains and genomes

Ten *Folini* strains were isolated from flax straw or from vegetative plants cultivated in the Tver region (Russia). In addition, two isolates, F200 and F456, came from the Netherlands and France correspondingly, while the F365 strain was obtained

10.3389/fpls.2024.1383914

from China (Table 1). Three flax cultivars distinguished by contrasting disease susceptibility, namely A-29 - highly resistant, Tvertza - moderately resistant and, finally, Tost 3 – the highly susceptible type, were used to estimate strain virulence under greenhouse conditions by calculating the Disease Severity Index (DSI) (Table 2), where the DSI is a normalized proportion of genotypes with identical disease symptoms (see Section 2.1). Thus, *Folini* strains F282, F287, F324, F329, F483 and MI39 were classified as strongly virulent, while strains F200, F365, F418, F456, and F482 belog to the weak virulence group. Finally, strains F476 and F525 developed a moderate response to infection.

The ability of the hyphae of two individual fungal isolates to fuse and form viable heterokaryons (i.e., vegetative compatibility) may be considered indirect evidence of genetic similarity (Kistler, 1997; Katan and Primo, 1999). Because of the above, we interrogated 11 *Folini* strains to determine Vegetative Compatibility (VCG) groups (Table 2). Of the four VCGs revealed, the largest of them, i.e., group "004416" contains seven strains, including MI39. The next group by size, the "004417", has three members, while groups "004415" and "004418" are represented by one strain each (F365 and F482, correspondingly).

The MI39 reference genome was constructed from PacBio long reads and was later polished and corrected using short sequencing reads generated by Illumina technology as described in (Kanapin et al., 2020). Out of the 29 scaffolds, 20 scaffolds of the resulting reference genome assembly have been identified as chromosomes based on their homology to the *Fusarium oxysporum* f. sp. *lycopersici* reference genome and the similarity of the genome assemblies of other *F. oxysporum* f. sp. *lini* isolates, as elaborated in (Kanapin et al., 2020). The provisional attribution of the *Folini* chromosomes into two genomic compartments has been facilitated by the syntenic analyses of the MI39 strain that were previously reported (Kanapin et al., 2020; Samsonova et al., 2021). Consequently, chromosomes 1 – 11 and 16 – 19 are assigned to the conservative part, whereas chromosomes 12 –15 and 20 are allocated to the variable compartment.

TABLE 2 Strain virulence and VCGs.

Strain	DSI, %			VCG
	Tost 3	Tvertza	A-29	
F282	69,9	27,8	12,3	004416
F287	66,6	19,5	16,7	004416
F324	69,9	24,2	15,4	004416
F329	72,7	29,9	8,0	004416
MI39	86,3	25,3	6,5	004416
F200	12,5	0	0	004416
F365	15,6	0	0	004415
F418	18,3	5,6	0	004417
F456	16,7	19,0	0,2	004417
F482	20,0	15,3	1,0	004418
F476	31,4	15,1	6,2	004417
F525	32,0	14,1	14,7	004416
F483	62.4	15,3	12,7	Not available

We used the MI39 genome as a reference to reassemble the genomes of 12 *Folini* strains sequenced by different methods (Table 1). The sizes of assembled genomes vary from 53.2 to 69.5 Mbp, with average GC content equal to 48.1%. The N50 value ranges from 28,09 to 173,71 kbp. Both numbers of predicted chromosomes and gene models are similar across thirteen *Folini* genomes, with the latter ranging from 14,087 to 14,395. The majority of the strain genomes are comprised of twenty

TABLE 1 *Folini* strain characteristics.

Strain	Origin	Virulence	Sequencing	Genome size (Mbp)	Chromosome number	Gene number
MI39	Torzhok distr.	strong	Illumina+PacBio	69,5	20	14 234
F200	the Netherlands	weak	Illumina	64,0	20	14 352
F282	Tver' distr.	strong	Illumina	64,2	20	14 207
F287	Tver' distr.	strong	Illumina	64,1	20	14 304
F324	Tver' distr.	strong	Illumina	65,7	20	14 300
F329	Tver' distr.	strong	Illumina	64,9	19	14 332
F365	China	weak	Illumina	57,1	20	14 395
F418	Tver' distr.	weak	Illumina+PacBio	64,9	20	14 200
F456	France	weak	Illumina+NanoPore	55,7	20	14 334
F476	Tver' distr.	moderate	Illumina+NanoPore	57,9	20	14 260
F482	Tver' distr.	weak	Illumina+NanoPore	53,2	20	14 466
F483	Tver' distr.	strong	Illumina+NanoPore	53,7	20	14 087
F525	Tver' distr.	moderate	Illumina+NanoPore	59,5	20	14 382

chromosomes, while F329 has nineteen of them in the predicted karyotype.

To gain insight into patterns of synteny and orthology across *Folini* isolates we compared MI39 and F418 strains as a) their genome sequences resulted from hybrid *de novo* genome assembly, and b) the isolates demonstrate contrasting pathogenic potential. Specifically, MI39 is a highly virulent strain, while F418 exhibit weak virulence. To analyze syntenic patterns, we ran GENESPACE (Lovell et al., 2022) software on MI39 and F418 genome assemblies. The conservative chromosomes of the above strains are similar in size, while the dispensable chromosomes of the MI39 isolate, namely, chromosomes 12–15, differ in length from their counterparts in F418 (Figures 1A, B). As expected, the conservative chromosome sets of MI39 and F418 strains demonstrate a high degree of similarity in gene order. Also, the conservation pattern did not change once *F. oxysporum* Fo47 endophytic strain was added to the analysis (Wang et al., 2020). However, we observed at least eight whole chromosome inversions in the Fo47 genome (Figure 1A).

The dispensable chromosomes of fungal pathogens are associated with virulence and host-specificity (Frantzeskakis et al., 2019; Torres et al., 2020). Syntenic analysis of dispensable chromosomes in MI39 and F418 isolates revealed chromosomes 15 and 14 as the most and least conserved ones, respectively. Chromosome 15 showed the highest level (64.3%) of similarity in gene order between the aforementioned strains. In contrast, chromosome 14 shares syntenic blocks with dispensable chromosomes 13, 14, and 15 and core chromosomes 1, 6, and 8. It is also longer in MI39 as compared to F418. (Figure 1B). Similarly, other accessory chromosomes of MI39 share syntenic blocks with core and non-homologous dispensable chromosomes of F418, as shown in Figures 1A, B.

We performed the phylogenetic analysis to resolve the relationships and estimate genetic distances between *Folini* strains. Two phylogenetic trees were constructed: (1) a maximum likelihood (ML) tree for EF-1α sequence data for a group of 50 isolates, including 13 *Folini* genomes from this study, 20 *Folini* isolates from NCBI database (https://www.ncbi.nlm.nih.gov/

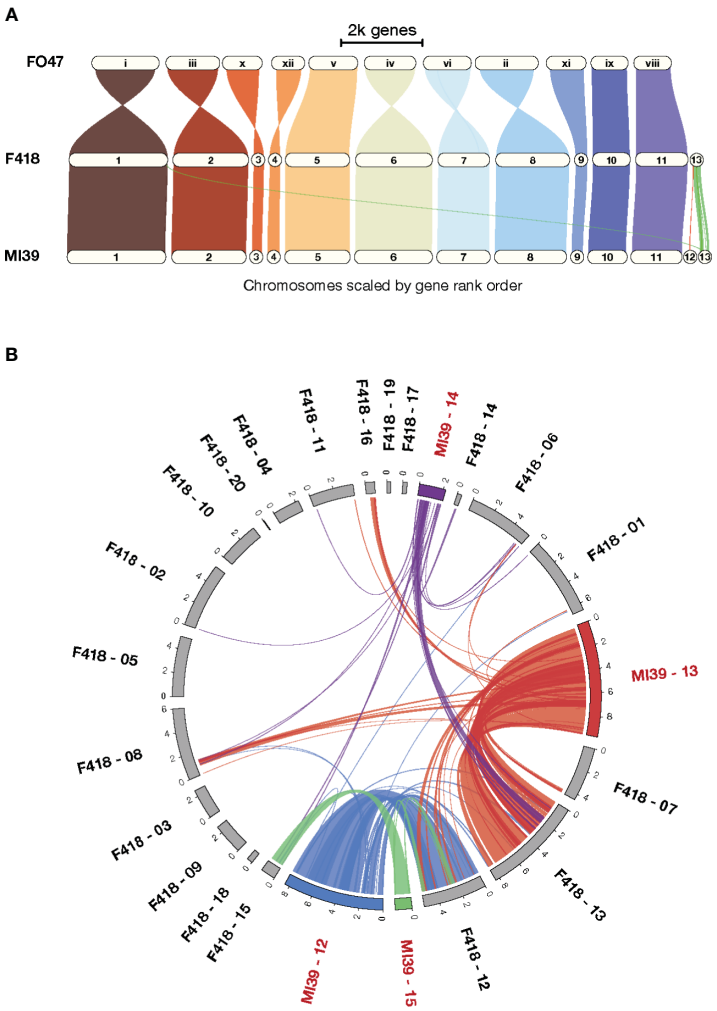

FIGURE 1
A comparison of the MI39 and F418 genome assemblies. **(A)** The GENESPACE syntenic map (i.e., riparian plot) of syntenic regions in the genome comparison of the *Folini* MI39 and F418 strains and Fo47 endophytic strain. **(B)** Circos plot (Krzywinski et al., 2009) presenting syntenic regions between MI39 and F418 dispensable chromosomes.

nucleotide/), and 26 different *F. oxysporum* ff. spp. isolates, while 4 other *Fusarium* species were used as an outgroup (Supplementary Table S1, Figure 2A), and (2) a neighbor-joining (NJ) cladogram based on a whole-genome SNP set for 12 *Folini* strains and MI39 genome as a reference (see Figure 2B). On both trees, most of the strains clustered into two distinct clades, while F482 appeared to form a separate branch. It is worth noting that the F365 isolate was in a separate branch on the NJ tree, but grouped together with other isolates obtained from flax and cotton plants on the ML tree, forming a clade.

3.2 *Folini* pangenome

To estimate the genomic diversity of *Folini* strains and gain insight into its gene repertoire, we constructed a pangenome by clustering 185,853 proteins identified in the 13 *Folini* genomes. We thus detected 17,731 non-redundant orthologous protein clusters (othogroups), of which 9388 (53%) are core orthogroups shared among all genomes (Figure 3A). Moreover, 4095 (23%) of all orthogroups are present in some but not all genomes (i.e., accessory orthogroups) and 24% of the orthogroups (4248) are

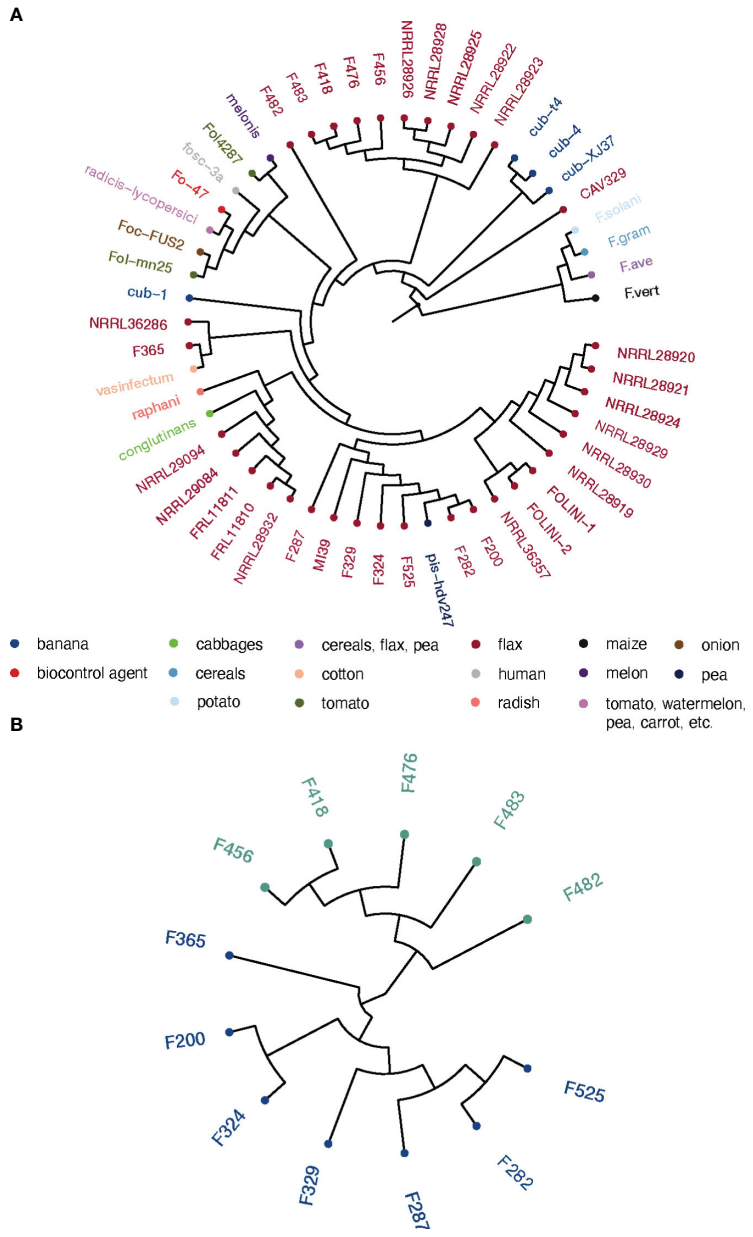

FIGURE 2
Phylogeny of *Folini* isolates. **(A)** The phylogeny of *F. oxysporum* isolates infecting flax and various other hosts as inferred with the maximum likelihood algorithm run on EF-1α gene sequences. **(B)** Neighbor-joining tree for 12 *Folini* genomes generated with whole-genome sets of SNPs as discovered in respective sequences.

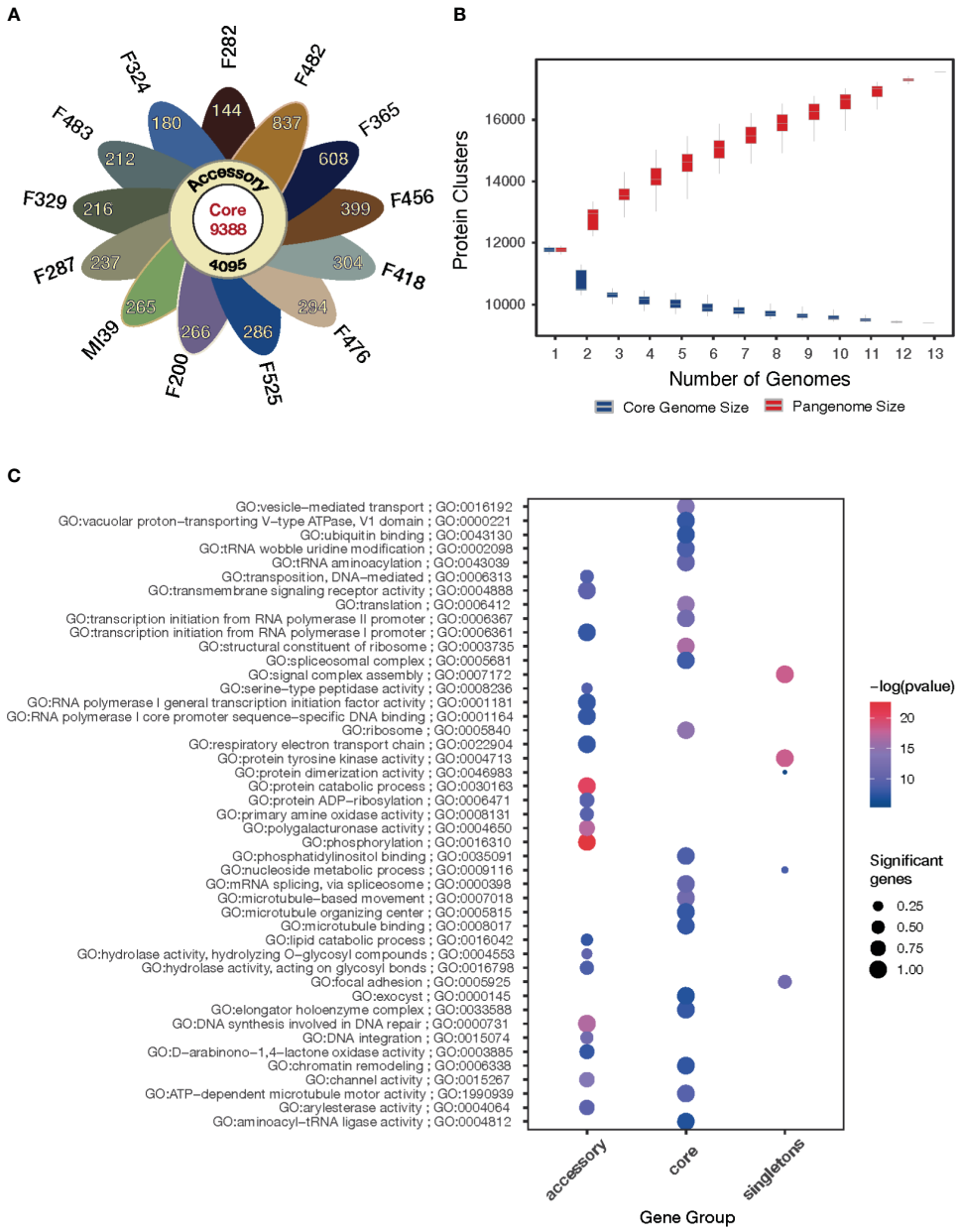

FIGURE 3
Pangenome of the *Folini* strains. **(A)** The flower plot shows the numbers of core proteins (center), accessory proteins (annulus) and singletons (petals) encoded by the genomes of the 13 *Folini* strains. **(B)** The *Folini* pangenome accumulation curves. **(C)** Functional annotation of core, accessory and singleton proteins.

singletons composed of genes found in one of the genomes only. Curiously, F482 and F365 strains have the highest proportion of singletons, 837 and 608 genes, respectively, while the lowest proportion of singletons (144 and 180 genes) is detected in F282 and F324 isolates, respectively. The rest of the strains contain comparable numbers of singletons in the interval sandwiched by 212 and 399 genes.

The gene accumulation curve (Figure 3B) demonstrates that the number of core genes continually decreases with the addition of new genomes. On the contrary, pangenome size, defined as a total number of non-redundant orthologous protein clusters, grows steadily with the iterative addition of new genomes, which eventually characterizes the *Folini* genome as open one.

The GO enrichment analysis (FDR< 0.001) of the core, accessory and singleton proteins encoded by the *Folini* pangenome reveals clear differences in their functions (Figure 3C). The core proteins are significantly enriched in terms associated with basic cellular and molecular functions, such as microtubule-based movement, ribosome, structural constituent of the ribosome, vesicle-mediated transport, spliceosomal complex, and chromatin remodeling. As expected, the accessory proteins demonstrate enrichment of GO categories linked to pathogenicity

10.3389/fpls.2024.1383914

and defense mechanisms (e.g. channel activity, D–arabinono–1,4 –lactone oxidase activity, hydrolase activity, phosphorylation, polygalacturonase activity, primary amine oxidase activity, protein ADP–ribosylation, serine-type peptidase activity, transmembrane signaling receptor activity), as well as to DNA transposition (e.g. DNA integration, DNA synthesis involved in DNA repair, transposition). Finally, singleton proteins are enriched in terms associated with pathogen recognition and immune signaling, such as cell adhesion, assembly of signal complexes, and protein tyrosine kinase activity.

3.3 Pansecretome and virulence

Fungus interaction with the plant immune system, as well as the digestion of plant cells to get nutrients, are accomplished by the secretion of specific proteins that make up an individual secretome (de Sain and Rep, 2015; Jashni et al., 2015; Berlemont, 2017; Kameshwar and Qin, 2018), which, incidentally, is roughly of the same size in different *Folini* strains. The pansecretome was assembled from 621 orthogroups of secreted proteins (3,5% of the *Folini* pangenome). The core and non-core orthogroups of secreted proteins comprise 40,3% and 59,7% of the pansecretome, i.e., 250 and 371 clusters, respectively. Among the non-core orthogroups, 229 clusters (36,9% of the pansecretome) are assigned to accessory orthogroups, while 142 orthogroups (22,6% of the pansecretome) are singletons.

The pansectretome primarily comprises three functional groups: CAZYmes, effector proteins, and proteases (see Table 3), where the non-core orthogroups dominate within each functional class (Figure 4A).

We classified CAZYmes into six groups according to their functions and analyzed their abundance and distribution among pansecretome categories (Figure 4B). The core genes dominate in the most abundant classes, which are glycosyl hydrolases (GH), auxiliary activities (AA) and carbohydrate esterases (CE).

The average number of effector proteins identified in individual *Folini* genomes is about 114 (Table 3). The *Folini* pansecretome contains 200 effector orthogroups. Of these, 88 are accessory, 40 belong to one isolate only and 72 are conserved between all strains (Figure 4C). The number of singletons agrees with the phylogenomic relationship between strains. For example, the F482 strain contains the maximum number of singletons (10 orthogroups), while the F365 strain and F456 isolate incorporate 7 and 5 singletons correspondingly. The number of singleton effectors in the remaining ten genomes ranges between 3 and 1.

The *Folini* genome has dual compartmentalization encompassing conserved and dispensable (i.e., lineage-specific) parts. Incidentally, the reference MI39 strain has 116 effector genes (Table 3; Supplementary Table S6), of which 63 and 53 genes belong to core and accessory pansecretome, respectively. F418, the second strain sequenced with LRS technology, has the same number of core effectors and 7 non-core effectors fewer than MI39. The majority of genes encoding these proteins are located on conserved chromosomes, while only 12 and 9 non-core effector genes map to dispensable chromosomes of MI39 and F418 correspondingly.

TABLE 3 A number of genes encoding secreted proteins, effectors, proteases and CAZYmes found in the individual *Folini* genomes.

Strain	Number of genes encoding			
	secreted proteins	effectors	proteases	CAZYmes
F200	368	110 + 7*	55	105
F282	350	109 + 7	47	99
F287	359	111 + 7	48	100
F324	372	112 + 7	48	103
F329	345	105 + 7	48	101
F365	356	112	46	94
MI39	340	108 + 8	47	93
F418	342	102 + 7	49	95
F456	346	109 + 7	50	94
F476	347	105 + 6	49	96
F482	367	109	51	112
F483	349	105 + 8	51	98
F525	371	113 + 6	50	102

*The number of *SIX* genes in a strain.

The expression level of predicted effectors in MI39 mycelia was assessed in both liquid culture and *in planta* by observing the infection progress in seedlings from resistant (Atalante) and susceptible (LM98) flax varieties over time. While all MI39 effectors were expressed, their levels varied. One-third of the effectors showed low expression in both mycelium and infected plants. The remaining effectors are divided into two categories: (1) those present in both the mycelium and the plant and (2) those only found in the plant (as shown in Supplementary Figure S1). The effector orthogroups' presence-absence heatmap in *Folini* strains indicates a clear separation between strongly and weakly virulent strains (Figure 4D). Notably, an orthogroup known as FOL004461, consists of eight proteins expressed only *in planta*. Of these proteins, five are present in MI39, as well as in other strongly virulent strains, while two proteins are found in weakly virulent strains, namely F365 and F200, and one is present in the medium virulent strain, F525. These proteins contain three specific PFAM domains: MANEC (PF07502), PAN_3 (PF08277), and PAN_4 (PF14295). PAN domains are ubiquitous in diverse proteins and are involved in protein-protein and protein-carbohydrate interactions (Tordai et al., 1999), while the MANEC domain may play a pivotal role in the formation of protein complexes that contain various protease activators and inhibitors (Guo et al., 2004).

We performed a genome-wide annotation of CAZYmes, effector proteins, and proteases using the PFAM database (Mistry et al., 2020). The results of hierarchical clustering of PFAM domain frequencies computed for strongly and moderately virulent *Folini* isolates in core, accessory and singleton categories highlight a remarkable difference in domain repertoire (Figure 4D; Supplementary Figure S2). It is noteworthy that certain PFAM domains are exclusive to specific virulence groups, with most of

10.3389/fpls.2024.1383914

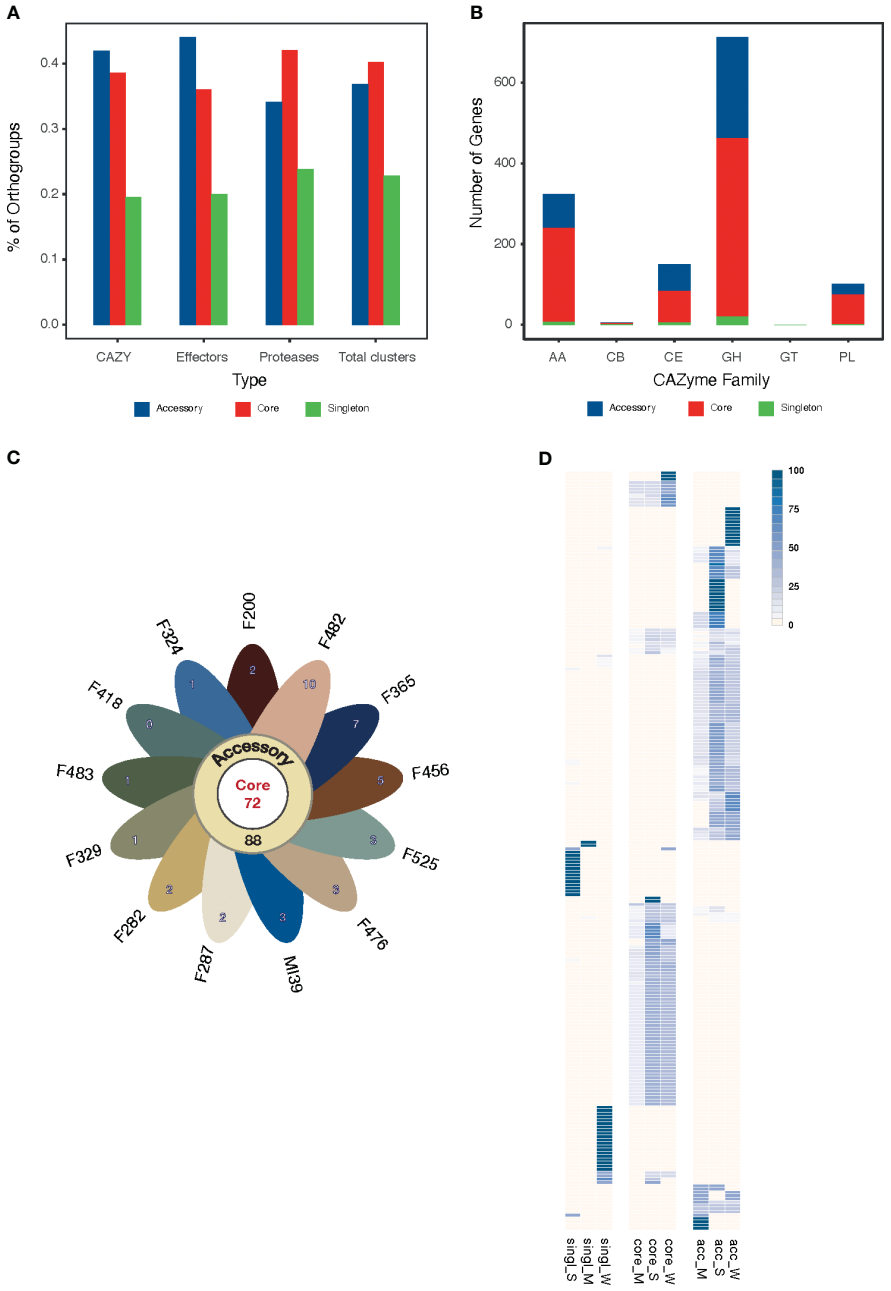

FIGURE 4
(A) The proportion of core, accessory and singleton orthogroups within the pansecretome functional classes. **(B)** Core, accessory and singleton protein numbers within the CAZYme functional classes: AA, auxiliary activities; GH, glycosyl hydrolases; CE, carbohydrate esterases; PL, polysaccharide lyases; GT, glycosyltransferases; CB, carbohydrate-binding modules. **(C)** Flower plot presenting the number of core (center), accessory (annulus) and singleton (petals) orthogroups in the effectome of the 13 *Folini* strains. **(D)** Heatmap of PFAM domain frequencies observed in core ("core") and non-core ("single" stands for singleton and "acc" stands for accessory) effectome and in strains with moderate (M) and strong (S) virulence. The intensity of the blue color is proportional to the PFAM domain frequency.

these domains being encoded by non-core genes. Among strongly virulent strains, the number of unique PFAMs found in CAZYmes and proteases is three times less than in weakly virulent strains (23 and 68 domains, respectively), as presented in Supplementary Table S4. This disparity can be attributed to the close genetic relationship of strongly virulent strains, as evident from most of them being grouped in one clade of the phylogenetic tree (Figure 2A). Despite the significant genetic similarity between strongly and weakly virulent strains, the number of unique PFAM domains found in effectors is similar for both, with 26 and 35, respectively (see Supplementary Table S5). The PFAM domains found in CAZYmes of strongly virulent strains are commonly found in transmembrane and extracellular proteins, as well as proteins participating in glycoside bond hydrolysis (PF01120, PF07477, PF03632, PF17851, etc.), carbohydrate synthesis (PF05691), and fatty acid metabolism (PF02737). Additionally, weakly virulent

strains also possess a functionally similar set of specific domains for CAZYmes, but with the added presence of domains characteristic of methyltransferases (e.g., PF08241, PF13489, PF13649) and host-pathogen recognition (PF13517). The functional diversity of PFAM domains found in effector proteins is particularly high (Supplementary Table S5), with strongly virulent strains possessing domains for proteins involved in signaling (PF07645, PF13923) and regulation of transcription (PF05086), while weakly virulent strains exhibit protein domains involved in tyrosine and phenylalanine biosynthesis (PF01817) and chromatin remodeling (PF09011).

3.4 *SIX* gene analysis

The pathogen's virulence is modulated by cysteine-rich small effector proteins called Secreted in Xylem (SIX) proteins (Rep et al., 2004; Houterman et al., 2009; Kashiwa et al., 2013; Schmidt et al., 2013; Ma et al., 2015; van Dam et al., 2017; Widinugraheni et al., 2018). SIX proteins were first discovered in xylem sap of tomato plants (Houterman et al., 2007; Schmidt et al., 2013). The coding of these proteins is attributed to *SIX* genes belonging to 14 gene families and located on pathogenic-specific chromosomes. Nonetheless, formae speciales have diverse SIX protein profiles and gene sequences (de Sain and Rep, 2015; Jangir et al., 2021). Thus, *SIX* genes can be utilized as markers for identifying pathogens.

Surprisingly, we could not find *SIX* genes in two weakly virulent strains (i.e., F365 and F482). Yet, the rest of the 11 *Folini* genomes considered in this study exhibit identical sets of the *SIX* gene families, namely *SIX1, SIX7, SIX10, SIX12* and *SIX13*, thus suggesting a conservation of the *SIX* gene repertoire (Table 4; Supplementary Figures S3, S7-S20).

The *SIX1* gene sequence is identical in all genomes except for F418 and F456. The Six1 protein in the F418 isolate has 12 amino acid substitutions, of which one, at position 238 (glutamate to glutamine), is also present in the Six1 protein of the F456 isolate. Also, there are two paralogs of the *SIX7* gene *(i.e., SIX7a* and *SIX7b)* on chromosomes 12 and 15, respectively (Table 4). Interestingly, all *Folini SIX*-containing strains have *SIX7a*, while the MI39 genome has three copies of this gene. We found *SIX7b* gene in genomes of the MI39, F418, F456, F476, F483 and F525 strains. The amino acid sequences of *SIX7a* and *SIX7b* are 82% identical. The *SIX10* gene is situated on chromosome 12 and includes one intron. It encodes two polypeptide variants, one with arginine and the other with glutamine at the C-terminus. Two paralogs of the *SIX12* gene, *SIX12a* and *SIX12b*, are present, with widely varying location and number of copies. Most *Folini* strains, M39, F282, F287, F324, F329 and F418 contain both paralogs. In all strains, except for F456 and F483, *SIX12a* maps to chromosome 12, while *SIX12b* is found on chromosome 13. In the F456 strain, two copies of *SIX12a* are located on chromosome 13, while in the F483, there are two *SIX12a* copies on chromosome 13 and only one copy on chromosome 12. In the F476 and the F525 strains, genes *SIX12b* and *SIX12a* are found on chromosomes 13 and 12, respectively (Table 4). The F200 strain has three copies of the *SIX12b* gene, all of which are located on chromosome 13. The Six12a and Six12b proteins are almost identical, differing only in two positions: 83 and 91. At these positions, Six12a has glutamate and lysine, while Six12b has lysine and asparagine, respectively. The *SIX13* gene has two introns and is always present as a single copy on chromosome 12 (as shown in Table 4). This gene is strongly conserved across strains.

We characterized the relative location of *SIX* genes in chromosome 12 using the genomes assembled with the LRS technology (M39 and F418 isolates, Figure 5A). The analyses revealed several gene clusters of similar architecture.

Recent results show that *SIX1* and *SIX13* gene families demonstrate host-related clustering, as revealed by phylogenetic analyses (Samsonova et al., 2021). Given these findings, we examined the remaining *SIX* genes to check if the aforementioned host-related grouping holds. The *SIX* gene dataset included members from different *F. oxysporum* ff. spp. alongside three other *Folini* isolates from Australia and Canada (Supplementary Table S3). The phylogeny analyses conducted on the *SIX7*, *SIX10* and *SIX12* genes demonstrate that the *Folini* isolates are separate from other ff. spp. (see Supplementary Figures S4, S5). The phylogeny of the *SIX7* (Supplementary Figure S4A) and *SIX12* (Supplementary Figure S5) gene families distinctly highlights the difference between *SIX7a* and *SIX7b*, as well as *SIX12a* and *SIX12b* sequence variants, since they occupy separate clades on the trees. We thus conclude that the *SIX7* and *SIX12* gene homologs are of polyphyletic origin. In contrast, as demonstrated in the respective phylogenetic tree, the origin of *SIX10* is monophyletic.

We used RNAseq technology to assess the expression levels of *SIX* genes during the 5-day infection process of flax plants. We conducted this evaluation on seedlings from both resistant (Atalante) and susceptible (LM98) varieties, as shown in Figure 5B. *SIX1* and *SIX13* exhibit higher expression levels than other *SIX* genes. *SIX13* expression in LM98 exhibits variable levels of activity over replicates. In contrast to the Atalante variety, in LM98, it is slightly lower and reaches high levels only by the fifth day. The remaining *SIX* genes (and their copies) are either expressed at low or moderate levels. Interestingly, the latter is detected in two copies of *SIX7a*, a copy of *SIX12* and *SIX10* on day five post-infection in the susceptible flax cultivar.

Thus the characterization of the *SIX* gene diversity in *Folini* strains revealed the conservation of their repertoire: most strains had the same set of *SIX* genes regardless of their virulence status. However two *Folin*i isolates lacked any of the *SIX* genes in spite of weak virulence.

3.5 Mating-type idiomorphs

It is widely accepted that *F. oxysporum* is a species that reproduces asexually (Gordon and Martyn, 1997). However, the fungus contains a conserved set of genes involved in sexual development and reproduction in other fungi, including mating-type idiomorphs (Yun et al., 2000). We found that twelve of thirteen *Folini* strains have *MAT1–2* idiomorph, while only the F365 strain is *MAT1–1* positive (Supplementary Figure S6). In all strains considered, the *MAT1–2* locus contains two genes oriented in

10.3389/fpls.2024.1383914

TABLE 4 *SIX* gene repertoires identified in each of the 13 *Folini* genomes.

Strain	Chromosome	*SIX1*	*SIX7*		*SIX10*	*SIX12*		*SIX13*
			a	b		a	b	
M39	12	+	+ (x3)	–	+	+	–	+
	13	–	–	–	–	–	+	–
	15	–	–	+	–	–	–	–
F200	12	+	+	–	+	–	–	+
	13	–	–	–	–	–	+ (x3)	–
F282, F287, F324, F329	12	+	+	–	+	+	–	+
	13	–	–	–	+	–	+	–
F365		–	–	–	–	–	–	–
F418	12	+	+	–	+	+	–	+
	13	–	–	–	–	–	+	–
	15	–	–	+	–	–	–	–
F456	12	+	+	–	+	_	–	–
	13	–	–	–	–	+ (x2)	–	–
	15	–	–	+	–	_	–	–
F476	12	+	+	–	+	–	–	+
	13	–	–	–	–	–	+	–
	15	–	–	+	–	–	–	–
F482		–	–	–	–	–	–	–
F483	12	+	+	–	+	+	–	+
	13	–	–	–	–	+ (x2)	–	–
	15	–	–	+	–	–	–	–
F525	12	+	+	–	+	+	–	+
	15	–	–	+	–	–	–	–

"+" and "-" indicate gene presence or absence, (xn) shows the number of copies.

opposite directions at its ends. The first gene is *MAT1–2-1*, highly conserved across Sordariomycetes. The second gene encodes a protein exhibiting a high level of homology with Mat1–2-3 protein from *F. avenaceum* and hence was identified as *MAT1–2-3* (Lysøe et al., 2014) The F482 strain has the truncated version of this gene, *MAT1–2-3m*, which lacks the whole third exon and part of the second intron. PCR analysis revealed that *MAT1–2-3* and *MAT1–2-3m* transcripts in liquid mycelial cultures of MI39 were of the expected gene length.

The F365 strain's *MAT1–1* locus conforms to the architecture characteristic of heterothallic Sordariomycetes (Supplementary Figure S6), apart from the fact that the *MAT1–1-3* gene lacks an intron.

4 Discussion

In this study, we created a pangenome for 13 isolates of *F. oxysporum* f. sp. *lini (Folini)* at the intra-species level. An average *Folini* genome contains 14,296 genes, contrary to our baseline assessment of the gene repertoire in the pangenome of 17,731 genes. The number of genes found in the genomes of all isolates considered in this study is even smaller – 9,388, which amounts to 54% of the pangenome gene repertoire. Recently, it has been shown that the pangenome of *F. graminearum* is made up of 20,807 non-redundant sequences from 20 isolates. Out of these, 11,560 genes (56%) are non-core genes. Also, the genome of an isolate varies between 12,729 and 13,316 predicted genes (Alouane et al., 2021). According to a study, the *Z. tritici* pangenome constructed with 19 genomes has about 15,474 orthogroups. However, only 60% of these orthogroups (around 9,193) are present in all studied isolates. Additionally, each genome has a gene count ranging between 11,657 and 12,787 (Badet et al., 2020). Despite having a larger number of individual genes, which is an average of 20,645, and a larger pangenome size of 34,639 genes (Fayyaz et al., 2023), the pangenome of 99 F. *oxysporum* f. sp. *ciceris* strains still contains a similar number of core genes as 10,435. Given these findings, the number of core genes in the *Folini* genome stands in the same range

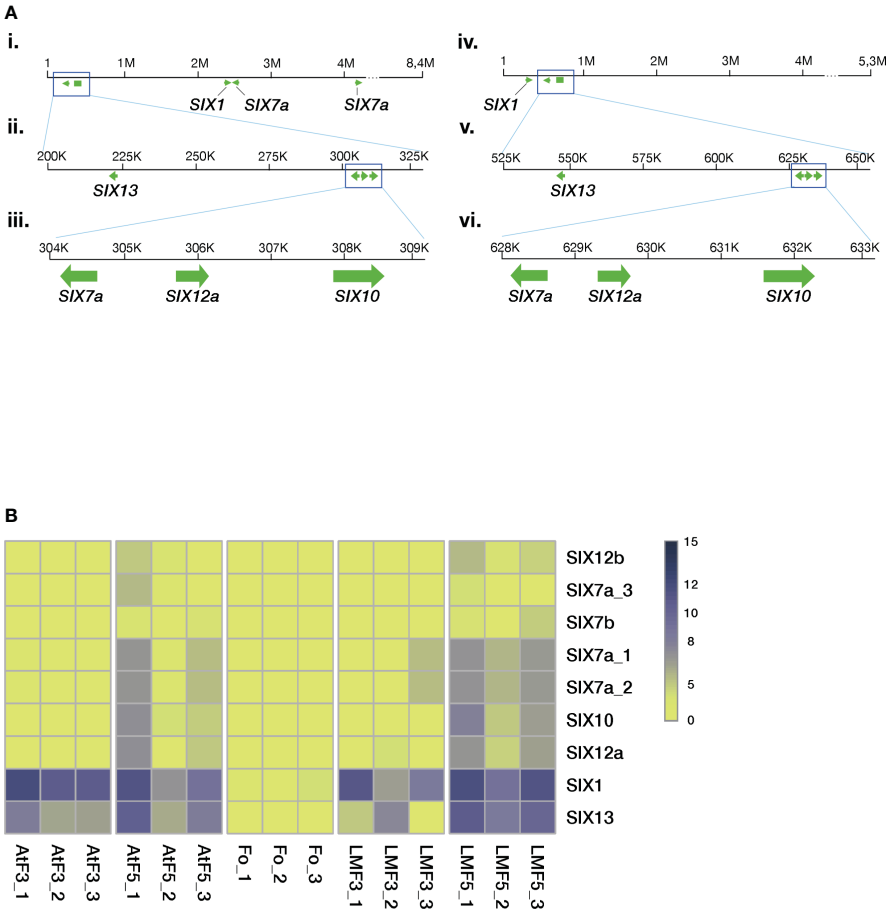

FIGURE 5
The *Folini SIX* genes. **(A)**. *SIX* gene mapping to chromosome 12 of MI39 (panels i, ii, iii) and F418 genomes (panels iv, v, vi) assembled with the long-read sequencing technology. Note the similarity of the *SIX7a-SIX12a-SIX10* gene cluster between the genomes and the positioning of the *SIX13* gene. **(B)** Heatmap presenting normalized *SIX* gene expression levels in different genomes, where *Fo* samples correspond to mycelia in liquid culture, AtF stands for Atalante flax cultivar (resistant to infection) on the third and the fifth day post-inoculation, and, finally, LMF shows LM98 flax variety (susceptible) on the third and the fifth day post-inoculation. All experiments were carried out in three biological replicates.

as in the genomes of *F. oxysporum* f. sp. *ciceris*, *F. graminearum* and *Z. tritici* (10,435, 9,388 and 9,193, respectively). Most notably, as the analyses of enriched GO terms clearly demonstrate (Alouane et al., 2021; Fayyaz et al., 2023), proteins attributed to the core part of the above pangenomes are associated with primary metabolism, which points to the conservation of essential gene repertoire in genomes of phytopathogenic mycelial fungi.

Our results demonstrate that the *Folini* pangenome is open and has not yet captured the overall diversity of the f. sp. At present, the *Folini* pangenome captures gene content from 4 clonal lineages. Yet, a survey of vegetative compatibility conducted on 74 isolates in wilt nurseries in western Canada identified 12 vegetative compatibility groups (Mpofu and Rashid, 2001), thus emphasizing the need for further research, including sequencing of new strains from different regions.

The *Folini* pangenome contains a relatively high proportion of accessory and singleton genes (46%), indicating the presence of considerable genomic diversity within individual isolates. This observation is further supported by the syntenic analyses of the genomes of MI39 and F418, which revealed significant genomic rearrangements in dispensable chromosomes, as shown in Figure 1B. The spectrum of enriched GO terms commonly associated with non-core *Folini* genes highlights their involvement in processes concerned with plant immunity and pathogenicity (Figure 3C). It is possible to hypothesize that the virulence potential and adaptation of individual strains to the environment is upheld by a high level of genetic variability that is intrinsic to them. It's worth noting that the conjecture is strongly supported by the fact that PFAM domains specific to virulence groups are predominantly encoded by non-core genes (as shown in Figure 4D; Supplementary Figure S2, Supplementary Table S4).

The genomes of filamentous plant pathogens are divided into two parts - conservative and dispensable, which creates a concept called the "two-speed genome" (Raffaele et al., 2010; Torres et al., 2020). This genome compartmentalization speeds up the evolution of genomic loci on variable chromosomes, which is crucial for virulence. It's worth noting that only a small percentage (0.2%) of

core genes are found in the dispensable part of both MI39 and F418 genomes. Meanwhile, the proportion of non-core genes located on these chromosomes is much larger (namely, 23.5% in MI39 and 15.5% in F418 - as shown in Supplementary Table S6). Despite this, most of the genes that encode the preponderate pansecretome classes - CAZYmes, effectors, and proteases are situated in the conservative part of both genomes and depending on the functional category, between 20 and 40 percent of these genes are non-core.

The fungus pansecretome is an indispensable player shaping host-pathogen interactions (de Sain and Rep, 2015; Jashni et al., 2015; Berlemont, 2017; Kameshwar and Qin, 2018). The *Folini* pansecretome amounts to 3.5% of pangenome and is almost exclusively made of CAZYmes, effector proteins and proteases (Table 3), which are distributed nonuniformly over core and non-core orthogroups. Glycosyl hydrolases (GH), auxiliary activities (AA), and carbohydrate esterases (CE) (Figure 4B) are abundant classes in CAZYmes. They are involved in cellulose, hemicelluloses, pectin and lignin degradation and are essential for successful invasion and pathogenesis (Berlemont, 2017; Kameshwar and Qin, 2018). Incidentally, the prevalence of the same functional classes over other types of enzymes was also found in ff. spp. infecting legumes (Roy et al., 2020)

To establish a stable infection, fungi secrete effector proteins that suppress the host's immune response or manipulate the host's cell physiology (Presti et al., 2015). Somewhat surprisingly, despite their crucial role in understanding the mechanisms driving fungal invasion, the majority of *Folini* effector proteins are still uncharacterized (Jangir et al., 2021). At present, 14 families of SIX proteins have been identified (Does et al., 2008; Schmidt et al., 2013). Most importantly, the repertoire of SIX proteins is diverse in different ff. spp (van Dam et al., 2016). A selected number of SIX proteins found in *F. oxysporum* ff. spp. *lycopersici*, *cubensis* and *conglutinans* were experimentally shown to enhance virulence and are, therefore, genuine effectors (Rep et al., 2004; Houterman et al., 2009; Kashiwa et al., 2013; Ma et al., 2015; Li et al., 2016; van Dam et al., 2017; Widinugraheni et al., 2018). An in-depth analysis of the *Folini SIX* genes revealed the conservation of their repertoire since all strains except two isolates contain an identical set of five gene families, namely, *SIX1, SIX7, SIX10, SIX12* and *SIX13* (Table 4; Supplementary Figure S3). Notably, multiple copies of *SIX7* and *SIX12*, along with paralogous genes, exist in various isolates. Furthermore, when infecting flax cultivars with the MI39 strain, we observed *in planta* expression for nearly all *SIX* genes (Figure 5B). Interestingly, the two mildly virulent strains, F365 and F482, lacked any of the *SIX* genes (Tables 2, 4). This implies that *SIX* genes are not always present in pathogenic *F. oxysporum* strains. Likewise, the absence of *SIX* genes was reported in two weakly virulent isolates of *F. oxysporum* f. sp. *cepae* (Taylor et al., 2016), in the genomes of endophytic isolates of *F. oxysporum* f. sp. *ciceris* (Fayyaz et al., 2023) and the *F. oxysporum* isolates obtained from the diseased pea plants collected from the fields in the UK (Jenkins et al., 2021). Also, a low frequency of *SIX* genes is observed in natural populations of *F. oxysporum* isolates sampled across the Australian continent (Rocha et al., 2016). It is possible that the absence of *SIX* genes in *Folini* strains is a result of their distinct origin. However, this seems unlikely as F365 belongs to the same clade as the NRRL36286 that infects flax and the *F. oxysporum* f. sp. *vasinfectum* isolate that infects cotton (as shown in Figure 2A). Also, no correlation between *SIX* gene presence and virulence was reported for endophytic isolates of *F. oxysporum* f. sp. *ciceris* (Fayyaz et al., 2023). Thus *F. oxysporum* isolates can be pathogenic in the absence of *SIX* genes, which puts a high priority on analyzing other effectors as potential virulence factors.

F. oxysporum is an exclusively asexual species, though it contains a conserved set of mating-type idiomorphs (Yun et al., 2000; Gordon, 2017). We found that 12 of 13 *Folini* strains have *MAT1–2* idiomorph, while F365 is the only *MAT1–1* positive one (Supplementary Figure S6). The predominance of *MAT1–2* idiomorph could be due to a geographic factor, as the majority of the strains come from the Tver region in Russia. In contrast to *F. oxysporum* ff. spp. *lycopersici* and *ciceris*, all *MAT1–2 Folini* strains contain additional gene *MAT1–2-3*. Conservation of *MAT* idiomorphs in *F. oxysporum* goes hand in hand with the conservation of other genes required for sexual reproduction (Yun et al., 2000; Zhang et al., 2020). In this context, the evolutionary stability of a functional sex pheromone synthesis and perception pathway is of particular interest (Turrà et al., 2015).

Our study focuses on the gene repertoire of *F. oxysporum* f. sp. *lini*, shedding new light on its genomic diversity. We discovered significant chromosomal rearrangements that are specific to individual genomes. Moreover, our study provides strong support for the hypothesis that *F. oxysporum* isolates utilize different virulence factors during crop infection, allowing them to evade plant defense mechanisms efficiently. Most importantly, our findings clearly demonstrate no relationship between the *SIX* gene content and virulence, which enhances our understanding of the role of *SIX* genes in pathogenicity. However, analysis of the core and accessory pan-genome gene repertoire of *Folini* indicates the open state of the genome and highlights the importance of further research that includes sequencing of new diverse strains from different regions. Charting the *Folini* pangenome blueprint and studying its diversity is an essential and imperative initial step towards uncovering the mechanisms that underlie plant-fungal interactions, and devising new strategies for controlling diseases.

Data availability statement

The datasets presented in this study can be found in online repositories. The names of the repository/repositories and accession number(s) can be found below: BioProject, PRJNA630722 and PRJNA721899.

Author contributions

AL: Investigation, Writing – original draft. AK: Conceptualization, Formal Analysis, Methodology, Validation, Writing – review & editing. TR: Funding acquisition, Resources, Writing – original draft. VS:

Validation, Writing – original draft. MB: Data curation, Writing – original draft. AS: Software, Visualization, Writing – review & editing. EO: Project administration, Writing – original draft. MS: Writing – review & editing, Supervision, Conceptualization, Methodology.

Funding

The author(s) declare that financial support was received for the research, authorship, and/or publication of this article. This research was funded by Russian Science Foundation, grant number 23–16-00037.

Acknowledgments

The authors would like to thank the St. Petersburg State Polytechnic University Centre for Supercomputing (scc.spbstu.ru) for providing excellent computational resources and support for this project. They would also like to express their thanks to the shared services center "The analytical center of nano- and biotechnologies of SPbPU" for the use of specialized lab equipment.

Conflict of interest

The authors declare that the research was conducted in the absence of any commercial or financial relationships that could be construed as a potential conflict of interest.

Publisher's note

Supplementary material

The Supplementary Material for this article can be found online at: https://www.frontiersin.org/articles/10.3389/fpls.2024.1383914/full#supplementary-material

References

Alonge, M., Lebeigle, L., Kirsche, M., Jenike, K., Ou, S., Aganezov, S., et al. (2022). Automated assembly scaffolding using RagTag elevates a new tomato system for high-throughput genome editing. *Genome Biol.* 23, 258. doi: 10.1186/s13059-022-02823-7

Alouane, T., Rimbert, H., Bormann, J., González-Montiel, G. A., Loesgen, S., Schäfer, W., et al. (2021). Comparative genomics of eight fusarium graminearum strains with contrasting aggressiveness reveals an expanded open pangenome and extended effector content signatures. *Int. J. Mol. Sci.* 22, 6257. doi: 10.3390/ijms22126257

Armitage, A. D., Taylor, A., Sobczyk, M. K., Baxter, L., Greenfield, B. P. J., Bates, H. J., et al. (2018). Characterisation of pathogen-specific regions and novel effector candidates in Fusarium oxysporum f. sp. cepae. *Sci. Rep-uk* 8, 13530. doi: 10.1038/s41598-018-30335-7

Ayukawa, Y., Komatsu, K., Taga, M., and Arie, T. (2018). Cytological karyotyping of Fusarium oxysporum by the germ tube burst method (GTBM). *J. Gen. Plant Pathol.* 84, 254–261. doi: 10.1007/s10327-018-0784-5

Baayen, R. P., O'Donnell, K., Bonants, P. J. M., Cigelnik, E., Kroon, L. P. N. M., Roebroeck, E. J. A., et al. (2000). Gene genealogies and AFLP analyses in the fusarium oxysporum complex identify monophyletic and nonmonophyletic formae speciales causing wilt and rot disease. *Phytopathology®* 90, 891–900. doi: 10.1094/PHYTO.2000.90.8.891

Badet, T., and Croll, D. (2020). The rise and fall of genes: origins and functions of plant pathogen pangenomes. *Curr. Opin. Plant Biol.* 56, 65–73. doi: 10.1016/j.pbi.2020.04.009

Badet, T., Oggenfuss, U., Abraham, L., McDonald, B. A., and Croll, D. (2020). A 19-isolate reference-quality global pangenome for the fungal wheat pathogen Zymoseptoria tritici. *BMC Biol.* 18, 12. doi: 10.1186/s12915-020-0744-3

Berlemont, R. (2017). Distribution and diversity of enzymes for polysaccharide degradation in fungi. *Sci. Rep.* 7, 222. doi: 10.1038/s41598–017-00258-w

Bray, N. L., Pimentel, H., Melsted, P., and Pachter, L. (2016). Near-optimal probabilistic RNA-seq quantification. *Nat. Biotechnol.* 34, 525–527. doi: 10.1038/nbt.3519

Burge, C. B., and Karlin, S. (1998). Finding the genes in genomic DNA. *Curr. Opin. Struct. Biol.* 8, 346–354. doi: 10.1016/S0959-440X(98)80069-9

Chen, Y., Chen, Y., Shi, C., Huang, Z., Zhang, Y., Li, S., et al. (2017). SOAPnuke: A MapReduce Acceleration supported Software for integrated Quality Control and Preprocessing of High-Throughput Sequencing Data. *Gigascience* 7, gix120. doi: 10.1093/gigascience/gix120

Dean, R., Van Kan, J. A., Pretorius, Z. A., Hammond-Kosack, K. E., Di Pietro, A., Spanu, P. D., et al. (2012). The Top 10 fungal pathogens in molecular plant pathology. *Mol. Plant Pathol.* 13, 414–430. doi: 10.1111/j.1364-3703.2011.00783.x

de Sain, M., and Rep, M. (2015). The role of pathogen-secreted proteins in fungal vascular wilt diseases. *Int. J. Mol. Sci.* 16, 23970–23993. doi: 10.3390/ijms161023970

Does, H. C. V. D., Lievens, B., Claes, L., Houterman, P. M., Cornelissen, B. J. C., and Rep, M. (2008). The presence of a virulence locus discriminates Fusarium oxysporum isolates causing tomato wilt from other isolates. *Environ. Microbiol.* 10, 1475–1485. doi: 10.1111/j.1462-2920.2007.01561.x

Dvorianinova, E. M., Pushkova, E. N., Novakovskiy, R. O., Povkhova, L. V., Bolsheva, N. L., Kudryavtseva, L. P., et al. (2021). Nanopore and Illumina Genome Sequencing of Fusarium oxysporum f. sp. lini Strains of Different Virulence. *Front. Genet.* 12. doi: 10.3389/fgene.2021.662928

Edel-Hermann, V., and Lecomte, C. (2019). Current status of fusarium oxysporum formae speciales and races. *Phytopathology* 109, 512–530. doi: 10.1094/PHYTO-08-18-0320-RVW

Fayyaz, A., Robinson, G., Chang, P. L., Bekele, D., Yimer, S., Carrasquilla-Garcia, N., et al. (2023). Hiding in plain sight: Genome-wide recombination and a dynamic accessory genome drive diversity in Fusarium oxysporum f.sp. ciceris. *Proc. Natl. Acad. Sci.* 120, e2220570120. doi: 10.1073/pnas.2220570120

Fokkens, L., Guo, L., Dora, S., Wang, B., Ye, K., Sánchez-Rodríguez, C., et al. (2020). A chromosome-scale genome assembly for the fusarium oxysporum strain fo5176 to establish a model arabidopsis-fungal pathosystem. *G3 Genes Genomes Genet.* 10, 3549–3555. doi: 10.1534/g3.120.401375

Frantzeskakis, L., Kusch, S., and Panstruga, R. (2019). The need for speed: compartmentalized genome evolution in filamentous phytopathogens. *Mol. Plant Pathol.* 20, 3–7. doi: 10.1111/mpp.12738

Gordon, T. R. (2017). Fusarium oxysporum and the fusarium wilt syndrome. *Annu. Rev. Phytopathol.* 55, 23–39. doi: 10.1146/annurev-phyto-080615-095919

Gordon, T. R., and Martyn, R. D. (1997). The evolutionary biology of Fusarium oxysporum. *Annu. Rev. Phytopathol.* 35, 111–128. doi: 10.1146/annurev.phyto.35.1.111

Grabherr, M. G., Russell, P., Meyer, M., Mauceli, E., Alföldi, J., Palma, F. D., et al. (2010). Genome-wide synteny through highly sensitive sequence alignment: Satsuma. *Bioinformatics* 26, 1145–1151. doi: 10.1093/bioinformatics/btq102

Guallar, M. A. B., Fokkens, L., Rep, M., Berke, L., and van Dam, P. (2022). Fusarium oxysporum effector clustering version 2: An updated pipeline to infer host range. *Front. Plant Sci.* 13. doi: 10.3389/fpls.2022.1012688

Guo, J., Chen, S., Huang, C., Chen, L., Studholme, D. J., Zhao, S., et al. (2004). MANSC: a seven-cysteine-containing domain present in animal membrane and extracellular proteins. *Trends Biochem. Sci.* 29, 172–174. doi: 10.1016/j.tibs.2004.02.007

Gurevich, A., Saveliev, V., Vyahhi, N., and Tesler, G. (2013). QUAST: quality assessment tool for genome assemblies. *Bioinformatics* 29, 1072–1075. doi: 10.1093/bioinformatics/btt086

Henry, P. M., Pincot, D. D. A., Jenner, B. N., Borrero, C., Aviles, M., Nam, M., et al. (2021). Horizontal chromosome transfer and independent evolution drive diversification in Fusarium oxysporum f. sp. fragariae. *N. Phytol.* 230, 327–340. doi: 10.1111/nph.17141

Houterman, P. M., Ma, L., Ooijen, G. V., Vroomen, M. J. D., Cornelissen, B. J. C., Takken, F. L. W., et al. (2009). The effector protein Avr2 of the xylem-colonizing fungus Fusarium oxysporum activates the tomato resistance protein I-2 intracellularly. *Plant J.* 58, 970–978. doi: 10.1111/j.1365-313X.2009.03838.x

Houterman, P. M., Speijer, D., L.Dekker, H., Koster, C. G., Cornelissen, B. J. C., and Rep, M. (2007). The mixed xylem sap proteome of Fusarium oxysporum-infected tomato plants. *Mol. Plant Pathol.* 8, 215–221. doi: 10.1111/j.1364-3703.2007.00384.x

Jangir, P., Mehra, N., Sharma, K., Singh, N., Rani, M., and Kapoor, R. (2021). Secreted in xylem genes: drivers of host adaptation in fusarium oxysporum. *Front. Plant Sci.* 12. doi: 10.3389/fpls.2021.628611

Jashni, M. K., Mehrabi, R., Collemare, J., Mesarich, C. H., and de Wit, P. J. G. M. (2015). The battle in the apoplast: further insights into the roles of proteases and their inhibitors in plant–pathogen interactions. *Front. Plant Sci.* 6. doi: 10.3389/fpls.2015.00584

Jenkins, S., Taylor, A., Jackson, A. C., Armitage, A. D., Bates, H. J., Mead, A., et al. (2021). Identification and Expression of Secreted In Xylem Pathogenicity Genes in Fusarium oxysporum f. sp. pisi. *Front. Microbiol.* 12. doi: 10.3389/fmicb.2021.593140

Kameshwar, A. K. S., and Qin, W. (2018). Comparative study of genome-wide plant biomass-degrading CAZymes in white rot, brown rot and soft rot fungi. *Mycology* 9, 93–105. doi: 10.1080/21501203.2017.1419296

Kanapin, A., Samsonova, A., Rozhmina, T., Bankin, M., Logachev, A., and Samsonova, M. (2020). The Genome Sequence of Five Highly Pathogenic Isolates of Fusarium oxysporum f. sp. lini. *Mol. Plant-Microbe Interact.* 33, 1112–1115. doi: 10.1094/MPMI-05-20-0130-SC

Kashiwa, T., Inami, K., Fujinaga, M., Ogiso, H., Yoshida, T., Teraoka, T., et al. (2013). An avirulence gene homologue in the tomato wilt fungus Fusarium oxysporum f. sp. lycopersici race 1 functions as a virulence gene in the cabbage yellows fungus F. oxysporum f. sp. conglutinans. *J. Gen. Plant Pathol.* 79, 412–421. doi: 10.1007/s10327-013-0471-5

Katan, T., and Primo, P. D. (1999). Current status of vegetative compatibility groups inFusarium oxysporum: Supplemen. *Phytoparasitica* 27, 273–277. doi: 10.1007/BF02981483

Kistler, H. C. (1997). Genetic diversity in the plant-pathogenic fungus fusarium oxysporum. *Phytopathology* 87, 474–479. doi: 10.1094/PHYTO.1997.87.4.474

Kommedahl, T., Christensen, J. J., and Frederiksen, R. A. (1970). *A half century of research in Minnesota on flax wilt caused by Fusarium oxysporum* (USA: Minnesota Agricultural Experiment Station. Retrieved from the University of Minnesota Digital Conservancy). Available at: https://hdl.handle.net/11299/108280.

Koren, S., Walenz, B. P., Berlin, K., Miller, J. R., Bergman, N. H., and Phillippy, A. M. (2017). Canu: scalable and accurate long-read assembly via adaptive k-mer weighting and repeat separation. *Genome Res.* 27, 722–736. doi: 10.1101/gr.215087.116

Krogh, A., Larsson, B., von Heijne, G., and Sonnhammer, E. L. L. (2001). Predicting transmembrane protein topology with a hidden markov model: application to complete genomes11Edited by F. Cohen. *J. Mol. Biol.* 305, 567–580. doi: 10.1006/jmbi.2000.4315

Krzywinski, M., Schein, J., Birol, İ., Connors, J., Gascoyne, R., Horsman, D., et al. (2009). Circos: An information aesthetic for comparative genomics. *Genome Res.* 19, 1639–1645. doi: 10.1101/gr.092759.109

Kumar, M., UK, T., Tomer, A., Kumar, P., and Singh, A. (2014). Screening of Linseed Germplasm for Resistance/Tolerance against Fusarium oxysporum F Sp. Lini (Bolley) Disease. *J. Plant Pathol. Microbiol.* 05. doi: 10.4172/2157–7471.1000235

Li, H., and Durbin, R. (2009). Fast and accurate short read alignment with Burrows–Wheeler transform. *Bioinformatics* 25, 1754–1760. doi: 10.1093/bioinformatics/btp324

Li, J., Fokkens, L., Conneely, L. J., and Rep, M. (2020a). Partial pathogenicity chromosomes in Fusarium oxysporum are sufficient to cause disease and can be horizontally transferred. *Environ. Microbiol.* 22, 4985–5004. doi: 10.1111/1462-2920.15095

Li, J., Fokkens, L., van Dam, P., and Rep, M. (2020b). Related mobile pathogenicity chromosomes in Fusarium oxysporum determine host range on cucurbits. *Mol. Plant Pathol.* 21, 761–776. doi: 10.1111/mpp.12927

Li, E., Wang, G., Xiao, J., Ling, J., Yang, Y., and Xie, B. (2016). A SIX1 Homolog in Fusarium oxysporum f. sp. conglutinans Is Required for Full Virulence on Cabbage. *PLoS One* 11, e0152273. doi: 10.1371/journal.pone.0152273

Lovell, J. T., Sreedasyam, A., Schranz, M. E., Wilson, M., Carlson, J. W., Harkess, A., et al. (2022). GENESPACE tracks regions of interest and gene copy number variation across multiple genomes. *eLife* 11, e78526. doi: 10.7554/eLife.78526.sa2

Lysøe, E., Harris, L. J., Walkowiak, S., Subramaniam, R., Divon, H. H., Riiser, E. S., et al. (2014). The genome of the generalist plant pathogen fusarium avenaceum is enriched with genes involved in redox, signaling and secondary metabolism. *PLoS One* 9, e112703. doi: 10.1371/journal.pone.0112703

Ma, L.-J., Does, H. C., Borkovich, K. A., Coleman, J. J., Daboussi, M.-J., Pietro, A. D., et al. (2010). Comparative genomics reveals mobile pathogenicity chromosomes in Fusarium. *Nature* 464, 367–373. doi: 10.1038/nature08850

Ma, L., Houterman, P. M., Gawehns, F., Cao, L., Sillo, F., Richter, H., et al. (2015). The AVR2–SIX5 gene pair is required to activate I-2-mediated immunity in tomato. *New Phytol.* 208, 507–518. doi: 10.1111/nph.13455

Miele, V., Penel, S., and Duret, L. (2011). Ultra-fast sequence clustering from similarity networks with SiLiX. *BMC Bioinform.* 12, 116. doi: 10.1186/1471-2105-12-116

Minh, B. Q., Schmidt, H. A., Chernomor, O., Schrempf, D., Woodhams, M. D., Haeseler, A., et al. (2020). IQ-TREE 2: New models and efficient methods for phylogenetic inference in the genomic era. *Mol. Biol. Evol.* 37, 1530–1534. doi: 10.1093/molbev/msaa015

Mistry, J., Chuguransky, S., Williams, L., Qureshi, M., Salazar, G. A., Sonnhammer, E. L. L., et al. (2020). Pfam: The protein families database in 2021. *Nucleic Acids Res.* 49, gkaa913. doi: 10.1093/nar/gkaa913

Mpofu, S. I., and Rashid, K. Y. (2001). Vegetative compatibility groups within Fusarium oxysporum f.sp. lini from Linum usitatissimum (flax) wilt nurseries in western Canada. *Can. J. Bot.* 79, 836–843. doi: 10.1139/b01–058

Nielsen, H., Tsirigos, K. D., Brunak, S., and von Heijne, G. (2019). A brief history of protein sorting prediction. *Protein J.* 38, 200–216. doi: 10.1007/s10930-019-09838-3

O'Donnell, K., Kistler, H. C., Cigelnik, E., and Ploetz, R. C. (1998). Multiple evolutionary origins of the fungus causing Panama disease of banana: Concordant evidence from nuclear and mitochondrial gene genealogies. *Proc. Natl. Acad. Sci.* 95, 2044–2049. doi: 10.1073/pnas.95.5.2044

Oksanen, J., Blanchet, F. G., Friendly, M., Kindt, R., Legendre, P., McGlinn, D., et al. (2018) *Vegan: community ecology package*. Available online at: https://github.com/vegandevs/vegan.

Pierleoni, A., Martelli, P. L., and Casadio, R. (2008). PredGPI: a GPI-anchor predictor. *BMC Bioinform.* 9, 392. doi: 10.1186/1471-2105-9-392

Pimentel, H., L., B. N., Puente, S., Melsted, P., and Pachter, L. (2016). Differential analysis of RNA-Seq incorporating quantification uncertainty. *bioRxiv*, 058164. doi: 10.1101/058164

Plissonneau, C., Benevenuto, J., Mohd-Assaad, N., Fouché, S., Hartmann, F. E., and Croll, D. (2017). Using population and comparative genomics to understand the genetic basis of effector-driven fungal pathogen evolution. *Front. Plant Sci.* 8. doi: 10.3389/fpls.2017.00119

Presti, L. L., Lanver, D., Schweizer, G., Tanaka, S., Liang, L., Tollot, M., et al. (2015). Fungal effectors and plant susceptibility. *Plant Biol.* 66, 513–545. doi: 10.1146/annurev-arplant-043014-114623

Puhalla, J. E. (1985). Classification of strains of Fusarium oxysporum on the basis of vegetative compatibility. *Can. J. Bot.* 63, 179–183. doi: 10.1139/b85-020

Raffaele, S., Farrer, R. A., Cano, L. M., Studholme, D. J., MacLean, D., Thines, M., et al. (2010). Genome evolution following host jumps in the irish potato famine pathogen lineage. *Science* 330, 1540–1543. doi: 10.1126/science.1193070

Rawlings, N. D., Barrett, A. J., Thomas, P. D., Huang, X., Bateman, A., and Finn, R. D. (2017). The MEROPS database of proteolytic enzymes, their substrates and inhibitors in 2017 and a comparison with peptidases in the PANTHER database. *Nucleic Acids Res.* 46, gkx1134. doi: 10.1093/nar/gkx1134

Rep, M., Does, H. C. V. D., Meijer, M., Wijk, R. V., Houterman, P. M., Dekker, H. L., et al. (2004). A small, cysteine-rich protein secreted by Fusarium oxysporum during colonization of xylem vessels is required for I-3-mediated resistance in tomato. *Mol. Microbiol.* 53, 1373–1383. doi: 10.1111/j.1365-2958.2004.04177.x

Rocha, L. O., Laurence, M. H., Ludowici, V. A., Puno, V. I., Lim, C. C., Tesoriero, L. A., et al. (2016). Putative effector genes detected in Fusarium oxysporum from natural ecosystems of Australia. *Plant Pathol.* 65, 914–929. doi: 10.1111/ppa.12472

Roy, A., Jayaprakash, A., Rajeswary, T. R., Annamalai, A., and Lakshmi, P. (2020). Genome-wide annotation, comparison and functional genomics of carbohydrate-active enzymes in legumes infecting Fusarium oxysporum formae speciales. *Mycology* 11, 56–70. doi: 10.1080/21501203.2019.1706656

Rozhmina, T., Samsonova, A., Kanapin, A., and Samsonova, M. (2022). An account resistance in flax of Fusarium wilt Linum usitatissimum: the disease severity data. *Data Brief* 41, 107869. doi: 10.1016/j.dib.2022.107869

Sabahi, F., Sain, M., Banihashemi, Z., and Rep, M. (2021). Comparative genomics of Fusarium oxysporum f. sp. melonis strains reveals nine lineages and a new sequence type of AvrFom2. *Environ. Microbiol.* 23, 2035–2053. doi: 10.1111/1462-2920.15339

Sakane, K., Akiyama, M., Jogaiah, S., Ito, S., and Sasaki, K. (2023). Pathogenicity chromosome of Fusarium oxysporum f. sp. cepae. *Fungal Genet. Biol.* 170, 103860. doi: 10.1016/j.fgb.2023.103860

Samsonova, A., Kanapin, A., Bankin, M., Logachev, A., Gretsova, M., Rozhmina, T., et al. (2021). A Genomic Blueprint of Flax Fungal Parasite Fusarium oxysporum f. sp. lini. *Int. J. Mol. Sci.* 22, 2665. doi: 10.3390/ijms22052665

Schmidt, S. M., Houterman, P. M., Schreiver, I., Ma, L., Amyotte, S., Chellappan, B., et al. (2013). MITEs in the promoters of effector genes allow prediction of novel virulence genes in Fusarium oxysporum. *BMC Genom.* 14, 119. doi: 10.1186/1471-2164-14-119

Seppey, M., Manni, M., and Zdobnov, E. M. (2019). Gene prediction, methods and protocols. *Methods Mol. Biol.* 1962, 227–245. doi: 10.1007/978–1-4939–9173-0_14

Simpson, J. T., Wong, K., Jackman, S. D., Schein, J. E., Jones, S. J. M., and Birol, İ. (2009). ABySS: A parallel assembler for short read sequence data. *Genome Res.* 19, 1117–1123. doi: 10.1101/gr.089532.108

Sperschneider, J., and Dodds, P. N. (2022). EffectorP 3.0: prediction of apoplastic and cytoplasmic effectors in fungi and oomycetes. *Mol. Plant-Microbe Interact.* 35, 146–156. doi: 10.1094/MPMI-08-21-0201-R

Sun, X., Fang, X., Wang, D., Jones, D. A., and Ma, L. (2022). Transcriptome Analysis of Fusarium–Tomato Interaction Based on an Updated Genome Annotation of Fusarium oxysporum f. sp. lycopersici Identifies Novel Effector Candidates That Suppress or Induce Cell Death in Nicotiana benthamiana. *J. Fungi* 8, 672. doi: 10.3390/jof8070672

Tamura, K., Stecher, G., and Kumar, S. (2021). MEGA11: molecular evolutionary genetics analysis version 11. *Mol. Biol. Evol.* 38, msab120. doi: 10.1093/molbev/msab120

Taylor, A., Vágány, V., Jackson, A. C., Harrison, R. J., Rainoni, A., and Clarkson, J. P. (2016). Identification of pathogenicity-related genes in Fusarium oxysporum f. sp. cepae: Pathogenicity in Fusarium oxysporum f. sp. cepae. *Mol. Plant Pathol.* 17, 1032–1047. doi: 10.1111/mpp.12346

Tello, D., Gonzalez-Garcia, L. N., Gomez, J., Zuluaga-Monares, J. C., Garcia, R., Angel, R., et al. (2022). NGSEP 4: efficient and accurate identification of orthogroups and whole-genome alignment. *bioRxiv*. doi: 10.1101/2022.01.27.478091

Tordai, H., Bányai, L., and Patthy, L. (1999). The PAN module: the N-terminal domains of plasminogen and hepatocyte growth factor are homologous with the apple domains of the prekallikrein family and with a novel domain found in numerous nematode proteins. *FEBS Lett.* 461, 63–67. doi: 10.1016/S0014-5793(99)01416-7

Torres, D. E., Oggenfuss, U., Croll, D., and Seidl, M. F. (2020). Genome evolution in fungal plant pathogens: looking beyond the two-speed genome model. *Fungal Biol. Rev.* 34, 136–143. doi: 10.1016/j.fbr.2020.07.001

Turrà, D., Ghalid, M. E., Rossi, F., and Pietro, A. D. (2015). Fungal pathogen uses sex pheromone receptor for chemotropic sensing of host plant signals. *Nature* 527, 521–524. doi: 10.1038/nature15516

van Dam, P., de Sain, M., Ter Horst, A., van der Gragt, M., and Rep, M. (2018). Use of comparative genomics-based markers for discrimination of host specificity in fusarium oxysporum. *Appl. Environ. Microb.* 84. doi: 10.1128/aem.01868–17

van Dam, P., Fokkens, L., Ayukawa, Y., van der Gragt, M., Ter Horst, A., Brankovics, B., et al. (2017). A mobile pathogenicity chromosome in Fusarium oxysporum for infection of multiple cucurbit species. *Sci. Rep.* 7, 9042. doi: 10.1038/s41598–017-07995-y

van Dam, P., Fokkens, L., Schmidt, S. M., Linmans, J. H. J., Kistler, H. C., Ma, L., et al. (2016). Effector profiles distinguish formae speciales of Fusarium oxysporum. *Environ. Microbiol.* 18, 4087–4102. doi: 10.1111/1462-2920.13445

Vlaardingerbroek, I., Beerens, B., Rose, L., Fokkens, L., Cornelissen, B. J. C., and Rep, M. (2016). Exchange of core chromosomes and horizontal transfer of lineage-specific chromosomes in Fusarium oxysporum. *Environ. Microbiol.* 18, 3702–3713. doi: 10.1111/1462-2920.13281

Walker, B. J., Abeel, T., Shea, T., Priest, M., Abouelliel, A., Sakthikumar, S., et al. (2014). Pilon: an integrated tool for comprehensive microbial variant detection and genome assembly improvement. *PLoS One* 9, e112963. doi: 10.1371/journal.pone.0112963

Wang, B., Yu, H., Jia, Y., Dong, Q., Steinberg, C., Alabouvette, C., et al. (2020). Chromosome-scale genome assembly of fusarium oxysporum strain fo47, a fungal endophyte and biocontrol agent. *Mol. Plant-Microbe Interact.* 33, 1108–1111. doi: 10.1094/MPMI-05-20-0116-A

Widinugraheni, S., Niño-Sánchez, J., van der Does, H. C., van Dam, P., García-Bastidas, F. A., Subandiyah, S., et al. (2018). A SIX1 homolog in Fusarium oxysporum f.sp. cubense tropical race 4 contributes to virulence towards Cavendish banana. *PLoS One* 13, e0205896. doi: 10.1371/journal.pone.0205896

Williams, A. H., Sharma, M., Thatcher, L. F., Azam, S., Hane, J. K., Sperschneider, J., et al. (2016). Comparative genomics and prediction of conditionally dispensable sequences in legume–infecting Fusarium oxysporum formae speciales facilitates identification of candidate effectors. *BMC Genomics* 17, 191. doi: 10.1186/s12864-016-2486-8

Yang, H., Yu, H., and Ma, L.-J. (2020). Accessory chromosomes in fusarium oxysporum. *Phytopathology®* 110, 1488–1496. doi: 10.1094/PHYTO-03-20-0069-IA

Yun, S.-H., Arie, T., Kaneko, I., Yoder, O. C., and Turgeon, B. G. (2000). Molecular organization of mating type loci in heterothallic, homothallic, and asexual gibberella/fusarium species. *Fungal Genet. Biol.* 31, 7–20. doi: 10.1006/fgbi.2000.1226

Zhang, Y., and Ma, L.-J. (2017). Deciphering pathogenicity of Fusarium oxysporum from a phylogenomics perspective. *Adv. Genet.* 100, 179–209. doi: 10.1016/bs.adgen.2017.09.010

Zhang, Y., Yang, H., Turra, D., Zhou, S., Ayhan, D. H., DeIulio, G. A., et al. (2020). The genome of opportunistic fungal pathogen Fusarium oxysporum carries a unique set of lineage-specific chromosomes. *Commun. Biol.* 3, 50. doi: 10.1038/s42003-020-0770-2

Zheng, J., Ge, Q., Yan, Y., Zhang, X., Huang, L., and Yin, Y. (2023). dbCAN3: automated carbohydrate-active enzyme and substrate annotation. *Nucleic Acids Res.* 51, W115–W121. doi: 10.1093/nar/gkad328

frontiers | Frontiers in Plant Science

TYPE Original Research
PUBLISHED 06 August 2024
DOI 10.3389/fpls.2024.1444195

OPEN ACCESS

EDITED BY
Franco Nigro,
University of Bari Aldo Moro, Italy

REVIEWED BY
Samia Gargouri,
Institut National de la Recherche Agronomique de Tunisie (INRAT), Tunisia
Filippo De Curtis,
University of Molise, Italy

*CORRESPONDENCE
Mahyar Mirmajlessi
mahyar.mirmajlessi@ugent.be

RECEIVED 05 June 2024
ACCEPTED 19 July 2024
PUBLISHED 06 August 2024

CITATION
Mirmajlessi M, Najdabbasi N, Sigillo L and Haesaert G (2024) An implementation framework for evaluating the biocidal potential of essential oils in controlling *Fusarium* wilt in spinach: from *in vitro* to *in planta*. *Front. Plant Sci.* 15:1444195. doi: 10.3389/fpls.2024.1444195

An implementation framework for evaluating the biocidal potential of essential oils in controlling *Fusarium* wilt in spinach: from *in vitro* to *in planta*

Mahyar Mirmajlessi[1]*, Neda Najdabbasi[1], Loredana Sigillo[2] and Geert Haesaert[1]

[1]Department of Plants and Crops, Ghent University, Faculty of Bioscience Engineering, Ghent, Belgium, [2]Council for Agricultural Research and Economics (CREA), Research Centre for Vegetable and Ornamental Crops, Pontecagnano, Italy

Fusarium wilt, caused by *Fusarium oxysporum* f. sp. *spinaciae*, causes a significant challenge on vegetative spinach and seed production. Addressing this issue necessitates continuous research focused on innovative treatments and protocols through comprehensive bioassays. Recent studies have highlighted the potential of plant-based compounds in controlling fungal diseases. The present work aims to conduct a series of experiments, encompassing both *in vitro* and *in planta* assessments, to investigate the biocontrol capabilities of different essential oils (EOs) at various application rates, with the ultimate goal of reducing the incidence of *Fusarium* wilt in spinach. The inhibitory effect of four plant EOs (marjoram, thyme, oregano, and tea tree) was initially assessed on the spore germination of five unknown *Fusarium* strains. The outcomes revealed diverse sensitivities of *Fusarium* strains to EOs, with thyme exhibiting the broadest inhibition, followed by oregano at the highest concentration (6.66 µL/mL) in most strains. The tested compounds displayed a diverse range of median effective dose (ED50) values (0.69 to 7.53 µL/mL), with thyme and oregano consistently showing lower ED50 values. The direct and indirect inhibitory impact of these compounds on *Fusarium* mycelial growth ranged from ~14% to ~100%, wherein thyme and oregano consistently exhibiting the highest effectiveness. Following the results of five distinct inoculation approaches and molecular identification, the highly pathogenic strain F-17536 (*F. oxysporum* f.sp. *spinaciae*) was chosen for *Fusarium* wilt assessment in spinach seedlings, employing two promising EO candidates through seed and soil treatments. Our findings indicate that colonized grain (CG) proved to be a convenient and optimal inoculation method for consistent *Fusarium* wilt assessment under greenhouse conditions. Seed treatments with thyme and oregano EOs consistently resulted in significantly better disease reduction rates, approximately 54% and 36% respectively, compared to soil treatments ($P > 0.05$). Notably, thyme, applied at 6.66 µL/mL, exhibited a favorable emergence rate (ERI), exceeding seven, in both treatments,

emphasizing its potential for effective disease control in spinach seedlings without inducing phytotoxic effects. This study successfully transitions from *in vitro* to *in planta* experiments, highlighting the potential incorporation of EOs into integrated disease management for *Fusarium* wilt in spinach production.

KEYWORDS

anti-fungal activity, disease management, *Fusarium oxysporum* f.sp. *spinaciae*, fusarium wilt, plant-based compounds

Introduction

Fungal diseases caused by *Fusarium* species cause significant economic threats, contributing to a wide range of plant diseases such as damping off, root rot, stem rot, leaf spots, crown rot, and vascular wilts, thereby posing challenges to crops cultivation worldwide. Furthermore, the secondary metabolites produced by the genus *Fusarium*, known as mycotoxins, exhibit a broad range of toxic effects, leading to both acute and chronic diseases in animals and humans (Antonissen et al., 2014). Over 50 species of *Fusarium* have been identified, encompassing both plant and animal pathogens, but only a few of these species are known to cause infections in humans (Nucci and Anaissie, 2007). Spinach (*Spinacia oleracea* L.) is prone to various diseases, leading to reduced production worldwide. Amongst them, *Fusarium* wilt, caused by the fungus *Fusarium oxysporum* f. sp. *spinaciae*, is recognized as the most prevalent and severe disease of spinach. It leads to symptoms ranging from seed decay, wilting, stunted growth, and discoloration of the vascular system to damping-off and plant death, in both young seedlings and fully grown plants (Mowlick et al., 2013; Ekwomadu and Mwanza, 2023). This disease is also a concern in spinach seed production because the pathogen is readily seedborne and can spread through soil, enabling its survival for very long periods even in the absence of host plants (Larena et al., 2003; Sharma et al., 2017). Additionally, the long-lasting chlamydospores, which can persist for over 10 years, pose a significant challenge in controlling *Fusarium* wilt disease (Egel and Martyn, 2007; Bahadur, 2022). Despite the development of various control strategies, their effectiveness in controlling *Fusarium* diseases has been insufficient. Specifically, the use of synthetic fungicides to fight *Fusarium* wilt has been discouraged as they can harm soil health and potentially affect humans and other non-target organisms in the environment (De Cal et al., 2009; Sharma et al., 2017). Hence, exploring potent bioactive compounds for controlling *Fusarium* diseases directly or in combination with other strategies has become the new emphasis.

Plant-derived bioactive compounds are highlighted for their environmental safety, as they are biodegradable and exhibit minimal to no toxicity towards mammals and non-target organisms (Linde et al., 2010; Kumar et al., 2014; Sharma et al., 2017; Moungthipmalai et al., 2023). Essential oils (EOs), derived from organic sources, offer a range of benefits such as low residue levels, broad-range antimicrobial effectiveness and diverse mechanisms of action, making them promising eco-friendly green preservative agents and alternatives to synthetic fungicides (Han et al., 2019; Najdabbasi et al., 2020; Prakash et al., 2024). They possess remarkable permeability and high volatility, and are composed of a diverse array of secondary metabolites obtained from aromatic plants. Indeed, aromatic plants are abundant sources of bioactive compounds, including tannins, sterols, carvacrol, flavonoids, phenols, alkaloids, quinones, and saponins (Khan et al., 2015; Han et al., 2019). These compounds have demonstrated strong antifungal impacts by affecting cell wall/membrane, inhibiting quorum sensing, altering hyphal morphology, preventing biofilm formation, and suppressing mycotoxin synthesis/production (Chen et al., 2013; Sardi et al., 2014; Haque et al., 2016; Najdabbasi et al., 2020; Abdi-Moghadam et al., 2023). EOs may exert their effects through the active components, either directly influencing the pathogen or inducing systemic resistance in host plants, ultimately leading to a reduction in disease development. Previous studies have reported the antifungal activity of different EOs against various phytopathogens, such as *Didymella bryoniae, Colletotrichum lupini, C. lindemuthianum, Penicillium digitatum*, *Botrytis cinerea, Pleiochaeta setosa, Rhizoctonia solani, Sclerotinia sclerotiorum, Pythium ultimum* and *Fusarium* spp (Fiori et al., 2000; Soylu et al., 2007; Sharma et al., 2017; Dewitte et al., 2018; Bounar et al., 2020; Najdabbasi et al., 2020; Khaleil et al., 2021; Parikh et al., 2021). Many EOs and their major components are classified as "generally recognized as safe" (GRAS) by regulatory authorities such as the Food and Drug Administration (FDA) and the Environmental Protection Agency (EPA), underlining their safety and highlighting their potential effectiveness in combatting fungal pathogens (Tolouee et al., 2010; Lu et al., 2013). Besides extensive research on various target pathogens, the potential of EOs to be used in combination with other EOs or biocontrol agents (Abdel-Kader et al., 2011; Tejeswini et al., 2014; Pane et al., 2017; Zimmermann et al., 2023) makes them promising for controlling *Fusarium* diseases. In addition, given the modest biological activity of individual components and the synergistic or antagonistic interactions among them, it is important to consider the entire

EO for disease management rather than isolating and synthesizing individual components (Bi et al., 2012; Stevic et al., 2014; Nazzaro et al., 2017; Perczak et al., 2019). Despite these, the existing literature on the utilization of EOs for controlling *Fusarium* wilt in spinach is currently limited. Similarly, there is less information available on the efficiency of artificial inoculation methods for pathogenicity assessment of *Fusarium oxysporum* f. sp. *spinaciae*, thereby establishing an optimal inoculation technique is crucial in evaluating the effectiveness of biological control strategies.

Consequently, the objectives of this study were i) to assess the potential of pure EOs as a safe and environmentally-friendly alternative to synthetic chemicals. This encompassed a series of *in vitro* bioassays that examined the fungitoxicity of EOs on spore germination and mycelial growth of *Fusarium* strains; ii) to compare various pathogenicity tests and determine the optimal inoculation method for assessing disease severity of *Fusarium oxysporum* f. sp. *spinaciae* on spinach; and iii) to investigate the efficacy of chosen EOs in reducing *Fusarium* wilt of spinach through *in planta* bioassays.

Materials and methods

Fungal isolates, inoculum preparation and plant EOs

A total of 11 unknown *Fusarium* strains were isolated from various host plants and diverse geographical locations. Among these, eight were obtained from Enza Zaden (Vegetable-Breeding Company) in the Netherlands, and three from the Research Centre for Vegetable and Ornamental Crops (CREA) in Italy. However, only five strains out of the total of eleven were randomly selected for use in the *in vitro* experiments, with selection criteria based on their respective host plants and geographical origins. To prepare spore suspensions, each isolate was sub-cultured onto a Potato Dextrose Agar (PDA, 39 gr/L) (Sigma Aldrich, Overijse, Belgium) plate and incubated at 25°C in darkness for 5 days. The mature mycelium was then transferred to fresh PDA plates and subjected to near-ultraviolet (NUV) light and dark cycles, following a 12-hour photoperiod, for 10 days to induce sporulation (International Seed quality Assurance (ISTA) (2023). Afterward, the mycelial surface was gently rubbed with 10 mL of sterile distilled water (SDW), and the resulting mixture was filtered through a sterilized Mira-cloth layer (Merck, Darmstadt, Germany). The spore suspensions were quantified using a hemocytometer and diluted to a concentration of 5×10^5 conidia/mL. Five commercially pure pharmaceutical grade EOs (Omega Pharma, Phytosun aroms, France) including tea tree (*Melaleuca alternifoliai*), thyme (*Thymus vulgaris*), oregano (*Origanum vulgare*) and marjoram (*Origanum majorana*) were examined for their antifungal activity against *Fusarium* strains. The EOs were stored at low temperature (4°C) and kept protected from light and humidity for future use. To obtain suitable preparations, the aforementioned EOs were dissolved in SDW at the following concentrations: 0.83, 1.66, 3.33, and 6.66 µL/mL, with 0.1% Tween 80 (Sigma-Aldrich) added.

Inhibitory effects of EOs on spore germination

Agar well diffusion method

For the initial screening, the standard well diffusion assay was employed by incorporating each EO into molten PDA (at approximately 50°C) to assess their antifungal activity against five *Fusarium* strains. For each strain, spore suspension (5×10^5 conidia/mL) was dispensed onto the surface of solidified PDA plate. Following a drying period of approximately 5 minutes, two wells with a diameter of 6 mm were created on each agar plate (90 mm) using a sterile cork-borer. These wells were then filled with 100 µL of EOs at different concentrations (0.83, 1.66, 3.33, and 6.66 µL/mL). Subsequently, the culture plates were incubated at 25°C for 10 days, and screened for the presence of a zone of inhibition, also known as the zone of clearance. The effectiveness of the tested EOs activity was obtained based on diameter of zone of inhibition (with 6 mm of the well) around the well.

Microtiter plate method

The inhibitory effect of EOs at various concentrations on the spore germination of *Fusarium* species was assessed using a 96-well microtiter plate assay, based on photometric measurements, following a previously described method (Najdabbasi et al., 2020). In each well of the microtiter plate, a mixture of 20 µL of the respective compound's concentrations, 180 µL of potato dextrose broth (Potato dextrose broth, 24 g/L) (Sigma Aldrich, Overijse, Belgium), and 20 µL of spore suspension (5×10^5 conidia/mL) was added. The negative control wells in each replicate block contained 20 µL of water instead of the spore suspension. After 8 days of incubation, spore germination in each plate was quantified using a microplate photometer (Asys UVM 330 Plate Reader) to measure the optical density at 620 nm (OD 620). Consequently, the median effective dose (ED50) was derived from the net OD, representing the point at which spore germination was reduced by 50% compared to the control.

Inhibitory effects of EOs on mycelial growth

Agar dilution method

The mycelial growth of *Fusarium* strains was evaluated through a dose-response assay using petri plates containing PDA media supplemented with different concentrations of the EOs. Mycelial plugs (6 mm) of fungal isolates were taken from the actively growing edges of the cultures and transferred to the center of each pre-amended PDA petri plate. The control comprised PDA without any EO. Following incubation in darkness at 25°C, the average radial growth was determined by measuring the diameters of the colonies in two perpendicular directions using a digital caliper (Solna, Sweden) every two days, until the mycelia fully covered the medium in the control petri plate. Consequently, the inhibitory percentage of different concentrations of EOs was calculated using Abbott's formula (Abbott, 1925):

$$MI\ (\%) = \frac{C - T}{C}\ X\ 100$$

wherein, MI represents the percentage of mycelial growth inhibition, and C and T refer to the diameter of the fungus colony (mm) in the control and the relevant treatment, respectively. Furthermore, the minimum inhibitory concentration (MIC) and the minimum fungicidal concentration (MFC) of each EO were determined by sub-culturing the inhibited fungal plugs from the EO-treated plates to newly prepared PDA plates without EO (Najdabbasi et al., 2020). After incubation for an additional seven days at 25°C, the lowest EO concentration that inhibited mycelial growth but allowed growth revival upon transfer was identified as the MIC. Conversely, the lowest EO concentration that prevented mycelial growth after transfer to fresh EO-free PDA plates was recognized as the MFC.

Volatile method

The impact of the volatile compounds from the same EOs on the mycelial growth of *Fusarium* strains was also evaluated at different concentrations, according to a previously reported method (Parikh et al., 2021). Briefly, a mycelial plug (6 mm) obtained from a 10-day-old culture grown on PDA was transferred to the center of a new PDA plate. A volume of 10 µl of the EOs was applied to the inner side of the inverted lid of the fresh PDA plate, and then the plate containing the mycelial plug was inverted and placed onto the lid. The control plates were left untreated without any addition of EO. To prevent any leakage of the active components, the petri plates were tightly sealed with parafilm. The percentage of mycelial growth inhibition was determined for each treatment by measuring the colony diameter of each pathogen 10 days after inoculation, as previously described. Furthermore, the fungal plugs from treatments showing no fungal growth were transferred to untreated PDA culture medium and placed in an incubator at 25°C for an additional week for further evaluation to ascertain fungistatic or fungicidal activity of each EO, as described earlier. The *in vitro* bioassays were conducted twice, and each treatment was subjected to six replications. Following the evaluation of results obtained from *in vitro* bioassays, the EO that exhibited the most effective antifungal activity against *Fusarium* strains at its applied concentrations was chosen for subsequent investigation in *in vivo* bioassays.

Molecular identification

The subsequent molecular analysis aimed to confirm the identity of *Fusarium* strains, which was critical for designing the subsequent *in planta* experiments targeting disease control. The identification process was carried out for all 11 unidentified strains. Total genomic DNA was extracted from mycelia cultured in PDB for seven days at 22°C using a DNeasy Plant Mini Kit (Qiagen, USA) according to the manufacturer's instructions. The identification of each fungus involved amplification of the internal transcribed spacer (ITS) region (*ITS1-5.8SITS4*) of the ribosomal RNA (rRNA) using primers ITS1 (5'-TCCGTAGGTGAACCCTGCGG-3') and ITS4 (5'-TCCTCCGCTTATTGATATGC-3') (White et al., 1990), along with amplification of the elongation factor (*TEF-1α*) using primers EF-1α (5'-ATGGGTAAGGAAGACAAGAC-3') and EF2 (5'-GGAAGTACCAGTGATCATGTT-3') (O'Donnell et al., 1998). For PCR, all samples were amplified with a final volume of 25 µl, consisting of 12.5 µl of GoTaq® Colorless Master Mix (Promega Corporation, Madison, WI), 0.25 µl each of 50 µM forward and 50 µM reverse primers, 2 µl of DNA template, and 10 µl of nuclease-free water, and the amplification was performed using the GeneAmp PCR system 97,000 PCR (Applied Biosystem, Foster City, CA, USA). The amplification parameters for ITS1/4 included an initial denaturation step at 94°C for 5 min, followed by 30 cycles of denaturation at 94°C for 40 s, annealing at 58°C for 40 s, and elongation at 72°C for 40 s, with a final extension step at 72°C for 5 min. The amplification conditions for EF1/2 involved an initial denaturation at 94°C for 5 min, followed by 33 cycles of denaturation at 94°C for 30 s, annealing at 51°C for 30 s, elongation at 72°C for 30 s, and a final extension at 72°C for 5 min. After PCR amplification, the amplicons were separated on a 1% (w/v) agarose gel, stained with ethidium bromide for 30 minutes, and visualized using the Molecular Imager® Gel Doc™ XR+ System with Image Lab™ Software (BIO-RAD, Hercules, CA, USA). Following that, the amplicons were purified using the E.Z.N.A.® Cycle-Pure Kit (VWR International, Leuven, Belgium), and the resulting purified PCR products were sent to LGC Genomics (LGC group, Berlin, Germany) for Sanger sequencing. Identification of *Fusarium* strains was accomplished by performing a BLAST-search on NCBI (National Center for Biotechnology Information) database.

Assessments of the antifungal activity of EOs - in planta

Inoculation method

Following molecular identification, various inoculation methods were performed on a single strain of *Fusarium* species isolated from spinach host plant. This aimed to identify the most effective and efficient assessment method suitable for subsequent greenhouse experiments. To set up plant materials, spinach seeds were placed on two layers of blotting paper in petri plates, and subsequently transplanted into standard potting soil after germination. In the first pathogenicity test, the soil drench (SD) method, the fungus spore suspension (5×10^5 conidia/mL) was drenched using a repeater syringe onto the root plugs of two-week-old spinach seedlings (var. Crosstrek F1) grown in 0.5 L plastic pots containing standard potting soil (organic/mineral fertilizers NPK 14-16-18, pH (H2O) 5–6.5, organic and dry matters: 25% and 20%, respectively), with three seedlings per pot. In pathogenicity test 2, the root-dip inoculation (RD) method, the bottom 20% of the root plugs of two-week-old seedlings were cut manually to provide wounding for infection, then swirled in 100 ml of the fresh spore suspension for two minutes. Inoculated seedlings were then transplanted into plastic pots containing standard potting soil. The pathogenicity test 3, seed soaking (SS) method, involved soaking spinach seeds in spore suspension for one hour. Following this soaking period, the seeds were allowed to dry before being planted into the soil. In pathogenicity test 4, the mycelial plug (MP) inoculation method, seedlings roots

were inoculated with fungal mycelial plugs. Two weeks after transplantation, the root zones of the seedlings were inoculated with 6 mm fungal mycelial plugs. In pathogenicity test 5, the colonized grain (CG) method, spinach seeds were planted in pots filled with the mixture of standard potting soil and ground wheat grains colonized by the fungus at a ratio of 10 g inoculum/L of substrate. *Fusarium* strain had been grown on sterilized wheat grains at 25°C for two weeks. Throughout all tests, a non-inoculated treatment was also included in each pathogenicity test as a negative control. Pots were maintained in the growth chamber at 21°C and 12 h photoperiod for four weeks. A rating scale was developed to qualitatively determine the disease severity index (DSI) based on visual foliar symptoms, ranging from 0 to 3: 0 for a healthy plant, 1 for slight wilting, 2 for severe wilting, and 3 for a dead plant. The pathogenicity tests were conducted twice with 10 pots per treatment. The assessment was conducted on a percentage basis using the following formula:

$$DSI\ (\%) = \left[\frac{\Sigma(class\ occurrence \times grading\ class\ score)}{(total\ plants\ in\ a\ set) \times (maximum\ disease\ grading)}\right] X\ 100$$

Phytotoxic effect assessment

The phytotoxicity of the tested oils on spinach seeds was also assessed using a germination test following the standard "top of paper method" detailed in the International Seed Testing Association (ISTA), with slight modifications. Two EOs, at concentrations of 3.33 and 6.66 µL/mL, were chosen due to their superior efficacy observed across all strains *in vitro*, aiming for potential application in future *in vivo* experiments. To conduct the experiment, a total of 240 previously disinfected spinach seeds (var. Crosstrek F1) were immersed in aqueous EO solutions for 10 minutes, then air-dried on sterile filter paper (Whatman no. 1) under controlled, sterile conditions at room temperature. For each treatment, sets of 15 seeds were placed on top of two layers of filter paper in 140 mm petri plate, ensuring uniform spacing. Petri plates were pre-moistened with 2 ml sterile distilled water (SDW), and covered with lids. Petri plates containing only distilled water served as the control group. The set up was kept in the growth chamber under suitable consistent conditions (85–90% RH, 20°C, and 12 h photoperiod). The experiment followed a completely randomized design (CRD) with four replicates. Seeds were considered germinated once 1 mm of the radicle had protruded through the seed coat. The seed germination percentage was evaluated seven days post-treatment according to the equation stated below.

$$Germination\ percentage\ (\%) = \frac{Total\ number\ of\ germinated\ seeds}{Total\ number\ of\ seeds}\ X\ 100$$

Fusarium wilt control

Two types of pot experiments were conducted to assess the effectiveness of promising EOs in mitigating *Fusarium* wilt. These experiments involved treatments applied to both seeds and soil, enabling a comprehensive evaluation of their impact on disease development. As mentioned earlier, fungal inoculum was incorporated into the soil at a rate of 1%, thoroughly mixed, and filled into sterile plastic pots two weeks prior to sowing. For the seed treatment, EOs were prepared in conical flasks at concentrations of 3.33 and 6.66 µL/mL. Spinach seeds were immersed in the prepared oils and shaken for 10 minutes using a shaker to ensure thorough saturation. Following this, the seeds were air-dried and planted with four seeds per pot (0.5 L). In the control treatment, seeds were soaked in SDW. Moreover, the same concentrations of these EOs, as used for seed treatment, were applied for soil treatment. During the planting process, the oils (15 ml) were initially added to each planting hole until saturation. As a control treatment, SDW was employed prior to planting. Pots were subjected to a temperature of 21°C and a photoperiod of 12 h in the growth chamber for a period of four weeks to monitor the development of *Fusarium* wilt. Disease incidence was evaluated using the aforementioned 0-3 scale for foliar symptoms, and subsequently the disease incidence reduction (DIR) was determined by using the following formula:

$$DIR\ (\%) = \frac{[DSI\ (control) - DSI\ (treatment)]}{DSI\ (control)} X\ 100$$

The values calculated for DSI on the assessment day were used to compute the DIR in the respective experiment. Additionally, daily assessments were conducted over a period of 14 days post-sowing to determine the seedling emergence rate index (ERI), using the formula outlined by the Association of Official Seed Analysts (AOSA) (2002):

$$Emergence\ index = \sum(Gt/Dt)$$

where Gt is the number of the germinated seed on day t and Dt is time corresponding to Gt in days. The irrigation process was performed as necessary, and all experiments were repeated twice.

Statistical analyses

All experiments followed a randomized complete block design (RCBD), and the data are presented as means ± standard deviations (SD) and visually represented using box plots. Due to the lack of normality (Shapiro-Wilk test) and homogeneity of variances (Levene's test), non-parametric hypothesis testing, specifically the Kruskal-Wallis test, was employed to assess the statistical significance of differences between treatments. In cases where significant differences were observed ($p < 0.05$), pairwise comparisons of the groups were conducted using Dunn's test in the "R" software package (version 2.15.3). Probit analysis was utilized to calculate the ED50 values based on the OD values.

Results

Agar well diffusion

A sensitivity assessment using a well diffusion assay evaluated the response of five *Fusarium* strains (AL64, AK181, F17536,

AT014, and L20-076) to four different EOs at concentrations ranging from 0.83 to 6.66 µL/mL, with clearance zones measured to determine their effects, as shown in Figure 1. The susceptibility of the selected fungal strains varied ($P< 0.05$) across different concentrations of EOs. Thyme and oregano EOs exhibited the highest level of antifungal activity among the tested oils. Marjoram also exhibited effectiveness, albeit to a lesser extent, by inhibiting only one strain (AK181). For strains AL64, L20-076, and F17536, thyme EO displayed the broadest inhibition zones, with average diameters of 15.46, 14.54, and 14.01 mm, respectively, followed by oregano at the highest concentrations (6.66 µL/mL). Similarly, for strains AT014 and AK181, oregano EO produced the widest inhibition zones of 15.33 and 14.01 mm (at 6.66 µL/mL), respectively, followed by thyme. Overall, among *Fusarium* strains, thyme and oregano EOs exhibited heightened antifungal activity in most cases, with AK181 emerging as particularly susceptible to marjoram. Conversely, marjoram and tea tree EOs demonstrated minimal variations in sensitivity across the tested strains, with some strains showing little to no response.

Microtiter plate

The baseline assay investigating the impact of four EOs on spore germination of *Fusarium* strains unveiled a spectrum of ED50 values ranging from 0.69 to 7.53 µL/mL. The statistical analysis revealed significant variations ($p< 0.05$) in the ED50 values among the tested compounds, indicating highly significant effects of different EOs on the response of various strains (Figure 2). Thyme and oregano EOs consistently exhibited lower ED50 values, indicating robust antifungal properties, while other EOs demonstrated varying levels of efficacy. Tea tree displayed moderate activity, with ED50 values ranging from 1.62 to 6.71 µL/mL across different *Fusarium* strains. In contrast, marjoram EO generally yielded higher ED50 values, averaging 3.78 µL/mL, suggesting comparatively lower effectiveness against spore germination. Notably, it exhibited an ED50 value of 7.53 µL/mL against AT014, indicating its weaker inhibitory effect in this particular instance.

Agar dilution

The inhibitory effect of EOs on the mycelial growth of various *Fusarium* strains was also investigated, revealing a dose-dependent response. As the concentration of EOs increased, the antifungal activity notably improved, resulting in inhibition of mycelial growth ranging from approximately 14% to 100% after seven days of incubation (Figure 3). All tested *Fusarium* strains exhibited similar sensitivity to the EOs. Notably, thyme and oregano EOs demonstrated complete inhibition (100% mycelial inhibition) against all *Fusarium* strains, even at the lowest concentration of 0.84 µL/mL. Marjoram EO also exhibited significant ($p< 0.05$) antifungal activity, with complete growth inhibition observed at concentrations of 3.33 and 6.66 µL/mL, while even at a lower concentration of 1.66 µL/mL, it considerably reduced mycelial growth of most tested strains. In contrast, tea tree EO displayed the weakest inhibitory effect, failing to entirely suppress mycelial growth in some strains, particularly AL64 and F17536, even at its maximum concentration of 6.66 µL/mL.

Furthermore, the assessment of fungistatic activity revealed that tee tree and marjoram EOs were effective at inhibiting the fungal growth at a concentration of 3.33 µL/mL. Thyme and oregano oils, however, displayed this activity even at 0.84 µL/mL, unlike the other EOs (Table 1). Indeed, tee tree and marjoram exhibited the highest MICs, indicating a lack of fungicidal impact on the fungal strains. Thyme EO displayed fungicidal activity ranging between 1.66 and 6.66 µL/mL, while Oregano ranged from 0.84 to 6.66 µL/mL across all strains tested. However, the importance of the surfactant Tween 80 added to the growth medium should not be overlooked, as it facilitated the even dispersion of the EOs, resulting in reducing the risk of inaccurately elevated MICs and MFCs. Overall, thyme and oregano consistently demonstrated the highest effectiveness among the four EOs, with a MIC of 0.84 µL/mL against nearly all tested strains in this study.

Volatile

The antifungal activity of tea tree, thyme, oregano, and marjoram EOs was investigated to detect their indirect effects in the vapor phase against *Fusarium* strains (Figure 4), contrasting with direct contact in the agar dilution method. Our results indicate that tea tree and marjoram oils had minimal to negligible effects on all strains, with mycelial growth inhibition consistently below 20% across all concentrations. In contrast, thyme and oregano notably EOs triggered complete growth inhibition in AL64 and L20-076 when applied at the highest concentration tested (6.66 µL/mL). Furthermore, volatiles from these oils consistently ($P< 0.05$) inhibited growth by over 80% across all strains at this concentration. Notably, the volatile compound derived from thyme exhibited the highest inhibitory potency, effectively halting the mycelial growth of at least one strain (AL64) at a concentration of 3.33 µL/mL.

Determining the lowest EO concentration resulting in 100% mycelial growth inhibition classified whether the effect was fungicidal or fungistatic. Fungistatic characterization involved observing growth upon transfer from the amended PDA plates to fresh PDA, while the absence of regrowth on fresh PDA indicated fungicidal activity. In this assay, thyme and oregano EOs, particularly at their highest concentration (6.66 µL/mL), exhibited varying degrees of antifungal activity. They demonstrated fungistatic effects against the tested *Fusarium* strains, except for AL64 and L20-076, where they showed a fungicidal effect (Table 2). Notably, thyme at a concentration of 3.33 µL/mL also displayed fungicidal activity against AL64. Additionally, while these oils effectively inhibited mycelial growth by 100% at the higher concentration, they did not demonstrate fungicidal or fungistatic effects on the *Fusarium* strains at lower concentrations. After comprehensive assessment of the outcomes derived from the *in vitro* bioassays, it was concluded that thyme and oregano EOs exhibited superior antifungal efficacy against *Fusarium* strains, particularly at concentrations of 3.33 and 6.66 µL/mL, prompting their selection for subsequent investigation in *in vivo* bioassays.

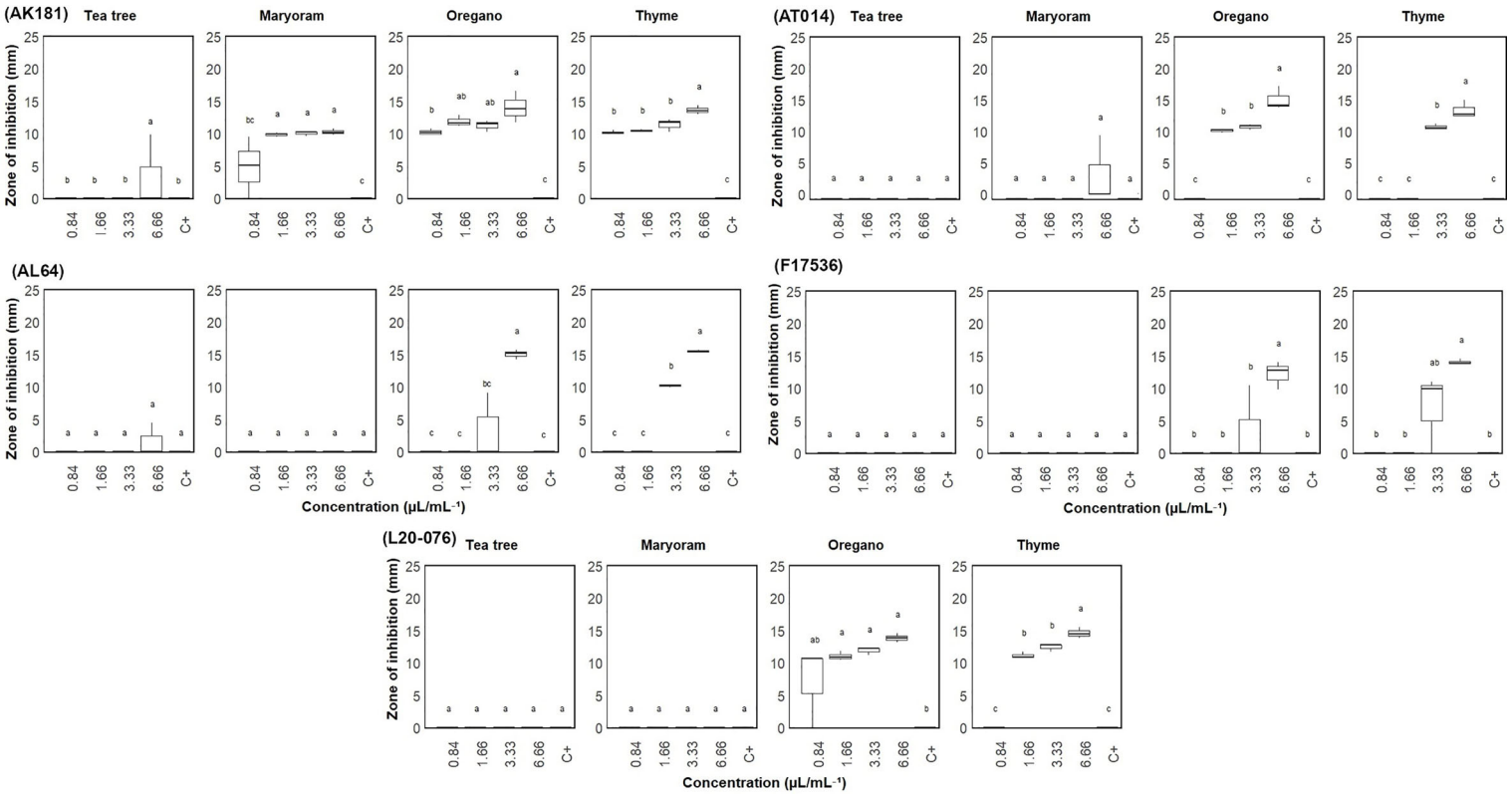

FIGURE 1
Zone of inhibition (mm) of *Fusarium* sp. measured via the agar well diffusion test on plates treated with varied concentrations (0.84-6.66 µL/mL) of essential oils. C+: Sterile distilled water served as positive control. Vertical bars represent the standard error (SE) of mean values of six replicates each including 2 wells. Boxes sharing the identical letters indicate values that do not differ significantly based on Dunn's test ($P > 0.05$).

10.3389/fpls.2024.1444195

10.3389/fpls.2024.1444195

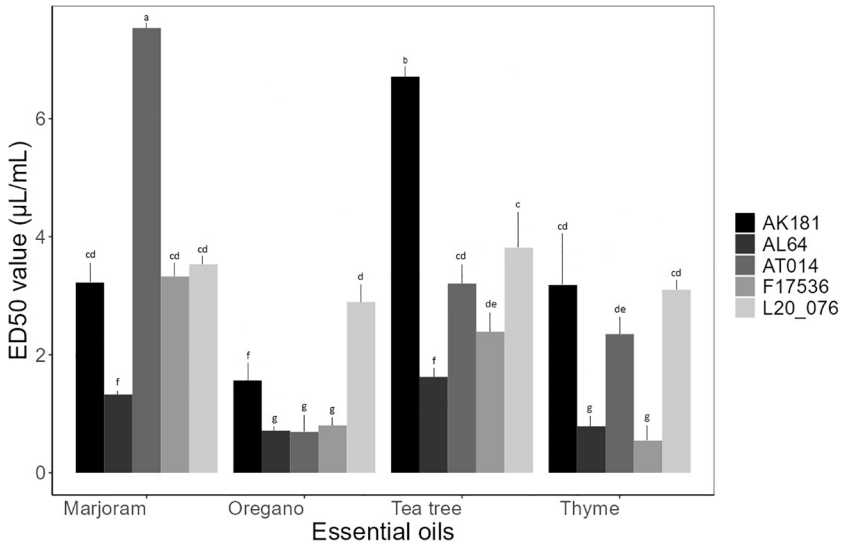

FIGURE 2
Mean effective dose (µL/mL) of essential oils for spore germination of *Fusarium* strains. Bars sharing the identical letters indicate values that do not differ significantly based on Dunn's test (P > 0.05).

Molecular identification of *Fusarium* strains

To strengthen confidence in strains identification and minimize the risk of result misinterpretation, we amplified the ITS rDNA and TEF-1α regions of all isolates. The BLAST search showed the PCR products from three major *Fusarium* species including *F. equiseti, F. oxysporum*, and *F. incarnatum-equiseti* exhibited a 99-100% homology with the associated sequences in the GenBank database (Table 3). Our analysis identified three strains belonging to the *F. oxysporum* species complex (L20-076, AS-109, and L20-080), three strains belonging to *F. equiseti* (AT-014, L20-92 and L21-014), one strain belonging to *F. oxysporum* f.sp. *cepae* (AK-181), one strain belonging to the *F. incarnatum-equiseti* species complex (AL-64), and three strains belonging to *F. oxysporum* f.sp. *spinaciae* (F-100.2, F14157 and F-17536). Consequently, we selected a single strain of *F. oxysporum* f.sp. *spinaciae* (F-17536) for *in planta* experiments involving spinach, considering its relevance to the target plant and its prior assessment in *in vitro* experiments.

Assessments of the antifungal activity of EOs - in planta

Inoculation method

To ascertain the most efficient approach for greenhouse-based inoculation, an assessment was conducted on five distinct inoculation methods, namely SD, RD, SS, MP, and CG. This evaluation was performed on a specific strain of *F. oxysporum* f.sp. *spinaciae* (F-17536) following preliminary *in vitro* bioassays and considering its original host plant. All five inoculation techniques induced symptoms of *Fusarium* wilt in the spinach plants, resulting in significantly varied levels of disease severity (P< 0.05) (Figure 5). Reddening attributed to the presence of fungal mycelium was observed alongside the root vascular tissue in infected seedlings, which exhibited a water-soaked appearance or brown to black discoloration. All inoculation methods displayed initial disease symptoms approximately 14 days after inoculation (DAI), except for the CG method, which manifested symptoms at 9 DAI, characterized by poor germination, stunted growth, and post-emergence damping off. However, the RD, SD, and MP methods displayed comparable levels of disease severity which were significantly (P< 0.05) different from the control. Though the SS method did induce mild foliar symptoms, it was inconsistent throughout the experiments. All of the non-inoculated control plants remained asymptomatic over the duration of each pathogenicity test. As a general observation, the effectiveness of inoculating methods could be arranged in the following order: CG method exhibited the highest efficacy, succeeded by methods MP, RD, SD, and SS, respectively. Consequently, the GC method was selected for conducting further *in vivo* experiments.

Phytotoxic effect

The impact of thyme and oregano EOs on the germination rate of spinach seeds is presented in Table 4. By comparing the average germination rates of different treatments, including various concentrations of EOs, with those of the control group, we could determine if there were any harmful effects on seed germination. At 6.66 µL/mL, oregano oil showed a marginal 2% decrease in germination percentage compared to the control, which is practically negligible and might be compensated for by increasing the seed amount. Thyme oil at 3.33 and 6.66 µL/mL and oregano oil at 3.33 µL/mL did not affect germination rates, indicating no phytotoxic impact of treatments on seed germination across all concentrations used when compared to the untreated control.

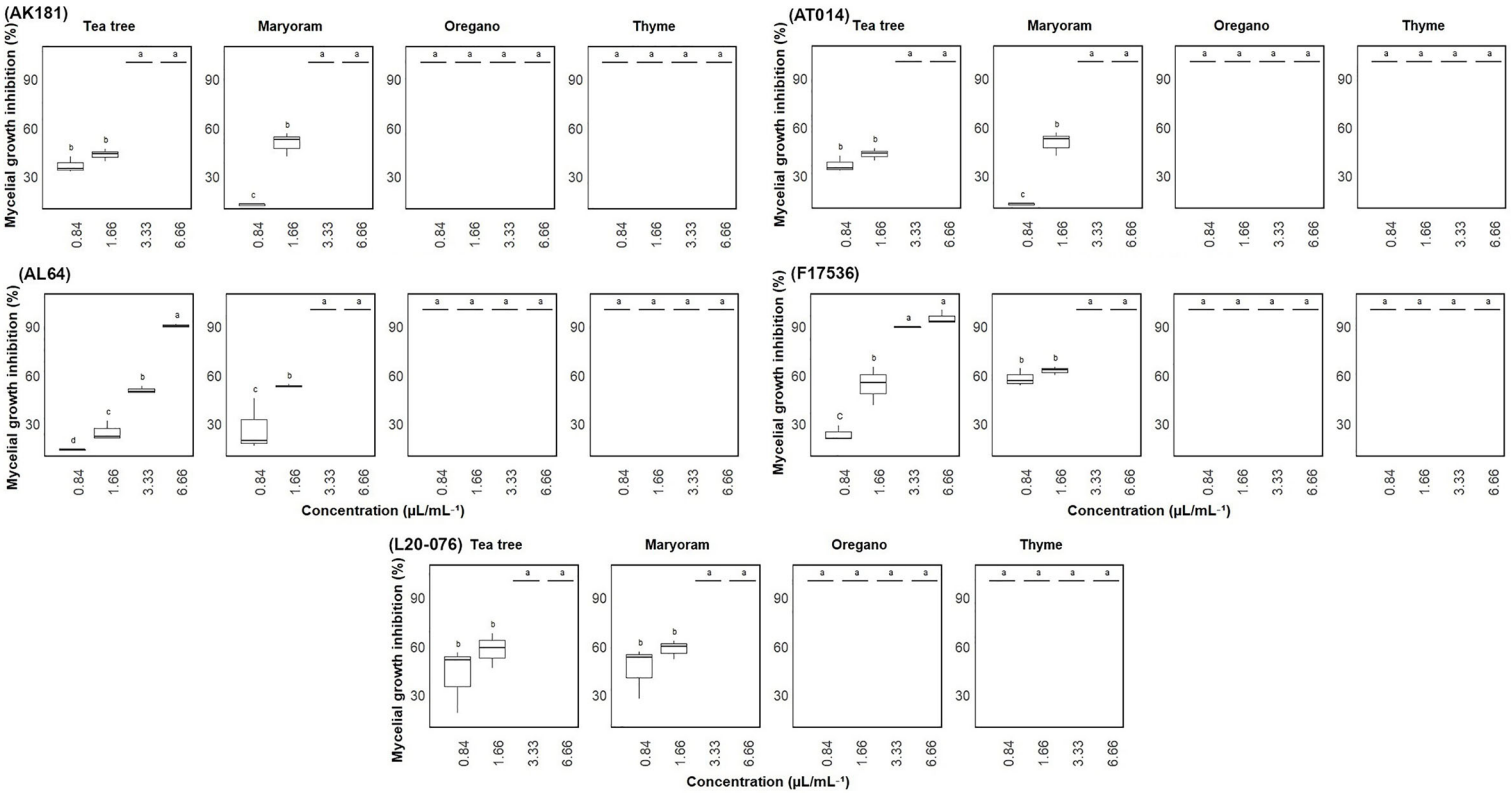

FIGURE 3
Mycelial growth inhibition (%) of *Fusarium* sp. on media amended with varied concentrations (0.84-6.66 µL/mL) of essential oils. Vertical bars represent the standard error (SE) of mean values of six replicates for each compound concentration. Boxes sharing the identical letters indicate values that do not differ significantly based on Dunn's test ($P > 0.05$).

10.3389/fpls.2024.1444195

TABLE 1 Minimum inhibitory concentrations (MIC) and minimum fungicidal concentrations (MFC) of tee tree, thyme, oregano, and marjoram EOs (µL/mL) against the tested *Fusarium* strains.

Fusarium sp.	Tee tree		Thyme		Oregano		Marjoram	
	MIC	MFC	MIC	MFC	MIC	MFC	MIC	MFC
AL64	ND	ND	0.84	1.66	0.84	1.66	3.33	ND
AK181	3.33	ND	0.84	1.66	0.84	1.66	3.33	ND
F17536	ND	ND	0.84	1.66	0.84	1.66	3.33	ND
AT014	3.33	ND	0.84	1.66	0.84	0.84	3.33	ND
L20-076	3.33	ND	0.84	1.66	0.84	0.84	3.33	ND

ND, not detected.

Fusarium wilt control

In this phase of our study, the primary aim was to mitigate *Fusarium* wilt in spinach seedlings through the application of two efficient EOs candidates in both seed and soil treatments. Focusing on oregano and thyme at concentrations of 3.33 and 6.66 µL/mL, we sought to evaluate the impact of these treatments on disease incidence and the emergence rate of seedlings. There was no significant difference ($p > 0.05$). in the mean ERI values 14 days after sowing spinach seeds treated with EOs compared to the untreated control (Table 5). Soil treatment with varying concentrations of EOs also resulted in no significant difference in the ERI values, indicating that the pathogen was not able to interfere the development of spinach seeds. Additionally, a clear relationship found between the application of these EOs and their concentrations in terms of DIR. Indeed, thyme and oregano EOs consistently reduced disease occurrence across various concentration levels ($P< 0.05$), with no discernible impact on seeds emergence. For instance, thyme, in seed treatment at 6.66 µL/mL, exhibited an ERI of ≈ 7 and the highest DIR of ≈ 54%. The remarkable performance of thyme emphasizes its potential for effective disease control in spinach seedlings, making it a promising candidate for further exploration in *Fusarium* wilt management strategies. The data from the experiment also revealed that seed treatments with thyme and oregano EOs at various concentrations consistently led to considerable DIR compared to soil treatments, highlighting the superior efficacy of seed-based interventions in controlling disease occurrence. In essence, using EOs as seed dressing proved more effective than soil treatment, with thyme oil showing the most promising outcomes among the oils tested.

Discussion

In response to the growing need to reduce reliance on chemical substances for plant protection and combat resistance to existing chemicals, there has been a notable increase in the investigation of natural-based compounds. This aims to alleviate the adverse impacts of synthetic pesticides on human health and the environment. Additionally, spinach, an important leafy green crop, is predominantly threatened by soilborne diseases that target its vascular tissue, posing a considerable challenge to its cultivation worldwide. Therefore, the current study aimed to assess antifungal activity of certain plant-derived EOs through both *in vitro* and *in planta* experiments, with the overarching objective of managing *Fusarium* wilt disease in spinach. Fungal growth was influenced by all the tested EOs, although the degree of inhibition differed depending on the specific oil and the strains investigated. The EOs utilized in our study, commercially produced, are known for their effectiveness as biocontrol agents against various phytopathogens. Also, their extraction through standardized procedures enhances the reliability and repeatability of outcomes. Nevertheless, aside from environmental factors, inconsistencies in the efficiency of EOs may occur as a result of their extraction from different plant parts and under varying laboratory conditions, as indicated in previous studies (Dan et al., 2010; Amini et al., 2016; Sarkhosh et al., 2018; Najdabbasi et al., 2020).

We found notable efficacy in inhibiting spore germination and mycelial growth across strains for both thyme and oregano EOs. Oregano EO revealed the most extensive inhibition zone and consistently lower ED50 values, highlighting its potent antifungal attribute. Following oregano, thyme EO also showed considerable effectiveness, while other EOs demonstrated varying levels of efficacy against the tested strains. Such inhibitory effects could be linked to the enzymatic activity of the EOs by disrupting cell wall structure and impeding membrane synthesis (Rasooli et al., 2006; Li et al., 2014). In a study by Parikh et al. (2021), the inhibitory effects of 38 EOs on 10 important pathogenic fungi and oomycetes were examined, revealing that thyme, clove, lemongrass, cinnamon, and oregano EOs exhibited the most potent inhibitory effects on spore germination, sporangia production, and mycelial growth of the pathogens. However, the levels of inhibitory effect varied among the different plant pathogens. In our investigation, thyme and oregano EOs could also effectively suppress *Fusarium* growth through fungicidal activity, at concentrations exceeding 0.84 µL/mL, as opposed to the fungistatic effects observed with tea tree and marjoram at 3.33 µL/mL. Diverse volatile bioactive compounds such as tannins, carvacrol, flavonoids, borneol, sterols, quinones, saponins, alkaloids, and phenols present in EOs cause a range of biological activities, including antibacterial, insecticidal, antiviral, and antifungal properties (Daferera et al., 2003; Kim et al., 2003; Burt, 2004; Schnitzler et al., 2007; Halmer, 2008; Kerekes et al., 2013; Nazzaro et al., 2017). For instance, the antifungal capability of

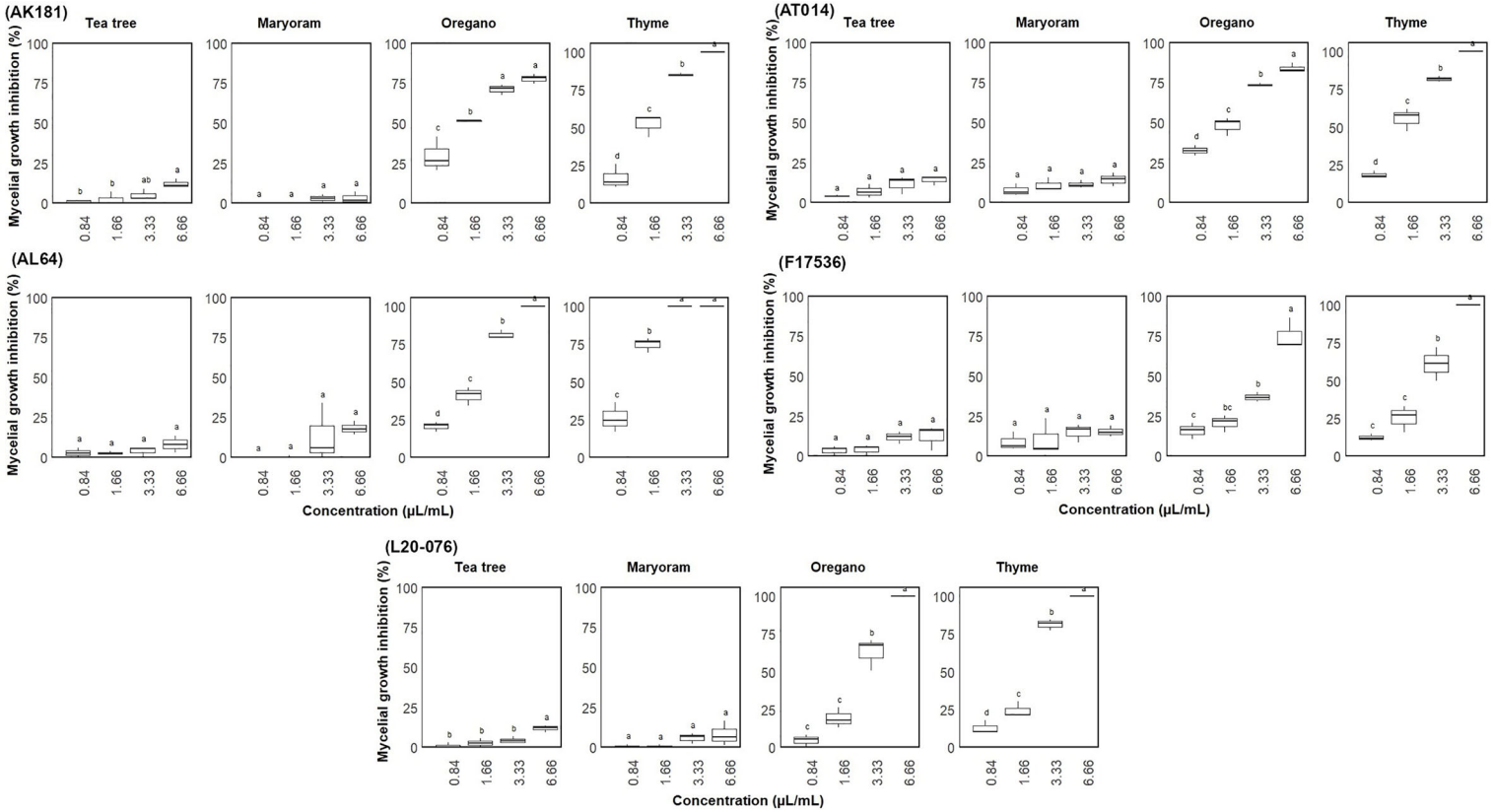

FIGURE 4
Mycelial growth inhibition (%) of *Fusarium* sp. on media through exposure to different concentrations (0.84-6.66 µL/mL) of essential oils. Vertical bars represent the standard error (SE) of mean values of six replicates for each compound concentration. Boxes sharing the identical letters indicate values that do not differ significantly based on Dunn's test ($P > 0.05$).

10.3389/fpls.2024.1444195

TABLE 2 Fungicidal or fungistatic effects of volatiles from thyme and oregano essential oils against the tested *Fusarium* strains.

Fusarium sp.	Thyme (µL/mL)		Oregano (µL/mL)	
	3.33 *	6.66	3.33	6.66
AL64	–	–	ND	–
AK181	ND	+	ND	+
F17536	ND	+	ND	+
AT014	ND	+	ND	+
L20-076	ND	–	ND	–

+, Fungistatic effect as mycelial regrowth observed on fresh PDA; -, fungicidal effect; ND, not detected.
*: Concentrations of thyme and oregano essential oils as µL/mL.

oregano oil may be linked to the presence of its primary components, carvacrol and thymol, which are phenolic compounds known for their antioxidant effects (Mechergui et al., 2010). Utilizing GC-MS analysis, Soylu et al. (2006) also identified 16 bioactive compounds in thyme oil, with carvacrol constituting the major component at 37.9%. Considering the significant presence and activity of phenols and monoterpenic alcohols, it was not surprising that oregano and thyme oils were among the most effective in inhibiting all tested *Fusarium* strains in our study, consistent with previous research (Kishore et al., 2007; Regnier et al., 2014; Dewitte et al., 2018; Najdabbasi et al., 2020). In our study, a uniform level of MFC values exhibiting fungicidal activity was observed for most strains, with the exception of oregano, which showed reduced activity for two *Fusarium* strains (AT014 and L20-076). EOs with the lower MFCs are not only more effective and preferable for disease management but are also desirable for reducing both the volume and cost of applications. On the contrary, their efficacy without fungicidal activity might be weakened upon initial contact with the pathogen, especially through evaporation and washing away (Parikh et al., 2021).

TABLE 3 Molecular identification of 11 *Fusarium* strains obtained from different sources.

Strain	Fungal taxa	Host	Provider*
AT-014	*F. equiseti*	Spinach	Enza Zaden
L20-076	*F. oxysporum*	Leafy green	Enza Zaden
AS-109	*F. oxysporum*	Spinach	Enza Zaden
L20-080	*F. oxysporum*	Leafy green	Enza Zaden
L20-192	*F. equiseti*	Spinach	Enza Zaden
L21-014	*F. equiseti*	Lamb lettuce	Enza Zaden
AK-181	*F. oxysporum* f.sp. *cepae*	Leafy green	Enza Zaden
AL-64	*F. incarnatum-equiseti*	Lamb lettuce	Enza Zaden
F-100.2	*F. oxysporum* f.sp. *spinaciae*	Spinach	CREA
F-14157	*F. oxysporum* f.sp. *spinaciae*	Spinach	CREA
F-17536	*F. oxysporum* f.sp. *spinaciae*	Spinach	CREA

* Enza Zaden: Vegetable Breeding Company, Netherlands; CREA; Research Centre for Vegetable and Ornamental Crops, Italy.

To assess the possible phytotoxic impact of the chosen EOs on germination, spinach seeds were subjected to seed treatments with the EOs. Indeed, treating seeds to prevent soil-borne pathogens when planting leafy green vegetables is a widespread disease management practice. In our study, a standard germination rate exceeding 90% was observed across all treated seeds, affirming that even at a concentration of 6.66 µL/mL, these oils do not exhibit phytotoxic effects on spinach seeds germination. Similar findings were observed by Parikh et al. (2021), where EOs derived from oregano, clove, cinnamon, palmarosa, and thyme did not affect the germination of chickpea seeds, with a germination rate of 90 to 95%, comparable to that of untreated control seeds. Orzali et al. (2020) also reported no influence of *Origanum vulgare* EO on the germination rate of tomato seeds, consistent with the findings of Flores et al. (2018), who investigated the antibacterial efficacy of oregano, thyme, and cinnamon EOs without observing any phytotoxic effects on tomato seedlings. However, the phytotoxic impacts of EOs on various crop seeds have been previously documented (Mahdavikia and Saharkhiz, 2015; Boukaew et al., 2017; Ibáñez and Blázquez, 2018; Perczak et al., 2019; Jouini et al., 2020), which are mainly associated with allelopathy, a non-selective phenomenon that becomes serious only if seeds or plants possess enzymatic mechanisms of eliminating toxicogenic potential (Sumalan et al., 2019; Benarab et al., 2020; Bota et al., 2022). Overall, the type and concentration of the EO, along with the plant species exposed to it, determine the phytotoxic level (Somda et al., 2007; Orzali et al., 2014),. Hence, establishing the ideal concentration of EOs possessing potent antifungal properties yet are free of phytotoxicity is always crucial.

To delve deeper into controlling *Fusarium* wilt in greenhouse settings, we initially assessed different inoculation methods employing a specific strain of *F. oxysporum* f.sp. *spinaciae*, F-17536, to induce the infection in spinach, aiming to establish a reliable and reproducible methodology. An optimal inoculation technique guarantees effective colonization of the host plant, enabling a thorough disease assessment. In the comparison of the five inoculation methods, we suggest seeding spinach in a mixture of *Fusarium*-colonized ground wheat (GC) and substrate at a ratio of 1%. As the preferred protocol for *Fusarium* wilt screening, we effectively exposed spinach to a concentrated pathogen load, thereby intensifying disease pressure from the soil. This resulted in symptoms appearing as early as 9 DAI, in contrast to the 14 DAI observed with other inoculation methods. However, the presence of conidia in the mycelia might have interfered with this outcome. This inoculation method also simulates the presence of soil-borne fungal inoculum in natural field conditions, representing a primary source of infections (Hörberg, 2002; Hoheneder et al., 2022). Lai et al. (2020) showed that introducing *Fusarium*-colonized barley inoculum during sugar beet seed planting led to the development of more severe disease symptoms in a shorter timeframe compared to the root-dipping technique. Although the colonized grain-based inoculum technique has been demonstrated as suitable for studying various soil-borne pathogens and host plants (Holmes and Benson, 1994; Bai and Shaner, 2004; Kirk et al., 2008; Mirmajlessi et al., 2012; Zhang et al., 2014; Noor and Khan, 2015; Koch et al., 2020; Lai et al., 2020; Hoheneder et al., 2022), it was applied for the first time

10.3389/fpls.2024.1444195

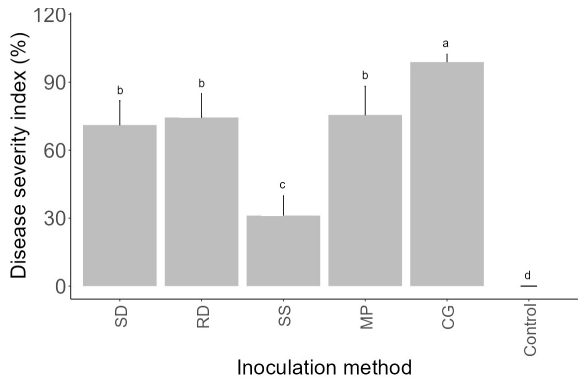

FIGURE 5
Mean *Fusarium* wilt severity index (%) on spinach (var. Crosstrek F1) induced by *F. oxysporum* f.sp. *spinaciae* 22 days post-inoculation using five distinct inoculation methods. SD: soil drenching; RD: root dipping; SS: seed soaking; MP: mycelial plug; CG: colonized grain. Vertical bars represent the standard error (SE) of mean values of 10 pots each including 3 plants. Barplots sharing the identical letters indicate values that do not differ significantly based on Dunn's test (P > 0.05).

to test the pathogenicity of *F. oxysporum* f.sp. *spinaciae* on spinach, leveraging strengths from previous studies. The disease symptom induced by MP, RD, and SD inoculation methods also led to comparable severe *Fusarium* infections. The observed uniformity in DSI among these three methods is likely because of their shared capacity to infiltrate the root epidermis and colonize tissues intracellularly and intercellularly, as reported by previous studies (Van Peer and Schippers, 1992; Mendgen et al., 1996; Czymmek et al., 2007; Lai et al., 2020). However, despite their effectiveness, these methods are time consuming and resource-intensive, requiring large quantities of inoculant and nursery preparation. In contrast, the SS method was found to be less effective, likely due to factors such as limited survival of the inoculant, inadequate spore quantities on seeds, or the removal of attached spores during watering. Nonetheless, it offers cost savings for large-scale experiments as it needs low amount of inoculant compared to other methods (Rocha et al., 2019).

Continuing with greenhouse experiments, we evaluated the effects of the most potent EOs (thyme and oregano), determined *in vitro*, on the *F. oxysporum* f.sp. *spinaciae*-spinach pathosystem *in vivo*, laying the groundwork for future field experiments. Since greenhouse experiments can be adjusted to mitigate environmental variables, creating optimal growth conditions and gaining fresh insights into disease management within a shorter time frame, they can yield comparable assessments to field evaluations, as reported by previous studies (La Torre et al., 2016; Borrero et al., 2017; Gonçalves et al., 2021). For instance, Ribeiro et al. (2015) found that while field evaluations for testing genotype resistance to *Fusarium oxysporum* f. sp. *cubense* isolates typically span two years, greenhouse experiments could achieve similar assessments in approximately three months. We observed that at the highest concentration, thyme oil exhibited greater efficacy against *F. oxysporum* f.sp. *spinaciae* compared to oregano oil. This resulted in approximately 54% and 17% reductions in disease incidence on spinach in both seed and soil treatments, respectively, without causing any phytotoxic effects. Indeed, the antifungal activities of these EOs are primarily due to high levels of carvacrol and thymol,

TABLE 4 Percentage of germination rate on day seven after treatment of spinach seeds with thyme and oregano essential oils.

Thyme (µL/mL)	Germination rate(%)		Oregano (µL/mL)	Germination rate (%)	
0	97 ± 2.0	a	0	97 ± 2.0	a
3.33	97 ± 2.0	a	3.33	97 ± 3.82	a
6.66	97 ± 3.82	a	6.66	95 ± 2.0	a

Means (± SD) sharing the identical letter in a column denote no significant differences compared to the untreated control (0 µL/mL), according to Dunn's test (P > 0.05).

TABLE 5 Emergence rate index and reduction of *Fusarium* wilt incidence in spinach seedlings through the application of oregano and thyme EOs in seed and soil treatments.

Essential oil	Concentration (µL/mL)	Seed treatment		Soil treatment	
		ERI	DIR (%)	ERI	DIR (%)
Oregano	3.33	$7.7 \pm 0.79^{a}_{a}$	16.66^{a}_{c}	$6.34 \pm 1.69^{a}_{a}$	$8.33 \pm 9.62^{b}_{c}$
	6.66	$5.77 \pm 3.56^{a}_{a}$	$36.11 \pm 5.55^{a}_{b}$	$5.24 \pm 2.68^{a}_{a}$	$16.66 \pm 13.6^{b}_{a}$
Thyme	3.33	$6.34 \pm 0.96^{a}_{a}$	$30.55 \pm 5.55^{a}_{b}$	$6.71 \pm 2.25^{a}_{a}$	$12.5 \pm 15.95^{b}_{b}$
	6.66	$7.07 \pm 2.02^{a}_{a}$	$54.16 \pm 9.48^{a}_{a}$	$7.8 \pm 1.38^{a}_{a}$	$18.05 \pm 2.77^{b}_{a}$
	0	$6.69 \pm 0.71^{a}_{a}$	0^{a}_{d}	$7.06 \pm 1.29^{a}_{a}$	0^{a}_{d}
CV (%)		21.48	12.77	29.52	85.04

DIR, Disease incidence reduction in percentage; ERI, Emergence rate index; CV, Coefficient of variation in percentage. Values represent mean ± SD. Identical superscript letters within a row denote no significant differences (P > 0.05), Duncan's multiple-range test) in each concentration for the same treatment. Different subscript letters within a column denote significant differences (p< 0.05), Duncan's multiple-range test) between concentrations for the same treatment.

as reported in several studies (Bouchra et al., 2003; Neri et al., 2006; Combrinck et al., 2011; Pérez-Alfonso et al., 2012; Zhang et al., 2019). Carvacrol suppresses Cyclooxygenase (COX-2) expression and activates peroxisome proliferator-activated receptors (PPAR) α and γ (Hotta et al., 2010; Mączka et al., 2023), while thymol induces the production of reactive oxygen species (ROS) and lipid peroxidation (LPO) in fungal cells (Ma et al., 2019; Shcherbakova et al., 2021). The reduced efficacy of soil treatment may result from the uneven distribution of EOs in the soil matrix, leading to varying concentrations around treated seeds and limiting their effectiveness in inhibiting fungal growth. Besides, the interaction between EO and soil components can also affect the bioavailability and stability of active compounds, thereby reducing its antifungal activity. In contrast, immersing seeds in the EO could potentially create a protective obstacle against contaminated soil during the germination process. These could explain why *Fusarium* wilt was satisfactorily inhibited in seeds treated with relatively high concentrations of these oils, which is consistent with findings from other studies (Mbega et al., 2012; Karaca et al., 2017; Cadena et al., 2018; Terzić et al., 2023). Van Der Wolf et al. (2008) demonstrated the antifungal properties of thyme, oregano, cinnamon, and Clove EOs against various seed-borne pathogens, highlighting thyme as the most effective natural compound for mitigating infections in cabbage seeds. In a study conducted by Ben-Jabeur et al. (2015), thyme EO also revealed effective control of gray mold and *Fusarium* wilt in tomato seedlings. It resulted in a reduction of *Botrytis cinerea* colonization by 64% and significantly lowered *Fusarium* wilt severity by 30.76%, compared to the untreated control, especially seven days post-treatment. In practice, adjusting the treatment duration and dosage is crucial when applying oil to seeds before sowing to maximize antifungal action against soil-borne pathogens without causing phytotoxicity. Furthermore, the susceptibility of EOs to environmental factors like light, temperature, and humidity, along with their high volatility, can lead to instability, potentially affecting their effectiveness over time (Turek and Stintzing, 2013; Najdabbasi et al., 2020). To address these challenges, EOs can be integrated into novel formulations like microemulsions, nanoparticles, and encapsulation techniques, which enhance their physicochemical stability, reinforce biocidal effectiveness, and prolong their activity against plant pathogenic fungi and bacteria (Zhang et al., 2014; Pavoni et al., 2019; Weisany et al., 2019; Basavegowda et al., 2020; Tu et al., 2020; Weisany et al., 2022). For instance, Sivalingam et al. (2024) showed that essential oil-loaded nanostructured lipid carriers displayed antifungal activity against *Fusarium oxysporum* f.sp. *lycopersici*, comparable to the positive control carbendazim. Taken together, these aspects suggest that although seed treatment with EOs holds promise as a control strategy, improving application methods and formulations is essential to enhance their effectiveness in managing *Fusarium* wilt in spinach cultivation.

Conclusion

This study collectively assessed various artificial inoculation methods to induce *Fusarium* wilt in spinach under greenhouse conditions. It found that the colonized grain-based inoculum method was the most effective approach in eliciting symptoms, which appeared at approximately 9 DAI, thus providing valuable insight for future *Fusarium* research on spinach. Furthermore, given that previous studies have primarily focused on other *Fusarium* species when assessing the fungitoxicity of EOs, our research provides additional evidence supporting the potential use of thyme and oregano oils for controlling *F. oxysporum* f.sp. *spinacia*. To our knowledge, this study is the first to investigate the application of these EOs for treating spinach seeds and soil in a greenhouse environment, resulting in a reduction in *Fusarium* wilt incidence without adverse effects on plant health. Supported by *in vivo* experiments, these findings highlight the potential of thyme EO as a green fungicide for integrated pest management in spinach cultivation. However, successful large-scale application of such compounds requires formulation optimization, suitable farm facilities, and consideration of various biological and environmental factors.

Data availability statement

The raw data supporting the conclusions of this article will be made available by the authors, without undue reservation.

Author contributions

MM: Conceptualization, Data curation, Investigation, Methodology, Supervision, Validation, Visualization, Writing – original draft, Writing – review & editing. NN: Data curation, Formal analysis, Investigation, Methodology, Software, Writing – original draft, Writing – review & editing. LS: Resources, Writing – review & editing. GH: Funding acquisition, Project administration, Resources, Writing – review & editing.

Funding

The author(s) declare that no financial support was received for the research, authorship, and/or publication of this article.

Acknowledgments

We are grateful to Sacha Kofman (Enza Zaden) for providing the spinach seeds for the plant experiments.

Conflict of interest

The authors declare that the research was conducted in the absence of any commercial or financial relationships that could be construed as a potential conflict of interest.

The author(s) declared that they were an editorial board member of Frontiers, at the time of submission. This had no impact on the peer review process and the final decision.

Publisher's note

References

Abbott, W. S. (1925). A method of computing the effectiveness of an insecticide. *J. Econ. Entomol.* 18, 265–267. doi: 10.1093/jee/18.2.265a

Abdel-Kader, M. M., El-Mougy, N. S., and Lashin, S. M. (2011). Essential oils and *Trichoderma harzianum* as an integrated control measure against faba bean root rot pathogens. *J. Plant Prot. Res.* 51, 306–313. doi: 10.2478/v10045-011-0050-8

Abdi-Moghadam, Z., Mazaheri, Y., Rezagholizade-Shirvan, A., Mahmoudzadeh, M., Sarafraz, M., Mohtashami, M., et al. (2023). The significance of essential oils and their antifungal properties in the food industry: A systematic review. *Heliyon.* 9, e21386. doi: 10.1016/j.heliyon.2023.e21386

Amini, J., Farhang, V., Javadi, T., and Nazemi, J. (2016). Antifungal effect of plant essential oils on controlling Phytophthora species. *Plant Pathol. J.* 32, 16. doi: 10.5423/PPJ.OA.05.2015.0091

Antonissen, G., Martel, A., Pasmans, F., Ducatelle, R., Verbrugghe, E., Vandenbroucke, V., et al. (2014). The impact of *Fusarium* mycotoxins on human and animal host susceptibility to infectious diseases. *Toxins (Basel).* 6, 430–452. doi: 10.3390/toxins6020430

Association of Official Seed Analysts (AOSA). (2002). *Seed vigor testing handbook: contribution no. 32 to the Handbook on seed testing* (Las Cruces, NM: Association of Official Seed Analysts).

Bahadur, A. (2022). "urrent status of *Fusarium* and their management strategies," in Fusarium - *an overview of the genus*. Ed. S. M. Mirmajlessi (IntechOpen, London, United Kingdom), 1–17. doi: 10.5772/intechopen.100608

Bai, G., and Shaner, G. (2004). Management and resistance in wheat and barley to *Fusarium* head blight. *Annu. Rev. Phytopathol.* 42, 135–161. doi: 10.1146/annurev.phyto.42.040803.140340

Basavegowda, N., Patra, J. K., and Baek, K. H. (2020). Essential oils and mono/bi/trimetallic nanocomposites as alternative sources of antimicrobial agents to combat multidrug-resistant pathogenic microorganisms: an overview. *Molecules.* 25, 1058. doi: 10.3390/molecules25051058

Benarab, H., Fenni, M., Louadj, Y., Boukhabti, H., and Ramdani, M. (2020). Allelopathic activity of essential oil extracts from *Artemisia Herba-Alba* Asso. on seed and seedling germination of weed and wheat crops. *Acta Sci. Nat.* 7, 86–97. doi: 10.2478/asn-2020-0009

Ben-Jabeur, M., Ghabri, E., Myriam, M., and Hamada, W. (2015). Thyme essential oil as a defense inducer of tomato against gray mold and *Fusarium* wilt. *Plant Physiol. Biochem.* 94, 35–40. doi: 10.1016/j.plaphy.2015.05.006

Bi, Y., Jiang, H., Hausbeck, M. K., and Hao, J. J. (2012). Inhibitory effects of essential oils for controlling *Phytophthora capsici*. *Plant Dis.* 96, 797–803. doi: 10.1094/PDIS-11-11-0933

Borrero, C., Bascón, J., Gallardo, M.Á., Orta, M. S., and Avilés., M. (2017). New foci of strawberry *Fusarium* wilt in Huelva (Spain) and susceptibility of the most commonly used cultivars. *Sci. Hortic.* 226, 85–90. doi: 10.1016/j.scienta.2017.08.034

Bota, V., Sumalan, R. M., Obistioiu, D., Negrea, M., Cocan, I., Popescu, I., et al. (2022). Study on the sustainability potential of thyme, oregano, and coriander essential oils used as vapours for antifungal protection of wheat and wheat Products. *Sustainability.* 14, 4298. doi: 10.3390/su14074298

Bouchra, C., Achouri, M., Hassani, L. M. I., and Hmamouchi, M. (2003). Chemical composition and antifungal activity of essential oils of seven Moroccan Labiatae against *Botrytis cinerea* Pers. *Fr. J. Ethnopharmacol.* 89, 165–169. doi: 10.1016/S0378-8741(03)00275-7

Boukaew, S., Prasertsan, P., and Sattayasamitsathit, S. (2017). Evaluation of antifungal activity of essential oils against aflatoxigenic *Aspergillus flavus* and their allelopathic activity from fumigation to protect maize seeds during storage. *Ind. Crop Prod.* 97, 558–566. doi: 10.1016/j.indcrop.2017.01.005

Bounar, R., Krimat, S., Boureghda, H., and Dob, T. (2020). Chemical analyses, antioxidant and antifungal effects of oregano and thyme essential oils alone or in combination against selected *Fusarium* species. *Int. Food Res. J.* 27, 66–77. Available at: https://api.semanticscholar.org/CorpusID:229321802.

Burt, S. (2004). Essential oils: their antibacterial properties and potential applications in foods-a review. *Int. J. Food Microbiol.* 94, 223–253. doi: 10.1016/j.ijfoodmicro.2004.03.022

Cadena, M. B., Preston, G. M., van der Hoorn, R. A., Flanagan, N. A., Townley, H. E., and Thompson, I. P. (2018). Enhancing cinnamon essential oil activity by nanoparticle encapsulation to control seed pathogens. *Ind. Crops Prod.* 124, 755–764. doi: 10.1016/j.indcrop.2018.08.043

Chen, Y., Zeng, H., Tian, J., Ban, X., Ma, B., and Wang, Y. (2013). Antifungal mechanism of essential oil from *Anethum graveolens* seeds against *Candida albicans*. *J. Med. Microbiol.* 62, 1175–1183. doi: 10.1099/jmm.0.055467-0

Combrinck, S., Regnier, T., and Kamatou, G. P. P. (2011). *In vitro* activity of eighteen essential oils and some major components against common postharvest fungal pathogens of fruit. *Ind. Crop Prod.* 33, 344–349. doi: 10.1016/j.indcrop.2010.11.011

Czymmek, K. J., Fogg, M., Powell, D. H., Sweigard, J., Park, S. Y., and Kang, S. (2007). *In vivo* time-lapse documentation using confocal and multi-photon microscopy reveals the mechanisms of invasion into the Arabidopsis root vascular system by *Fusarium oxysporum*. Fungal Genet. *Biol.* 44, 1011–1023. doi: 10.1016/j.fgb.2007.01.012

Daferera, D. J., Basil, N., Ziogas, N., and Polissiou, M. G. (2003). The effectiveness of plant essential oils on Botrytis cinerea, Fusarium sp. and *Clavibacter michiganensis* subsp. *michiganensis*. *Crop Protect.* 22, 39–44. doi: 10.1016/S0261-2194(02)00095-9

Dan, Y., Liu, H.-Y., Gao, W.-W., and Chen, S.-L. (2010). Activities of essential oils from *Asarum heterotropoides* var. *mandshuricum* against five phytopathogens. *Crop Protect.* 29, 295–299. doi: 10.1016/j.cropro.2009.12.007

De Cal, A., Sztejnberg, A., Sabuquillo, P., and Melgarejo, P. (2009). Management *Fusarium* wilt on melon and watermelon by *Penicillium oxalicum*. *Biol. Control.* 51, 480–486. doi: 10.1016/j.biocontrol.2009.08.011

Dewitte, K., Landschoot, S., Carrette, J., Audenaert, K., and Haesaert, G. (2018). Exploration of essential oils as alternatives to conventional fungicides in lupin cultivation. *Organic Agric.* 9, 107–116. doi: 10.1007/s13165-018-0212-3

Egel, D. S., and Martyn, R. D. (2007). *Fusarium* wilt of watermelon and other cucurbits. *Plant Health Instr.* 10, 1094. doi: 10.1094/PHI-I-2007-0122-01

Ekwomadu, T. I., and Mwanza, M. (2023). *Fusarium* fungi pathogens, identification, adverse effects, disease management, and global food security: a review of the latest research. *Agric.* 13, 1810. doi: 10.3390/agriculture13091810

Fiori, A., Schwan-Estrada, K., Stangarlin, J., Vida, J., Scapim, C., Cruz, M., et al. (2000). Antifungal activity of leaf extracts and essential oils of some medicinal plants against *Didymella bryoniae*. *J. Phytopathol.* 148, 483–487. doi: 10.1046/j.1439-0434.2000.00524.x

Flores, J. B., García, J. O., Becheleni, F. R. C., Espinoza, A. V., Wong-Corral, F. J., and Rueda-Puente, E. O. (2018). Effect of essential oils in the control of the *Clavibacter michiganensis* subespecie *michiganensis* in tomato (*Lycopersicum esculentum* L.) plants. *Biotecnia.* 20, 96–101. doi: 10.18633/biotecnia.v20i3.704

Gonçalves, D. C., Tebaldi de Queiroz, V., Costa, A. V., Lima, W. P., Belan, L. L., Moraes, W. B., et al. (2021). Reduction of fusarium wilt symptoms in tomato seedlings following seed treatment with *origanum vulgare* L. *essential Oil carvacrol. Crop Prot.* 141, 105487. doi: 10.1016/j.cropro.2020.105487

Halmer, P. (2008). Seed technology and seed enhancement. *Acta Hortic.* 771, 17–26. doi: 10.17660/ActaHortic.2008.771.1

Han, X.-B., Zhao, J., Cao, J.-M., and Zhang, C.-S. (2019). Essential oil of *Chrysanthemum indicum* L.: potential biocontrol agent against plant pathogen *Phytophthora nicotianae*. Environ. *Sci. pollut. Control Ser.* 26, 7013–7023. doi: 10.1007/s11356-019-04152-y

Haque, E., Irfan, S., Kamil, M., Sheikh, S., Hasan, A., Ahmad, A., et al. (2016). Terpenoids with antifungal activity trigger mitochondrial dysfunction in *Saccharomyces cerevisiae*. *Microbiol.* 85, 436–443. doi: 10.1134/S0026261716040093

Hoheneder, F., Biehl, E. M., Hofer, K., Petermeier, J., Groth, J., Herz, M., et al. (2022). Host genotype and weather effects on *Fusarium* head blight severity and mycotoxin load in spring barley. *Toxins.* 14, 125. doi: 10.3390/toxins14020125

Holmes, K. A., and Benson, D. M. (1994). Evaluation of *Phytophthora parasitica* var. *nicotianae* for biocontrol of *Phytophthora parasitica* on *Catharanthus roseus*. *Plant Dis.* 78, 193–199. doi: 10.1094/PD-78-0193

Hörberg, H. M. (2002). Patterns of splash dispersed conidia of *Fusarium poae* and *Fusarium culmorum*. *Eur. J. Plant Pathol.* 108, 73–80. doi: 10.1023/A:1013936624884

Hotta, M., Nakata, R., Katsukawa, M., Hori, K., Takahashi, S., and Inoue, H. (2010). Carvacrol, a component of thyme oil, activates PPARalpha and gamma and suppresses COX-2 expression. *J. Lipid Res.* 51, 132–139. doi: 10.1194/jlr.M900255-JLR200

Ibáñez, M., and Blázquez, M. (2018). Phytotoxicity of essential oils on selected weeds: Potential hazard on food crops. *Plants.* 7, 79. doi: 10.3390/plants7040079

International Seed quality Assurance (ISTA) (2023). *International rules for seed testing*. Available online at: https://www.seedtest.org/en/international-rules-for-seed-testing-rubric-3.html (Accessed February 15, 2023).

Jouini, A., Verdeguer, M., Pinton, S., Araniti, F., Palazzolo, E., Badalucco, L., et al. (2020). Potential effects of essential oils extracted from mediterranean aromatic plants on target weeds and soil microorganisms. *Plants.* 9, 1–24. doi: 10.3390/plants9101289

Karaca, G., Bilginturan, M., and Olgunsoy, P. (2017). Effects of some plant essential oils against fungi on wheat seeds. *Indian J. Pharm. Educ. Res.* 51, 385–388. doi: 10.5530/ijper.51.3s.53

Kerekes, E. B., Deák, É., Takó, M., Tserennadmid, R., Petkovits, T., Vágvölgyi, C., et al. (2013). Anti-biofilm forming and anti-quorum sensing activity of selected essential oils and their main components on food-related micro-organisms. *J. Appl. Microbiol.* 115, 933–942. doi: 10.1111/jam.2013.115.issue-4

Khaleil, M. M., Alnoman, M. M., Elrazik, E. S. A., Zagloul, H., and Khalil, A. M. A. (2021). Essential oil of *Foeniculum vulgare* Mill. as a green fungicide and defense-inducing agent against *Fusarium* Root Rot Disease in *Vicia faba* L. *Biol. (Basel).* 10, 696. doi: 10.3390/biology10080696

Khan, A., Ahmad, A., Khan, L. A., Padoa, C. J., van Vuuren, S., and Manzoor, N. (2015). Effect of two monoterpene phenols on antioxidant defense system in *Candida albicans*. *Microb. Pathog.* 80, 50–56. doi: 10.1016/j.micpath.2015.02.004

Kim, S.-I., Park, C., Ohh, M.-H., Cho, H.-C., and Ahn, Y.-J. (2003). Contact and fumigant activities of aromatic plant extracts and essential oils against *Lasioderma serricorne* (Coleoptera: anobiidae). *J. Stored Prod. Res.* 39, 11–19. doi: 10.1016/S0022-474X(02)00013-9

Kirk, W. W., Wharton, P. S., Schafer, R. L., Tumbalam, P., Poindexter, S., Guza, C., et al. (2008). Optimizing fungicide timing for the control of *Rhizoctonia* crown and root rot of sugar beet using soil temperature and plant growth stages. *Plant Dis.* 92, 1091–1098. doi: 10.1094/PDIS-92-7-1091

Kishore, G. K., Pande, S., and Harish, S. (2007). Evaluation of essential oils and their components for broad-spectrum antifungal activity and control of late leaf spot and crown rot diseases in peanut. *Plant Dis.* 91, 375–379. doi: 10.1094/PDIS-91-4-0375

Koch, E., Zink, P., Pfeiffer, T., von Galen, A., Linkies, A., Drechsel, J., et al. (2020). Artificial inoculation methods for testing microorganisms as control agents of seed- and soil-borne *Fusarium*-seedling blight of maize. *J. Plant Dis. Prot.* 127, 883–893. doi: 10.1007/s41348-020-00350-w

Kumar, V., Mathela, C. S., Tewari, A. K., and Bisht, K. S. (2014). *In vitro* inhibition activity of essential oils from some Lamiaceae species against phytopathogenic fungi. *Pestic. Biochem. Phys.* 114, 67–71. doi: 10.1016/j.pestbp.2014.07.001

Lai, X., Qi, A., Liu, Y., Mendoza, L. E. D. R., Liu, Z., Lin, Z., et al. (2020). Evaluating inoculation methods to infect sugar beet with *Fusarium oxysporum* f. *betae* and *F. secorum*. *Plant Dis.* 104, 1312–1317. doi: 10.1094/PDIS-09-19-1895-RE

Larena, I., Sabuquillo, P., Melgarejo, P., and De Cal, A. (2003). Biocontrol of *Fusarium* and *Verticillium* wilt of tomato by *Penicillium oxalicum* under greenhouse and field conditions. *J. Phytopathol.* 151, 507–512. doi: 10.1046/j.1439-0434.2003.00762.x

La Torre, A., Caradonia, F., Matere, A., and Battaglia, V. (2016). Using plant essential oils to control *Fusarium* wilt in tomato plants. *Eur. J. Plant Pathol.* 144, 487–496. doi: 10.1007/s10658-015-0789-2

Li, Y., Fabiano-Tixier, A.-S., and Chemat, F. (2014). "Essential oils: from conventional to green extraction," in *Essential oils as reagents in green chemistry*. Eds. Y. Li, A. S. Fabiano-Tixier and F. Chema (Switzerland: Springer Cham), 9–20.

Linde, J. H., Combrinck, S., Regnier, T. J. C., and Virijevic, S. (2010). Chemical composition and antifungal activity of the essential oils of *Lippia rehmannii* from South Africa. *S. Afr. J. Bot.* 76, 37–42. doi: 10.1016/j.sajb.2009.06.011

Lu, M., Han, Z., and Yao, L. (2013). *In vitro* and in *vivo* antimicrobial efficacy of essential oils and individual compounds against *Phytophthora parasitica* var. *nicotianae*. *J. Appl. Microbiol.* 115, 187–198. doi: 10.1111/jam.12208

Ma, D., Cui, X., Zhang, Z., Li, B., Xu, Y., Tian, S., et al. (2019). Honokiol suppresses mycelial growth and reduces virulence of *Botrytis cinerea* by inducing autophagic activities and apoptosis. *Food Microbiol.* 88, 103411. doi: 10.1016/j.fm.2019.103411

Mączka, W., Twardawska, M., Grabarczyk, M., and Wińska, K. (2023). Carvacrol-a natural phenolic compound with antimicrobial properties. *Antibiotics.* 12, 824. doi: 10.3390/antibiotics12050824

Mahdavikia, F., and Saharkhiz, M. J. (2015). Phytotoxic activity of essential oil and water extract of peppermint (Mentha × piperita L. CV. Mitcham). *J. Appl. Res. Med. Aromat. Plants.* 2, 146–153. doi: 10.1016/j.jarmap.2015.09.003

Mbega, E. R., Mabagala, R. B., Mortensen, C. N., and Wulff, E. G. (2012). Evaluation of essential oils as seed treatment for the control of Xanthomonas spp. associated with the bacterial leaf spot of tomato in Tanzania. *J. Plant Pathol.* 94, 273–281.

Mechergui, K., Coelho, J. A., Serra, M. C., Lamine, S. B., BoukhChina, S., and Khouja, M. L. (2010). Essential oils of *Origanum vulgare* L. subsp. *glandulosum* (Desf.) Ietswaart from Tunisia: chemical composition and antioxidant activity. *J. Sci. Food. Agric.* 90, 1745–1749. doi: 10.1002/jsfa.v90:10

Mendgen, K., Hahn, M., and Deising, H. (1996). Morphogenesis and mechanisms of penetration by plant pathogenic fungi. *Annu. Rev. Phytopathol.* 34, 367–386. doi: 10.1146/annurev.phyto.34.1.367

Mirmajlessi, S. M., Safaie, N., Mostafavi, H., Mansouripour, S. M., and Mahmoudy, S. B. (2012). Genetic diversity among crown and root rot isolates of *Rhizoctonia solani* isolated from cucurbits using PCR based techniques. *Afr. J. Agric. Res.* 7, 583–590. doi: 10.5897/AJAR11.1453

Moungthipmalai, T., Puwanard, C., Aungtikun, J., Sittichok, S., and Soonwera, M. (2023). Ovicidal toxicity of plant essential oils and their major constituents against two mosquito vectors and their non-target aquatic predators. *Sci. Rep.* 13, 2119. doi: 10.1038/s41598-023-29421-2

Mowlick, S., Inoue, T., Takehara, T., Kaku, N., Ueki, K., and Ueki, A. (2013). Changes and recovery of soil bacterial communities influenced by biological soil disinfestation as compared with chloropicrin-treatment. *AMB Express.* 3, 1–12. doi: 10.1186/2191-0855-3-46

Najdabbasi, N., Mirmajlessi, S. M., Dewitte, K., Landschoot, S., Mänd, M., Audenaert, K., et al. (2020). Biocidal activity of plant-derived compounds against *Phytophthora infestans*: An alternative approach to late blight management. *Crop Prot.* 138, 105315. doi: 10.1016/j.cropro.2020.105315

Nazzaro, F., Fratianni, F., Coppola, R., and Feo, V. D. (2017). Essential oils and antifungal activity. *Pharm. (Basel).* 10, 86. doi: 10.3390/ph10040086

Neri, F., Mari, M., and Brigati, S. (2006). Control of *Penicillium expansum* by plant volatile compounds. *Plant Pathol.* 55, 100–105. doi: 10.1111/j.1365-3059.2005.01312.x

Noor, A., and Khan, M. F. R. (2015). Efficacy and safety of mixing azoxystrobin and starter fertilizers for controlling *Rhizoctonia solani* in sugar beet. *Phytoparasitica.* 43, 51–55. doi: 10.1007/s12600-014-0416-3

Nucci, M., and Anaissie, E. (2007). *Fusarium* infections in immunocompromised patients. *Clin. Microbiol. Rev.* 20, 695–704. doi: 10.1128/CMR.00014-07

O'Donnell, K., Kistler, H. C., Cigelnik, E., and Ploetz, R. C. (1998). Multiple evolutionary origins of the fungus causing Panama disease of banana: concordant evidence from nuclear and mitochondrial gene genealogies. *PNAS.* 95, 2044–2049. doi: 10.1073/pnas.95.5.204

Orzali, L., Forni, C., and Riccioni, L. (2014). Effect of chitosan seed treatment as elicitor of resistance to *Fusarium graminearum* in wheat. *Seed Sci. Technol.* 42, 132–149. doi: 10.15258/sst.2014.42.2.03

Orzali, L., Valente, M. T., Scala, V., Loreti, S., and Pucci, N. (2020). Antibacterial activity of essential oils and Trametes versicolor extract against *Clavibacter michiganensis* subsp. *michiganensis* and *Ralstonia solanacearum* for seed treatment and development of a rapid *in vivo* assay. *Antibiotics.* 9, 628. doi: 10.3390/antibiotics9090628

Pane, C., Villecco, D., and Zaccardelli, M. (2017). Combined use of *Brassica carinata* seed meal, thyme oil and a *Bacillus amyloliquefaciens* strain for controlling three soil-borne fungal plant diseases. *J. Plant Pathol.* 99, 77–84. doi: 10.4454/jpp.v99i1.3829

Parikh, L., Agindotan, B. O., and Burrows, M. E. (2021). Antifungal activity of plant-derived essential oils on pathogens of pulse crops. *Plant Dis.* 105, 1692–1701. doi: 10.1094/PDIS-06-20-1401-RE

Pavoni, L., Maggi, F., Mancianti, F., Nardoni, S., Ebani, V. V., Cespi, M., et al. (2019). Microemulsions: an effective encapsulation tool to enhance the antimicrobial activity of selected EOs. *J. Drug Deliv. Sci. Technol.* 53, 101101. doi: 10.1016/j.jddst.2019.05.050

Perczak, A., Gwiazdowska, D., Gwiazdowski, R., Juś, K., Marchwińska, K., and Waśkiewicz, A. (2019). The inhibitory potential of selected essential oils on Fusarium spp. growth and mycotoxins biosynthesis in maize seeds. *Pathogens.* 9, 23. doi: 10.3390/pathogens9010023

Pérez-Alfonso, C. O., Martínez-Romero, D., Zapata, P. J., Serrano, M., Valero, D., and Castillo, S. (2012). The effects of essential oils carvacrol and thymol on growth of *Penicillium digitatum* and *P. italicum* involved in lemon decay. *Int. J. Food Microbiol.* 158, 101–106. doi: 10.1016/j.ijfoodmicro.2012.07.002

Prakash, B., Gupta, V., and Raghuvanshi, T. S. (2024). Essential oils as green promising alternatives to chemical preservatives for agri-food products: New insight into molecular mechanism, toxicity assessment, and safety profile. *Food Chem. Toxicol.* 183, 114241. doi: 10.1016/j.fct.2023.114241

Rasooli, I., Rezaei, M. B., and Allameh, A. (2006). Growth inhibition and morphological alterations of *Aspergillus Niger* by essential oils from *Thymus eriocalyx* and *Thymus xporlock*. *Food Contr* 17, 359–364. doi: 10.1016/j.foodcont.2004.12.002

Regnier, T., Combrinck, S., Veldman, W., and Du Plooy, W. (2014). Application of essential oils as multi-target fungicides for the control of *Geotrichum citri-aurantii* and other postharvest pathogens of citrus. *Ind. Crops Prod.* 61, 151–159. doi: 10.1016/j.indcrop.2014.05.052

Ribeiro, L. R., da Luz, L. A., Silva, S. O., Bragança, C. A. D., Amorim, E. P., and Haddad, F. (2015). "Teste de agressividade de haplótipos de *Fusarium oxysporum* f. sp. *cubense* oriundos de regiões produtoras," in *II Simpósio Internacional de Fruticultura - Pragas Quarentenárias e Melhoramento Preventivo*. Eds. D. Haroldo, R. C. Reinhardt and F. L. Ferraz (Salvador-BA: Embrapa Brasília), 51–52.

Rocha, I., Ma, Y., Souza-Alonso, P., Vosátka, M., Freitas, H., and Oliveira, R. S. (2019). Seed coating: a tool for delivering beneficial microbes to agricultural crops. *Front. Plant Sci.* 6. doi: 10.3389/fpls.2019.01357

Sardi, J. D. C. O., Pitangui, N. D. S., Rodríguez-Arellanes, G., Taylor, M. L., Fusco-Almeida, A. M., and Mendes-Giannini, M. J. S. (2014). Highlights in pathogenic fungal biofilms. *Rev. Iberoam. De. Micol.* 31, 22–29. doi: 10.1016/j.riam.2013.09.014

Sarkhosh, A., Schaffer, B., VargaS, A. I., Palmateer, A. J., Lopez, P., and Soleymani, A. (2018). *In vitro* evaluation of eight plant essential oils for controlling *Colletotrichum, Botryosphaeria, Fusarium* and *Phytophthora* fruit rots of avocado, mango and papaya. *Plant Protect. Sci.* 54, 153–162. doi: 10.17221/49/2017-PPS

Schnitzler, P., Koch, C., and Reichling, J. (2007). Susceptibility of drug-resistant clinical herpes simplex virus type 1 strains to essential oils of ginger, thyme, hyssop, and sandalwood. *Antimicrob. Agents Chemother.* 51, 1859–1862. doi: 10.1128/AAC.00426-06

Sharma, A., Rajendran, S., Srivastava, A., Sharma, S., and Kundu, B. (2017). Antifungal activities of selected essential oils against *Fusarium oxysporum* f. sp. lycopersici 1322, with emphasis on *Syzygium aromaticum* essential oil. *J. Biosci. Bioeng.* 123, 308–313. doi: 10.1016/j.jbiosc.2016.09.011

Shcherbakova, L., Mikityuk , O., Arslanova , L., Stakheev , A., Erokhin , D., Zavriev , S., et al. (2021). Studying the ability of thymol to improve fungicidal effects of tebuconazole and difenoconazole against some plant pathogenic fungi in seed or foliar treatments. *Front. Microbiol.* 12. doi: 10.3389/fmicb.2021.629429

Sivalingam, S., Sharmila, J. S., Golla, G., Arunachalam, L., Singh, T., Karthikeyan, G., et al. (2024). Encapsulation of essential oil to prepare environment friendly nanobio-fungicide against *Fusarium oxysporum* f.sp. *lycopersici*: An experimental and molecular dynamics approach. Colloids and Surfaces A: Physicochemical and Engineering Aspects. *Colloid Surface A*. 681, 132681. doi: 10.1016/j.colsurfa.2023.132681

Somda, I., Leth, V., and Sereme, P. (2007). Antifungal effect of *Cymbopogon citratus*, *Eucalyptus camaldulensis* and *Azadirachta indica* oil extracts on sorghum seed-borne fungi. *Asian J. Plant Sci.* 6, 1182–1189. doi: 10.3923/ajps.2007.1182.1189

Soylu, E. M., Soylu, S., and Kurt, S. (2006). Antimicrobial activities of the essential oils of various plants against tomato late blight disease agent *Phytophthora infestans*. *Mycopathologia.* 161, 119–128. doi: 10.1007/s11046-005-0206-z

Soylu, S., Yigitbas, H., Soylu, E. M., and Kurt, S. (2007). Antifungal effects of essential oils from oregano and fennel on *Sclerotinia sclerotiorum*. *J. Appl. Microbiol.* 103, 1021–1030. doi: 10.1111/jam.2007.103.issue-4

Stevic, T., Berić, T., Šavikin, K., Soković, M., Gođevac, D., Dimkić, I., et al. (2014). Antifungal activity of selected essential oils against fungi isolated from medicinal plant. *Ind. Crops Prod.* 55, 116–122. doi: 10.1016/j.indcrop.2014.02.011

Sumalan, R. M., Alexa, E., Popescu, I., Negrea, M., Radulov, I., Obistioiu, D., et al. (2019). Exploring ecological alternatives for crop protection using *Coriandrum sativum* essential oil. *Molecules.* 24, 2040. doi: 10.3390/molecules24112040

Tejeswini, M. S., Sowmya, H. V., Swarnalatha, S. P., and Negi, P. S. (2014). Antifungal activity of essential oils and their combinations in *in vitro* and in *vivo* conditions. *Arch. Phytopathol. Plant Prot.* 47, 564–570. doi: 10.1080/03235408.2013.814235

Terzić, D., Tabaković, M., Oro, V., Poštić, D., Štrbanović, R., and Filipović,V.R. (2023). Impact of essential oils on seed quality and seed-borne pathogens of Althea officinalis seeds of different ages. *Chem. Biol. Technol. Agric.* 10, 33. doi: 10.1186/s40538-023-00405-8

Tolouee, M., Alinezhad, S., Saberi, R., Eslamifar, A., Zad, S. J., Jaimand, K., et al. (2010). Effect of *matricaria chamomilla* L. flower essential oil on the growth and ultrastructure of *Aspergillus Niger* van Tieghem. *Int. J. Food Microbiol.* 139, 127–133. doi: 10.1016/j.ijfoodmicro.2010.03.032

Tu, Q. B., Wang, P. Y., Sheng, S., Xu, Y., Wang, J.-Z., You, S., et al. (2020). Microencapsulation and antimicrobial activity of plant essential oil against *Ralstonia solanacearum*. *Waste Biomass Valor.* 11, 5273–5282. doi: 10.1007/s12649-020-00987-6

Turek, C., and Stintzing, F. C. (2013). Stability of essential oils: a review. *Comp. Rev. Food Sci. Food Safe.* 12, 40–53. doi: 10.1111/1541-4337.12006

Van Der Wolf, J. M., Birnbaum, Y., van der Zouwen, P. S., and Groot, S. P. C. (2008). Disinfection of vegetable seed by treatment with essential oils, organic acids and plant extracts. *Seed Sci. Technol.* 36, 7688. doi: 10.15258/sst.2008.36.1.08

Van Peer, R., and Schippers, B. (1992). Lipopolysaccharides of plant-growth promoting Pseudomonas sp. strain WCS417r induce resistance in carnation to *Fusarium* wilt. *Eur. J. Plant Pathol.* 98, 129–139. doi: 10.1007/BF01996325

Weisany, W., Amini, J., Samadi, S., Hossaini, S., Yousefi, S., and Struik, P. C. (2019). Nano silver-encapsulation of *Thymus daenensis* and *Anethum graveolens* essential oils enhances antifungal potential against strawberry anthracnose. *Ind. Crop Prod.* 141, 111808. doi: 10.1016/j.indcrop.2019.111808

Weisany, W., Yousefi, S., Tahir, N. A. R., Zadeh, N. G., McClements, D. J., Adhikari, B., et al. (2022). Targeted delivery and controlled released of essential oils using nanoencapsulation: A review. *Adv. Colloid Interface Sci.* 303, 102655. doi: 10.1016/j.cis.2022.102655

White, T. J., Bruns, T. D., Lee, S. B., and y Taylor, J. W. (1990). "Amplification and direct sequencing of fungal ribosomal RNA genes for phylogenetics," in *PCR protocols: A Guide to Methods and Applications*. Eds. M. A. Innis, D. H. Gelfand, J. J. Sninsky and T. J. White (Academic Press, New York, NY), 315–322.

Zhang, J., Ma, S., Du, S., Chen, S., and Sun, H. (2019). Antifungal activity of thymol and carvacrol against postharvest pathogens *Botrytis cinerea*. *J. Food Sci. Technol.* 56, 2611–2620. doi: 10.1007/s13197-019-03747-0

Zhang, Y., Niu, Y., Luo, Y., Ge, M., Yang, T., Yu, L., et al. (2014). Fabrication, characterization and antimicrobial activities of thymol loaded zein nanoparticles stabilized by sodium caseinate chitosan hydrochloride doub layers. *Food Chem.* 142, 269–275. doi: 10.1016/j.foodchem.2013.07.058

Zimmermann, R. C., Poitevin, C. G., da Luz, T. S., Mazarotto, E. J., Furuie, J. L., Martinset, C. E. N., et al. (2023). Antifungal activity of essential oils and their combinations against storage fungi. *Environ. Sci. pollut. Res.* 30, 48559–48570. doi: 10.1007/s11356-023-25772-5

frontiers | Frontiers in Plant Science

TYPE Original Research
PUBLISHED 26 September 2024
DOI 10.3389/fpls.2024.1446062

OPEN ACCESS

EDITED BY
Mahyar Mirmajlessi,
Ghent University, Belgium

REVIEWED BY
Yogesh Vikal,
Punjab Agricultural University, India
Hong-Bin Zhang,
Texas A and M University, United States

*CORRESPONDENCE
Yuanzhang Guo
hbsesameg@sina.com

RECEIVED 08 June 2024
ACCEPTED 05 September 2024
PUBLISHED 26 September 2024

CITATION
Xu G, Cui Y, Li S, Guan Z, Miao H and Guo Y (2024) High-density genetic map construction and QTL mapping to identify genes for blight defense- and yield-related traits in sesame (*Sesamum indicum* L.). *Front. Plant Sci.* 15:1446062. doi: 10.3389/fpls.2024.1446062

High-density genetic map construction and QTL mapping to identify genes for blight defense- and yield-related traits in sesame (*Sesamum indicum* L.)

Guizhen Xu[1], Yanqin Cui[1], Sida Li[1], Zhongbo Guan[1], Hongmei Miao[2] and Yuanzhang Guo[1]*

[1]Hebei Laboratory of Crop Genetics and Breeding, Institute of Cereal and Oil Crops, Hebei Academy of Agriculture and Forestry Sciences, Shijiazhuang, China, [2]Henan Sesame Research Center, Henan Academy of Agricultural Sciences, Zhengzhou, China

Sesame (*Sesamum indicum* L.) is an important oilseed crop widely cultivated in subtropical and tropical areas. Low genetic yield potential and susceptibility to disease contribute to low productivity in sesame. However, the genetic basis of sesame yield- and disease-related traits remains unclear. Here, we represent the construction of a high-density bin map of sesame using whole genome sequencing of an F2 population derived from 'Yizhi' and 'Mingdeng Zhima'. A total of 2766 Bins were categorized into 13 linkage groups. Thirteen significant QTLs were identified, including ten QTLs related to yield, two QTLs related to Sesame Fusarium wilt (SFW) disease, and one QTL related to seed color. Among these QTLs, we found that SFW-QTL1.1 and SFW-QTL1.2 were major QTLs related to Fusarium wilt disease, explaining more than 20% of the phenotypic variation with LOD > 6. SCC-QTL1.1 was related to seed coat color, explaining 52% of the phenotypic variation with LOD equal to 25.3. This suggests that seed color traits were controlled by a major QTL. Candidate genes related to Fusarium wilt disease and seed color in the QTLs were annotated. We discovered a significant enrichment of genes associated with resistance to late blight. These genes could be spectral disease resistance genes and may have a role in the regulation of Fusarium wilt disease resistance. Our study will benefit the implementation of marker-assisted selection (MAS) for the genetic improvement of disease resistance and yield-related traits in sesame.

KEYWORDS

***Sesamum indicum* L, genetic map, QTL mapping, fusarium wilt disease, yield-related traits**

Introduction

Sesame (*Sesamum indicum* L.), an indispensable oilseed crop renowned for its versatility and nutritional richness, belongs to the genus *Sesamum*, nestled within the expansive Pedaliaceae family of flowering plants. Sesame seeds have a high oil content, ranging from 50% to 60%. They also contain multiple biologically active values of sesame peptides, making them a healthy and nutritious oil crop (Wei et al., 2022). The oil extracted from sesame seeds, known as sesame oil, has a pleasant fragrance. It serves multiple purposes, including being used as a direct food ingredient, a base for ointments, a lubricant, and a detoxifier. Additionally, sesame is abundant in natural antioxidants such as sesamin, sesamol, and sesaminol. These antioxidants have the potential to be utilized as active ingredients in a range of products, such as preservatives, disinfectants, antiviral agents, insecticides, and anti-tuberculosis agents (Mili et al., 2021; Wei et al., 2022). Despite its excellent characteristics, sesame remains under-researched compared to other crops. This is one of the reasons for its low and unstable yield. Since sesame seeds are the primary raw material for production, enhancing the yield of sesame seeds is a subject of concern in both agricultural production and scientific research.

The growth cycle of sesame requires high temperature and high humidity, making it highly susceptible to various pathogenic fungi and resulting in multiple sesame diseases (Chinchilla et al., 2009). Stem rot disease and wilt disease are considered the most serious diseases in sesame production (Kwon et al., 2013; Zhang et al., 2020). *Sclerotinia sclerotiorum* and *Fusarium oxysporum* are the pathogens responsible for stem rot disease and wilt disease, respectively (Duan et al., 2020; Aguilar-Pérez et al., 2022). Current approaches to plant disease defense involve the use of chemical pesticides and improved cultivation methods. However, these methods are costly and fail to address the root causes of plant diseases. Biotechnological approaches, utilizing molecular biology techniques, have emerged as a precise and expedited methods for enhancing disease resistance in plants. Plants primarily employ pathogen-associated molecular patterns (PAMPs)-triggered immunity and effector-triggered immunity in response to pathogen invasion (Asai et al., 2002; Boller and He, 2009; Chinchilla et al., 2009). The CaAMP1 gene enhances the resistance to stem wilt disease in soybeans, while ZmWRKY83 enhances resistance to *Fusarium graminearum* rot infection in maize (Niu et al., 2020; Bai et al., 2021). Although plant-pathogen interaction pathways have been established in model plants, there is still a significant amount of unknown information.

Currently, significant progress has been made in sequencing and assembly of high-quality plant genomes, providing necessary gene sequence references for genome resequencing (Huang et al., 2009; Li et al., 2020; Sun et al., 2022). Genome resequencing provides a large number of variant sites, such as single nucleotide polymorphisms (SNPs), copy number variations (CNVs), and insertion/deletion (InDel) mutations, enabling efficient and accurate acquisition of genetic characteristics of biological populations (Huang et al., 2009; Zegeye et al., 2018). Analyzing the genetic characteristics of biological populations reveals the population's evolutionary history, gene flow, and adaptation to environmental changes. This understanding helps us comprehend the mechanisms and patterns of biological evolution (Chen and Narum, 2021; North et al., 2021; Wang et al., 2022). These genetic characteristics can assess the species adaptability, genetic health status, and degree of endangerment, leading to the development of effective conservation strategies and promoting biodiversity protection and sustainable utilization (Chen and Narum, 2021; Wang et al., 2022). Moreover, they can identify genes with beneficial traits, improving crop varieties, enhancing yield, resistance, and other economic traits, and promoting sustainable agricultural development (Huang et al., 2009; Zegeye et al., 2018; Pawlowski et al., 2020). Obtaining the genetic characteristics of biological populations provides fundamental data and references for scientific research and practical applications in plant science, with wide-ranging applications in plant research.

Materials and methods

Plant materials and growing environment

In total, 169 individuals and two parents ('Yizhi' and 'Mingdeng Zhima') were collected for genome resequencing. Plants were grown on sandy or loamy soil with medium to high fertility. Plants were 16.5 cm apart with a row-to-row distance of 40 cm, totaling 10,000 plants per acre.

Collection and analysis of phenotypic data

Data were collected on eleven phenotypic traits, including plant height (PH), first capsule height (CH), capsules length (CL), infertile top length (ITL), seeds per capsule (SPC), capsules per plant (CPP), 1000-seed weight (SW), yield per plant (YPP), number of capsule layers (NCL), sesame fusarium wilt (SFW) and seed coat color (SCC). To determine the phenotypic traits of sesame more accurately, we divided its growth cycles into ten stages, as shown in Supplementary Table S11. The criteria for the measurement of 11 phenotypic traits are shown in Supplementary Table S12. Three biological replicates were recorded.

Genomic DNA extraction and genotyping

Young leaves were collected from parental plants and F2 progeny in liquid nitrogen and stored at −80°C. The plant DNA extraction Kit (Tiangen Biotech, Beijing, China) was used to extract the genomic DNA. The quality of the isolated DNA was checked using agarose gel electrophoresis and assessed using a Qubit 2.0 Fluorometer (Thermo Fisher, CA, USA). Paired-end sequencing libraries with 150 bp insert-sizes were constructed. Over 10 Gb clean data were generated for each sample using the Illumina Casava 1.8 platform. The parental DNA samples were replicated to detect SNPs and estimate marker segregation types. The raw sequencing data were filtered to get high-quality clean reads. Clean reads of all samples of parents and offspring were mapped to the

reference genome of *S. indicum* Zhongzhi13_v2.0 using Burrows-Wheeler Aligner (BWA) v0.7.10. Calibrated alignments were used to call genomic variants using the HaplotypeCaller Genome Analysis Toolkit (GATK) v4.2. The raw SNPs and Indel variants were filtered using the following parameters: 'QD < 2.0 || MQ < 40.0 || FS > 60.0 || QUAL <30.0 ||-clusterSize 2-clusterWindowSize 5'. The identified SNPs and indels were annotated using SnpEff v4.3T tool software.

Linkage map construction using the F2 population

To ensure the accuracy of the linkage map, we selected markers that were homozygous and inconsistent between parents with a sequencing depth of more than four and removed non-chromosomal markers. Markers with more than 30% missing data were filtered. A total of 110345 SNPs were obtained to construct linkage map. Chromosome number and order of markers were anchored according to the physical map. HighMap was used to estimate the genetic distance between markers (Liu et al., 2014). The process involved: (1) data input and preprocessing; (2) Identifying linkage groups; (3) sorting and reordering markers to optimize their positions along the linkage groups; (4) performing genotype error correction to further improve the genetic map's quality; (5) estimating the genetic distance between markers based on the corrected marker order; (6) Assessing the quality of the genetic map. Recombination frequency was converted into map distance by the Kosambi mapping function. R package LinkageMapView was used for visualization of the linkage map.

QTL mapping for fusarium wilt defense- and yield-related traits

The algorithm of composite interval mapping (CIM) for the F2 population implemented by R/qtl was used for QTL mapping of the eleven traits. The LOD threshold was set at 3.0. The scanning step was 0.5 cM. The two probabilities for entering and removing variables were set at 0.001 and 0.002, respectively. Comparison of QTL mapping results among the eleven traits was conducted. QTLs in different traits were considered to be common if the genetic positions were close enough (linkage map was less than 20 cM in terms of QTL positions. ShinyCircos was used for the visualization of QTL positions on the linkage map.

Candidate gene identification and annotation

We detected the genes in the QTL region based on the functional annotation of *S. indicum* reference genome Zhongzhi13_v2.0 (Basak et al., 2019). The gene annotations were screened for polymorphism at the amino acid level between the re-sequenced parents. Genes showing more than one changes at the amino acid level were considered candidates. For detailed functional annotation, we compared the candidates with the NR protein sequences available at UniProt database using the BLASTX algorithm, with an E-value threshold of 10^{-01}. The associated hits were then searched for their respective Gene Ontology (GO) terms at www.geneontology.org and Kyoto Encyclopedia of Genes and Genomes (KEGG) pathway at https://www.genome.jp/kegg/.

Results

Phenotypic evaluation and correlation analysis among eleven traits

Phenotypic data were collected for 11 agronomic traits of sesame to examine the correlation among them. All traits exhibited normal distributions, with no significant skewness (Figure 1A). All the traits showed a small skewness and kurtosis values with low standard error. However, seeds per capsule stood out with high skewness and kurtosis values (Supplementary Table S1). Strong correlations were among between several traits (Figure 1B). For instance, there were significant positive correlations between 1000-seed weight (SW) and capsule length (CL), Number of capsule layers (NCL), and plant height (PH), NCL. There were positive correlations between capsules per plant (CPP), as well as yield per plant (YPP) and CPP. On the other hand, NCL and infertile top length (ITL) showed strong negative correlations (Figure 1B).

Genome resequencing and genotyping

Parent 'Yizhi' produced a total of 10.35 Gb of clean data, and parent 'Mingdeng Zhima' produced 9.23 Gb of clean data. The total data volume of the 169 descendants was 486.10 Gb. The GC percentage ranged from 33.74% to 41.13% and the Q30 was above 88% (Supplementary Table S2).

The data reliability can be seen from a negligible single base error rate along the read position, which was maintained under 0.006% (Supplementary Figure S1A). The total GC content was well below 40% (Supplementary Figure S1B). Moreover, the AT and CG bases were basically not separated, and the curve was relatively flat, indicating that the sequencing results were normal (Supplementary Figure S1B).

The average depth of coverage of parents and offspring and the corresponding proportion of genome coverage are shown in Supplementary Table S3. It ccan be seen that the average coverage depth of the parent genome was more than 20X. The average coverage of the genome was more than 90% (at least 1X coverage). The average coverage depth of the offspring samples was 9.01X, and the coverage was more than 97.79% (at least 1X coverage). Poor coverage may be due to improper assembly of the reference genome or a distant relation to the parent, making it impossible to compare sequencing data to the reference genome. In general, the distribution of base coverage depth on the genome indicates a higher level of sequencing randomness.

Construction of high-density linkage bin map and evaluation

Based on the available information, a total of 2766 bins were divided into 13 linkage groups (Figure 2A). The HighMap software analysis enabled the determination of the linear arrangement of markers within each linkage group, and estimation of the genetic distance between adjacent markers. Ultimately, a genetic map with a total map distance of 1850.52 cM was obtained.

The statistics of the number of bins, total genetic distance, average genetic distance, maximum gap distance and proportion of gap less than 5 cM of each linkage group are shown in Table 1. Graphical genotype analysis was performed on 169 offsprings using 2766 bin loci, as shown in the Supplementary Figure S2. Most strains had a small number of chromosomes in their genomes that hadn't undergone recombination, meaning they originated entirely from a single parental genome. There were also some strains with chromosomal segments that are heterozygous, which might be related to incomplete repair or incorrect repair after chromosome exchange.

Collinearity analysis was performed by the position of the marker on the genome and the genetic map (Figure 2B). Spearman correlation coefficient of each linkage group and the physical graph showed the collinear quality (Supplementary Table S4). The closer the Spearman coefficient is to 1, the better the collinearity of the map and the physical map. The correlation coefficient values were all above 0.97, suggesting significant collinearity between linkage groups and physical map.

Population SNP detection and annotation

A total of 1,09,696 alleles were identified among all the samples (Supplementary Table S5). The percentage of 'aa' genotype ranged from 44.82% to 84.24%. However, the 'bb' genotype was less common, accounting for 9.44%–52.25%. The 'ab' genotype showed a narrow range, varying from 2.39% to 23.26%. The rate of missing alleles ranged from 1.41% to 15.8%, indicating a relatively low proportion of missing alleles (Supplementary Table S5). The SNP variation had two types, including conversion and reversal. A total of 5,56,668 SNPs were detected with a conversion/reversal (Ti/Tv) ratio of 1.78 (Supplementary Table S6). The ratio of heterozygosity ranged from 21.48% to 68.16%.

By determining the location of the variant site on the reference genome and using gene position information, we identified the specific region in the genome where the variant occured. Additionally, this allowed us to determine the impact of mutation (Supplementary Figure S3). Most abundant SNP variants occurred in the intergenic (29.29%), upstream (27.83%) and downstream (22.50%) regions. The CDS contained 6.84% of SNP variant sites, which further included synonymous_coding (49.39%) and non-synonymous_coding (48.67%) regions as the effects of mutations (Supplementary Figure S3A). The major distribution sites for InDels included upstream (33.40%), downstream (24.51) and intergenic (24.13%) regions (Supplementary Figure S3B). However, compared to SNPs, only 2.17% of InDels were situated on CDS, which further covered frame_shift (67.68%), codon_deletion (9.18%), and codon_insertion (8.81%) as major effects of mutations (Supplementary Figure S3B).

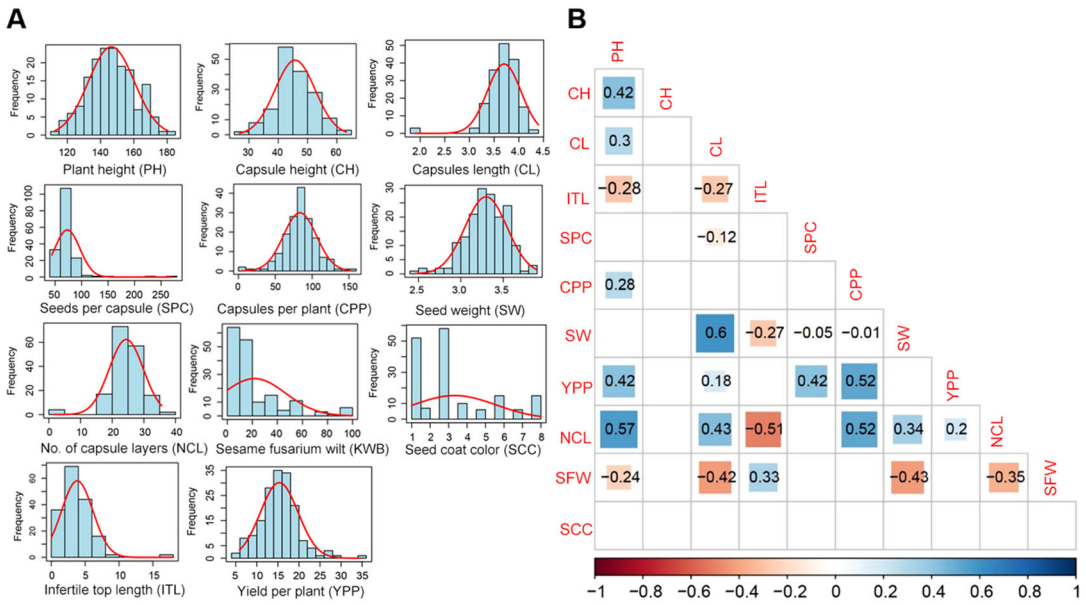

FIGURE 1
Analysis of eleven traits related to growth, yield, and disease resistance. **(A)** Histograms for the frequency distribution of the traits. **(B)** Correlation coefficients and level of significance for the traits of sesame. PH, Plant height; CH, first capsule height; CL, capsule length; ITL, infertile top length; SPC, seeds per capsule; CPP, capsules per plant; SW, 1000-seed weight; YPP, yield per plant; NCL, number of capsule layers; SFW, sesame fusarium wilt; SCC, seed coat color.

10.3389/fpls.2024.1446062

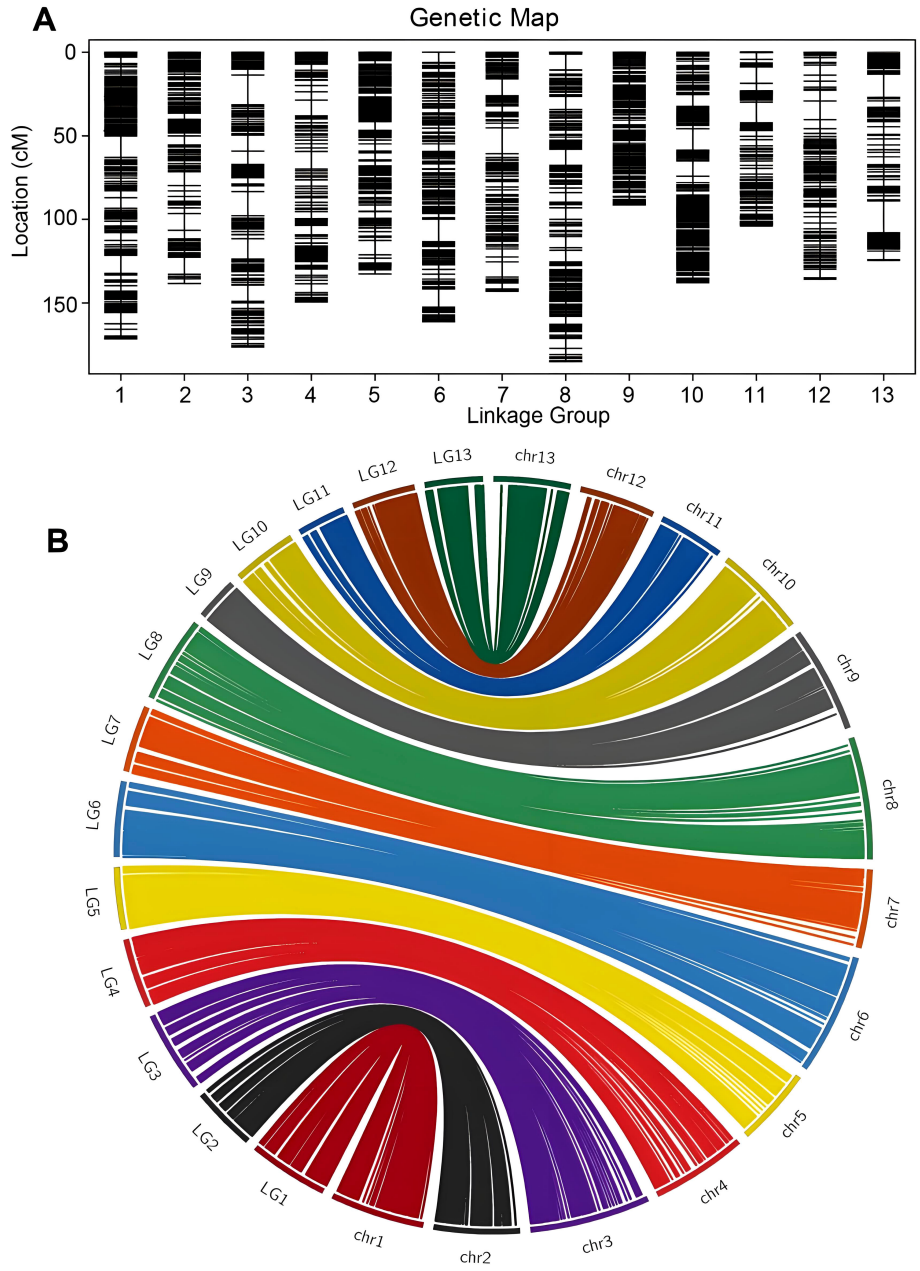

FIGURE 2
High-density genetic bin map construction based on genome resequencing and collinearity analysis of the markers between the genetic map and the physical map. **(A)** Distribution of markers with unique block loci in the genetic linkage bin map of sesame. **(B)** Syntenic analysis of makers between sesame genetic map and *Sesamum indicum* genome via circle diagram.

Detection of QTLs associated with key agronomic traits

Statistical analysis method was used for the identification of significant QTLs that incorporates LOD (Logarithm of Odds) scores and confidence intervals. The text outlines a procedure for using the IM interval mapping method to locate traits. The LOD thresholds were set based on the results of permutation test performed 1000 times. The process considers different confidence levels (0.99, 0.95, and 0.90) for LOD thresholds. If a mapping interval could not be found, the text recommends manually adjusting the threshold. It suggested starting from 3.0 and gradually decreasing it to 2.5 or 2.0 if necessary. Using a threshold of 3, we identified 14 significant QTL sites associated with the agronomic traits of *S. indicum* (Table 2; Figure 3). SS, SG, SW, NCL, and SFW each contained two potential QTL sites; while each of the remaining trait possessed one site. The PVE (phenotypic variance explained) for these QTL sites ranged from 9.16% for NCL-QTL1.1 to 18.23% for SPC-QTL1.1 (Table 2). Except for NCL-QTL1.1, all other QTL sites showed a PVE greater than 10%. SFW-QTL1.1 and SFW-QTL1.2 showed a significant PVE above 20%, while SCC-QTL1.1 had a PVE of 52.72%. The QTL distribution over the genome was not uniform.

10.3389/fpls.2024.1446062

TABLE 1 Summary of the bin map in sesame F2 population.

LG	nloc	nind	sum	gap_5	gap_5 (%)	max gap	Distance (cM)	aver. Distance (cM)
1	355	169	59995	350	0.9887	12.87	171.45	0.48
2	190	169	32110	184	0.9735	10.26	138.3	0.73
3	235	169	39715	228	0.9744	17.78	176.2	0.75
4	149	169	25181	143	0.9662	10.51	149.39	1
5	207	169	34983	204	0.9903	8.6	132.66	0.64
6	233	169	39377	229	0.9871	13.52	161.12	0.69
7	178	169	30082	174	0.9831	15.48	143.02	0.8
8	269	169	45461	260	0.9701	9.58	184.93	0.69
9	215	169	36335	214	1	2.81	91.26	0.42
10	282	169	47658	278	0.9893	12.88	137.93	0.49
11	156	169	26364	153	0.9871	12.19	103.97	0.67
12	155	169	26195	150	0.974	11.2	135.87	0.88
13	142	169	23998	138	0.9787	19.01	124.41	0.88

Among the 14 potential QTL sites, three were located on chromosome 1, whereas each of the chromosome 4, 6, 9 and 13, contained 2 potential QTL sites.

Identification of overlapping QTLs associated with SFW and SCC traits

Two most significant QTLs were identified for sesame fusarium wilt and seed coat color. Two major QTLs of sesame fusarium wilt (SFW-QTL1.1 and SFW-QTL1.2) were located on chromosome 1, each explaining 23.84%–24.8% of the PVE, with an LOD score above 6. These QTLs contained 28 bin markers from locus 121 to 153 (Supplementary Table S7). QTL1.1 occupied 20 loci and the QTL1.2 engaged the remaining 8 loci. The other most important trait was seed coat color with one QTL (SCC-QTL1.1), which was also located on chromosome 1. SCC-QTL1.1 had the highest PV above 50%. This SCC-QTL1.1 contained 11 intervals (Block2445-Block2403) (Supplementary Table S7). However, decreasing the threshold to 3 increased the number of QTLs for sesame fusarium wilt and seed coat color, each accounting for more than 30 QTL bin makers (Figure 4).

TABLE 2 List of QTLs for eight traits identified in sesame F_2 population.

Trait	QTL name	LOD Threshold	Group ID	Start (cM)	End	Peak position (cM)	MaxLOD	ADD	DOM	PVE(%)
PH	PH-QTL1.1	3.2	6	61.761	62.648	62.057	3.649	6.225	-1.108	15.233
CH	CH-QTL1.1	4.5	4	118.264	129.633	124.538	5.554	-2.938	-0.863	13.852
CH	CH-QTL2.1	4.7	11	89.937	102.782	94.713	6.765	-3.362	-0.218	17.906
CL	CL-QTL1.1	3.0	1	34.301	45.547	39.985	3.153	-0.093	0.176	11.017
CL	CL-QTL2.1	4.1	13	110.185	124.408	124.112	6.010	-0.169	0.045	18.621
SPC	SPC-QTL1.1	3.0	8	37.529	39.425	39.425	7.166	32.874	-31.521	18.259
CPP	CPP-QTL1.1	3.0	4	45.176	50.728	49.456	3.605	-6.933	8.873	10.384
SW	SW-QTL1.1	4.7	5	33.403	37.909	36.069	5.704	-0.110	-0.027	14.658
SW	SW-QTL2.1	4.9	13	116.698	124.408	124.112	5.881	-0.121	-0.001	17.588
NCL	NCL-QTL1.1	3.0	9	0.357	1.009	1.009	3.192	-1.857	0.691	9.159
NCL	NCL-QTL1.2	3.0	9	9.828	17.045	14.078	4.287	-2.109	1.832	13.828
SFW	SFW-QTL1.1	6.5	1	36.372	39.985	37.912	7.503	11.909	-15.298	24.852
SFW	SFW-QTL1.2	6.5	1	41.169	44.068	41.760	7.588	11.276	-16.051	23.839
SCC	SCC-QTL1.1	22.2	6	123.487	127.109	125.270	25.294	-1.529	2.059	52.720

10.3389/fpls.2024.1446062

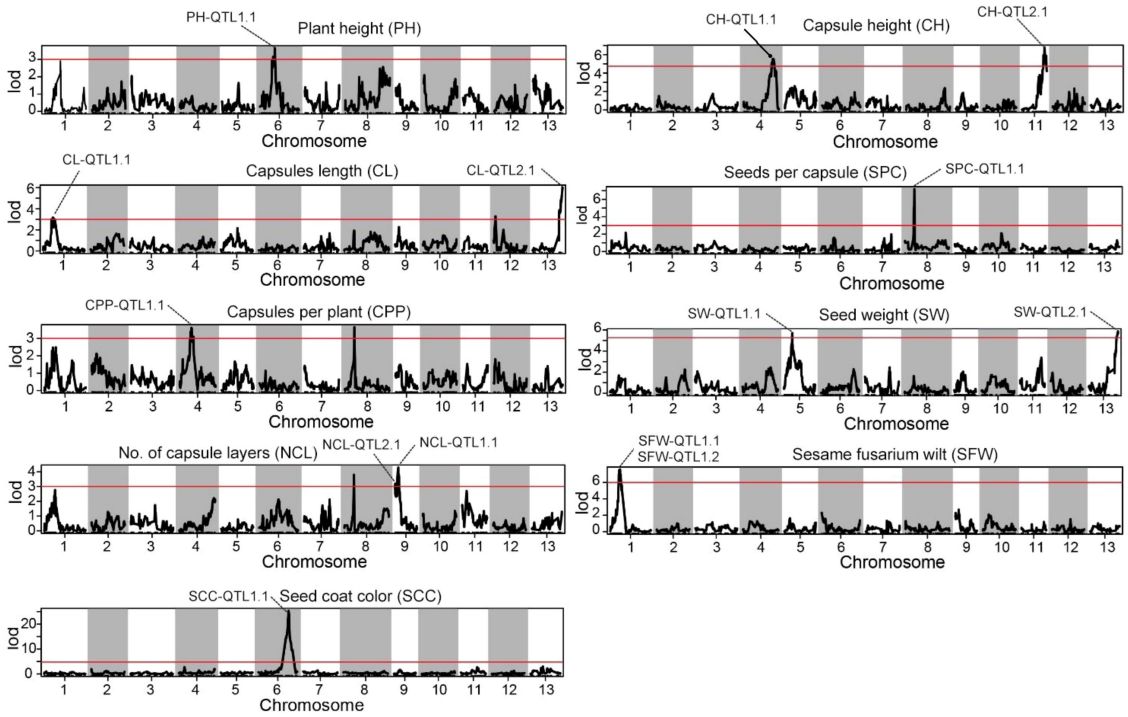

FIGURE 3
Distribution of mapping QTLs with ten different traits on the sesame genetic map. The red lines indicate confidence interval of QTLs with LOD score above threshold 3.0.

Identification and annotation of genes in the QTL intervals

The gene sets associated with QTL intervals were annotated using different annotation platforms and NR annotations of 2762 genes were obtained (Supplementary Table S8). Pentatricopeptide repeat-containing (PPR) proteins were the most abundant annotations among the annotated genes (Figure 5A). PPR proteins regulate plant defense-pathway genes by modulating RNA processing and translation and fine tune the expression of stress-responsive genes. Cytochrome P450 (CYPs) and zinc finger proteins were the second most abundant categories. Regarding the disease resistance, CYPs played important roles. These enzymes involved the biosynthesis of phytoalexins, which were potential secondary metabolites helping plants to cope with pathogenic attack. Moreover, CYPs also contribute to the detoxification of dangerous compounds produced by pathogens and regulate plant defense responses. Among the other categories, protein DETOXIFICATION, LRR receptor-like serine/threonine kinase, putative disease resistance protein, disease resistance protein and late blight resistance protein were the most important gene annotations for plant disease control (Supplementary Table S8; Figure 5A). The annotated genes were located on 8 chromosomes (Figure 5B). Of the 2762 genes, 980 were associated with the QTL intervals positioned on chromosome 13 and 593 were linked with chromosome 6. The lowest were allied with chromosome 8, containing only 9 genes.

sesame fusarium wilt and seed coat color were identified as the most important QTLs and functional annotation of the genes associated with these QTLs were significantly involved in plant immune responses and signal transductions (Figures 5C, D). Two distinct annotation categories were observed in the genes connected with SFW-QTL1.1 and SFW-QTL1.2 (Figure 5C). These were the 'defense mechanisms' and 'secondary metabolite biosynthesis, transport and catabolism', suggesting that SFW could specifically be involved in plant defense and immunity responses. However, multiple regulatory processes were linked with SCC-QTL1.1, including 'signal transduction mechanism', 'posttranslational modification, protein turnover, chaperones', 'cell wall/membrane/envelope biogenesis', 'translation, ribosomal structure and biogenesis', 'lipid transport and metabolism' and 'defense mechanisms' (Figure 5D). This suggested a multi-directional role of SCC-QTL1.1.

Discussion

Genetic analysis of Fusarium wilt defense- and yield-related traits

Plant height, capsule characteristic, yield per plant, and sesame Fusarium wilt disease are important agronomic traits. We used F_2 population from parents with significant differences in traits for an intraspecific cross, and a new sesame high-density genetic map was constructed with 2766 bin loci and identified significant QTLs. For precise QTL mapping results, we performed segregation analysis with a large experimental group and multiple phenotypic indexes. The frequency distribution of phenotypic characters was analyzed,

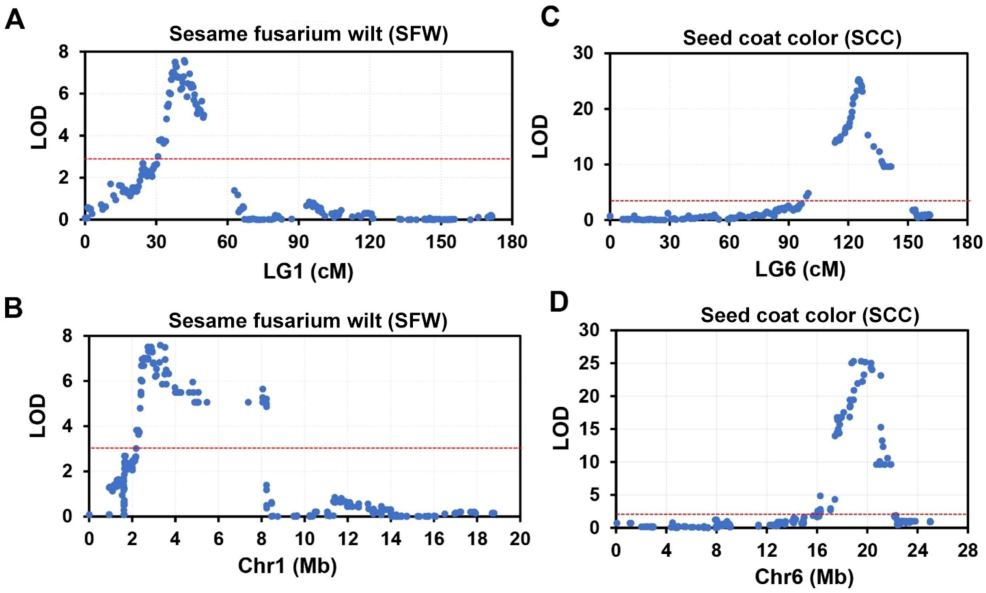

FIGURE 4
The top two significant QTLs for sesame fusarium wilt (SFW) and seed coat color (SCC) on linkage group (LG) 1 and LG6. **(A, B)** Significant QTLs responsible for SFW trait on LG 1 **(A)** and its corresponding physical position on chromosome (Chr) 1 **(B)**. **(C, D)** Significant QTLs responsible for SCC trait on LG 6 **(C)** and its corresponding physical position on Chr6 **(D)**.

revealing a normal distribution and a significant correlation between different traits. This suggests a polygene mode of genetic control.

Significant positive correlations ($P \leq 0.05$) were observed among NCL, PH, CL, CPP, SW. Meanwhile, sesame fusarium wilt related trait SFW was negatively correlated with PH, CL, SW, NCL ($P \leq 0.05$), while it was positively correlated with infertile top length (ITL). Plant height, capsule length, capsules per plant, 1000-seed weight are important factors of sesame yield composition (Monpara, 2016). We analyzed the correlation between the eleven important traits. The results showed that plant height, seeds per capsule, and capsules per plant were positively correlated with yield per plant ($P \leq 0.05$).

The high-yield and disease-resistant varieties are important achievements in sesame breeding, increasing food security. Fusarium wilt of sesame, caused by *Fusarium oxysporum* f. sp. sesami, is a destructive soil-born fungal disease that causes huge economic losses in China (Zhang et al., 2001). Developing a high-yielding, stress-resistant variety is a viable option to address these challenges. Previous studies about Fusarium wilt mainly focused on the molecular characterization of *F. oxysporum* f. sp. Sesami, field trials evaluating and screening sesame resistance to fusarium wilt (Herrera and Laurentin, 2014; Silme and ÇAĞIrgan, 2010; Jyothi et al., 2011; Li et al., 2012). In the genetic and genomic analysis, seven positive markers (five RAPD and two ISSR) linked to Fusarium wilt resistance were found in the line C3.8 (Anter and Ghada, 2021). Transcriptome comparison of resistant and susceptible sesame varieties inoculated with *F. oxysporum* f.sp.sesami showed that phenylpropanoid biosynthesis pathway may play more important role in Fusarium wilt resistance in early stage infection (Wei et al., 2016). A genome-wide association study (GWAS) of an interspecific population and genome comparisons revealed a long terminal repeat insertion and a sequence deletion in DIR genes of wild *Sesamum angustifolium*, while the cultivated sesame independently cause high susceptibility to Fusarium wilt disease (Miao et al., 2024). A study on the inheritance of resistance to Fusarium wilt in sesame indicated that the genetic effect of Fusarium wilt resistance was complex and controlled by dominant, additive, and recessive effect (Wang, 1993; El-Bramawy, 2006).

In the F_2 population, we investigated the segregation of individuals in Fusarium wilt disease resistance. Based on the phenotyping and linkage map, QTLs were identified in LG1, suggesting their important role in disease resistance. The number of genes regulating the Fusarium wilt disease varies in different species of sesame, and different genes and genetic variations are detected for controlling the trait (Wei et al., 2016; Miao et al., 2024). The genetic mechanism of Fusarium wilt disease is still unclear.

Genetic linkage map

QTL mapping is an important method applied to locate the candidate genes controlling specific traits. Genotyping-by-sequencing (GBS) is a high-throughput technique employed to develop SNP markers in a short time for high-density genetic map construction and QTL mapping. To date, this technique has been widely used for locating the key traits in sesame (Zhang et al., 2013; Wu et al., 2014; Du et al., 2019; Yol et al., 2021).

In this study, we constructed a high-density bin map for sesame using the whole genome resequencing approach, achieving mass identification of SNPs and InDels for sesame. We discovered 5,56,668 SNPs. Most of SNPs occurred in the noncoding region of the genome, including intergenic (29.29%), upstream (27.83%) and downstream (22.50%) regions. While only 6.84% of SNPs were located in protein coding region, including synonymous_coding (49.39%) and non-synonymous_coding (48.67%) as the effects of mutations. This

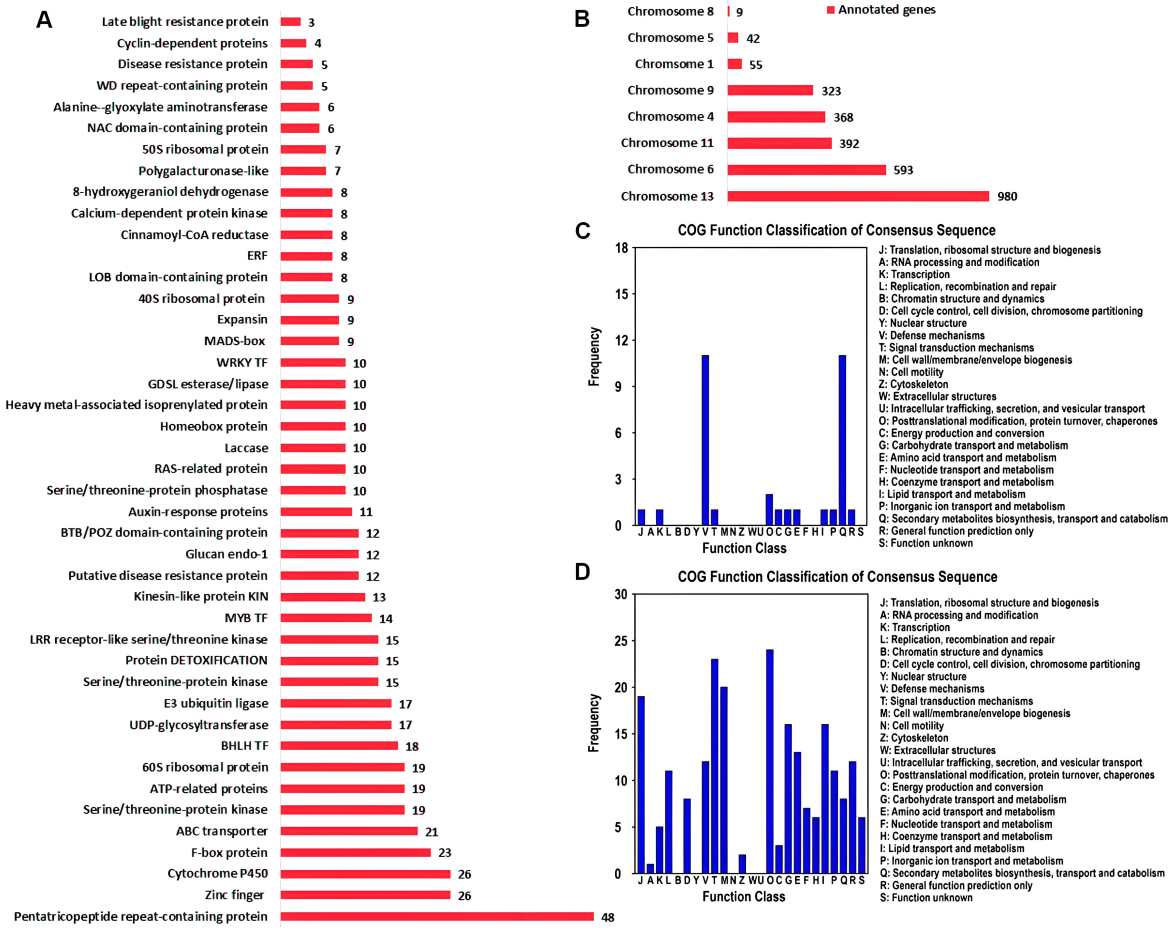

FIGURE 5
Functional enrichment of genes located in the QTL intervals. **(A)** NR annotation summary showing the most abundant gene families. **(B)** The frequency of annotated genes on individual chromosome. **(C)** COG function classification of genes in SFW-QTL1.1 and SFW-QTL1.2 QTL intervals related to SFW trait. **(D)** COG function classification of genes in SCC-QTL1.1 related to SCC trait.

new map has several advantageous features compared to other published genetic maps in sesame. Firstly, larger F_2 segregating populations of 169 individuals were used. Secondly, the map is an ultra-high-density genetic map with 2766 bins, including 1,10,345 SNPs with a sequencing depth more than 4×. Thirdly, the 13 LGs (linkage groups) corresponded to the 13 chromosomes in the sesame karyotype (2n = 26), allowing for precise gene mapping. Lastly, the estimated size of the sesame genome is 1850.52 cM with an average marker distance of 0.67 cM per bin. The marker density is significantly higher than that of previously published maps. Therefore, the map in this study is superior to previously published sesame maps and it can contribute to the development for QTL analysis, gene mapping, and map-based cloning.

QTL identification of seed-related traits

In this study, QTL analysis of 11 important traits in sesame (ten yield related traits and one Fusarium wilt disease evaluation) identified 14 associated regions. All of these QTLs contributed above 10% of the phenotypic variation with LOD > 3, except for NCL-QTL1.1. Eleven QTLs were related to yield, two QTLs were associated with disease resistance, and one QTL was associated with seed coat color.

In the QTLs for yield, PH-QTL1.1, CH-QTL2.1, CL-QTL2.1, SPC-QTL1.1, SW-QTL2.1 played major roles, explaining more than 15.0% of the phenotypic variation. SFW-QTL1.1 and SFW-QTL1.2 are responsible for Fusarium wilt, and explained 24.9% and 23.8% phenotypic variation. These Fusarium wilt related QTLs are reported for the first time in sesame, and their genetic control was mostly comprised of major QTLs with R2 ≥ 20%. An important QTL of seed coat color was detected in LG6 with LOD value equal to 22.2, explaining 52.7% of phenotypic variation. Similar to previous study (Zhang et al., 2013; Wei et al., 2015; Wang et al., 2016; Du et al., 2019; Li et al., 2021), our results also showed that seed color of sesame was controlled by major QTL. However, the number of QTLs regulating seed colors is different among these studies. Zhang et al. (2013) detected four QTLs on three LGs controlling the seed coat color using an F_2 population (Zhang et al., 2013). Wei et al. (2015) identified seven QTLs distributed on three LGs using GWAS strategy (Wei et al., 2015). Du et al. (2019) found seven seed coat color related QTLs on three LGs (Du et al.,

2019). However, only one major QTL on LG6 was identified, suggesting that seed coat color is controlled by multiple major QTLs and their genetic mechanism might be different.

Candidate gene function analysis

In total, there were 2762 candidate genes in the confidence interval with R2 ≥ 9% (Supplementary Tables S8). For yield-related trait, there were 22 functional categories in COG analysis. Carbohydrate transport and metabolism, signal transduction mechanisms, and lipid transport and metabolism harbored a large number of candidate genes. In KEGG analysis, the largest number of genes were enriched in biosynthesis of secondary metabolites and carbon metabolism, harboring 69 genes and 19 genes, respectively. SFW-QTL1.1/SFW-QTL1.2 and SCC-QTL1.1 were identified as the most significant QTLs involved in plant immune responses and signal transduction (Figures 5C, D). KEGG analysis showed two key genes involved in plant-pathogen interaction. One was annotated as putative late blight resistance protein R1A-4 (gene.SIN_1021452), and another was annotated as Rust resistance kinase Lr10 (gene.SIN_1021460). We suggest that genes in SFW-QTL1.1 loci may also play an important role in Sesame Fusarium wilt resistance.

In addition, pentatricopeptide repeat-containing (PPR) proteins were the most abundant annotations among the annotated genes (Figure 5A). PPR proteins regulate plant defense-pathway genes by modulating RNA processing and translation and fine tune the expression of stress-responsive genes. Recently, studies indicated that PPR proteins are essential for plant disease resistance, such as *Fusarium pseudograminearum* in wheat (Wang et al., 2021), *Ralstonia solanacearum* in potato (Park et al., 2016). Moreover, several other genes, including CYPs, DETOXIFICATION, LRR receptor-like serine/threonine kinase, also contribute to the detoxification of dangerous compounds produced by pathogens and might be involved in regulating plant defense responses. The signaling pathways of plant hormones also exhibit cross-talk in plant defense responses, which is an important and efficient strategy to resist the invasion of pathogens (Robert-Seilaniantz et al., 2007). These genes could contribute to disease resistance, plant growth, and ultimately yield-related traits. Our study has identified the QTLs and candidate genes. However, further study is needed to verify the markers nearest to the genes and their functions.

Conclusions

This study is the first to map QTLs for yield-related traits, seed color, and Sesame Fusarium wilt disease in sesame using an F2 population. A high-density map was constructed using 3129 SNP markers. QTL analysis revealed 13 major-effect QTLs, with ten related to yield, two related to Sesame Fusarium wilt disease, and one related to seed color. These QTLs individually explained more than 10% of the phenotypic variation with LOD > 3. Additionally, three QTLs were identified with similar regions and partially explained the correlations among disease-related traits. Two key genes controlling Sesame Fusarium wilt disease were found in the SFW-QTL1.1 and SFW-QTL1.2 intervals (R2 ≥ 20%). This study establishes a strong foundation for further genetic analyses of Fusarium wilt disease related traits in sesame, including map-based gene cloning and marker-assisted selection breeding.

Data availability statement

The data presented in the study are deposited in the National Genomics Data Center (https://ngdc.cncb.ac.cn/) repository, accession number PRJCA025796 and in the Figshare (https://figshare.com/) repository, accession number figshare.27038404 (https://doi.org/10.6084/m9.figshare.27038404).

Author contributions

GX: Conceptualization, Formal analysis, Methodology, Writing – original draft. YC: Investigation, Writing – review & editing. SL: Data curation, Writing – review & editing. ZG: Data curation, Writing – review & editing. HM: Writing – review & editing. YG: Conceptualization, Funding acquisition, Writing – review & editing.

Funding

The author(s) declare financial support was received for the research, authorship, and/or publication of this article. This research was funded by China Agriculture Research System of MOF and MARA (CARS-14) and HAAFS Science and Technology Innovation Project (2022KJCXZX-LYS-16) and Key R&D project of Hebei Province (21326334D).

Conflict of interest

The authors declare that the research was conducted in the absence of any commercial or financial relationships that could be construed as a potential conflict of interest.

Publisher's note

Supplementary material

The Supplementary Material for this article can be found online at: https://www.frontiersin.org/articles/10.3389/fpls.2024.1446062/full#supplementary-material

References

Aguilar-Pérez, V. H., García-León, E., Solano-Báez, A. R., Beltran-Peña, H., Tovar-Pedraza, J. M., and Márquez-Licona, G. (2022). First Report of Collar Rot Caused by Sclerotinia sclerotiorum on Sesame (Sesamum indicum) in Mexico. *Plant Dis*. 107, 957. doi: 10.1094/pdis-06-22-1316-pdn

Anter, A. S., and Ghada, S. M. (2021). Possibility of combining high yield and resistance to fusarium wilt disease using molecular markers in 4 Élite sesame lines. *Turkish. J. Of. Field Crops* 26, 129–138. doi: 10.17557/tjfc.954499

Asai, T., Tena, G., Plotnikova, J., Willmann, M. R., Chiu, W. L., Gomez-Gomez, L., et al. (2002). MAP kinase signalling cascade in Arabidopsis innate immunity. *Nature* 415, 977–983. doi: 10.1038/415977a

Bai, H., Si, H., Zang, J., Pang, X., Yu, L., Cao, H., et al. (2021). Comparative proteomic analysis of the defense response to gibberella stalk rot in maize and reveals that zmWRKY83 is involved in plant disease resistance. *Front. Plant Sci.* 12. doi: 10.3389/fpls.2021.694973

Basak, M., Uzun, B., and Yol, E. (2019). Genetic diversity and population structure of the Mediterranean sesame core collection with use of genome-wide SNPs developed by double digest RAD-Seq. *PloS One* 14, e0223757. doi: 10.1371/journal.pone.0223757

Boller, T., and He, S. Y. (2009). Innate immunity in plants: an arms race between pattern recognition receptors in plants and effectors in microbial pathogens. *Science* 324, 742–744. doi: 10.1126/science.1171647

Chen, Z., and Narum, S. R. (2021). Whole genome resequencing reveals genomic regions associated with thermal adaptation in redband trout. *Mol. Ecol.* 30, 162–174. doi: 10.1111/mec.15717

Chinchilla, D., Shan, L., He, P., de Vries, S., and Kemmerling, B. (2009). One for all: the receptor-associated kinase BAK1. *Trends Plant Sci.* 14, 535–541. doi: 10.1016/j.tplants.2009.08.002

Du, H., Zhang, H., Wei, L., Li, C., Duan, Y., and Wang, H. (2019). A high-density genetic map constructed using specific length amplified fragment (SLAF) sequencing and QTL mapping of seed-related traits in sesame (Sesamum indicum L.). *BMC Plant Biol.* 19, 588. doi: 10.1186/s12870-019-2172-5

Duan, Y., Qu, W., Chang, S., Li, C., Xu, F., Ju, M., et al. (2020). Identification of Pathogenicity Groups and Pathogenic Molecular Characterization of Fusarium oxysporum f. sp. sesami in China. *Phytopathology* 110, 1093–1104. doi: 10.1094/phyto-09-19-0366-r

El-Bramawy, M. A. S. (2006). Inheritance of resistance to Fusarium wilt in some sesame crosses under field conditions. *Plant Prot. Sci.* 42, 99. doi: 10.17221/2755-PPS

Herrera, I., and Laurentin, H. (2014) Sesame evaluation of (*Sesamum indicum* L.) germplasm of the infection caused by Fusarium oxysporum f.sp. sesame. *Revista de la Facultad de Agronomia* 31, 23–38. Available at: https://www.researchgate.net/publication/285255513

Huang, X., Feng, Q., Qian, Q., Zhao, Q., Wang, L., Wang, A., et al. (2009). High-throughput genotyping by whole-genome resequencing. *Genome Res.* 19, 1068–1076. doi: 10.1101/gr.089516.108

Jyothi, B., Ansari, N. A., Vijay, Y., Anuradha, G., Sarkar, A., Sudhakar, R., et al. (2011). Assessment of resistance to Fusarium wilt disease in sesame (*Sesamum indicum* L.) germplasm. *Australas. Plant Pathol.* 40, 471–475. doi: 10.1007/s13313-011-0070-x

Kwon, J. H., Choi, O., and Kim, J. (2013). Fusarium oxysporum Causing Wilt and Stem Rot in Chrysanthemum × morifolium in Korea. *Plant Dis.* 97, 1118. doi: 10.1094/pdis-01-13-0067-pdn

Li, C., Duan, Y., Miao, H., Ju, M., Wei, L., and Zhang, H. (2021). Identification of candidate genes regulating the seed coat color trait in sesame (*Sesamum indicum* L.) using an integrated approach of QTL mapping and transcriptome analysis. *Front. Genet.* 12. doi: 10.3389/fgene.2021.700469

Li, D. H., Wang, L. H., Zhang, Y. X., Lv, H. X., Qi, X. Q., Wei, W. L., et al. (2012). Pathogenic variation and molecular characterization of *Fusarium* species isolated from wilted sesame in China. *Afr. J. OF. Microbiol. Res.* 6, 149–154. doi: 10.5897/AJMR11.1081

Li, X., Yang, J., Shen, M., Xie, X. L., Liu, G. J., Xu, Y. X., et al. (2020). Whole-genome resequencing of wild and domestic sheep identifies genes associated with morphological and agronomic traits. *Nat. Commun.* 11, 2815. doi: 10.1038/s41467-020-16485-1

Liu, D., Ma, C., Hong, W., Huang, L., Liu, M., Liu, H., et al. (2014). Construction and analysis of high-density linkage map using high-throughput sequencing data. *PloS One* 9, e98855. doi: 10.1371/journal.pone.0098855

Miao, H., Wang, L., Qu, L., Liu, H., Sun, Y., Le, M., et al. (2024). Genomic evolution and insights into agronomic trait innovations of Sesamum species. *Plant Commun.* 5, 100729. doi: 10.1016/j.xplc.2023.100729

Mili, A., Das, S., Nandakumar, K., and Lobo, R. (2021). A comprehensive review on Sesamum indicum L.: Botanical, ethnopharmacological, phytochemical, and pharmacological aspects. *J. Ethnopharmacol.* 281, 114503. doi: 10.1016/j.jep.2021.114503

Monpara, B. A. (2016). Sesame germplasm evaluation for reproductive period and harvest index. *Genetika-belgrade* 48, 665–674. doi: 10.2298/GENSR1602665M

Niu, L., Zhong, X., Zhang, Y., Yang, J., Xing, G., Li, H., et al. (2020). Enhanced tolerance to Phytophthora root and stem rot by over-expression of the plant antimicrobial peptide CaAMP1 gene in soybean. *BMC Genet.* 21, 68. doi: 10.1186/s12863-020-00872-0

North, H. L., McGaughran, A., and Jiggins, C. D. (2021). Insights into invasive species from whole-genome resequencing. *Mol. Ecol.* 30, 6289–6308. doi: 10.1111/mec.15999

Park, S., Gupta, R., Krishna, R., Kim, S. T., Lee, D. Y., Hwang, D. J., et al. (2016). Proteome Analysis of Disease Resistance against Ralstonia solanacearum in Potato Cultivar CT206-10. *Plant Pathol. J.* 32, 25–32. doi: 10.5423/ppj.Oa.05.2015.0076

Pawlowski, M. L., Vuong, T. D., Valliyodan, B., Nguyen, H. T., and Hartman, G. L. (2020). Whole-genome resequencing identifies quantitative trait loci associated with mycorrhizal colonization of soybean. *Theor. Appl. Genet.* 133, 409–417. doi: 10.1007/s00122-019-03471-5

Robert-Seilaniantz, A., Navarro, L., Bari, R., and Jones, J. D. (2007). Pathological hormone imbalances. *Curr. Opin. IN. Plant Biol.* 10, 372–379. doi: 10.1016/j.pbi.2007.06.003

Silme, R. S., and ÇAĞIrgan, M.İ. (2010). Screening for resistance to Fusarium wilt in induced mutants and world collection of sesame under intensive management. *Turkish. J. Field Crops* 15, 89–93. doi: 10.3906/tar-0911-59

Sun, Y., Shang, L., Zhu, Q. H., Fan, L., and Guo, L. (2022). Twenty years of plant genome sequencing: achievements and challenges. *Trends Plant Sci.* 27, 391–401. doi: 10.1016/j.tplants.2021.10.006

Wang, L., Xia, Q., Zhang, Y., Zhu, X., Zhu, X., Li, D., et al. (2016). Updated sesame genome assembly and fine mapping of plant height and seed coat color QTLs using a new high-density genetic map. *BMC Genomics* 17, 1–13. doi: 10.1186/s12864-015-2316-4

Wang, L., Xie, S., Zhang, Y., Kang, R., Zhang, M., Wang, M., et al. (2021). The fpPPR1 gene encodes a pentatricopeptide repeat protein that is essential for asexual development, sporulation, and pathogenesis in fusarium pseudograminearum. *Front. Genet.* 11. doi: 10.3389/fgene.2020.535622

Wang, Q. W. Z., Liu, R., and Tu, C. (1993). Study on the Inheritance of Resistance to Fusarium Wilt in Sesame. *Acta Agriculturae Universitatis Henanensis.* 27, 84–8927, 84-89. doi: 10.16445/j.cnki.1000-2340.1993.01.016

Wang, X., Hu, Y., He, W., Yu, K., Zhang, C., Li, Y., et al. (2022). Whole-genome resequencing of the wheat A subgenome progenitor Triticum urartu provides insights into its demographic history and geographic adaptation. *Plant Commun.* 3, 100345. doi: 10.1016/j.xplc.2022.100345

Wei, L. B., Zhang, H. Y., Duan, Y. H., Li, C., Chang, S. X., and Miao, H. M. (2016). Transcriptome comparison of resistant and susceptible sesame (*Sesamum indicum* L.) varieties inoculated with *Fusarium oxysporum* f.sp. sesami. *Plant Breed.* 135, 627–635. doi: 10.1111/pbr.12393

Wei, P., Zhao, F., Wang, Z., Wang, Q., Chai, X., Hou, G., et al. (2022). Sesame (sesamum indicum l.): A comprehensive review of nutritional value, phytochemical composition, health benefits, development of food, and industrial applications. *Nutrients* 14, 4079. doi: 10.3390/nu14194079

Wei, X., Liu, K., Zhang, Y., Feng, Q., Wang, L., Zhao, Y., et al. (2015). Genetic discovery for oil production and quality in sesame. *Nat. Commun.* 6, 8609. doi: 10.1038/ncomms9609

Wu, K., Liu, H., Yang, M., Tao, Y., Ma, H., Wu, W., et al. (2014). High-density genetic map construction and QTLs analysis of grain yield-related traits in Sesame (Sesamum indicum L.) based on RAD-Seq techonology. *BMC Plant Biol.* 14, 274. doi: 10.1186/s12870-014-0274-7

Yol, E., Basak, M., Kızıl, S., Lucas, S. J., and Uzun, B. (2021). A high-density SNP genetic map construction using ddRAD-seq and mapping of capsule shattering trait in sesame. *Front. Plant Sci.* 12. doi: 10.3389/fpls.2021.679659

Zegeye, W. A., Zhang, Y., Cao, L., and Cheng, S. (2018). Whole genome resequencing from bulked populations as a rapid QTL and gene identification method in rice. *Int. J. Mol. Sci.* 19, 4000. doi: 10.3390/ijms19124000

Zhang, R., Xu, K., Li, X., Gao, Y., Sun, Y., and Huang, Q. (2020). Ginger wilt and rot disease caused by Ceratocystis fimbriata in China. *Plant Dis.* 105, 1569. doi: 10.1094/pdis-08-20-1647-pdn

Zhang, X., Cheng, Y., Liu, S., Feng, X., Jin, L., Jin, Q., et al. (2001). Evaluation of sesame germplasm resistance to Macrophomina phaseolina and Fusarium oxysporium. *Chin. J. Oil Crop Sci.* 23, 23–27. Available at: http://europepmc.org/abstract/CBA/356747

Zhang, Y., Wang, L., Xin, H., Li, D., Ma, C., Ding, X., et al. (2013). Construction of a high-density genetic map for sesame based on large scale marker development by specific length amplified fragment (SLAF) sequencing. *BMC Plant Biol.* 13, 141. doi: 10.1186/1471-2229-13-141

frontiers | Frontiers in Plant Science

TYPE Original Research
PUBLISHED 10 October 2024
DOI 10.3389/fpls.2024.1415534

OPEN ACCESS

EDITED BY
Mahyar Mirmajlessi,
Ghent University, Belgium

REVIEWED BY
Martijn Rep,
University of Amsterdam, Netherlands
Maryam Rafiqi,
Independent Researcher, Richmond,
United Kingdom

*CORRESPONDENCE
Helen J. Bates
helen.bates@niab.com

†PRESENT ADDRESSES
Andrew Armitage,
Natural Resources Institute, University of Greenwich, Chatham, United Kingdom
Richard J. Harrison,
Plant Science Group, Wageningen University and Research, Wageningen, Netherlands

RECEIVED 10 April 2024
ACCEPTED 19 September 2024
PUBLISHED 10 October 2024

CITATION
Bates HJ, Pike J, Price RJ, Jenkins S, Connell J, Legg A, Armitage A, Harrison RJ and Clarkson JP (2024) Comparative genomics and transcriptomics reveal differences in effector complement and expression between races of *Fusarium oxysporum* f.sp. *lactucae*.
Front. Plant Sci. 15:1415534.
doi: 10.3389/fpls.2024.1415534

Comparative genomics and transcriptomics reveal differences in effector complement and expression between races of *Fusarium oxysporum* f.sp. *lactucae*

Helen J. Bates[1]*, Jamie Pike[2], R. Jordan Price[1], Sascha Jenkins[2], John Connell[1], Andrew Legg[2], Andrew Armitage[1†], Richard J. Harrison[1†] and John P. Clarkson[2]

[1]NIAB, Cambridge, United Kingdom, [2]Warwick Crop Centre, School of Life Sciences, University of Warwick, Wellesbourne, United Kingdom

This study presents the first genome and transcriptome analyses for *Fusarium oxysporum* f. sp. *lactucae* (Fola) which causes Fusarium wilt disease of lettuce. Long-read genome sequencing of three race 1 (Fola1) and three race 4 (Fola4) isolates revealed key differences in putative effector complement between races and with other *F. oxysporum* ff. spp. following *mimp*-based bioinformatic analyses. Notably, homologues of *Secreted in Xylem* (*SIX*) genes, also present in many other *F. oxysporum* ff. spp, were identified in Fola, with both *SIX9* and *SIX14* (multiple copies with sequence variants) present in both Fola1 and Fola4. All Fola4 isolates also contained an additional single copy of *SIX8*. RNAseq of lettuce following infection with Fola1 and Fola4 isolates identified highly expressed effectors, some of which were homologues of those reported in other *F. oxysporum* ff. spp. including several in *F. oxysporum* f. sp. *apii*. Although *SIX8*, *SIX9* and *SIX14* were all highly expressed in Fola4, of the two *SIX* genes present in Fola1, only *SIX9* was expressed as further analysis revealed that *SIX14* gene copies were disrupted by insertion of a transposable element. Two variants of Fola4 were also identified based on different genome and effector-based analyses. This included two different *SIX8* sequence variants which were divergently transcribed from a shared promoter with either *PSE1* or *PSL1* respectively. In addition, there was evidence of two independent instances of HCT in the different Fola4 variants. The involvement of helitrons in Fola genome rearrangement and gene expression is discussed.

KEYWORDS

***Fusarium oxysporum* f. sp. *lactucae*, lettuce, secreted in xylem, effector, accessory genome, helitron, *SIX* genes, plant pathogen**

1 Introduction

Fusarium oxysporum is a globally important fungal species complex that includes plant pathogens, human pathogens, and non-pathogens (Edel-Hermann and Lecomte, 2019). Plant pathogenic isolates are grouped into different *formae speciales* (ff. spp.) depending on their host range (generally one species) and are of major significance as they cause vascular wilts, crown and root rots of many important horticultural crops and ornamental plants (Edel-Hermann and Lecomte, 2019).

Lettuce (*Lactuca sativa*) is a globally significant vegetable crop, cultivated in over 150 countries worldwide (FAOSTAT) with a substantial market value of more than €3.3 billion in Europe (Eurostat, 2019) and $2 billion in the USA (United States Department of Agriculture - National Agricultural Statistics Service, 2021). However, lettuce production is becoming increasingly affected by Fusarium wilt disease caused by *F. oxysporum* f. sp. *lactucae* (Fola) which causes plant yellowing, stunting, wilting and death with losses of more than 50% commonly reported (Gilardi et al., 2017a). Fusarium wilt of lettuce was first described in Japan in 1955 (Motohashi, 1960) and since then has been identified in many lettuce producing areas of the world with an increasing number of outbreaks recently reported for the first time. Four races are described for Fola with race 1 (Fola1) the most established and widespread, primarily causing disease in field-grown lettuce in warmer parts of the world such as Asia, USA, Southern Europe and South America while races 2 and 3 are confined to Japan and Taiwan (Gilardi et al., 2017a). In contrast, Fola race 4 (Fola4) only emerged relatively recently in Northern Europe where Fusarium wilt of lettuce was previously completely absent and was first reported in 2015 affecting greenhouse-grown (protected) lettuce in the Netherlands (Gilardi et al., 2017a) and Belgium (Claerbout et al., 2018). Since then, Fola4 has been reported in other areas of Europe including the UK (Taylor et al., 2019b), Italy (Gilardi et al., 2019) and Spain (Gálvez et al., 2023). Notably, Fola4 initially only affected protected lettuce although has now also been identified in the open field in both Italy and Spain (Gilardi et al., 2019; Gálvez et al., 2023). In addition, Fola1 also seems to be spreading into Northern Europe with new reports on protected lettuce in both Norway (Herrero et al., 2021) and Northern Ireland (van Amsterdam et al., 2023). This suggests that in the near-future both Fola1 and Fola4 may co-exist in many locations affecting both protected and field-grown lettuce, as is currently the case in some European countries such as Italy (Gilardi et al., 2017b), Belgium (Claerbout et al., 2023) and Spain (Guerrero et al., 2020; Gálvez et al., 2023). Fola4 and Fola1 are very closely related based on phylogenetic analyses of DNA sequences of standard loci such as the translation elongation factor 1α, while Fola2 and Fola3 are in separate distinct clades (Gilardi et al., 2017a; Claerbout et al., 2023). Interestingly Fola4 has been shown to be more aggressive at lower temperatures than Fola1 (Gilardi et al., 2021). The four races of Fola can be distinguished based on their virulence on a differential set of lettuce cultivars (Gilardi et al., 2017a), which has recently been updated by the International Seed Federation (Worldseed.org). Moreover, there are also specific PCR assays published for both Fola1 (Pasquali et al., 2007) and Fola4 (Gilardi et al., 2017b). Although resistance to Fola1 is available within commercial cultivars (Garibaldi et al., 2004; Scott et al., 2010; Murray et al., 2021), these are not always adapted or suitable for some locations and are often also susceptible to Fola4. Moreover, the lettuce cultivars commonly used in indoor production in Europe are highly susceptible to Fola4 and hence the plant breeding industry has had to try and react quickly to identify and deploy resistant cultivars to this new race.

It is now well established that *F. oxysporum* has a compartmentalised genome consisting of both core and accessory (or lineage specific, LS) chromosomes with the former highly conserved and syntenous between different *F. oxysporum* ff. spp. In contrast, the accessory chromosomes are highly variable, are dispensable for viability and are enriched with an abundance of transposable elements (Ma et al., 2010; Yang et al., 2020) which makes assembly of these regions difficult. It is also apparent through *F. oxysporum* genome analyses that some accessory chromosomes (referred to as pathogenicity chromosomes) contain the majority of effectors known to have a role in disease and are therefore associated with pathogenicity and host specificity (Vlaardingerbroek et al., 2016a; van Dam et al., 2017; Armitage et al., 2018; Li et al., 2020a, 2020b; Ayukawa et al., 2021). An important finding initially for *F. oxysporum* f. sp. *lycopersici* (Fol) was that effectors were frequently found downstream of miniature impala elements (*mimps*), a specific family of miniature inverted-repeat transposable elements (MITEs) (Schmidt et al., 2013) and since then this has been used as a successful bioinformatics approach to identify the effector complement within other *F. oxysporum* ff. spp (van Dam et al., 2016, 2017; van Dam and Rep, 2017; Armitage et al., 2018; Taylor et al., 2019a; Chang et al., 2020). Interestingly, non-pathogenic *F. oxysporum* strains including the well-studied endophyte and biological control agent Fo47 (Aimé et al., 2013) also have accessory chromosomes and some effector genes, but are reported to have far fewer than pathogenic ff. spp (Constantin et al., 2021). Of the effectors identified in *F. oxysporum*, the most studied are the *Secreted in Xylem* (*SIX*) genes first identified in Fol which encode small, secreted proteins that are released into the xylem upon infection (Houterman et al., 2007). Since then, homologues of 14 Fol *SIX* genes have been identified in different numbers and complements in most *F. oxysporum* ff. spp. and have therefore been used to differentiate between them based on presence/absence or sequence variation (Jangir et al., 2021). A further *SIX* gene, designated *SIX15* was identified in the Fol genome following comparison with the *F. oxysporum* f. sp. *physali* (infects cape gooseberry) genome (Simbaqueba et al., 2021). Moreover, *SIX* gene complement and sequence can also vary between races within a single *F. oxysporum* f. sp. For instance, the breaking of I gene-mediated resistance in tomato by Fol race 2 was shown to be associated with loss of the avirulence gene *SIX4* (*Avr 1*) or in the case of Fol race 3 by mutations in *SIX3* (*Avr 2*) (Takken and Rep, 2010). Similarly, in *F. oxysporum* f. sp. *cubense* (Focub) races affecting banana, *SIX1*, *SIX6*, *SIX9*, and *SIX13* were detected in race 1, *SIX1*, *SIX2*, *SIX7*, *SIX8*, and *SIX9* in race 4, while tropical race (TR) 4 carries *SIX1*, *SIX2*, *SIX6*, *SIX8*, *SIX9*, and *SIX13* (Czislowski et al., 2018). Three copies and four sequence variations of *SIX1* were also identified in Focub race 4 compared with one copy and two

variants in race 1 (Guo et al., 2014). The *SIX8* sequence is also different between Focub races 4, TR4 and subtropical (STR4) races (Fraser-Smith et al., 2014). There is evidence that both horizontal chromosome transfer (HCT) and horizontal gene transfer (HGT) play a role in shuffling pathogenicity genes and chromosomes between different members of the *F. oxysporum* species complex (FOSC) potentially enabling host jumps and the emergence of new races within a f. sp (Ma et al., 2010; van Dam and Rep, 2017; Henry et al., 2020), although the mechanism for this is not clear.

Despite the global importance of Fola and the recent emergence of Fola 4 that has expanded the pathogen's geographic range, there are no published genomes. Moreover, determining the genetic differences between the most significant races Fola1 and Fola4 would further our understanding of the evolution of the pathogen and could inform breeding more durable resistance in lettuce. In this study we present the first genome and transcriptome analyses for Fola 1 and Fola 4. Long-read genome sequencing of three isolates of each race revealed differences in putative effector complement in Fola 1 and Fola 4 and with other F. oxysporum ff. spp. following mimp-based bioinformatic analyses. Notably, homologues of both SIX9 and SIX14 (multiple copies with sequence variants) were present in both Fola 1 and Fola 4 isolates but all Fola 4 isolates also contained an additional single copy of SIX8. RNAseq of lettuce inoculated with Fola 1 and Fola 4 identified highly expressed effectors, some of which were homologues of those reported in other F. oxysporum ff. spp. including several in F. oxysporum f. sp. apii. Although SIX8, SIX9 and SIX14 were all highly expressed in Fola 4, of the two SIX genes present in Fola 1 only SIX9 was expressed as further analysis revealed that copies of SIX14 were disrupted by either insertion of a helitron or another transposable element. Two variants of Fola4 were also identified based on different genome and effector-based analyses. This included two different SIX8 sequence variants which were divergently transcribed from a shared promoter with either PSE1 or PSL1 respectively which suggested HCT from different sources.

2 Materials and methods

2.1 *Fusarium oxysporum* isolates

The Fola and other *F. oxysporum* isolates used in this study were obtained from other researchers and industry collaborators or were directly isolated from host plants as described by Taylor et al. (2019c) (Table 1). Briefly, this involved surface sterilising sections of symptomatic stem or tap root tissue that exhibited typical vascular browning in 70% ethanol followed by washing twice in sterile distilled water (SDW) and placing on potato dextrose agar (PDA) containing 20 µg/ml of chlorotetracycline. Plates were incubated for 4 days at 20°C, from which emerging *Fusarium* colonies were then sub-cultured from hyphal tips onto fresh PDA. Spore suspensions of all isolates were prepared from two-week-old PDA cultures grown at 25°C in potato dextrose broth (PDB) amended with 20% glycerol (v/v) for long-term storage on ceramic beads at −80°C. In total, three Fola1 isolates (AJ520, AJ718, AJ865) and three Fola4 isolates (AJ516, AJ592, AJ705) were selected as the focus of this study. Fola 1 isolates represented different European locations (France Italy, Spain) while Fola 4 isolates were from England (AJ516, AJ592) and the Netherlands (AJ705). Fola 4 isolates were also selected based on preliminary research which had shown that AJ516 had a different SIX8 sequence compared with AJ592 and AJ705, hence suggesting variation within this race. Fola

TABLE 1 *Fusarium oxysporum* f.sp. *lactucae* and other *F. oxysporum* isolates used in this study.

Isolate code	Identity	Race	Host source	Country of origin	Other code/Reference/ Source
AJ520	*F. oxysporum* f.sp. *lactucae*	1	Lettuce (*Lactuca sativa*)	Italy	ATCCMya-3040 Gilardi et al., 2017
AJ718	*F. oxysporum* f.sp. *lactucae*	1	Lettuce (*Lactuca sativa*)	France	Fyto 7211 BASF, NL
AJ865	*F. oxysporum* f.sp. *lactucae*	1	Lettuce (*Lactuca sativa*)	Spain	PF1 Gs Espana, SP
AJ516	*F. oxysporum* f.sp. *lactucae*	4	Lettuce (*Lactuca sativa*)	England	LANCS1 Taylor et al., 2019c
AJ592	*F. oxysporum* f.sp. *lactucae*	4	Lettuce (*Lactuca sativa*)	England	
AJ705	*F. oxysporum* f.sp. *lactucae*	4	Lettuce (*Lactuca sativa*)	Netherlands	AD035 Enza Zaden, NL
AJ260	*F. oxysporum* f.sp. *matthiolae*	–	Column stocks (*Matthiola incana*)	England	
AJ275	*F. oxysporum* f.sp. *narcissi*	–	Daffodil (*Narcissus pseudonarcissus*)	England	FON63 Taylor et al., 2019a
AJ174	*F. oxysporum*	–	Rocket (*Diplotaxis tenuifolia*)	England	Taylor et al., 2019b
AJ937	*F. oxysporum*	–	Endophyte	France	Fo47, Aimé et al., 2013

isolates were subject to genome sequencing, effector identification and RNAseq *in planta* alongside an isolate of *F. oxysporum* f. sp *matthiolae* (Foma isolate AJ260) which infects column stocks (*Matthiola incana*). Isolates of *F. oxysporum* infecting *Narcissus* spp. (*F. oxysporum* f. sp. *narcissi*; Fon isolate AJ275 [FON63], Taylor et al., 2019a) and wild rocket (*Diplotaxis tenuifolia*; *F. oxysporum* rocket isolate AJ174, Taylor et al., 2019b) were used for genome sequencing and comparison of effector complement only. The non-pathogenic *F. oxysporum* endophyte isolate Fo47 used in other genome studies (e.g. Armitage et al., 2018; van Dam et al., 2016) was also used for comparative purposes and RNAseq. All isolates were confirmed as *F. oxysporum* by PCR and sequencing of the translation elongation factor (TEF) gene as described by Taylor et al. (2016). Fola isolate race identity and virulence was confirmed by testing on a standard lettuce differential set (Gilardi et al., 2017a) by isolate suppliers or in previous studies and also by confirming the presence of *SIX9* and *SIX14* in Fola1 and *SIX8*, *SIX9* and *SIX14* in Fola4 isolates by PCR as described by Taylor et al. (2016) using modified primers for Fola (Supplementary Table SD1-T1). These different complements of *SIX* genes for Fola1 and Fola4 were consistent across multiple Fola isolates in initial studies (unpublished). The Foma and *F. oxysporum* rocket isolates were confirmed to be pathogenic on their respective hosts using standard root dip inoculations with conidial suspensions as described by Taylor et al. (2019b) while Fon isolate AJ275 was previously confirmed to be pathogenic on daffodil bulbs (Taylor et al., 2019a).

2.2 Genome sequencing, assembly and analyses

2.2.1 DNA extraction

Fusarium oxysporum isolates (Table 1) were grown on PDA plates at 25°C for 4 days and 5 mm mycelial plugs from growing tips then used to inoculate 50 ml potato dextrose broth (PDB) containing 20 µg/ml streptomycin which were incubated for 4 days in the dark at 25°C at 180 rpm. The resulting mycelium for each isolate was harvested on filter paper (Fisherbrand 11556873, Fisher Scientific UK Ltd.), washed with distilled water, blotted dry and snap frozen in liquid nitrogen prior to freeze drying and storing at -80°C. Freeze-dried mycelium (20 mg) was used for DNA extraction using a Macherey-Nagel NucleoSpin Plant II kit (Fisher Scientific) following the manufacturer's instructions. DNA samples were eluted in 30 µl 10 mM Tris HCl pH 8 and analysed for purity and quantity using the Nanodrop spectrophotometer (NanoDrop One, ThermoFisher Scientific) and Qubit fluorometer (Invitrogen) and for integrity using the Agilent TapeStation (TS 4150, Agilent Technologies). DNA samples with Nanodrop ratios 260/280 between 1.8-2.0, 260/230 between 2.0-2.2 and molecular weight >50 kb were selected for sequencing.

2.2.2 Genome sequencing

Illumina PCR-free genome sequencing was carried out for isolates Foma AJ260, Fon AJ275, Fola1 AJ520 and Fola4 AJ516 as previously described (Armitage et al., 2018). Long-read genome sequencing was carried out using 1 µg input DNA into Oxford Nanopore Technologies (ONT) ligation sequencing kit LSK108 (Foma AJ260, Fon AJ275) or LSK110 (Fola1 isolates AJ520, AJ718, AJ865; Fola4 isolates AJ516, AJ592, AJ705 and *F. oxysporum* rocket) as described and flow cells FLO-MIN106 R9.4 (Foma AJ260, Fon AJ275) or FLO-MIN106 R9.4.1 (all other isolates). Enzymes were purchased from New England Biolabs (NEBNext Companion Module #E7180) and Omega Bio-Tek Mag-bind TotalPure NGS magnetic beads were from VWR International. All ONT sequencing runs were performed on the GridION with live high-accuracy base calling. Data were re-base called using super-high accuracy mode post-run and prior to genome assembly.

2.2.3 Genome assembly

De novo genome assemblies for the six Fola (3 x Fola1, 3 x Fola4), and the single isolates of Foma, and *F. oxysporum* rocket were generated from long-read Oxford Nanopore Technologies sequence data (Wang et al., 2021). Quality control of ONT data was performed using NanoPlot v1.30.1 (De Coster et al., 2018). Adapter trimming was performed using Porechop v0.2.4 (https://github.com/rrwick/Porechop) with default parameters, followed by removal of reads shorter than 1 kb or with a quality score less than Q9 using Filtlong v0.2.1 (https://github.com/rrwick/Filtlong). Long read data were assembled using NECAT v0.0.1_update20200803 (Chen et al., 2021) with a genome size of 60 Mb, with other parameters left as default. Long read error correction was performed by aligning reads to the assemblies with Minimap2 v2.17-r941 (Li, 2018) to inform one iteration of Racon v1.4.20 (Vaser et al., 2017), followed by one iteration of Medaka v1.5.0 (https://github.com/nanoporetech/medaka) using the r941_min_high_g360 model. Quality control of Illumina paired-end reads was performed using FastQC v0.11.9 (https://www.bioinformatics.babraham.ac.uk/projects/fastqc/), with adapters and low-quality regions trimmed using Fastq-Mcf v1.04 (Aronesty, 2013). Bowtie2 v2.2.5 (Langmead and Salzberg, 2012) and SAMtools v1.13 (Li et al., 2009) were used to align short reads to the long-read assemblies. Three iterations of polishing were carried out using Pilon v1.24 (Walker et al., 2014) to allow correction of single base call errors and small insertions or deletions. Assembly statistics were generated using a custom Python script, with assembly quality also assessed through single copy ortholog analysis performed using BUSCO v5.2.2 (Simão et al., 2015), with the hypocreales_odb10 database. Genome assembly of the Fon isolate AJ275 was performed prior to this study using the pipeline described in Armitage et al. (2020).

2.2.4 Gene prediction in Fola1, Fola4 and Foma isolates

Prior to gene prediction repetitive sequences were masked using RepeatMasker version 4.1.2 (Smit et al., 2013-2015) and RepeatModeler version 2.0.5 (Smit and Hubley, 2008-2015) to produce both hard and soft masked genome assemblies. Gene models were annotated using both BRAKER version 2.16 (Brůna et al., 2021) and CodingQuarry version 2 gene prediction

tools (Testa et al., 2015). RNAseq reads (see below) were adapter trimmed and poor-quality reads removed using Fastq-Mcf version 1.04 (Aronesty, 2013). Pre-processed reads were aligned to respective *F. oxysporum* assemblies using STAR version 2.7.10 (Dobin et al., 2013) with the flags –winAnchorMultimapNmax set to 200 and –seedSearchStartLmax set to 30 to improve mapping sensitivity. An initial round of gene prediction was performed using the BRAKER 2 method with flags –fungus to specify a fungal organism, and –softmasking to specify a soft masked genome assembly. RNAseq alignments generated for Fola infection of lettuce (as described below) were used as inputs to BRAKER to provide additional evidence to improve gene prediction accuracy. A second round of gene prediction was performed using the CodingQuarry pathogen method. Genome alignment files produced by STAR as described above were used as inputs to Cufflinks version 2.2.1 (Trapnell et al., 2010) to produce a *de novo* transcriptome which was used as a guide for CodingQuarry. Gene predictions for both BRAKER and CodingQuarry were investigated using the BEDTools intersect function (Quinlan and Hall, 2010) with the -v flag to separate CodingQuarry predictions where no overlap to a BRAKER prediction was found. Resulting gene predictions were combined and ordered with any duplicated annotations removed using a custom-made Python script to retain BRAKER gene models and integrate CodingQuarry predictions that were located in intergenic regions (Python Software Foundation, 2021). Following this, predicted genes were functionally annotated using InterProScan version 5.62-94.0 (Jones et al., 2014). Orthologous gene families were identified using OrthoFinder version 2.5.4 (Emms and Kelly, 2019) with the Fola1 (AJ520, AJ718, AJ865), Fola4 (AJ516, AJ592, AJ705), Foma AJ260 genomes, along with the *F. oxysporum* Fo47 genome.

2.2.5 Identification and visualisation of genomic features for Fola1 and Fola4 isolates

Annotation of genomic features including transposable elements, carbohydrate active enzymes (CAZymes), fungal effector proteins, secreted signal peptides and secondary metabolite clusters was carried out for Fola1 and Fola4 isolates. Transposable elements were identified using transposonPSI version 1.0.0 (Haas, 2010) with the default settings. CAZymes were identified using the hmmscan tool from HMMER version 3.3.2 (Finn et al., 2011) with HMM models from the dbCAN2 version 11 database (Zhang et al., 2018). Candidate fungal effector proteins were identified using EffectorP version 3.0 (Sperschneider et al., 2016) with default settings. Secreted signal peptides were predicted by taking a unique list of genes from the combined output of SignalP versions 2, 3, 4 and 5 (Almagro Armenteros et al., 2019; Bendtsen et al., 2004; Nielsen and Krogh, 1998; Petersen et al., 2011). A custom python script was used to identify the presence and position of the [SG]PC[KR]P motif in proteins that were predicted to contain signal peptides as this has been specifically associated with the *Fusarium* genus (Sperschneider et al., 2015; Rafiqi et al., 2022). Secondary metabolite clusters were identified using the antiSMASH version 6.0 webserver (Blin et al., 2021) with the addition of the cluster-border prediction based on transcription factor binding sites feature enabled. Individual secondary metabolite genes were pulled out from the genebank file produced by antiSMASH using a custom python script. Visualisation of core and pathogenicity chromosomes was performed for Fola1 AJ520 and Fola4 AJ516 using Circos software version 0.69-9 (Krzywinski et al., 2009). The locations of genomic features including CAZymes, transposable elements, secondary metabolite clusters, miniature impala sequences, and *SIX* gene homologs that were identified as described above, were plotted on the ideogram based on their genomic position. The putative effector gene locations generated by the *mimp*-associated pipeline described below, were mapped to the annotated genome to identify genes and those genes filtered by EffectorP and SignalP predictions to produce the list of putative effector genes shown. To visualise reads that map to both Fola1 AJ520 and Fola4 AJ516 genomes from the other *F. oxysporum* isolates, short read data was simulated from the long reads for each genome by generating 300 bp fragments with a 50 bp step. This simulated short read data for Fola1 isolates AJ718 and AJ865, Fola4 isolates AJ592 and AJ705, Foma AJ260 and the non-pathogenic *F. oxysporum* Fo47 were aligned using BWA-MEM version 0.7.17-r1188 (Li, 2013) using default parameters. Genome alignment coverage was calculated using BEDTools genomecov function (Quinlan and Hall, 2010) with the flag -d to specify that a per base coverage should be calculated. A custom python script was employed to calculate a per window sum of genome coverage at a window size of 10,000 bp.

2.2.6 Phylogenetic reconstruction of *F. oxysporum* core and accessory genomes

To investigate the genetic relatedness of core and accessory genome sequences for the *F. oxysporum* genomes included in this study (Supplementary Table SD1-T2), alignment-free phylogenetic reconstruction was performed using SANS ambages v2.3_9A (Rempel and Wittler, 2021). Highly contiguous genome sequences were aligned to the core chromosomes of the reference *F. oxysporum* f.sp. *lycopersici* isolate 4287 using Minimap2 v2.17-r941 (Li, 2018). Contigs with continuous alignments of more than 100 kb were then extracted as core genome sequences. To prevent interference from repetitive and unplaced contigs, sequences less than 100 kb were removed from the remaining contigs following extraction of core genome sequences. The remaining contigs were considered as accessory genome sequences. Using these core and accessory sequences, SANS ambages v2.3_9A was run with 1000 bootstrap replicates and the option 'strict' to output a Newick format file, and all other options left as default. Phylogenetic trees were visualised using iTOL v6 (Letunic and Bork, 2021).

2.2.7 Synteny of Fola core and accessory genomes

To compare the synteny across core and accessory genomes of all the Fola1 and Fola4 isolates, collinearity analysis was performed using the core and accessory contigs extracted for phylogenetic reconstruction as described above. Pairwise alignments were performed using Minimap2 v2.17-r941 (Li, 2018) and prior to visualisation, core genome alignments smaller than 100 kb and

accessory genome alignments smaller than 10 kb were discarded. The results were visualised using NGenomeSyn v1.41 (He et al., 2023).

2.3 *Mimp*-associated putative effector identification in Fola and other *F. oxysporum* genome assemblies

As highlighted previously, miniature impala elements (*mimps)* have been used previously to predict potential effectors in *F. oxysporum* including the majority of *SIX* genes in different *F. oxysporum* f.spp (Armitage et al., 2018; Brenes Guallar et al., 2022; van Dam et al., 2016; van Dam and Rep, 2017; Schmidt et al., 2013). We therefore adapted a *mimp*-associated effector identification pipeline as utilised by van Dam et al. (2016), to find putative effectors in genomes of all the Fola isolates and other *F. oxysporum* f.spp. generated in this study (Fon AJ275, Foma AJ260, and *F. oxysporum* rocket AJ174). Alongside these assemblies, publicly available representative high-quality genomes (minimum ≤50 contigs and a reported BUSCO of >97%) for the *F. oxysporum* endophyte Fo47, and the *F. oxysporum* f.spp. *cepae, conglutinans, coriandrii, cubense, lini, lycopersici, niveum, rapae* and *vasinfectum* were downloaded from GenBank (https://www.ncbi.nlm.nih.gov/data-hub/genome/) (Supplementary Table SD1-T2).

Two methods of searching for *mimps* were employed for each *F. oxysporum* genome. The first used a custom python script to search for the *mimp* TIR sequences, "CAGTGGG.GCAA[TA]AA" and "TT[TA]TTGC.CCCACTG". Where sequences matching this pattern occurred within 400 nucleotides of each other a *mimp* was recorded. The second *mimp* searching method employed a Hidden Markov Model (HMM) which was developed using the HMM tool HMMER (3.3.1) (Wheeler and Eddy, 2013). Briefly, publicly available *mimp* sequences (Supplementary Table SD1-T3) and further sequences identified using the regular expression method in the *Fusarium* assemblies were used to build a *mimp* profile-HMM. This profile-HMM was used as the input for an NHMMER search of each genome. Using *mimps* identified by both *mimp* finding methods, sequences 2.5 kb upstream and downstream of each *mimp* were extracted and subjected to gene prediction using AUGUSTUS (3.3.3) (Stanke et al., 2006) with the "*Fusarium*" option enabled, and open reading frames (ORFs) within this region identified using the EMBOSS (6.6.0.0) tool, getorf (https://www.bioinformatics.nl/cgi-bin/emboss/getorf). ORFs and gene models from each genome with a signal peptide predicted using SignalP (4.1, default settings) (Petersen et al., 2011) were then clustered using CD-HIT (4.8.1) (Fu et al., 2012) to create a non-redundant candidate effector set for each genome. Sequences of between 30 aa and 300 aa were then extracted from the individual, non-redundant candidate effector sets for all isolates and were combined and clustered using CD-HIT (4.8.1) at 65% identity. The longest sequence from each cluster was then subject to effector prediction using EffectorP (2.0.1) (Sperschneider et al., 2016), generating a collective candidate *mimp*-associated-effector set. To determine the presence/absence of the candidate effectors across all of the *Fusarium* genomes, the collective candidate *mimp*-associated-pan-effector set was used to search for effector homologues across all genomes using TBLASTN (Camacho et al., 2009), with a cut-off $1e^{-6}$ and a percentage identity and coverage threshold of 65%. TBLASTN hits were extracted, translated using transeq from EMBOSS (6.6.0.0), and filtered by the presence of a signal peptide (SignalP version 1.4, default settings) and effector prediction using EffectorP (2.0.1, default settings). Candidates were classified into effector groups at 65% identity CD-HIT (4.8.1) and a presence/absence data matrix was generated using the candidate effector clusters. The R functions dist(method = binary) and hclust were used to cluster the binary effector matrix and the R package Pheatmap (1.0.12) (Kolde and Kolde, 2015) used to create the heatmap (R version 3.6.3).

2.4 Identification of *SIX* genes in Fola and other *F. oxysporum* genome assemblies

The complement of *SIX* gene homologues was determined in all the Fola and other *F. oxysporum* isolate genomes generated in this study as well as in publicly available genomes for the *F. oxysporum* endophyte Fo47, and for *F. oxysporum* f.spp. *capsici, cepae, conglutinans, coriandrii, cubense, lini, luffae, lycopersici, matthiolae, niveum, rapae* and *vasinfectum* which were downloaded from GenBank following a genome search (https://www.ncbi.nlm.nih.gov/data-hub/genome/) (Supplementary Table SD1-T2). Reference sequences for *SIX1-SIX15* from *F. oxysporum* f.sp *lycopersici* (isolate 4287) were downloaded from the NCBI database (Supplementary Table SD1-T4) and homologues of each *SIX* gene identified in each assembly using tBLASTx (1e-6 cut-off). A binary data matrix indicating presence ("+") or absence ("-") was generated using the tBLASTx hit data. *SIX* gene phylogenies were then constructed for the *SIX* genes present in Fola1 (*SIX9*, *SIX14*) and Fola4 (*SIX8*, *SIX9*, *SIX14*). The locations of *SIX8*, *SIX9*, and *SIX14* tBLASTx (1e-6 cut-off) hits were recorded, and the sequence within this region extracted using Samtools (version 1.15.1). Extracted regions from each genome were added to a multiFASTA file for each *SIX* gene. MAFFT (version 7.505) (Katoh et al., 2019) was used to construct a multiple sequence alignment using the "—adjustdirectionaccurately" and "–reorder" options. To ensure correct alignment, any overhanging regions were inspected and trimmed manually. IQ-TREE (Version 2.2.0.3) (Nguyen et al., 2015) was used to infer a maximum-likelihood phylogeny using the ultrafast bootstrap setting for 1000 bootstrap replicates and was visualised using iTOL (Letunic and Bork, 2021).

2.5 Expression of predicted Fola effectors in lettuce

2.5.1 Inoculation of lettuce seedlings with Fola and non-pathogenic *F. oxysporum*

Lettuce seedlings were grown and inoculated with isolates of Fola1 AJ520 and two variants of Fola4 (AJ516, AJ705) on an agar medium using a method adapted from Taylor et al. (2016) for subsequent RNA extraction and sequencing. As controls, two

F. oxysporum isolates non-pathogenic on lettuce were also used for inoculations; these were Foma AJ260 which is pathogenic on column stocks where the genome contains homologues of *SIX8* and *SIX9* also both present in Fola4, and the endophyte *F. oxysporum* Fo47 which is a 'standard' non-pathogenic isolate used in other studies (Constantin et al., 2021) where the genome contains no *SIX* genes. A non-inoculated control treatment (no *F. oxysporum*) was also set up. Autoclaved ATS medium [5 mM KNO_3, 2.5 mM KPO_4, 3 mM $MgSO_4$, 3 mM $Ca(NO_3)^2$, 50 uM Fe-EDTA, 70 uM H_3BO_3, 14 uM $MnCl_2$, 0.5 uM $CuSO_4$, 1 uM $ZnSO_4$, 0.2 uM Na_2MoO_4, 10 uM NaCl, 0.01 uM $CoCl_2$, 0.45% Gelrite (Duchefa Biochemie, Haarlem, The Netherlands)] was used to three-quarter fill square petri dishes (12 x 12 x 1.7 cm, Greiner Bio-One, UK) and once set, the top 5 cm of the gel was removed with a sterile spatula. Lettuce seeds of a Fola susceptible cultivar (cv. Kordaat) were surface sterilised in a 10% bleach water (v/v) solution for 5 min and then rinsed three times with SDW before they were placed across the cut edge of the agar in each plate (12 seeds per plate) after which the lid was replaced and secured with tape. Stacks of five plates were wrapped in cling film and placed at 4°C in the dark for 4 days. Plates were then incubated at 15°C in 16 h light/dark for 8 days, before the temperature was increased to 25°C for six days. Conidial suspensions of each *F. oxysporum* isolate were prepared by releasing spores from two-week-old cultures grown on PDA at 25°C with 10 mL SDW and filtering through three layers of Miracloth. Spore suspensions were adjusted to 1 x 10^6 spores ml^{-1} in SDW with the addition of 200 µl of Tween20 l^{-1} and 1.5 ml pipetted directly onto the lettuce roots on each plate and spread by tilting, before being dried briefly under sterile air flow. Non-inoculated control treatments consisted of SDW + Tween only. In total, seven agar plates of lettuce seedlings were inoculated for each *F. oxysporum* isolate, of which four were used for RNAseq and three were incubated further to confirm that disease developed for the Fola isolates and not for the non-pathogenic Foma AJ260 and the *F. oxysporum* endophyte isolate Fo47. Plates were placed in a randomised design within an incubator at 25°C (16 h photoperiod). Lettuce roots from each treatment for RNAseq were harvested 96 hours post-inoculation and pooled into one sample of 12 plants per plate. This time point corresponded to a peak in expression of *SIX8*, *SIX9* and *SIX14* as quantified through RT-PCR assays of a time-course study using the same bioassay for lettuce seedlings cv. Temira inoculated with Fola4 AJ516 (data not shown). Roots were rinsed in SDW, blotted dry and flash frozen in liquid nitrogen and stored at -80°C prior to RNA extraction and sequencing. Lettuce seedlings from each treatment retained at 25°C for disease assessment were inspected for root browning and death two weeks post -inoculation. To provide data for gene expression *in vitro* in order to identify upregulated genes *in planta*, spore suspensions of each *F. oxysporum* isolate (Fola1 AJ520, Fola4 AJ516/AJ705, Foma AJ260 and *F. oxysporum* Fo47) were prepared as above, and 500 µL of 1 x 10^6 spores ml^{-1} pipetted onto a PDA plate containing an autoclaved cellulose disc placed on the surface and incubated for 96h at 25˚C. Six replicate plates were prepared and the resulting mycelium harvested by scraping off the layer growing on the cellulose surface before immediately flash freezing. Four replicate samples were then used for RNA extraction.

2.5.2 RNA extraction and sequencing

Lettuce roots were ground to a fine powder using a pestle and mortar filled with liquid nitrogen and approximately 100 mg of tissue transferred to a 2 ml tube. Frozen root material was ground further using a Dremel drill (model 398, with a rounded drill bit) and then RNA extracted using Trizol ® reagent (Thermo Fisher Scientific) following the manufacturer's guidelines. Extracted RNA was precipitated using 900 µl of lithium chloride to 100 µl RNA (250 µl LiCl2 + 650 µl DEPC treated water) and any DNA was removed from samples using DNase 1 (Sigma-Aldrich, UK). RNA samples were visualised on a 2% agarose gel (containing GelRedTM at 2 µl per 100 ml of gel) with the addition of loading dye (Orange G, Sigma-Aldrich, UK) to check for degradation. RNA samples (four replicates for each isolate) were sent to Novogene for polyA-enrichment, followed by Illumina PE150 sequencing at a depth of 23 Gb raw data per sample for *in planta* samples and 9 Gb per sample for *in vitro* mycelial RNA samples.

2.5.3 RNAseq data analyses

RNAseq reads containing transcripts from both *F. oxysporum* isolates and lettuce were trimmed using Fastq-Mcf as described above. To separate *F. oxysporum* reads from lettuce, the lettuce genome (*Lactuca sativa*, NCBI accession: GCF_002870075.3) was downloaded from NCBI and used for alignment of pre-processed RNAseq reads using STAR as described above with the addition of the flag –outReadsUnmapped which was used to specify that a file of non-mapping reads should be created. Non-mapping putative *F. oxysporum* RNAseq reads were pseudo-aligned to the respective reference genome and quantified using Kallisto version 0.48.0 (Bray et al., 2016). Differential gene expression analysis was conducted using R version 4.1.3 (R core team, 2021) with the DESeq2 package version 1.34.0 (Love et al., 2014) using the contrast function to give a list of differentially expressed genes. Results were filtered to identify putative effectors that were upregulated *in planta*. Firstly, all genes upregulated *in planta* with a log 2 fold change (L2FC) greater than 2.0 (compared to PDB grown controls) were identified for each isolate. These were then sorted for genes containing a signal peptide and with gene length less than 1 kb to identify small, secreted proteins. Genes identified as CAZymes, secondary metabolites, transposons or those with homologues of greater than 70% identity in the non-pathogen Fo47 were discarded from the analysis. Remaining genes were then sorted based on level of induction based on L2FC, identification as a putative effector from the previously described effector discovery pipeline and presence on an accessory contig. Expressed candidate effectors were grouped by orthogroup (Supplementary Table SD1-T12) and all members of the orthogroup were cross-referenced for level of expression. Putative effectors by orthogroup were also cross-referenced to gene locations of candidate effector clusters (CECs) identified by the effector discovery pipeline.

3 Results

3.1 Core and accessory genome phylogenies support a single Fola1 and Fola4 clade

Three isolates of both Fola 1 (AJ520, AJ718, AJ865) and Fola 4 (AJ516, AJ592, AJ705) were selected for long-read genome sequencing (Table 1) based on different geographic origins and, for Fola 4, because preliminary data indicated that AJ516 had a different SIX8 sequence compared with AJ592 and AJ705. Nanopore sequencing produced high quality and highly contiguous genome assemblies for Fola as well as the other F. oxysporum isolates sequenced; Foma, Fon and *F. oxysporum* rocket isolates (Supplementary Table SD1-T6). To identify core and accessory genome sequences, these *de novo* genome assemblies and selected high quality genome sequences from other *F. oxysporum* ff. spp. (Supplementary Table SD1-T2) were aligned to the reference *F. oxysporum* f. sp. *lycopersici* isolate 4287 genome. Core genome contigs comprised approximately 45-55 Mb across all isolates (Table 2), consistent with observations in other *F. oxysporum* ff. spp. Following removal of contigs less than 100 kb to prevent confounding results from unplaced core sequences and/or highly repetitive contigs, the size of the accessory genomes varied considerably across all the *F. oxysporum* isolates, from 1.3 Mb for *F. oxysporum* f. sp. *cubense* 16052 to 23.5 Mb for *F. oxysporum* f. sp. *lini* 39 (Table 2). The putative accessory genomes of all Fola1 isolates had similar sizes of around 15 Mb, while the Fola4 isolates had larger accessory genome sizes, with 21 Mb for AJ516 and approximately 18 Mb for AJ705 and AJ592.

Phylogenies based on the identified core and accessory genome sequences were generated using an alignment free reconstruction method (Figure 1). Based on our sampling of three Fola 1 and three Fola 4 isolates, both phylogenies demonstrated a single well supported clade for all the Fola isolates. The topology of the Fola clade in the core and accessory trees were congruent, with Fola1 and Fola4 as sister clades. Within each Fola race there was further separation into two groups. Within the Fola1 clade, AJ718 represented a separate group to AJ520 and AJ865, while in the Fola4 clade AJ516 was separated from AJ705 and AJ592 (Figure 1). In both the core genome (Figure 1A) and the accessory genome (Figure 1B) phylogenies, the Fola isolates were part of a larger clade that also included Foma AJ260 and *F. oxysporum* f. sp. *apii* 207.A.

TABLE 2 Number and sizes of core and accessory *Fusarium oxysporum* (*Fo*) genome sequences used for phylogenetic reconstruction.

F. oxysporum f.sp./isolate	Core genome		Accessory genome	
	Contigs	Size (Mb)	Contigs	Size (Mb)
Fo f.sp. *apii* 207.A	12	46.1	26	18.3
Fo f.sp. *cepae* Fus2	21	45.5	8	7.2
Fo f.sp. *conglutinans* Fo5176	14	54.8	4	12.0
Fo f.sp. *coriandrii* 3-2	9	46.3	22	15.5
Fo f.sp. *cubense* 16052	11	49.9	1	1.3
Fo f.sp. *cubense* UK0001	11	47.1	2	1.4
Fo f.sp. *lactucae* race4 AJ516	14	47.5	17	20.9
Fo f.sp. *lactucae* race1 AJ520	17	45.2	14	15.5
Fo f.sp. *lactucae* race4 AJ592	19	46.2	11	18.2
Fo f.sp. *lactucae* race4 AJ705	17	46.5	12	17.7
Fo f.sp. *lactucae* race1 AJ718	20	46.3	12	15.2
Fo f.sp. *lactucae* race1 AJ865	20	45.6	11	15.7
Fo f.sp. *lini* 39	11	45.8	8	23.5
Fo f.sp. *lycopersici* 4287	12	45.8	13	14.5
Fo f.sp. *matthiolae* AJ260	11	46.0	23	13.9
Fo f.sp. *narcissus* FON63	12	44.6	19	14.8
Fo f.sp. *niveum* 110407-3-1-1	24	46.5	6	3.1
Fo f.sp. *vasinfectum* TF1	12	45.9	3	4.0
Fo rocket AJ174	19	50.4	10	12.1
F. oxysporum Fo47	11	46.1	1	4.3

10.3389/fpls.2024.1415534

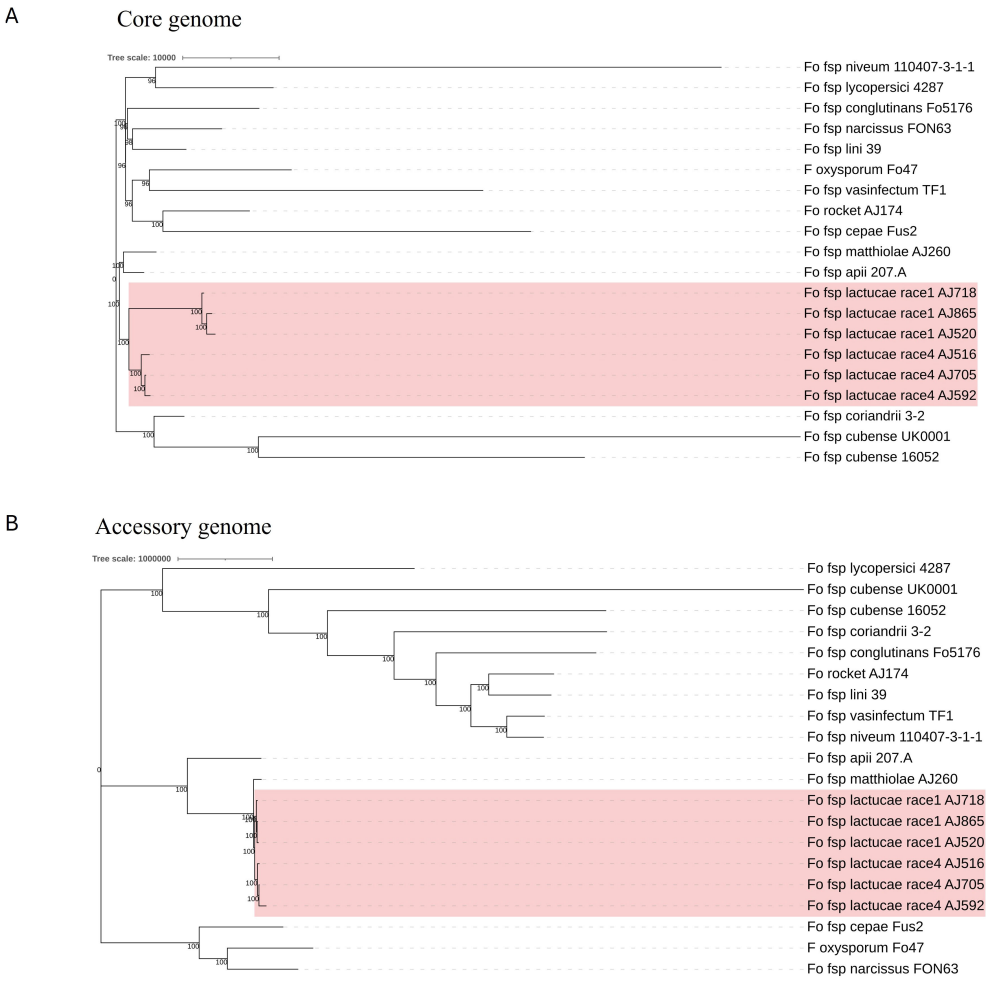

FIGURE 1
Core **(A)** and accessory **(B)** genome phylogenies for *Fusarium oxysporum* f. sp. *lactucae* (Fola) and other *F. oxysporum* f.spp. The monophyletic Fola clades are highlighted in the red boxes. Numbers at nodes represent percentage bootstrap support following 1000 replicates. The scale represents SNP count.

3.2 Fola1 and Fola4 isolates cluster separately based on *mimp*-associated candidate effector profiles

To investigate differences in effector repertoire between Fola1 and Fola4, we used a *mimp*-based effector discovery pipeline to analyse six Fola genomes (3 x race 1 and 3 x race 4), along with 15 other *F. oxysporum* ff.spp. with high quality genome assemblies (Table 3). The total number of candidate effectors across all these *F. oxysporum* genomes ranged from 52 in *F. oxysporum* f.sp. *cubense* race 1 isolate 160527 to 277 in Fola4 isolate AJ592 (Table 3). Interestingly the *F. oxysporum* (non-pathogenic) endophyte isolate Fo47 yielded 66 candidate effectors, which was 14 more than for *F. oxysporum* f. sp. *cubense* isolate 160527. Fewer candidate effectors were identified in the three Fola1 isolates compared with the three Fola4 isolates with 215, 230, 247 and 274, 276, 277 candidate effectors found, respectively (Table 3).

Candidate effectors were clustered into groups using CD-HIT (65% identity) resulting in 238 clusters, including 101 candidate effector clusters for Fola. Of these, 48 were shared amongst all Fola isolates, 18 were unique to Fola4 while 11 were unique to Fola1. The 24 remaining Fola candidate effector clusters (CECs) did not show a consistent presence based on race (Figure 2). Of these 24 non-race specific clusters, eight displayed an interesting distribution pattern within the Fola4 isolates. Candidate effector clusters CEC_153, CEC_173, and CEC_232 were found in Fola4 AJ516, but not in Fola4 AJ592 or AJ705, whereas candidate effector clusters CEC_10, CEC_32, CEC_185, CEC_212 were present in Fola4 AJ592 and AJ705 but not identified in Fola4 isolate AJ516. Of these clusters, CEC_10, CEC_212, and CEC_232 were found in all of the Fola1 isolates, while the remaining clusters (CEC_32, CEC_153, CEC_173, 185) were not identified in any of the Fola1 isolates. Effector complement therefore distinguished between Fola1 and Fola4 isolates, but also suggested that there were two variants of

TABLE 3 Effector candidates and *SIX* gene distribution for *Fusarium oxysporum* genomes.

Species	Race	Host Species	No. candidate effectors	*SIX* gene presence/absence														
				SIX 1	*SIX 2*	*SIX 3*	*SIX 4*	*SIX 5*	*SIX 6*	*SIX 7*	*SIX 8*	*SIX 9*	*SIX 10*	*SIX 11*	*SIX 12*	*SIX 13*	*SIX 14*	*SIX 15*
F. oxysporum Fo47*		Endophyte	66	–	–	–	–	–	–	–	–	–	–	–	–	–	–	–
Fo fsp. *apii* 207.A*	2	*Apium graveolens* (celery)	252	+	–	–	–	–	–	+	–	+	–	–	–	–	+	+
Fo fsp. *cepae* Fus2*		*Allium cepae* (onion)	175	–	–	+	–	+	–	+	–	+	+	–	+	–	+	–
Fo fsp. *conglutinans* Fo517*		*Brassica oleracea* (cabbage), *Arabidopsis thaliana*	264	+	–	–	+	–	–	–	+	+	–	–	–	–	–	+
Fo fsp. *coriandrii* 3-2*		*Coriandrum sativum* (coriander)	235	+	–	–	–	+	–	+	–	+	–	–	–	–	+	–
Fo fsp. *cubense* 16052*	1	*Musa* spp. (banana)	52	+	–	–	+	–	+	–	–	+	–	–	–	+	–	–
Fo fsp. *cubense* UK0001*	TR4	*Musa* spp. (banana)	83	+	+	–	+	–	+	–	+	+	–	–	–	+	–	–
Fo fsp. *lactucae* AJ520†	1	*Lactuca sativa* (lettuce)	230	–	–	–	–	–	–	–	–	+	–	–	–	–	+	–
Fo fsp. *lactucae* AJ718†	1	*Lactuca sativa* (lettuce)	215	–	–	–	–	–	–	–	–	+	–	–	–	–	+	–
Fo fsp. *lactucae* AJ856†	1	*Lactuca sativa* (lettuce)	247	–	–	–	–	–	–	–	–	+	–	–	–	–	+	–
Fo fsp. *lactucae* AJ516†	4	*Lactuca sativa* (lettuce)	274	–	–	–	–	–	–	–	+	+	–	–	–	–	+	–
Fo fsp. *lactucae* AJ592†	4	*Lactuca sativa* (lettuce)	277	–	–	–	–	–	–	–	+	+	–	–	–	–	+	–
Fo fsp. *lactucae* AJ705†	4	*Lactuca sativa* (lettuce)	276	–	–	–	–	–	–	–	+	+	–	–	–	–	+	–
Fo fsp. *lini* 39*		*Linum usitatissiumum* (flax)	210	+	–	–	–	–	–	+	–	+	–	–	+	+	+	–
Fo fsp. *lycopersici* 4287*	2	*Solanum lycopersicum* (tomato)	183	+	+	+	-‡	+	+	+	+	+	+	+	+	+	+	+
Fo fsp. *matthiolae* AJ260†		*Matthiola incana* (stocks)	185	+	–	–	–	–	–	–	+	+	–	–	–	–	–	–
Fo fsp. *narcissus* FON63†		*Narcissus* spp. *(Narcissus)*	190	–	–	–	–	–	–	+	–	+	+	–	+	+	–	–
Fo fsp. *niveum* 110407-3-1-1*		*Citrullus lanatus* (watermelon)	40	–	–	–	–	+	–	–	–	+	–	–	–	–	–	+

(Continued)

10.3389/fpls.2024.1415534

10.3389/fpls.2024.1415534

TABLE 3 Continued

Species	Race	Host Species	No. candidate effectors	*SIX* gene presence/absence													
				SIX 1	*SIX 2*	*SIX 3*	*SIX 4*	*SIX 5*	*SIX 6*	*SIX 7*	*SIX 8*	*SIX 9*	*SIX 10*	*SIX 11*	*SIX 12*	*SIX 13*	*SIX 14*	*SIX 15*
Fo f.sp. *rapae* Tf1208*		*Brassica rapa*	144	–	–	–	–	–	–	–	–	+	–	–	–	–	+	–
Fo f.sp. *vasinfectum* TF1*	1	*Gossypium* spp. (cotton)	73	+	–	–	–	–	–	–	–	+	–	–	–	–	–	–
Fo rocket AJ174†		*Diplotaxis tenuifolia* (Wild Rocket)	196	–	–	–	–	–	+	–	+	+	–	–	–	+	+	+

*Genome sequence publicly available and was downloaded from GenBank, †Genomes sequenced as part of this study, ‡Not found in this assembly, supported by previous publications e.g.,Czislowski et al. (2018).
Candidate effectors identified using TBLASTN (1e-6 cut-off, 65% identity and 65% coverage) of *Fusarium* isolate *mimp*-associated 'pan-effectorome' followed by SignalP and EffectorP filtering. *SIX* genes identified using TBLASTN (cut off 1-e^6) using *SIX* genes from *F. oxysporum* f.sp. *lycopersici* isolate 4287 as a reference.

Fola4, one represented by isolate AJ516 and the other by isolates AJ705 and AJ592.

3.3 *SIX* gene phylogenies reveal variation between Fola1 and Fola4, and differences in *SIX8* between Fola4 isolates

Fola races displayed different *SIX* gene profiles with homologs of *SIX8, SIX9*, and *SIX14* in all Fola4 isolates, and homologs of *SIX9* and *SIX14* in all Fola1 isolates. Phylogenetic analysis of *SIX8*, *SIX9*, and *SIX14* revealed sequence variation between Fola races in *SIX9* and *SIX14* as well as variation in *SIX8* sequences amongst the Fola4 isolates (Figure 3). Fola4 isolates had a single copy of *SIX8* which was identical for isolates AJ705 and AJ592, but different for isolate AJ516, with 16 base substitutions and one indel from position 528 to 535 (Supplementary Table SD1-T4). The Fola4 *SIX8* sequences were most closely related to the *F. oxysporum* isolate from rocket (AJ174), *F. oxysporum* f. sp. *conglutinans* (Fo5176), and *F. oxysporum* f. sp. *matthiolae* (AJ260 and PHW726 1). The two different *SIX8* sequence variants within Fola4 were consistently identified within 29 isolates obtained from Italy, Ireland, Netherlands, Spain and UK following PCR and sequencing with 23 isolates having the same sequence as Fola4 isolate AJ516 and 6 isolates having the AJ592/AJ705 sequence (data not shown). Two copies of *SIX9 (SIX9.1 and SIX9.4)* were identified in the Fola1 isolates, with four copies identified in Fola4 isolate AJ516, and five copies in Fola4 isolates AJ705 and AJ592. There was variation in the two copies of *SIX9* in the Fola1 isolates, which were in separate clades, but there was no variation in these copies between isolates (Figure 4). One of the copies of *SIX9 (SIX9.4)* appears to have been duplicated in Fola4, with two copies of *SIX9.4* in each isolate identical to the Fola1 copy. The two additional copies of *SIX9* (*SIX9.2 and SIX9.3*) were found in all Fola4 isolates but were not identified in Fola1 and were similar to copies of *SIX9* identified in *F. oxysporum* from rocket (AJ174), *F. oxysporum* f. sp. *conglutinans* (Fo5176), and *F. oxysporum* f. sp. *matthiolae* (AJ260 and PHW726 1), as observed for *SIX8*. Copies of *SIX9* from *F. oxysporum* ff. spp. *luffae, coriandrii*, and *capsici* were also similar to *SIX9.2 and SIX9.3* identified in Fola4. The remaining sequence variant of *SIX9* (*SIX9.1*) identified was only present in Fola4 isolates AJ705 and AJ592 but was absent in Fola4 isolate AJ516, where the different *SIX8* sequence was identified in comparison with Fola4 isolates AJ705 and AJ592. All Fola4 isolates each had one identical copy of *SIX14* which was the same as the two copies of *SIX14* present in each of the Fola1 isolates (Figure 5). The Fola1 isolates also had an additional third copy of *SIX14*. The different sequence variants of *SIX14* in all Fola isolates were more closely related to each other than to homologues of *SIX14* in other *F. oxysporum* ff. spp.

In summary, the *SIX* gene phylogenies showed clear differences between the two Fola races in terms of gene copy number and sequence; the absence of *SIX8* in Fola1, only two *SIX9* gene variants in Fola1 compared to up to four *SIX9* gene variants in Fola4 isolates, and three *SIX14* gene copies in Fola1 compared to a single copy of *SIX14* in Fola4. Furthermore, differences between Fola4 AJ516 *SIX8* gene sequence and *SIX9* gene variants, compared to AJ705 and

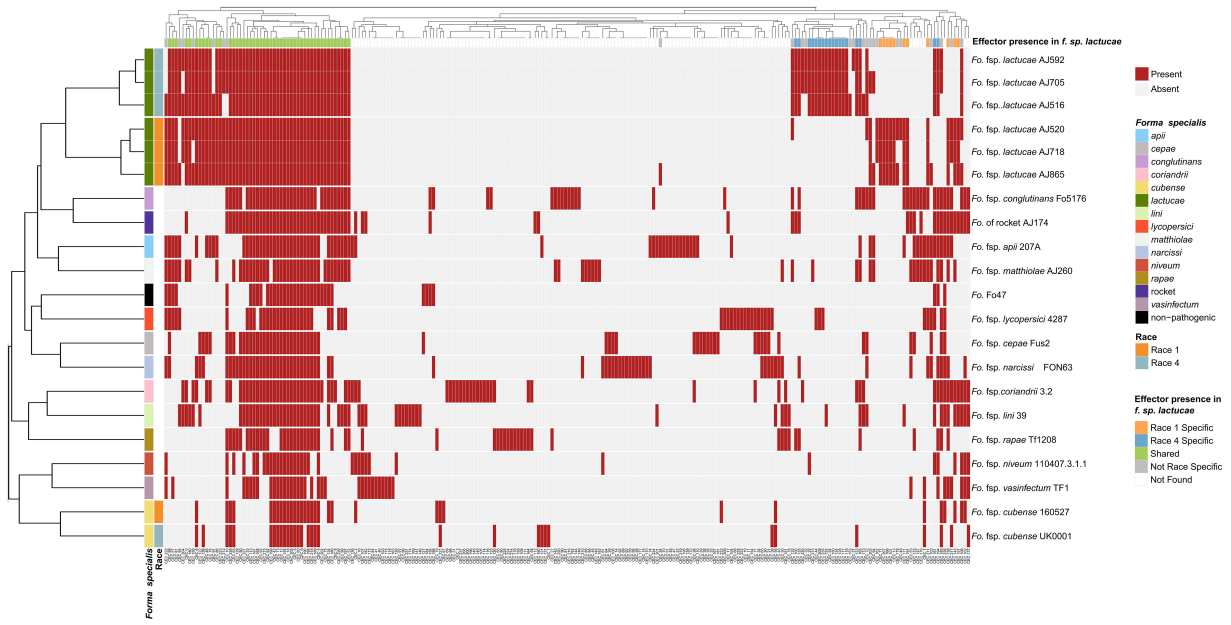

FIGURE 2
Fusarium oxysporum f.sp. *lactucae* races 1 and 4 and other *F. oxysporum* f.spp. clustered based on *mimp*-based effector profile. *Mimps* were identified in the *F. oxysporum* assemblies using either a custom Python script or NHMMER (version 3.3.1) search using a *mimp*-profile Hidden Markov Model. Predicated gene models (Augustus, version 3.3.3) and open reading frames (EMBOSS getorf, version 6.6.6) were filtered for a predicted signal peptide using SignalP (version 4.1) and clustered (CD-HIT, version 4.8.1) to generate a non-redundant protein set for each assembly. Likely effectors were identified using EffectorP (version 2.0.1) and searched against the assemblies using TBLASTN (1e-6 cut-off, 65% identity and 65% coverage). Blast hits were then extracted, sequences filtered (SignalP and EffectorP, default parameters), and clustered into effector groups at ≥65% identity), generating a binary data matrix used to create a heatmap (R Package, Pheatmap). Fola1 isolates are indicated in orange and Fola4 in blue-grey. Red indicates effector presence, grey indicates absence.

AJ592, supported the evidence from the genome phylogenies and the candidate effector profiles for two variants of Fola4.

3.4 Collinearity analysis highlights differences in accessory genomes of Fola isolates

To further understand genome evolution across the Fola isolates, we determined large scale synteny across both core and accessory regions through collinearity analysis. When Fola core sequences were aligned to the Fol 4287 core chromosomes, all Fola isolates demonstrated high collinearity (Supplementary Figure 1), as has been previously observed in other *F. oxysporum* f.spp. However, we observed a possible translocation event in Fola1 AJ520, whereby sequence syntenic with Fol 4287 chromosome 9 was joined to AJ520 contig 2, the rest of which was syntenic with Fol 4287 chromosome 5. This potential translocation region was supported by approximately 30x coverage of long read sequencing data (data not shown) but was not investigated any further. When Fola accessory genome sequences were examined, all three of the Fola1 isolates were found to share a high level of collinearity, with large blocks of syntenic sequences and evidence of some structural variations across the larger contigs (Figure 6). However, collinearity analysis between Fola1 AJ520 and Fola4 AJ516 demonstrated an overall absence of large-scale synteny between these two races, with only small-scale alignments scattered throughout both isolates (Figure 6). Fola4 AJ592 and AJ705 also demonstrated high collinearity, with the majority of contigs being highly syntenic and evidence of only a small number of rearrangements. However, the relationship between Fola4 AJ705 and AJ516 was much more variable. While some contigs shared large blocks of synteny, the remaining contigs displayed evidence of numerous structural variations, including large fragment inversions, translocations, insertions and deletions. These results further highlighted that despite the high collinearity across the core genome sequences, much more genomic variation was observed throughout the accessory genome sequences across the Fola isolates with clear lack of synteny between Fola1 and Fola4. The results also again identified differences between the two Fola4 variants represented by AJ516 and AJ705/AJ592.

3.5 Fola accessory chromosomes are enriched for *mimps*, predicted effectors, *SIX* genes and transposable elements

Genome organisation in Fola1 and Fola4 followed a similar pattern to previously reported *F. oxysporum* genomes (Armitage et al., 2018). *Mimp* sequences (Figure 7, track B), which have previously been shown to be associated with known effectors in *F. oxysporum* f.spp (Schmidt et al., 2013), were enriched on accessory contigs, notably contigs 9, 6, 15, 17, 19, 20, 22 and 27 of Fola4 AJ516, and contigs 4, 5, 19, 24, 27 and 29 of Fola1 AJ520 (Figure 7,

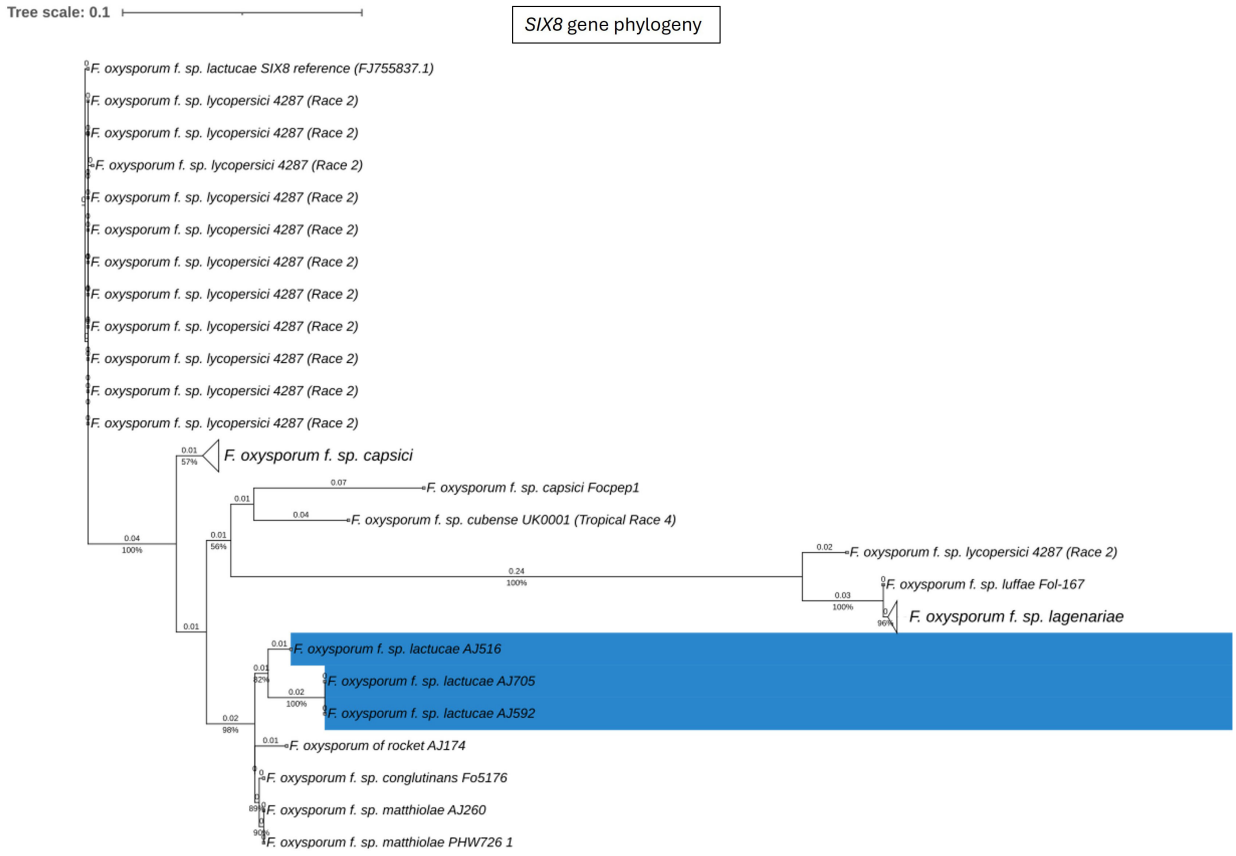

FIGURE 3
Phylogenetic tree of *Fusarium oxysporum SIX8* sequences. ModelFinder, using Bayesian information criterion, was used to calculate the best model of sequence evolution, selecting K2P+G4. IQ-tree2 was used to estimate the maximum likelihood (ML) tree under this model, with 1000 ML bootstrap replicates expressed as a percentage (UFBoot2). The tree is rooted through the *F. oxysporum* f.sp. *lycopersici* SIX8 reference FJ755837.1. *F. oxysporum* f.sp. *lactucae* race 4 isolates are highlighted in blue. Branch lengths are shown above the branch and the scale bar indicates 0.1 substitutions per site. Collapsed clades are denoted by the white triangle.

track B). *SIX* gene homologues were located on contigs 6 and 9 for Fola4 AJ516 (Figure 7A, track D) and contig 5 for Fola1 AJ520 (Figure 7B, track D) indicating that these are putative pathogenicity contigs. Predicted *mimp*-associated effector genes were found in clusters on contigs 6, 9, 15, 19 and 27 for Fola4 AJ516, and on contig 5 in Fola1 AJ520 (Figure 7, track C). Helitrons and other transposons were also enriched on accessory contigs (Figure 7, tracks E, F). In contrast, the frequency of secreted carbohydrate active enzymes (CAZymes) and secondary metabolite clusters (track H) were reduced on the accessory contigs compared to the core (Figure 7, track G). Fola4 AJ516 core contigs 7, 13 and 12 and Fola1 AJ520 core contigs 9, 11 (and 17, 23, 28) showed enrichment of CAZymes as observed for *F. oxysporum* f.sp. *cepae* by Armitage et al. (2018). Very few *mimps* or predicted effectors were present on Fola core contigs. Although helitrons were enriched on accessory contigs, they were also present on core contigs for both Fola1 AJ520 and Fola4 AJ516. The N-terminal [SG]PC[KR]P motif has previously been associated with rapidly evolving genes in *Fusarium* species and was also suggested to play a role in pathogenesis (Sperschneider et al., 2015). An *in silico* analysis showed the motif is found in some secreted proteins in *Fo* f. sp. *albedinis* and may be involved in interactions with host membranes (Rafiqi et al., 2022). However, in this study, only 1.4% (47-49 proteins) of the approximately 3500 proteins with a signal peptide found in each of the Fola race isolates contained the N-terminal [SG]PC[KR]P motif. Of these, 10-12 were identified as putative effectors by EffectorP, but only 1 or 2 were located on accessory contigs in each Fola isolate, while none were identified as putative effectors by our analysis pipeline and hence none were investigated further (Supplementary Table SD1-T7 Fola4 AJ516, T8 Fola4 AJ705 and T9 Fola1 AJ520).

Core contigs showed a consistent level of alignment across all comparative genomes (Fola4 AJ516 and AJ705, Fola1 AJ520 and AJ865, Foma AJ260 and Fo47; Figure 7, tracks I - M). In contrast, accessory contigs of Fola4 AJ516 and Fola1 AJ520 generally showed the most consistent levels of alignment with isolates of the same race, while more variable alignment indicating duplication or loss events, was evident with isolates of the opposite Fola race (Figures 7A, B tracks J-K, tracks I-J) or with Foma AJ260 (track L). Low levels of alignment were observed for all Fola isolates with the non-pathogen Fo47 (Figure 7, track M). Interestingly, accessory contigs 21 and 28 from Fola4 AJ516 (Figure 7A) show a lower level of alignment against Fola4 isolate AJ705 (track I) than it does to either Fola1 AJ520 (track J) or Foma AJ260 (track L), with levels of

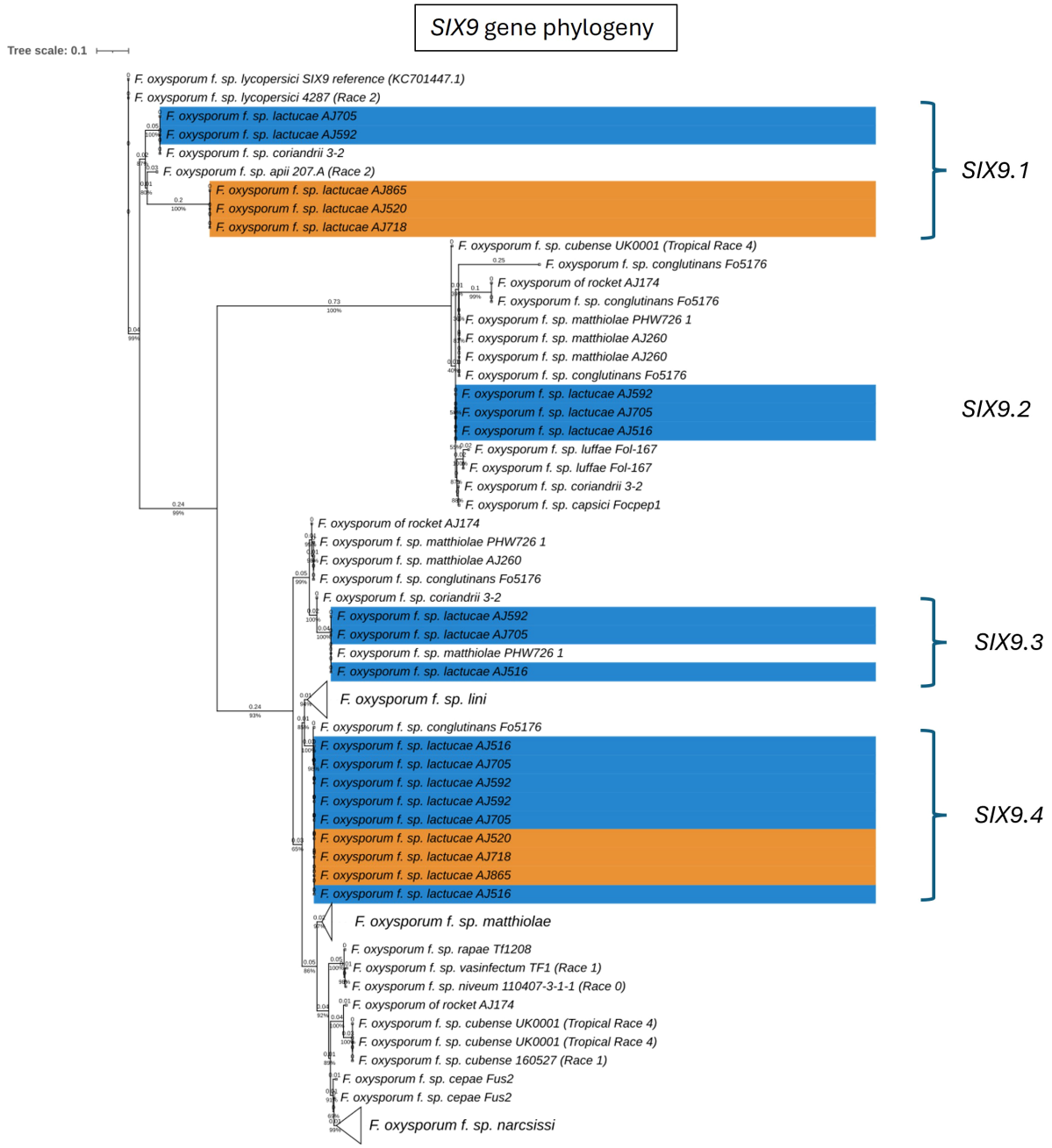

FIGURE 4
Phylogenetic tree of *Fusarium oxysporum SIX9* sequences. ModelFinder, using Bayesian information criterion, was used to calculate the best model of sequence evolution, selecting TPM3+G4. IQ-tree2 was used to estimate the maximum likelihood (ML) tree under this model, with 1000 ML bootstrap replicates expressed as a percentage (UFBoot2). The tree is rooted through the *F. oxysporum* f.sp. *lycopersici SIX9* reference KC701447.1. *F. oxysporum* f.sp. *lactucae* race 1 and race 4 isolates are highlighted in orange and blue respectively. Branch lengths are shown above the branch and the scale bar indicates 0.1 substitutions per site. Collapsed clades are denoted by the white triangle.

alignment against Fola4 AJ705 being more similar to the non-pathogen Fo47 for these two contigs. On further investigation it was found that the subtelomeric 7.5 kb sequences of these two contigs (5' telomere for contig 21 and 3' telomere for contig 28) differed to all other subtelomeric sequences of AJ516, but were very similar to each other. This suggests that these two contigs may be related and possibly part of the same chromosome. Subtelomeric sequences are rapidly evolving regions of the genome (Rahnama et al., 2021) which tend to differ between isolates of different *F. oxysporum* f.sp. while being very similar within a f.sp (Huang, 2023). Phylogenetic analysis of all sub-telomere 7.5 kb regions found in Fola4 AJ516, AJ705 and Fola1 AJ520, showed that Fola1 subtelomeric sequences clustered separately from Fola4 isolates, while Fola4 isolates AJ516 and AJ705 subtelomeric sequences clustered together with the notable exception of AJ516 contigs 21 and 28 which clustered separately (Supplementary Figure 2). This suggests that contigs 21

10.3389/fpls.2024.1415534

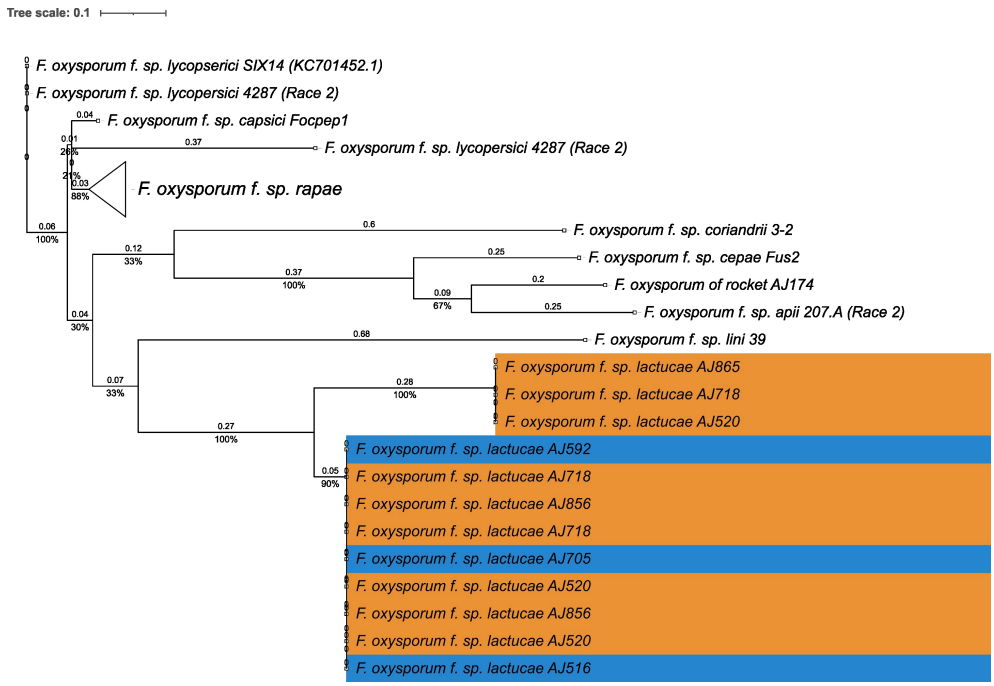

FIGURE 5
Phylogenetic tree of *Fusarium oxysporum SIX14* sequences. ModelFinder, using Bayesian information criterion, was used to calculate the best model of sequence evolution, selecting K2P+G4. IQ-tree2 was used to estimate the maximum likelihood (ML) tree under this model, with 1000 ML bootstrap replicates expressed as a percentage (UFBoot2). The tree is rooted through the *F. oxysporum* f.sp. *lycopersici SIX14* reference KC701452.1. *F. oxysporum* f.sp. *lactucae* race 1 and race 4 isolates are highlighted in orange and blue respectively. Branch lengths are shown above the branch and the scale bar indicates 0.1 substitutions per site. Collapsed clades are denoted by the white triangle.

and 28 from Fola4 AJ516 may have been acquired by HCT from an unknown donor. Although we do not know how recently this HCT event occurred, this provides further evidence that separates the two Fola4 variants.

3.6 RNAseq identifies key shared and unique effectors expressed by Fola1 and Fola4 in lettuce

Genomic mimp-based analysis identified a large number of candidate effectors. To further narrow this list and identify putative effectors of biological importance in Fola pathogenesis, in planta RNAseq of a Fola susceptible lettuce variety was carried out using one Fola1 isolate (AJ520), isolates representing the two variants of Fola4 (AJ516 and AJ705), a closely related non-host pathogenic isolate (Foma AJ260) and the non-pathogen Fo47. RNAseq data were filtered to identify putative effectors highly upregulated *in planta* in each isolate (Supplementary Table SD1-T6-T11). To simplify the comparison of expressed effectors across multiple isolates, often with multiple gene copies, an orthogroup analysis was carried out to identify homologues and therefore orthogroup number is used to refer to unknown putative expressed effectors. The gene ID for each isolate in the orthogroup can be found in Supplementary Table SD1-T12. This analysis identified 14 putative expressed effectors shared between Fola1 AJ520 and Fola4 AJ516 and AJ705, including the known effectors *SIX9* (OG0001312) and *SIX14* (OG0017931, Figure 8). Of these effectors, all but one (OG0017028) showed homology to hypothetical proteins or putative effector proteins from other members of the FOSC following a blastx search of the NCBI database, with several homologues identified in *F. oxysporum* ff. spp. *apii*, *raphani*, *cubense* and *narcissi*. Seven putative effectors were identified as Fola4 specific, including the previously reported divergently transcribed effector pair *SIX8* (OG0019701) and *PSE/PSL1* (OG0021533) (Ayukawa et al., 2021), and one of the *SIX9* (OG0017710) homologues. An additional effector (OG0022521) was identified as present and expressed only in Fola4 AJ705 with homology to a hypothetical protein in *F. oxysporum* f. sp. *cepae*. Three putative effectors were identified as specific to Fola1, two of which had homologues in *F. oxysporum* ff. spp. *vasinfectum*, *raphani* and *matthiolae*.

SIX8, SIX9 and *SIX14* genes were located on contigs 6 and 9 of Fola4 AJ516, with the other expressed putative effectors located mainly on contigs 6, 9, with a few on 15, 19, 27 and 34. In Fola4 AJ705, *SIX* genes were located on contig 2 and contig 20, with the majority of expressed putative effectors located on contig 2, with fewer on contigs 20, 24, 15, 12, and 13. *SIX9* and *SIX14* in Fola1 AJ520 were located on contig 5, with other expressed putative effectors also located mainly on contig 5, with some on contig 4. This identified the main putative pathogenicity contigs as contigs 6 and 9 in Fola4 AJ516, contigs 2 and 20 in Fola4 AJ705 (corresponding to contigs 9, 4 and 24 in Fola4 AJ592) and contigs 4 and 5 for Fola1 AJ520.

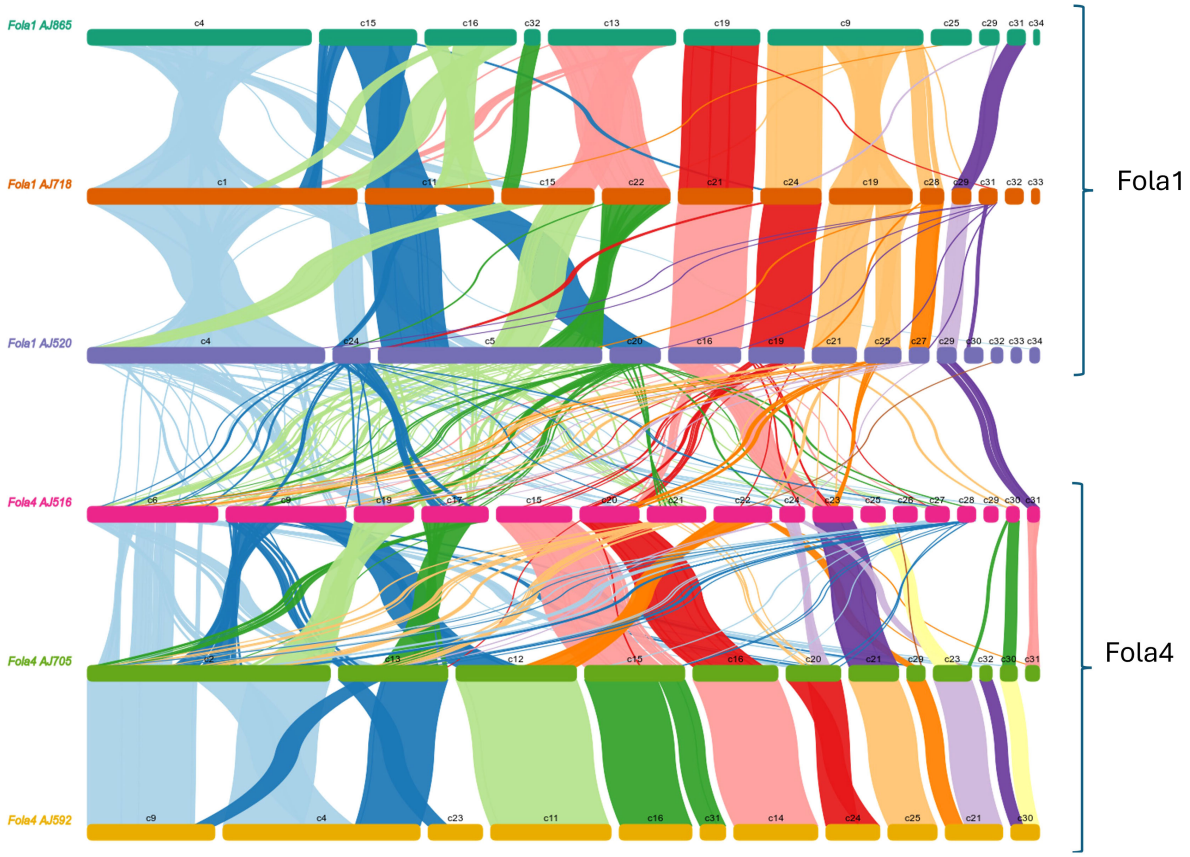

FIGURE 6
Collinearity analysis of *Fusarium oxysporum* f.sp. *lactucae* (Fola) race 1 and race 4 accessory genome sequences, showing syntenic alignments larger than 10 Kb.

Several of the highly expressed putative effectors were found to be arranged as gene pairs divergently transcribed from a shared promoter. This included the Fola4 specific genes *SIX8* and *PSL1*, and the gene pair OG0000519 - OG0018947/OG0016261, which showed evidence of duplication, being present in Fola1 AJ520 and Fola4 AJ705 as three copies and in Fola4 AJ516 as two copies. In Fol, *Avr2* (*SIX3*) is also arranged as a paired effector with *SIX5* sharing a promoter (Cao et al., 2018). Both *SIX8* and *Avr2* are members of the same ToxA-like structural family (Yu et al., 2024) with their paired partner (*PSE1*/*PSL1* and *SIX5* respectively) being members of another structural group, family 4. Further analysis will show if the newly identified paired putative effectors present in Fola will fall into the same categories. In addition, Fola4 carried a head-to-head pair of identical genes with a shared promoter that is duplicated to give four copies of the gene (OG0001121). Moreover, orthogroups OG0000926, OG0001047, OG0001099, OG0000220, OG0001312 and OG0017710 were all present as multiple copies showing evidence of duplications.

Orthogroup analysis also highlighted multiple differences in copy number and sequence variation for some of the expressed putative effectors. Of the multiple *SIX9* copies identified in the DNA phylogeny in the two Fola races (Figure 4), only *SIX9.2* (present in Fola4 only) and *SIX9.4* (present in all Fola isolates) were differentially expressed *in planta*. For the *SIX9.1* copy (present in Fola1 and Fola4 AJ592/AJ705 only), it was found that although the full gene was annotated and present in Fola4 AJ705 and AJ592, it was not expressed *in planta*. Only a partial copy of SIX9.1 was present on contig 5 in Fola1 (which was not annotated) with no RNAseq reads aligned to it. The Fola4 *SIX9.3* gene copies were all partial copies with no gene annotation. In summary, Fola1 AJ520 contained one full-length *SIX9* gene copy (*SIX9.4*) that is upregulated *in planta* and identical to a duplicated upregulated *SIX9* gene copy in Fola4 isolates (*SIX9.4*). Fola4 isolates also contained an additional *SIX9* gene copy (*SIX9.2*) that was also upregulated *in planta*.

Although *SIX14* (OG0017931) had identical DNA sequences for both Fola races, there were differences in both copy number and expression level between Fola1 and Fola4. Despite Fola1 AJ520 having three copies of *SIX14* all located on accessory contig 5, RNAseq indicated that there was low basal expression of these genes with only 30 transcripts per million (TPM) and no upregulation *in planta* (10 TPM). In contrast, the single copy of *SIX14* found in Fola4 AJ516 (contig 9) showed a L2FC of 4.3 with high level of expression, rising from a basal level of 483 TPM to 6309 TPM *in planta* (Supplementary Table SD1). Further investigation of the genome showed that Fola4 AJ516 *SIX14* has a *mimp* sequence 151

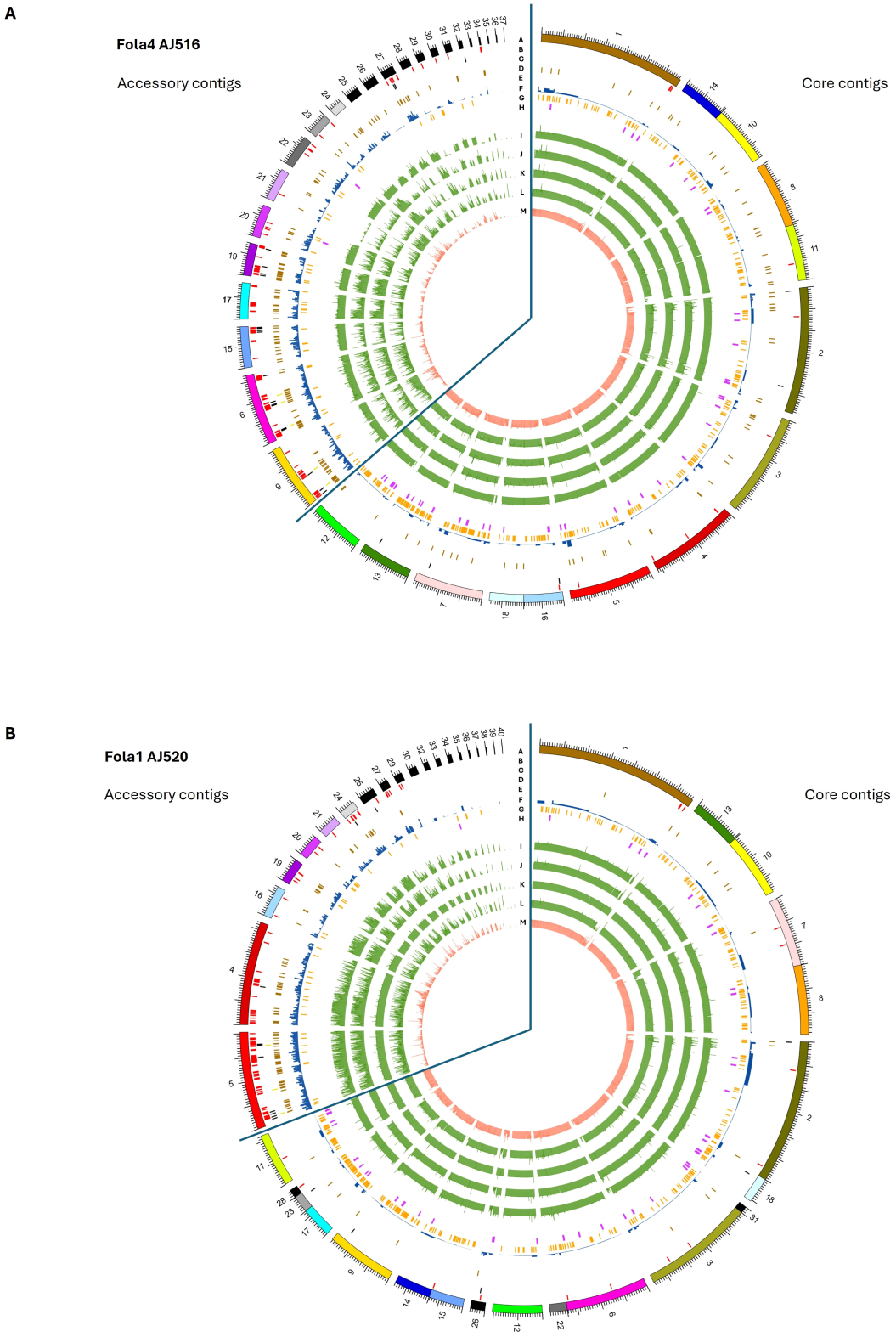

FIGURE 7
Genomic features on core and accessory contigs for **(A)** *Fusarium oxysporum* f. sp. *lactucae* race 4 (Fola4) isolate AJ516 and **(B)** *F. oxysporum* (f) sp. *lactucae* race 1 (Fola1) isolate AJ520. Inner tracks moving in from the outside (Track A) genome assembly contigs, (Track B) *mimp* sequences, (Track C) predicted effector genes (Track D) *SIX* gene homologues (Track E) Helitron transposable elements f) other transposable elements (Track F) secreted carbohydrate active enzymes (Track H) secondary metabolite clusters. Inner tracks (I-M) showing alignment of assemblies to A) Fola4 AJ516 from Fola4 AJ705 (Track I), Fola1 AJ520 (Track J), Fola1 AJ865 (Track K), Foma AJ260 (Track L) and non-pathogen Fo47 (Track M), and B) Fola1 AJ520 from Fola4 AJ516 (Track I) Fola4 AJ705 (Track J), Fola1 AJ865 (Track K) Foma AJ260 (Track L) and non-pathogen Fo47 (Track M).

10.3389/fpls.2024.1415534

		Fola4 AJ516	Fola4 AJ705	Fola1 AJ520	Foma AJ260	Fo47 non-pathogen	Top Blastx hits (% identity)	Candidate effector cluster
Fola1 and Fola4 shared putative effectors	OG0015992	1	1	1	1		hypothetical protein in f. sp. *matthiolae* (100%)	
	OG0018947 OG0016261	2	3	3			effector protein ff. spp. *apii (99%),* cepae (95%)	C46
	OG0000926	3	3	2			effector protein ff. spp. *apii* (55%), albedinis (55%)	
	OG0017027	1	1	1			hypothetical protein ff. spp. *cubense (88%), narcissus (87%)*	C6
	OG0016083	1	1	1	1		hypothetical protein ff. spp. *raphani* (88%), *rapae* (82%)	
	OG0019093	1	1	1			no significant similarity	
	OG0001047	1	2	2	1		hypothetical protein ff. spp. *raphani* (80%), *albedinis* (76%)	C86
	OG0001099	2	2	2			hypothetical protein f. sp. *narcissus* (96%)	C126
	OG0000519	2	3	3			effector protein ff. spp. *apii, physalis, cepae* (99%)	C76
	OG0000220	6	8	1	1		hypothetical protein ff. spp. *vasinfectum (100%) conglutinans (98%)*	C50
	OG0016869	1	1	1	1		Uncharacterised protein *F. redolans* (98%),	C180
	OG0001312	2	2	1	2		SIX9a *ff. spp. conglutinans (100%), sesame* (99%)	C63
	OG0017931	1	1	3			SIX14 **Blastn** 99% identity f. sp. *sesami*	
	OG0017028	1	1	1			No significant homology	
Fola4 putative effectors	OG0019913	1	1				hypothetical protein f. sp. *albedinis* (100%)	
	OG0001121	4	4				hypothetical protein f. sp. *vasinfectum* (98%)	C22
	OG0017710	1	1		2		(SIX9.2) ff. spp. *matthiolae* (98%), conglutinans (98%)	C123
	OG0019884	1	1				No significant homology	
	OG0017138	2	2				hypothetical protein - RALF-like domain	C117
	OG0019701	1	1		1		SIX8 ff.spp. *sesami* (83%), *conglutinans* (83%),	
	OG0021533	1	1		2		PSE1 ff. spp. *lycopersici (94%), conglutinans* (69%)	
	OG0022521		1				hypothetical protein f. sp. *cepae* (94%)	
Fola1 putative effectors	OG0020732			1			no signif homology	
	OG0018816			1			hypothetical protein ff. spp. *raphani* (93%), *vasinfectum* (91%)	C101
	OG0018844			1	1		hypothetical protein ff. spp. *vasinfectum* (98%), *matthiolae* (97%)	

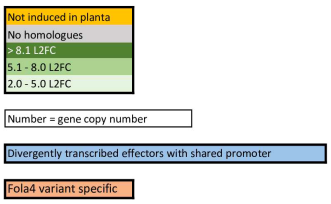

FIGURE 8
Filtered shared and unique candidate effectors upregulated *in planta* for *Fusarium oxysporum* f.sp. *lactucae* race 1 (Fola1) and race 4 (Fola4) isolates in comparison with *Fusarium oxysporum* f.sp. *matthiolae* (Foma) and non-pathogenic *F. oxysporum* Fo47. Candidate effectors are listed by orthogroup and matched to the relevant candidate effector cluster on the effector heatmap (Figure 2) where applicable. Orthogroup numbers coloured blue indicate genes with divergently transcribed paired effectors. Orthogroup OG0022521 (highlighted in pink) is only present in Fola4 AJ705 and AJ592. Numbers indicate gene copy number. Colours indicate level of induction by log 2 fold change (L2FC). Dark green = L2FC >8.1, mid-green = L2FC 5.1 - 8.0, light-green = L2FC 2.0 - 5.0, orange = no induction *in planta*, grey = no homologues.

bp upstream of the start codon, while the two full-length copies of *SIX14* in Fola1 AJ520 on contig 5 have a helitron transposon inserted into the promoter region immediately upstream of the start codon. The third copy of *SIX14* in Fola1 AJ520 has transposon Tf2-9 inserted into the intron between exon 1 and exon 2. In addition, the *mimp* sequence is 1 kb upstream of the start codon. Thus, all copies of *SIX14* in Fola 1 have disruptions or changes to the promoter region with one copy also having a disruption to the gene sequence which prevents expression of this putative effector *in planta*. Other orthogroups that showed differences in expression between races (OG0016083, OG0001047, and OG0019028) require further investigation.

3.7 Fola4 isolates show differences in SIX8-PSE1/PSL1 effector pair sequence

The putative effector gene *PSE1* has previously been reported as divergently transcribed *in planta* from the same promoter as *SIX8* in *F. oxysporum* f.sp. *conglutinans* (Focn, isolate Cong1-1), with both genes being required for virulence on *Arabidopsis* (Ayukawa et al., 2021). Furthermore, the authors reported a similar gene, *PSL1* (PSE1-like) paired with *SIX8* in the tomato infecting isolate Fol 4287 that differed in ten amino acids at the C-terminal (Ayukawa et al., 2021). Both *SIX8* and *PSE1/PSL1* divergently transcribed genes were identified as putative effectors that were induced *in planta* for both Fola4 isolates AJ705 and AJ516 in our RNAseq analysis. As described previously, Fola4 isolates all contain homologues of *SIX8* that are closely related to those present in Focn, Foma and *F. oxysporum* from rocket. These *SIX8* sequence differences identified between Fola4 AJ516 compared with AJ705 and AJ592 result in 7 amino acid substitutions in the SIX8 protein sequence (Figure 9A). All Fola4 isolates also showed differences in the amino acid sequence of *SIX8* compared to Focn and Foma, with Fola4 AJ516 having 4 amino acid substitutions and AJ705/AJ592 having 3 different amino acid substitutions. Alignment of the PSE1 and PSL1 protein sequences (Figure 9B) showed that the PSL1 found in Fola4 AJ516 is more closely related to that from the tomato infecting isolate Fol 4287 than to the PSE1 in either of the other Fola4 isolates AJ705 or AJ592 which in turn are identical to the PSE1 from Focn isolate 5176 and the Foma AJ260 isolate. Notably, isolate Fola4 AJ516 shares the same ten amino acid difference at the C-terminus of PSL1 as the tomato infecting isolate Fol 4287 as previously described (Ayukawa et al., 2021). DNA sequence alignment of a 4 kb region encompassing the *SIX8-PSL1* gene pair (Figure 9C) from all Fola4 isolates, Fol 4287, Focn 5176 (100% sequence identity to isolate Cong1-1 for the *SIX8 - PSE1* gene pair locus), Foma AJ260 and *F. oxysporum* AJ174 from rocket showed that sequence homology between these *F. oxysporum* f.spp. is confined to the region of the genes and, to a lesser extent, the intergenic region, while alignment was quickly lost outside of this region. Interestingly, the only *F. oxysporum* isolate that had a full *mimp* sequence present in the shared promoter was Foma AJ260 (Figure 9C). All isolates that harboured the *SIX8-PSE1/PSL1* gene pair, had a *mimp*TIR. Furthermore, sequence alignment between the Fola4 isolate AJ516 compared to isolates AJ705 and AJ592 was also lost outside of the *SIX8-PSL1* gene pair. The *SIX8-PSE1* gene pair is located on contig 20 of AJ705 and contig 24 of AJ592 which are both telomere to telomere contigs with 99.92% identity to one another. These 1.12 Mb chromosomes also harboured the *SIX9.1* gene copy that is absent in AJ516. Overall these data strongly suggest that Fola4 AJ705 has potentially gained the *SIX8-PSE1* gene

10.3389/fpls.2024.1415534

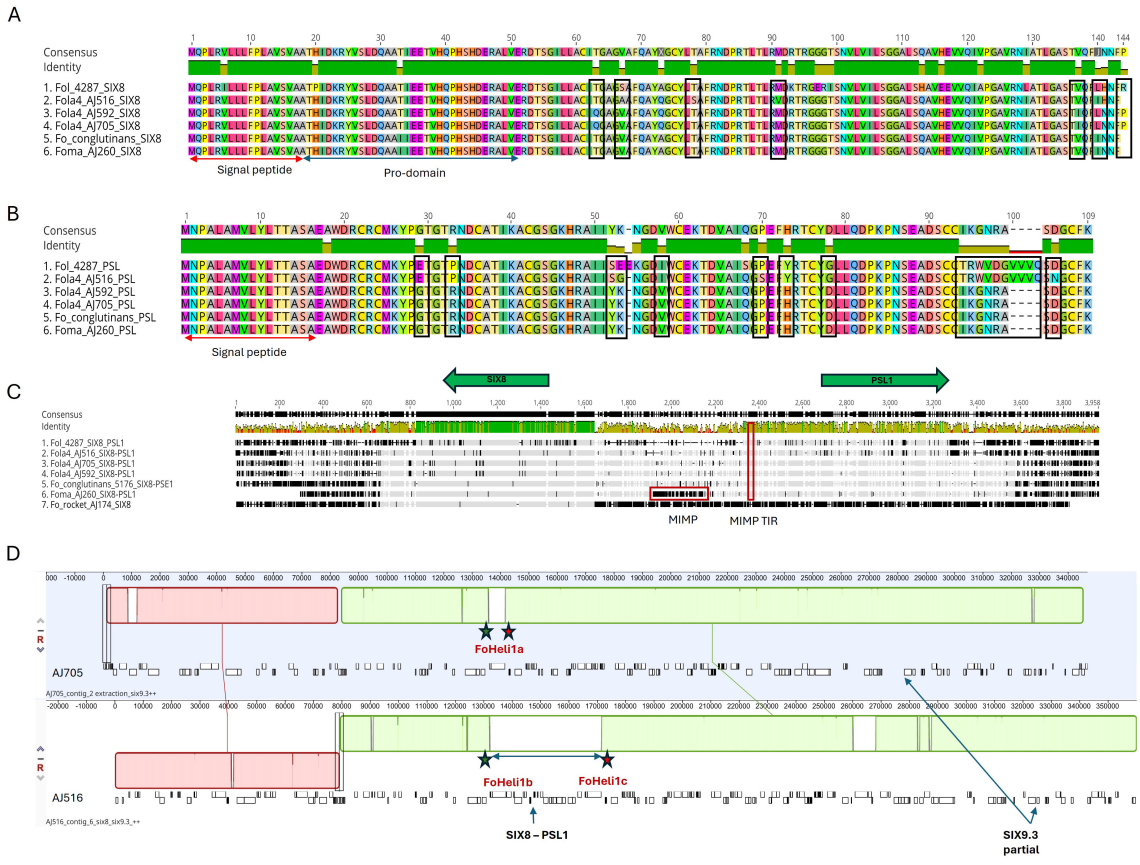

E

FolHeli	5’ insertion site - HAIRPIN	3’ HAIRPIN - insertion site
1a	aatTCAGCCGAAGGCTGACTCTACATTAATCCATAAGTTTCC	TGTACCCCTTGCACCACCGCTCTAAAGTGCAAGGGGTGACGTAGTATTTTtgt
1b	aatTCAGCCGAAGGCTGACTCTACATTAATCCATAAGTTTCC	TGTACCCCTTGCACCACCGCTCTAAAGTGCAAGGGGTGACGTAGTATTTTaat
1c	catTCAGCCGAAGGCTGACTCTACATTAATCCATAAGTTTCC	TGTACCCCTTGCACCACCGCTCTAAAGTGCAAGGGGTGACGTAGTATTTTtgt

FIGURE 9
Comparison of *SIX8* and *PSE1/PSL1* gene pair partition for two *Fusarium oxysporum* f.sp. *lactucae* race 4 (Fola 4) variants represented by isolates AJ516 and AJ592/AJ705 compared with *F. oxysporum* f.sp. *conglutinans* (Focn) isolate 5176 and *F. oxysporum* f.sp. *mathiolae* isolate (Foma) isolate AJ260. Geneious Prime (2023.2.1) alignment of **(A)** SIX8 and **(B)** PSE1/PSL1 protein sequences for Fol 4287, Fola4 AJ516, AJ705 and AJ592, Focn 5176 and Foma AJ260. Amino acid differences between the two Fola4 subgroups are outlined in black. **(C)** Geneious alignment using progressive pairwise alignment and the neighbour-joining method of tree building on default settings to create the tree was carried on the 4kb genomic region covering the *six8 – psl1* genes. *mimp* and *mimp*TIR sequences are outlined in red. **(D)** Anchored genome alignment of locally collinear blocks of 350 kb genomic regions for Fola4 AJ705 contig 2 using Mauve default settings within Geneious Prime 2023.2.1 (top panel) and AJ516 contig 6 (bottom panel). The location of identical FoHeli1-like helitrons are shown. The green and red stars show location of identical 5’ and 3’ insertion sequences respectively. **(E)** 5’ and 3’ insertion sequences of each FoHeli1 with FoHeli1 termini shown in capitals and genomic sequence in lower case.

pair (along with *SIX9*.1 gene copy) by HCT or HGT from a different source to that for the Fola4 AJ516 *SIX8-PSL1* gene pair. This is again supporting evidence for two variants of Fola4. In addition, collinearity analysis (Figure 6) identified a region of synteny between Fola4 AJ516 contig 6 and Fola4 AJ705 contig 9 that appears to span the location of AJ516 *SIX8-PSL1*. Further investigation found that 39 kb of additional genetic material was present in Fola4 AJ516 at the site of a *F. oxysporum* specific helitron sequence in Fola4 AJ705 (Figure 9D). The additional 39 kb present in Fola4 AJ516 was flanked by identical helitrons to that present at this site in AJ705. These helitrons have similar terminal sequences to FoHeli1 (Chellapan et al., 2016) and contain intact rep and hel domains for autonomous replication. The arrangement of the FoHeli sequences and insertion sites suggest either gene gain in Fola4 AJ516 or gene loss in Fola4 AJ705, possibly by homologous recombination at the helitron site (Figures 9D, E). Helitrons usually insert at a TA site so the immediate 5’ nucleotide to the helitron sequence is usually a T and 3’ is usually an A. This was not the case for Fola4 AJ705 which has a TT insertion site, with AAT-5’ and 3’-TGT flanking FoHeli1a (Figure 9E). In Fola4 AJ516 the FoHeli1b 5’ matches the AA T-5’ of AJ705 FoHeli1a and the FoHeli1c 3’-TGT matches AJ705 FoHeli1a. Recombination between FoHeli1b and FoHeli1c could therefore have produced a single FoHeli1 as in AJ705 FoHeli1a, thus losing the *SIX8-PSL1* gene pair.

4 Discussion

4.1 Fola1 and Fola4 have emerged independently from a common ancestor

This research has presented the first full genome and transcriptome data for Fola, which has enabled the identification of key differences in effector repertoire and expression in the globally significant races Fola1 and Fola4 for the first time. Four lines of evidence suggest that the more recently identified Fola4 did not evolve from Fola 1. Firstly, based on our current sampling, phylogenetic analysis of both core and accessory genomes indicated that Fola1 and Fola4 were sister clades, suggesting that Fola4 is not derived from Fola1. This is also supported by a previous report where Fola1 and Fola4 isolates were consistently shown to be in distinct vegetative compatibility groups (Pintore et al., 2017) and by GBS based phylogenetic analysis (Claerbout et al., 2023). Secondly, the *mimp*-associated effector profile for Fola1 and Fola4 also separates them into separate clusters. However, of those predicted effectors that are shared between the two races, the majority are also present in the non-pathogen Fo47 along with many other ff. spp. and so are not pathogen or host specific. Thirdly, collinearity analysis of the accessory genome also suggested that Fola4 did not emerge from Fola1. Here, the larger accessory genome size of Fola4 (17.7 – 20.9 Mb) compared with Fola1 (15.2 – 15.5 Mb) might suggest that Fola4 arose from Fola1 by gain of additional genetic material via HCT/HGT; however, collinearity analysis showed large blocks of synteny between isolates of the same race, in contrast to extremely fragmented and rearranged small islands of synteny between the two races represented by Fola1 AJ520 and Fola4 AJ516. If Fola4 evolved from Fola1, then larger blocks of synteny might be expected between the accessory contigs that originated from Fola1. A final piece of evidence suggesting that Fola4 did not evolve from Fola1, is the difference in the subtelomeric sequences between the two races. Although telomeric regions are highly variable regions prone to transposon insertion, duplications, and rearrangements (Chiara et al., 2015), some fungi, including *Magnaportha oryzae*, *Metarhizium anisopliae* and *Ustilago maydis*, have remarkably stable telomeric regions that also harbour RecQ-like telomere-linked helicase (TLH) genes within ~10 kb of the telomere (Sánchez-Alonso and Guzmán, 1998; Gao et al., 2002; Inglis et al., 2005). More recently, the presence of RecQ-like TLH genes associated with stable, telomere-adjacent sequences specific to *F. oxysporum* ff. spp. has been reported (Huang, 2023; Salimi et al., 2024) where it was suggested that these regions were common between isolates adapted to the same host. In contrast, preliminary comparisons of sequences of the subtelomeric 7.5 kb region from Fola1 AJ520 and AJ718 with Fola4 AJ516 and AJ705, that includes a RecQ-like helicase gene, suggested that these regions were generally in separate race-specific clusters. Overall, these four distinct lines of evidence suggest that Fola4, which was identified more recently, did not evolve directly from Fola1. Two potential evolutionary scenarios could explain the differences between Fola 1 and Fola 4; first that both races inherited their accessory genomes from a common origin which then underwent very different rearrangements/recombination hence resulting in loss of synteny, or second, that the accessory regions were acquired independently, via HCT. It is most likely, however, that Fola1 and Fola4 acquired their accessory genome by a combination of these two scenarios.as this would explain why the races are highly related in sequence (Figure 1B) but show low levels of synteny (Figure 6). Without more extensive sampling of Fola isolates, it is not possible to determine whether the most recent common ancestor of Fola1 and Fola 4 would have been pathogenic on lettuce, or whether this evolved subsequently in both races.

4.2 Identification of both shared and race-specific *SIX* genes and novel putative effectors upregulated *in planta* differentiates the Fola races

Genomic and transcriptomic analyses of Fola1 and Fola4 isolates identified different *SIX* gene complements and expression for the first time. All Fola1 and Fola4 isolates harboured copies of *SIX9* and *SIX14*. Of the two copies of *SIX9* found in Fola1, only one (*SIX9.4*), was found to be expressed *in planta*. The Fola 4 isolates contained different copies of *SIX9*; *SIX9.2* and *SIX9.4* were both expressed *in planta* in all Fola4 isolates while *SIX9.3* was a partial gene copy (pseudogene) not annotated in the genomes. Fola4 isolates AJ705 and AJ592 also harboured *SIX9.1* (unlike the other FOL4 variant isolate AJ516) but this was not expressed *in planta*. *SIX9* has been shown to be structurally similar to *SIX11* (Yu et al., 2024) and its presence was recently found to be associated with highly virulent *F. oxysporum* f. sp. *vasinfectum* race 4 isolates (Jobe et al., 2024). Three copies of *SIX14* were identified in the genome of Fola1 AJ520, but transcriptomic analysis showed that none of these were expressed *in planta*, due to disruptions in the promoter and gene sequences by transposon insertion. In contrast, the single copy of *SIX14* present in Fola4 AJ516 and AJ705 was highly upregulated *in planta*. Loss of *SIX14* expression by pseudogenesis for all copies in Fola1 is a potential key difference between the Fola races that could contribute to their differential virulence on lettuce cultivars. Currently, there is no information on cellular location or interacting proteins for SIX14 although Yu et al. (2024) placed *SIX14* in 'effector family 4' alongside SIX5 and PSE1/PSL1, based on structural similarity of the proteins. However, unlike other members of this group, which are divergently transcribed with another paired effector, Fola *SIX14* does not appear to have a similarly paired transcribed gene. An important finding was that all Fola4 isolates contained a single copy of *SIX8* which was highly induced *in planta* but was absent in Fola1. Two different sequence variations of *SIX8* were also identified within multiple Fola4 isolates, which contributed with other evidence to the conclusion that there are two Fola4 variants. *SIX8* has been reported to be required for virulence of *F. oxysporum* f. sp. *cubense* tropical race 4 (Focub TR4) on Cavendish banana and is absent in Focub race1 (An et al., 2019) and interestingly, two sequence variants of *SIX8* have been identified that separate Focub TR4 from subtropical race 4 (Fraser-Smith et al., 2014). *SIX8* has also been shown to be required for virulence of Focn (isolate cong1-1) on *Arabidopsis* where it may also interact with the divergently transcribed effector PSE1 (paired with *SIX8*; Ayukawa et al., 2021). More recently,

evidence has suggested that two specific members of the TOPLESS gene family in tomato act as susceptibility factors via interaction with SIX8 (Aalders et al., 2024).

RNAseq of Fola1 and Fola4 during lettuce infection identified both shared and race specific expressed putative effectors in addition to the *SIX* genes that require further investigation and characterisation to determine their potential role in pathogenicity. The majority of these corresponded to either candidate effector clusters (CECs) identified using the *mimp*-based effector discovery pipeline (Supplementary Table SD2) or to putative effectors identified in other *F. oxysporum* ff. spp. Of the 25 putative effectors identified as highly expressed *in planta* across all Fola isolates, 12 corresponded to CECs identified using the effector pipeline. Five of these 25 putative effectors were not within 2.5kb of a *mimp*, and of these, two (OG0000220, OG0001047) corresponded to CECs; given the way the pipeline was implemented, this implied that these were orthologues of effectors in other *F. oxysporum* ff. spp. that were associated with a *mimp*. The lack of any DNA or protein sequence similarity between effectors in *F. oxysporum* emphasises the importance of understanding effector protein structure (Yu et al., 2024) and highlighted some short-comings of the *mimp*-based effector discovery pipeline employed here. *Mimp*-associated candidate effectors from each *F. oxysporum* genome were clustered at 65% identity using CD-HIT which designates the longest sequence within each cluster as the representative sequence, which is then submitted to EffectorP for identification. Consequently, if the representative sequence does not meet the EffectorP probability threshold for effector identification, other sequences within the cluster which do are discarded with the entire CEC and this was the case for *SIX14*, *SIX8*, and *PSE1*. This highlights the importance of RNAseq expression data to further inform genome and effectorome analyses to enable more reliable identification of expressed putative effectors.

4.3 Fola4 consists of two different variant forms

This study presented evidence that there are two Fola4 variants represented by Fola4 isolate AJ516 and Fola4 isolates AJ705/AJ592 and this is also supported genotyping by sequencing data for Fola1 and Fola 4 which also suggested two groups of Fola4 (Claerbout et al., 2023). Firstly, our work showed that Fola4 AJ516 diverges from isolates AJ705 and AJ592 in phylogenies of both core and accessory genomes. Synteny analysis of the accessory contigs then demonstrated extremely high similarity between Fola4 AJ705 and AJ592 while in contrast, although a few Fola4 AJ516 accessory genome contigs shared large blocks of synteny with AJ705 contigs, there were many rearrangements and regions of little or no synteny between the two isolates. This could suggest some common vertical inheritance of the accessory genome for both Fola4 variants followed by different recombination and HGT/HCT events. The evidence for different HGT events in the two Fola4 variants is supported by the differences in isolate AJ516 *SIX8-PSL1* gene pair compared with the SIX8-PSE1 pair in Fola4 isolates AJ705/AJ592.

Sanger sequencing of this region showed that the *SIX8-PSE1* and *SIX8-PSL1* sequence differences were consistent across 13 Fola4 isolates (data not shown), partitioning them into two variant groups. Of particular interest is the 10 amino acid difference at the C-terminus of PSE1 (AJ705/AJ592) compared to PSL1 (AJ516). *PSE1* has been identified in Focn isolates virulent on *Arabidopsis* while *PSL1* was found in the tomato-infecting isolate Fol 4287 (Ayukawa et al., 2021). It was then demonstrated that PSL1 could not be substituted for PSE1 in Focn mutants to confer virulence on *Arabidopsis* (Ayukawa et al., 2021). The authors therefore suggested that *PSE/PSL1* might play a role in host specificity, although no evidence of a direct interaction between SIX8 and PSE1 proteins was found in a yeast 2-hybrid assay. More recently however, Yu et al. (2024) demonstrated a direct interaction between SIX8-PSE1 proteins *in vitro*, by co-incubation of expressed proteins and size exclusion chromatography. Given this information, the difference in the *SIX8-PSE1/PSL1* pairs in the two Fola4 variants suggests that they could differ in host range, potentially affecting different lettuce cultivars or even different host species. The two Fola4 variants might also have gained the *SIX8-PSE1/PSL1* gene pairs from different sources. In the Fola4 AJ705/AJ592 variant, the presence of the *SIX8-PSE1* gene pair is close to the *SIX9.1* gene copy on a small accessory chromosome (contig20, 1.12 Mb), which may suggest that this variant has acquired these versions of *SIX8, PSE1* and *SIX9* together by HCT. In contrast, the Fola4 AJ516 variant may have gained the *SIX8-PSL1* pair by the involvement of (identical) FoHeli1-like helitrons that flank a 39 kb block containing the *SIX8-PSL1* locus. This may have been either by helitron insertion of the block following gene capture or by recombination with a helitron already present. Helitrons replicate by a rolling-circle mechanism and are capable of capturing other genes in large fragments, sometimes containing many genes, thus facilitating movement, rearrangement or duplication of genes (Thomas and Pritham, 2015; Barro-Trastoy and Köhler, 2024). Five classes of non-canonical helitrons with distinct end terminal sequences have been identified in the FOSC, with both autonomous and non-autonomous elements present in varying numbers and evidence of circular intermediates suggesting active helitron elements (Chellapan et al., 2016). Helitrons have also been shown to affect gene expression (Castanera et al., 2014) and were implicated in the loss of *SIX4* (*Avr1*) which resulted in a new race of Fol by homologous recombination (Biju et al., 2017). Transfer of chromosomes and partial chromosomes between members of the FOSC has also been demonstrated (Ma et al., 2010; Vlaardingerbroek et al., 2016b; van Dam et al., 2017; Li et al., 2020a, 2020b; Henry et al., 2021) and there is also evidence for the transfer of genes or blocks of genes (Simbaqueba et al., 2018; Liu et al., 2019). The mechanism by which this happens is not clear and needs further investigation but the involvement of recombination, or transposon (including helitrons) activity is implicated. The FoHeli1-like helitrons flanking the 39 kb block in Fola4 AJ516 that contains the *SIX8-PSL1* locus also appear to be currently active. A BLAST search of the Fola genomes revealed that other than these three identical copies, Fola4 AJ516 contains 79 additional copies of this FoHeli1-like helitron that differ by a single synonymous SNP, and a further eight copies with a non-synonymous SNP, while Fola4 AJ705/AJ592 contains 4 identical copies, and a further 80 copies with the same synonymous SNP. In contrast, Fola1 AJ520 has only

16 identical copies of this FoHeli1-like helitron and another 3 with single SNPs, Focn 5176 contains 28 and Fol 4287 has no identical copies. Other FoHeli helitron variants are present in both Fola1 and Fola4 genomes and require a further, more detailed study to understand their involvement in genome reorganisation and the evolution of Fola races. Finally, in addition to the above differences between the two Fola4 variants, there is further provisional evidence of HCT in Fola4 AJ516 that is not present in Fola4 AJ705/AJ592. Accessory genome contigs 21 and 28 in Fola4 AJ516 each have a telomere and, across their length, show very low levels of homology to AJ705. The subtelomere sequences of these two contigs in Fola4 AJ516 were identical and unique while all other Fola4 subtelomere sequences we were able to assemble fell into a single clade. This suggests that contigs 21 and 28 in Fola4 AJ516 might be a recent acquisition from an unknown source. Interestingly, a preliminary search for similarity to other subtelomeric sequences from other Nanopore genome assemblies, found that these two AJ516 contig subtelomere sequences grouped very closely with those from *F. oxysporum* rocket AJ174 (data not shown). With more high quality Nanopore assemblies becoming available, the number of full-length accessory chromosomes or large contigs containing telomeric sequences will enable a more thorough analysis of these regions and potentially increase our understanding of HCT between members of the FOSC.

In summary we have presented the first comparative genome and transcriptome analyses of two globally important Fola races and presented evidence forthe presence of two Fola4 variant forms. In addition, we identified some key putative effectors that are highly upregulated *in planta*, which are common to both races, as well as others that are potentially important in differentiating between Fola1 and Fola4, hence providing essential information for future functional studies. We also provided evidence of potential HCT in each of the two Fola4 variants, as well as the potential involvement of helitrons in affecting gene movement and expression, all of which suggests that Fola is rapidly evolving. A comprehensive genomics study of multiple Fola isolates from all four known races would enable even greater insights into race evolution and a much better understanding of the potential role of HCT and helitrons in driving this process.

Data availability statement

The datasets generated for this study can be found in the article and Supplementary Material. All raw sequencing data and new genome assemblies presented have been submitted to the NCBI under the BioProject ID PRJNA1092066. Further enquiries can be directed to the corresponding author.

Author contributions

HB: Conceptualization, Formal analysis, Investigation, Methodology, Project administration, Validation, Visualization, Writing – original draft, Writing – review & editing. JP: Formal analysis, Investigation, Methodology, Software, Visualization, Writing – original draft, Writing – review & editing. RP: Data curation, Formal analysis, Investigation, Methodology, Visualization, Writing – original draft, Writing – review & editing. SJ: Investigation, Writing – original draft, Writing – review & editing. JC: Formal analysis, Visualization, Writing – original draft, Writing – review & editing. AL: Investigation, Writing – review & editing. AA: Formal analysis, Writing – review & editing. RH: Conceptualization, Funding acquisition, Project administration, Supervision, Writing – original draft, Writing – review & editing. JPC: Conceptualization, Funding acquisition, Project administration, Supervision, Writing – original draft, Writing – review & editing.

Funding

The author(s) declare financial support was received for the research, authorship, and/or publication of this article. This research was funded by the BBSRC project BB/V017608/1, AHDB Horticulture projects CP204 and FV PE 458.

Acknowledgments

We very gratefully acknowledge Giovanna Gilardi (University of Turin), Mathieu Pel (Enza Zaden, NL), Bart Geraats (BASF, NL) and G's Espana for supplying isolates. We also thank Laura Baxter (University of Warwick) for advice on RNAseq analysis. The authors acknowledge Research Computing at the James Hutton Institute for providing computational resources and technical support for the "UK's Crop Diversity Bioinformatics HPC" (BBSRC grants BB/S019669/1 and BB/X019683/1), use of which has contributed to the results reported within this paper.

Conflict of interest

The authors declare that the research was conducted in the absence of any commercial or financial relationships that could be construed as a potential conflict of interest.

Publisher's note

Supplementary material

The Supplementary Material for this article can be found online at: https://www.frontiersin.org/articles/10.3389/fpls.2024.1415534/full#supplementary-material

References

Aalders, T. R., de Sain, M., Gawehns, F., Oudejans, N., Jak, Y. D., Dekker, H. L., et al. (2024). Specific members of the TOPLESS family are susceptibility genes for Fusarium wilt in tomato and Arabidopsis. *Plant Biotechnol. J.* 22, 248–261. doi: 10.1111/pbi.14183

Aimé, S., Alabouvette, C., Steinberg, C., and Olivain, C. (2013). The endophytic strain *Fusarium oxysporum* Fo47: a good candidate for priming the defense responses in tomato roots. *Mol. Plant-Microbe Interact.* 26, 918–926. doi: 10.1094/MPMI-12-12-0290-R

Almagro Armenteros, J. J., Tsirigos, K. D., Sønderby, C. K., Petersen, T. N., Winther, O., Brunak, S., et al. (2019). SignalP 5.0 improves signal peptide predictions using deep neural networks. *Nat. Biotechnol.* 37, 420–423. doi: 10.1038/s41587-019-0036-z

An, B., Hou, X., Guo, Y., Zhao, S., Luo, H., He, C., et al. (2019). The effector SIX8 is required for virulence of *Fusarium oxysporum* f.sp. *cubense* tropical race 4 to Cavendish banana. *Fungal Biol.* 123, 423–430. doi: 10.1016/j.funbio.2019.03.001

Armitage, A. D., Cockerton, H. M., Sreenivasaprasad, S., Woodhall, J., Lane, C. R., Harrison, R. J., et al. (2020). Genomics, evolutionary history and diagnostics of the *Alternaria alternata* species group including apple and asian pear pathotypes. *Front. Microbiol.* 10. doi: 10.3389/fmicb.2019.03124

Armitage, A. D., Taylor, A., Sobczyk, M. K., Baxter, L., Greenfield, B. P. J., Bates, H. J., et al. (2018). Characterisation of pathogen-specific regions and novel effector candidates in *Fusarium oxysporum* f.sp. *cepae*. *Sci. Rep.* 8, 13530. doi: 10.1038/s41598-018-30335-7

Aronesty, E. (2013). Comparison of sequencing utility programs. *Open Bioinf. J.* 7. doi: 10.2174/1875036201307010001

Ayukawa, Y., Asai, S., Gan, P., Tsushima, A., Ichihashi, Y., Shibata, A., et al. (2021). A pair of effectors encoded on a conditionally dispensable chromosome of *Fusarium oxysporum* suppress host-specific immunity. *Commun. Biol.* 4, 707. doi: 10.1038/s42003-021-02245-4

Barro-Trastoy, D., and Köhler, C. (2024). Helitrons: genomic parasites that generate developmental novelties. *Trends Genet.* 0. doi: 10.1016/j.tig.2024.02.002

Bendtsen, J. D., Nielsen, H., Von Heijne, G., and Brunak, S. (2004). Improved prediction of signal peptides: SignalP 3.0. *J. Mol. Biol.* 340, 783–795. doi: 10.1016/j.jmb.2004.05.028

Biju, V. C., Fokkens, L., Houterman, P. M., Rep, M., and Cornelissen, B. J. C. (2017). Multiple evolutionary trajectories have led to the emergence of races in *Fusarium oxysporum* f.sp. *lycopersici*. *Appl. Environ. Microbiol.* 83, e02548–e02516. doi: 10.1128/AEM.02548-16

Blin, K., Shaw, S., Kloosterman, A. M., Charlop-Powers, Z., Van Wezel, G. P., Medema, M. H., et al. (2021). antiSMASH 6.0: improving cluster detection and comparison capabilities. *Nucleic Acids Res.* 49, W29–W35. doi: 10.1093/nar/gkab335

Bray, N. L., Pimentel, H., Melsted, P., and Pachter, L. (2016). Near-optimal probabilistic RNA-seq quantification. *Nat. Biotechnol.* 34, 525–527. doi: 10.1038/nbt.3519

Brenes Guallar, M. A., Fokkens, L., Rep, M., Berke, L., and van Dam, P. (2022). *Fusarium oxysporum* effector clustering version 2: An updated pipeline to infer host range. *Front. Plant Sci.* 13. doi: 10.3389/fpls.2022.1012688

Brůna, T., Hoff, K. J., Lomsadze, A., Stanke, M., and Borodovsky, M. (2021). BRAKER2: automatic eukaryotic genome annotation with GeneMark-EP+ and AUGUSTUS supported by a protein database. *NAR Genomics Bioinf.* 3, 108. doi: 10.1093/nargab/iqaa108

Camacho, C., Coulouris, G., Avagyan, V., Ma, N., Papadopoulos, J., Bealer, K., et al. (2009). BLAST+: architecture and applications. *BMC ioinformatics* 10, 1–9. doi: 10.1186/1471-2105-10-421

Castanera, R., Pérez, G., López, L., Sancho, R., Santoyo, F., Alfaro, M., et al. (2014). Highly expressed captured genes and cross-kingdom domains present in helitrons create novel diversity in *Pleurotus ostreatus* and other fungi. *BMC Genomics* 15, 1071. doi: 10.1186/1471-2164-15-1071

Cao, L., Blekemolen, M. C., Tintor, N., Cornelissen, B. J. C., and Takken, F. L. W. (2018). The *Fusarium oxysporum* Avr2-Six5 effector pair alters plasmodesmatal exclusion selectivity to facilitate cell-to-cell movement of Avr2. *Mol. Plant.* 11, 691–705. doi: 10.1016/j.molp.2018.02.011

Chang, W., Li, H., Chen, H., Qiao, F., and Zeng, H. (2020). Identification of *mimp*-associated effector genes in *Fusarium oxysporum* f. sp. *cubense* race 1 and race 4 and virulence confirmation of a candidate effector gene. *Microbiological Res.* 232, 126375. doi: 10.1016/j.micres.2019.126375

Chellapan, B. V., van Dam, P., Rep, M., Cornelissen, B. J. C., and Fokkens, L. (2016). Non-canonical helitrons in *Fusarium oxysporum*. *Mobile DNA* 7, 27. doi: 10.1186/s13100-016-0083-7

Chen, Y., Nie, F., Xie, S.-Q., Zheng, Y.-F., Dai, Q., Bray, T., et al. (2021). Efficient assembly of nanopore reads via highly accurate and intact error correction. *Nat. Commun.* 12, 60. doi: 10.1038/s41467-020-20236-7

Chiara, M., Fanelli, F., Mulè, G., Logrieco, A. F., Pesole, G., Leslie, J. F., et al. (2015). Genome sequencing of multiple isolates highlights subtelomeric genomic diversity within *Fusarium fujikuroi*. *Genome Biol. Evol.* 7, 3062–3069. doi: 10.1093/gbe/evv198

Claerbout, J., Van Poucke, K., Mestdagh, H., Delaere, I., Vandevelde, I., Venneman, S., et al. (2023). *Fusarium* isolates from Belgium causing wilt in lettuce show genetic and pathogenic diversity. *Plant Pathol.* 72, 593–609. doi: 10.1111/ppa.13668

Claerbout, J., Venneman, S., Vandevelde, I., Decombel, A., Bleyaert, P., Volckaert, A., et al. (2018). First report of *Fusarium oxysporum* f.sp. lactucae race 4 on lettuce in Belgium. *Plant Dis.* 102, 1037. doi: 10.1094/pdis-10-17-1627-pdn

Constantin, M. E., Fokkens, L., de Sain, M., Takken, F. L. W., and Rep, M. (2021). Number of candidate effector genes in accessory genomes differentiates pathogenic from endophytic *Fusarium oxysporum* strains. *Front. Plant Sci.* 12. doi: 10.3389/fpls.2021.761740

Czislowski, E., Fraser-Smith, S., Zander, M., O'Neill, W. T., Meldrum, R. A., Tran-Nguyen, L. T. T., et al. (2018). Investigation of the diversity of effector genes in the banana pathogen, *Fusarium oxysporum* f.sp. *cubense*, reveals evidence of horizontal gene transfer. *Mol. Plant Pathol.* 19, 1155–1171. doi: 10.1111/mpp.12594

De Coster, W., D'Hert, S., Schultz, D. T., Cruts, M., and Van Broeckhoven, C. (2018). NanoPack: visualizing and processing long-read sequencing data. *Bioinformatics* 34, 2666–2669. doi: 10.1093/bioinformatics/bty149

Dobin, A., Davis, C. A., Schlesinger, F., Drenkow, J., Zaleski, C., Jha, S., et al. (2013). STAR: ultrafast universal RNA-seq aligner. *Bioinformatics* 29, 15–21. doi: 10.1093/bioinformatics/bts635

Edel-Hermann, V., and Lecomte, C. (2019). Current status of *Fusarium oxysporum formae speciales* and races. *Phytopathology* 109, 512–530. doi: 10.1094/phyto-08-18-0320-rvw

Emms, D. M., and Kelly, S. (2019). OrthoFinder: phylogenetic orthology inference for comparative genomics. *Genome Biol.* 20, 1–14. doi: 10.1186/s13059-019-1832-y

Finn, R. D., Clements, J., and Eddy, S. R. (2011). HMMER web server: interactive sequence similarity searching. *Nucleic Acids Res.* 39, W29–W37. doi: 10.1093/nar/gkr367

Fraser-Smith, S., Czislowski, E., Meldrum, R. A., Zander, M., O'Neill, W., Balali, G. R., et al. (2014). Sequence variation in the putative effector gene SIX8 facilitates molecular differentiation of *Fusarium oxysporum* f. sp. *cubense*. *Plant Pathol.* 63, 1044–1052. doi: 10.1111/ppa.12184

Fu, L., Niu, B., Zhu, Z., Wu, S., and Li, W. (2012). CD-HIT: accelerated for clustering the next-generation sequencing data. *Bioinformatics* 28, 3150–3152. doi: 10.1093/bioinformatics/bts565

Gálvez, L., Brizuela, A. M., Garcés, I., Cainarca, J. S., and Palmero, D. (2023). First report of *Fusarium oxysporum* f.sp. *lactucae* race 4 causing lettuce wilt in Spain. *Plant Dis.* 107, 2549. doi: 10.1094/pdis-12-22-2819-pdn

Gao, W., Khang, C. H., Park, S.-Y., Lee, Y.-H., and Kang, S. (2002). Evolution and organization of a highly dynamic, subtelomeric helicase gene family in the rice blast fungus *Magnaporthe grisea*. *Genetics* 162, 103–112. doi: 10.1093/genetics/162.1.103

Garibaldi, A., Gilardi, G., and Gullino, M. L. (2004). Varietal resistance of lettuce to *Fusarium oxysporum* f.sp. *lactucae*. *Crop Prot.* 23, 845–851. doi: 10.1016/j.cropro.2004.01.005

Gilardi, G., Franco Ortega, S., Van Rijswick, P. C. J., Ortu, G., Gullino, M. L., and Garibaldi, A. (2017a). A new race of *Fusarium oxysporum* f.sp. *lactucae* of lettuce. *Plant Pathol.* 66, 677–688. doi: 10.1111/ppa.12616

Gilardi, G., Garibaldi, A., Matic, S., Senatore, M. T., Pipponzi, S., Prodi, A., et al. (2019). First report of *Fusarium oxysporum* f.sp. *lactucae* race 4 on lettuce in Italy. *Plant Dis.* 103, 2680–2680. doi: 10.1094/pdis-05-19-0902-pdn

Gilardi, G., Pons, C., Gard, B., Franco-Ortega, S., and Gullino, M. L. (2017b). Presence of Fusarium wilt, incited by *Fusarium oxysporum* f.sp. *lactucae*, on lettuce in France. *Plant Dis.* 101, 1053. doi: 10.1094/PDIS-12-16-1815-PDN

Gilardi, G., Vasileiadou, A., Garibaldi, A., and Gullino, M. L. (2021). Low temperatures favour Fusarium wilt development by race 4 of *Fusarium oxysporum* f.sp. *lactucae*. *J. Plant Pathol.* 103, 973–979. doi: 10.1007/s42161-021-00859-5

Guerrero, M. M., Martínez, M. C., León, M., Armengol, J., and Monserrat, A. (2020). First report of Fusarium wilt of lettuce caused by *Fusarium oxysporum* f.sp. *lactucae* race 1 in Spain. *Plant Dis.* 104, 1858–1858. doi: 10.1094/pdis-10-19-2143-pdn

Guo, L., Han, L., Yang, L., Zeng, H., Fan, D., Zhu, Y., et al. (2014). Genome and transcriptome analysis of the fungal pathogen *Fusarium oxysporum* f. sp. *cubense* causing banana vascular wilt disease. *PloS One* 9, e95543. doi: 10.1371/journal.pone.0095543

Haas, B. (2010). *TransposonPSI: an application of PSI-Blast to mine (Retro-) Transposon ORF homologies*. Available online at: http://transposonpsi.sourceforge.net/.

He, W., Yang, J., Jing, Y., Xu, L., Yu, K., and Fang, X. (2023). NGenomeSyn: an easy-to-use and flexible tool for publication-ready visualization of syntenic relationships across multiple genomes. *Bioinformatics* 39, btad121. doi: 10.1093/bioinformatics/btad121

Henry, P., Kaur, S., Pham, Q. A. T., Barakat, R., Brinker, S., Haensel, H., et al. (2020). Genomic differences between the new *Fusarium oxysporum* f.sp. *apii* (Foa) race 4 on celery, the less virulent Foa races 2 and 3, and the avirulent on celery f. sp. *coriandrii*. *BMC Genomics* 21, 1–23. doi: 10.1186/s12864-020-07141-5

Henry, P. M., Pincot, D. D. A., Jenner, B. N., Borrero, C., Aviles, M., Nam, M.-H., et al. (2021). Horizontal chromosome transfer and independent evolution drive diversification in *Fusarium oxysporum* f.sp. *fragariae*. *New Phytol.* 230, 327–340. doi: 10.1111/nph.17141

Herrero, M. L., Nagy, N. E., and Solheim, H. (2021). First Report of *Fusarium oxysporum* f.sp. *lactucae* race 1 causing Fusarium wilt of lettuce in Norway. *Plant Dis.* 105, 2239. doi: 10.1094/pdis-01-21-0134-pdn

Houterman, P. M., Speijer, D., Dekker, H. L., de Koster, C. G., Cornelissen, B. J. C., and Rep, M. (2007). The mixed xylem sap proteome of *Fusarium oxysporum*-infected tomato plants. *Mol. Plant Pathol.* 8, 215–221. doi: 10.1111/j.1364-3703.2007.00384.x

Huang, X. (2023). Host-specific subtelomere: structural variation and horizontal transfer in asexual filamentous fungal pathogens. *Preprint bioRxiv*. doi: 10.1101/2023.02.05.527183

Inglis, P. W., Rigden, D. J., Mello, L. V., Louis, E. J., and Valadares-Inglis, M. C. (2005). Monomorphic subtelomeric DNA in the filamentous fungus, *Metarhizium anisopliae*,contains a RecQ helicase-like gene. *Mol. Genet. genomics: MGG* 274, 79–90. doi: 10.1007/s00438-005-1154-5

Jangir, P., Mehra, N., Sharma, K., Singh, N., Rani, M., and Kapoor, R. (2021). Secreted in xylem genes: Drivers of host adaptation in *Fusarium oxysporum*. *Front. Plant Sci.* 12. doi: 10.3389/fpls.2021.628611

Jobe, T. O., Urner, M., Ulloa, M., Broders, K., Hutmacher, R. B., and Ellis, M. L. (2024). *Secreted in xylem* (*SIX*) gene *SIX9* is highly conserved in *Fusarium oxysporum* f. sp. *vasinfectum* race 4 isolates from cotton in the United States. *PhytoFrontiers*. doi: 10.1094/PHYTOFR-11-23-0143-SC

Jones, P., Binns, D., Chang, H.-Y., Fraser, M., Li, W., McAnulla, C., et al. (2014). InterProScan 5: genome-scale protein function classification. *Bioinformatics* 30, 1236–1240. doi: 10.1093/bioinformatics/btu031

Katoh, K., Rozewicki, J., and Yamada, K. D. (2019). MAFFT online service: multiple sequence alignment, interactive sequence choice and visualization. *Briefings Bioinf.* 20, 1160–1166. doi: 10.1093/bib/bbx108

Kolde, R., and Kolde, M. R. (2015). Package 'pheatmap'. *R Package* 1, 790.

Krzywinski, M., Schein, J., Birol, I., Connors, J., Gascoyne, R., Horsman, D., et al. (2009). Circos: an information aesthetic for comparative genomics. *Genome Res.* 19, 1639–1645. doi: 10.1101/gr.092759.109

Langmead, B., and Salzberg, S. L. (2012). Fast gapped-read alignment with Bowtie 2. *Nat. Methods* 9, 357–359. doi: 10.1038/nmeth.1923

Letunic, I., and Bork, P. (2021). Interactive Tree Of Life (iTOL) v5: an online tool for phylogenetic tree display and annotation. *Nucleic Acids Res.* 49, W293–W296. doi: 10.1093/nar/gkab301

Li, H. (2013). Aligning sequence reads, clone sequences and assembly contigs with BWA-MEM. *arXiv preprint arXiv:1303.3997*. doi: 10.48550/arXiv.1303.3997

Li, H. (2018). Minimap2: pairwise alignment for nucleotide sequences. *Bioinformatics* 34, 3094–3100. doi: 10.1093/bioinformatics/bty191

Li, J., Fokkens, L., Conneely, L. J., and Rep, M. (2020a). Partial pathogenicity chromosomes in *Fusarium oxysporum* are sufficient to cause disease and can be horizontally transferred. *Environ. Microbiol.* 22, 4985–5004. doi: 10.1111/1462-2920.15095

Li, J., Fokkens, L., van Dam, P., and Rep, M. (2020b). Related mobile pathogenicity chromosomes in *Fusarium oxysporum* determine host range on cucurbits. *Mol. Plant Pathol.* 21, 761–776. doi: 10.1111/mpp.12927

Li, H., Handsaker, B., Wysoker, A., Fennell, T., Ruan, J., Homer, N., et al. (2009). The sequence alignment/map format and SAMtools. *Bioinformatics* 25, 2078–2079. doi: 10.1093/bioinformatics/btp352

Liu, S., Wu, B., Lv, S., Shen, Z., Li, R., Yi, G., et al. (2019). Genetic diversity in FUB Genes of *Fusarium oxysporum* f. sp. *cubense* suggests horizontal gene transfer. *Front. Plant Sci.* 10. doi: 10.3389/fpls.2019.01069

Love, M. I., Huber, W., and Anders, S. (2014). Moderated estimation of fold change and dispersion for RNA-seq data with DESeq2. *Genome Biol.* 15, 1–21. doi: 10.1186/s13059-014-0550-8

Ma, L.-J., van der Does, H. C., Borkovich, K. A., Coleman, J. J., Daboussi, M.-J., Di Pietro, A., et al. (2010). Comparative genomics reveals mobile pathogenicity chromosomes in *Fusarium*. *Nature* 464, 367–373. doi: 10.1038/nature08850

Motohashi, S. (1960). Occurrence of lettuce root rot. *Ann. Phytopathological Soc. Japan* 25, 47.

Murray, J. J., Hisamutdinova, G., Sandoya, G. V., Raid, R. N., and Slinski, S. (2021). Genetic resistance of *Lactuca* spp. against *Fusarium oxysporum* f. sp. *lactucae* race 1. *HortScience* 56, 1552–1564. doi: 10.21273/hortsci16186-21

Nguyen, L.-T., Schmidt, H. A., Von Haeseler, A., and Minh, B. Q. (2015). IQ-TREE: a fast and effective stochastic algorithm for estimating maximum-likelihood phylogenies. *Mol. Biol. Evol.* 32, 268–274. doi: 10.1093/molbev/msu300

Nielsen, H., and Krogh, A. (1998). Prediction of signal peptides and signal anchors by a hidden Markov model. *Ismb*, 122–130.

Pasquali, M., Dematheis, F., Gullino, M. L., and Garibaldi, A. (2007). Identification of race 1 of *Fusarium oxysporum* f. sp. *lactucae* on lettuce by inter-retrotransposon sequence-characterized amplified region technique. *Phytopathology* 97, 987–996. doi: 10.1094/phyto-97-8-0987

Petersen, T. N., Brunak, S., Von Heijne, G., and Nielsen, H. (2011). SignalP 4.0: discriminating signal peptides from transmembrane regions. *Nat. Methods* 8, 785–786. doi: 10.1038/nmeth.1701

Pintore, I., Gilardi, G., Gullino, M. L., and Garibaldi, A (2017). Analysis of vegetative compatibility groups of Italian and Dutch isolates of Fusarium oxysporum f. sp. lactucae. *J. Plant Path.* 99, 517–521.

Quinlan, A. R., and Hall, I. M. (2010). BEDTools: a flexible suite of utilities for comparing genomic features. *Bioinformatics* 26, 841–842. doi: 10.1093/bioinformatics/btq033

R Core Team (2021). *R: A language and environment for statistical computing*. (Vienna, Austria: R Foundation for Statistical Computing). Available online at: https://www.R-project.org/.

Rafiqi, M., Jelonek, L., Diouf, A. M., Mbaye, A., Rep, M., and Diarra, A. (2022). Profile of the in *silico* secretome of the palm dieback pathogen, *Fusarium oxysporum* f. sp. *albedinis*, a fungus that puts natural oases at risk. *PloS One* 17, e0260830. doi: 10.1371/journal.pone.0260830

Rahnama, M., Wang, B., Dostart, J., Novikova, O., Yackzan, D., Yackzan, A., et al. (2021). Telomere roles in fungal genome evolution and adaptation. *Front. Genet.* 12. doi: 10.3389/fgene.2021.676751

Rempel, A., and Wittler, R. (2021). SANS serif: alignment-free, whole-genome-based phylogenetic reconstruction. *Bioinformatics* 37, 4868–4870. doi: 10.1093/bioinformatics/btab444

Salimi, S., Abdi, M. F., and Rahnama, M. (2024). Characterization and organization of telomeric-linked helicase (TLH) gene families in *Fusarium oxysporum*. *Preprint BioRxiv*. doi: 10.1101/2024.02.27.582403

Sánchez-Alonso, P., and Guzmán, P. (1998). Organization of chromosome ends in *Ustilago maydis* RecQ-like helicase motifs at telomeric regions. *Genetics* 148, 1043–1054. doi: 10.1093/genetics/148.3.1043

Schmidt, S. M., Houterman, P. M., Schreiver, I., Ma, L., Amyotte, S., Chellappan, B., et al. (2013). MITEs in the promoters of effector genes allow prediction of novel virulence genes in *Fusarium oxysporum*. *BMC Genomics* 14, 119. doi: 10.1186/1471-2164-14-119

Scott, J. C., Kirkpatrick, S. C., and Gordon, T. R. (2010). Variation in susceptibility of lettuce cultivars to fusarium wilt caused by *Fusarium oxysporum* f.sp. *lactucae*. *Plant Pathol.* 59, 139–146. doi: 10.1111/j.1365-3059.2009.02179.x

Simão, F. A., Waterhouse, R. M., Ioannidis, P., Kriventseva, E. V., and Zdobnov, E. M. (2015). BUSCO: assessing genome assembly and annotation completeness with single-copy orthologs. *Bioinformatics* 31, 3210–3212. doi: 10.1093/bioinformatics/btv351

Simbaqueba, J., Catanzariti, A. M., González, C., and Jones, D. A. (2018). Evidence for horizontal gene transfer and separation of effector recognition from effector function revealed by analysis of effector genes shared between cape gooseberry- and tomato-infecting *formae speciales* of *Fusarium oxysporum*. *Mol. Plant Pathol.* 19, 2302–2318. doi: 10.1111/mpp.12700

Simbaqueba, J., Rodríguez, E. A., Burbano-David, D., González, C., and Caro-Quintero, A. (2021). Putative novel effector genes revealed by the genomic analysis of the phytopathogenic fungus *Fusarium oxysporum* f. sp. *physali* (Foph) that infects cape gooseberry plants. *Front. Microbiol.* 11. doi: 10.3389/fmicb.2020.593915

Sperschneider, J., Gardiner, D. M., Dodds, P. N., Tini, F., Covarelli, L., Singh, K. B., et al. (2016). EffectorP: predicting fungal effector proteins from secretomes using machine learning. *New Phytol.* 210, 743–761. doi: 10.1111/nph.13794

Sperschneider, J., Gardiner, D. M., Thatcher, L. F., Lyons, R., Singh, K. B., Manners, J. M., et al. (2015). Genome-wide analysis in three *Fusarium* Pathogens Identifies Rapidly Evolving Chromosomes and Genes Associated with Pathogenicity. *Genome Biol. Evol.* 7, 1613–1627. doi: 10.1093/gbe/evv092

Stanke, M., Keller, O., Gunduz, I., Hayes, A., Waack, S., and Morgenstern, B. (2006). AUGUSTUS: ab initio prediction of alternative transcripts. *Nucleic Acids Res.* 34, W435–W439. doi: 10.1093/nar/gkl200

Takken, F., and Rep, M. (2010). The arms race between tomato and *Fusarium oxysporum*. *Mol. Plant Pathol.* 11, 309–314. doi: 10.1111/j.1364-3703.2009.00605.x

Taylor, A., Armitage, A. D., Handy, C., Jackson, A. C., Hulin, M. T., Harrison, R. J., et al. (2019a). Basal Rot of Narcissus: Understanding Pathogenicity in *Fusarium oxysporum* f. sp. *narcissi*. *Front. Microbiol.* 10. doi: 10.3389/fmicb.2019.02905

Taylor, A., Barnes, A., Jackson, A. C., and Clarkson, J. P. (2019b). First Report of *Fusarium oxysporum* and *Fusarium redolens* causing wilting and yellowing of wild rocket (*Diplotaxis tenuifolia*) in the United Kingdom. *Plant Dis.* 103, 1428–1428. doi: 10.1094/pdis-12-18-2143-pdn

Taylor, A., Jackson, A. C., and Clarkson, J. P. (2019c). First report of *Fusarium oxysporum* f. sp. *lactucae* race 4 causing lettuce wilt in England and Ireland. *Plant Dis.* 103, 1033–1033. doi: 10.1094/pdis-10-18-1858-pdn

Taylor, A., Vágány, V., Jackson, A. C., Harrison, R. J., Rainoni, A., and Clarkson, J. P. (2016). Identification of pathogenicity-related genes in *Fusarium oxysporum* f. sp. *cepae*. *Mol. Plant Pathol.* 17, 1032–1047. doi: 10.1111/mpp.12346

Testa, A. C., Hane, J. K., Ellwood, S. R., and Oliver, R. P. (2015). CodingQuarry: highly accurate hidden Markov model gene prediction in fungal genomes using RNA-seq transcripts. *BMC Genomics* 16, 1–12. doi: 10.1186/s12864-015-1344-4

Thomas, J., and Pritham, E. J. (2015). Helitrons, the Eukaryotic rolling-circle transposable elements. *Microbiol. Spectr.* 3. doi: 10.1128/microbiolspec.mdna3-0049-2014

Trapnell, C., Williams, B. A., Pertea, G., Mortazavi, A., Kwan, G., van Baren, M. J., et al. (2010). Transcript assembly and abundance estimation from RNA-Seq reveals thousands of new transcripts and switching among isoforms. *Nat. Biotechnol.* 28, 511. doi: 10.1038/nbt.1621

van Amsterdam, S., Jenkins, S., and Clarkson, J. P. (2023). First report of *Fusarium oxysporum* f. sp. *lactucae* race 1 causing lettuce wilt in Northern Ireland. *Plant Dis.* 107, 2524. doi: 10.1094/pdis-01-23-0196-pdn

van Dam, P., Fokkens, L., Ayukawa, Y., van der Gragt, M., Ter Horst, A., Brankovics, B., et al. (2017). A mobile pathogenicity chromosome in *Fusarium oxysporum* for infection of multiple cucurbit species. *Sci. Rep.* 7, 9042. doi: 10.1038/s41598-017-07995-y

van Dam, P., Fokkens, L., Schmidt, S. M., Linmans, J. H. J., Kistler, H. C., Ma, L.-J., et al. (2016). Effector profiles distinguish formae speciales of *Fusarium oxysporum*. *Environ. Microbiol.* 18, 4087–4102. doi: 10.1111/1462-2920.13445

van Dam, P., and Rep, M. (2017). The distribution of miniature impala elements and *SIX* genes in the *Fusarium* genus is suggestive of horizontal gene transfer. *J. Mol. Evol.* 85, 14–25. doi: 10.1007/s00239-017-9801-0

Vaser, R., Sović, I., Nagarajan, N., and Šikić, M. (2017). Fast and accurate *de novo* genome assembly from long uncorrected reads. *Genome Res.* 27, 737–746. doi: 10.1101/gr.214270.116

Vlaardingerbroek, I., Beerens, B., Rose, L., Fokkens, L., Cornelissen, B. J. C., and Rep, M. (2016a). Exchange of core chromosomes and horizontal transfer of lineage-specific chromosomes in *Fusarium oxysporum*. *Environ. Microbiol.* 18, 3702–3713. doi: 10.1111/1462-2920.13281

Vlaardingerbroek, I., Beerens, B., Schmidt, S. M., Cornelissen, B. J. C., and Rep, M. (2016b). Dispensable chromosomes in *Fusarium oxysporum* f. sp. *lycopersici*. *Mol. Plant Pathol.* 17, 1455–1466. doi: 10.1111/mpp.12440

Walker, B. J., Abeel, T., Shea, T., Priest, M., Abouelliel, A., Sakthikumar, S., et al. (2014). Pilon: an integrated tool for comprehensive microbial variant detection and genome assembly improvement. *PloS One* 9, e112963. doi: 10.1371/journal.pone.0112963

Wang, Y., Zhao, Y., Bollas, A., Wang, Y., and Au, K. F. (2021). Nanopore sequencing technology, bioinformatics and applications. *Nat. Biotechnol.* 39, 1348–1365. doi: 10.1038/s41587-021-01108-x

Wheeler, T. J., and Eddy, S. R. (2013). nhmmer: DNA homology search with profile HMMs. *Bioinformatics* 29, 2487–2489. doi: 10.1093/bioinformatics/btt403

Yang, H., Yu, H., and Ma, L.-J. (2020). Accessory chromosomes in *Fusarium oxysporum*. *Phytopathology* 110, 1488–1496. doi: 10.1094/phyto-03-20-0069-ia

Yu, D. S., Outram, M. A., Smith, A., McCombe, C. L., Khambalker, P. B., Rima, S. A., et al (2024). The structural repertoire of Fusarium oxysporum f. sp. lycopersici effectors revealed by experimental and computational studies. *eLife* 12, RP89280. doi: 10.7554/eLife.89280.3

Zhang, H., Yohe, T., Huang, L., Entwistle, S., Wu, P., Yang, Z., et al. (2018). dbCAN2: a meta server for automated carbohydrate-active enzyme annotation. *Nucleic Acids Res.* 46, W95–W101. doi: 10.1093/nar/gky418

frontiers | Frontiers in Plant Science

TYPE Original Research
PUBLISHED 14 April 2025
DOI 10.3389/fpls.2025.1366158

OPEN ACCESS

EDITED BY
Inmaculada Larena,
Instituto Nacional de Investigación y Tecnología Agraria y Alimentaria (INIA-CSIC), Spain

REVIEWED BY
Bharadwaj Chellapilla,
Indian Agricultural Research Institute (ICAR), India
Raghavendra Aminedi,
Indian Council of Agricultural Research (ICAR), India

*CORRESPONDENCE
Ying-Lien Chen
ychen28@ntu.edu.tw

†These authors have contributed equally to the work and share first authorship

RECEIVED 05 January 2024
ACCEPTED 19 March 2025
PUBLISHED 14 April 2025

CITATION
Hou Y-H, Zhang T-X and Chen Y-L (2025) Host-induced gene silencing targeting the calcineurin of *Fusarium fujikuroi* to enhance resistance against rice bakanae disease. *Front. Plant Sci.* 16:1366158. doi: 10.3389/fpls.2025.1366158

Host-induced gene silencing targeting the calcineurin of *Fusarium fujikuroi* to enhance resistance against rice bakanae disease

Yi-Hsuan Hou[1,2,3†], Ting-Xiang Zhang[4†] and Ying-Lien Chen[1,4*]

[1]Department of Plant Pathology and Microbiology, National Taiwan University, Taipei, Taiwan, [2]Institute of Biotechnology, National Taiwan University, Taipei, Taiwan, [3]Agricultural Biotechnology Research Center, Academia Sinica, Taipei, Taiwan, [4]Master Program for Plant Medicine, National Taiwan University, Taipei, Taiwan

Bakanae, or foolish seedling disease of rice, is caused by the ascomycetous fungus *Fusarium fujikuroi*, which is prevalent in many rice-growing countries. Current protection strategies depend on fungicides, but this results in chemical-resistant *F. fujikuroi* and detrimental environmental effects. It is known that calcineurin controls Ca^{2+} signaling, which mediates growth, stress responses, and pathogenicity in fungi. Based on the pharmacological inhibition of calcineurin in *F. fujikuroi*, we discovered that calcineurin inhibitor FK506 or cyclosporin A can intensely prevent the growth of *F. fujikuroi*, and further investigated the feasibility of silencing calcineurin genes of *F. fujikuroi* in rice using host-induced gene silencing (HIGS) to confer resistance to bakanae disease. The constructs *FfCNA1-Ri* and *FfCNB1-Ri* were introduced into rice plants by using *Agrobacterium*-mediated gene transformation, and the copy numbers of transgenes were examined by Southern blot hybridization in the transgenic lines. The results of pathogen inoculation assay and fungal biomass quantification demonstrated that the transgenic rice plants that carry the *FfCNA1-Ri* or *FfCNB1-Ri* construct had increased resistance against bakanae disease. We propose that RNAi-derived siRNAs might efficiently suppress the expression of calcineurin genes in *F. fujikuroi*, leading to impaired growth and poor colonization of *F. fujikuroi* in rice. These findings indicate that HIGS might be a potential disease management strategy for rice bakanae disease.

KEYWORDS

***Fusarium fujikuroi*, calcineurin, *Oryza sativa*, host-induced gene silencing, bakanae disease**

Introduction

Rice bakanae (also known as foolish seedling disease) caused by *Fusarium fujikuroi* [teleomorph: *Gibberella fujikuroi* (Sawada)] is widespread in the major rice-growing countries of Asia and Africa (Chen et al., 2016b; Sunani et al., 2019). As a disease that frequently occurs in rice-producing regions, the yield losses caused by the pathogen be up to 75%, posing a substantial threat to crop production (Matić et al., 2016; Piombo et al., 2020; Peng et al., 2022). The contaminated seeds primarily serve as the inoculum in the field. Furthermore, thick-walled hyphae and macroconidia can persist in plant debris and soil, leading to infections in the subsequent growing season (Carter et al., 2008; Chen et al., 2020; Tadasanahaller et al., 2023). Germinated conidia invade plants through seeds, stem bases, and root tips, subsequently establishing colonization within plant tissues (Sun, 1975). Under specific conditions, infected plants can produce a large quantity of conidia, which can be readily transmitted to nearby plants. Particularly during the heading stage, infected seeds initiate a new disease cycle in the subsequent season (Matic et al., 2017). During the seedling stage, infected rice plants show typical disease symptoms, such as spindly growth with thin and chlorotic leaves. As the disease progresses, *F. fujikuroi* colonies are aggregated in the vascular tissue and retard water transport, subsequently resulting in the severely infected seedlings dying at the early stages of grow or after transplanting into the field.

In crops, the predominant disease control strategy against *F. fujikuroi* is using fungicides to treat seeds. However, the increasing occurrence of the disease and developing resistance to fungicide in the fungal population have become a dilemma for disease management (Chen et al., 2016a; Niehaus et al., 2017). Thus, developing strategies providing credible, sustainable resistance to bakanae disease is necessary in crops, among which generation of *F. fujikuroi*-resistant cultivars might serve as one option.

An alternative approach to using fungicides involves RNA interference (RNAi), and is known as host-induced gene silencing (HIGS). RNAi has become a powerful tool for the characterization of gene function or generating disease resistant plants (Ghag, 2017). The RNAi processes are initiated with an RNase III enzyme (Dicer), which cuts the precursor double-stranded RNA (dsRNA) into double-stranded small interfering RNAs (siRNAs) of approximately 21 nucleotides (nt). These siRNAs are unwound into single-stranded siRNA by helicase, and the antisense siRNAs are then bound with several proteins, resulting in the formation of an RNA-induced silencing complex (RISC). The RISC is then base-paired with the endogenous complementary mRNA, leading to the cleavage of targeted mRNAs or blocking protein translation (Majumdar et al., 2017).

HIGS is the ectopic expression of siRNAs in transgenic plants in order to silence specific genes of pathogens or pests. HIGS generates siRNA molecules in plants targeting the specific mRNAs of pathogens and cause their degradation. Recently, the application of HIGS has been shown to be a powerful strategy for plants against phytopathogenic fungi and other pathogens (Nunes and Dean, 2012; Qi et al., 2018). During the pathogen-host interaction, the siRNA derived from transgenic plants can traffic into pathogens through an unidentified mechanism, which might result in targeted gene silencing, known as cross-kingdom RNA interference (ckRNAi) (Wang et al., 2016). The translocation mechanism of dsRNA/siRNA between the pathogen and the host relies on either a naked form or encapsulation within extracellular vesicles (EVs) (Wang and Dean, 2020; He et al., 2021; Mahanty et al., 2023). As a result, the efficiency of ckRNAi is positively correlated with the uptake of dsRNAs by fungi from the external environment. HIGS was used in wheat against *Fusarium* head blight with a specific chitin synthase gene from *Fusarium graminearum* constructed using RNAi and ectopic expression in transgenic wheat, and it was found that the chitin synthase gene was downregulated in *F. graminearum* and thereby conferred durable resistance to wheat head blight (Cheng et al., 2015). The dsRNA-derived siRNAs expressed in banana could silence two vital fungal genes *VEL* and *FTF1* in *Fusarium oxysporum* f. sp. *cubense* (Ghag et al., 2014), revealing that HIGS might be applicable for resistance against banana Fusarium wilt. The cyclic adenosine monophosphate protein kinase A (PKA) has been demonstrated to show vital roles in controlling pathogenicity, morphogenesis and development in phytopathogenic fungi (Fuller and Rhodes, 2012). The transgenic wheat plants expressing siRNAs targeting the *CPK1* (a PKA) gene of *Puccinia striiformis* f. sp. *tritici* (*Pst*) increased the resistance of wheat to stripe rust (Qi et al., 2018). The transgenic rice capable of expressing a specific dsRNA sequence was developed and evaluated for its effectiveness in combating *Rhizoctonia solani* AG-1 IA. The specific dsRNA sequence targets *AGLIP1*, an effector in the pathogen that induces cell death in rice protoplasts. The transgenic plant exhibited stable dsRNA expression and enhanced resistance against the pathogen, as evidenced by reduced infection areas and lower fungal biomass in the infected transgenic rice line (Mei et al., 2024). These studies provide important insight for developing stable transgenic plants using a HIGS-mediated silencing of specific genes in fungi.

Calcineurin is a calcium/calmodulin-dependent protein phosphatase and forms a heterodimer including a catalytic subunit A (Cna) and regulatory subunit B (Cnb) (Juvvadi et al., 2014). In the fungal kingdom, calcineurin maintains cellular processes as diverse as growth, morphogenesis, ion homeostasis, stress response, and virulence by triggering downstream targets (Hemenway and Heitman, 1999; Park et al., 2019). When fungal cells come across external stress, the cell compartment Ca^{2+} influx system is initiated and causes an augmented intracellular Ca^{2+} concentration. In the calcineurin signaling, calmodulin (CaM) and calcineurin Cnb subunit play as a sensor for the Ca^{2+} signal, then CaM/Ca^{2+} specifically binds to Cna and Cnb subunits of calcineurin to form a CaM/Ca^{2+}-calcineurin complex, resulting in the activation of protein phosphatase activity. The activated calcineurin then dephosphorylates the downstream targets, such as Crz1, permitting their nuclear import and inducing the expression of the target genes (Juvvadi and Steinbach, 2015; Liu et al., 2015).

For phytopathogenic fungi, calcineurin also acts crucial role in pathogenicity. The previous studies had shown that calcineurin signaling pathway involves in multiple cellular processes (Chen

et al., 2010; Juvvadi et al., 2014; Hou et al., 2020; Yadav and Heitman, 2023). Induction of antisense calcineurin expression in *Sclerotinia sclerotiorum* impaired sclerotial development at the prematuration phase. It resulted in the decrease of cell wall β-1,3-glucan content and attenuated pathogenesis in tomato and *Arabidopsis* (Harel et al., 2006). In *Magnaporthe grisea*, inhibition of calcineurin by cyclosporin A (CsA) was found to inhibit hyphal growth, appressorium development and retarded infection structure formation, indicating that calcineurin is vital for the formation of infection structure in *M. grisea* (Viaud et al., 2002, Viaud et al., 2003). In *Fusarium graminearum*, the calcium-calcineurin pathway involved in fungicide sensitivity. Either by chelating Ca^{2+} or inhibiting calcineurin with CsA, the inhibitory effect of tebuconazole was enhanced (Wang et al., 2023). Moreover, the Cna subunit of calcineurin was required for the morphogenesis and ear gall formation in *Ustilago maydis* (Egan et al., 2009). However, the roles of calcineurin in growth and pathogenicity have not yet been studied in *F. fujikuroi*.

In this study, we demonstrate the feasibility of HIGS-based silencing of calcineurin genes of *F. fujikuroi* in rice to confer resistance to bakanae disease. In bioassays, transgenic rice that carried the *FfCNA1*-RNAi or *FfCNB1*-RNAi construct showed a high level of resistance toward *F. fujikuroi* infection. Our results showed that RNAi-derived siRNAs might efficiently suppress the expression of calcineurin genes in *F. fujikuroi*, leading to impaired growth and poor colonization of *F. fujikuroi* in rice. These results indicate that HIGS might be a potential disease management strategy for rice bakanae disease.

Results

Identification of Cna1 and Cnb1 in *Fusarium fujikuroi*

To identify genes encoding calcineurin catalytic subunit Cna1 and regulatory subunit Cnb1 protein in *F. fujikuroi*, a BLAST search was conducted in NCBI (https://www.ncbi.nlm.nih.gov/) by using the amino acid sequences of Cna1 (XP_018243626) and Cnb1 (XP_018234243) in *F. oxysporum* f. sp. *lycopersici*. BLAST results revealed FoCna1 and FoCnb1 orthologs in *F. fujikuroi* (*Ff*) designated as FfCna1 (XP_023429196) and FfCnb1 (XP_023428777), respectively. The predicted *FfCNA1* has an open reading frame (ORF) of 1698 bp, encoding a protein with 565 amino acids, which contains a catalytic domain, an autoinhibitory domain, a Cnb1 binding helix, and a CaM-binding domain (Figure 1A). The *FfCNB1* has an ORF of 522 bp that encodes a protein of 173 amino acids, which contains four Ca^{2+}-binding motifs (Figure 1B). Sequence alignments of amino acid showed that FfCna1 shares 99%, 87%, and 86% identity with the calcineurin A subunit of *F. oxysporum* f. sp. *lycopersici*, *Sclerotinia sclerotiorum*, and *Magnaporth oryzae*, respectively. The FfCnb1 shared 99% identity with the calcineurin B subunit in *F. oxysporum* f. sp. *lycopersici*, and 94% to both *S. sclerotiorum* and *M. oryzae*. The phylogenetic trees revealed that *F. fujikuroi* calcineurin was closely related to the calcineurin of *F. oxysporum* f. sp. *lycopersici* but was distant to those in yeasts (Figure 2).

In vitro effect of calcineurin inhibitors on the growth of *F. fujikuroi*

Calcineurin inhibitors were used to examine the roles of calcineurin on the growth of *F. fujikuroi*. The mycelia agar discs of *F. fujikuroi* IL01 were inoculated on PDA medium in the absence or presence of FK506 (1 mg/mL) or cyclosporin A (CsA, 100 mg/mL), and incubated at 25°C for 7 days. The average diameter of the *F. fujikuroi* mycelia colony was able to extend 36.3 ± 2.1 mm in the inhibitor-free medium after 7 days of incubation (Figure 3). Whereas in the medium containing FK506 or CsA, the average diameter of the colonies was only 18.5 ± 0.2 and 16.9 ± 0.1 ($P< 0.001$). These results indicated that calcineurin is critical for *F. fujikuroi* growth.

Generation of RNAi constructs and transgenic rice

To investigate whether HIGS can be applied to combat rice bakanae disease, the RNAi strategy was performed for specific targeting of *F. fujikuroi* calcineurin mRNA transcripts. For the *FfCNA1*-RNAi construct, a 503 bp fragment of *FfCNA1* gene containing the 5'-untranslated region (328 bp) and 5'-coding sequence (175 bp) was PCR amplified from *F. fujikuroi* genomic DNA using primer sets JC1440/JC1441 and JC1442/JC1443. The 503 bp DNA fragment was fused up and downstream of the PDK intron in the vector pKANNIBAL (Helliwell and Waterhouse, 2003), and the inverted repeat of *FfCNA1* construct was expressed under the control of the CaMV 35S promoter (Figure 4A) to generate the *FfCNA1-Ri* construct in transgenic rice. Likewise, a 439 bp DNA fragment of *FfCNB1* containing the 3'-coding region (11 bp) followed by the 3'-untranslated region (428 bp) was amplified with primer pairs of JC1444/JC1445 and JC1446/JC1447. The construct of *FfCNB1-Ri* (Figure 4B) was similar to the *FfCNA1-Ri* described above. The *FfCNA1-Ri* and *FfCNB1-Ri* constructs were then cloned into the pBH binary vector (Ho et al., 2000) (Figure 4). The rice calli induced from the immature embryo were used for the *Agrobacterium*-mediated gene transformation. Under hygromycin B selection, 7 and 11 T0 independent antibiotic resistant transgenic lines of *FfCNA1-Ri* and *FfCNB1-Ri* were obtained, respectively, and used for further studies.

Molecular analysis of transformants

To confirm whether the hygromycin B resistant lines contained the transgenes, the antibiotic selection marker *hygromycin phosphotransferase gene* (*Hph*) contained in the transgene cassette was amplified by PCR. The genomic DNA was purified from the T1 seedlings of the putative transgenic

10.3389/fpls.2025.1366158

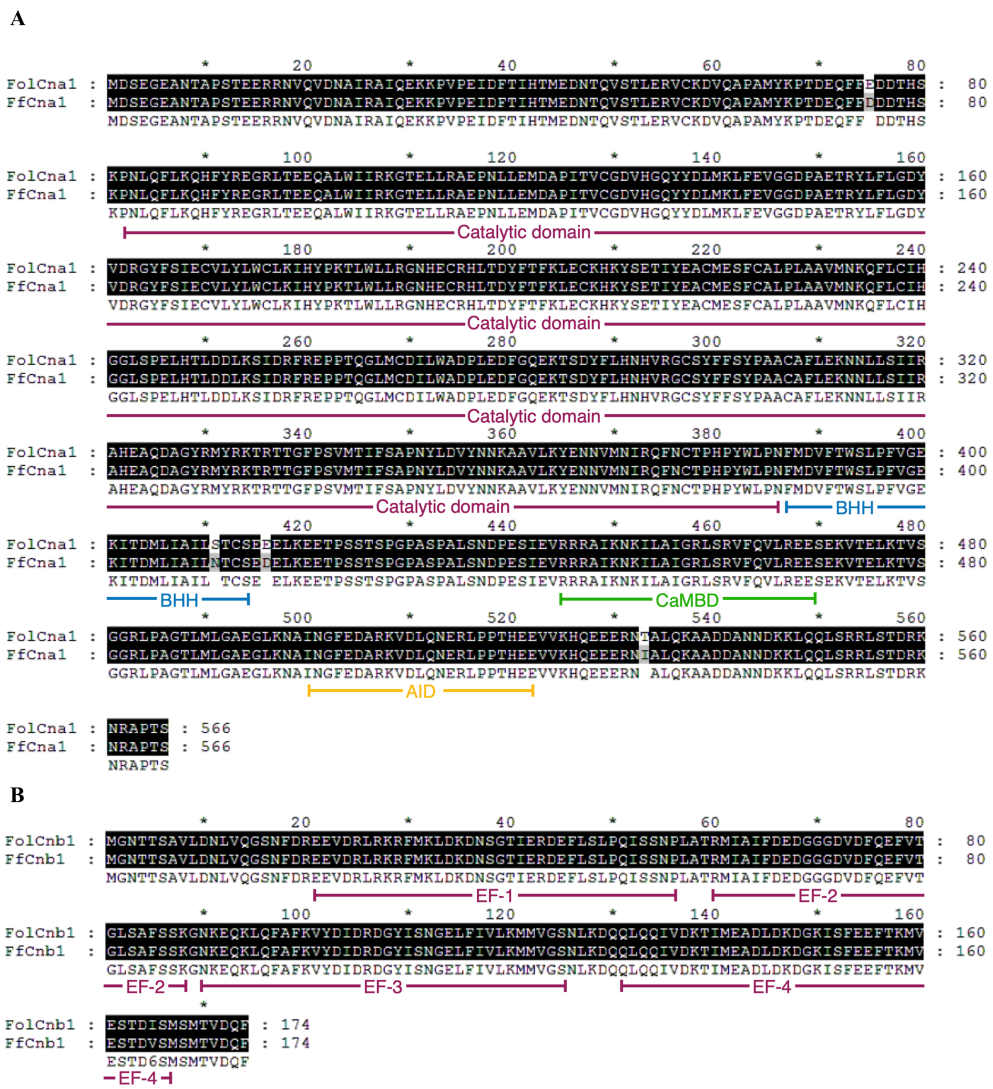

FIGURE 1
Domains and motifs of *Fusarium fujikiuroi* calcineurin catalytic (Cna1) and regulatory (Cnb1) subunits. Amino acid alignment of FfCna1 **(A)** and FfCnb1 **(B)** with homologs from *F. oxysporum* f. sp. *lycopersici*. Identical amino acids are shown by the white letters on the black background. The results indicate that FfCna1 contains a catalytic domain, a Cnb1 binding helix (BBH), a CaM-binding domain (CaMBD) and an autoinhibitory domain (AID), while FfCnb1 contains four Ca^{2+}-binding motifs (EF).

lines, and then used as template for PCR amplification As shown in Figure 5A, the results revealed that all the putative transgenic lines could produce the targeted DNA fragments (548 bp), whereas there was no signal detected in the wild-type control. These results demonstrated that all putative transgenic plants (*FfCNA1-Ri* and *FfCNB1-Ri* lines) contained the targeted transgenes. Moreover, to prevent the segregation and recombination of multiple copies of transgenes in the next generation of offspring, and to verify the transgenic lines that are consistent with the expression levels of transgenes, it is necessary to screen the transgenic lines carrying single copy of transgene. Southern blot analysis was performed to select single-copy transgenic lines, ensuring stable integration of the transgenes in the genome of transgenic rice plants. Because the T-DNA in the binary vector has only one restriction site *Pst*I, the number of hybridization signals detected on the x-ray films after chemiluminescence corresponded to the copy number of the T-DNAs integrated into the rice genome in these transgenic lines. After hybridization with an alkaline phosphatase-labeled *Hph* probe, in *FfCNA1-Ri* transgenic plants, we found that two independent lines, *FfCNA1-Ri*-2 and *FfCNA1-Ri*-11, exhibited a single copy of the transgene. In *FfCNB1-Ri* transgenic plants, we identified that three independent lines, *FfCNB1-Ri-2*, *FfCNB1-Ri-4* and *FfCNB1-Ri-5*, had one copy of the transgene (Figure 5B). All single-copy transgenic rice plants were healthy and showed a growth phenotype similar to the wild-type plants.

10.3389/fpls.2025.1366158

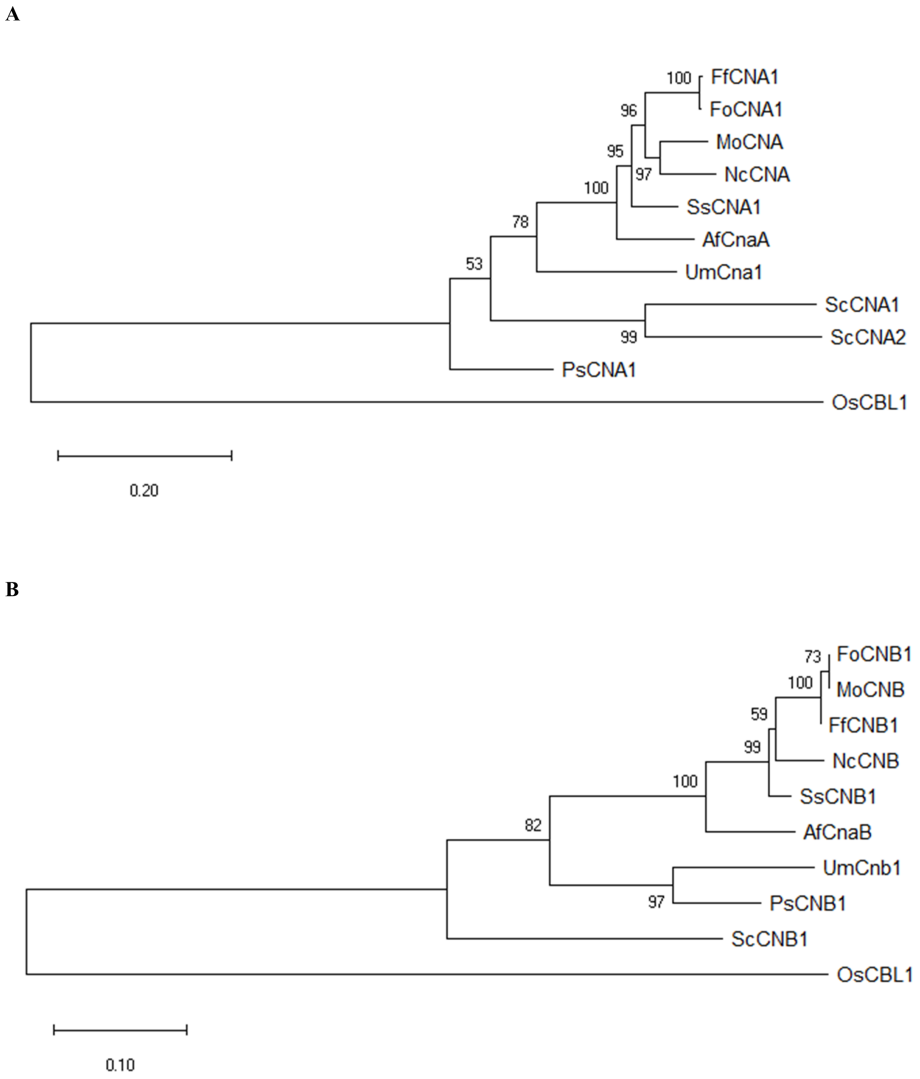

FIGURE 2
Phylogenetic analysis of *F. fujikuroi* CNA1 and CNB1 subunits. Phylogenetic tree of FfCNA1 **(A)** and FfCNB1 **(B)** with homologs from model organisms and phytopathogens. In addition, the calcineurin-B like protein of rice was also included. The phylogenetic tree was constructed in MEGA software using the neighbor-joining method. Confidence of groupings was estimated by using 1,000 bootstraps. GenBank accession number of proteins: FfCNA1 and FfCNB1 (*Fusarium fujikuroi*, XP_023429196 and XP_023428777), FoCNA1 and FoCNB1 (*Fusarium oxysporum* f. sp. *lycopersici* 4287, XP_018243626 and XP_018234243), MoCNA and MoCNB (*Magnaporthe oryzae* 70-15, XP_003711354 and XP_003709672), NcCNA and NcCNB (*Neurospora crassa* OR74A, XP_961193 and CAA73345), SsCNA1 and SsCNB1 (*Sclerotinia sclerotiorum* 1980 UF-70, XP_001597594 and XP_001598128), AfCnaA and AfCnaB (*Aspergillus fumigatus* Af293, XP_753703 and XP_747624), UmCna1 and UmCnb1 (*Ustilago maydis*, AAP48999 and EAK82139), ScCNA1 and ScCNA2 (*Saccharomyces cerevisiae*, NP_013537 and NP_013655), ScCNB1 (*Saccharomyces cerevisiae*, NP_012731), PsCNA1 and PsCNB1 (*Puccinia striiformis* **f**. sp. *tritici*, AFW98882 and AFW98883), OsCBL1 *(Oryza sativa* Japonica Group, NP_001391328).

FfCNA1-Ri and *FfCNB1-Ri* transgenic rice plants exhibit enhanced resistance to *F. fujikuroi* infection

To study the effects of *F. fujikuroi* IL01 on rice seedlings, a disease model of IL01 infected rice seedlings was established. Results showed typical bakanae symptoms in wild-type rice infected with *F. fujikuroi* IL01, such as internode elongation, large leaf angle, and seedling slender (Figure 6A). A pathogen infection assay was further conducted to evaluate the resistance toward *F. fujikuroi* between wild-type and transgenic rice seedlings. The T2 transgenic rice seeds derived from all the single-copy transgenic lines and the wild-type were dehulled and sterilized with sodium hypochlorite solution, and germinated on 1/2 MS medium with (transgenic lines) or without (wild-type) hygromycin B to remove the revertant seeds (wild-type). After culturing for 4 days, most of the wild-type and transgenic seeds had germinated, whereas the embryos from the revertant seeds became black. The seeds that had been germinated for 4 days were inoculated with *F. fujikuroi* (10^5 conidia/mL) and grown at 28°C. To determine the levels of disease severity on pathogen-infected rice seedlings, the disease severity index (DSI) was divided into 0–4 levels, and disease severity was calculated at 21 days post-infection(dpi). The disease severity (%) in wild-type was 58.3 ± 8.3% (DSI3), whereas in *FfCNA1-Ri*-2, -11

10.3389/fpls.2025.1366158

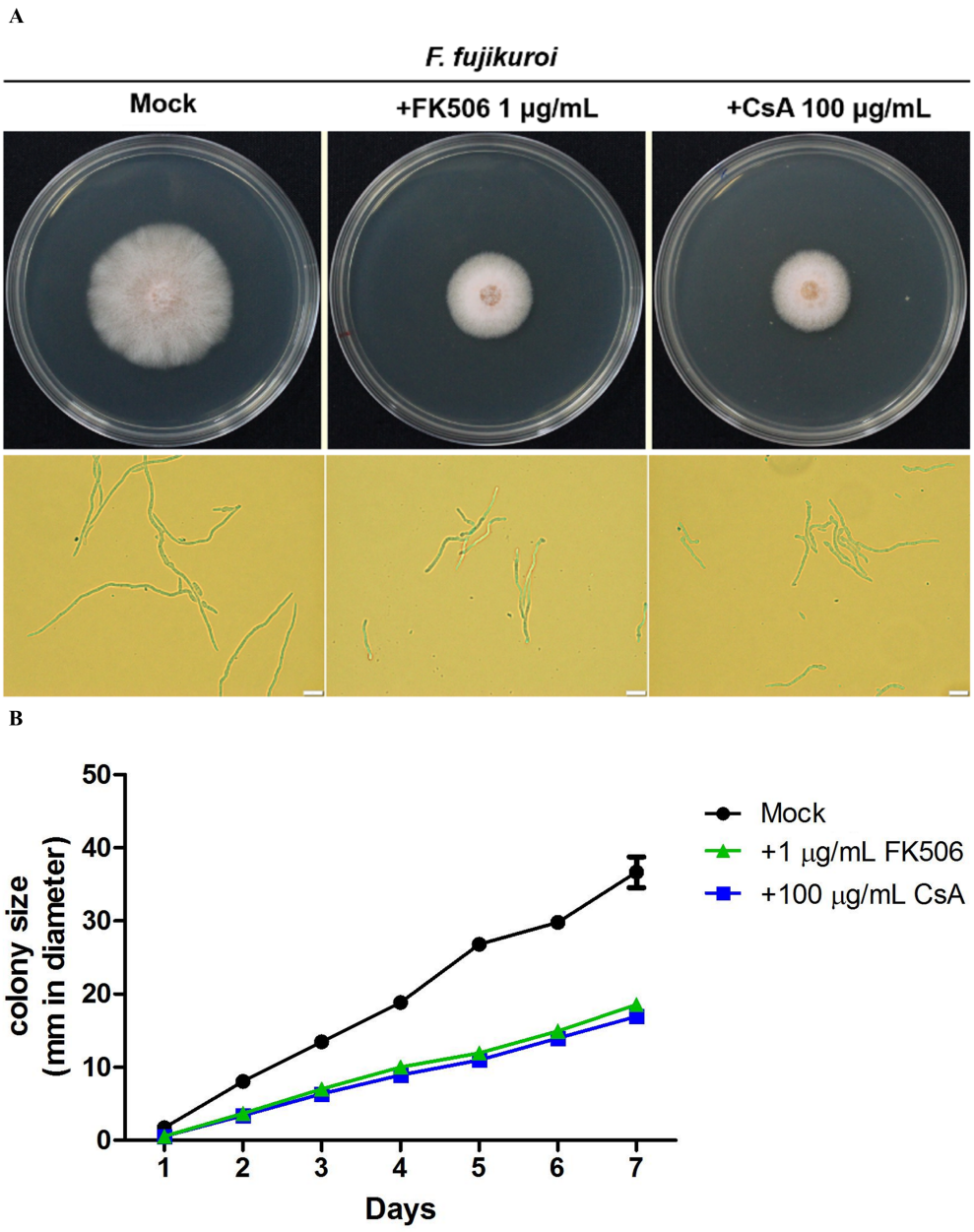

FIGURE 3
Pharmacological inhibition of *F. fujikuroi* calcineurin by calcineurin inhibitors. **(A)** Phenotypes of the *F. fujikuroi* IL01 in the presence or absence of a calcineurin inhibitor. The mycelia agar discs of *F. fujiluroi* IL01 were inoculated on plates containing either FK506 (1 μg/mL) or cyclosporin A (CsA, 100 μg/mL) and incubated at 25°C for 7 days. Bar, 20 μm. **(B)** Growth kinetics of *F. fujikuroi* were obtained from **(A)**. The experiments were performed in triplicate. Statistical significance was analyzed by ANOVA, compared to mock and calcineurin inhibitor treated *F. fujikuroi* ($P< 0.001$). Error bars represented standard deviations.

and, *FfCNB1-Ri*-2, -4, and -5 were 16.6±4.1% (DSI1), 12.5 ± 7.2% (DSI1), 12. 5 ± 7.2% (DSI1), 25.0 ± 0.0% (DSI1), and 25.0 ± 7.2% (DSI2), respectively (Figures 6B, C), that were significantly, 71.5%, 78.6%, 78.6%, 57.1% and 57.1% reduced in severity compared with that of the wild-type seedlings ($P< 0.01$ in *FfCNA1-Ri*-2, -11 and, *FfCNB1-Ri*-2; $P< 0.05$ in *FfCNB1-Ri*-4, and -5). Moreover, infected wild-type seedlings were wilted and died at 30 dpi, whereas all the *FfCNA1-Ri* and *FfCNB1-Ri* plants dramatically reduced disease symptoms and no dead plants were observed.

Quantification of *F. fujikuroi* biomass in transgenic rice plants

To further assess the effect of siRNA-mediated HIGS on pathogen-infected rice, real-time quantitative PCR (qPCR) was performed to quantify the fungal biomass in transgenic lines and the wild-type plant. After 21 dpi, the genomic DNA was purified from the *F. fujikuroi*-infected wild-type, *FfCNA1-Ri*, or *FfCNB1-Ri* seedlings. The qPCR was performed by using the species-specific

10.3389/fpls.2025.1366158

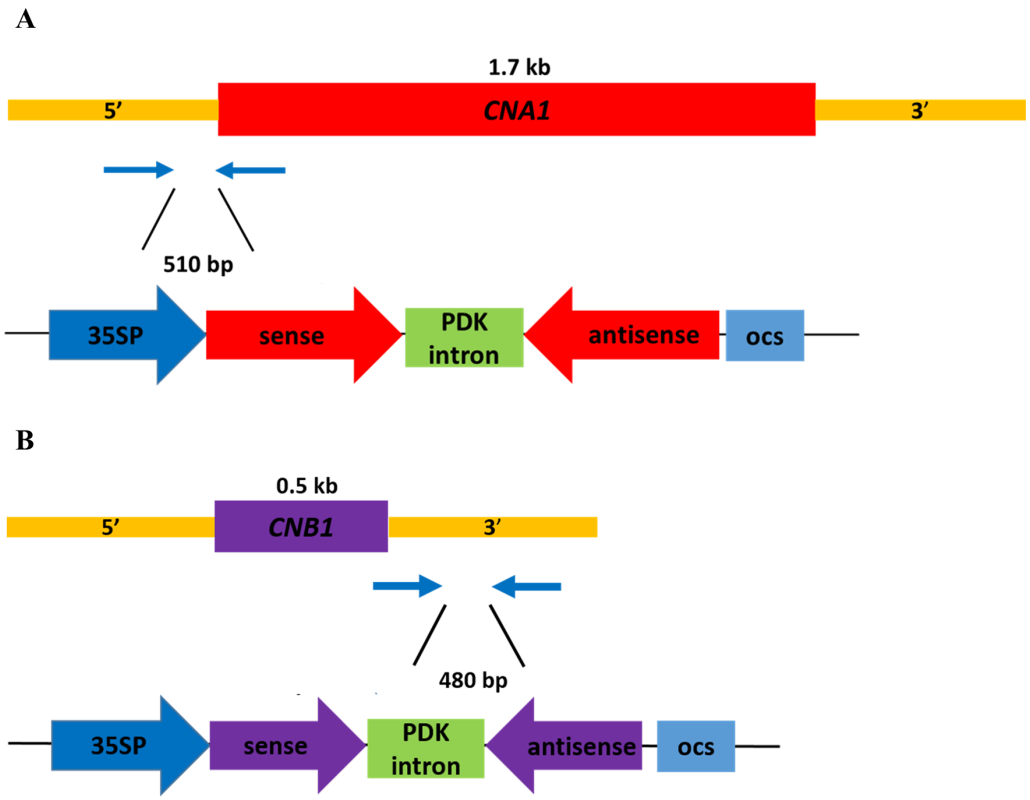

FIGURE 4
Schematic diagram of the RNA interference expression construct of calcineurin genes of *F. fujikuroi* in transgenic rice for HIGS analysis. The 510 bp DNA fragment containing the 5'-untranslated region and the 5'-coding sequence of *F. fujikuroi CNA1* **(A)**, and a 480 bp DNA fragment containing 3'-coding sequence and 3'-untranslated region of *F. fujikuroi CNB1* **(B)** were amplified by PCR, and inserted downstream of the 35S promoter in the sense and antisense orientation, with the PDK intron as the junction. 35SP, CaMV 35S promoter; PDK intron, pyruvate dehydrogenase kinase intron; ocs, octopine synthase terminator.

region of translation elongation factor 1-α (*TEF1-α*) gene in *F. fujikuroi*. The relative amount of *TEF1-α* was normalized with the rice *Actin 1* gene, and these values represent the biomass of *F. fujikuroi* in infected rice. As shown in Figure 6D, the relative biomass of *F. fujikuroi* in the wild-type seedling was 99.6 ± 60.3%. Whereas in the *FfCNA1-Ri*-2 and -11 and, the *FfCNB1-Ri*-2, -4 and -5 were 15.3 ± 2.3%, 5.6 ± 0.8%, 8 ± 0.5%, 16.6 ± 0.8%, and 17.6 ± 0.8%, respectively, that were significantly 84.7%, 94.4%, 91.9%, 83.4% and 82.4% reduced compared to that of the wild-type seedling ($P< 0.001$). These results revealed that expression of *FfCNA1-Ri* or *FfCNB1-Ri* in transgenic rice could enhance resistance against *F. fujikuroi* infection. Out of these, the transgenic lines *FfCNA1-Ri*-11 and *FfCNB1-Ri*-2 demonstrated higher disease resistance than other transgenic lines.

Discussion

Recently, HIGS has been used as an innovative approach for managing plant diseases. Numerous studies have shown the successful application of HIGS, and that genes crucial for morphogenesis or pathogenesis are the ideal targets for silencing (Nunes and Dean, 2012; Ghag, 2017). Calcineurin is well known for regulating hyphal growth, septation, and virulence in many plant and human pathogenic fungi. Moreover, calcineurin has been proven to be involved in the development of propagule or structure, which is required for infection, such as asexual/sexual spores, sclerotium, and appressorium (Chen et al., 2010; Park et al., 2019). Furthermore, our previous research showed that calcineurin plays an important role in the growth and virulence of *Fusarium oxysporum* f. sp. *lycopersici* (Hou et al., 2020). According to the pharmacological inhibition of calcineurin, our study revealed that both FK506 and CsA could lead to blunted and irregularly branched hyphae in *F. fujikuroi*, suggesting that calcineurin might be involved in hyphal development and further resulted in the defect of pathogenesis. To further evaluate the efficiency of dsRNA in RNAi-mediated gene silencing, naked dsRNA was applied to *F. fujikuroi* colony. The observed differences in colony growth under different dsRNA treatments suggest that the fungal growth was inhibited by exogenous dsRNA (Supplementary Figure S1). As a result, *F. fujikuroi* calcineurin could be the potential target for disease management via an RNAi approach.

Bioinformatic analysis and phenotypic assay were performed to assess the probability of off-target effects as the calcineurin cascade is conserved in eukaryotes and involved in many biological processes. To this end, 5' or 3' untranslated regions of *FfCNA1*

10.3389/fpls.2025.1366158

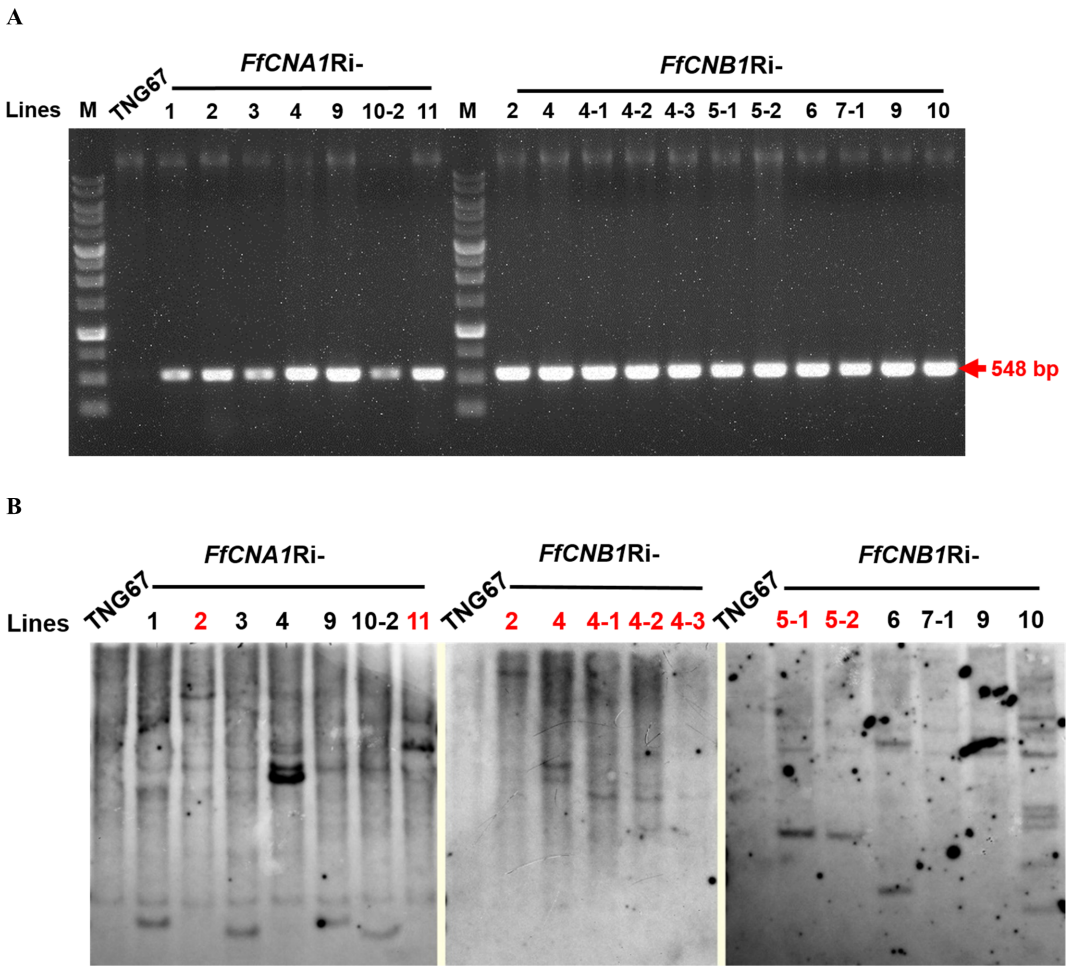

FIGURE 5
PCR and Southern blot analysis of rice wild-type (TNG67) and transgenic lines. Genomic DNAs were purified from the calli of TNG67, *FfCNA1*Ri, and *FfCNB1*Ri transgenic lines, respectively. **(A)** PCR analysis using the *FfCNA1-Ri* and *FfCNB1-Ri* specific primer sets. **(B)** Genomic DNAs were digested by *Pst*I and subjected to agarose gel electrophoresis, followed by Southern blot hybridization using the alkaline phosphatase-labeled hygromycin phosphotransferase (*Hph*) gene as the probe. The single-copied transgenic lines are marked with red letters.

and *FfCNB1* were chosen to build the RNAi constructs for the HIGS approach. According to phylogenetic analyses, results showed that rice calcineurin B-like protein (OsCBL1) was located at the most distance from *F. fujikuroi* and other fungal calcineurins. Furthermore, sequence alignment determined that our RNAi target sequences did not have any remarkable homology with the rice genome, and there was no difference in growth phenotype observed between the wild-type and transgenic rice lines (Figure 6A). Moreover, the expression of *OsCBL7*, which exhibited the highest sequence identity towards *FfCNB1* among rice calcineurin B-like protein family, showed no significant difference between wild-type and transgenic rice (Supplementary Figure S2). Taken together, these findings indicate that siRNA production does not influence the expression of specific genes or the physical state of rice. The off-target effect toward important genes in arbuscular mycorrhizal fungi (AMF) or plant growth-promoting rhizobacteria (PGPR) present in rice roots were also considered. The AMF species mostly belong to the *Glomeraceae* family, including *Rhizophagus* spp., *Glomus* spp. and *Funneliformis* spp. (Vallino et al., 2014; Wang et al., 2015). The results of alignment revealed poor similarity between the nucleotide sequence of calcineurin subunit A and B in *R. irregularis* compared with sequences used in *FfCNA1-Ri* and *FfCNB1-Ri* construct (Supplementary Figure S3). In contrast to eukaryotes, bacteria lack direct RNAi machinery, but instead use DNA as a gene silencing signal for the initiation of the CRISPR/Cas system, thus, it is unlikely that siRNA can affect the growth of PGPR. Moreover, the specificity of dsRNAs was evaluated. The results indicated that the presence of dsRNA has modestly impact on the virulence of *F. fujikuroi* when the dsRNA sequence was not homologous to the *F. fujikuroi* genome (Supplementary Figure S4). Taken together, siRNAs derived from the *FfCNA1*- or *FfCNB1-Ri* constructs might reduce the off-target effect on rice plants or nearby organisms.

As shown in Figure 6, the disease severity and the relative fungal biomass were lower in transgenic rice seedlings than in the wild-type. In addition to assessing disease severity, siRNA detection was conducted in transgenic rice to determine whether the observed

10.3389/fpls.2025.1366158

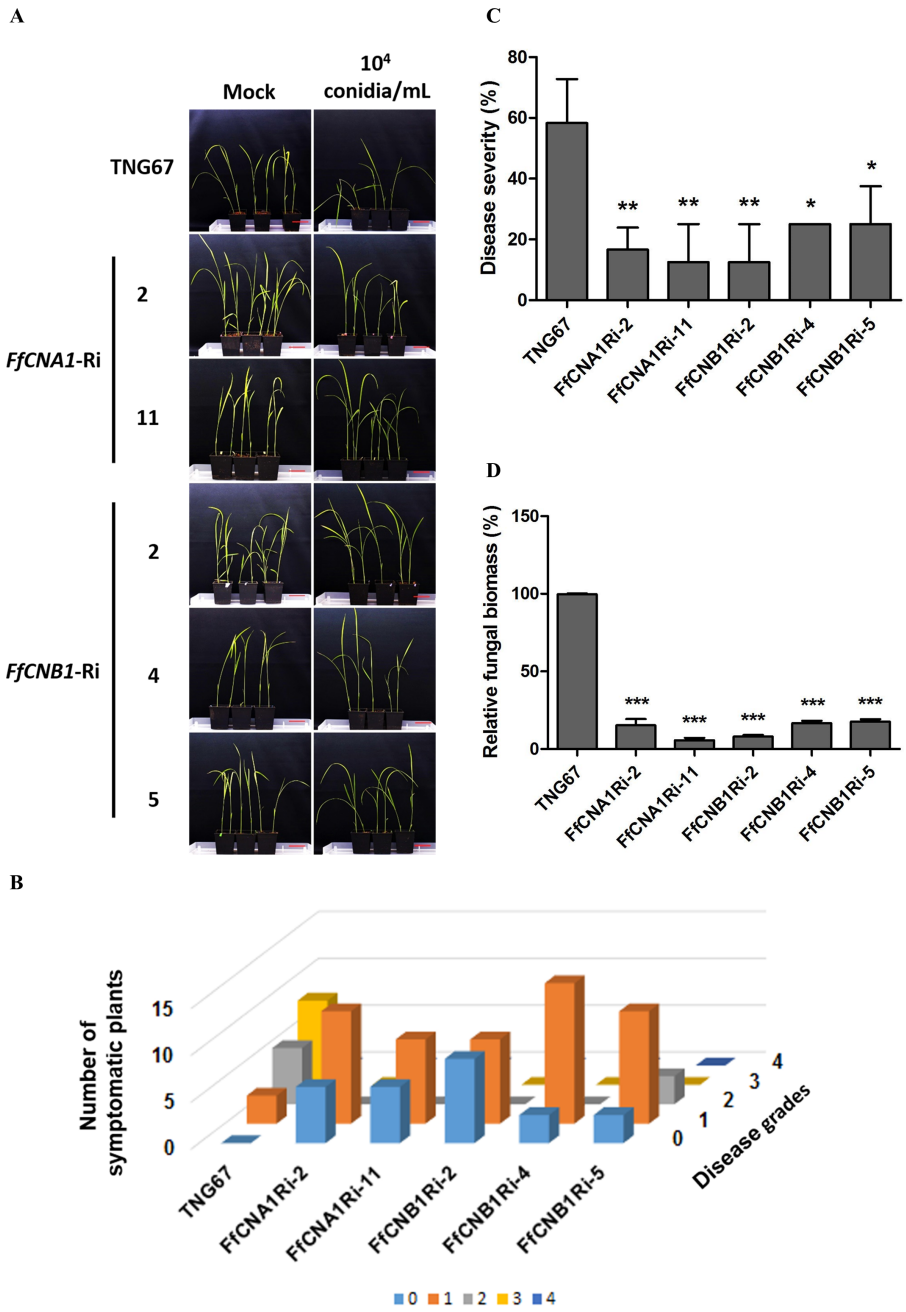

FIGURE 6
Ectopic expression of *FfCNA1-Ri* and *FfCNB1-Ri* in transgenic rice plants conferred enhanced resistance against rice bakanae disease. **(A)** The phenotypes of wild-type and transgenic rice lines at 21 dpi. Bar, 5 cm. The three days of germinated rice seeds were inoculated with *F. fujikuroi* (10^4 conidia/mL) for 1 h and incubated in a growth chamber at 28°C for 21 days. The disease index **(B)** and the disease severity **(C)** levels were calculated at 21 dpi based on criteria described in materials and methods. **(D)** The fungal biomass was determined by qPCR in rice seedlings at 21 dpi. Error bars represent standard deviations, and the relative fungal biomass was estimated by the expression levels of *F. fujikuroi TEF1-α*, which were normalized to the rice *Actin* gene expression level. These results were obtained from three biological replicates. Asterisks indicated significant differences compared to wild-type according to ANOVA. *, $P< 0.05$; **, $P< 0.01$; ***, $P< 0.001$.

enhancement in resistance was mediated by siRNAs derived from the sequences. Sequence alignment identified siRNAs ranging from 18 to 30 nucleotides in length that were complementary to the target sequence in *FfCNB1-Ri-4*, whereas no corresponding siRNAs were detected in WT (Supplementary Figure S5). These results indicated the expression of RNAi transgenes (*FfCNA1-Ris and FfCNB1-Ris*) in rice for the formation of anti-calcineurin siRNA induced the effect of HIGS to improve disease resistance in rice. Recently, HIGS in plants has been reported to combat diseases caused by *Fusarium* species. For instance, expression of the *F. graminearum* essential gene *Chs3b* (chitin synthase) using RNAi in wheat could increase resistance to Fusarium head blight (Cheng et al., 2015). Ectopic expression of fungal CYP51 (cytochrome P450 lanosterol C-14α-demethylase) RNAi construct in Arabidopsis and barley was able to

enhance resistance against *F. graminearum* (Koch et al., 2013). Resistance against banana Fusarium wilt was also achieved by using the HIGS strategy, via targeting the conserved domain of the fungal morphogenesis related genes, the velvet protein family, resulting in growth inhibition and reduced disease severity (Ghag et al., 2014). These studies also emphasized that genes which play a critical role in growth and virulence of pathogens can act as ideal HIGS targets to protect plants from pathogen attack (Qi et al., 2019).

In this study, by using a HIGS strategy in rice to directly silence *FfCNA1* and *FfCNB1* in *F. fujikuroi*, we found that the transgenic rice seedlings had enhanced resistance against *F. fujikuroi* infection, indicating calcineurin is critical for *F. fujikuroi* to infect rice plants. Furthermore, our results also provide insights into the mechanism of HIGS in plants and a strategy for improving resistance against rice bakanae disease.

Materials and methods

Fungal strain and culture condition

The *Fusarium fujikuroi* strain IL01 was used in this study (Hsu et al., 2013). *F. fujikuroi* was grown on potato dextrose agar (PDA; 0.4% potato starch from infusion, 2% dextrose, 1.5% agar) (BioShop, Burlington, ON, Canada). The growing temperature of *F. fujikuroi* was set at 25°C.

Colony morphology observation

F. fujikuroi was streaked out from -80°C stock, incubated on YPD at 25°C for one week, and cut to 7 mm in diameter with a hole punch (Bioshop, Canada). Agar discs having cultures were put on PDA plates, PDA with 1 µg/mL FK506 (Astellas Pharma, Tokyo, Japan) or 100 µg/mL cyclosporin A (LC Laboratories, Woburn, USA) with three replicates. All plates were incubated at 25°C for seven days, and the diameter of the fungal colony was measured daily. Data were analyzed by two-way ANOVA and Bonferroni post-test by using GraphPad Prism 5 (GraphPad Software, CA, USA). The representative plates were photographed.

Plant DNA isolation and Southern blotting

Rice genomic DNA was extracted from calli or young leaves. Tissues were frozen in liquid nitrogen and ground into powder. The powder was transferred to a 1.5 mL microcentrifuge tube followed by adding equal volume of urea extraction buffer [8M urea, 0.35M NaCl, 0.05M Tris-HCl (pH 7.5), 0.02M EDTA, 2% SDS] and a 3:2 ratio mixture of phenol:chloroform, mixed well and then centrifuged at 14,000 rpm for 10 min at 4°C Afterward, the upper phase was collected and an equal volume of isopropanol was added to precipitate the nucleic acid. The extracts were centrifuged at 14,000 rpm for 5 min. The supernatants were thrown away and the nucleic acid pellets were washed in 70% ethanol followed by 100% ethanol. The pellets were air dried for 5 min and dissolved with sterile water.

For Southern blot analyses of transgenic rice plants, 50 µg DNA was digested with *Pst*I and separated in a 0.8% agarose gel at 20V for 10 h. After electrophoresis, the gel was depurinated in 0.2N HCl for 10 min followed by soaking in denaturation solution (0.5 M NaOH, 1.5 M NaCl) and neutralization solution [0.5 M Tris-HCl (pH 8.0), 1.5 M NaCl] for 2 h, respectively. The hygromycin phosphotransferase (*Hph*) DNA probe was labeled with alkaline phosphatase by using Amersham AlkPhos Direct Labeling and Detection Systems (GE Healthcare, USA). The DNA fragments were transferred to a Hybond-N^+ membrane (GE Healthcare, USA). The primers used for the DNA probe generated by PCR are shown in Table 1.

Plant infection assay

The rice cultivar *Oryza sativa* L. cv Tainung 67 (TNG67, wild-type) and the transgenic rice seedlings were inoculated with *F. fujikuroi*. Three-day-old germinated seeds were inoculated with a suspension of 10^5 conidia/mL of *F. fujikuroi* for 1 h, and then planted in horticultural substrate [peat moss: Akadama soil (1:1)], and grown in the chamber at 28°C (16 h light/8 h dark). Disease severity was recorded at 21 days-post-inoculation (dpi). Data were plotted using software GraphPad Prism 5 (GraphPad Software, CA, USA). The disease severity index (DSI) was graded into five degrees from 0 to 4: 0 = no symptoms; 1 = only one symptom: internode elongation, large leaf angle, seedling slender or pale; 2 = two symptoms as described in 1; 3 = complex symptoms; and 4 = plant either wilted or dead. The DSI was modified from previous studies (Amatulli et al., 2010; Hsu et al., 2013; Chen et al., 2015). Six plants were used for each treatment. Data were analyzed by one-way ANOVA and Dunnett's post-test using GraphPad Prism 5. The formula of disease severity is shown below:

$$Disease\ \ severity = \frac{\sum (number\ \ of\ \ symptomatic\ \ plants \times disease\ \ grade)}{total\ \ number\ \ of\ \ disease\ \ scale \times maximum\ \ disease\ \ grade} \times 100\,\%$$

Pathogen biomass quantification in planta

Rice seeds were inoculated with or without *F. fujikuroi* and incubated in a growth chamber at 28°C (16 h light/8 h dark). After 21 dpi, seedlings were harvested and whole plants were cut in pieces and ground into a powder with liquid nitrogen for genomic DNA isolation as described above. Real-time quantitative PCR (qPCR) was carried out using 30 ng of genomic DNA as template with

TABLE 1 Primers used in this study.

Primer	Use	Sequence (5′ to 3′)
JC1440	F-*FfCNA1-Ri*-forward	ATACTCGAGCAGTGGCCCTTAGGTTCCTG
JC1441	R-*FfCNA1-Ri*-forward	ATAGGTACCCTTTGCACACACGCTCCAAG
JC1442	F-*FfCNA1-Ri*-reverse	ATATCTAGACAGTGGCCCTTAGGTTCCTG
JC1443	R-*FfCNA1-Ri*-reverse	ATCAAGCTTCTTTGCACACACGCTCCAAG
JC1444	F-*FfCNB1-Ri*-forward	ATACTCGAGACCAGTTCTAAACGATCGC
JC1445	R-*FfCNB1-Ri*-forward	ATAGGTACCAGACAGAATCAAGATGTTCG
JC1446	F-*FfCNB1-Ri*-reverse	ATATCTAGAACCAGTTCTAAACGATCGC
JC1447	R-*FfCNB1-Ri*-reverse	ATAGGATCCAGACAGAATCAAGATGTTCG
JC1676	F-*Hph* probe	TATGTTTATCGGCACTTTGC
JC1677	R-*Hph* probe	TGCTCCATACAAGCCAACCACG
JC1452	F-*FoAct* for qPCR	ATCCACGTCACCACTTTCAA
JC1453	R-*FoAct* for qPCR	TGCTTGGAGATCCACATTTG
JC1808	F-*FfTEF1*-α for qPCR	ATCCTGACCAAGATCTGGCGGGGTATATCTCA
JC1809	R-*FfTEF1*-α for qPCR	GCTCAGCGGCTTCCTATTGTCGAATGTTTAGTTTG
JC1814	F-*OsAct1* for qPCR	CCAGGCCGTCCTCTCTCTGTAT
JC1815	R-*OsAct1* for qPCR	AATGAGTAACCACGCTCCGTCA

The underline represents a restriction enzyme cutting site.

SYBR®Green PCR Master Mix (Thermo Fisher Scientific, Vilnius, Lithuania) in a StepOnePlus machine (Applied Biosystems, Foster City, CA, USA). The species-specific region of *F. fujikuroi TEF1-α* gene (Chen et al., 2016b) was amplified for fungal biomass measurement, and the rice *Actin* gene was used as internal control for sample equilibration, by using the $2^{-\Delta\Delta Ct}$ method. The average fungal biomass was examined using three plants for each line, and data were plotted using software GraphPad Prism 5. The primer sets that were used for detecting *FfTEF1-α* and *OsActin* genes are listed in Table 1.

Plant materials and callus induction

The rice cultivar TNG67 was used in this study. The immature seeds were de-hulled and sterilized with 2.4% NaOCl for 1 h, then washed with sterile water and cultured on N6 solid medium (pH 5.7) (Duchefa Biochemie, Netherlands) containing 2 mg/L of 2,4-dichlorophenoxyacetic (2,4-D) (N6D medium) and sucrose (30 g/L) for callus induction. One month after, the callus derived from scutellum was subcultured to fresh N6D medium plus sucrose (30 g/L) for 10 days for *Agrobacterium*-mediated gene transformation.

Construction of the *FfCNA1-Ri* and *FfCNB1-Ri* expression vectors

To construct the *35S::FfCNA1-RNAi* expression vector, a 0.5-kb DNA fragment including the 5'-untranslated region (328 bp) and 5' coding region (175 bp) of *FfCNA1* was PCR-amplified using the primer sets JC1440/JC1441 and JC1442/JC1443 (Table 1). Both ends of DNA fragments were cleaved either with *Xho*I and *Kpn*I, or with *Xba*I and *Hin*dIII, and introduced into the same cloning sites of the vector pKANNIBAL (Helliwell and Waterhouse, 2003) in an inverted repeat manner, respectively. To construct a vector for the ectopic expression of *35S::FfCNB1-RNAi* in rice, a 439-bp DNA fragment that included 3' coding region (11 bp) and 3'-untranslated region (428 bp) of *FfCNB1* was amplified using primer sets JC1444/JC1445 and JC1446/JC1447 (Table 1). Both ends of DNA fragments were cleaved either with *Xho*I and *Kpn*I, or with *Xba*I and *Bam*HI, and inserted into the vector pKANNIBAL in an inverted repeat manner, respectively, under the governor of 35S promoter. Both *35S::FfCNA1-Ri* and *35S::FfCNB1-Ri* constructs were linearized by *Pst*I digestion and introduced into the *Pst*I site of the pBH binary vector, respectively (Ho et al., 2000), followed by *Agrobacterium*-mediated transformation.

Rice transformation

The *FfCNA1-Ri* or *FfCNB1-Ri* vectors were transformed into *Agrobacterium tumefaciens* strain EHA101 through electroporation, and the rice calli were co-cultured with the transformed *Agrobacterium* strain in the solid N6D medium (pH 5.2) containing 100 μM acetosyringone for 3-5 days. The calli were then washed thoroughly with sterile water and thereafter incubated on N6D medium supplemented with hygromycin B (50 mg/L) and cefotaxime (250 mg/L) for 30 days. After incubation, the newly generated transformed

rice cells (callus) were treated with osmotic stress by transferring to the N6 medium plus sorbitol (90 g/L), 2,4-D (0.5 mg/L), Naphthalene acetic acid (NAA) (1 mg/L) and 6-Benzylaminopurine (0.5 mg/L) and incubated for 10 days under dark conditions. After stress treatment, the calli were transferred to the plant regeneration induction medium, which consisted of N6 agar medium supplemented with hygromycin B (50 mg/L), glucose (5 g/L), NAA (0.5 mg/L) and kinetin (5 mg/L), and then incubated for 30 days to induce the formation of shoots and roots from the callus. The regenerated rice seedlings were then transferred to the 1/2 Murashige and Skoog (MS) medium for further growth. The transgenic rice seedlings (T0 plants) were finally transferred and grown in the soil pot for further studies and the transgenic seeds (T1 seeds) were harvested.

Data availability statement

The raw data supporting the conclusions of this article will be made available by the authors, without undue reservation.

Author contributions

Y-HH: Conceptualization, Formal analysis, Investigation, Methodology, Software, Validation, Writing – original draft, Writing – review & editing. T-XZ: Conceptualization, Formal analysis, Investigation, Methodology, Software, Writing – original draft, Writing – review & editing. Y-LC: Conceptualization, Funding acquisition, Methodology, Resources, Supervision, Writing – original draft, Writing – review & editing.

Funding

The author(s) declare that financial support was received for the research and/or publication of this article. This work was financially supported by grants 113-2320-B-002-029-MY3, 110-2923-B-002-002-MY3, 110-2320-B-002-050-MY3 from the National Science and Technology Council and grant 112AS-14.5.2-CL-n1 from the Ministry of Agriculture, Executive Yuan, Taiwan.

Conflict of interest

The authors declare that the research was conducted in the absence of any commercial or financial relationships that could be construed as a potential conflict of interest.

Publisher's note

Supplementary material

The Supplementary Material for this article can be found online at: https://www.frontiersin.org/articles/10.3389/fpls.2025.1366158/full#supplementary-material

References

Amatulli, M. T., Spadaro, D., Gullino, M. L., and Garibaldi, A. (2010). Molecular identification of Fusarium spp. associated with bakanae disease of rice in Italy and assessment of their pathogenicity. *Plant Pathol.* 59, 839–844. doi: 10.1111/j.1365-3059.2010.02319.x

Carter, L., Leslie, J., and Webster, R. (2008). Population structure of Fusarium fujikuroi from California rice and water grass. *Phytopathology* 98, 992–998. doi: 10.1094/PHYTO-98-9-0992

Chen, C.-Y., Chen, S.-Y., Liu, C.-W., Wu, D.-H., Kuo, C.-C., Lin, C.-C., et al. (2020). Invasion and colonization pattern of Fusarium fujikuroi in rice. *Phytopathology* 110, 1934–1945. doi: 10.1094/PHYTO-03-20-0068-R

Chen, S. Y., Huang, K. J., Kuo, Y. F., Lai, M. H., Chen, Y. C., and Chung, C. L. (2015). Three modified methods for evaluation of bakanae disease resistance in rice seedlings. *Plant Pathol. Bull.* 24, 201–210.

Chen, W., Kastner, C., Nowara, D., Oliveira-Garcia, E., Rutten, T., Zhao, Y., et al. (2016a). Host-induced silencing of Fusarium culmorum genes protects wheat from infection. *J. Exp. Bot.* 67, 4979–4991. doi: 10.1093/jxb/erw263

Cheng, W., Song, X. S., Li, H. P., Cao, L. H., Sun, K., Qiu, X. L., et al. (2015). Host-induced gene silencing of an essential chitin synthase gene confers durable resistance to Fusarium head blight and seedling blight in wheat. *Plant Biotechnol. J.* 13, 1335–1345. doi: 10.6649/PPB.201512_24(3_4).0003

Chen, Y. C., Lai, M. H., Wu, C. Y., Lin, T. C., Cheng, A. H., Yang, C. C., et al. (2016b). The genetic structure, virulence, and fungicide sensitivity of Fusarium fujikuroi in Taiwan. *Phytopathology* 106, 624–635. doi: 10.1094/phyto-11-15-0285-r

Chen, Y. L., Kozubowski, L., Cardenas, M. E., and Heitman, J. (2010). On the roles of calcineurin in fungal growth and pathogenesis. *Curr. Fungal Infect. Rep.* 4, 244–255. doi: 10.1007/s12281-010-0027-5

Egan, J. D., García-Pedrajas, M. D., Andrews, D. L., and Gold, S. E. (2009). Calcineurin is an antagonist to PKA protein phosphorylation required for postmating filamentation and virulence, while PP2A is required for viability in Ustilago maydis. *Mol. Plant-Microbe Interact.* 22, 1293–1301. doi: 10.1094/MPMI-22-10-1293

Fuller, K. K., and Rhodes, J. C. (2012). Protein kinase A and fungal virulence: a sinister side to a conserved nutrient sensing pathway. *Virulence* 3, 109–121. doi: 10.4161/viru.19396

Ghag, S. B. (2017). Host induced gene silencing, an emerging science to engineer crop resistance against harmful plant pathogens. *Physiol. Mol. Plant Pathol.* 100, 242–254. doi: 10.1016/j.pmpp.2017.10.003

Ghag, S. B., Shekhawat, U. K., and Ganapathi, T. R. (2014). Host-induced post-transcriptional hairpin RNA-mediated gene silencing of vital fungal genes confers efficient resistance against Fusarium wilt in banana. *Plant Biotechnol. J.* 12, 541–553. doi: 10.1111/pbi.12158

Harel, A., Bercovich, S., and Yarden, O. (2006). Calcineurin is required for sclerotial development and pathogenicity of Sclerotinia sclerotiorum in an oxalic acid-independent manner. *Mol. Plant-Microbe Interact.* 19, 682–693. doi: 10.1094/MPMI-19-0682

He, B., Cai, Q., Qiao, L., Huang, C.-Y., Wang, S., Miao, W., et al. (2021). RNA-binding proteins contribute to small RNA loading in plant extracellular vesicles. *Nat. Plants* 7, 342–352. doi: 10.1038/s41477-021-00863-8

Helliwell, C., and Waterhouse, P. (2003). Constructs and methods for high-throughput gene silencing in plants. *Methods* 30, 289–295. doi: 10.1016/S1046-2023(03)00036-7

Hemenway, C. S., and Heitman, J. (1999). Calcineurin: structure, function, and inhibition. *Cell Biochem. Biophys.* 30, 115–151. doi: 10.1007/BF02737887

Ho, S. L., Tong, W. F., and Yu, S. M. (2000). Multiple mode regulation of a cysteine proteinase gene expression in rice. *Plant Physiol.* 122, 57–66. doi: 10.1104/pp.122.1.57

Hou, Y. H., Hsu, L. H., Wang, H. F., Lai, Y. H., and Chen, Y. L. (2020). Calcineurin regulates conidiation, chlamydospore formation and virulence in Fusarium oxysporum f. sp. lycopersici. *Front. Microbiol.* 11. doi: 10.3389/fmicb.2020.539702

Hsu, C. C., Lai, M. H., Lin, C. C., Huang, J. W., and Chen, C. Y. (2013). Standardization of the protocol for evaluating susceptibility of rice to the pathogen of bakanae disease. *Plant Pathol. Bull.* 22, 291–299. doi: 10.6649/PPB.201309_22(3).0005

Juvvadi, P. R., Lamoth, F., and Steinbach, W. J. (2014). Calcineurin as a multifunctional regulator: unraveling novel functions in fungal stress responses, hyphal growth, drug resistance, and pathogenesis. *Fungal Biol. Rev.* 28, 56–69. doi: 10.3390/pathogens4040883

Juvvadi, P. R., and Steinbach, W. J. (2015). Calcineurin orchestrates hyphal growth, septation, drug resistance and pathogenesis of Aspergillus fumigatus: where do we go from here? *Pathogens* 4, 883–893. doi: 10.1016/j.fbr.2014.02.004

Koch, A., Kumar, N., Weber, L., Keller, H., Imani, J., and Kogel, K. H. (2013). Host-induced gene silencing of cytochrome P450 lanosterol C14α-demethylase–encoding genes confers strong resistance to Fusarium species. *Proc. Natl. Acad. Sci. U. S. A.* 110, 19324–19329. doi: 10.1073/pnas.1306373110

Liu, S., Hou, Y., Liu, W., Lu, C., Wang, W., and Sun, S. (2015). Components of the calcium-calcineurin signaling pathway in fungal cells and their potential as antifungal targets. *Eukaryotic Cell* 14, 324–334. doi: 10.1128/ec.00271-14

Mahanty, B., Mishra, R., and Joshi, R. K. (2023). Cross-kingdom small RNA communication between plants and fungal phytopathogens-recent updates and prospects for future agriculture. *RNA Biol.* 20, 109–119. doi: 10.1080/15476286.2023.2195731

Majumdar, R., Rajasekaran, K., and Cary, J. W. (2017). RNA interference (RNAi) as a potential tool for control of mycotoxin contamination in crop plants: concepts and considerations. *Front. Plant Sci.* 8. doi: 10.3389/fpls.2017.00200

Matić, S., Bagnaresi, P., Biselli, C., Orru', L., Amaral Carneiro, G., Siciliano, I., et al. (2016). Comparative transcriptome profiling of resistant and susceptible rice genotypes in response to the seedborne pathogen Fusarium fujikuroi. *BMC Genomics* 17, 1–17. doi: 10.1186/s12864-016-2925-6

Matic, S., Gullino, M. L., and Spadaro, D. (2017). The puzzle of bakanae disease through interactions between Fusarium fujikuroi and rice. *Front. Biosci.* 9, 333–344. doi: 10.2741/e806

Mei, Z., Xiaoxue, L., Jun, W., Erxun, Z., and Canwei, S. (2024). Host-induced gene silencing of effector AGLIP1 enhanced resistance of rice to Rhizoctonia solani AG1-IA. *Rice Sci.* 31, 463–474. doi: 10.1016/j.rsci.2024.04.005

Niehaus, E. M., Kim, H. K., Münsterkötter, M., Janevska, S., Arndt, B., Kalinina, S. A., et al. (2017). Comparative genomics of geographically distant Fusarium fujikuroi isolates revealed two distinct pathotypes correlating with secondary metabolite profiles. *PLoS Pathog.* 13, e1006670. doi: 10.1371/journal.ppat.1006670

Nunes, C. C., and Dean, R. A. (2012). Host-induced gene silencing: a tool for understanding fungal host interaction and for developing novel disease control strategies. *Mol. Plant Pathol.* 13, 519–529. doi: 10.1111/j.1364-3703.2011.00766.x

Park, H. S., Lee, S. C., Cardenas, M. E., and Heitman, J. (2019). Calcium-calmodulin-calcineurin signaling: a globally conserved virulence cascade in eukaryotic microbial pathogens. *Cell Host Microbe* 26, 453–462. doi: 10.1016/j.chom.2019.08.004

Peng, Q., Waqas Younas, M., Yang, J., Zhu, H., Miao, J., Gu, B., et al. (2022). Characterization of prochloraz resistance in Fusarium fujikuroi from Heilongjiang Province in China. *Plant Dis.* 106, 418–424. doi: 10.1094/PDIS-02-21-0372-RE

Piombo, E., Bosio, P., Acquadro, A., Abbruscato, P., and Spadaro, D. (2020). Different phenotypes, similar genomes: three newly sequenced Fusarium fujikuroi strains induce different symptoms in rice depending on temperature. *Phytopathology* 110, 656–665. doi: 10.1094/PHYTO-09-19-0359-R

Qi, T., Guo, J., Peng, H., Liu, P., Kang, Z., and Guo, J. (2019). Host-induced gene silencing: a powerful strategy to control diseases of wheat and barley. *Int. J. Mol. Sci.* 20, 206. doi: 10.3390/ijms20010206

Qi, T., Zhu, X., Tan, C., Liu, P., Guo, J., Kang, Z., et al. (2018). Host-induced gene silencing of an important pathogenicity factor P s CPK 1 in Puccinia striiformis f. sp. tritici enhances resistance of wheat to stripe rust. *Plant Biotechnol. J.* 16, 797–807. doi: 10.1111/pbi.12829

Sun, S. K. (1975). The diseases cycle of rice bakanae disease in Taiwan *In Proc. Natl. Sci. Counc. Repub. China.* 8, 245–256.

Sunani, S. K., Bashyal, B. M., Rawat, K., Manjunatha, C., Sharma, S., Prakash, G., et al. (2019). Development of PCR and loop mediated isothermal amplification assay for the detection of bakanae pathogen Fusarium fujikuroi. *Eur. J. Plant Pathol.* 154, 715–725. doi: 10.1007/s10658-019-01694-2

Tadasanahaller, P. S., Bashyal, B. M., Yadav, J., Krishnan Subbaiyan, G., Ellur, R. K., and Aggarwal, R. (2023). Identification and characterization of Fusarium fujikuroi pathotypes responsible for an emerging bakanae disease of rice in India. *Plants* 12, 1303. doi: 10.3390/plants12061303

Vallino, M., Fiorilli, V., and Bonfante, P. (2014). Rice flooding negatively impacts root branching and arbuscular mycorrhizal colonization, but not fungal viability. *Plant Cell Environ.* 37, 557–572. doi: 10.1111/pce.12177

Viaud, M. C., Balhadère, P. V., and Talbot, N. J. (2002). A Magnaporthe grisea cyclophilin acts as a virulence determinant during plant infection. *Plant Cell* 14, 917–930. doi: 10.1105/tpc.010389

Viaud, M., Brunet-Simon, A., Brygoo, Y., Pradier, J. M., and Levis, C. (2003). Cyclophilin A and calcineurin functions investigated by gene inactivation, cyclosporin A inhibition and cDNA arrays approaches in the phytopathogenic fungus Botrytis cinerea. *Mol. Microbiol.* 50, 1451–1465. doi: 10.1046/j.1365-2958.2003.03798.x

Wang, M., and Dean, R. A. (2020). Movement of small RNAs in and between plants and fungi. *Mol. Plant Pathol.* 21, 589–601. doi: 10.1111/mpp.12911

Wang, H., Gai, Y., Zhao, Y., Wang, M., and Ma, Z. (2023). The calcium-calcineurin and high-osmolarity glycerol pathways co-regulate tebuconazole sensitivity and pathogenicity in Fusarium graminearum. *Pestic. Biochem. Physiol.* 190, 105311. doi: 10.1016/j.pestbp.2022.105311

Wang, Y., Li, T., Li, Y., Björn, L. O., Rosendahl, S., Olsson, P. A., et al. (2015). Community dynamics of arbuscular mycorrhizal fungi in high-input and intensively irrigated rice cultivation systems. *Appl. Environ. Microb.* 81, 2958–2965. doi: 10.1128/AEM.03769-14

Wang, M., Weiberg, A., Lin, F. M., Thomma, B. P., Huang, H. D., and Jin, H. (2016). Bidirectional cross-kingdom RNAi and fungal uptake of external RNAs confer plant protection. *Nat. Plants* 2, 1–10. doi: 10.1038/nplants.2016.151

Yadav, V., and Heitman, J. (2023). Calcineurin: the Achilles' heel of fungal pathogens. *PLoS Pathog.* 19, e1011445. doi: 10.1371/journal.ppat.1011445

Frontiers in
Plant Science

Cultivates the science of plant biology and its applications

The most cited plant science journal, which advances our understanding of plant biology for sustainable food security, functional ecosystems and human health.

Discover the latest Research Topics

See more →

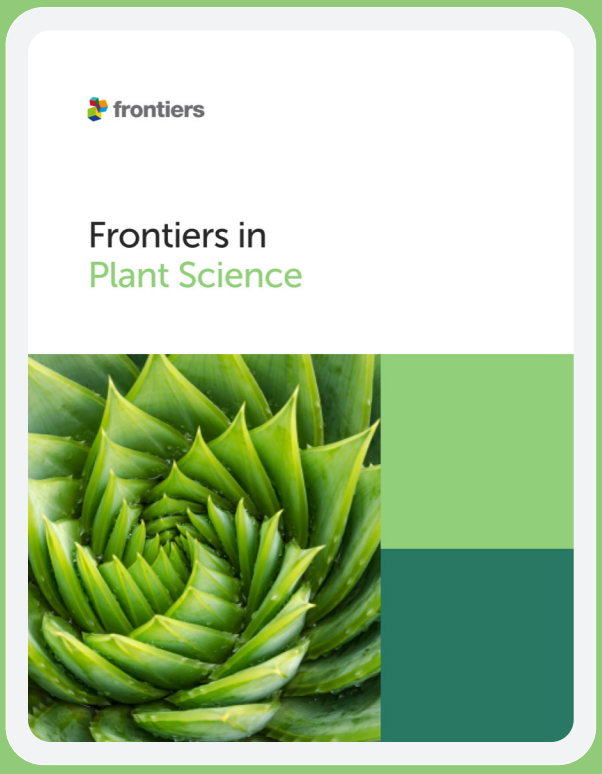

Frontiers

Avenue du Tribunal-Fédéral 34
1005 Lausanne, Switzerland
frontiersin.org

Contact us

+41 (0)21 510 17 00
frontiersin.org/about/contact